

**EVALUATING SITES FOR SUBSURFACE CO₂
INJECTION/SEQUESTRATION: TANGGUH,
BINTUNI BASIN, PAPUA, INDONESIA**

(VOLUME 2: Figures and Appendices)

Jonathan P. Salo

Supervisors:
Dr. Simon C. Lang
Dr. John G. Kaldi

**Australian School of Petroleum
University of Adelaide
South Australia
S.A. 5005**

May 2005

TABLE OF CONTENTS

TITLE PAGE	
ACKNOWLEDGMENTS.....	i
ABSTRACT.....	iii
TABLE OF CONTENTS.....	vi
PART I – INTRODUCTION.....	1
1. INTRODUCTION.....	2
1.0 Rationale and Aim.....	2
1.1 Background on Global Warming.....	2
1.2 Greenhouse Effect.....	4
1.3 Greenhouse Gases.....	6
1.4 Carbon Dioxide.....	11
1.5 Complete Carbon Cycle.....	13
1.6 Anthropogenic CO ₂	16
1.7 Non-geological CO ₂ Disposal Options.....	16
2. PROJECT AREA BACKGROUND.....	20
2.1 Location	20
2.2 Concession history and current status.....	21
3. EVALUATION OF GEOLOGICAL SEQUESTRATION OPTIONS.....	27
3.1 CUCS (CO ₂ in unmineable coal-bed sequestration).....	28
3.2 CECMP (CO ₂ for enhanced coal-bed methane production).....	29
3.3 CDOGR (CO ₂ in depleted oil/gas reservoirs).....	30
3.4 CCV (CO ₂ in cavity or void).....	31
3.4.1 Salt domes, mines, and tunnels.....	31
3.4.2 New Guinea Limestone Group member (NGLG)....	31
3.4.2.1 Eocene carbonates.....	31
3.4.2.2 Oligocene Limestone Formation.....	32
3.4.2.3 Faumai Formation.....	32
3.4.2.4 Kais Limestone Formation.....	32
3.4.2.5 Nonsuitability of the NGLG for CO ₂	33
3.4.2.6 Nonsuitability of CDOGR for CO ₂	34
3.4.2.6.1 Insufficient Storage Capacity	34
3.4.2.6.2 Supercritical Phase Instability...	35
3.4.2.6.3 Unsuitable Mineralogy.....	36

TABLE OF CONTENTS

3.4.2.6.4 Karstification.....	37
3.4.2.6.5 Salawati Basin Distance.....	37
3.5 CEOR (CO ₂ for enhanced oil recovery).....	38
3.6 CEGR (CO ₂ for enhanced gas recovery).....	38
3.7 CSA (CO ₂ in saline aquifer).....	39
3.7.1 CSA in non-hydrocarbon bearing structural traps....	39
3.7.2 CSA in hydrocarbon bearing structural traps.....	40
4. REGIONAL TECTONIC AND STRUCTURAL HISTORY.....	41
4.1 Paleozoic.....	41
4.2 Mesozoic.....	44
4.3 Cenozoic.....	50
5. LITHOSTRATIGRAPHY AND SEDIMENTOLOGY.....	55
5.1 Lithostratigraphic Overview Of The Bird's Head.....	55
5.2 Database Summary.....	58
5.3 Lithostratigraphy And Sedimentology Summary.....	60
5.3.1 Permian.....	60
5.3.2 Triassic.....	64
5.3.3 Early Jurassic.....	64
5.3.4 Middle Jurassic.....	64
5.3.4.i.1 Aalenian Sandstone.....	65
5.3.4.i.2 Roabiba Sandstone.....	66
5.3.5 Late Jurassic.....	69
5.3.5.i.1 Pre-Ayot Clastics Succession.....	69
5.3.5.i.2 Pre-Ayot Shale.....	69
5.3.5.i.3 Ayot Limestone Formation.....	71
5.3.5.i.4 Upper Late Jurassic Shales.....	72
5.3.5.i.5 Glauconitic Unconformity.....	73
5.3.6 Late Cretaceous.....	74
5.3.7 Late Paleocene Succession.....	76
5.3.7.i.1 Sand-Prone 'Lower Member' Interval....	78
5.3.7.i.2 Sand-Prone 'Middle Member' Interval...	80
5.3.7.i.3 Sand-Prone 'Upper Member' Interval....	83
5.3.7.i.4 Mud-Prone Interval.....	84
5.3.8 Eocene Succession.....	86

TABLE OF CONTENTS

5.3.9	New Guinea Limestone Group (NGLG).....	87
5.3.9.i.1	Oligocene Limestone Formation.....	87
5.3.9.i.2	Faumai Formation.....	88
5.3.9.i.3	Kais Limestone Formation.....	90
5.3.10	Steenkool Formation.....	91
PART II – INJECTIVITY.....		93
6.	STRATIGRAPHY.....	94
6.1	Stratigraphic Methodology.....	94
6.1.1	Seismic Stratigraphy.....	96
6.1.2	Palyнологical Biozonation.....	100
6.1.3	Wireline Log Motifs and Stratigraphic Correlations..	101
6.2	Paleogeographic Facies Maps for Tangguh Sequence Stratigraphy..	104
6.3	Detailed Sequence Stratigraphy Framework for Tangguh.....	107
6.3.1	Late Permian.....	116
6.3.2	Triassic and Early Jurassic.....	117
6.3.3	Aalenian MJ-4 (Middle Jurassic).....	120
6.3.4	Bajocian/Early Bathonian MJ-3 (Middle Jurassic)...	123
6.3.5	Late Bathonian MJ-2 (Middle Jurassic).....	131
6.3.6	Callovian MJ-1/LJ-11 (Middle-Late Jurassic).....	132
6.3.7	Ayot Limestone Formation LJ-9 (Late Jurassic).....	140
6.3.8	Upper Late Jurassic LJ-8 to LJ-2 (Late Jurassic).....	142
6.3.9	Late Cretaceous.....	143
6.3.10	Cenozoic Succession.....	145
6.4	Limitations and Alternatives.....	146
6.5	Re-interpretation of the Bird's Head Tectonic/Structural History....	147
7.	RESERVOIR CHARACTERIZATION.....	153
7.1	Whole Cores, Core Plug Analyses, and DST Data.....	153
7.2	Reservoir Quality.....	156
7.2.1	Late Permian Reservoir Quality.....	156
7.2.2	Aalenian Sandstone Formation Reservoir Quality....	163
7.2.3	Callovian and Bathonian/Bajocian Roabiba Sandstone Formation Reservoir Quality.....	165
7.2.4	Ayot Limestone Formation Reservoir Quality.....	170

TABLE OF CONTENTS

7.2.5 Late Cretaceous Reservoir Quality.....	171
7.2.6 Late Paleocene Reservoir Quality.....	172
7.2.7 NGLG Reservoir Quality.....	174
PART III – CONTAINMENT.....	176
8. ESSCI STRATA EVALUATION.....	177
8.1 Late Permian Reservoir ESSCI Potential.....	179
8.2 Middle Jurassic Reservoir ESSCI Potential.....	182
8.3 Late Cretaceous Reservoir ESSCI Potential.....	185
8.4 Late Paleocene Sand-Prone Interval ESSCI Potential.....	186
8.5 New Guinea Limestone Group Reservoir ESSCI Potential.....	188
8.6 ESSCI Stratum Rating and Ranking.....	190
9. ESSCI STRUCTURE EVALUATION.....	193
9.1 Vorwata Structure ESSCI Potential.....	194
9.2 Wiriagar Deep Structure ESSCI Potential.....	196
9.3 Ubadari Structure ESSCI Potential.....	198
9.4 Roabiba Structure ESSCI Potential.....	199
9.5 Ofaweri Structure ESSCI Potential.....	200
9.6 Wos Deep Structure ESSCI Potential.....	201
9.7 Kalitami Structure ESSCI Potential.....	201
9.8 Saritu Deep Structure ESSCI Potential.....	202
9.9 Ranking Structural Trap ESSCI Potentials.....	203
10. ESSCI SEAL EVALUATION.....	205
10.1 Overview of Reservoir/Seal Couplets and Seal Potential.....	205
10.2 Mercury Injection Capillary Pressure Methodology.....	207
10.3 Roabiba Reservoir Top and Lateral Seals.....	216
10.4 Roabiba Reservoir Regional Seals.....	224
10.5 Limitations.....	228
10.6 Discussions Regarding Seal Capacity, Geometry, and Integrity...	231
10.7 Seal Potential Conclusions.....	246
10.8 ESSCI Seal Evaluation.....	249
11. CO ₂ STORAGE CAPACITY ANALYSIS AND WEIGHTED DISTANCE FACTORING.....	252
11.1 ESSCI CO ₂ Storage Capacity Analysis And Evaluation.....	252

TABLE OF CONTENTS

11.2 Integrating ESSCI CO ₂ Storage Capacity Analysis with Reservoir, Structure, and Seal Potential ESSCI Evaluations.....	253
11.3 Distance/Economics Factor Weighted Rating and Ranking.....	257
12. CO ₂ INJECTION FAULT RE-ACTIVATION RISK EVALUATION.....	260
PART IV – CO₂ INJECTION-SITE RECOMMENDATION AND GEOLOGIC MODEL VERIFICATION.....	266
13. CO ₂ INJECTION SITE LOCATION RECOMMENDATIONS.....	267
14. TANGGUH GEO-CELLULAR MODEL.....	272
14.1 The Geological Test Model.....	273
14.2 The Preliminary Geological Model.....	275
14.3 The Final 3D Geologic Model.....	279
14.4 The Modeling Strategy.....	281
14.4.1 Zones Versus Layers in the Geological Model.....	281
14.4.2 Limitations on Volume of Active Cells in the Geological Model.....	285
i. Incorporation of Faults into the Final Tangguh 3D Geologic Model.....	286
ii. Attributes and Variograms in the Geological Model.....	287
14.5. Results of the Final 3D Geologic Model.....	291
14.6. Preliminary Reservoir Simulation Results.....	292
14.7. Conclusions.....	293
PART V – IMPLICATIONS FOR IMPLEMENTATION.....	294
15. DRILLING AND DATA RECOMMENDATIONS FOR EXPLORATION AND INJECTION WELLS.....	295
15.1. Recommendations on Future Tangguh Well Data Acquisitions.....	295
15.1.1. Steenkool/Sele Formations.....	296
15.1.2. Kais/Faumai Formations (NGLG).....	297
15.1.3. Eocene/Paleocene Formations.....	299
15.1.4. Late Cretaceous Interval.....	301
15.1.5. Jurassic Sequences.....	302
15.1.6. Triassic/Permian Sequences.....	303
15.1.7. Final Remarks on Data Acquisition.....	304

TABLE OF CONTENTS

15.1.8. Conclusions.....	305
16. EVALUATION OF SUBSURFACE CO₂ MONITORING.....	306
16.1. Surface Measurements.....	306
16.2. Smart Well Completions.....	307
16.3. Seismic.....	308
16.4. Time-Lapse 3D ('4D') Seismic Surveys.....	308
16.5. Downhole Seismic.....	309
16.5.1. VSP.....	309
16.5.2. Cross-well Seismic Tomography.....	310
16.5.3. Single-well Sonic Logging.....	310
16.5.4. Microseismic Imaging.....	311
16.6. Electromagnetic Methods.....	312
16.7. Surface Electromagnetic Measurements.....	312
16.8. Cross-well Electromagnetic Methods.....	313
16.9. Downhole to Surface Electromagnetic Methods.....	313
16.10. ERT (Electrical Resistance Tomography).....	313
16.11. Gravity.....	314
16.12. Tracers	314
16.13. Limitations and Advantages.....	315
16.14. Subsurface CO ₂ Monitoring Conclusions and Recommendations.....	315
PART VI – CONCLUSIONS, POSTSCRIPT, AND REFERENCES.....	320
17. Conclusions.....	321
18. Postscript.....	335
19. References.....	340
VOLUME 2 (FIGURES and APPENDICES)	
PART VII – FIGURES.....	1
PART VIII – APPENDICES.....	191
Appendix 1 :DST-PTA Summary.....	191
Appendix 2: Petrophysical Summary.....	205
Appendix 3: Porosity and Permeability Summary (V-10).....	229
Appendix 4: Core Plug/Chip Atlas.....	238

LIST OF TABLES

Volume 1

Table 1.1: Current averaged atmospheric gas composition	8
Table 5.1: Bintuni Basin gross intervals and formation/member	59
Table 6.1: Core and cuttings depth shifts at each well	95
Table 6.2a: Sequence stratigraphy zone/boundary depths at Tangguh	97
Table 6.2b: Sequence stratigraphy zone/boundary depths at Tangguh (cont.)	98
Table 6.3: Isopach thickness for zones/members	99
Table 6.4: Palynological zonation scheme used by Core Laboratories	103
Table 6.5: Palynological/Ichnological/Sedimentological/Log Motif charts	108-113
Table 7.1: List of all intervals cored and examined in Tangguh area	157
Table 7.2: Master list of new plug analyses (2002-2003)	158
Table 7.3: Core and cuttings depth shift for all wells	159
Table 7.4: Reservoir depth table	160
Table 7.5: New core plug porosity and permeability results	169
Table 7.6: Paleocene core plug porosity and permeability result summary	173
Table 8.1: Data confidence factor matrix for probabilistic HC exploration	178
Table 8.2: Data confidence factor matrix for ESSCI stratum at Tangguh	183
Table 8.3: Table of data confidence factor rating for ESSCI stratum	192
Table 9.1: Data confidence factor matrix for ESSCI structures at Tangguh	197
Table 9.2: Table of data confidence factor rating for ESSCI structures	204
Table 10.1: Core plug/chip MICP analyses results	208
Table 10.2: Example of GEODISC geochemical calculator	212
Table 10.3: CO ₂ column height calculator	213
Table 10.4: Measured salinities for major reservoirs	214
Table 10.5: Temperatures and pressures at datum for major reservoirs	215
Table 10.6a: Sensitivities to varied threshold pressures	218
Table 10.6b: Sensitivities to varied contact angles	219
Table 10.6c: Sensitivities to varied interfacial tension	220
Table 10.7: Comparison of seal capacities and column heights for various seals	226
Table 10.8: Bulk XRD analyses on core plug/chip seal samples	233
Table 10.9a: Petrographic analysis for V-1 and V-2 core plugs	235
Table 10.9b: Petrographic analysis for V-2 and V-7 core plugs	236
Table 10.9c: Petrographic analysis for V-10 core plugs	237
Table 10.9d: Petrographic analysis for V-10 core plugs (cont.)	238
Table 10.9e: Petrographic analysis for V-10 core plugs in aquifer leg	239
Table 10.10: Summary of seal capacity, geometry, integrity, and potential	248
Table 10.11: Data confidence factor matrix for ESSCI seals at Tangguh	251
Table 11.1: Calculator for CO ₂ storage volume in Tangguh structures	254
Table 11.2: Rating Product for ESSCI rankings	255
Table 11.2: Distance weighted rating	259
Table 12.1: List of Tangguh area leak-off tests/formation integrity tests	261
Table 12.2: Table of Tangguh area wells with FMI/FMS borehole image logs	262
Table 14.1: Zonation and layering scheme for preliminary geological model	278
Table 14.2: Zonation and layering scheme for final Tangguh geologic model	284
Table 14.3: Numerical facies codes used in the attribute ‘SimpleFacies_Use’	288
Table 14.4: Variogram models and numerical codes for paleodepositional facies	290
Table 14.5: Variogram models, structures, and parameters for stochastically populating cells in the final geologic model	290
Table 14.6: The search ellipse parameters for paleodepositional facies	291

LIST OF TABLES (Appendices) **Volume 2**

Appendix 1: DST-PTA Summary Tables	191
Appendix 2: Petrophysical Summary Tables	205
Appendix 3: Core Plug Porosity and Permeability Table 1998 (V-10 well)	229

LIST OF FIGURES **Volume 2**

Fig. 1.1: Changes in atmospheric CO ₂ composition plotted from ice core	2
Fig. 1.2: Change in CO ₂ concentrations over a millennium	3
Fig. 1.3: Change in CO ₂ concentrations and temperature over a millennium	3
Fig. 1.4: Change in CO ₂ concentrations and temperature over 400,000 yrs	4
Fig. 1.5: Change in GHG over a millennium	5
Fig. 1.6: Projected thermal expansion of sea level	6
Fig. 1.7: Projected sea level from thermal expansion and land-ice melt volume	6
Fig. 1.8: Projected SE coastal USA inundation from sea level rise	7
Fig. 1.9: Projected loss of polar ice caps (N. Pole)	8
Fig. 1.10: Map of global oceanic thermohaline circulation system	9
Fig. 1.11: CO ₂ PVT phase diagram	10
Fig. 1.12: LANDSAT image of Cameroon volcanic fields	11
Fig. 1.13: Aerial photograph of Lake Nyos and crater rim after CO ₂ bubble	11
Fig. 1.14: Temperature change relationship to GHG concentrations	12
Fig. 1.15: Schematic of the Complete Carbon Cycle (CCC)	13
Fig. 1.16: Schematic of the Bio-Geological Carbon Cycle	13
Fig. 2.1: Indonesia location map	14
Fig. 2.2: Map of Bird's Head PSC boundaries and gas/oil fields	15
Fig. 2.3: Map of Tangguh development area with gas fields	16
Fig. 3.1: ESSCI CO ₂ cross-sectional geological options schematic	17
Fig. 3.2: Bintuni Basin lithostratigraphic column	18
Fig. 3.3: Location map of production fields in Bintuni and Salawati Basins	19
Fig. 3.4: Map of shallow oil fields, seeps, and deep exploration wells in 1993	20
Fig. 3.5: Map of 'kitchen area' for source rock hydrocarbon generation	21
Fig. 4.1: Papua, Indonesia and Bird's Head area location map	22
Fig. 4.2: Paleotectonic map Cretaceous/Tertiary (K/T Boundary)	23
Fig. 4.3: Paleotectonic map Middle Oligocene	24
Fig. 4.4: Paleotectonic map Late Oligocene	25
Fig. 4.5: Paleotectonic map Early Miocene	26
Fig. 4.6: Paleotectonic map Middle Miocene	27
Fig. 4.7: Paleotectonic map Late Miocene of Banda Arc collision	28
Fig. 4.8: Paleotectonic map Pliocene	29
Fig. 4.9: Foreland and Piggyback basin formations map	30
Fig. 4.10: Kitchen area map of Bintuni and Berau basins	30
Fig. 4.11: Thermal maturity history plot for Bintuni Basin source rocks	31
Fig. 5.1: Early stratigraphic column for Bintuni Basin	31
Fig. 5.2: Examining the cores	32
Fig. 5.3: Fluvio-lacustrine Late Permian shale in core	33

Fig. 5.4: Late Permian marine sandstone in core (WD-3)	34
Fig. 5.5: Near-top Late Permian sandstone in core (WD-3)	35
Fig. 5.6: Late Permian sandstone in core (V-1)	36
Fig. 5.7: Late Permian/Middle Jurassic unconformity in core (WD-3)	37
Fig. 5.8: Aalenian Sandstone Formation and overlying MJ-4 shale (WD-3)	38
Fig. 5.9: Aalenian Sandstone Formation in core (WD-3)	39
Fig. 5.10: Various depositional facies Aalenian Sandstone Formation (WD-3)	40
Fig. 5.11: Roabiba Sandstone Formation in core (WD-2)	41
Fig. 5.12: Roabiba Sandstone Formation in core (WD-7)	42
Fig. 5.13: Sedimentological features Roabiba Sandstone Formation core (WD-3)	43
Fig. 5.14: Sedimentological features Roabiba Sandstone Formation core (V-2)	44
Fig. 5.15: <i>Helminthopsis</i> or <i>Helminthoida</i> ichnological fabric (V-2)	45
Fig. 5.16: Callovian (LJ-11) marine shale in core (V-10)	46
Fig. 5.17: Ayot Limestone Formation in core (WD-3)	47
Fig. 5.18: Ayot belemnite death assemblage in core (WD-3)	48
Fig. 5.19: Upper Late Jurassic altered volcanic tuff (WD-3)	49
Fig. 5.20: Base Late Cretaceous/Top Late Jurassic unconformity (WD-3)	50
Fig. 5.21: Near-Base Late Cretaceous carbonate (WD-3)	51
Fig. 5.22: Late Paleocene Sand-Prone Interval Middle Member in core (WD-2)	52
Fig. 5.23: Late Paleocene Sand-Prone Interval Middle Member in core (WD-2)	53
Fig. 5.24: Late Paleocene Mud-Prone Interval (WD-3)	54
Fig. 5.25: Oligocene Limestone Formation outcrop photograph (E. Onin-1)	55
Fig. 5.26: Near-top Faumai Formation coherency image 1632 ms TWT	56
Fig. 5.27: Faumai Formation coherency image 1660 ms TWT	57
Fig. 5.28: Faumai Formation coherency image 1892 ms TWT	58
Fig. 5.29: Kais Limestone Formation coherency image 1200 ms TWT	59
Fig. 5.30: Kais Limestone Formation coherency image 1320 ms TWT	60
Fig. 5.31: Kais Limestone Formation coherency image 1340 ms TWT	61
Fig. 5.32: LANDSAT image of Berau bay and Bintuni Bay	62
Fig. 5.33: Aerial photograph of the Wiriagar River and Wiriagar Swamp	63
Fig. 6.1: Stratigraphic geological cross-section A – A'	64
Fig. 6.2: Stratigraphic geological cross-section B – B'	65
Fig. 6.3: Stratigraphic geological cross-section C – C'	66
Fig. 6.4: Stratigraphic geological cross-section D – D'	67
Fig. 6.5: Stratigraphic geological cross-section E – E'	68
Fig. 6.6: Extensional Mesozoic rifting along Australian NW Shelf margin	69
Fig. 6.7: Bintuni Basin Mesozoic stratigraphic column	70
Fig. 6.8: A20 Aalenian isopach map	71
Fig. 6.9: Early A20 paleogeographic facies map	72
Fig. 6.10: Late A20 paleogeographic facies map	73
Fig. 6.11: Bajocian/Bathonian gross isopach map	74
Fig. 6.12: R10 isopach map	75
Fig. 6.13: R10 paleogeographic facies map	76
Fig. 6.14: R20 isopach map	77
Fig. 6.15: R20 paleogeographic facies map	78
Fig. 6.16: R30 isopach map	79
Fig. 6.17: R30 paleogeographic facies map	80
Fig. 6.18: R40 isopach map	81
Fig. 6.19: R40 paleogeographic facies map	82
Fig. 6.20: R50 isopach map	83

Fig. 6.21: Early R50 paleogeographic facies map	84
Fig. 6.22: Late R50 paleogeographic facies map	85
Fig. 6.23: R60 isopach map	86
Fig. 6.24: R60 paleogeographic facies map	87
Fig. 6.25: R70 isopach map	88
Fig. 6.26: R70 paleogeographic facies map	89
Fig. 6.27: R80 isopach map	90
Fig. 6.28: R80 paleogeographic facies map	91
Fig. 6.29: Base Pre-Ayot (MFS) GR correlation	92
Fig. 6.30: Callovian Roabiba gross isopach map	93
Fig. 6.31: CU10 isopach map	94
Fig. 6.32: CU10 paleogeographic facies map	95
Fig. 6.33: CU20 isopach map	96
Fig. 6.34: CU20 paleogeographic facies map	97
Fig. 6.35: CU30 isopach map	98
Fig. 6.36: CU30 paleogeographic facies map	99
Fig. 6.37: CU40 isopach map	100
Fig. 6.38: CU40 paleogeographic facies map	101
Fig. 6.39: CU50 isopach map	102
Fig. 6.40: CU50 paleogeographic facies map	103
Fig. 6.41: Pre-Ayot Formation gross isopach map	104
Fig. 6.42: PA10 isopach map	105
Fig. 6.43: PA10 paleogeographic facies map	106
Fig. 6.44: PA20 isopach map	107
Fig. 6.45: PA20 paleogeographic facies map	108
Fig. 6.46: PA30 isopach map (version 1)	109
Fig. 6.47: PA30 paleogeographic facies map	110
Fig. 6.48: PA30 isopach map (version 2)	111
Fig. 6.49: PA60/Ayot Limestone Formation isopach map	112
Fig. 6.50: PA60/Ayot Limestone Formation paleogeographic facies map	113
Fig. 6.51: BHMC paleotectonic migration map	114
Fig. 7.1: Wiriagar Deep/Ubadari cross-section with core & DST intervals	115
Fig. 7.2: Vorwata cross-section with core & DST intervals	116
Fig. 7.3: Permian well correlation cross-section V area	117
Fig. 7.4: Late Permian porosity vs. permeability cross-plot	118
Fig. 7.5: Aalenian well correlation cross-section WD-V area	119
Fig. 7.6: Aalenian Top Depth Structure Map	120
Fig. 7.7: Aalenian effective porosity map	121
Fig. 7.8: Aalenian porosity vs. permeability cross-plot	122
Fig. 7.9: Aalenian & Roabiba well correlation cross-section WD-V area	123
Fig. 7.10: Tangguh area seismic line W-E, surface to Base Cretaceous	124
Fig. 7.11: Cross-sectional schematic with simultaneous onlap & truncation	125
Fig. 7.12: Roabiba well correlation cross-section V area	126
Fig. 7.13: Bajocian/Bathonian/Callovian Roabiba Top Depth Structure Map	127
Fig. 7.14: Callovian Roabiba effective porosity map	128
Fig. 7.15: Bajocian/Bathonian Roabiba effective porosity map	129
Fig. 7.16: Roabiba porosity vs. permeability cross-plot	130
Fig. 7.17: Tangguh area Jurassic pressure gradients vs. depth graph	131
Fig. 7.18: Roabiba V-10 core porosity vs. permeability cross-plot	132
Fig. 7.19: Roabiba V-10 log and core porosity vs. permeability cross-plot	133

Fig. 7.20: Ayot porosity vs. permeability cross-plot	134
Fig. 7.21: Late Cretaceous Top Depth Structure Map	135
Fig. 7.22: Late Cretaceous porosity vs. permeability cross-plot	136
Fig. 7.23: Late Paleocene Middle Member porosity vs. permeability cross-plot	137
Fig. 7.24: Late Paleocene well correlation cross-section WD-V area	138
Fig. 7.25: Late Paleocene Sand-Prone well correlation cross-section WD area	139
Fig. 7.26: Kais Limestone Formation (NGLG) Top Depth Structure Map	140
Fig. 8.1: Kais-Faumai salinity difference map	141
Fig. 9.1: Distance to structures from LNG plant map	142
Fig. 10.1: Stratigraphic cross-section of regional seals	143
Fig. 10.2: Geological schematic of regional seals	144
Fig. 10.3: CO ₂ Column Height sensitivities due to varied contact angle	145
Fig. 10.4: CO ₂ Column Height sensitivities due to varied interfacial tension	146
Fig. 10.5: Map of areal extent for Roabiba top seals in the Tangguh area	147
Fig. 10.6: Photograph of severely altered core sample due to storage conditions	148
Fig. 10.7: Photograph of regional seals in slabbed cores	149
Fig. 10.8: Calculated seal capacity from wireline log analysis	150
Fig. 11.1: Relative storage capacity diagram	151
Fig. 11.2: Geologic cross-sectional schematic of proposed injection plan	152
Fig. 11.3: Graph of distance to proposed injection sites	153
Fig. 12.1: Leak-Off Test (LOT) gradient contour map	154
Fig. 12.2: Nafe-Drake Plot	155
Fig. 12.3: Vorwata vertical stress profile with depth	156
Fig. 12.4: Wiriagar Deep vertical stress profile with depth	157
Fig. 12.5: Tangguh area vertical stress contour map	158
Fig. 12.6: Formation pore pressure distribution with depth	159
Fig. 12.7: Rose diagram and depth vs. directional orientation graph	160
Fig. 12.8: Mohr diagram and planes-to-poles diagram	161
Fig. 12.9: Map of the in-situ horizontal stress orientations	162
Fig. 12.10: Fault risk of re-activation map for Tangguh area	163
Fig. 12.11: Fault risk of re-activation depth-slice map at ~14,000 ft TVDss	164
Fig. 13.1: Map of recommended surface injection site locations	165
Fig. 13.2: Subsurface location map of recommended Vorwata injection sites	166
Fig. 13.3: Map of subsurface CO ₂ reservoir volume at Vorwata	167
Fig. 13.4: Map of subsurface CO ₂ reservoir total volume at Vorwata	168
Fig. 14.1: Map of test model area	169
Fig. 14.2: Test model populating geo-cells with sonic values	170
Fig. 14.3: Base Late Cretaceous surface	171
Fig. 14.4: Tangguh coarse grid model with wells/base Late Cretaceous	172
Fig. 14.5: 2D mesh draped on base Late Cretaceous surface	173
Fig. 14.6: Fence display through wells and surfaces from model	174
Fig. 14.7: Wireline log display through surfaces at wells	175
Fig. 14.8: Bounding surfaces menu	176
Fig. 14.9: Work flow diagram	177
Fig. 14.10: Scheme and codes for facies polygons within the model	178
Fig. 14.11: Example of digitized paleogeographic map facies polygons	179
Fig. 14.12: Facies polygons displayed in GEOCARD as an attribute	180
Fig. 14.13: Example of paleogeographic map and facies attribute in model	181
Fig. 14.14: Fault compartment polygons	182
Fig. 14.15: Fault compartment polygons as an attribute	183

Fig. 14.16: Fault compartment boundaries for transmissibility multipliers	184
Fig. 14.17: Reservoir simulator screen capture of grids, zones, and attributes	185
Fig. 14.18: Reservoir simulator screen capture at Year 0 from injection	186
Fig. 14.19: Reservoir simulator screen capture at Year 5 from injection	187
Fig. 14.20: Reservoir simulator screen capture at Year 20 from injection	188
Fig. 14.21: Reservoir simulator screen capture at Year 25 from injection	189
Fig. 18.1: Vorwata Mesozoic core palynology/biostratigraphy chart	190

LIST OF FIGURES (Appendix 4) Volume 2

Fig. 1: Core Plug/Chip Atlas Guide	239
Fig. 2: Core Plug/Chip Atlas: WD-2, 7377' 11"	240-241
Fig. 3: Core Plug/Chip Atlas: WD-2, 7380' 0"	242-243
Fig. 4: Core Plug/Chip Atlas: WD-2, 8681' 3"	244-245
Fig. 5: Core Plug/Chip Atlas: WD-2, 8753' 2"	246
Fig. 6: Core Plug/Chip Atlas: WD-3, 7548' 9"	247-248
Fig. 7: Core Plug/Chip Atlas: WD-3, 7549' 2"	249-250
Fig. 8: Core Plug/Chip Atlas: WD-3, 7552' 7"	251-252
Fig. 9: Core Plug/Chip Atlas: WD-3, 7558' 8"	253-254
Fig. 10: Core Plug/Chip Atlas: WD-3, 7956' 3"	255
Fig. 11: Core Plug/Chip Atlas: WD-3, 9238' 0"	256-257
Fig. 12: Core Plug/Chip Atlas: WD-3, 9272' 1"	258-259
Fig. 13: Core Plug/Chip Atlas: WD-3, 9274' 1"	260-261
Fig. 14: Core Plug/Chip Atlas: WD-3, 9286' 2"	262-263
Fig. 15: Core Plug/Chip Atlas: WD-3, 9309' 8"	264-265
Fig. 16: Core Plug/Chip Atlas: WD-3, 9325' 0"	266-267
Fig. 17: Core Plug/Chip Atlas: WD-3, 9328' 4"	268-269
Fig. 18: Core Plug/Chip Atlas: WD-3, 9344' 1"	270-271
Fig. 19: Core Plug/Chip Atlas: WD-3, 9364' 9"	272-273
Fig. 20: Core Plug/Chip Atlas: WD-5, 9509' 0"	274
Fig. 21: Core Plug/Chip Atlas: WD-5, 9509' 5"	275-276
Fig. 22: Core Plug/Chip Atlas: WD-7, 7962' 6"	277-278
Fig. 23: Core Plug/Chip Atlas: WD-7, 7981' 6"	279-280
Fig. 24: Core Plug/Chip Atlas: WD-7, 8452' 5"	281-282
Fig. 25: Core Plug/Chip Atlas: WD-7, 8471' 1"	283-284
Fig. 26: Core Plug/Chip Atlas: WD-7, 8497' 9"	285-286
Fig. 27: Core Plug/Chip Atlas: WD-7, 8524' 7"	287
Fig. 28: Core Plug/Chip Atlas: V-1, 11765' 9"	288
Fig. 29: Core Plug/Chip Atlas: V-1, 11787' 7"	289
Fig. 30: Core Plug/Chip Atlas: V-1, 11790' 9"	290 -291
Fig. 31: Core Plug/Chip Atlas: V-1, 11797' 7"	292
Fig. 32: Core Plug/Chip Atlas: V-1, 11902' 3"	293-294
Fig. 33: Core Plug/Chip Atlas: V-1, 11904' 3"	295-297
Fig. 34: Core Plug/Chip Atlas: V-1, 11909' 7"	298
Fig. 35: Core Plug/Chip Atlas: V-1, 11914' 6"	299
Fig. 36: Core Plug/Chip Atlas: V-2, 12582' 7"	300-301
Fig. 37: Core Plug/Chip Atlas: V-2, 12584' 8"	302-303
Fig. 38: Core Plug/Chip Atlas: V-2, 12585' 8"	304-305
Fig. 39: Core Plug/Chip Atlas: V-2, 12594' 4"	306-307

Fig. 40: Core Plug/Chip Atlas: V-2, 12600' 3"	308-309
Fig. 41: Core Plug/Chip Atlas: V-2, 12757' 6"	310-311
Fig. 42: Core Plug/Chip Atlas: V-2, 12865' 7"	312-313
Fig. 43: Core Plug/Chip Atlas: V-2, 12901' 5"	314-315
Fig. 44: Core Plug/Chip Atlas: V-2, 13020' 6"	316-318
Fig. 45: Core Plug/Chip Atlas: V-2, 13025' 6"	319-321
Fig. 46: Core Plug/Chip Atlas: V-2, 13030' 1"	322-324
Fig. 47: Core Plug/Chip Atlas: V-7, 13118' 3"	325-326
Fig. 48: Core Plug/Chip Atlas: V-7, 13123' 8"	327
Fig. 49: Core Plug/Chip Atlas: V-7, 13136' 10"	328-329
Fig. 50: Core Plug/Chip Atlas: V-7, 13143' 6"	330
Fig. 51: Core Plug/Chip Atlas: V-7, 13152' 5"	331-333
Fig. 52: Core Plug/Chip Atlas: V-10, 3944.43 m	334-336
Fig. 53: Core Plug/Chip Atlas: V-10, 3947.64 m	337-339
Fig. 54: Core Plug/Chip Atlas: V-10, 3954.46 m	340-342
Fig. 55: Core Plug/Chip Atlas: V-10, 3965.57 m	343-345
Fig. 56: Core Plug/Chip Atlas: V-10, 3966.82 m	346-348
Fig. 57: Core Plug/Chip Atlas: V-10, 3967.10 m	349-351
Fig. 58: Core Plug/Chip Atlas: V-10, 4021.25 m	352-353
Fig. 59: Core Plug/Chip Atlas: V-10, 4021.86 m	354
Fig. 60: Core Plug/Chip Atlas: V-10, 4022.20 m	355
Fig. 61: Core Plug/Chip Atlas: V-10, 4025.08 m	356
Fig. 62: Core Plug/Chip Atlas: V-10, 4025.80 m	357
Fig. 63: Core Plug/Chip Atlas: V-10, 4025.98 m	358
Fig. 64: Core Plug/Chip Atlas: V-10, 4026.18 m	359-361
Fig. 65: Core Plug/Chip Atlas: V-10, 4028.15 m	362
Fig. 66: Core Plug/Chip Atlas: V-10, 4029.58 m	363
Fig. 67: Core Plug/Chip Atlas: V-10, 4029.70 m	364
Fig. 68: Core Plug/Chip Atlas: V-10, 4031.55 m	365-366
Fig. 69: Core Plug/Chip Atlas: V-10, 4034.51 m	367-369
Fig. 70: Core Plug/Chip Atlas: V-10, 4035.40 m	370
Fig. 71: Core Plug/Chip Atlas: V-10, 4036.23 m	371
Fig. 72: Core Plug/Chip Atlas: V-10, 4039.62 m	372-373
Fig. 73: Core Plug/Chip Atlas: V-10, 4040.20 m	374-375
Fig. 74: Core Plug/Chip Atlas: V-10, 4042.62 m	376-377
Fig. 75: Core Plug/Chip Atlas: V-10, 4044.81 m	378-379
Fig. 76: Core Plug/Chip Atlas: V-10, 4045.92 m	380-381
Fig. 77: Core Plug/Chip Atlas: V-10, 4049.40 m	382-383
Fig. 78: Core Plug/Chip Atlas: V-10, 4052.13 m	384-385
Fig. 79: Core Plug/Chip Atlas: V-10, 4052.64 m	386-387
Fig. 80: Core Plug/Chip Atlas: V-10, 4056.02 m	388
Fig. 81: Core Plug/Chip Atlas: V-10, 4057.32 m	389
Fig. 82: Core Plug/Chip Atlas: V-10, 4058.58 m	390
Fig. 83: Core Plug/Chip Atlas: V-10, 4059.26 m	391
Fig. 84: Core Plug/Chip Atlas: V-10, 4060.90 m	392
Fig. 85: Core Plug/Chip Atlas: V-10, 4063.45 m	393
Fig. 86: Core Plug/Chip Atlas: V-10, 4067.60 m	394
Fig. 87: Core Plug/Chip Atlas: V-10, 4068.50 m	395
Fig. 88: Core Plug/Chip Atlas: V-10, 4076.30 m	396-397
Fig. 89: Core Plug/Chip Atlas: V-10, 4081.32 m	398-399

Fig. 90: Core Plug/Chip Atlas: V-10, 4082.85 m	400-401
Fig. 91: Core Plug/Chip Atlas: V-10, 4090.85 m	402-403
Fig. 92: Core Plug/Chip Atlas: V-10, 4093.80 m	404-405
Fig. 93: Core Plug/Chip Atlas: V-10, 4095.50 m	406
Fig. 94: Core Plug/Chip Atlas: V-10, 4101.30 m	407-408
Fig. 95: Core Plug/Chip Atlas: V-10, 4117.70 m	409-410
Fig. 96: Core Plug/Chip Atlas: V-10, 4126.30 m	411-412
Fig. 97: Core Plug/Chip Atlas: V-10, 4126.69 m	413-414
Fig. 98: Core Plug/Chip Atlas: V-10, 4128.92 m	415-417
Fig. 99: Core Plug/Chip Atlas: Fractured & Faulted Cores of Seals	418-419
Fig. 100: Core Plug/Chip Atlas Guide	420

PART VII
FIGURES

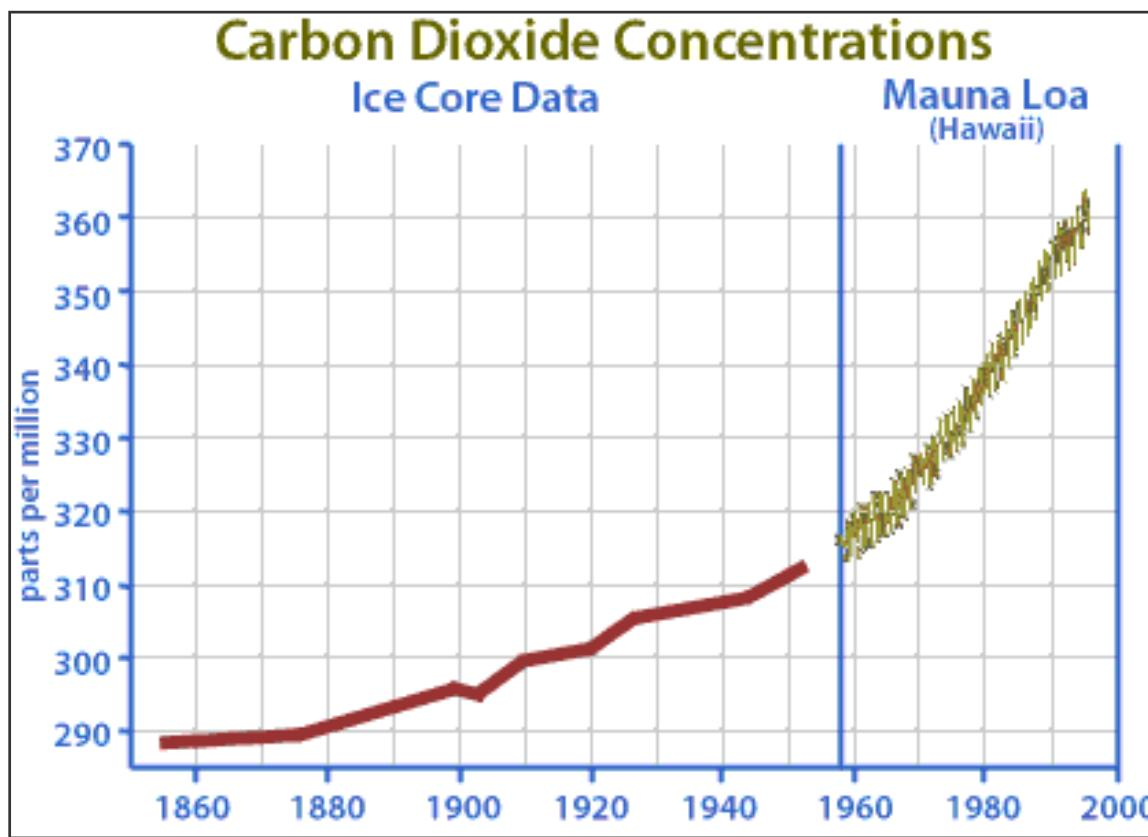


Figure 1.1: Changes in global atmospheric CO₂ composition plotted from Greenland and Antarctic ice core gas inclusion analyses (red), and recent (1950-2004) direct atmospheric measurements (green) at Mauna Loa Observatory, Hawaii (IPCC, 2001; after World Meteorological Organization, 2001).

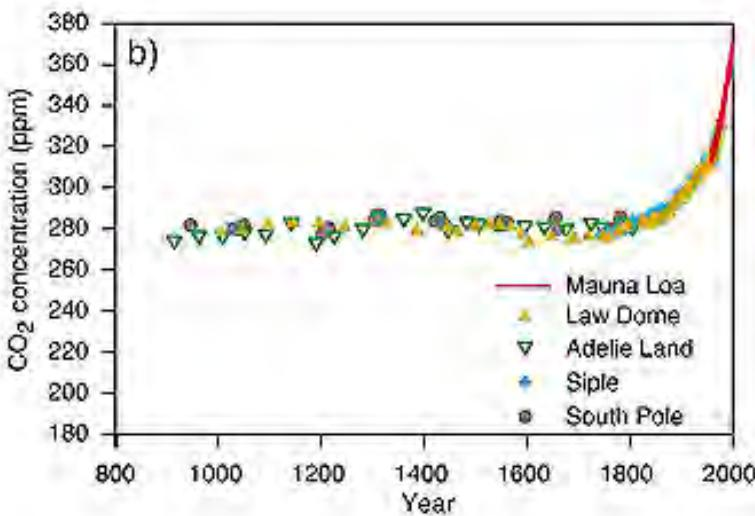


Figure 1.2: Changes in global atmospheric CO₂ composition for the last 1000 years plotted from ice core (Greenland and Antarctic) gas inclusion analyses, and calibrated to recent (1950-2004) direct atmospheric measurements at Mauna Loa Observatory, Hawaii (IPCC, 2001; after Mann, et. al., 1999).

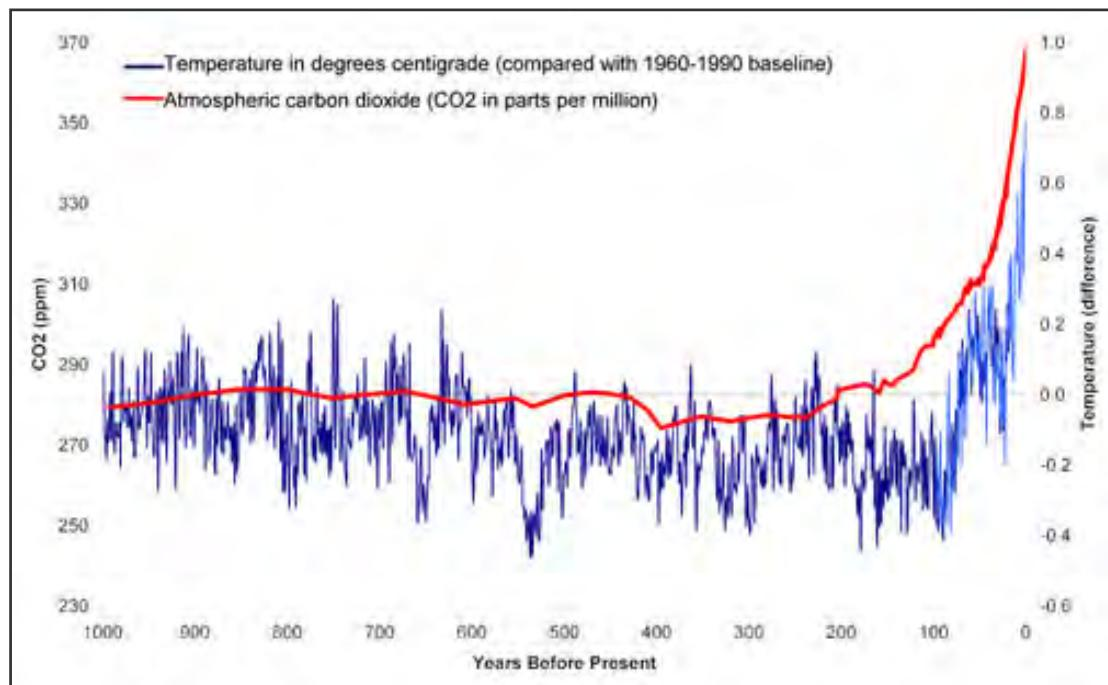


Figure 1.3: Changes in global mean temperature (red curve) and atmospheric CO₂ concentrations (purple curve) for the last 1000 years plotted from ice core (Greenland and Antarctic) gas inclusion and oxygen isotope analyses, and calibrated to recent (1900-2004) direct atmospheric gas (blue curve) and temperature measurements at Mauna Loa Observatory (IPCC, 2001; after Mann, et al., 1999).

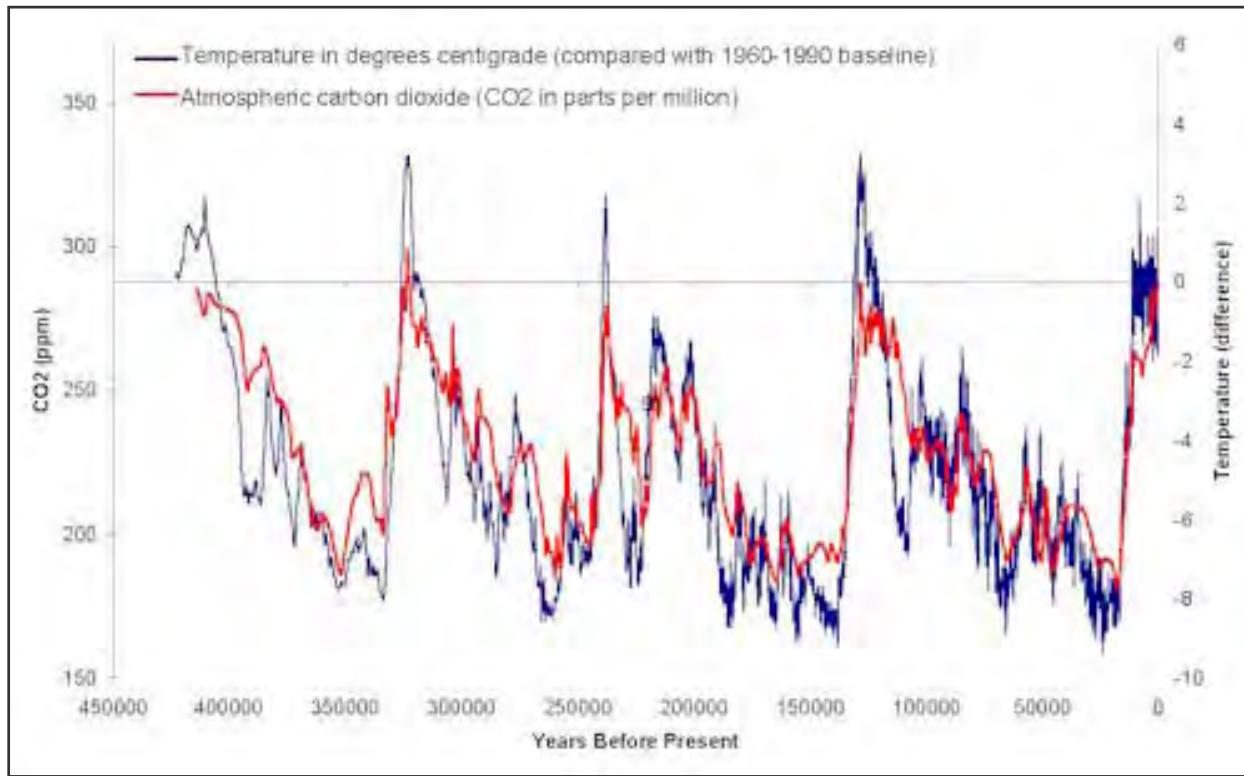
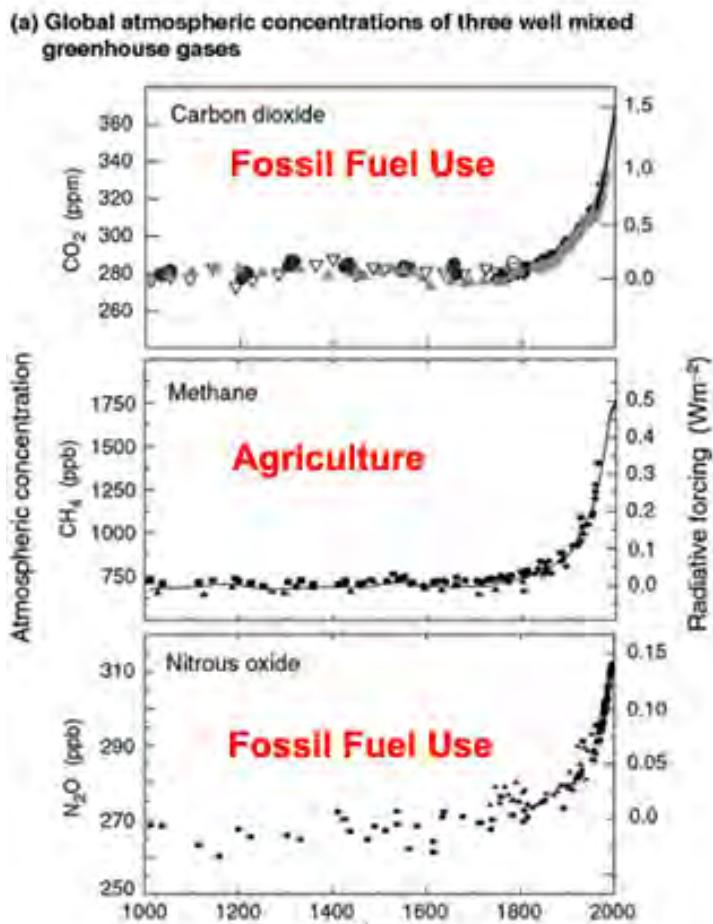


Figure 1.4: Changes in global mean temperature (red curve) and atmospheric CO₂ concentrations (purple curve) for the last 400,000 years plotted from ice core (Vostok) gas inclusion and oxygen isotope analyses, and calibrated to Siple, Adelie, and Law Dome ice core data (IPCC, 2001; after Petit, et al., 2000).



(b) Sulphate aerosols deposited in Greenland ice

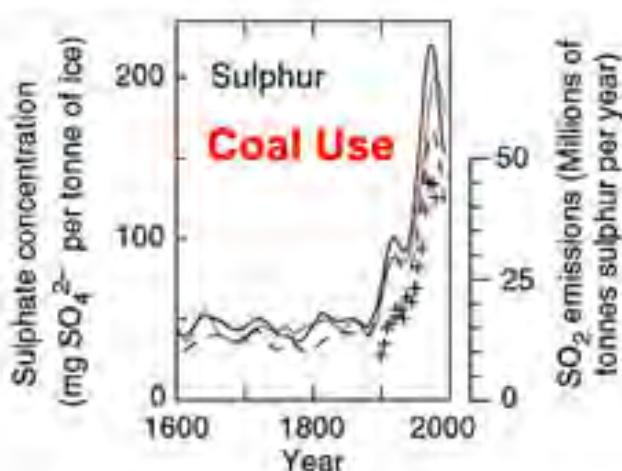


Figure 1.5: Global mean atmospheric GHG concentrations over 1000 years (a), including carbon dioxide (CO_2), methane (CH_4), and nitrous oxide (NO_2), plotted from ice core (Siple, Adelie, Law Dome, and South Pole ice cores) gas inclusion analyses (IPCC, 2001; after Mann, et al., 1999), and concentrations of sulphate aerosols (b) in ice cores from Greenland (Siple) deposited from atmospheric ‘fallout’ from coal-combustion particles (IPCC, 2001).

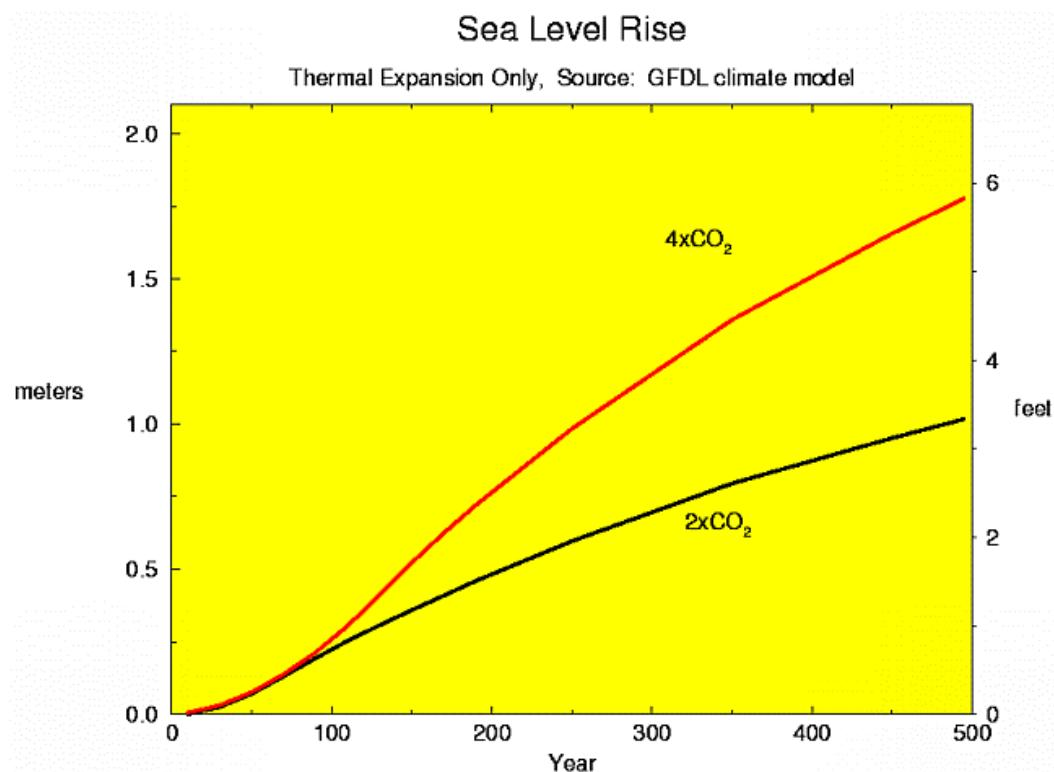


Figure 1.6: Projected thermal expansion minimum sea level rise based on the predicted doubling (2 x CO₂) and quadrupling (4 x CO₂) of atmospheric CO₂ content only, based on the Geophysical Fluid Dynamics Laboratory (GFDL) modelling. Continental and alpine glacial runoff volume not included in model (ESR, 2004, after NOAA, 2004).

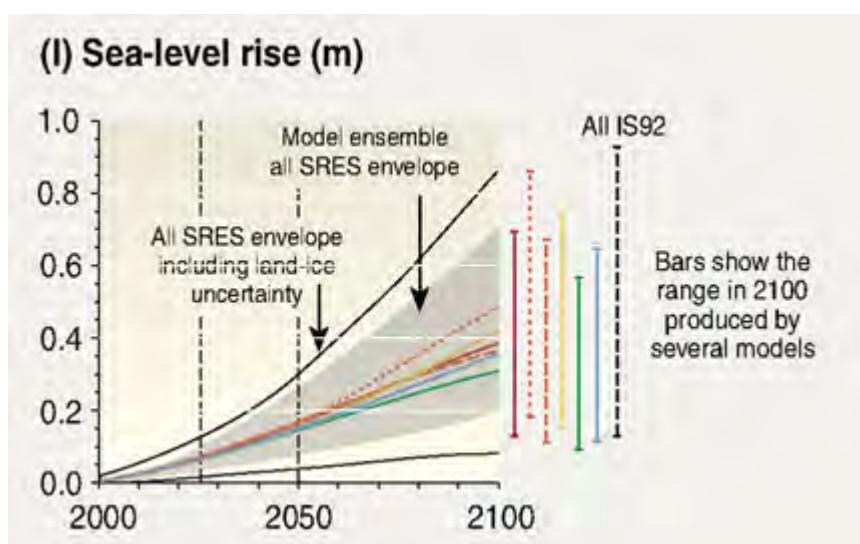


Figure 1.7: Present and projected minimum sea level rise (based on the forward modelling scenarios presented in Figures 1.7-1.8), includes thermal expansion and land-ice volume uncertainty envelope boundary (EEA, 2004).

Sea Level Rise

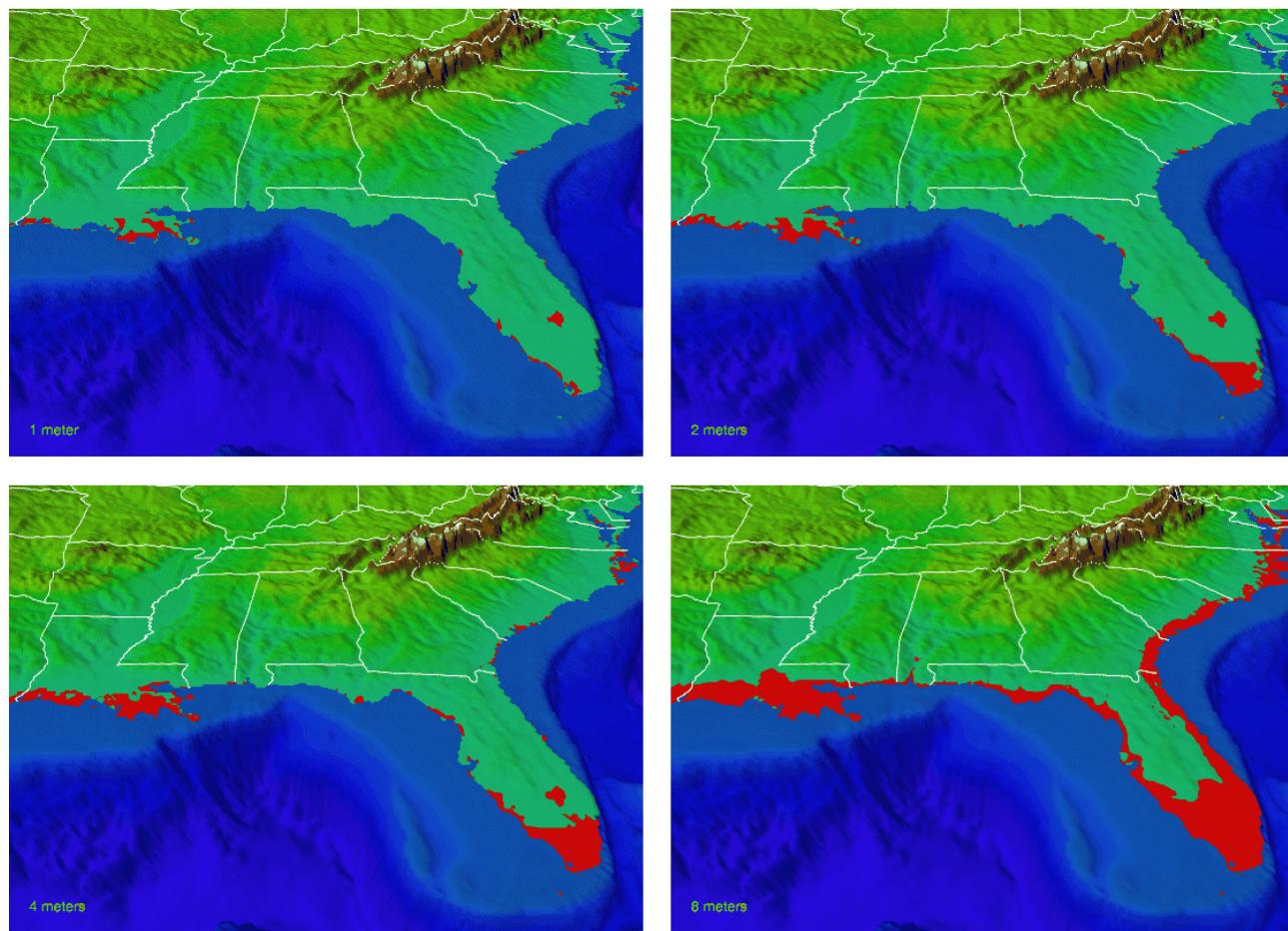


Figure 1.8: Projected coastal land loss along the Gulf of Mexico and SE Atlantic seaboard in the USA due to: 1 m sea level rise, 2 meter sea level rise, 4 meter sea level rise, and 8 meter sea level rise. Some major cities such as New Orleans, Louisiana are greatly affected by a 1m rise, 20% of Florida peninsula is lost with a 4m rise, and almost 50% of Florida peninsula is lost with an 8m rise (NOAA, 2004).

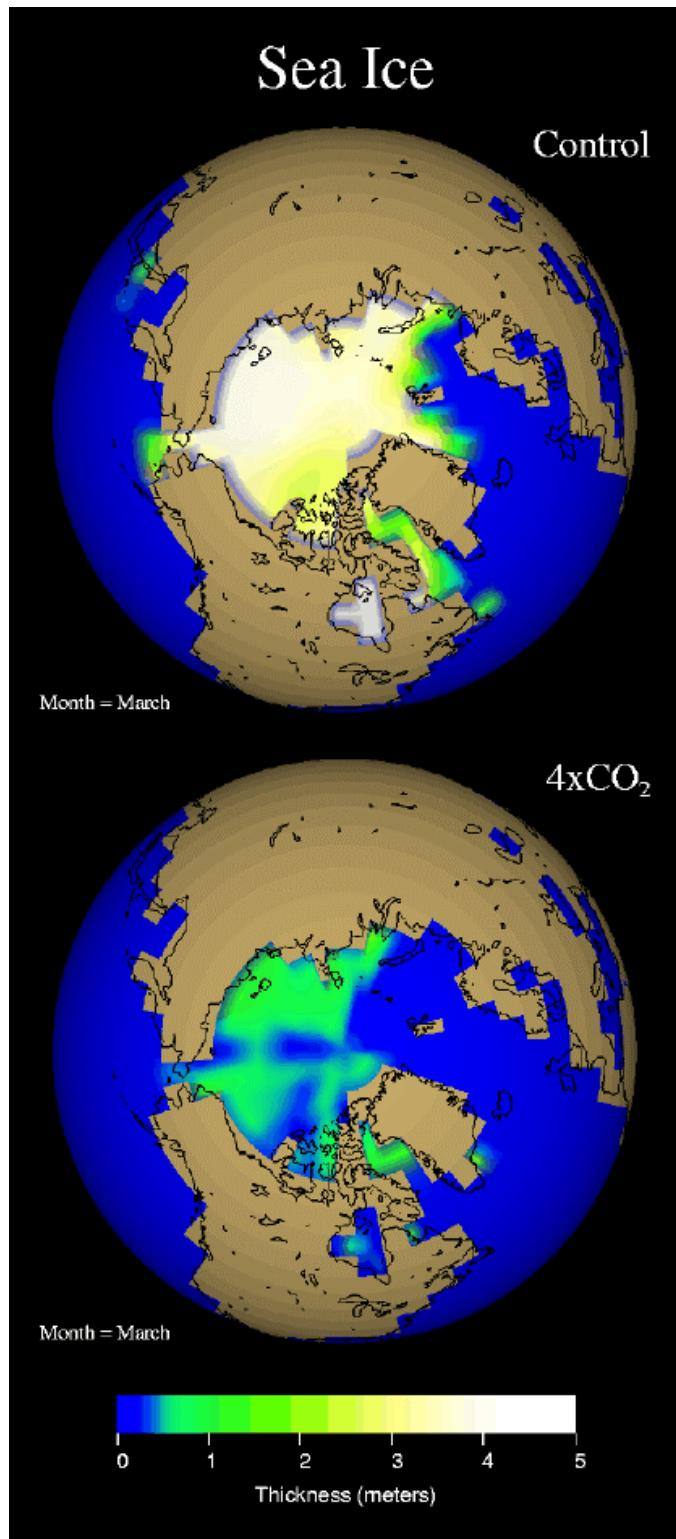


Figure 1.9: The loss of polar ice shelf at the North Pole is predicted in forward modelling if the atmospheric content of CO₂ is quadrupled and global warming accelerates further (NOAA, 2004). The top figure shows the current northern polar ice distribution and the lower figure shows only thin patchy regions of polar ice with the quadrupling of atmospheric CO₂.

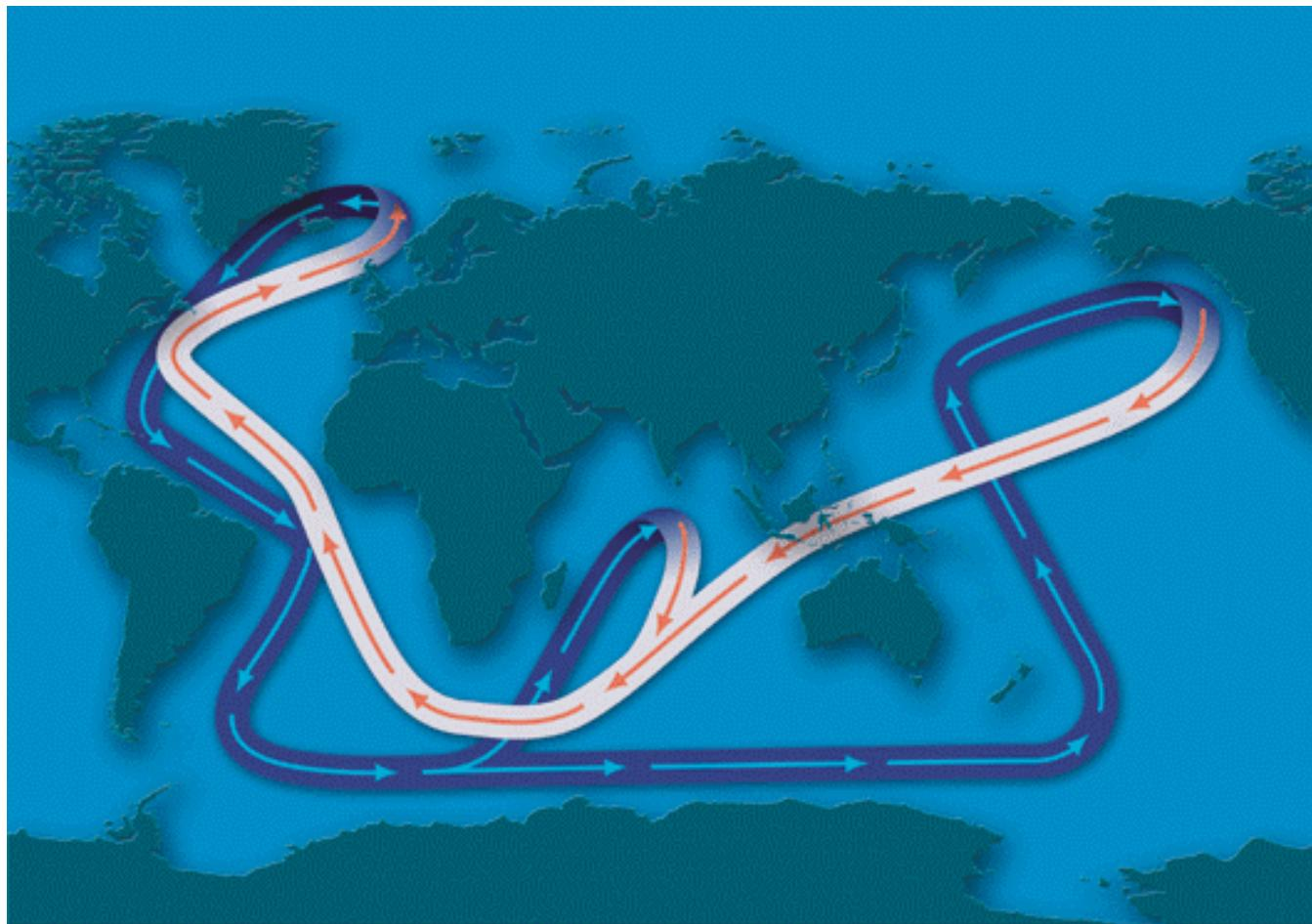


Figure 1.10: The Atlantic Ocean thermohaline system for ocean circulation, a system that could potentially be disrupted by global warming and melting polar ice caps, with dire consequences. Warm currents with red arrows; cold, higher-salinity currents with blue arrows (after Broeker, 2001; by WHOI, 2004).

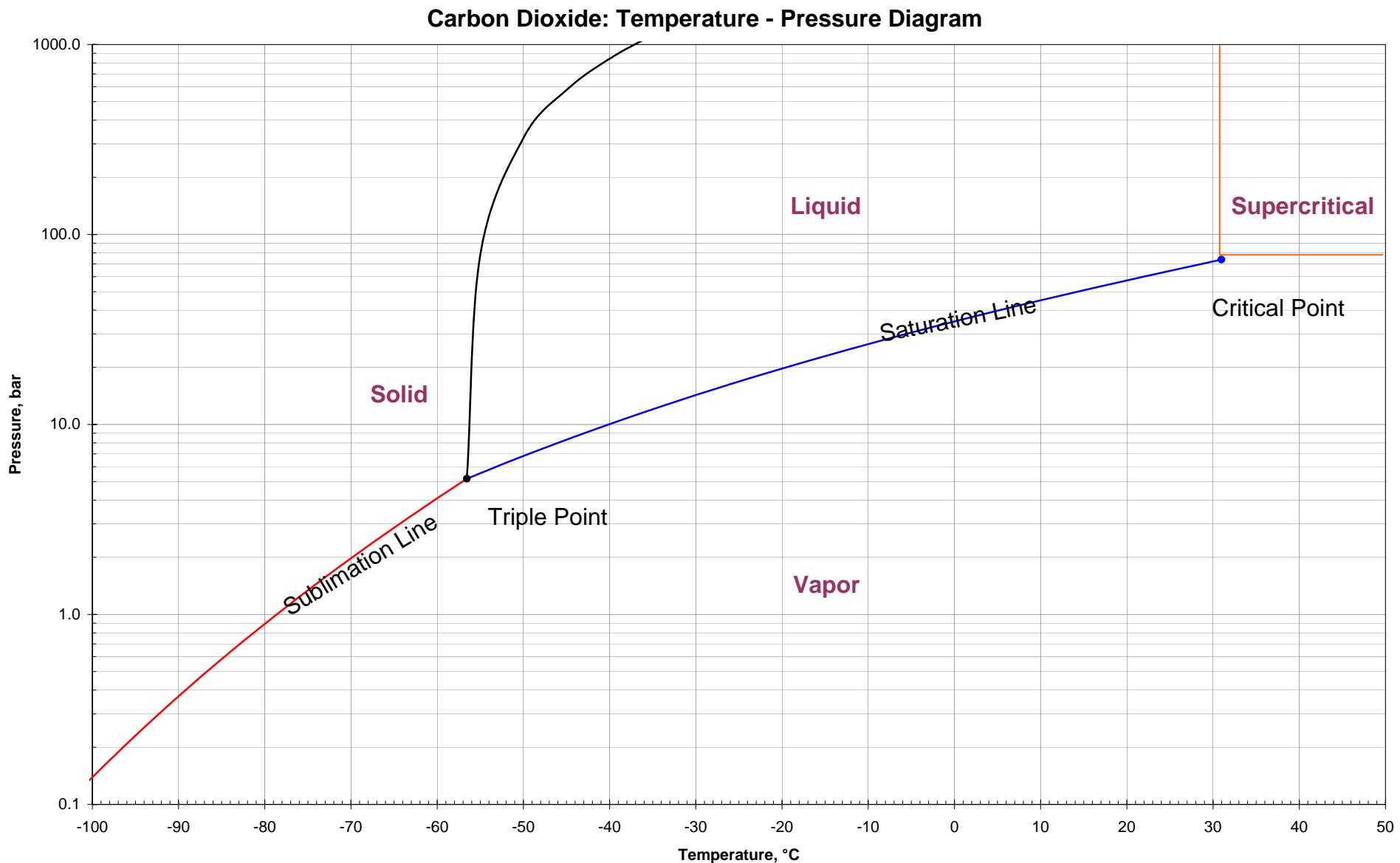


Figure 1.11: Temperature and pressure phase diagram for pure carbon dioxide. Critical point for supercriticality is shown at P=72.8 bar and T=31.1 degree C (after Chemicalogic, 2004).

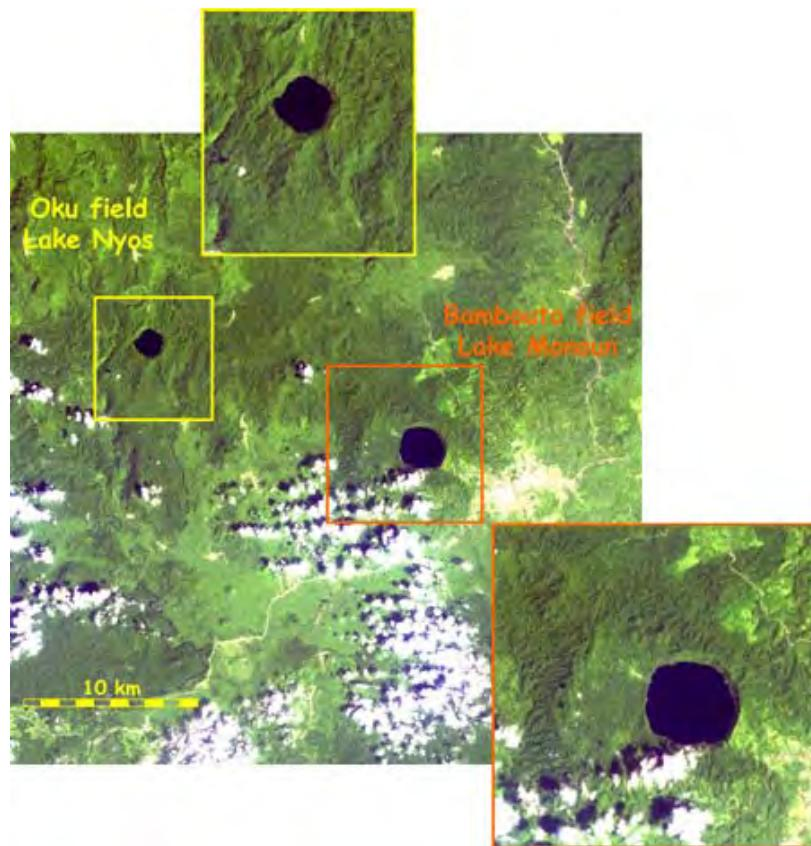


Figure 1.12: Cameroon volcanic fields from composite LANSAT image mosaic, with Lake Nyos shown in the mouth of a volcanic vent (LANSAT image processed by Sarah Sherman, 2000; from UND, 2004).



Figure 1.13: Aerial photograph of Lake Nyos, two days after the CO₂ bubble breached the lake algal seal (Photo by Jack Lockwood of the USGS; from UND, 2004).

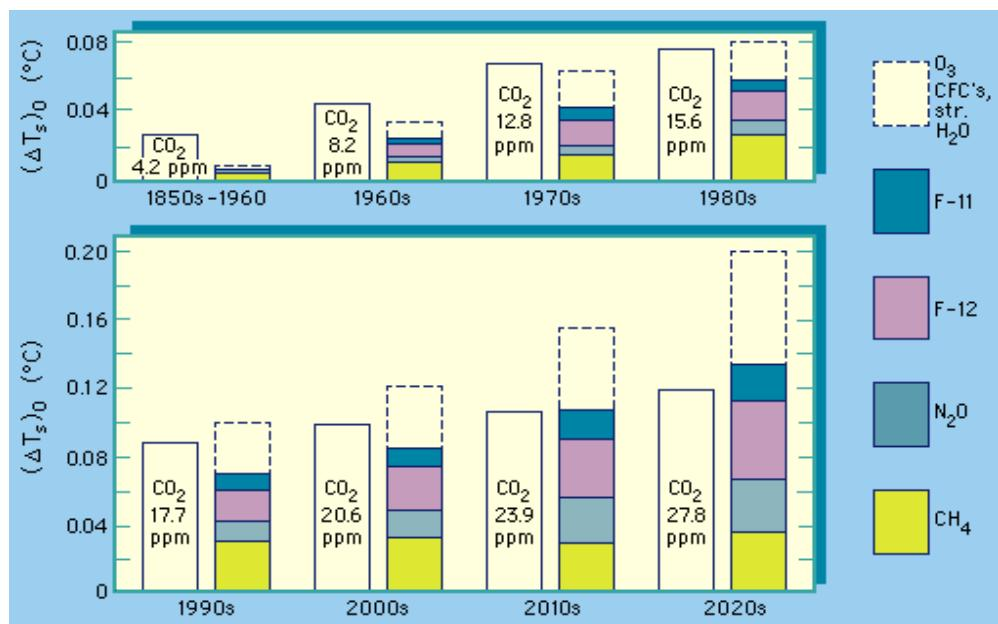


Figure 1.14: Atmospheric changes in global temperature based on the atmospheric concentrations of the major greenhouse gases and CO₂. The top histogram shows past and recent changes in global temperatures relative to the concentrations of major GHG and concentrations of atmospheric CO₂, from 1850 through 1989. The bottom histogram shows projected (2000-2030) increases in global temperature due to forecast changes in future concentrations of major greenhouse gases and CO₂ (World Meteorological Organization, 1989).

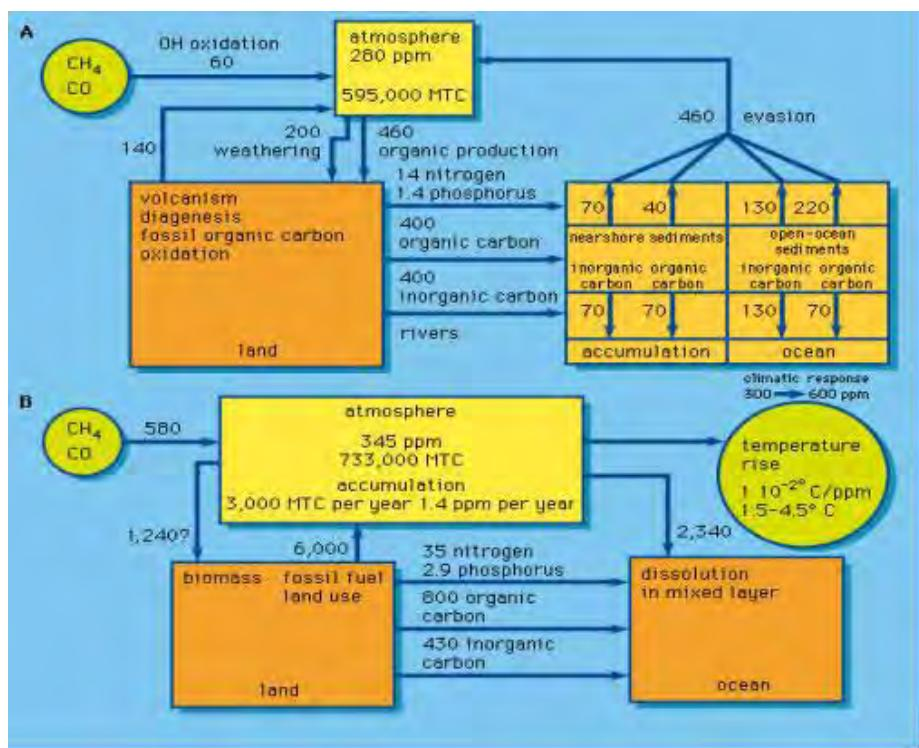


Figure 1.15: Global Complete Carbon Cycle past (A) and present (B) (Wollast and MacKenzie, 1989).

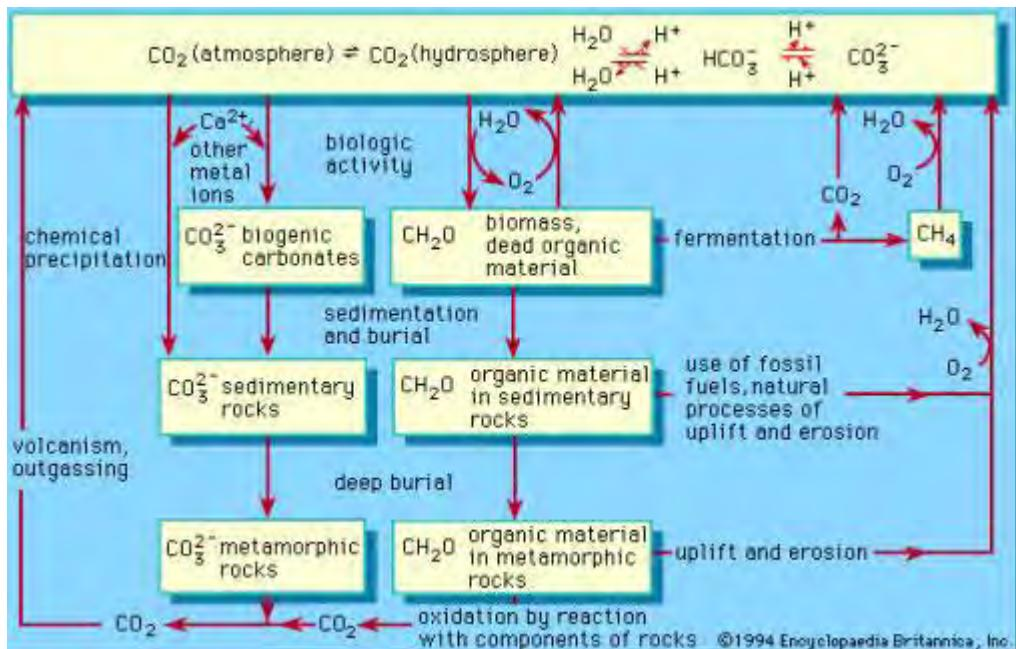


Figure 1.16: A schematic of the Bio-Geological Carbon Cycle (Encyclopaedia Britannica, 2001).



Figure 2.1 Papua, Indonesia geographical location map. Irian Jaya Province was renamed Papua Province by act of the Indonesian Parliament (MPR) in 2001. It is located in the western half of the island of New Guinea, with the eastern half being the independent sovereignty of Papua New Guinea (Geographix, 1997).

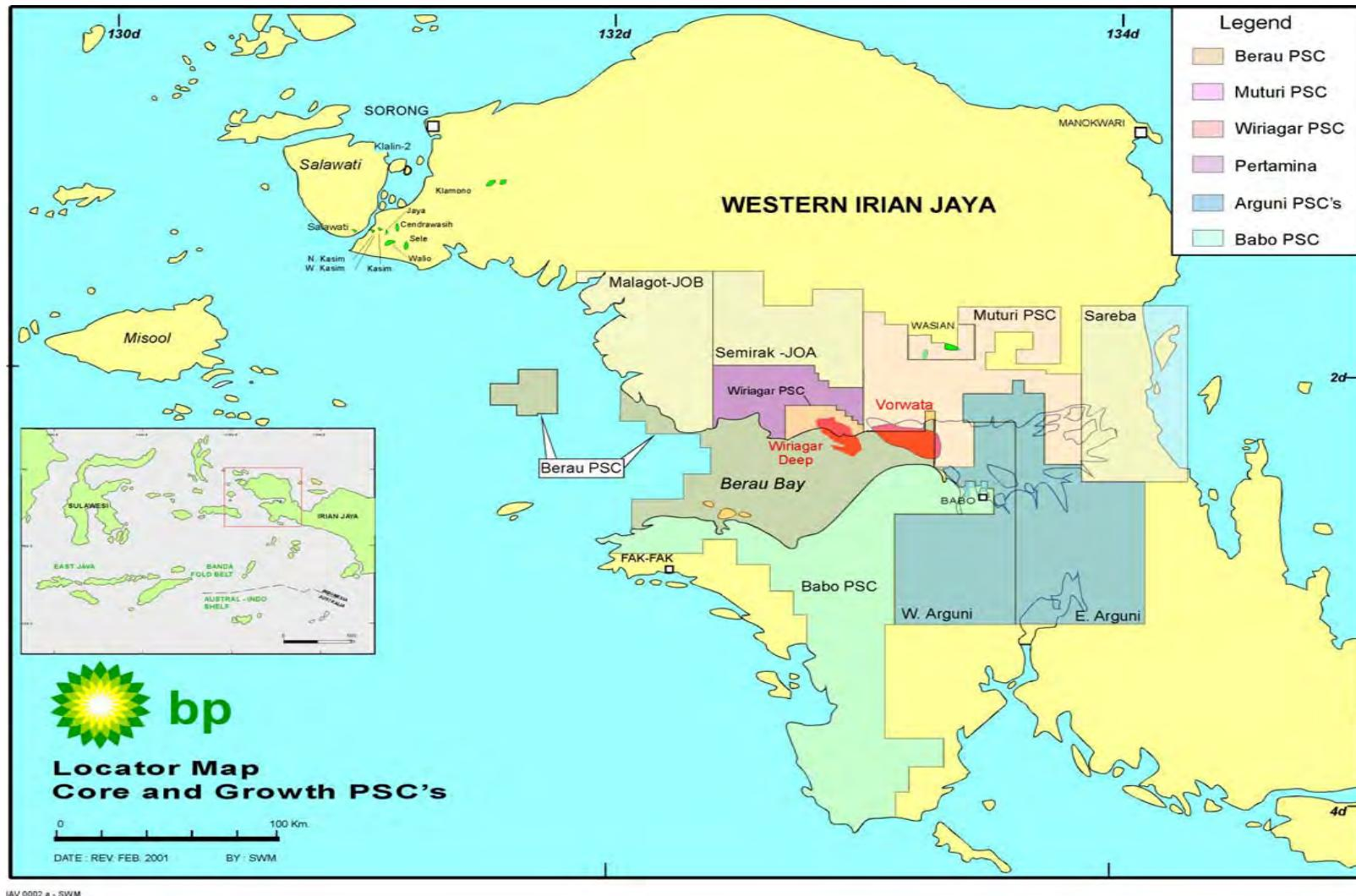


Figure 2.2: Location map of the Bird's Head (Kepala Burung) region in the extreme northwest Papua Province (formerly Irian Jaya), with the Production Sharing Contract (PSC) boundaries prior to 2001 shown according to the legend color scheme. The gas fields are in red, and oil fields are in green (courtesy BP, 2001).

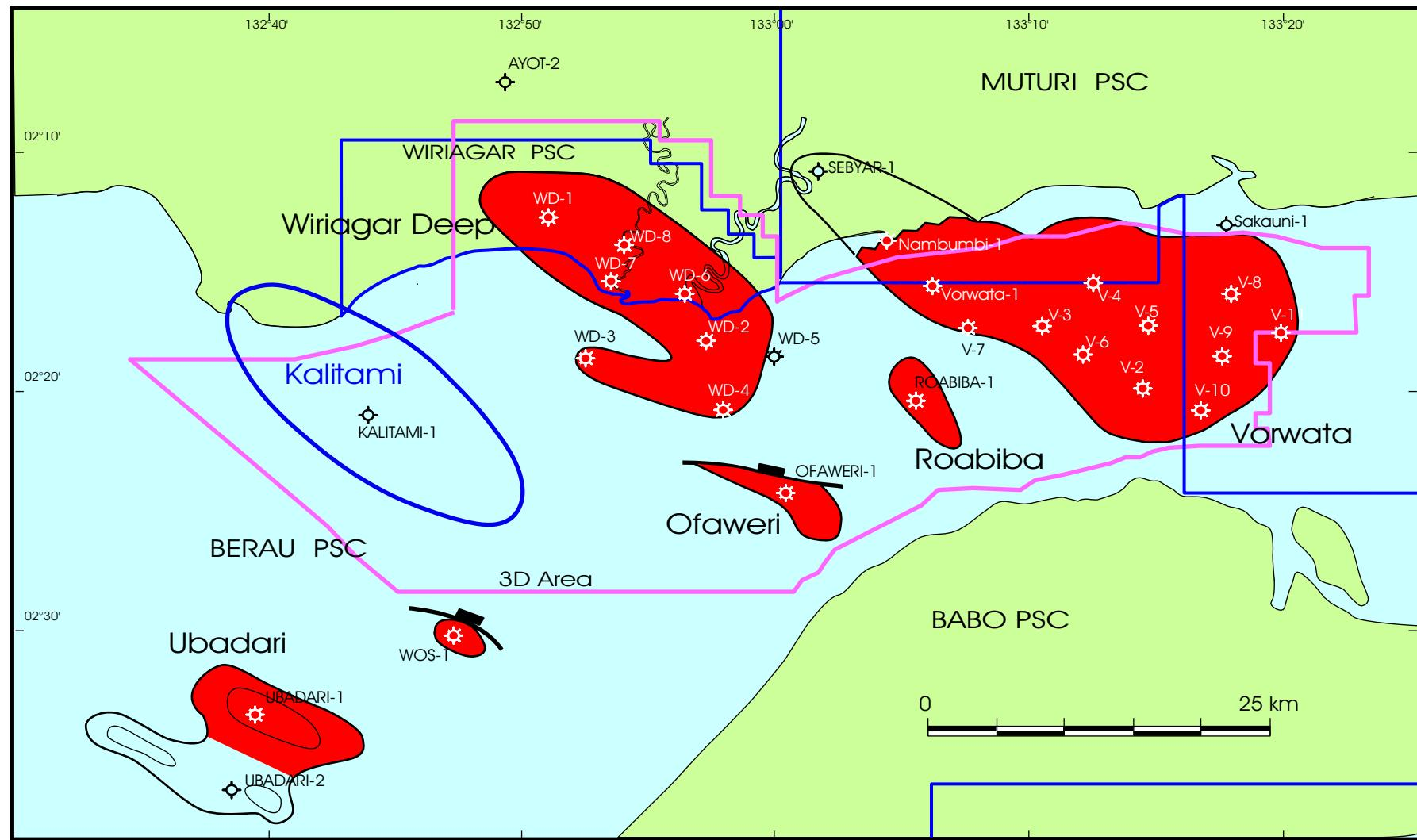
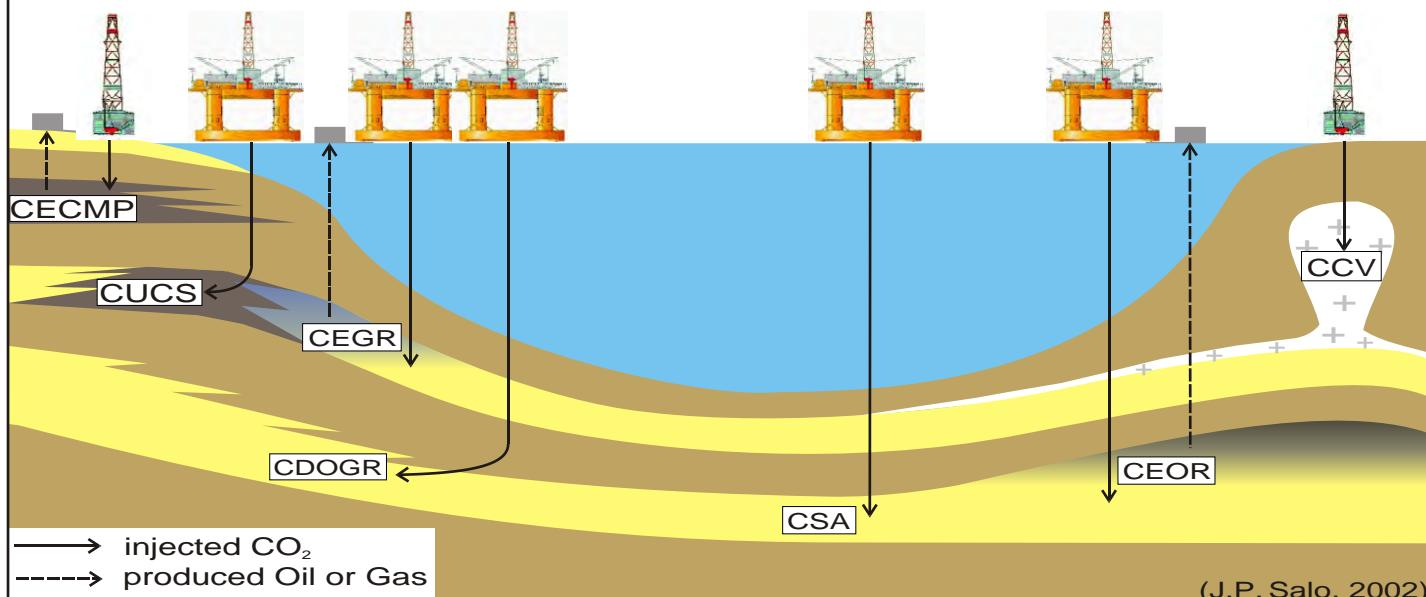


Figure 2.3: Map of the portion of Berau/Bintuni Bay where the Tangguh Project is located. Gas field accumulations are colored red. The area of a 3D seismic survey is outlined in purple. Onshore areas of land are green and the PSC block boundaries are also shown in dark blue. The gas accumulations are in 'en echelon' anticlinal structures trending NW-SE. The Kalitami structure, outlined as a blue oval has no known gas accumulation, but also trends NW-SE.

**ENVIRONMENTALLY-SAFE GEOLOGICAL OPTIONS
FOR
SUBSURFACE CO₂ INJECTION AND SEQUESTRATION**



LEGEND

[CEOR]	CO ₂ for Enhanced Oil Recovery	[CUCS]	CO ₂ in Unminable Coal Seams
[CEGR]	CO ₂ for Enhanced Gas Recovery	[CSA]	CO ₂ in Saline Aquifers
[CECMP]	CO ₂ for Enhanced Coal-bed Methane Production	[CCV]	CO ₂ in Caverns OR Voids
[CDOGR]	CO ₂ in Depleted Oil OR Gas Reservoirs		

Figure 3.1: Cross-sectional schematic illustrating the various subsurface geological ESSCI CO₂ sequestration/storage methods considered environmentally-sustainable, technologically feasible, and economically viable in some areas (modified from Bradshaw; et al., 2000; Bradshaw and Rigg, 2001).

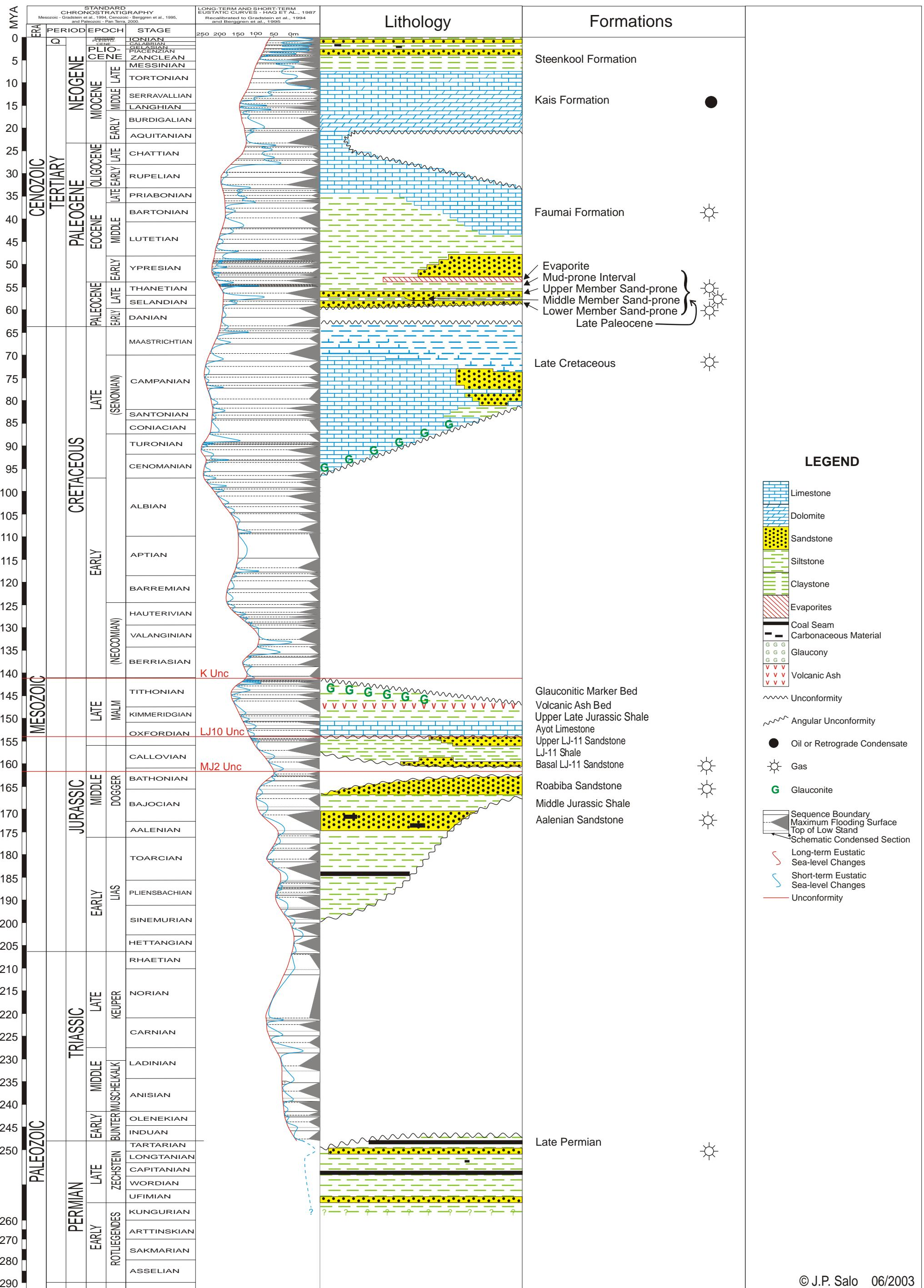


Figure 3.2: Generalized stratigraphic column for the Berau/Bintuni Basins area.

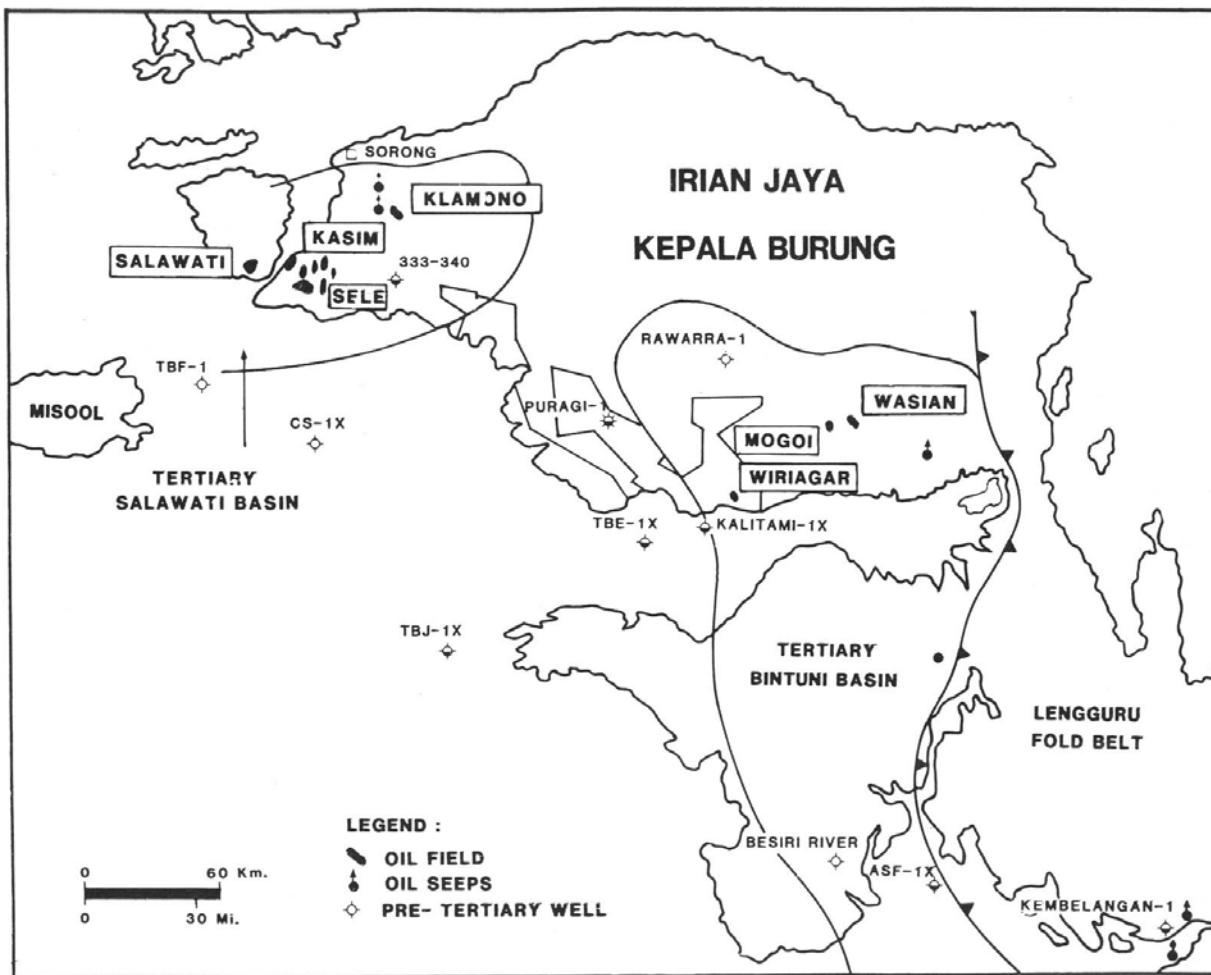


Figure 3.3 Location map of production fields in Bintuni and Salawati Basins, as of 1988. Bintuni Basin hydrocarbon discoveries were limited to Wasian and Mogoi fields, discovered by NNGPM, and Wiriagar shallow field, discovered by Conoco (Dolan and Hermann, 1988). The Tangguh gas fields are located approximately where the well name Kalitami-1X is written on the map.

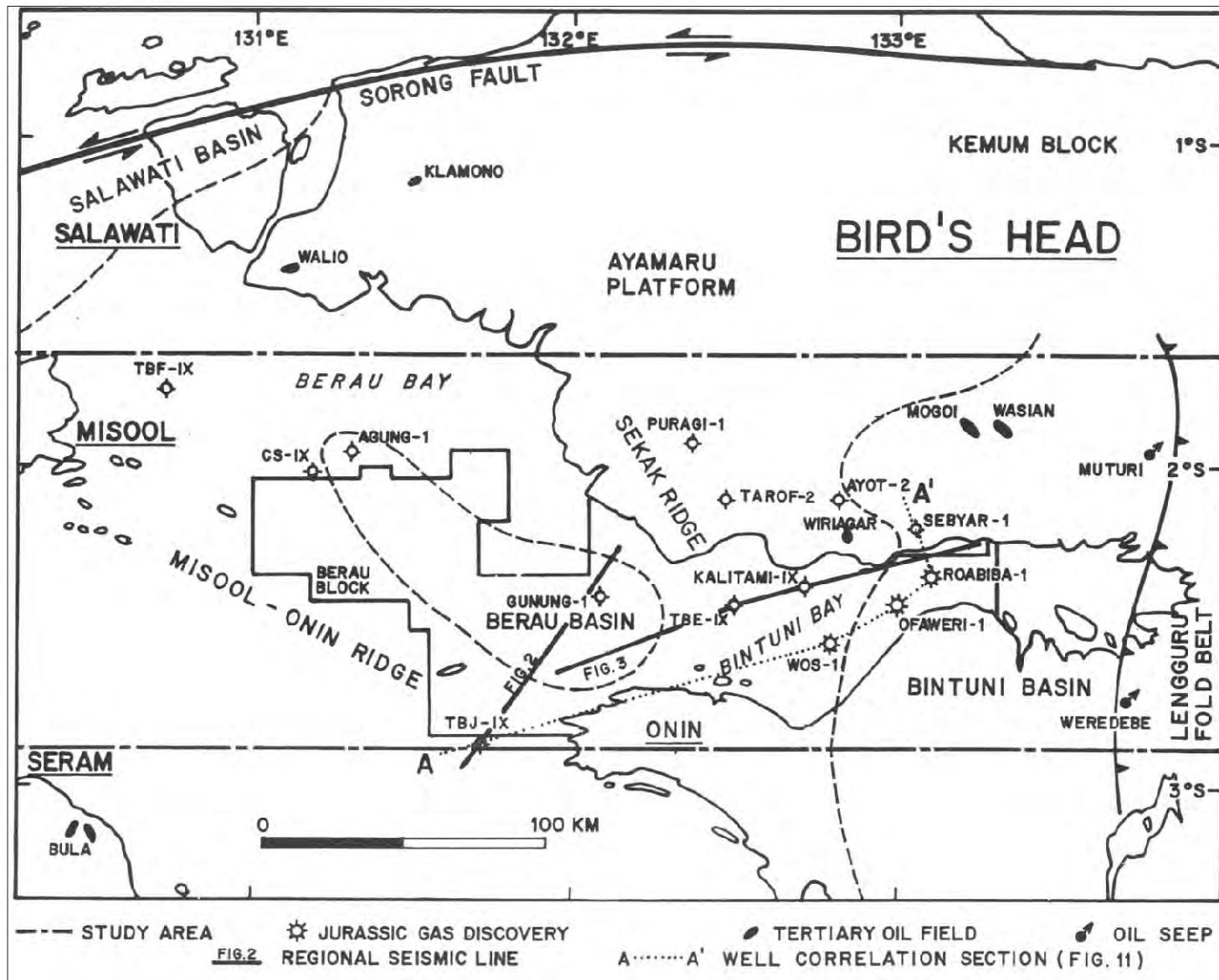


Figure 3.4: Location map of shallow oil fields, oil seeps, and deep exploration wells up to 1993, in Bintuni Basin. Additional seeps not noted on this Occidental Petroleum map occur at the Wiriagar, Mogoi, Wasian fields, and the Ayot-2 well location (Perkins and Livsey, 1993).

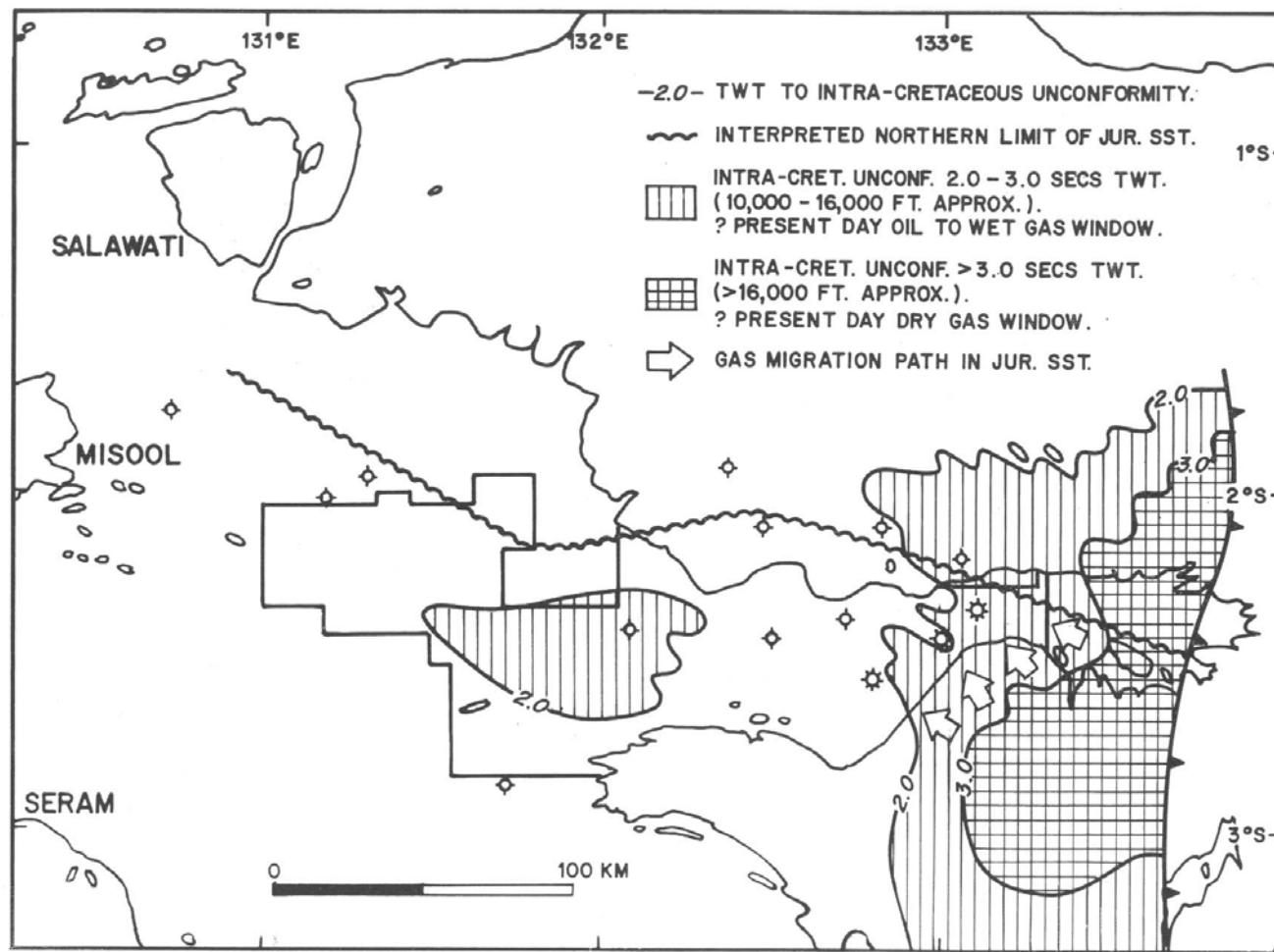


Figure 3.5: Map of 'kitchen area' for source rock hydrocarbon generation in the Bintuni and Berau Basins. The third arrow from the left, lies directly over the location of the 'S' structure and the proposed LNG plant (Perkins and Livsey, 1993).

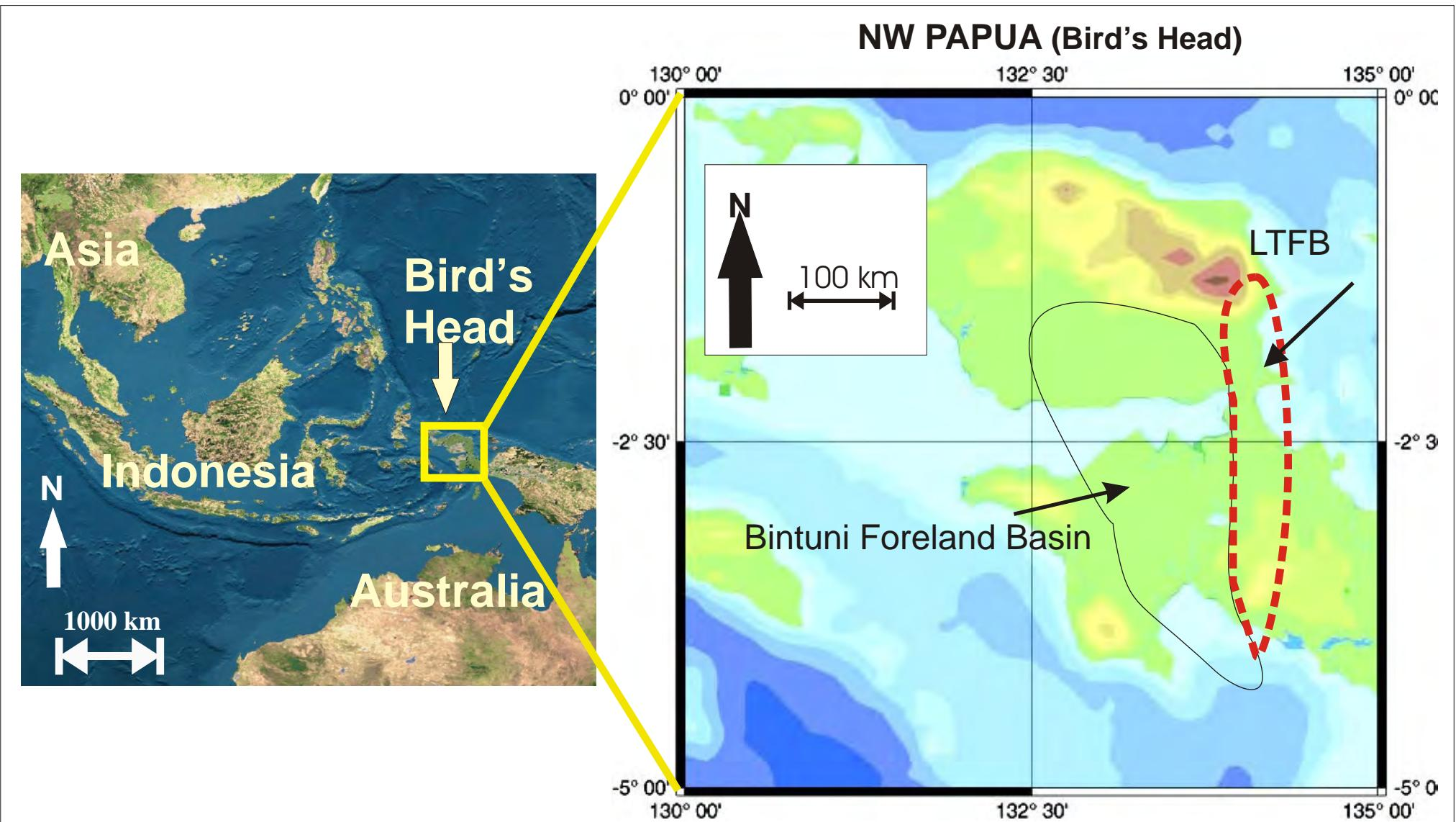


Figure 4.1: Location map for the area of interest, Bintuni Basin. Map on left is a bathymetry base map of S.E. Asia and northern Australia (base map modified from Fournilab, 2002). Map on right is bathymetry base map of the Bird's Head (Kepala Burung) area located in northwest Papua, Indonesia (base map modified from Reinecker, et al., 2004). LTFB is the Lengguru Thrust/Fold Belt, with the Bintuni Foreland Basin located directly to the west of the LTFB.

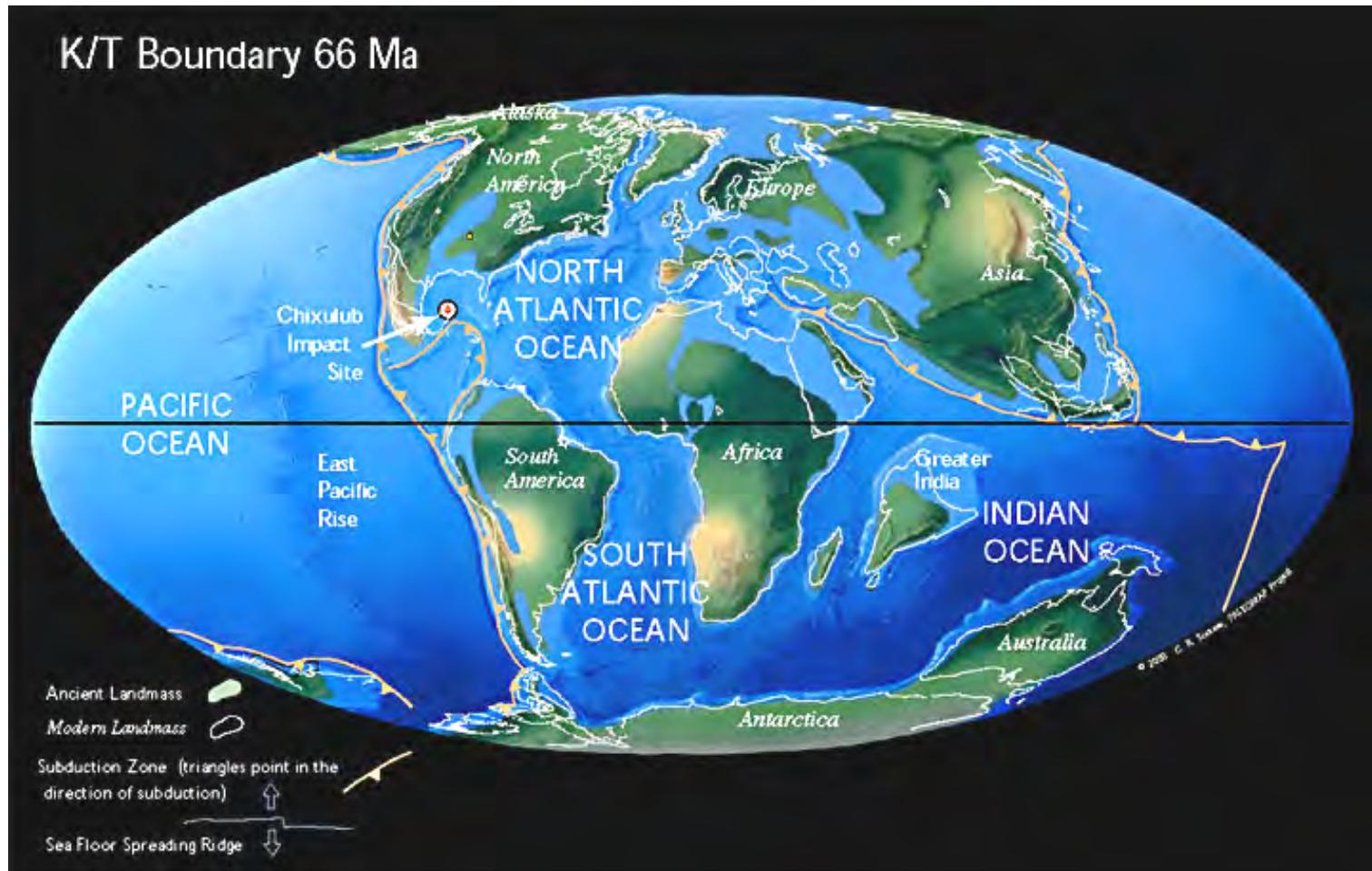


Figure 4.2: Paleotectonic map showing global tectonic plate geography in relation to the Bird's Head region at the Cretaceous/Tertiary Boundary (K/T Boundary), 65 Ma (Scotese, 2000). Paleo-landmasses are green and tan, modern landmasses are outlined in white. Subduction zones are indicated by tan lines with triangles, and sea floor ridges are represented by pale blue lines with blue arrows indicating direction of movement.

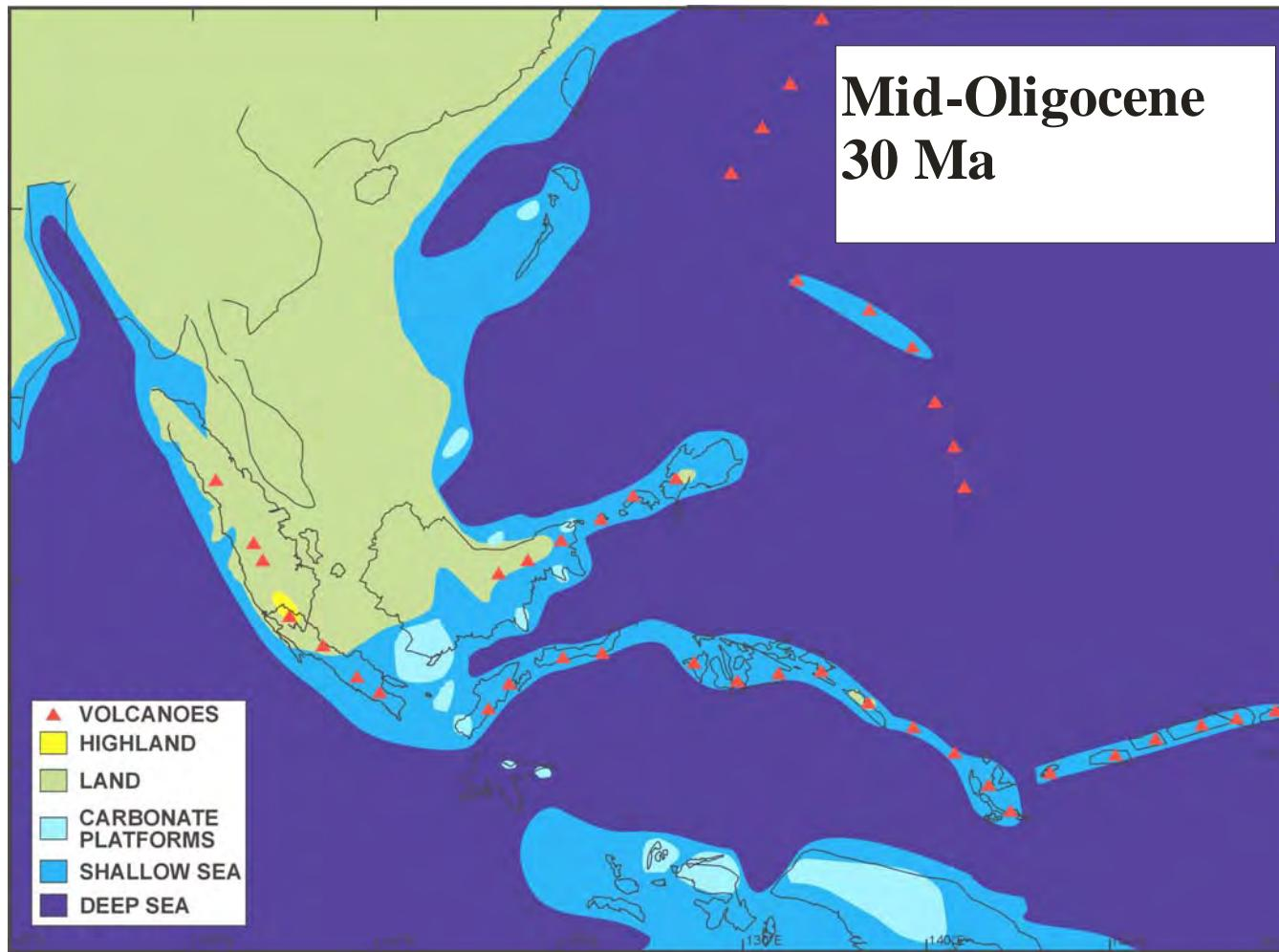


Figure 4.3: Mid-Oligocene paleotectonic map showing marine and subaerially exposed areas of SE Asia including location of paleo-volcanic sedimentation, continental landmasses and highlands, and carbonate marine platform formation during the Middle Oligocene. Note the carbonate platform deposition over New Guinea including the Bird's Head area (bottom center right). The Late Eocene and Oligocene carbonates are the oldest members of the New Guinea Limestone Group, or NGLG (Hall, 2000).

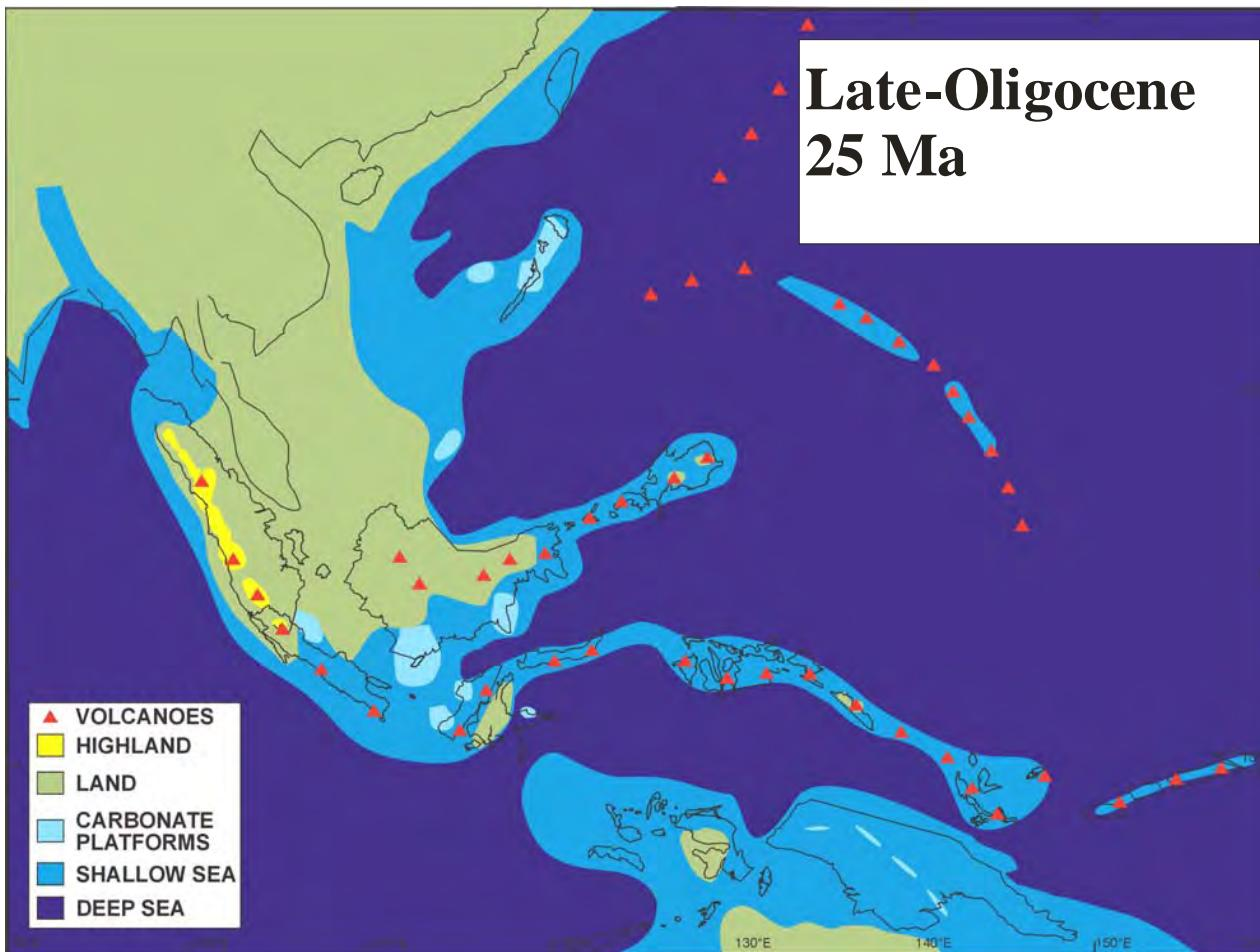


Figure 4.4: Paleotectonic map showing marine areas and subaerially exposed areas of SE Asia and the Bird's Head region including location of landmasses at the end of the Oligocene. Note that the Bird's Head region (bottom center right) was continental at the end of the Oligocene, which resulted in a peneplaning of most Oligocene sediments due to erosional subaerial exposure (Hall, 2000).

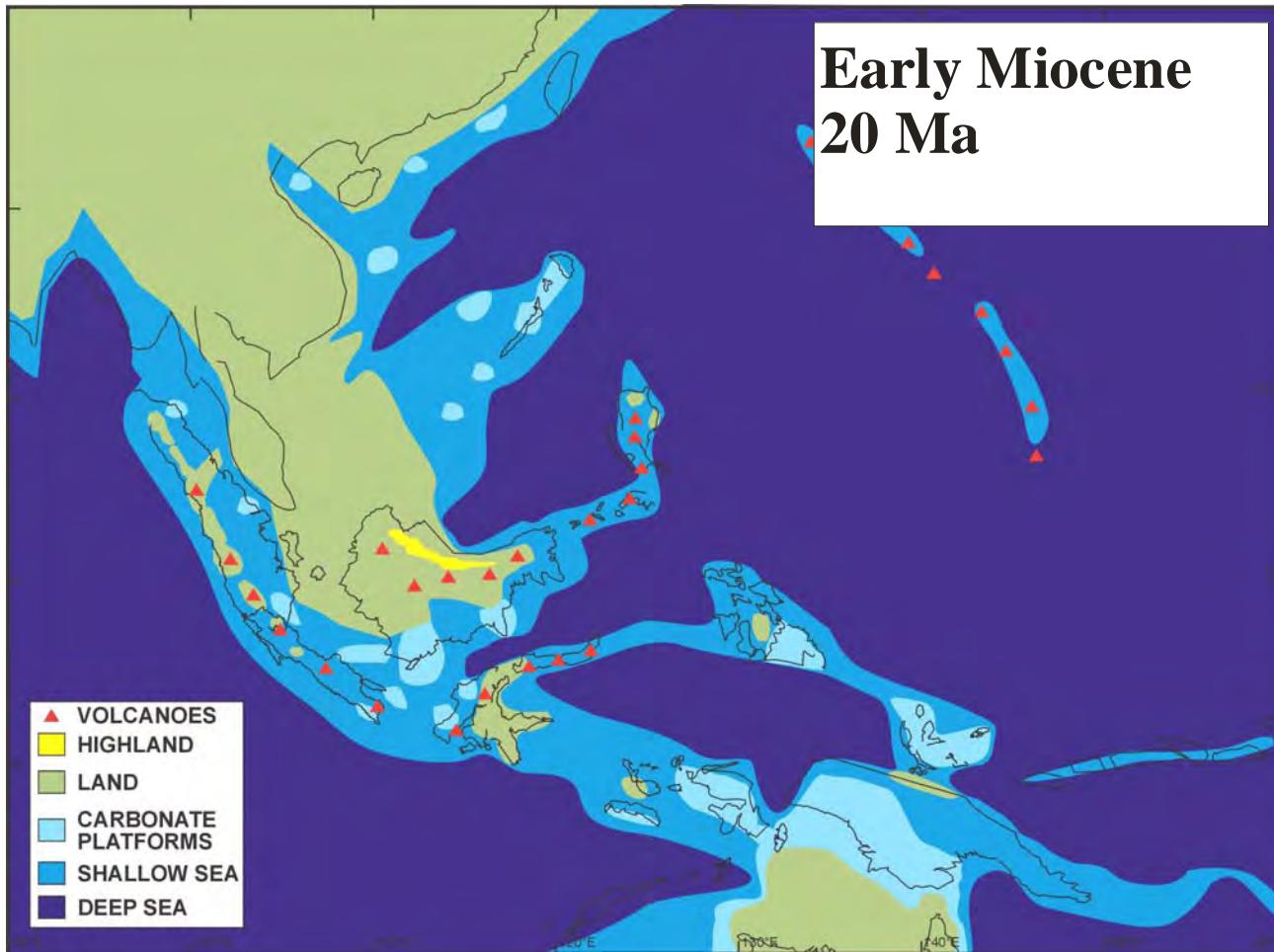


Figure 4.5: Early Miocene paleotectonic map showing carbonate platform areas of Bird's Head region (bottom center right) with the submergence of the Bird's Head area once again. The areal extent of the New Guinea Limestone Group ranges from the Bird's Head to Papua New Guinea. During the Miocene, the Kais Limestone Formation member of the NGLG was deposited in the Bintuni Basin area (Hall, 2000).

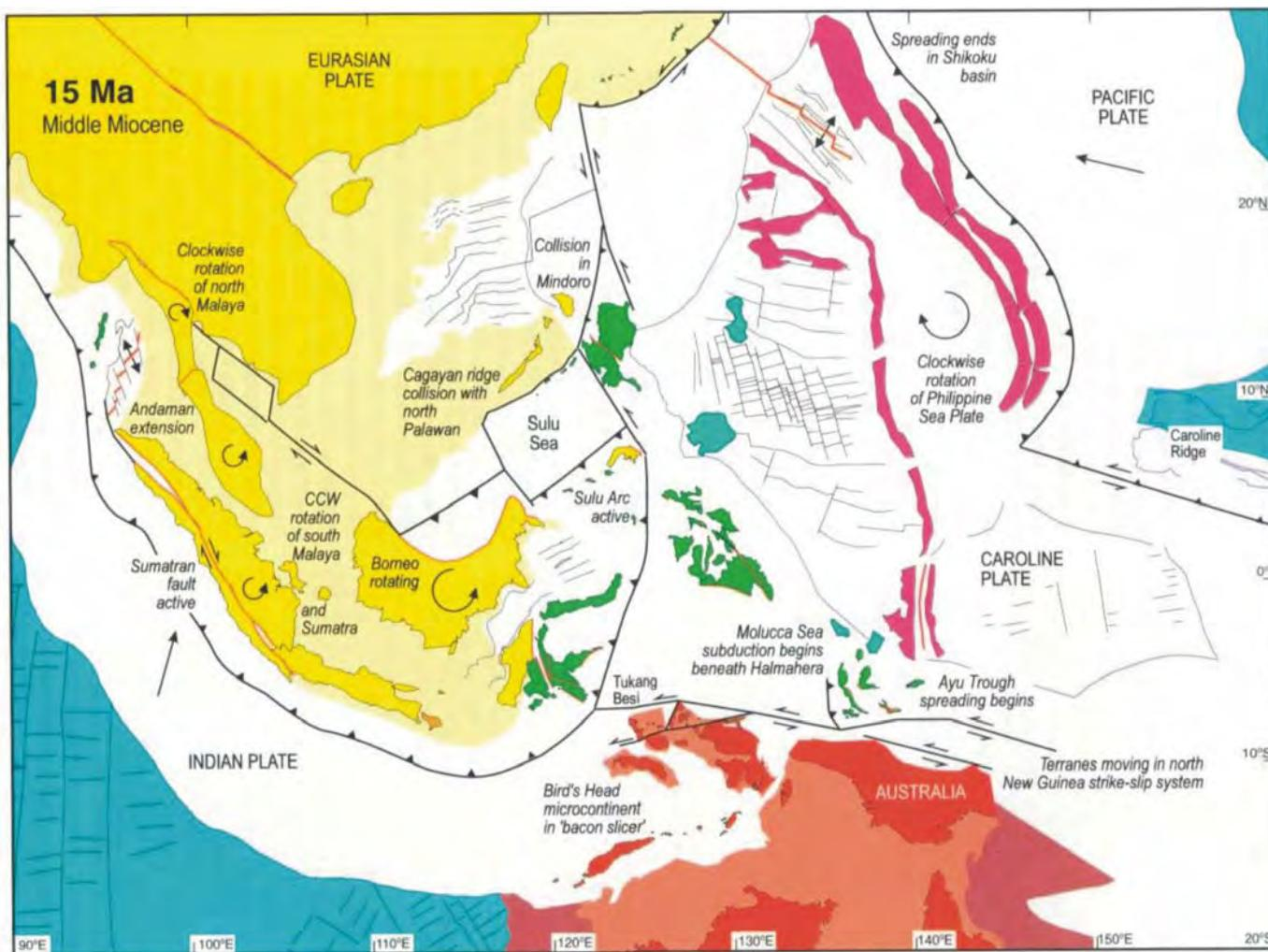


Figure 4.6: Detailed paleotectonic map of Eurasian, Pacific, and the Australian-New Guinea plates at the mid-Miocene, showing the onset of the Eurasian plate (Sundaland sub-plate) collision with the northern Australian-New Guinea plate and Pacific plate (Caroline sub-plate), and Hall's 'bacon-slicer' theory for Bird's Head detachment and subsequent re-aggregation during the Miocene (Hall, 1996).

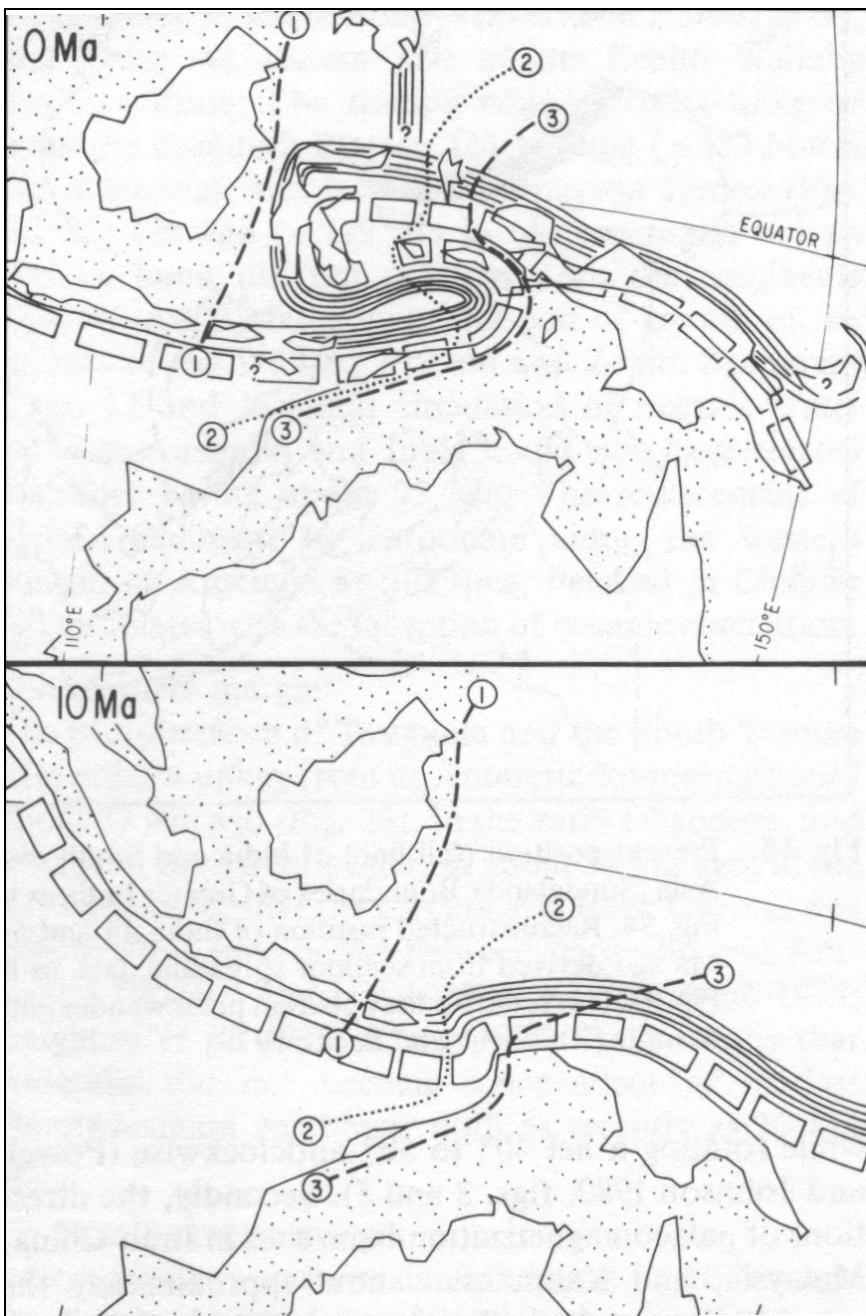


Figure 4.7: Two tectonic schematics, one from the Late Miocene (bottom figure -10 Ma), and the present-day (top figure -0 Ma), illustrating the Eurasian plate (Sundaland sub-plate) and the Pacific plate (Caroline sub-plate) collisions with the northern margin of the Australian-New Guinean Plate forming the Banda Arc fore arc island chain and re-accreting the Bird's Head micro-continent previously rifted from Australian-New Guinea plate. The Bird's Head was deformed in the east resulting in the Lengguru Fold/Thrust Belt (LFTB) approximately 5 to 7 Ma. Dashed and dotted lines labelled 1, 2, and 3 indicate progressive movement of the Sunda sub-plate margins from T1 (10 Ma) to present, T3 (0 Ma). Bird's Head deformation from the collision contributed in the formation of the Bintuni foreland basin and the Berau 'piggyback' basin in the fore of the LFTB (Veevers, 1986).

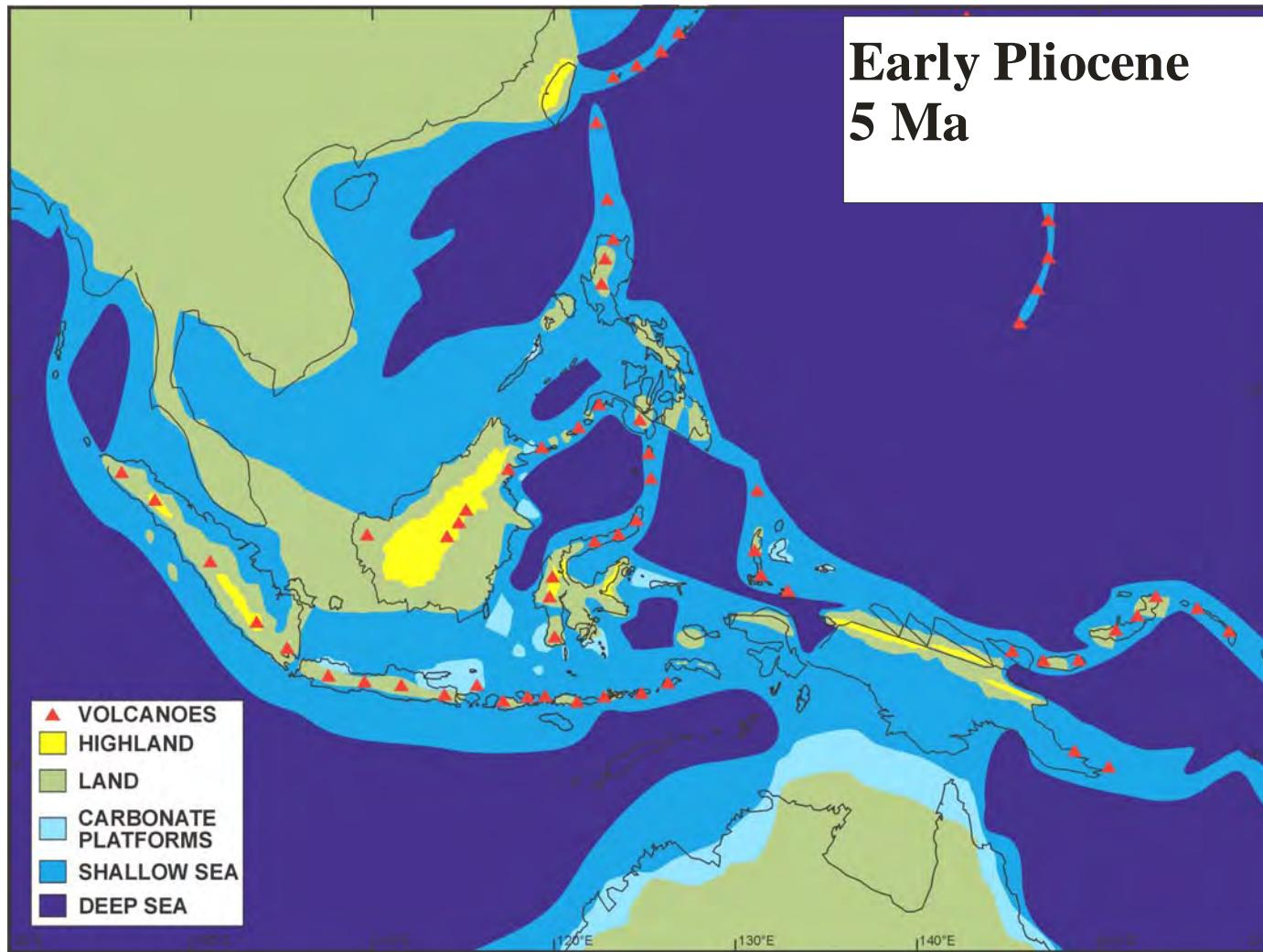


Figure 4.8: Paleotectonic map of Eurasian, Pacific, and Australian-New Guinea plates during the Pliocene (5 Ma). The Banda Arc collision has already, during the Late Miocene, caused substantial deformation to the Bird's Head region (center right). The tectonic deformation resulted in the Bintuni forebasin 'kitchen deep' entering the thermal 'oil and gas generation window' at depth approximately 5 Ma (Hall, 2000).

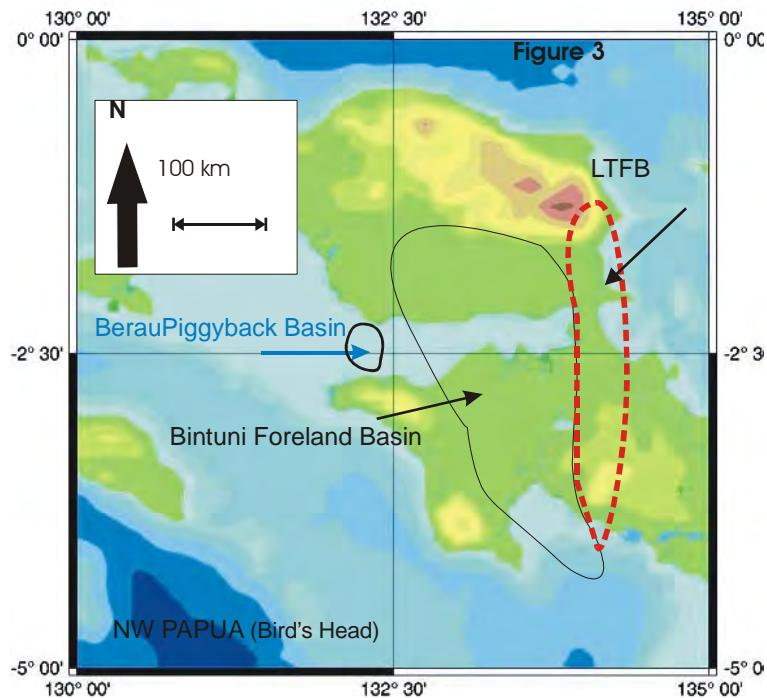


Figure 4.9: Tectonic collisions between the northward moving Australian-New Guinea plate, the eastward moving Sundaland subplate, and the southerly moving Caroline plate, resulted in tectonic deformation of the Bird's Head microplate, and orogenic/basinal structuring resulting in the creation of the Bintuni Foreland Basin and the Berau Piggyback Basin to the west of the LTFB. (bathymetry base map modified from Reinecker, et al., 2004).

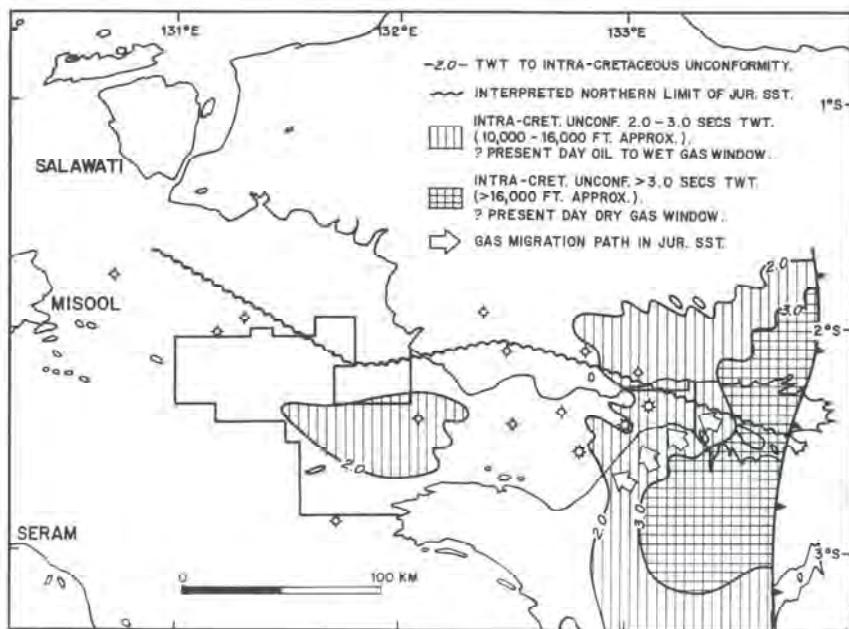


Figure 4.10: Map showing thermally mature 'kitchen' areas of the Bintuni foredeep, and Berau piggyback basin, for hydrocarbon generation (Perkins and Livsey, 1993).

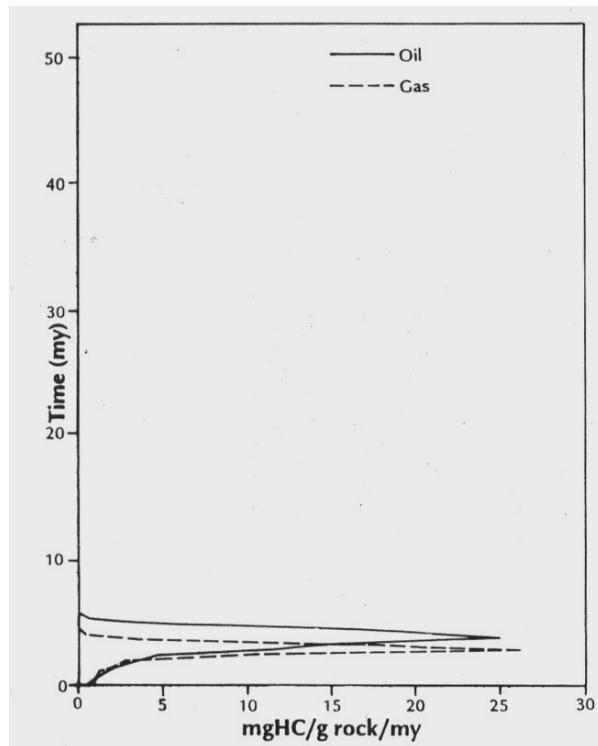


Figure 4.11: Graph showing thermal maturity history for oil generation and gas generation from geochemical analysis of known source rock samples in ‘kitchen’ areas of the Bintuni basin foredeep (Perkins and Livsey, 1993).

AGE	LITH.	FM/THICK	SIGNIFICANCE	ENVIRON.	SEQUENCE
REC.-		STEENKOOl			
MIOC.		1000' - 15,000'+	SEAL	SHALLOW MARINE	SYN - OROGENIC
MIOC - EOC.	● NEW GUINEA LIMESTONE	1250' - 8000'	RES.*	SHALLOW MARINE	
EOC.			S.R.*		
EOC. - LATE CRET.	● UPPER KEMBE-LANGAN	700' - 4000'	S.R.* SEAL RES.*	DEEP MARINE	POST-RIFT
E.CRET. - LATE TRIASSIC	● LOWER KEMB.	0' - 5000'	SEAL RES.* S.R.*	SHALLOW MARINE - NON MARINE	
TRIASSIC-	TIPUMA - AINIM.	0' - 2000'	S.R.*	NON - MARINE	
PERMIAN	AIFAT - AIMAU	4000' +	ECON. BSMT.	SHALLOW MARINE	RIFT
PERM. - CARBONI-FEROUS					

* S.R. = SOURCE ROCK RES. = RESERVOIR

Figure 5.1: Example of early stratigraphic column for Bintuni Basin from Perkins and Livsey (1993). All of the Jurassic formations are lumped together with the Early Cretaceous and the Late Triassic, and called the Lower Kembelangan. The Upper Kembelangan includes all of the Eocene, Paleocene and Late Cretaceous sedimentological sequences.



Figure 5.2: Examination of almost 3,000 ft of core and review of the core logs of G. Pemberton and C. Cook, by the author at Core Laboratories facility in Jakarta, Indonesia. Pictured, from left to right Dr. G. Perez (BP), the author, and Dr. Simon Lang (ASP) in 2001. Cores were digitally photographed and examined in 2001 and again in 2002, in addition to new core plugs selected and analyzed in 2003.

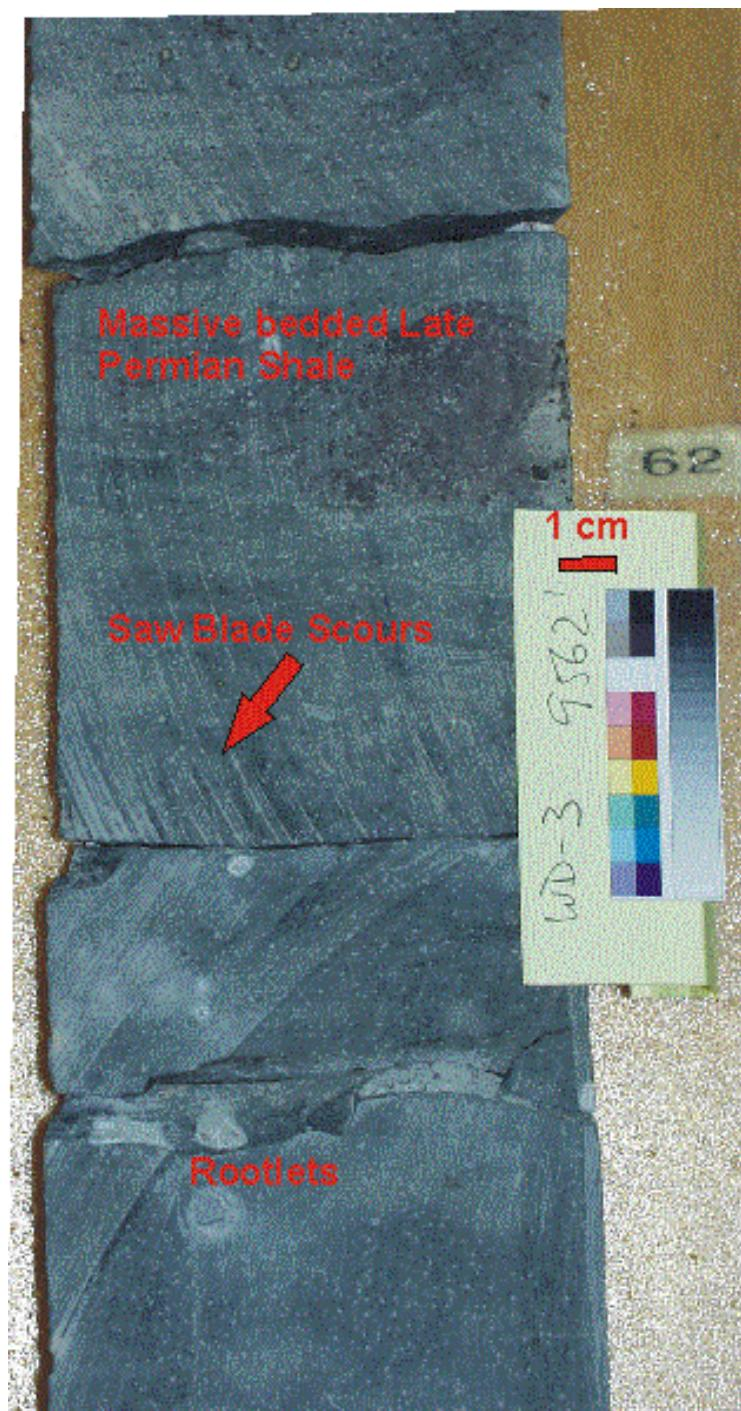


Figure 5.3: Massively bedded fluvio-lacustrine Late Permian shale, at driller's measured depth 9562 ft, from Core No.15 in the Wiriagar Deep #3 well.

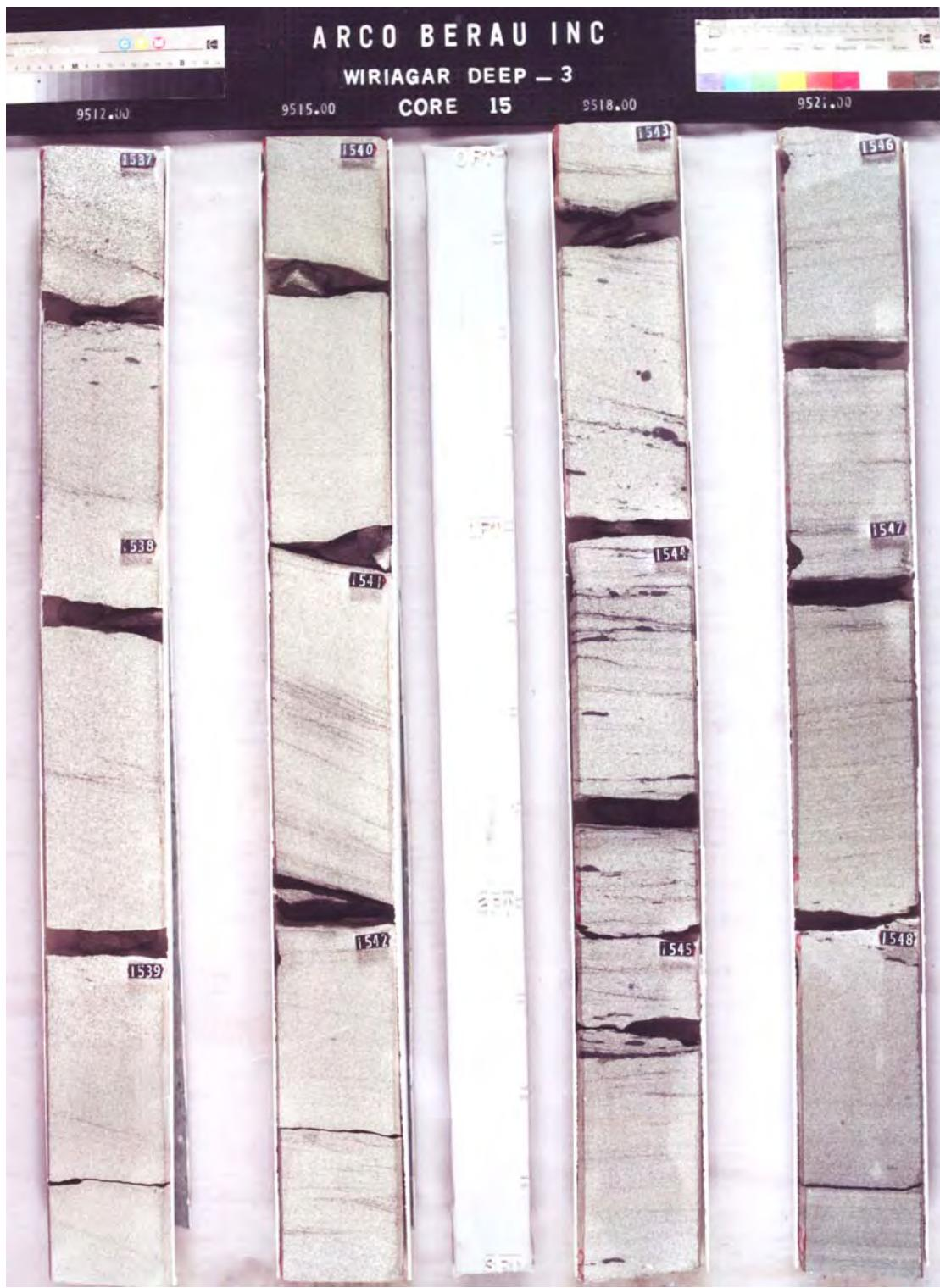


Figure 5.4: Photograph of near-top Late Permian marine sandstone interval depth 9512 ft to 9524 ft in Core No.15 from the Wiriagar Deep #3. Note the cross-bedding and flaser drapes (black paneled numbers displayed on the slabbed core are Core Lab's inventory ID tags at one foot intervals, and not core depths) (courtesy of Core Labs, 1996).

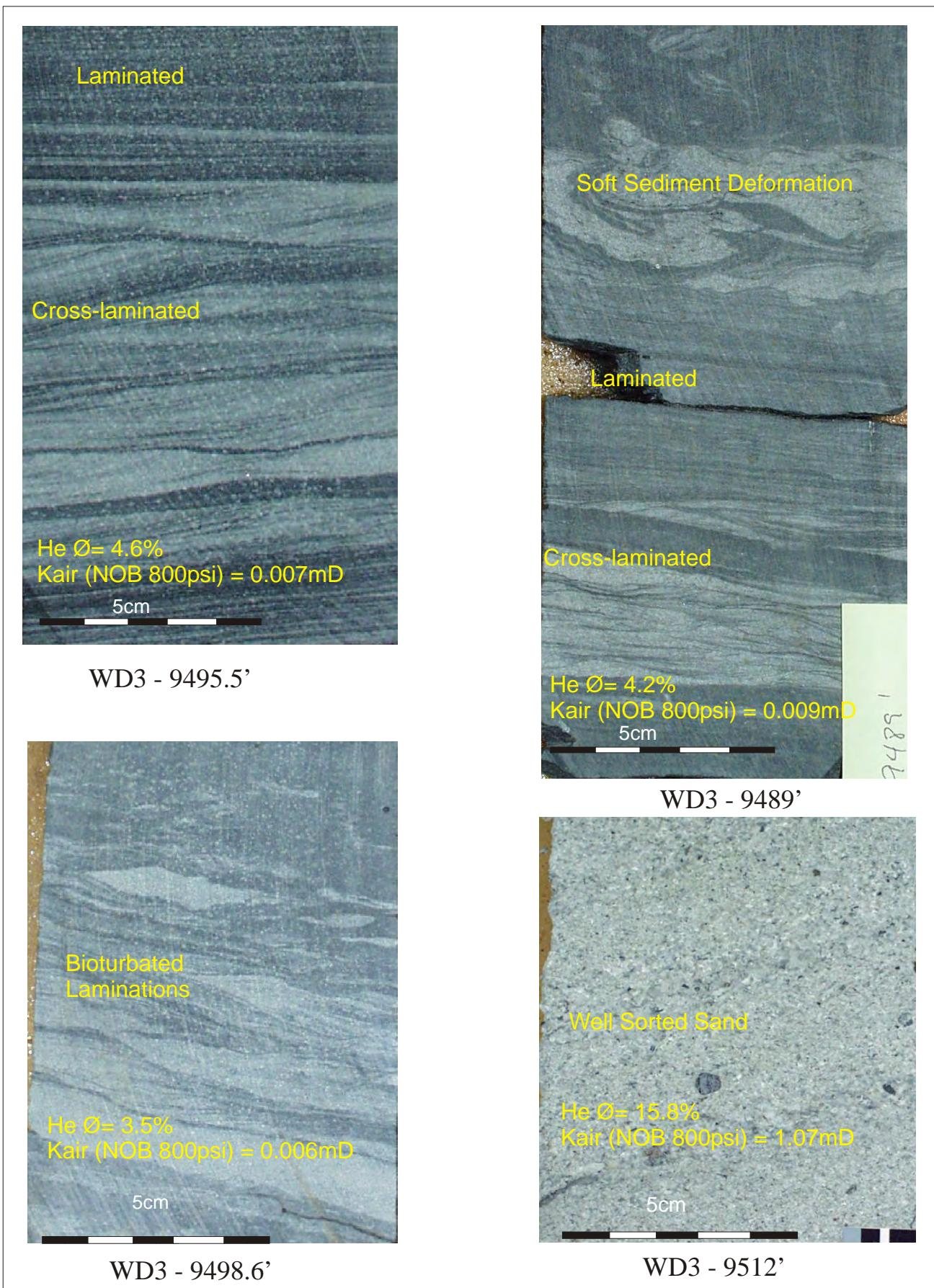
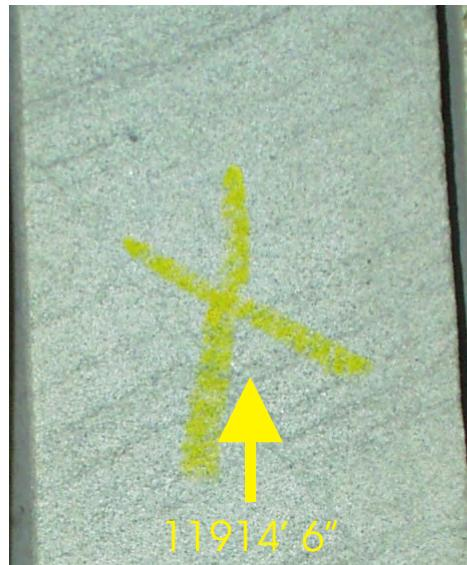
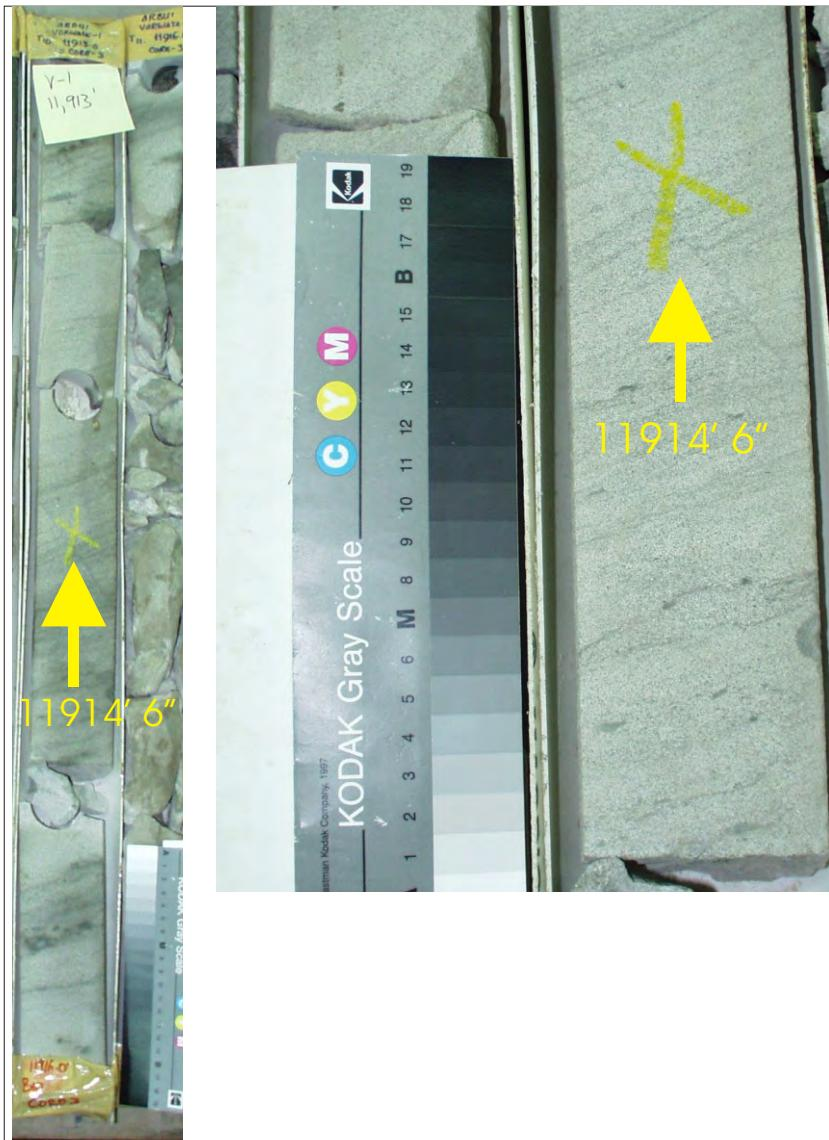


Figure 5.5: Near-top Late Permian sandstone cores with reservoir characteristics from core plug analysis. Pictures are of slabbed cores from the Wiriagar Deep #3 well (Core Labs, 1996).



Sample Depth: 11914' 6"
Shifted Depth: 11924' 6"
He-Ø: 6.9%
k air: 1.0 mD (NOB 800 psia)

WHOLE CORE PLUG
ANALYSES
WELL: VORWATA - 1
DEPTH: 11914' 6"

Figure 5.6: Core plug analyses for Permian sample 11914' 6" on Vorwata#1.



Figure 5.7: The Late Permian/Middle Jurassic nonconformable contact in WD-3 well, from Core No.15 at 9472 ft (driller's measured depth). Pebble lag at the base of the Jurassic is clearly visible.



Figure 5.8: Contact at the top of the Aalenian Sandstone Formation and the overlying MJ-4 shale break, which separates the Aalenian Sandstone Formation and the Roabiba Sandstone Formation. Photograph is from 9419 ft wireline log depth (9411 ft driller's measure core depth) in Core No.14 from the Wiriagar Deep #3 well. The shale has oxidized during storage resulting in a rust brown tint.

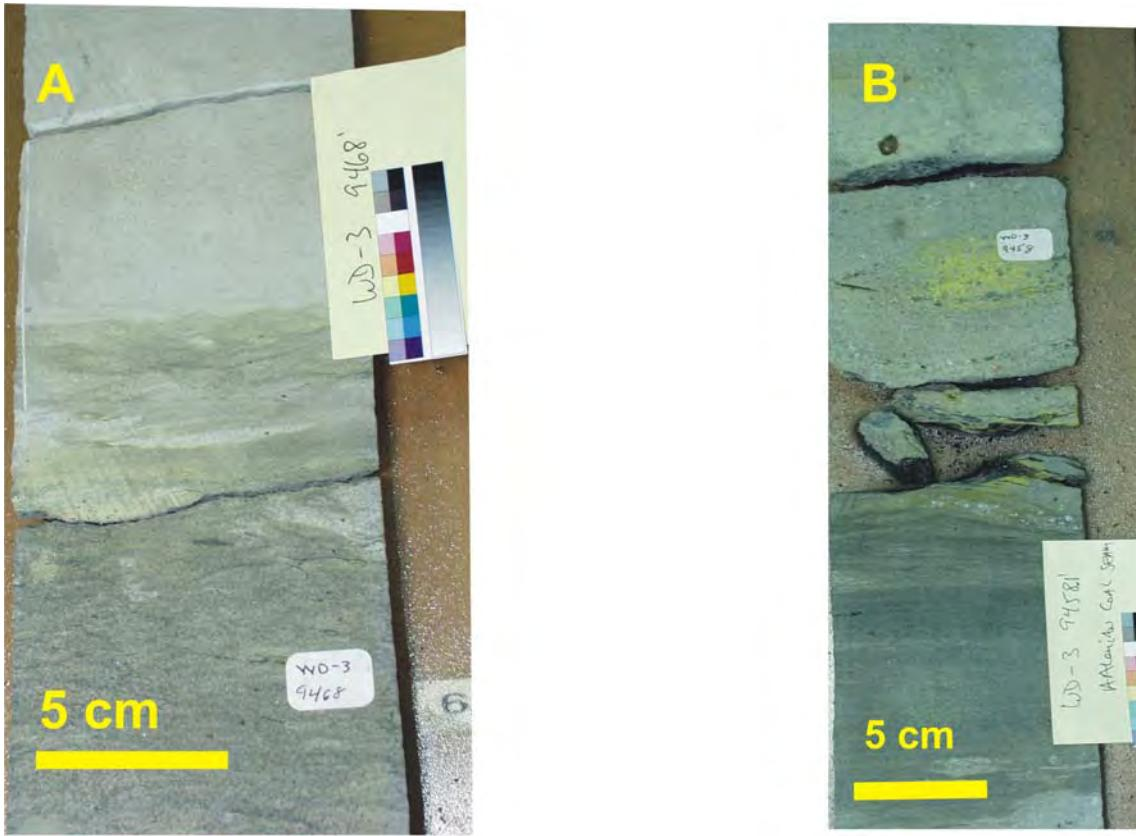


Figure 5.9: (A) Aalenian Sandstone Formation at 9475 ft wireline log depth (9468 ft driller's measured core depth) in Core No.14 on the Wiriagar Deep #3 well. (B) The Aalenian Sandstone Formation from 9457 ft wireline log depth (9450 ft driller's measure core depth) in Core No.14 on the Wiriagar Deep #3 well. Intervals shown are approximately in the middle of the Aalenian Sandstone Formation at the WD-3 well location. Yellow and green tints are due to organic growths on cores during storage between 1995 and 2002 (when digital photos were taken). Note the flaser bedding and clay microlaminations visible in the middle of (A) and the bottom third of (B).

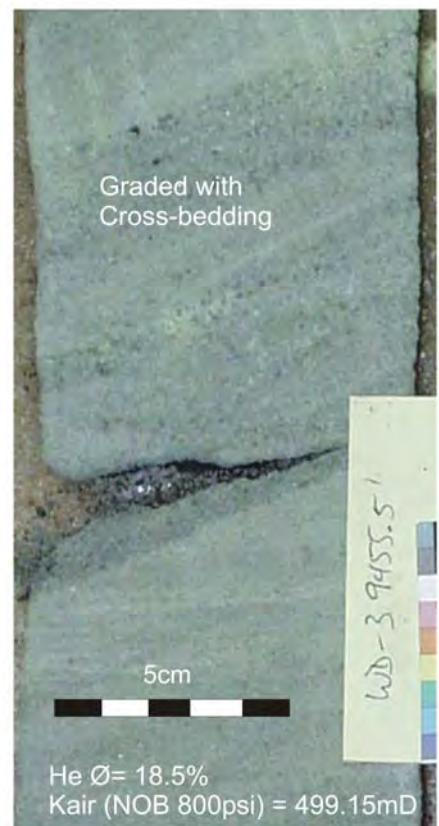
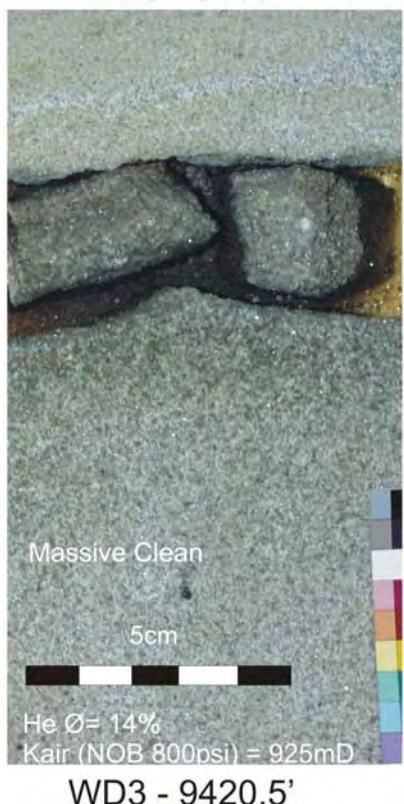
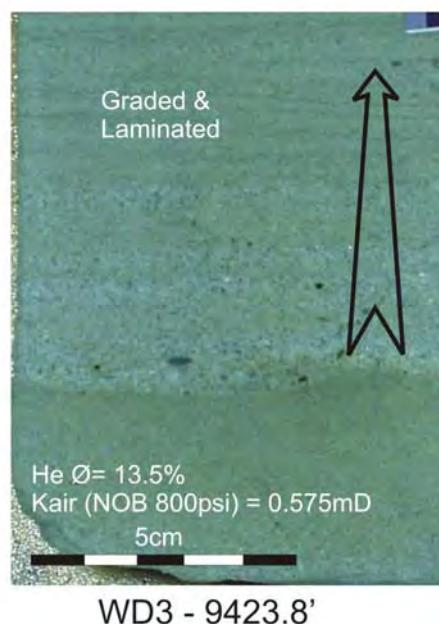
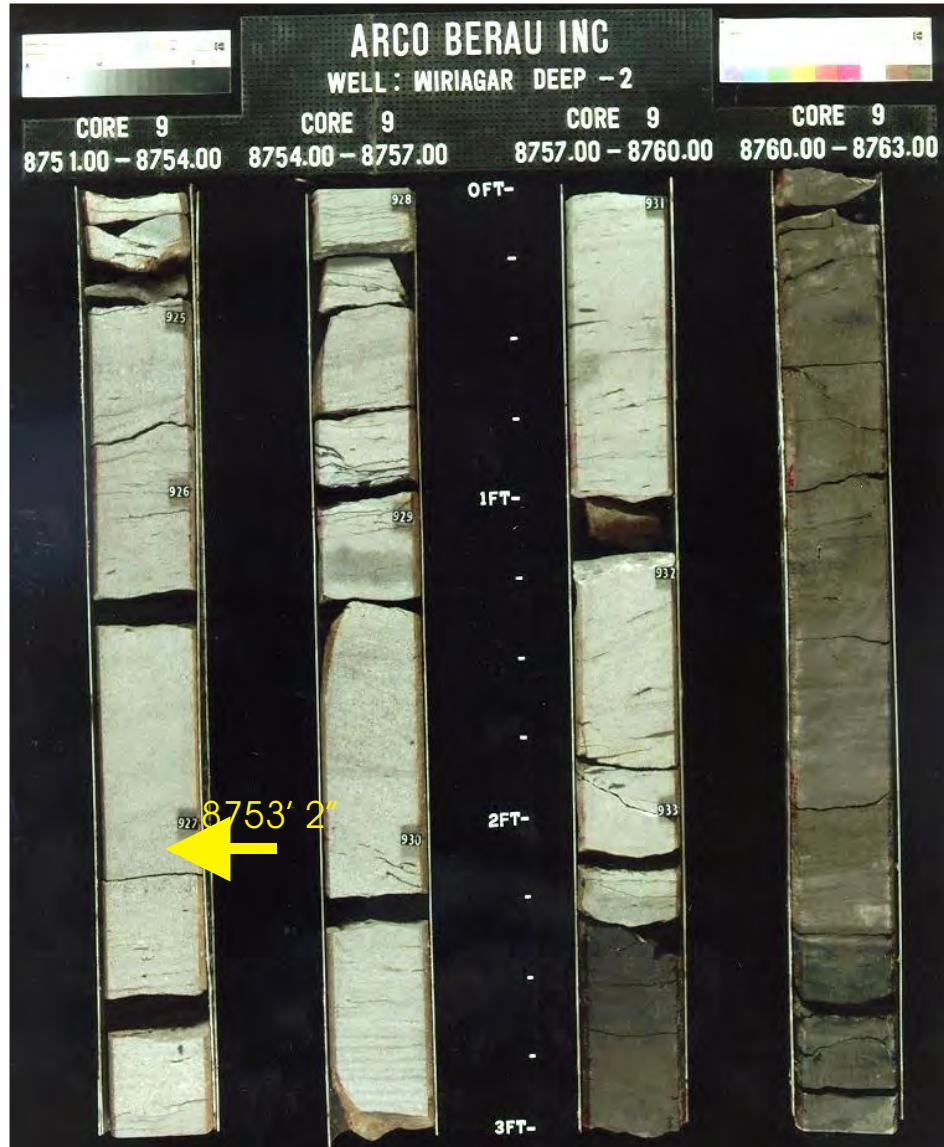


Figure 5.10: Different depositional facies are apparent in the pictures of the Aalenian Sandstone Formation from the WD-3 well, with depth respective sedimentological and reservoir character annotations noted for Core No.14. All depths are driller's measured depths from RKB.



Sample Depth: 8753' 2"
Shifted Depth: 8771' 2"
He-Ø: 14.8%
k air: 529 mD (NOB 800 psia)

WHOLE CORE PLUG
ANALYSES
WELL:WIRIAGAR DEEP #2
DEPTH: 8753' 2"

Figure 5.11:Core plug analysis from sample 8753' 2" on Wiriagar Deep#2.



Sample Depth: 8524' 7"
Shifted Depth: 8534' 7"
He-Ø: 19%
k air: 2264 mD (sc)

**WHOLE CORE PLUG ANALYSES
WELL:WIRIAGAR DEEP #7
DEPTH: 8524' 7"**

Figure 5.12: Core plug analyses for sample 8524' 7" from Wiriagar Deep #7.

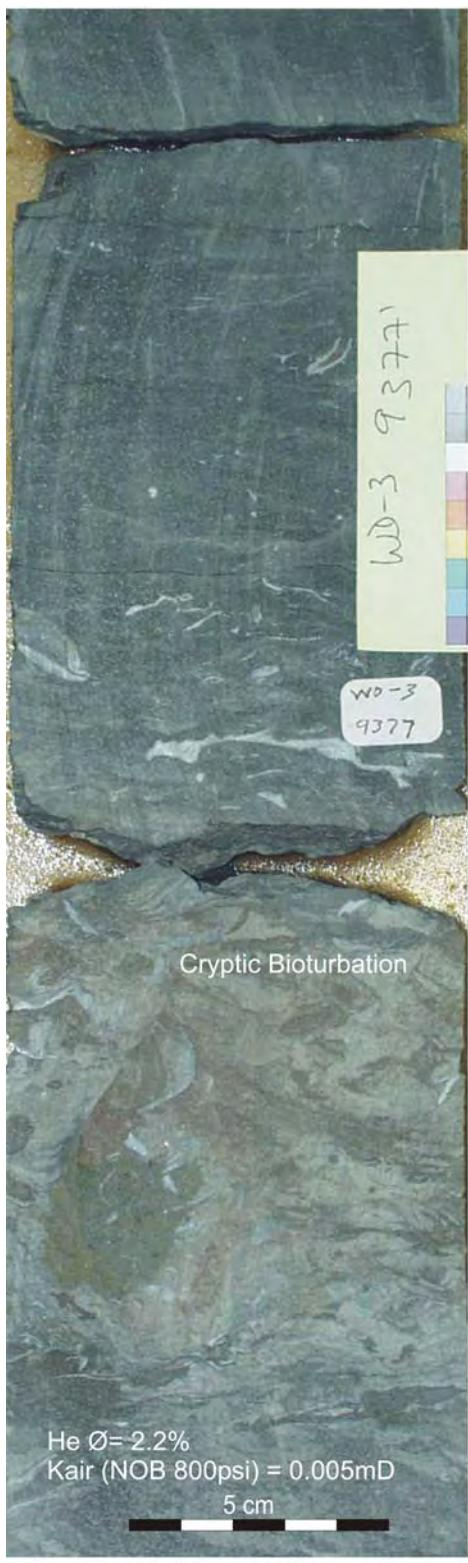


Figure 5.13: Roabiba Sandstone Formation from Wiriagar Deep #3 in slabbed core, annotated with sedimentological features and reservoir characteristics from their respective depths. All depths are driller's measured depths.

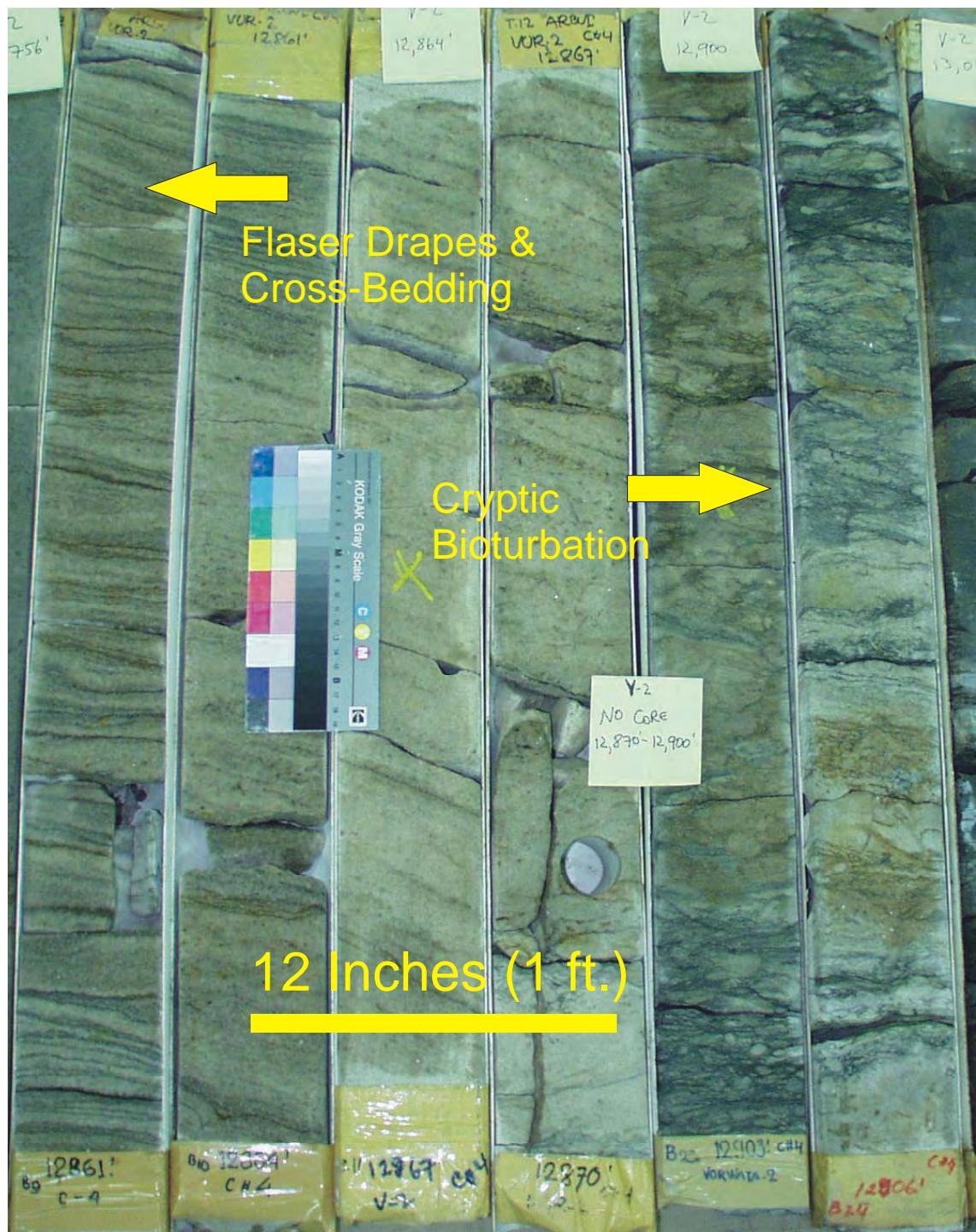


Figure 5.14: Core No.4 on the Vorwata #2 well, Roabiba Sandstone Formation, interval 12,858 ft through 12,906 ft (driller's measured depth). Zone of cryptic bioturbation is overlaid by a massive, 'clean' sandstone interval, overlaid in turn by a sandstone interval characterized by prominent flaser drapes, cross-bedding, and shale microlaminations.

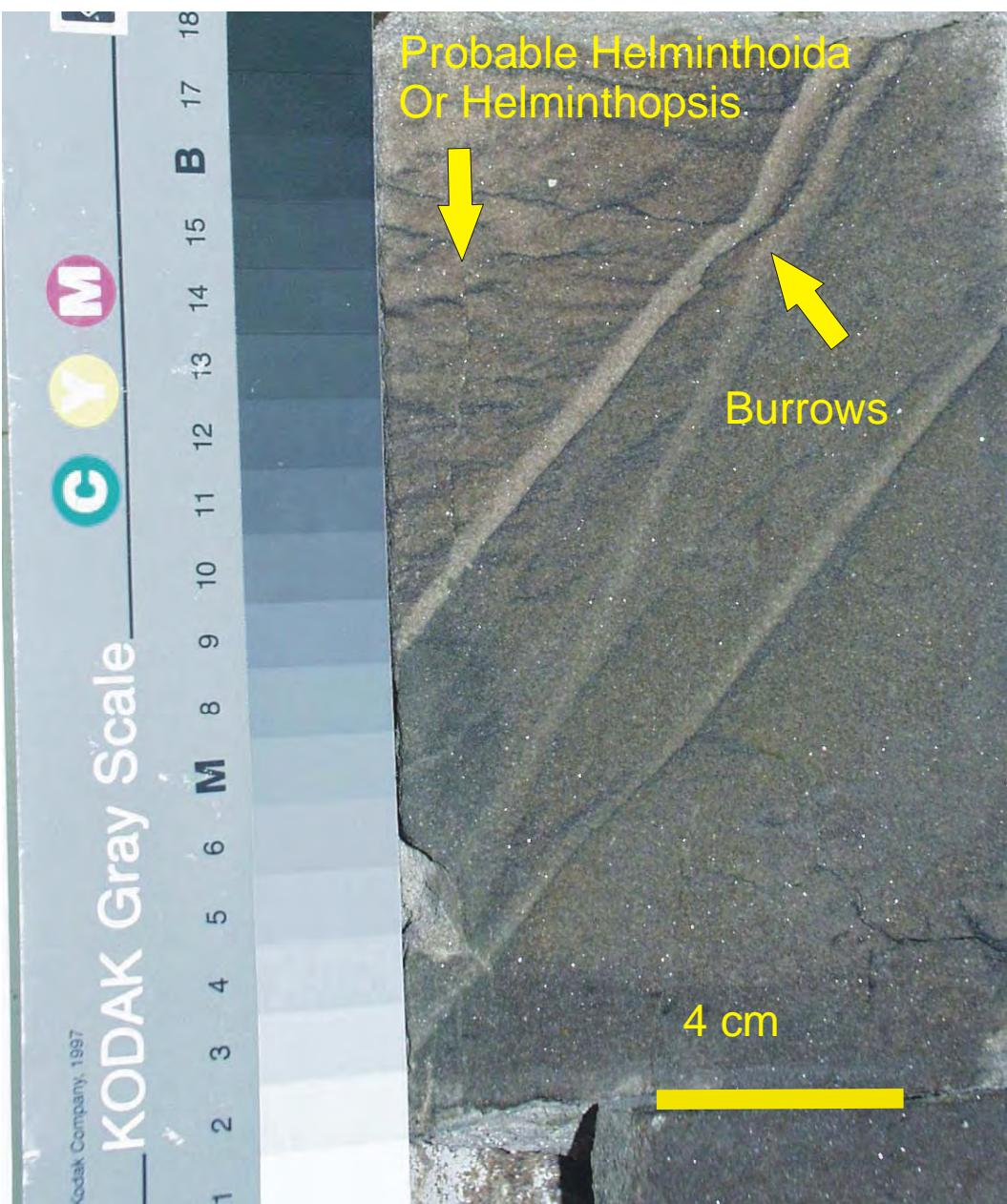


Figure 5.15: The Roabiba Sandstone Formation on the Vorwata #2 well, showing *Helminthopsis* or *Helminthoida* ichnological fabric at depth 12,599 ft (driller's measure depth). This marks the very top of the "Main Roabiba", which is now identified as an intra-reservoir unconformity between the Callovian Roabiba Sandstone and Bathonian/Bajocian Roabiba Sandstone (Ichnological interpretation; Dr. K. Bann, personal communication, 2003).

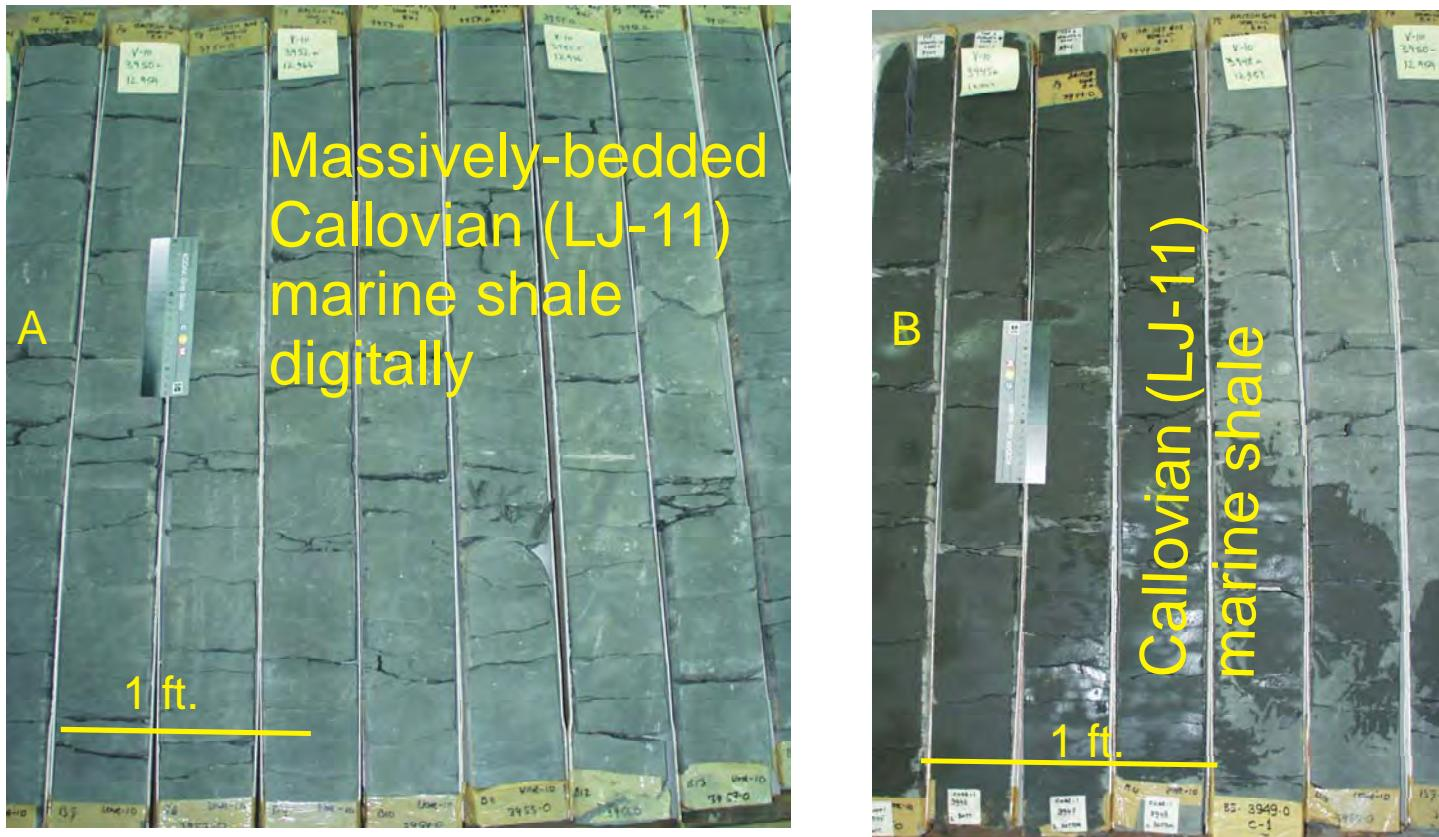


Figure 5.16: The massively bedded Callovian (LJ-11) marine shale is pervasive over the entire Vorwata area, but was captured in only a single core, Core No.1 on the Vorwata #10 well. This lithostratigraphic unit is the top-seal ‘cap-rock’ for the Roabiba Sandstone Formation at the Vorwata structure. Photograph ‘A’ shows the whole core dry, and photograph ‘B’ shows the whole core after wetting (it is beginning to dry out rapidly on the top left portion of the photo. The unit is relatively featureless sedimentologically.

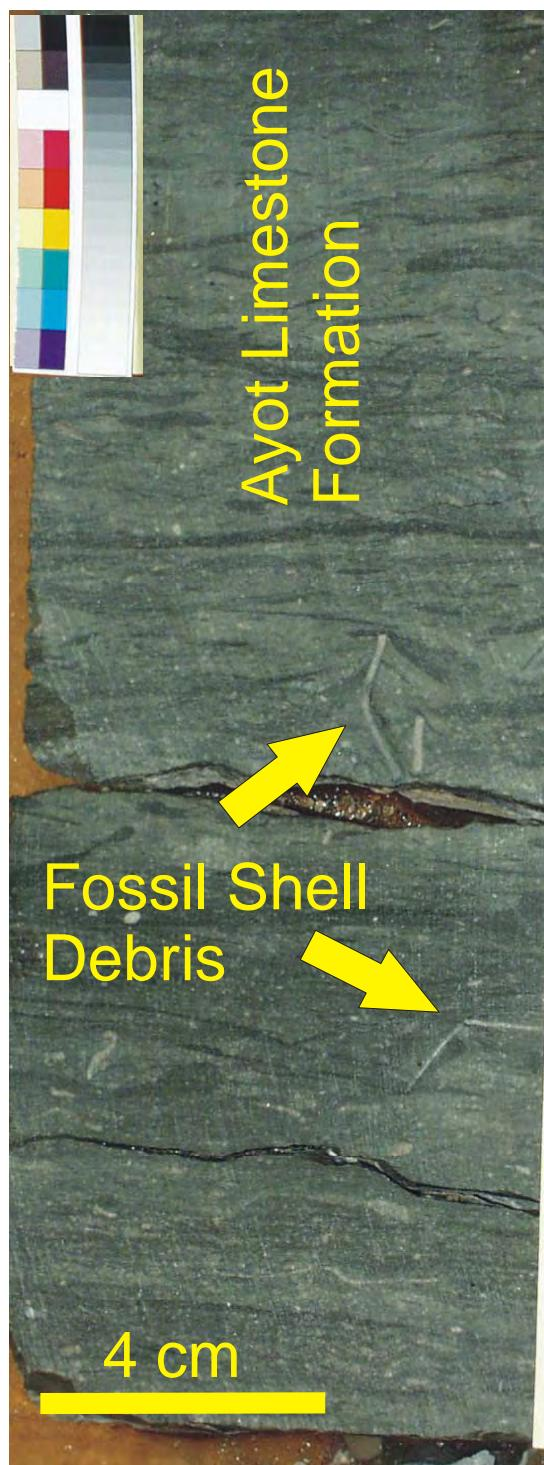


Figure 5.17: Slabbed core captured in Core No. 13 from Wiriagar Deep #3 well, showing the fossiliferous nature of the Ayot Limestone Formation.

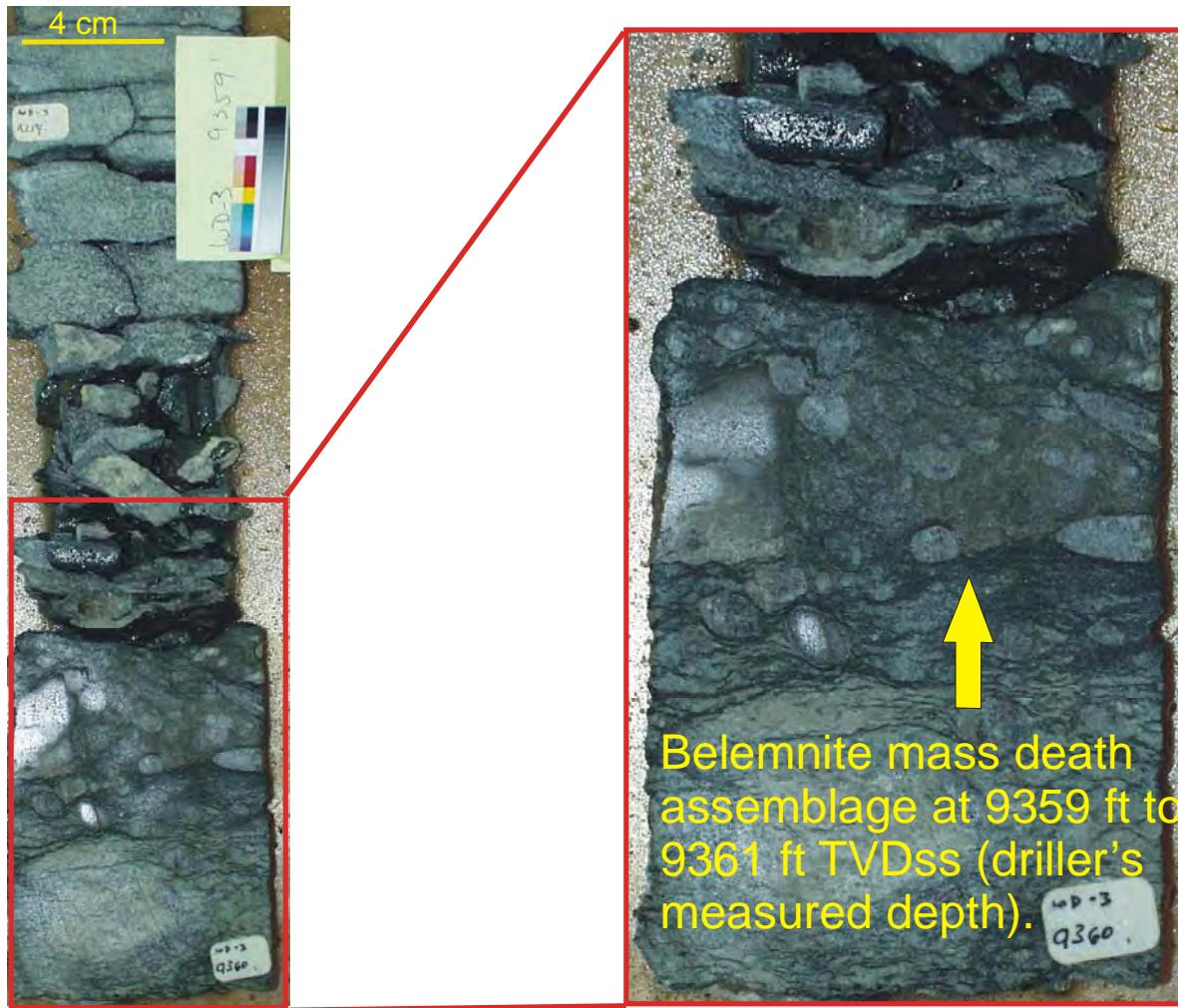


Figure 5.18: Photograph of interval 9359 ft to 9360 ft, (with high resolution close-up on right), showing belemnite ‘mass death assemblage’ just above the base (at 9367 ft) of the Ayot Limestone Formation on the Wiriagar Deep #3 well, in Core No.13.

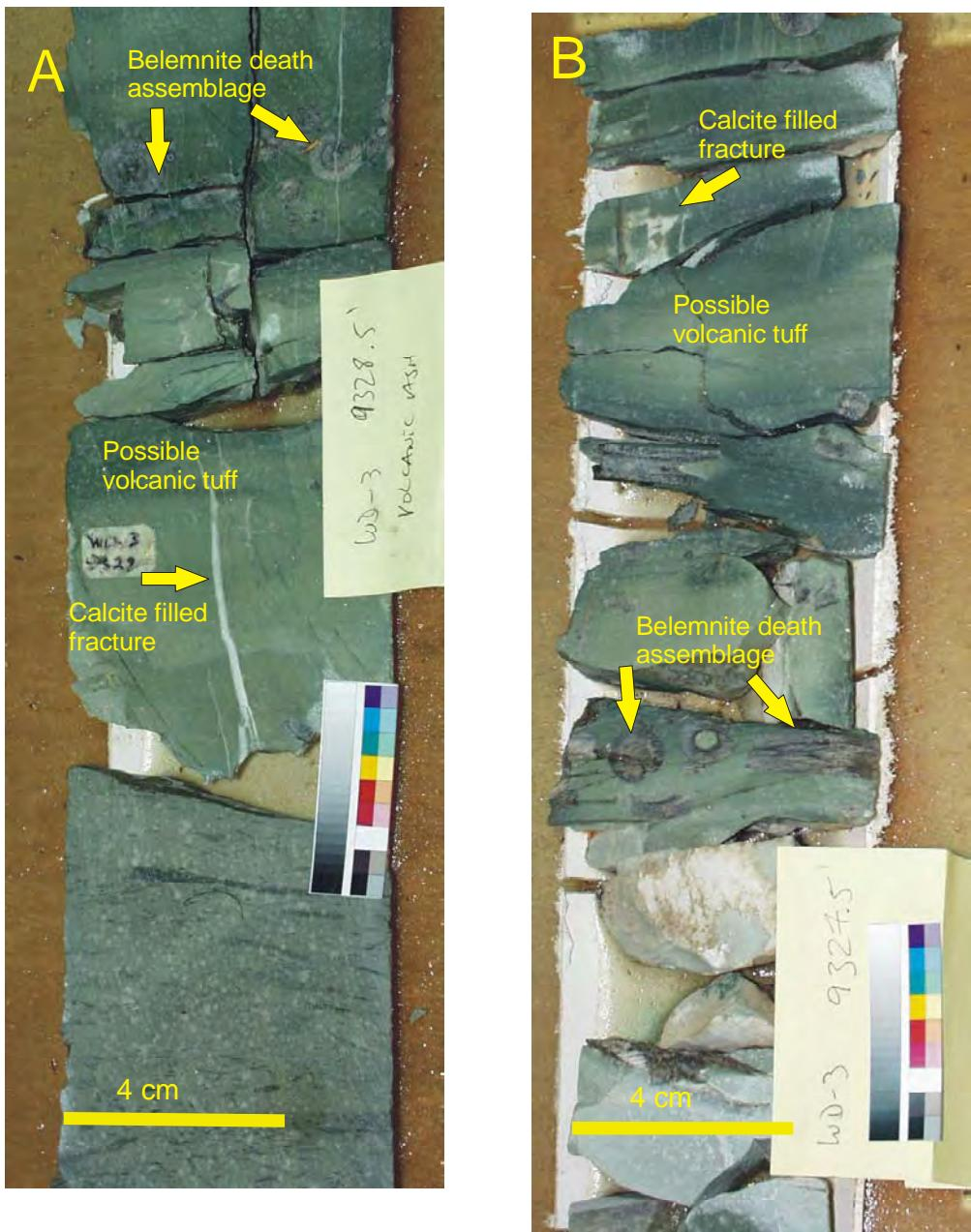


Figure 5.19: Possible altered tuff associated with a belemnite mass death assemblage, found between depths 9327 ft and 9328 ft, in slabbed cores from the Wiriagar Deep #3 well. Note calcite-filled fractures present. Some fracture surfaces also appear slickensided.

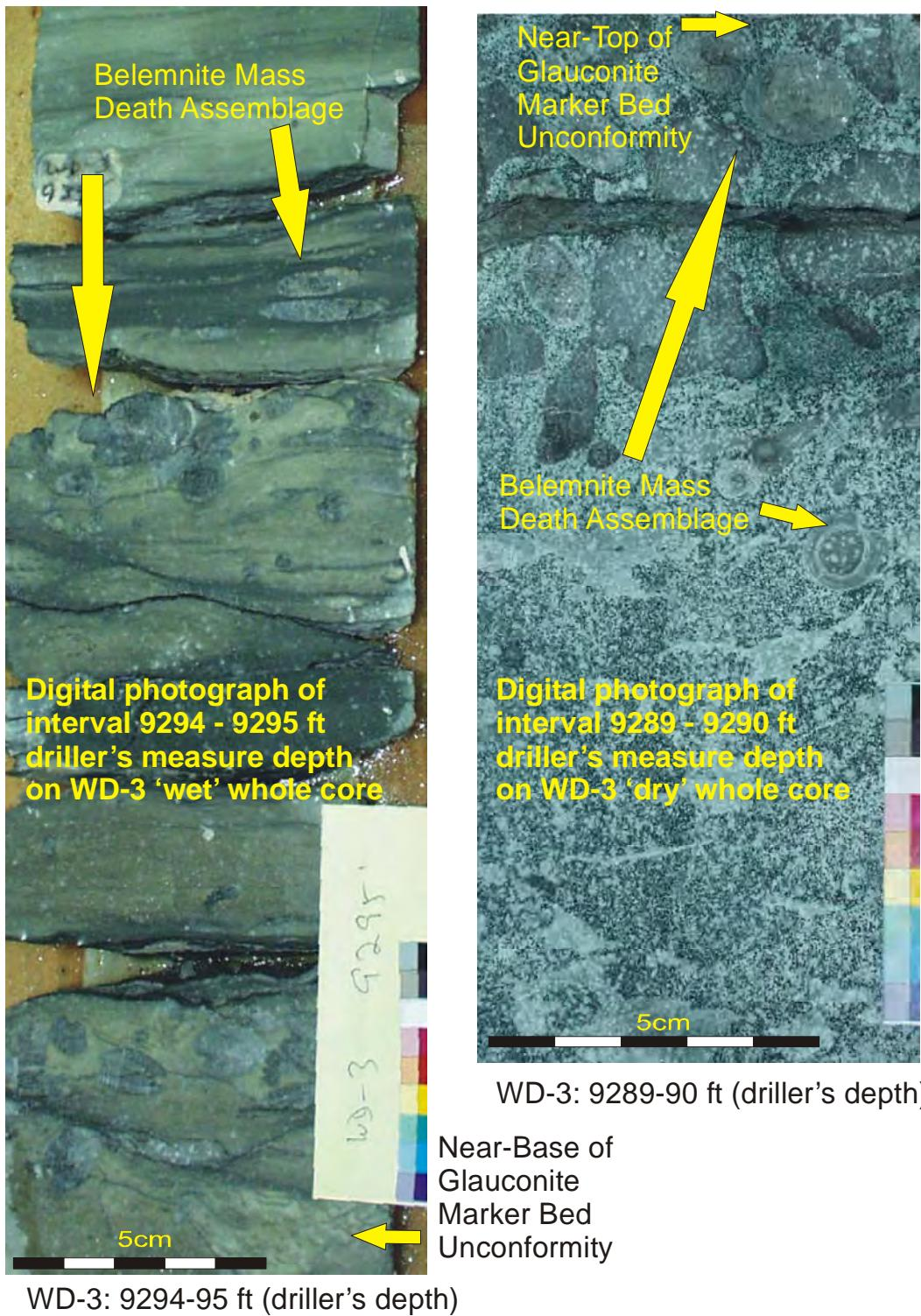


Figure 5.20: Slabbed core from the Wiriagar Deep #3 showing the Base Late Cretaceous/Top Late Jurassic Regional Unconformity. The unconformity is an excellent regional marker bed due to the appearance of abundant green glauconite nodules (>50% usually) in rock samples (ie. drill-cuttings and cores), and the distinctive wireline log signature of the bed.



Figure 5.21: Near-Base Late Cretaceous carbonate from Core No. 12 in the Wiriagar Deep #3 well. Dark reddish brown-gray color is due to high Fe carbonate content of the carbonate (siderite and ankerite, plus some dolomite).

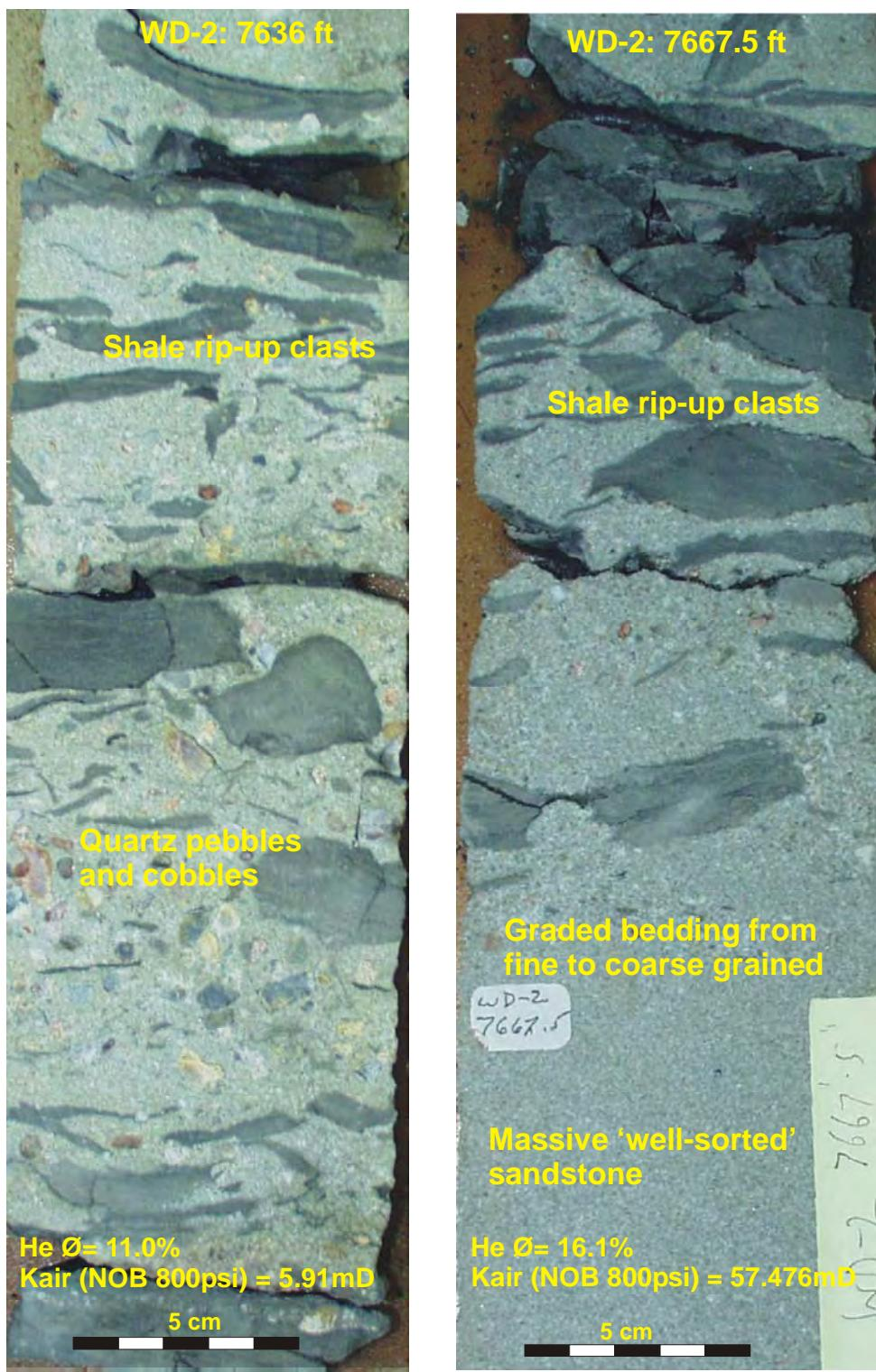


Figure 5.22: Whole core from Wiriagar Deep #2 showing Late Paleocene Sand-Prone Interval ‘Middle Member’ stacked channel sequence consisting of a series of stacked turbidite flows, found only in the WD-2 and WD-4 wells indicating a NE-SW trending turbidite channel. Lowe (1998) described the conglomerate pebbles and shale rip-up clast interval as being the coarser fraction that ‘floats’ on the top of a finer-grained sandstone due to greater turbidity.

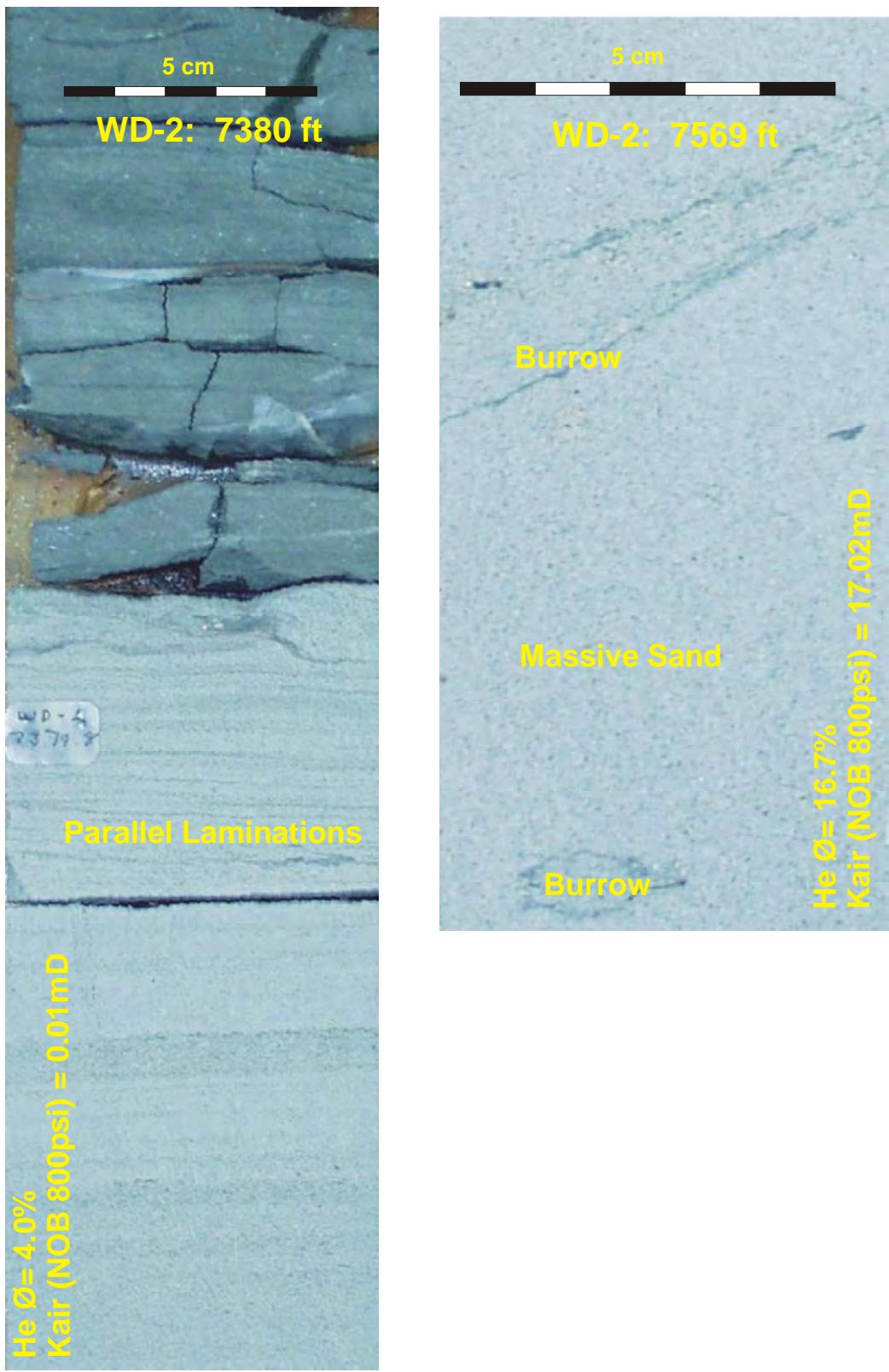


Figure 5.23: Turbidite member of the stacked channel sequence in the Late Paleocene Sand-Prone ‘Middle Member’ as seen in slabbed core from the Wiriagar Deep #2 well. Porosities and permeabilities listed were derived from core plugs at their respective depths where listed.

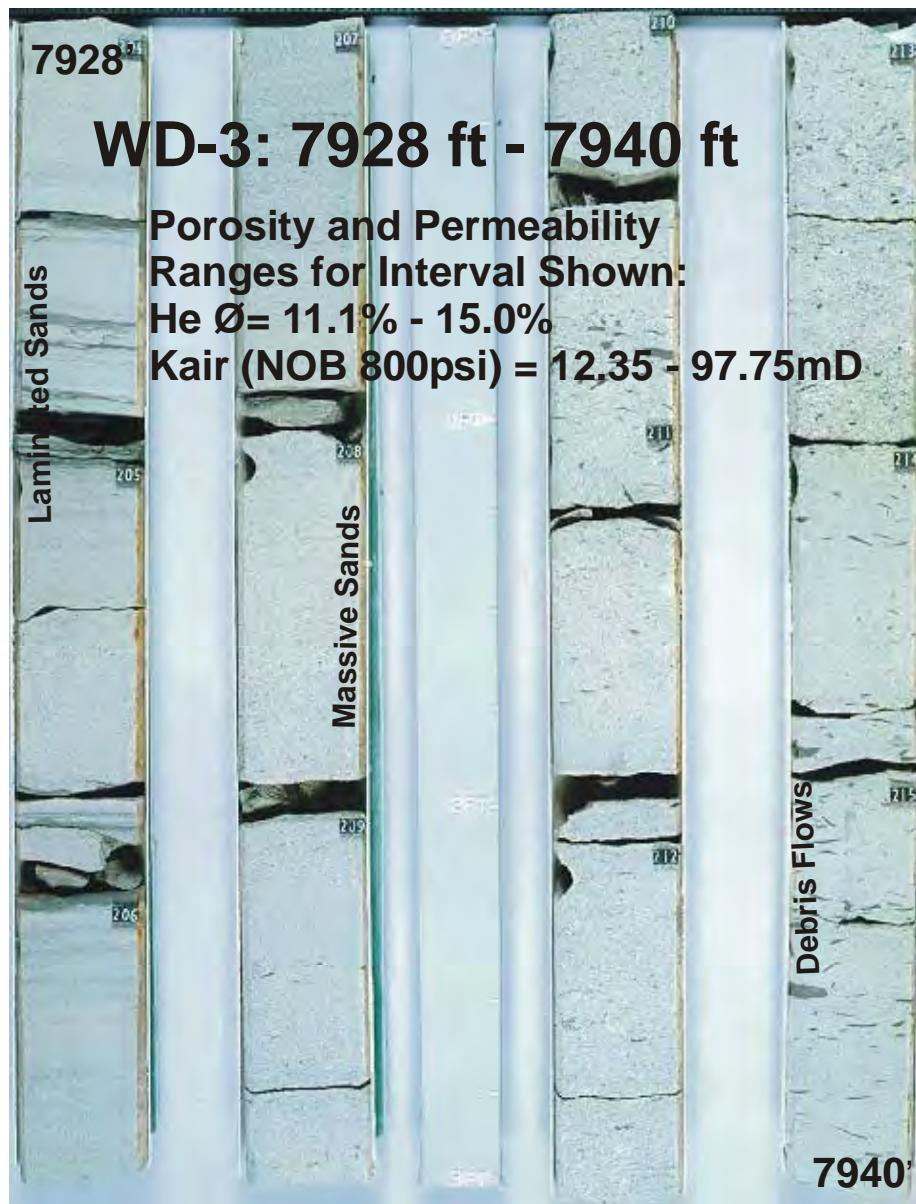


Figure 5.24: Core of a turbidite sandstone in the Late Paleocene ‘Mud-Prone Interval’ from the Wiriagar Deep #3 well. Minor rip-up clasts can be seen in an overall slightly graded series of cycles.



Figure 5.25: The outcropping Oligocene Limestone Formation, at the East Onin #1 (EO-1) well location, on the Bomberai Peninsula (south of Berau/Bintuni Bay). The fold exposed is near the axial crest of the Kumawa-Onin-Misool compressional structure (known as both the KOM or MOK ridge). The KOM Bomberai Peninsula forms the 'lower jaw' of the Bird's Head, and parallels the Banda Arc curvature offshore to the SW, separating the Arafura Sea from Berau/Bintuni Bay. Oligocene dating was done via palynofloral analysis (Dr P. Waton, personal communication, 1994) at the request of the author. (Photo by J. Salo; *in* Salo, 1994).

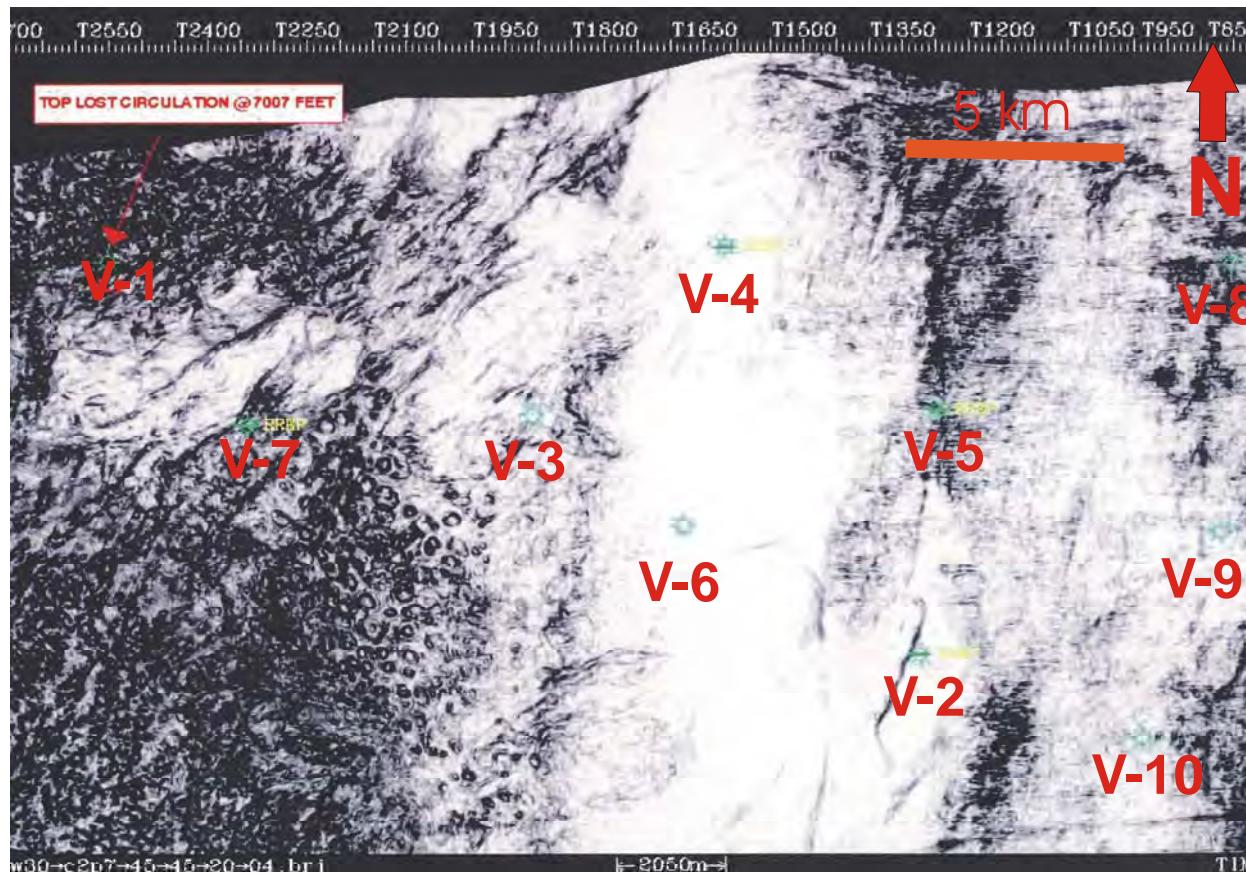


Figure 5.26: Coherency image slice from 3D seismic survey dataset, at 1632 ms TWT, clearly showing the faulted/fractured and vuggy nature of the Near-Top Faumai Formation, a member of the NGLG. Linaments striking N-S and NE-SW are interpreted as fractures/faults. Note the ‘sinkhole’ appearance and massive size of the dissolution cavities cluster in the lower left of the photo. The image covers the Vorwata anticline area with the Vorwata-1 well location noted on the top left of the image (modified from BP, 2002).

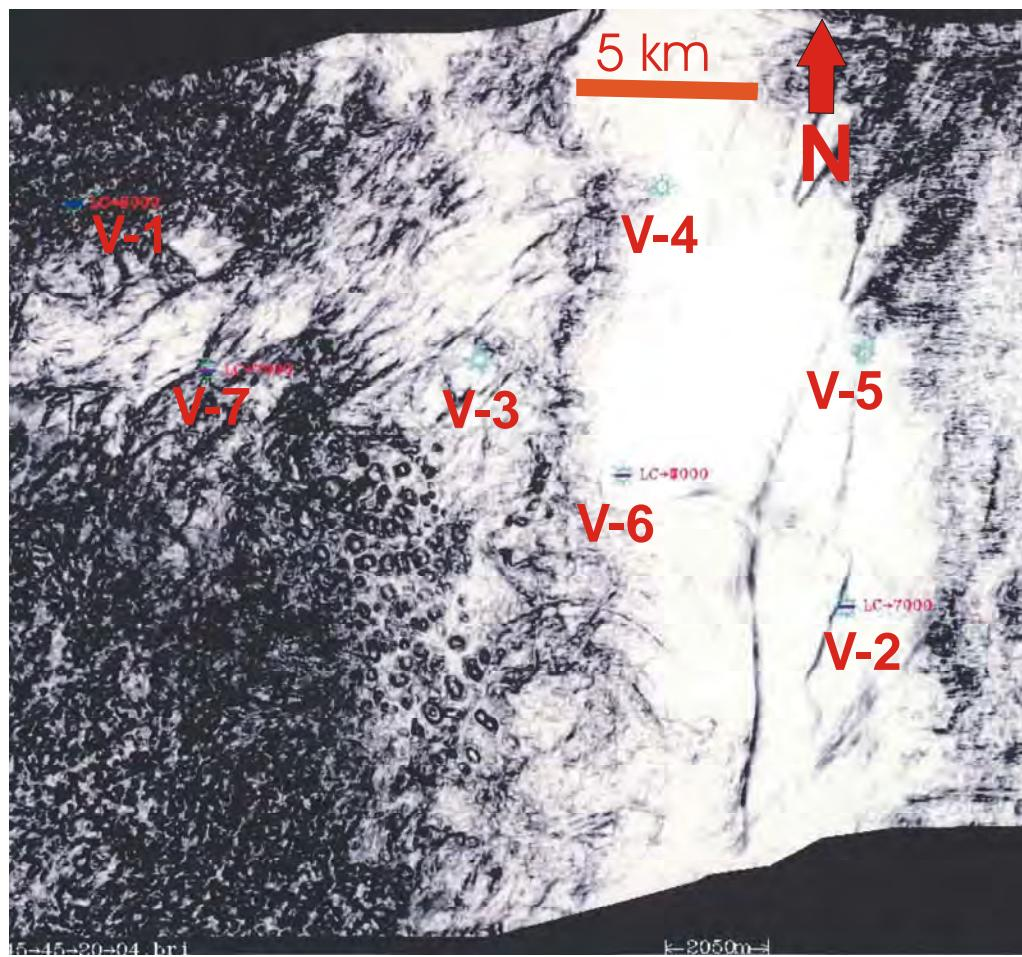


Figure 5.27: Coherency image slice from 3D seismic survey dataset, at 1660 ms, clearly showing major fractures/faults and dissolution cavities near the top of the Faumai Formation over the western two-thirds of the Vorwata anticline. Note the large uninterpreted circular feature just south of the V-6 well location (modified from BP, 2002).

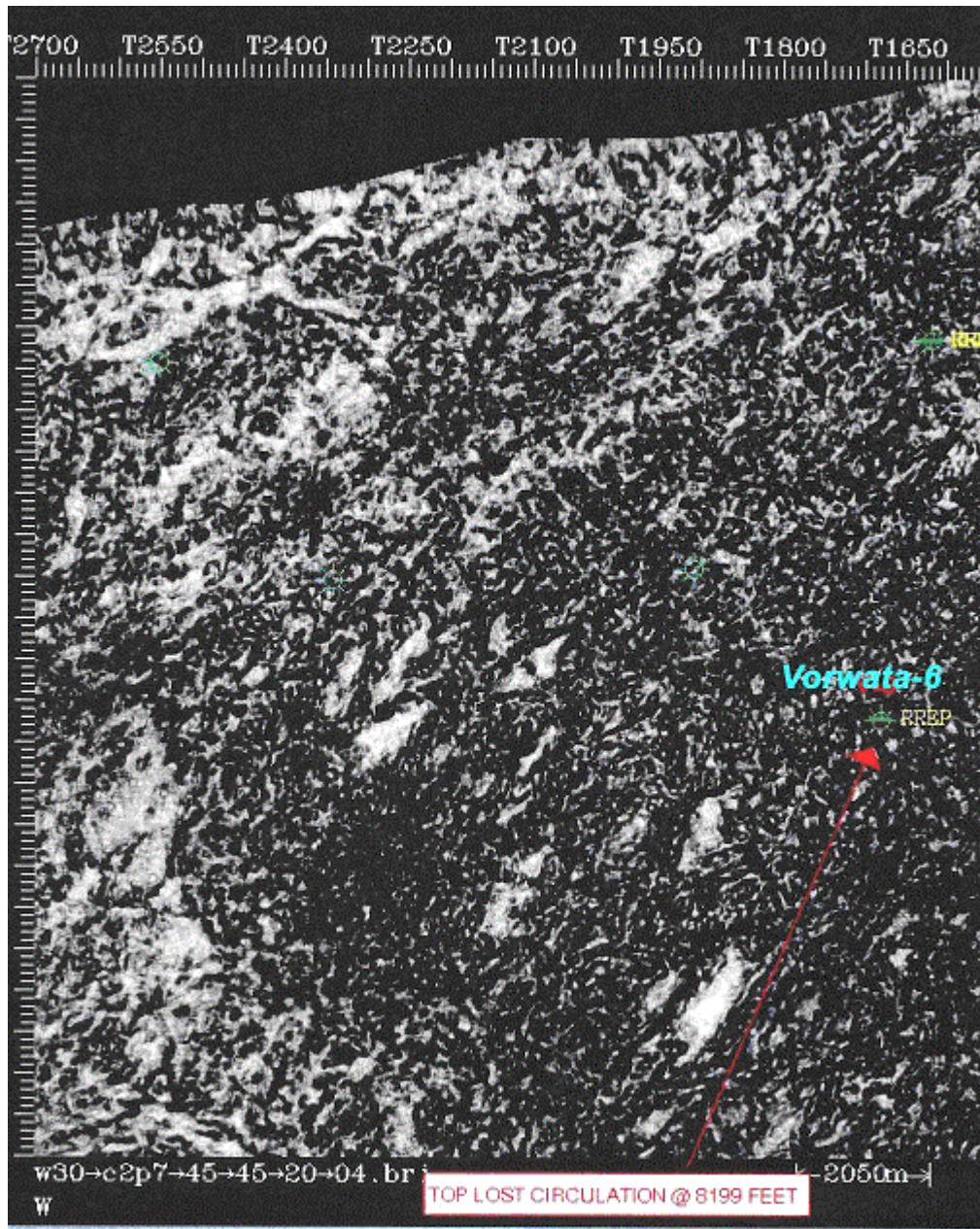


Figure 5.28: Coherency image slice from 3D seismic survey dataset, at 1892 ms, showing the massive vuggy nature of the middle Faumai Formation over the western half of the Vorwata anticline. Note the Vorwata-6 well, on right side of image, lost total circulation in this interval, at 8199 ft driller's measured depth, whilst drilling. Most Vorwata wells had lost total circulation by this depth equivalent due to the vugs and fractures in the Faumai Formation (modified from BP, 2002).

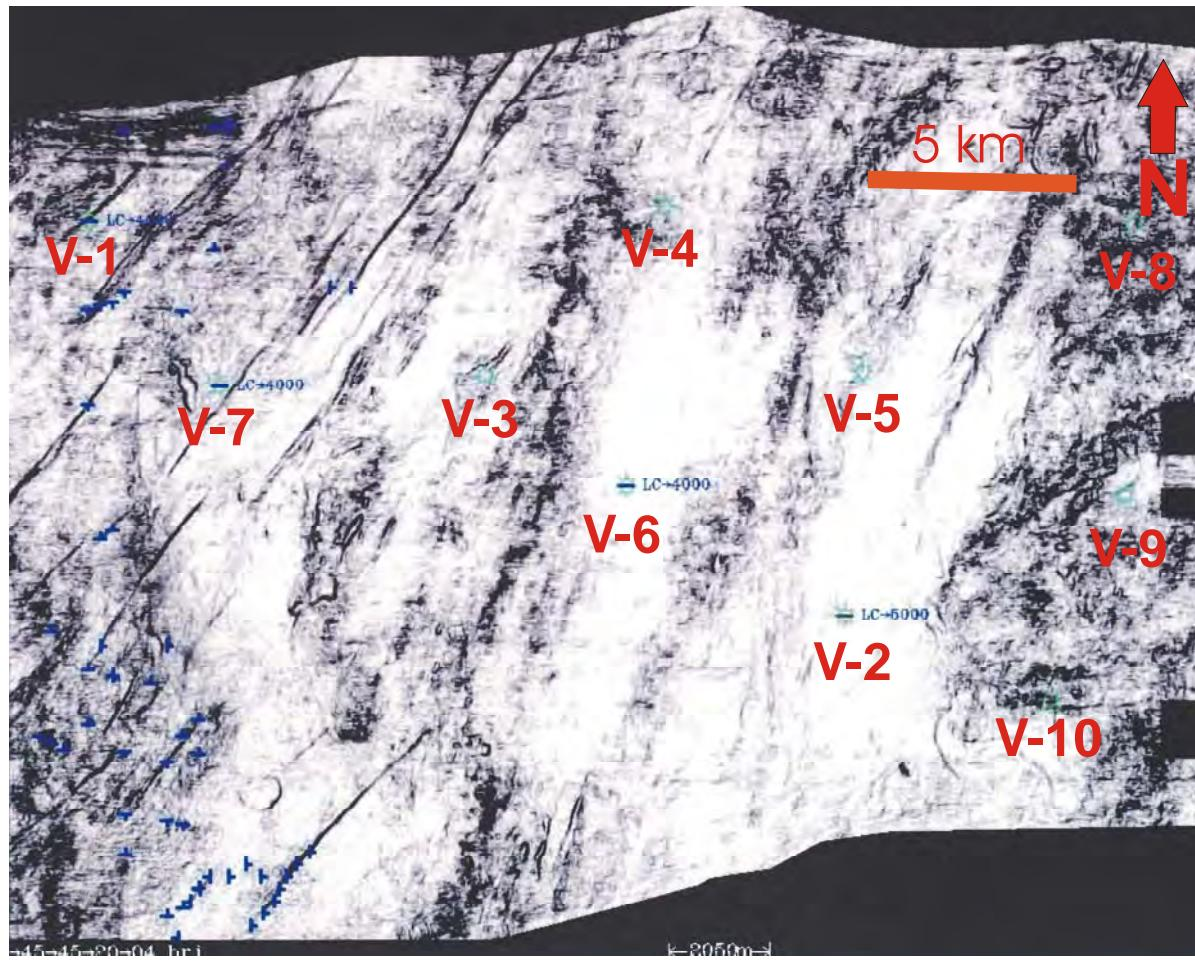


Figure 5.29: Coherency image of middle Kais Formation, at 1200 ms over the Vorwata anticline. Interpretation of the coherency image includes a major series of SW-NE trending fractures present, as well as dissolution vugs and cavities south of the V-7 and V-3 well locations (modified from BP, 2002).

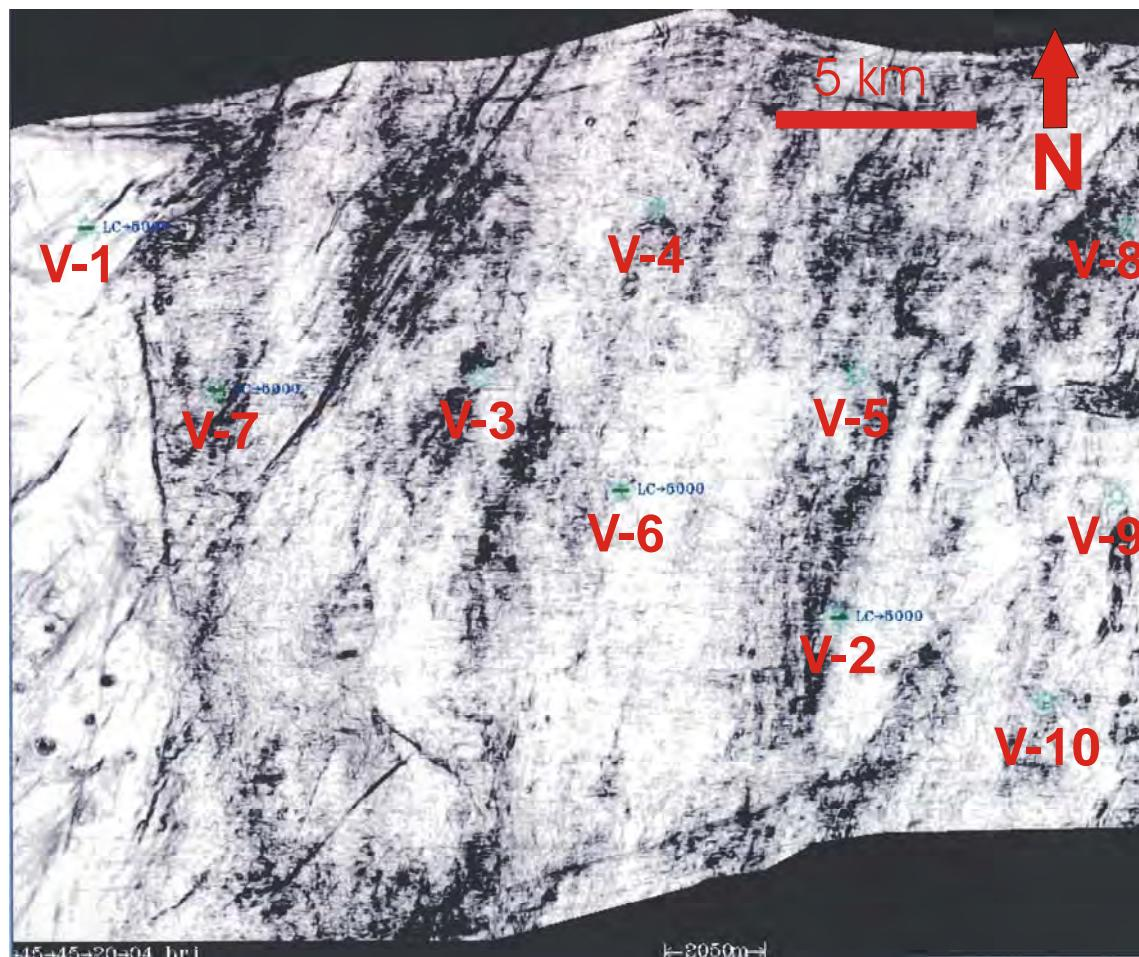


Figure 5.30: Coherency image of middle Kais Formation, at 1320 ms over the Vorwata anticline. This time slice is in the basal portion of the Kais Limestone Formation, and fracture systems and dissolution vugs are more prominent (modified from BP, 2002).

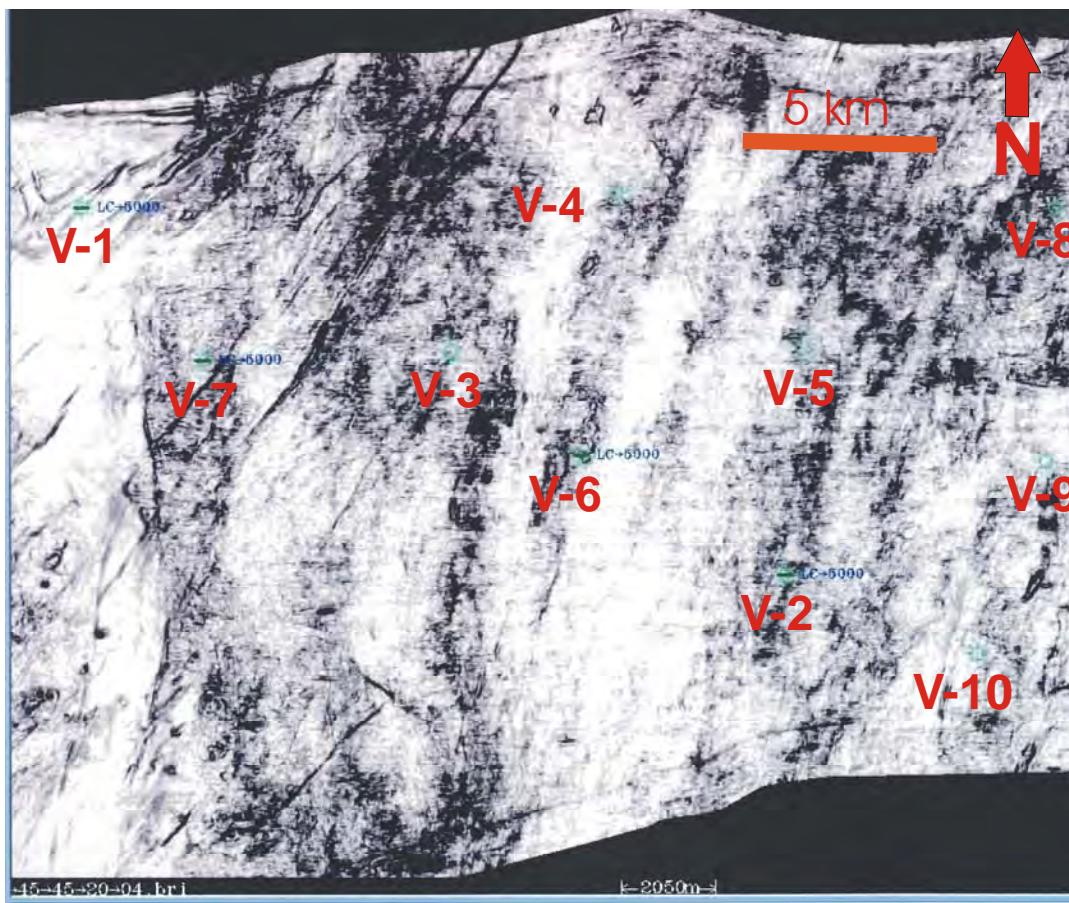


Figure 5.31: Coherency image of middle Kais Formation, at 1340 ms over the Vorwata anticline. The image shown is at the near-base of the Kais Formation and shows extensive fractures and cavities in the limestone lithostratigraphic unit (modified from BP, 2002).

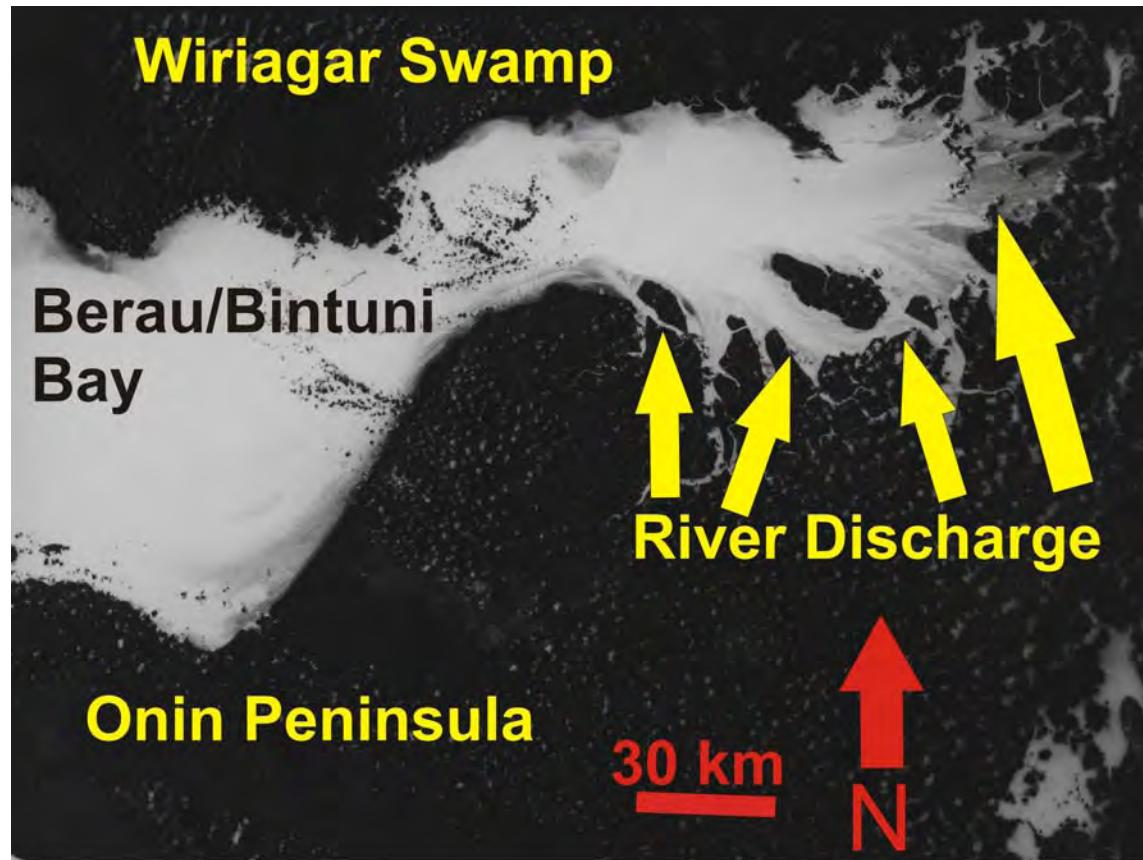


Figure 5.32: LANDSAT image, presented as a negative image, of Berau/Bintuni Bay showing massive sediment discharge from adjacent rivers. The LANDSAT satellite photograph was taken on January 22nd, 1979 with an estimated 40% cloud cover over the region. (NASA/EROS, 1979).



Figure 5.33: Wiriagar Swamp, the largest mangrove swamp in the world, as seen from the air. Meandering river system with oxbow lakes shown is the Wiriagar River (photo by J. Marcou, 1995).

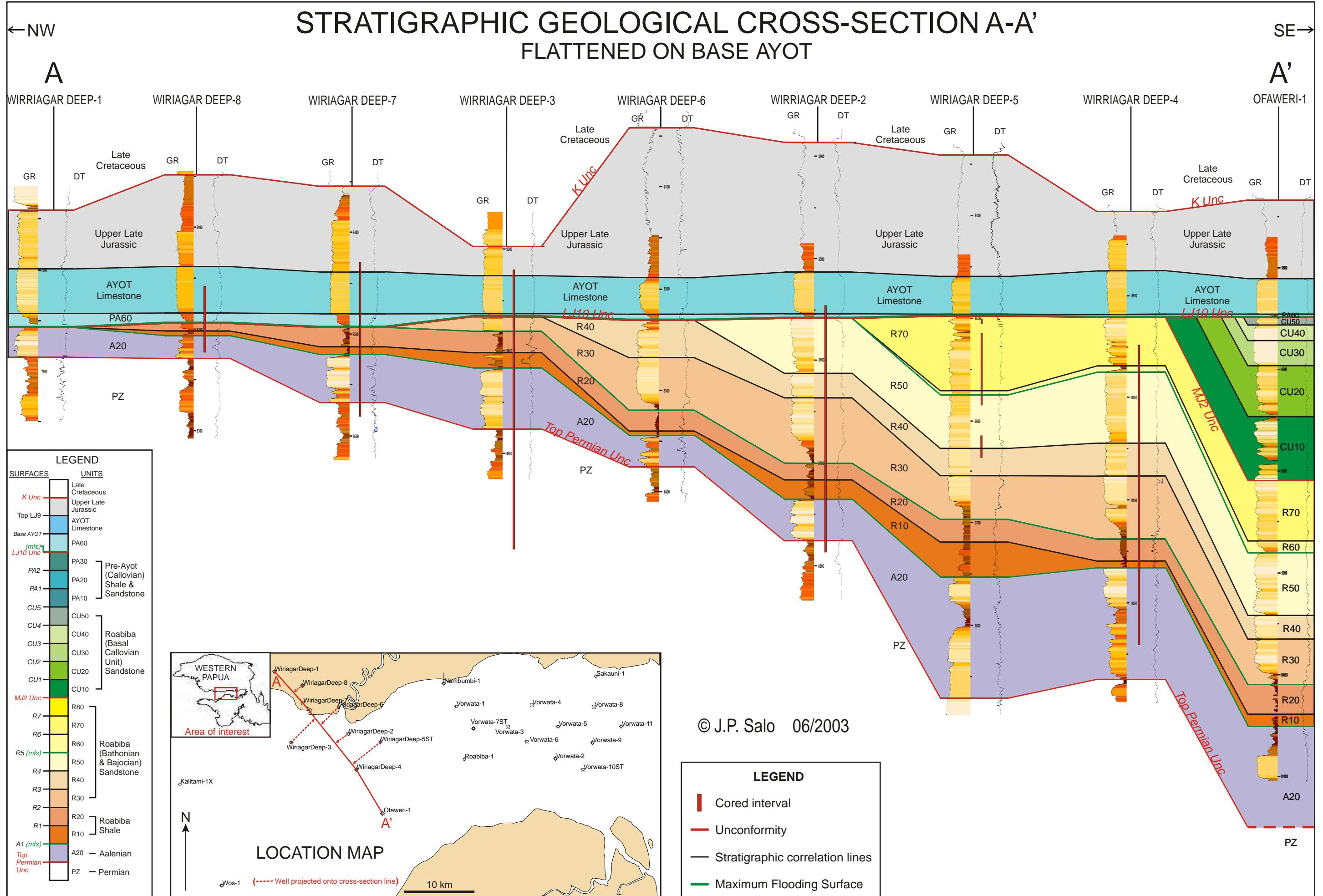


Figure 6.1: Stratigraphic cross-section NW-SE through the Mesozoic interval at Wiriagar Deep area.

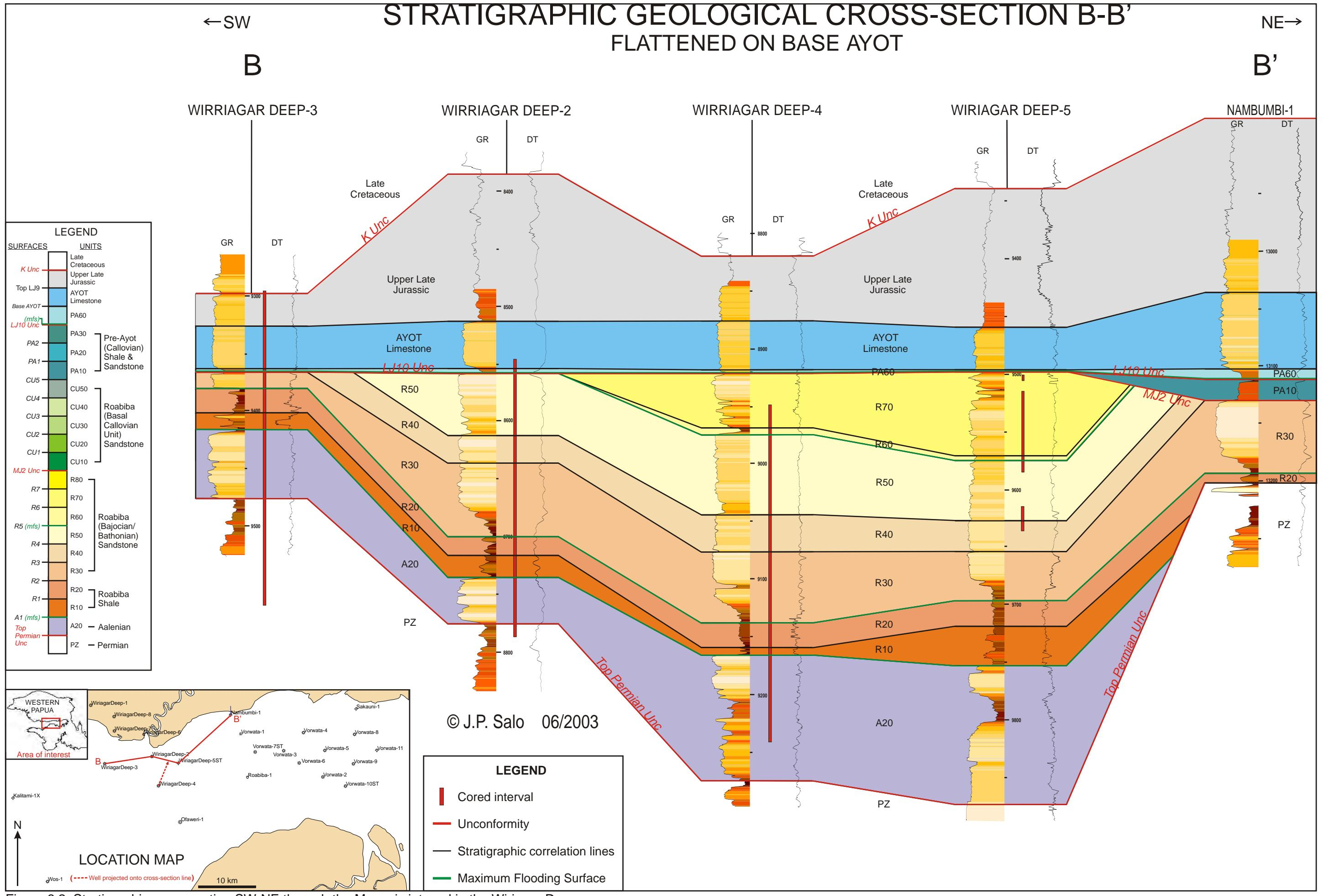


Figure 6.2: Stratigraphic cross-section SW-NE through the Meozoic interval in the Wiriagar Deep area.

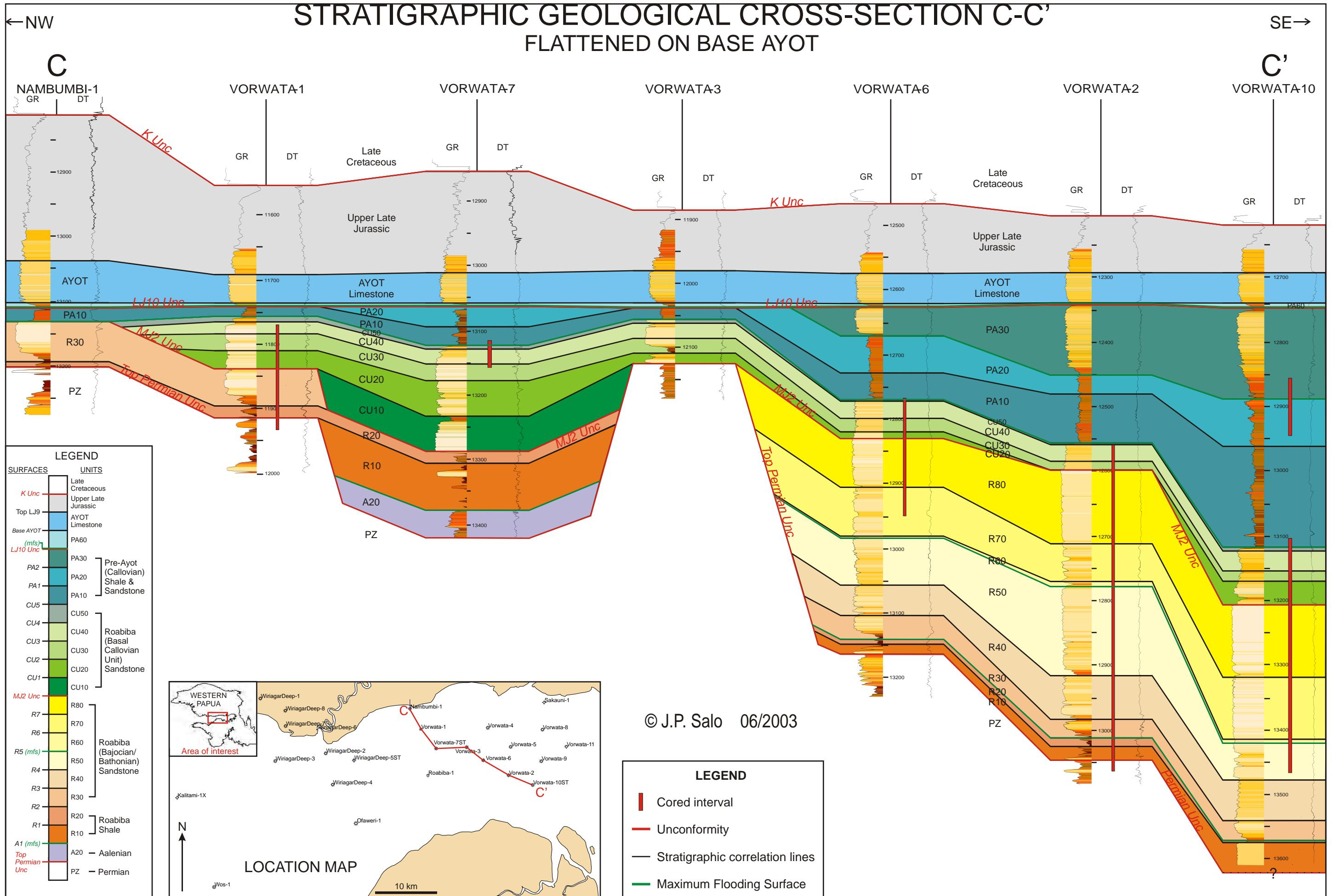


Figure 6.3: Stratigraphic cross-section NW-SE through the Mesozoic interval at the Vorwata area.

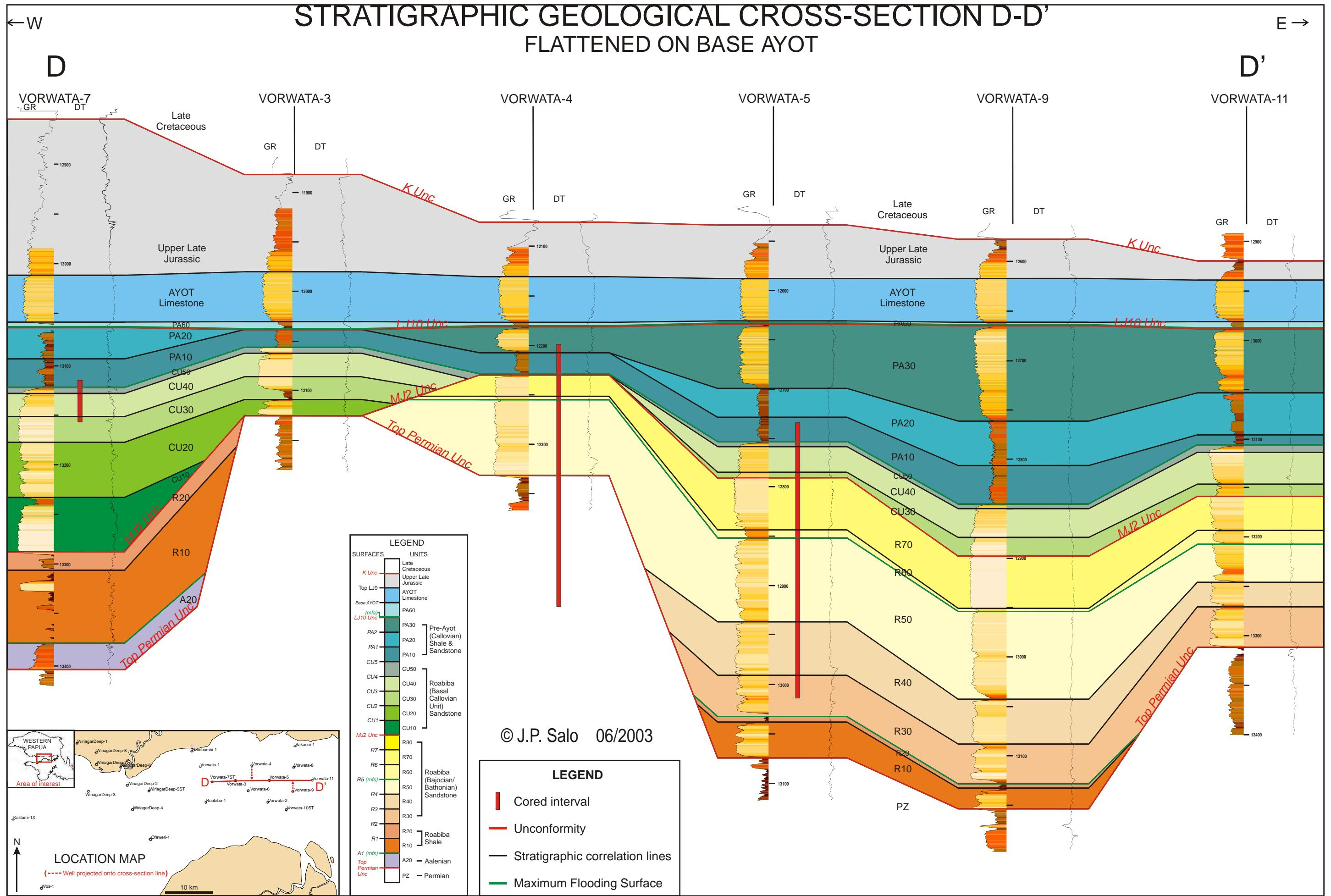


Figure 6.4: Stratigraphic cross-section W-E through the Mesozoic interval at the Vorwata area.

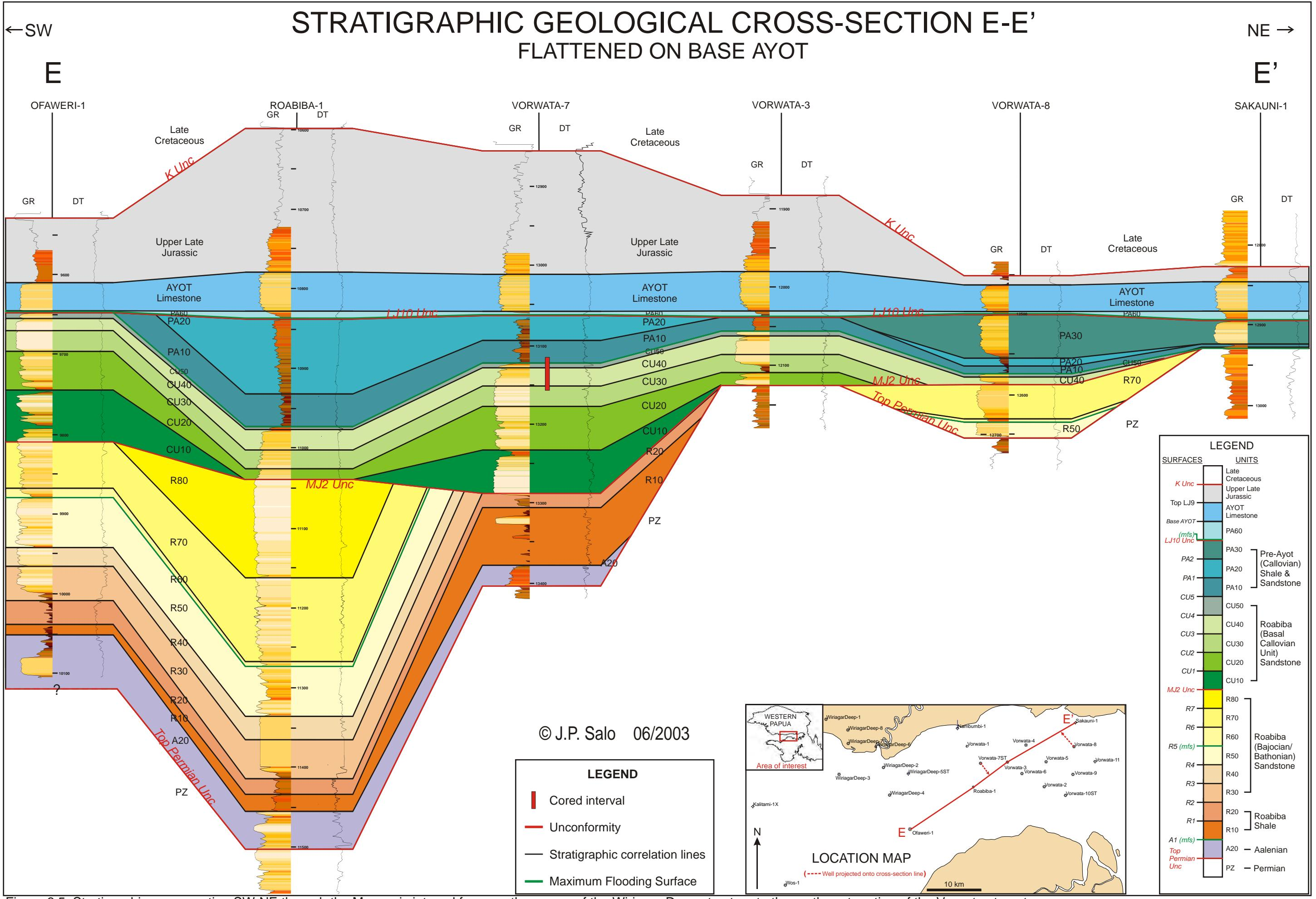


Figure 6.5: Stratigraphic cross-section SW-NE through the Mesozoic interval from southern area of the Wiriagar Deep structure to the northwest portion of the Vorwata structure.

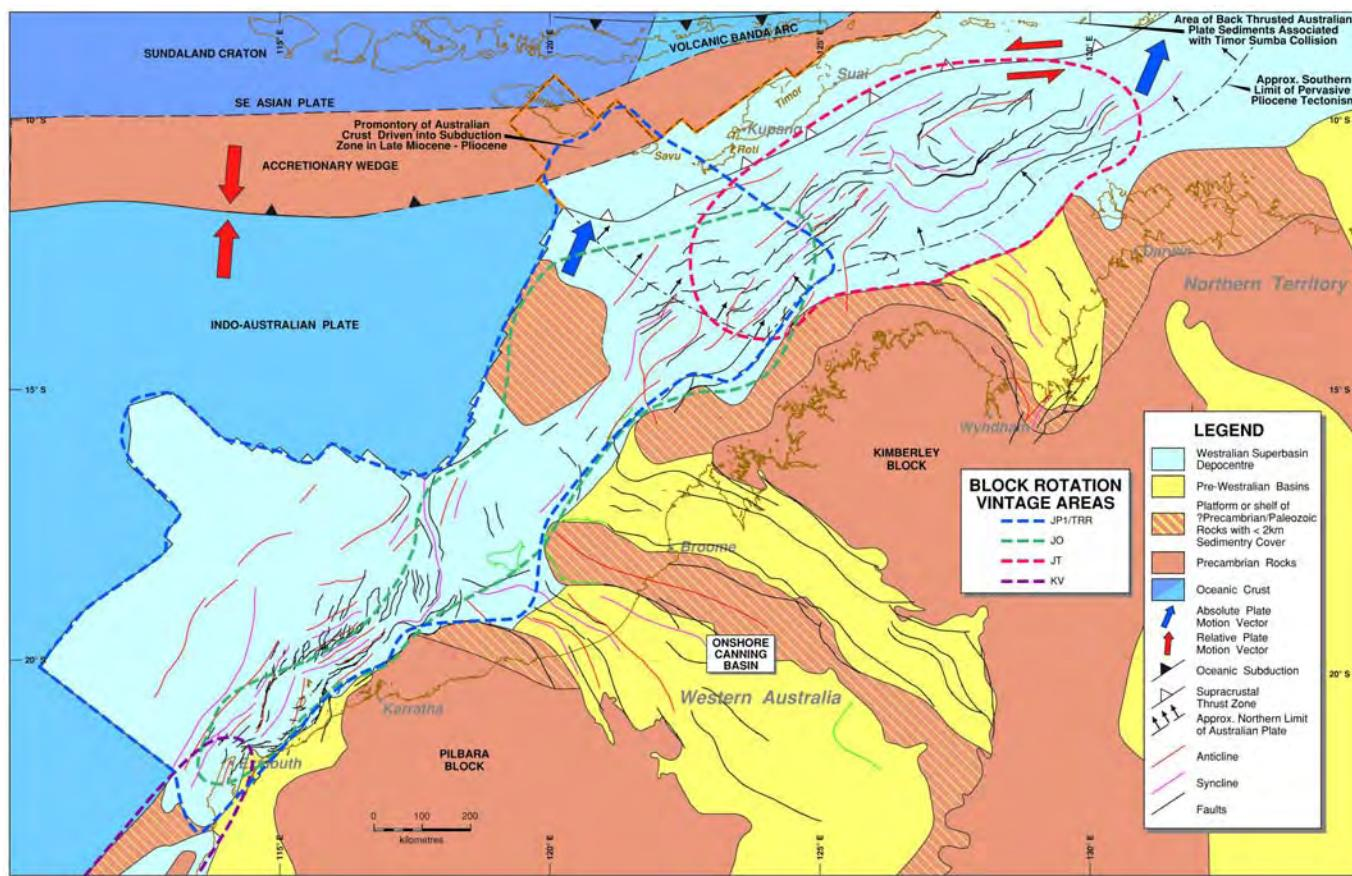


Figure 6.6: Extensional rifting of microplates and blocks from the NW Shelf margin of the ANGP margin during the Mesozoic. JP/TRR is Jurassic (Pliensbachian)/Triassic (Rhaetian); JO is Jurassic (Oxfordian); JT is Jurassic (Tithonian); and KV is Cretaceous (Valanginian) (Longley, et al., 2002; modified after Bradshaw, et al., 1994b).

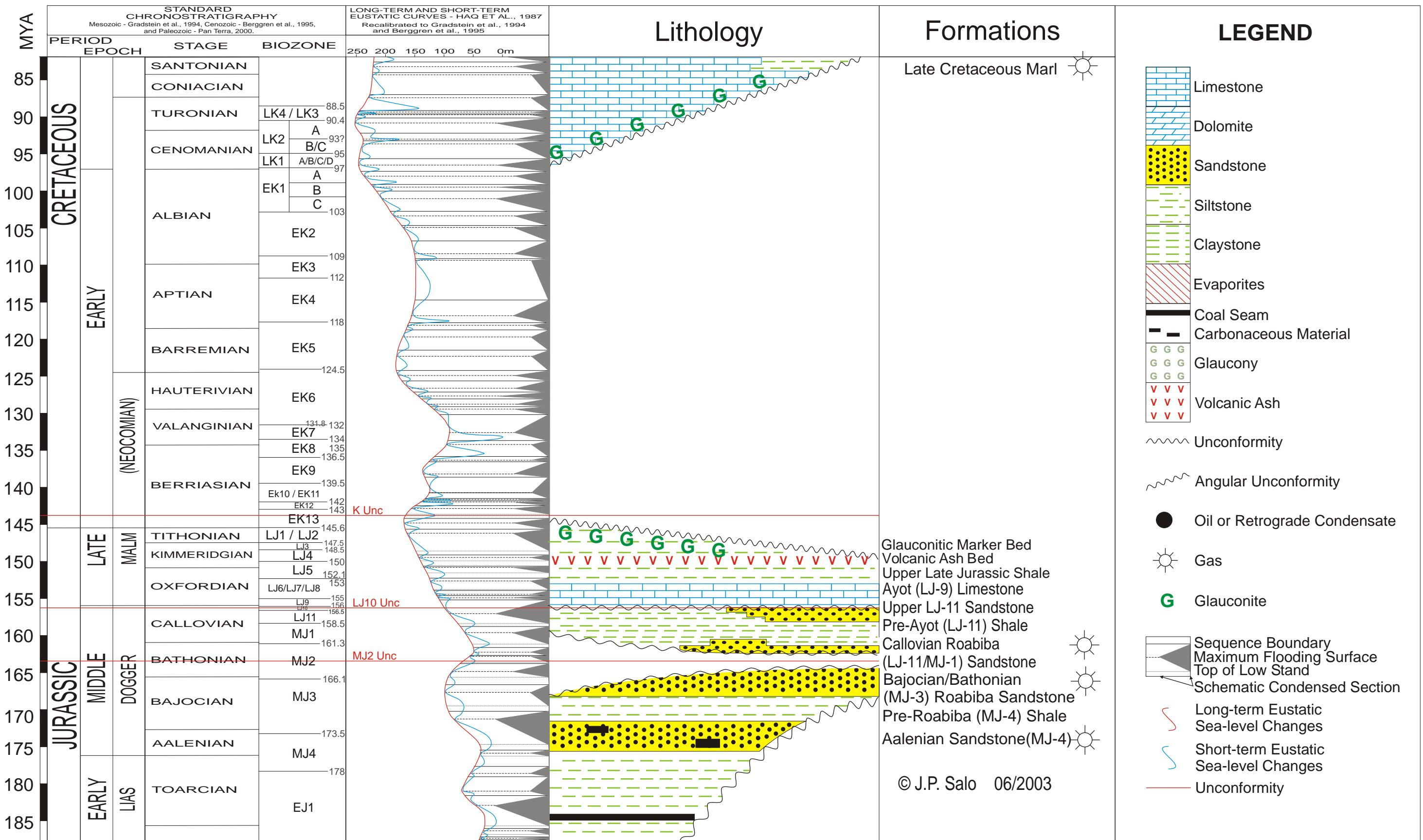


Figure 6.7: General stratigraphic column of the Mesozoic interval in the Berau/Bintuni Basins area.

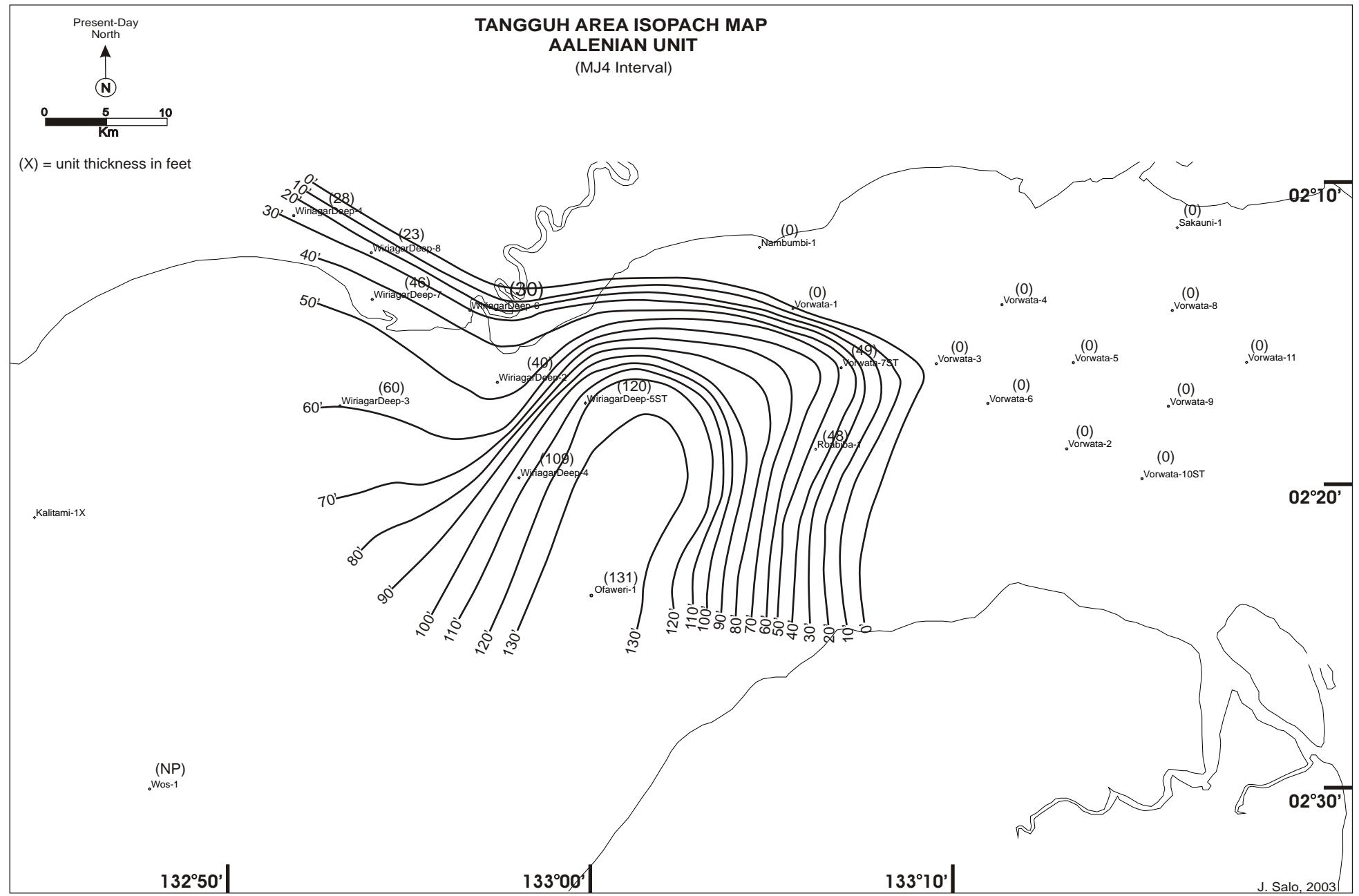


Figure 6.8: Isopach of the Aalenian A20 zone at Tangguh. Onlapping paleo-deposition appears to be due to a marine transgression.

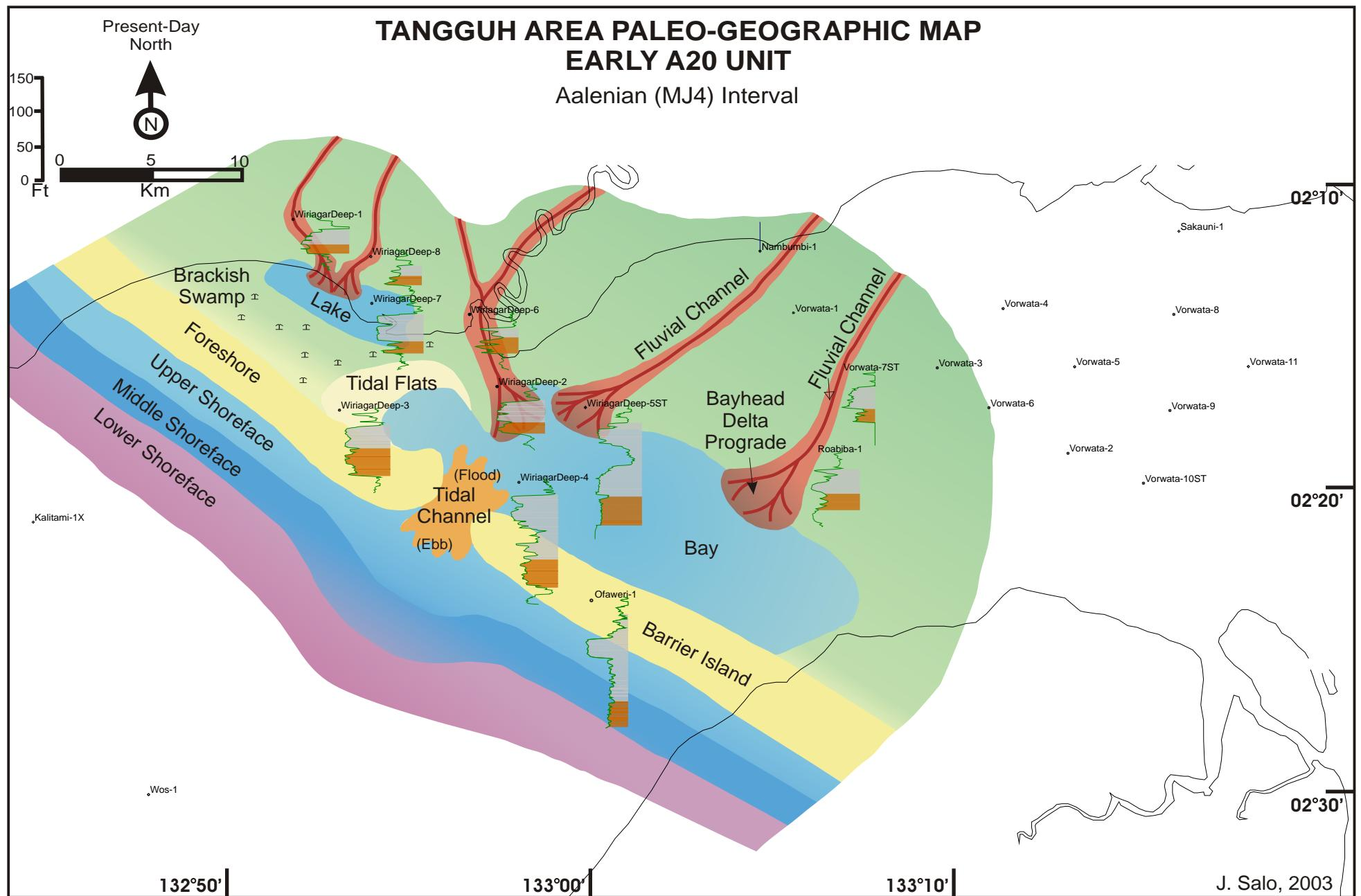


Figure 6.9: Paleogeographic map of depositional facies during the Early Aalenian (Early A20). Marine transgression appears to initiate from the SW.

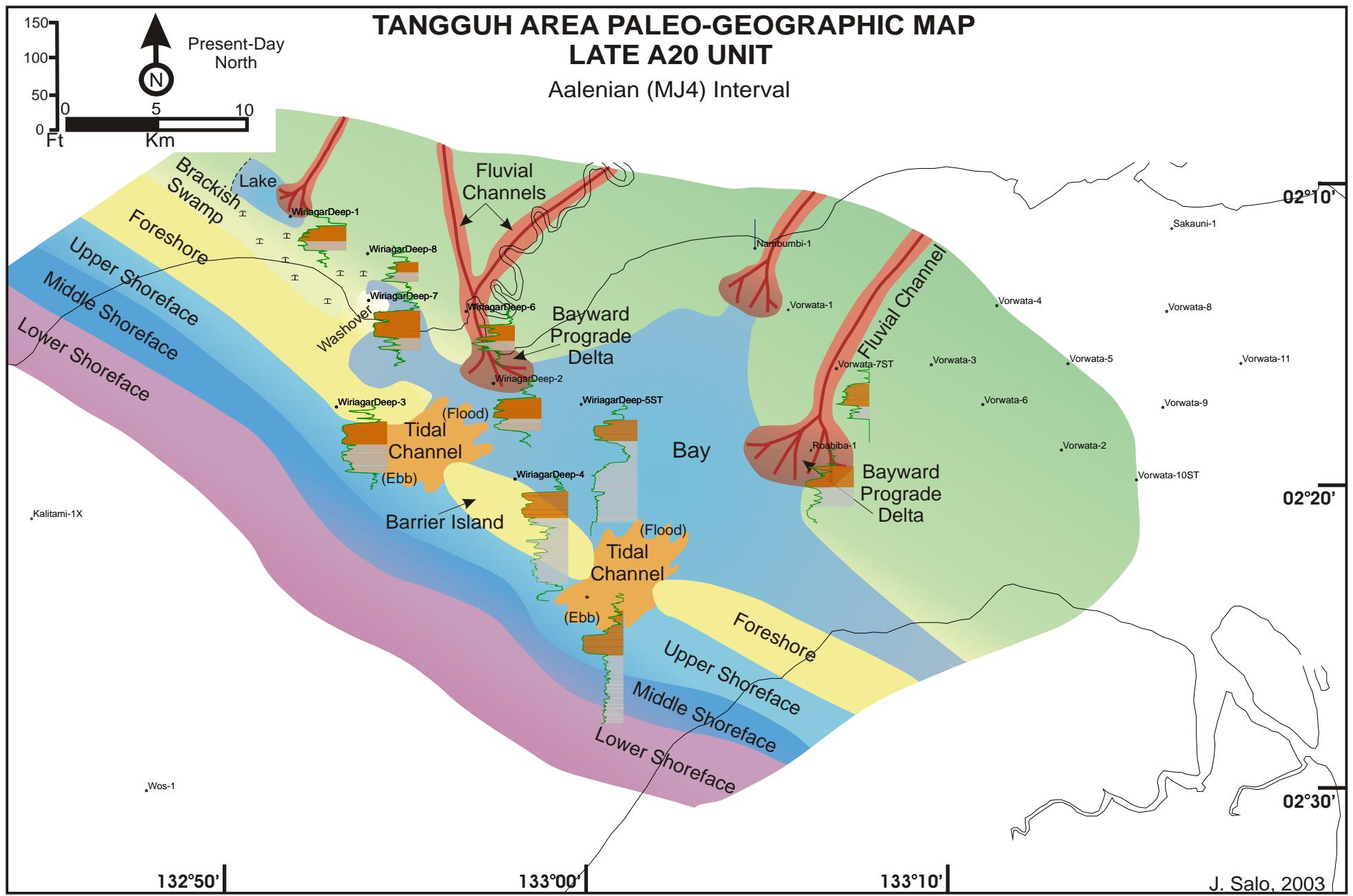


Figure 6.10: Paleogeographic map of depositional facies during the Late A20 Aalenian at Tangguh. Paleo-coastline is oriented present-day NW-SE.

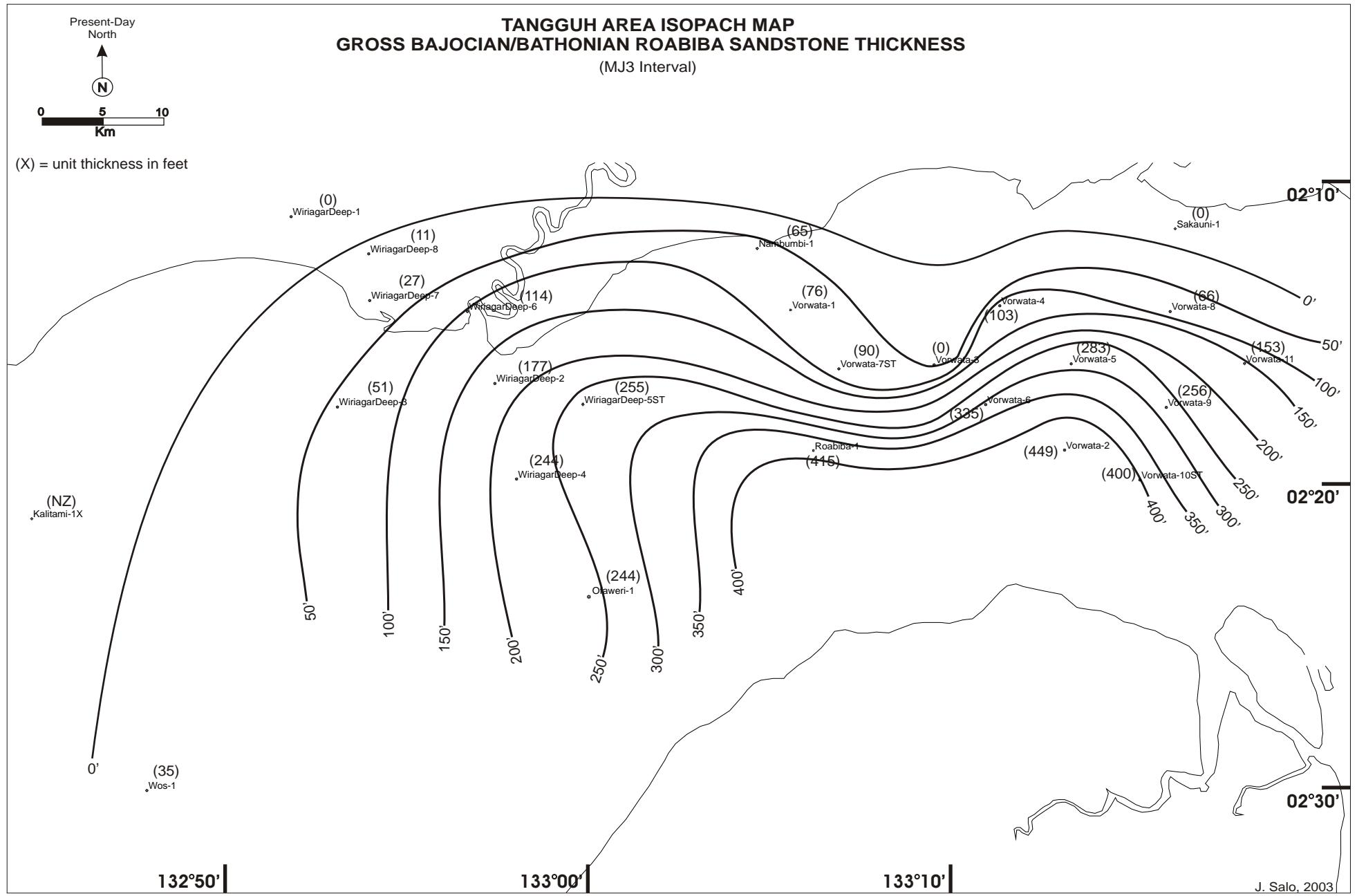


Figure 6.11: Gross isopach of the Bajocian/Bathonian Roabiba sandstone sequence. An unconformity has eroded the Roabiba over Wiriagar Deep

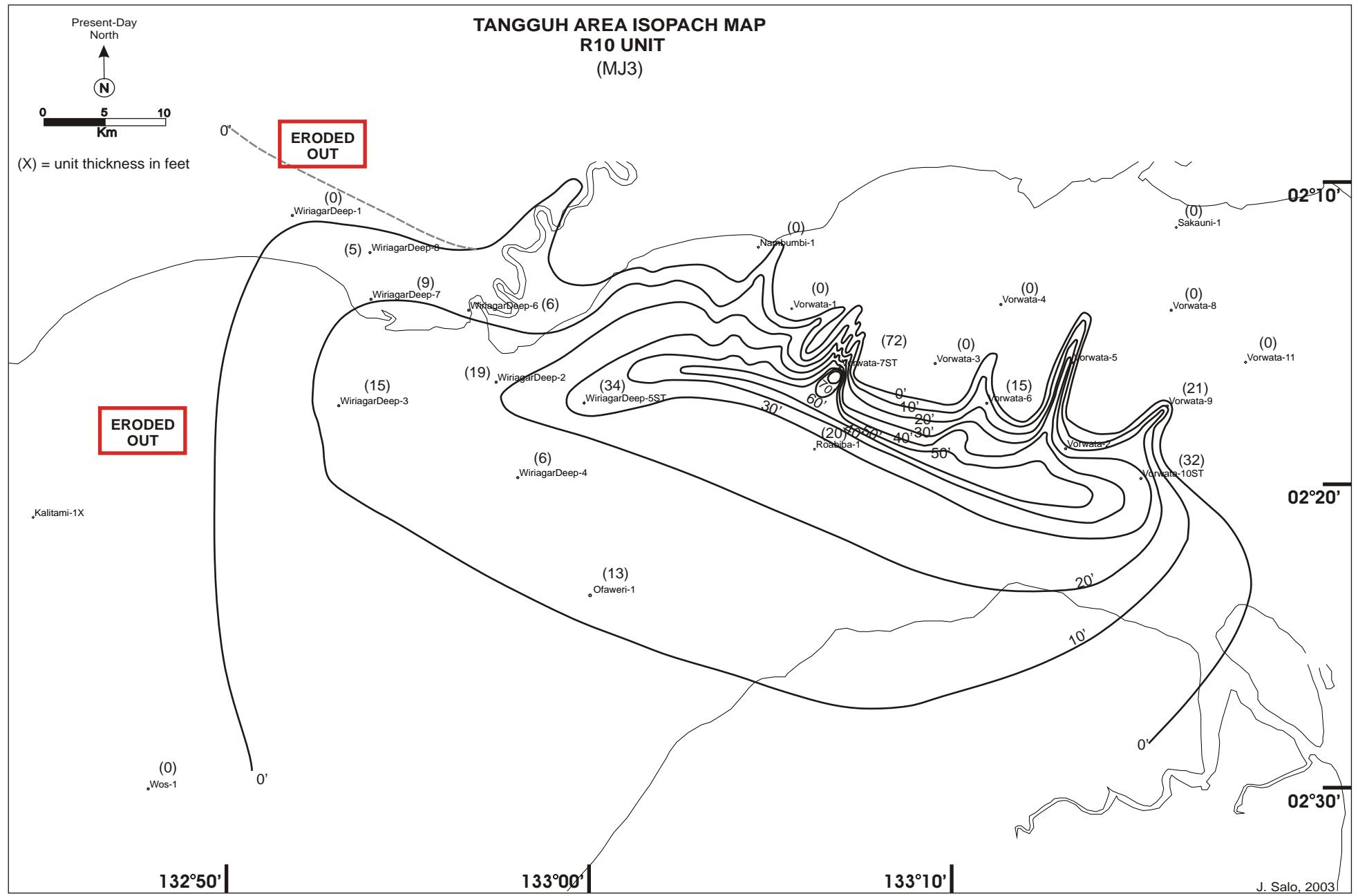


Figure 6.12: Isopach of the R10 zone at Tangguh. CI = 10 ft.

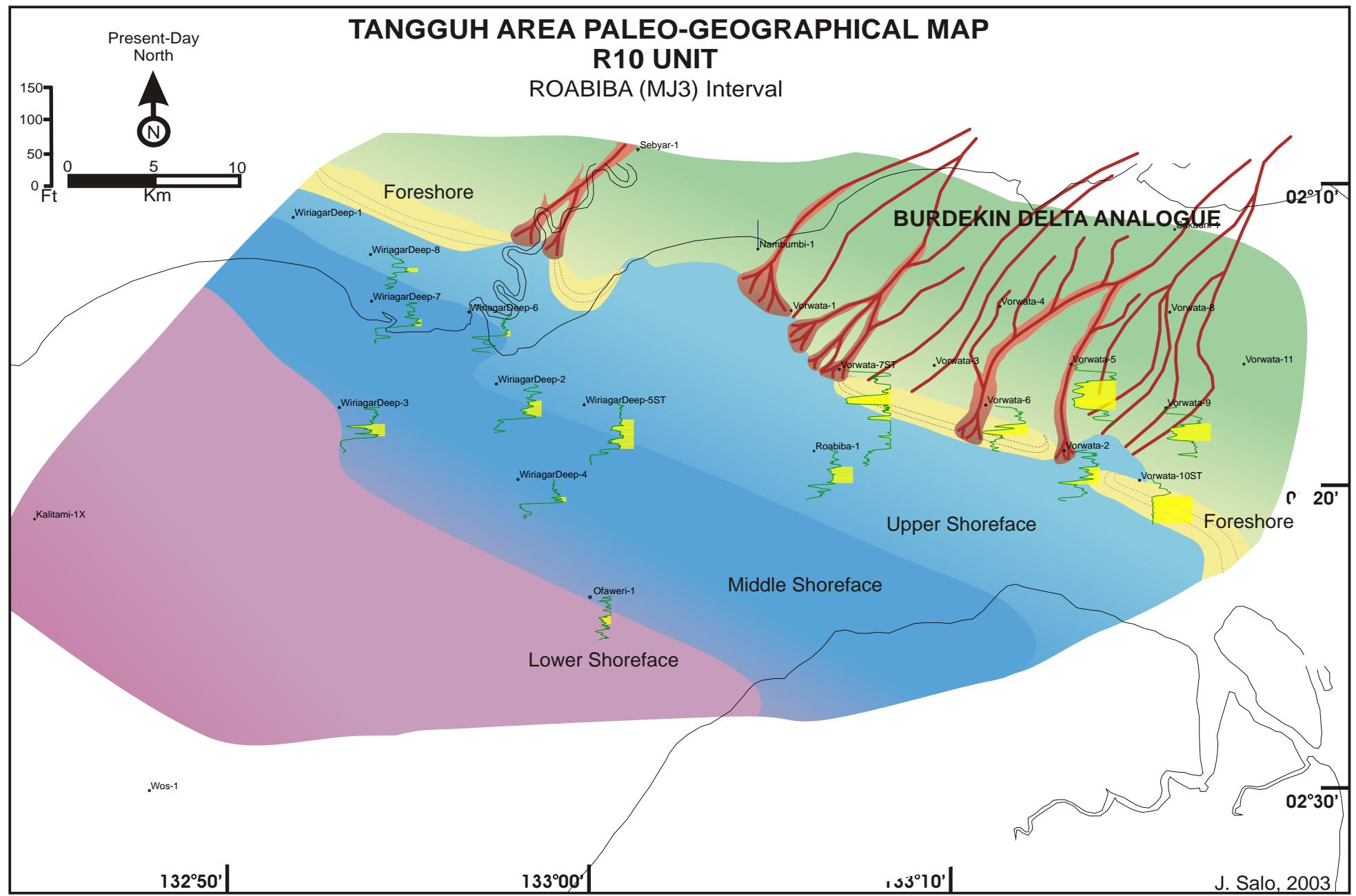


Figure 6.13: Paleogeographic map of depositional facies of the R10 zone at Tangguh. Fluvio-deltaic sediments at Vorwata.

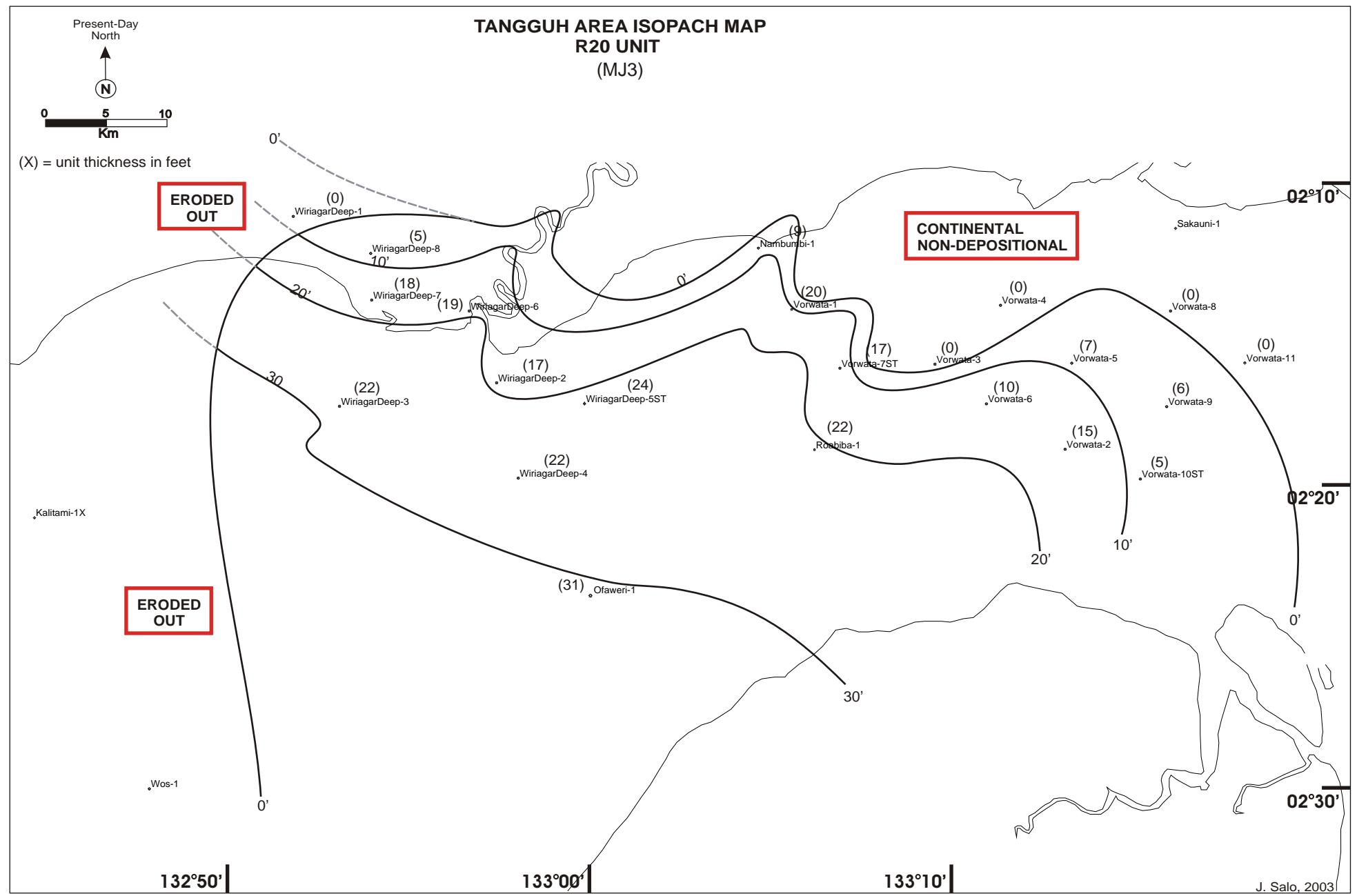


Figure 6.14: Isopach of the R20 zone at Tangguh. Erosion is due to uplift along the N-S Sekak Ridge (west of Kalitami-1X), and E-W Kemum High.

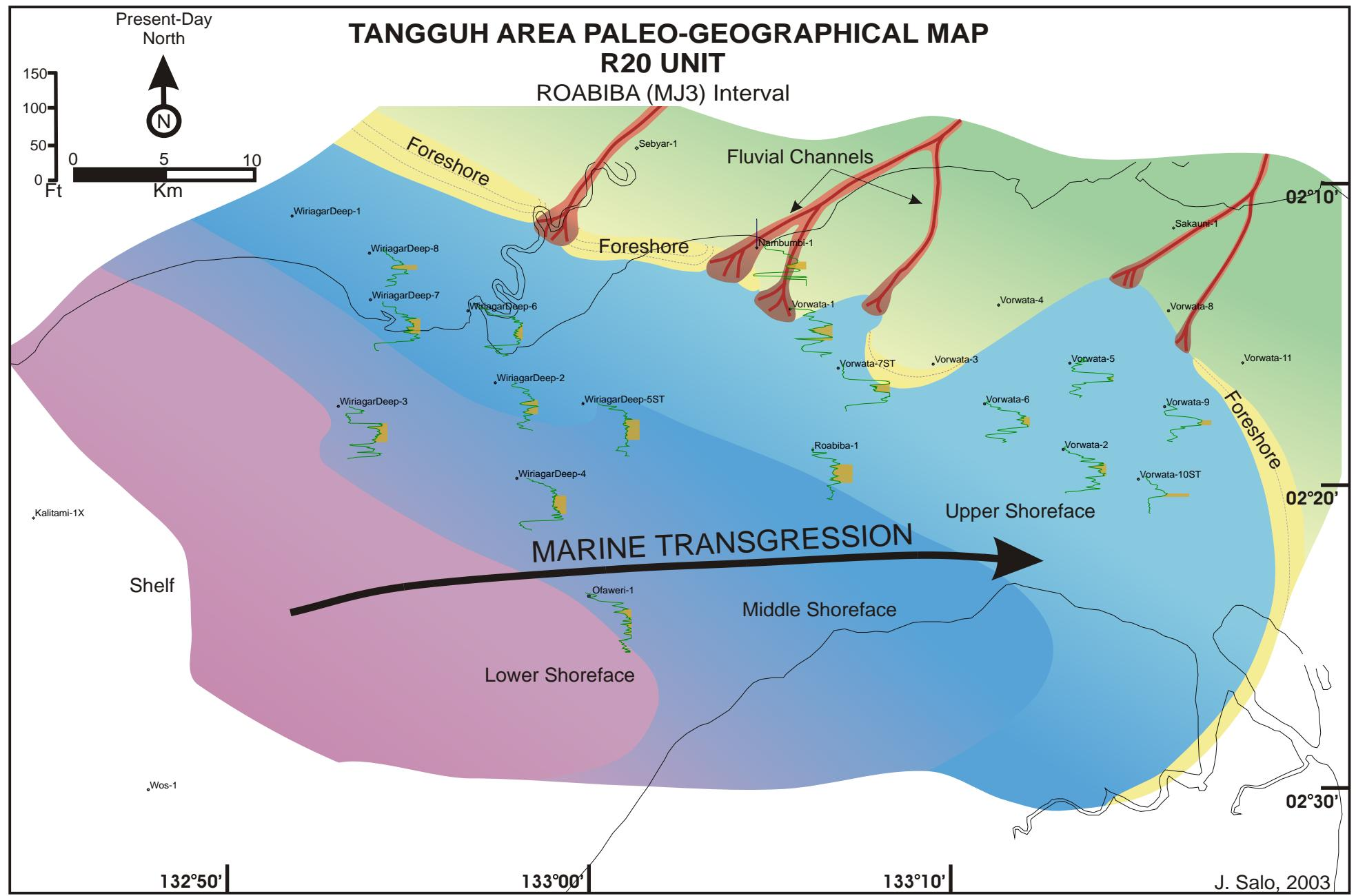


Figure 6.15: Paleogeographic map of R20 facies during the Bajocian/Bathonian. Most of the Wiriagar Deep and Vorwata area is marine.

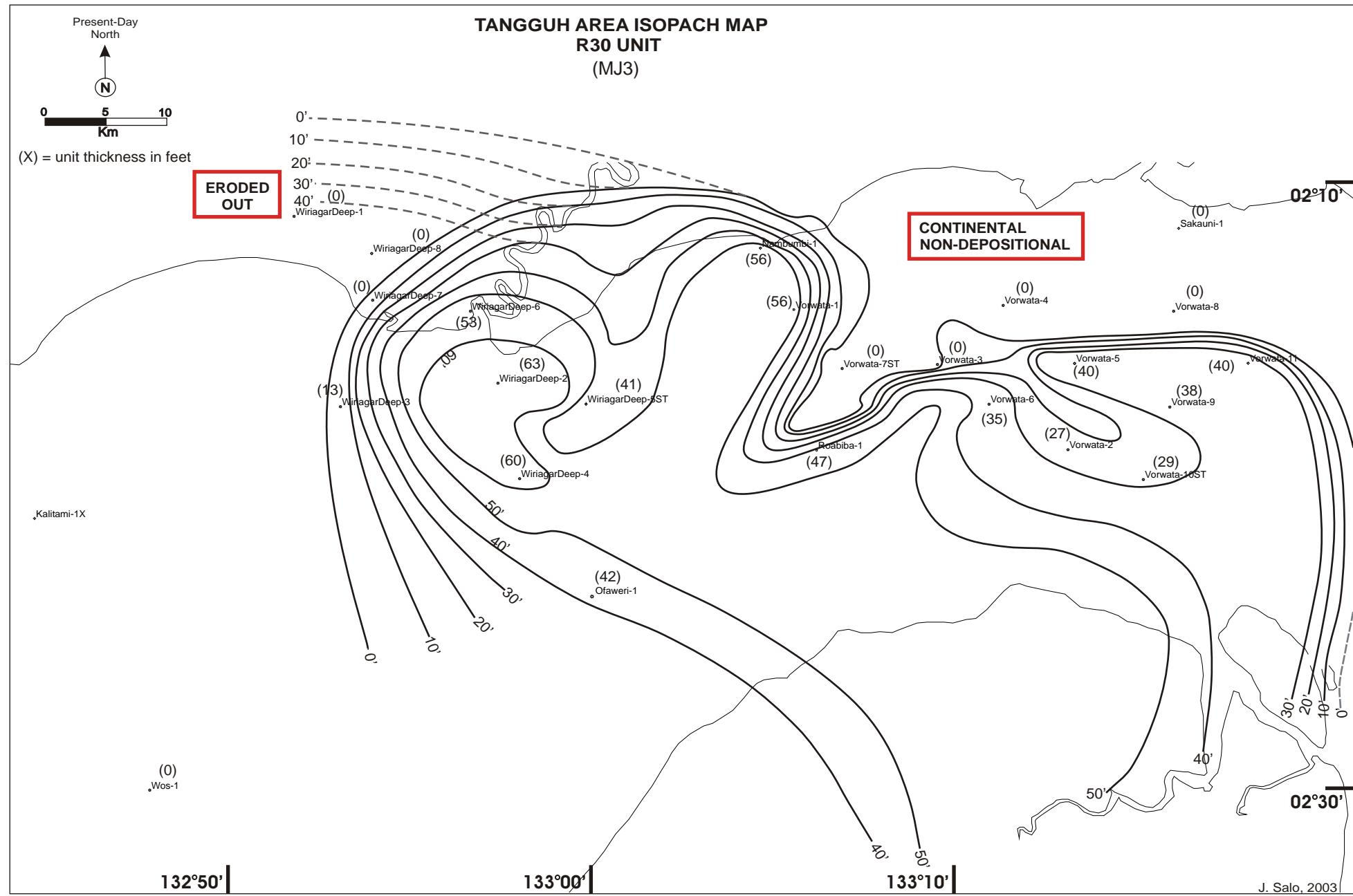


Figure 6.16: Isopach of the R30 zone at Tangguh. CI=10 ft. Present-day CI is shown with solid lines, conjectured paleo-CI's are indicated by dashed lines.

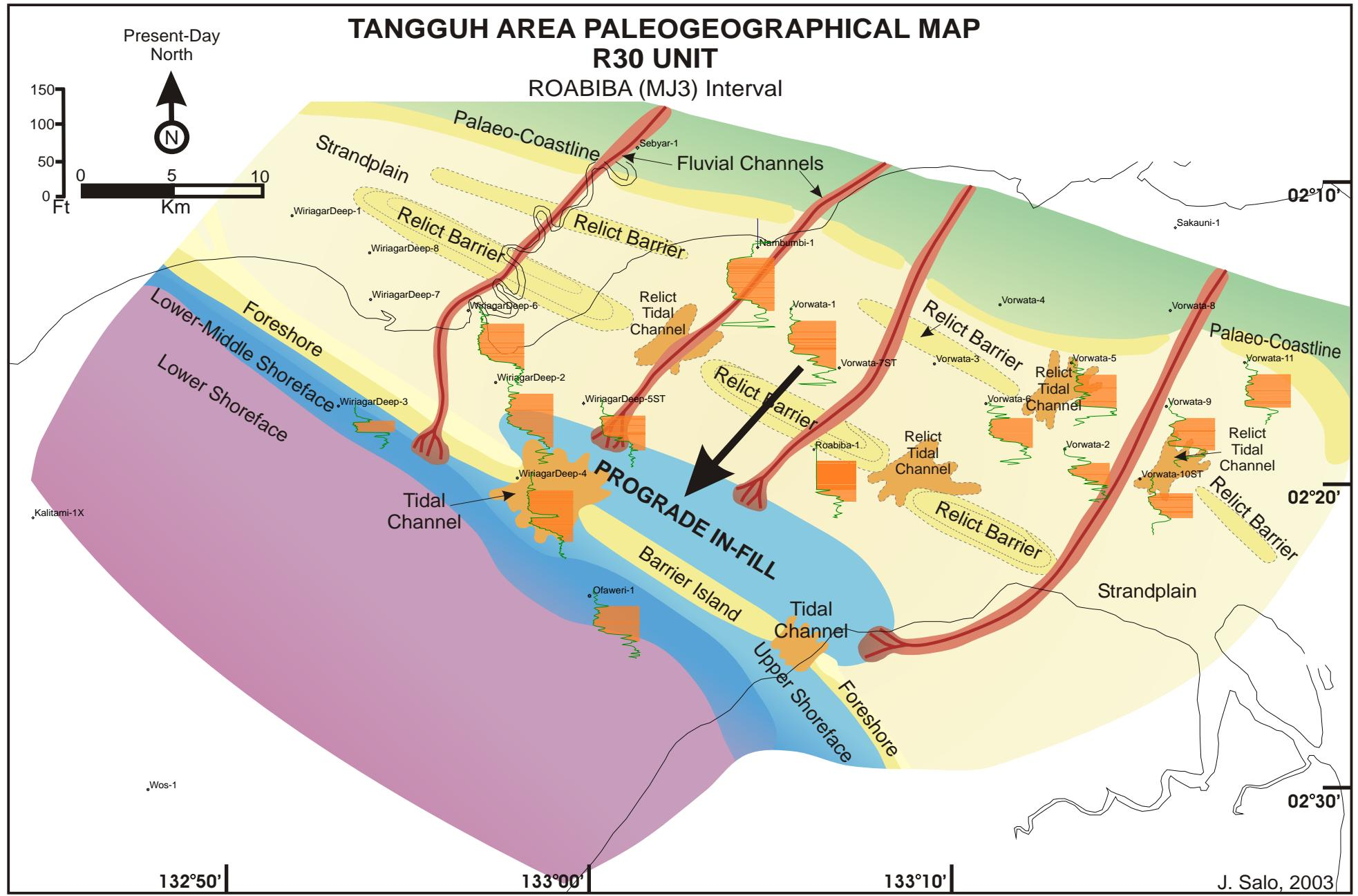


Figure 6.17: Paleogeographic map of R30 zone depositional facies. Prograding coastline indicates sediment supply is outpacing accommodation space.

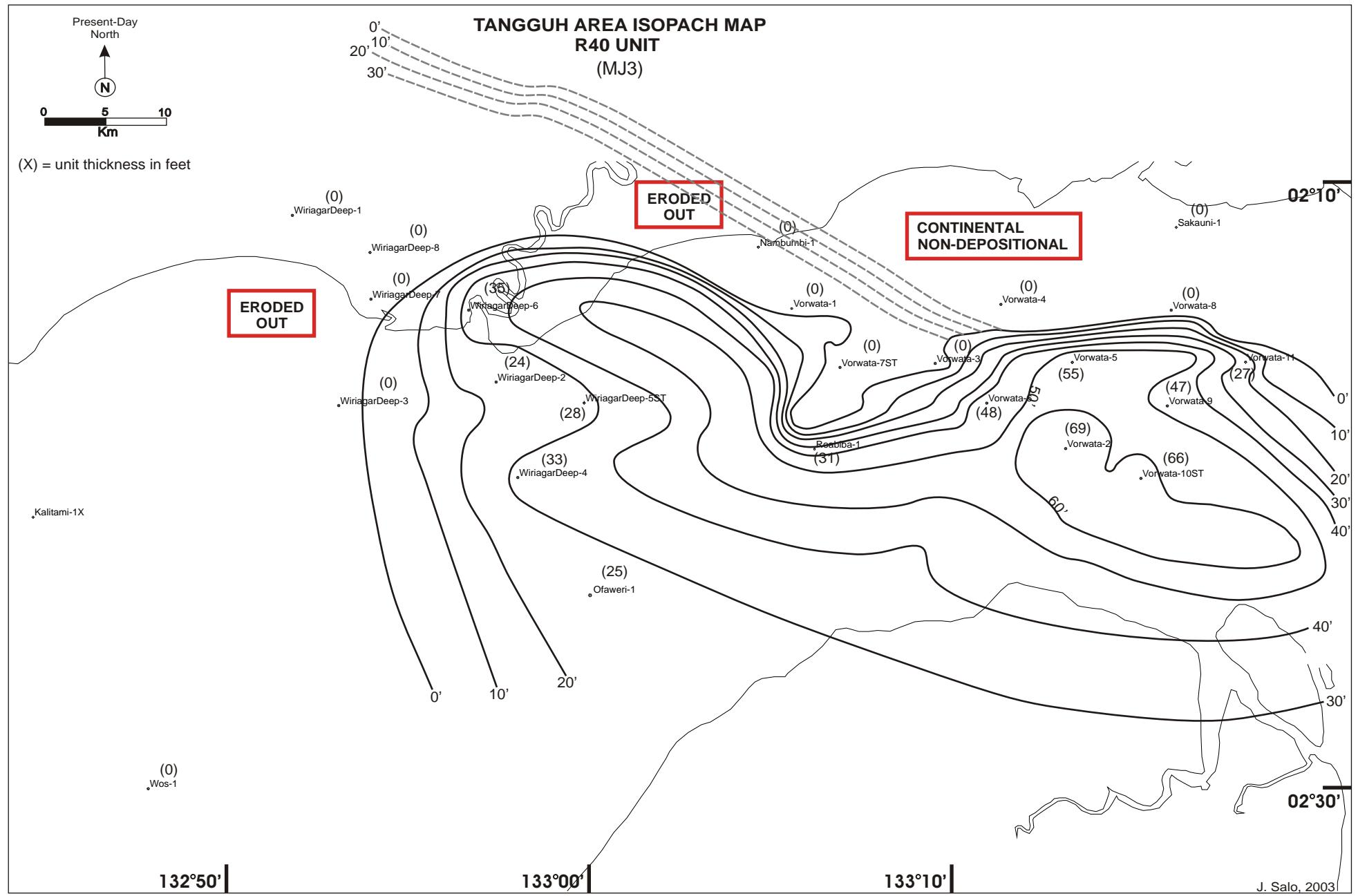


Figure 6.18: Isopach of the R40 zone. Erosional unconformity subsequently removed R40 sediments to the north and the west.

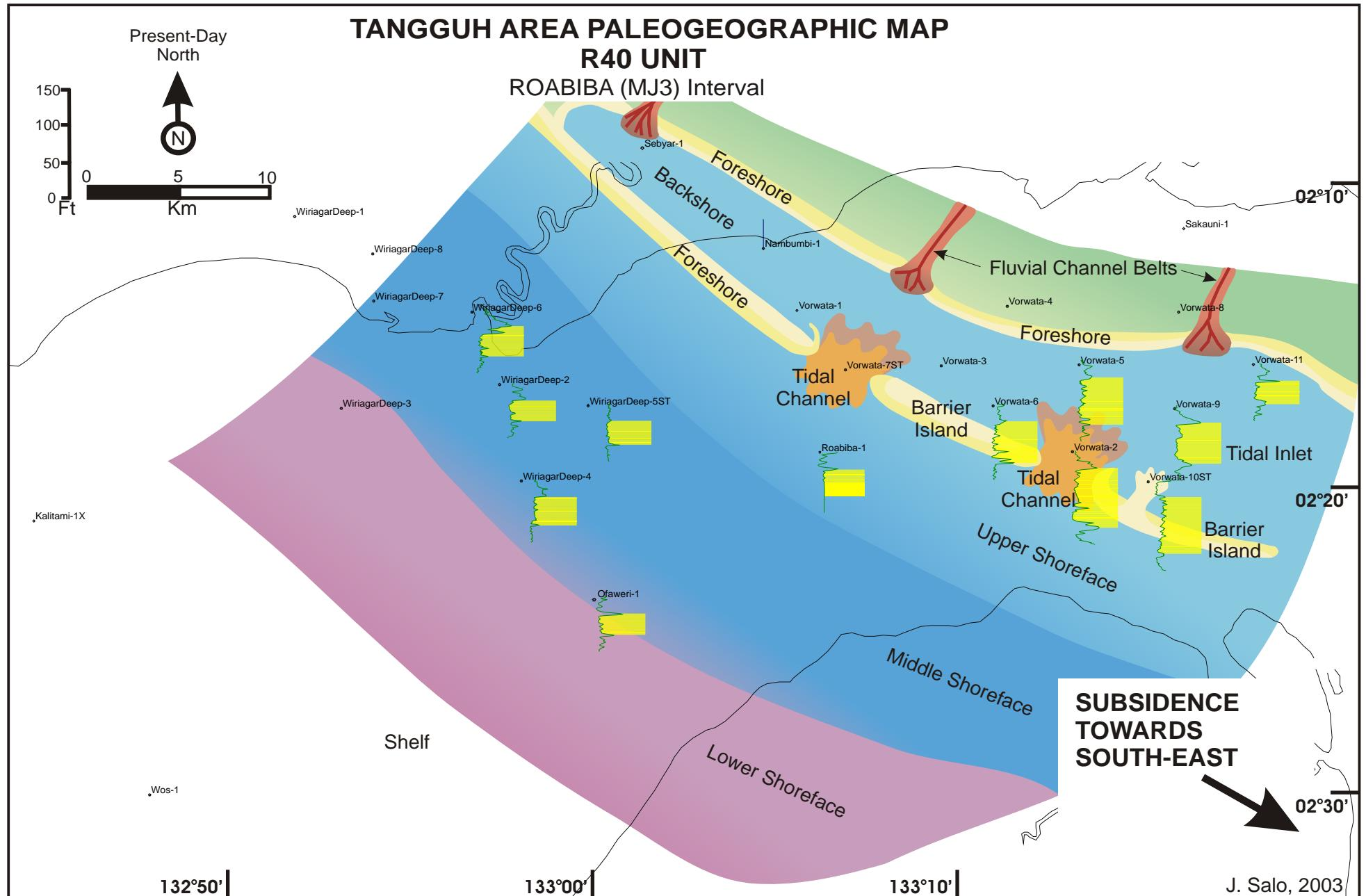


Figure 6.19: Paleogeographic map of the R40 zone. Tectonics are resulting in uplift to the west and north, and subsidence (e.g. accommodation space) to the SE.

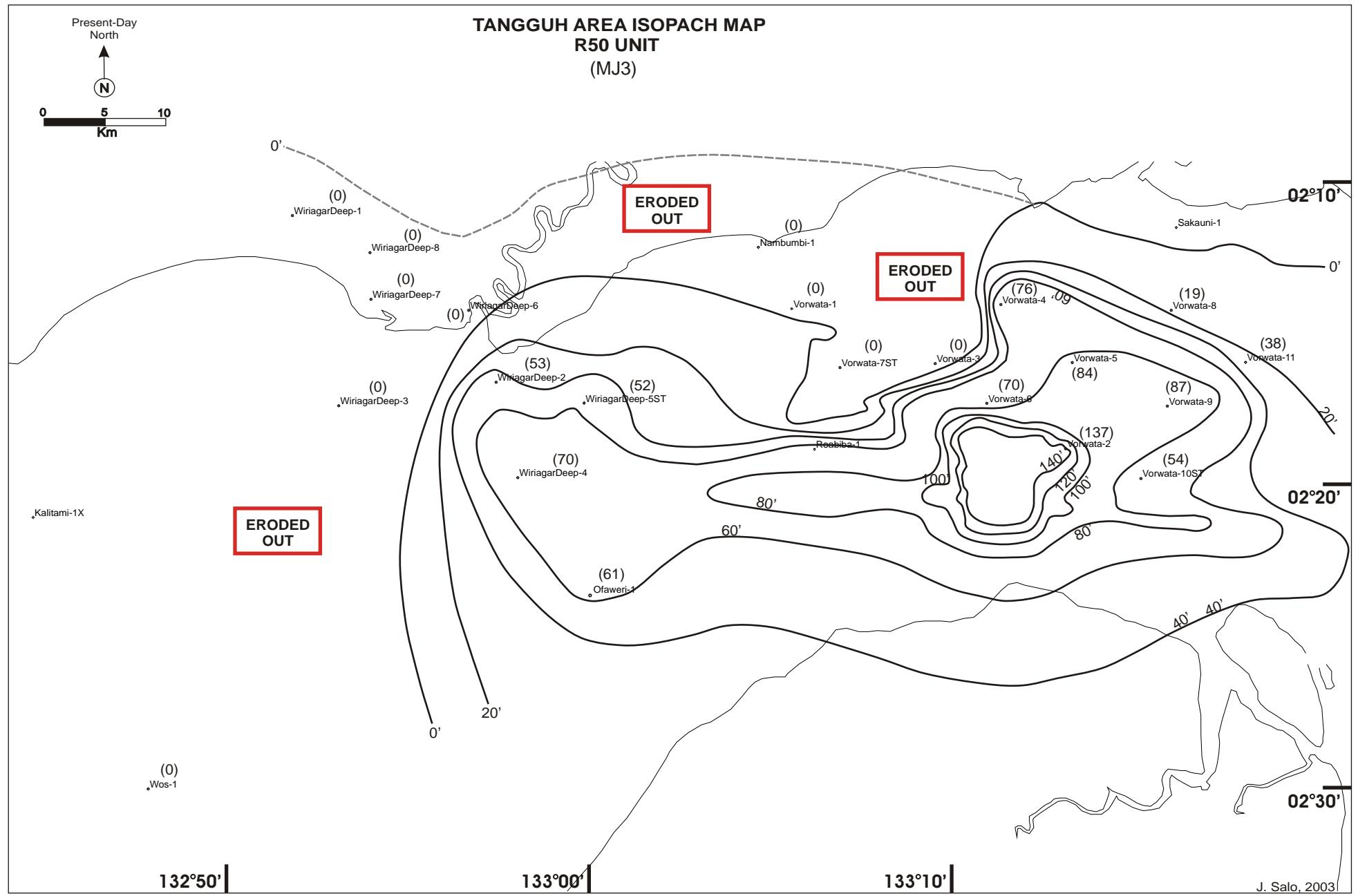


Figure 6.20: Isopach of the R50 zone at Tangguh. CI = 20 ft.

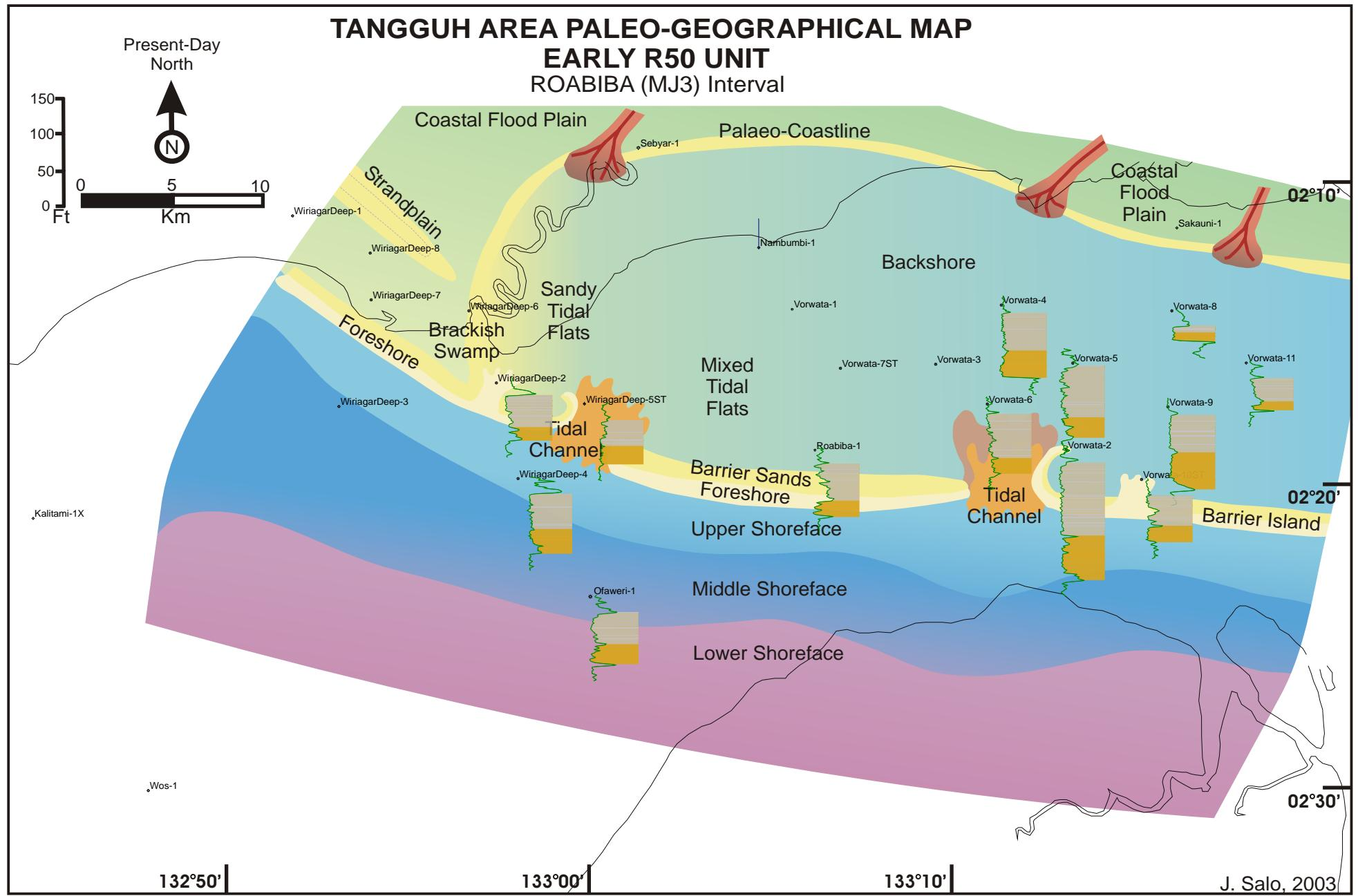


Figure 6.21: Paleogeographic map of early R50. The Wiragar Deep area is prograding with sandy tidal flat depositional facies identified in WD-6 core.

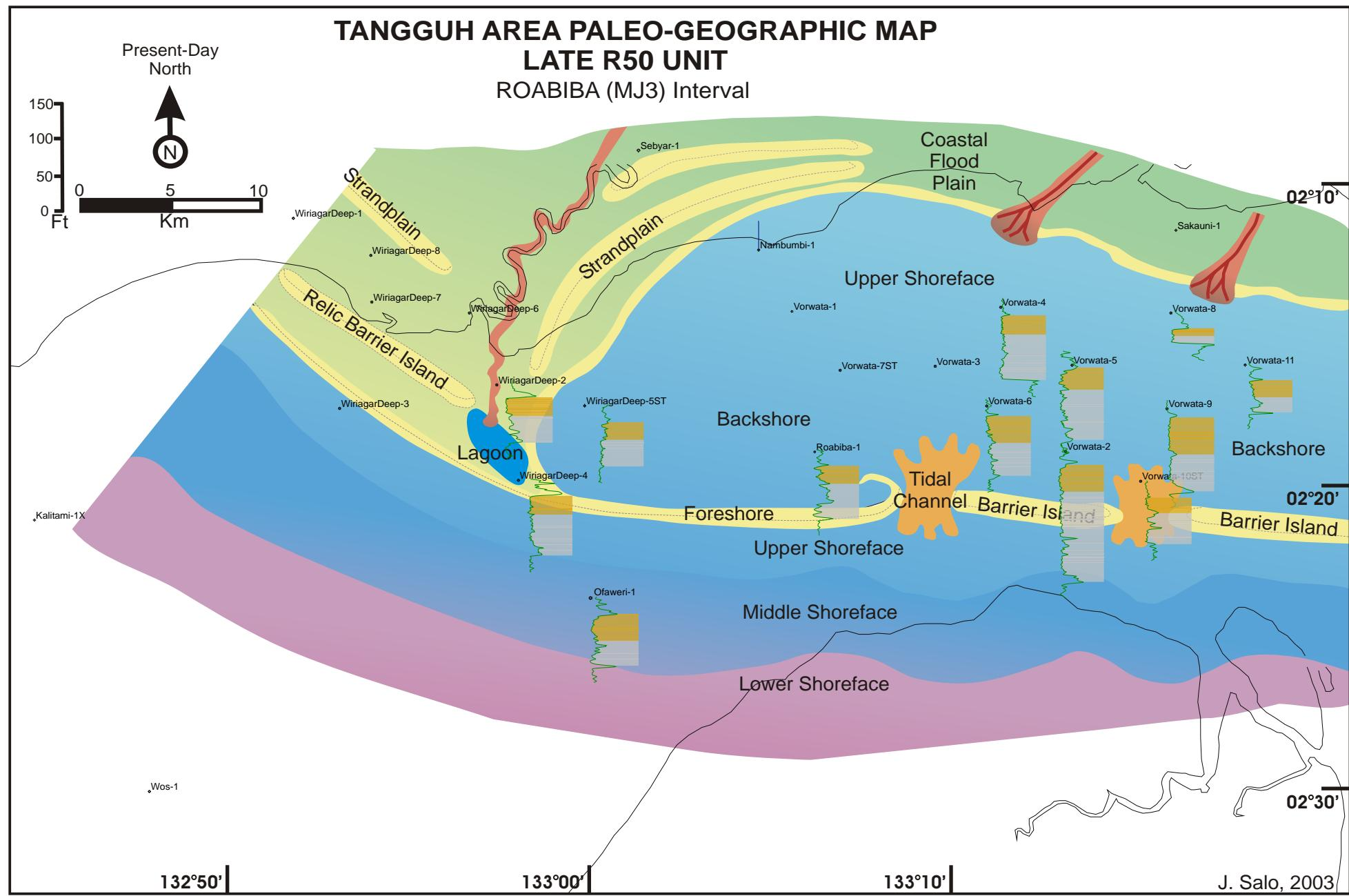


Figure 6.22: Paleogeographic map of the Late R50 zone. An areally extensive backshore area is well developed over the Vorwata area, and fluvio-lacustrine sediments are identified in WD-2 core.

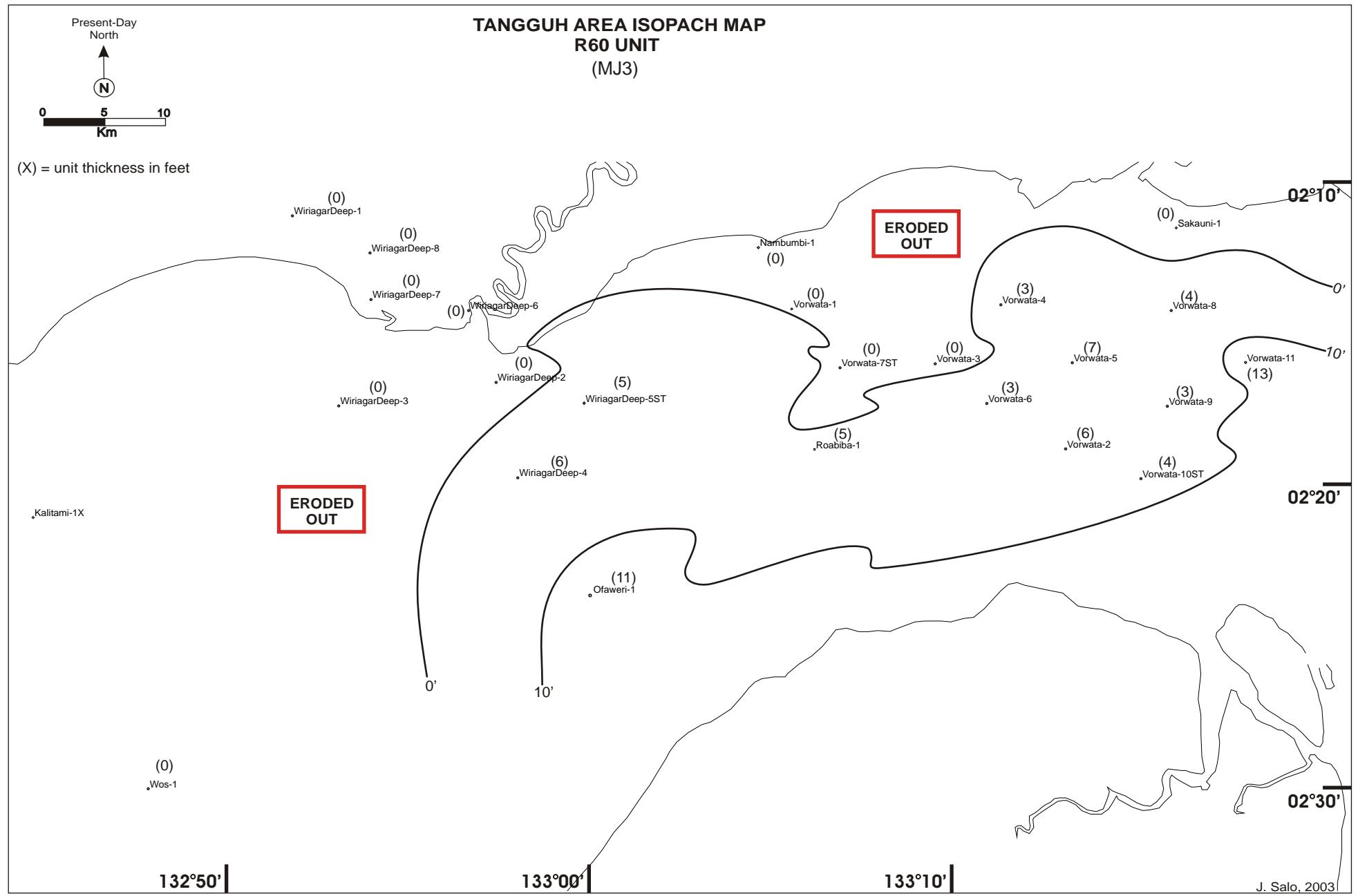


Figure 6.23: Isopach of the R60 zone at Tangguh. The R60, a thin-bedded shale break, is eroded from much of the northern and western areas

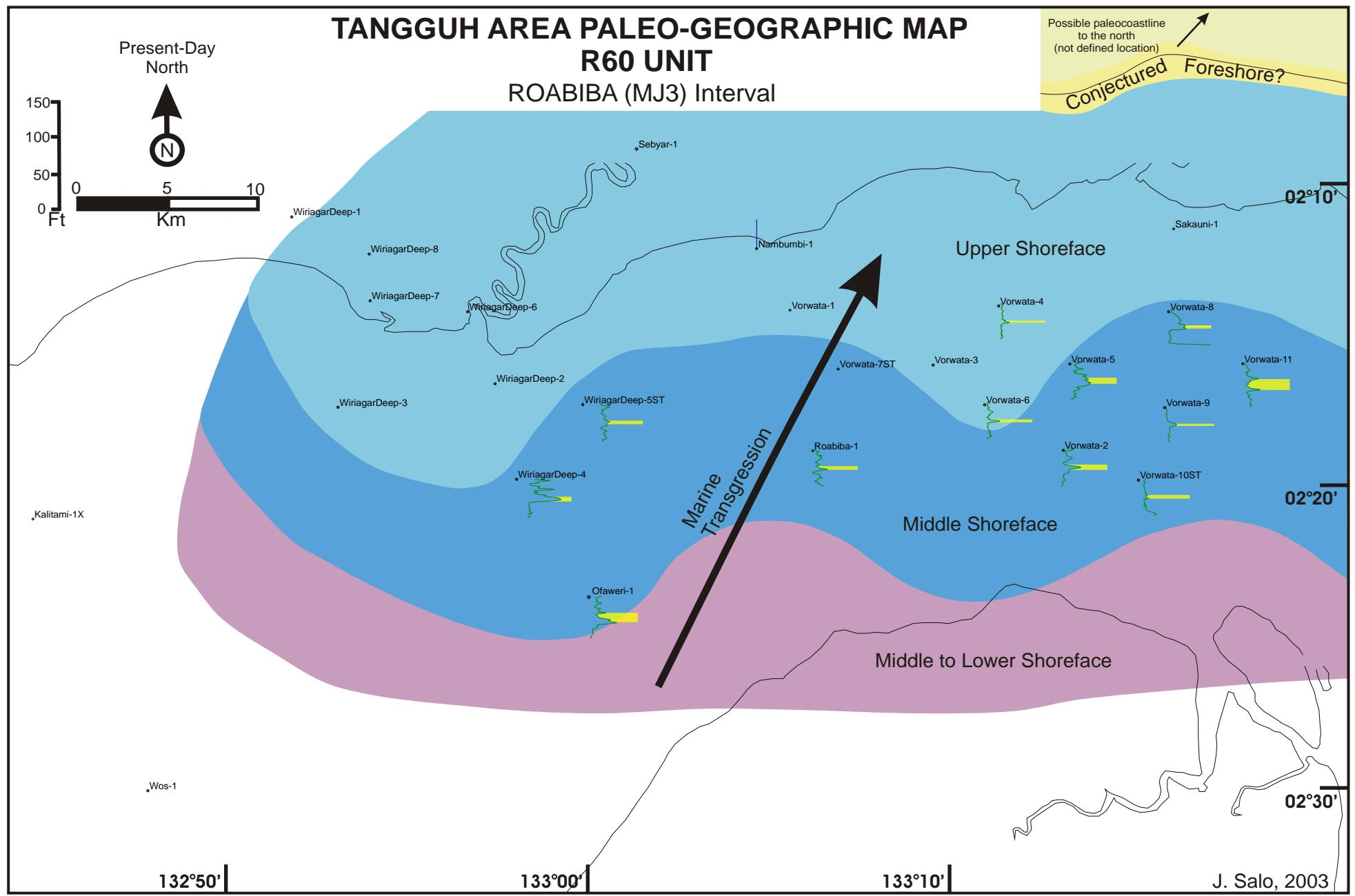


Figure 6.24: Paleogeographic map of the R60 shale break. It has been interpreted as a MSF, and is a significant intra-Roabiba sequence boundary.

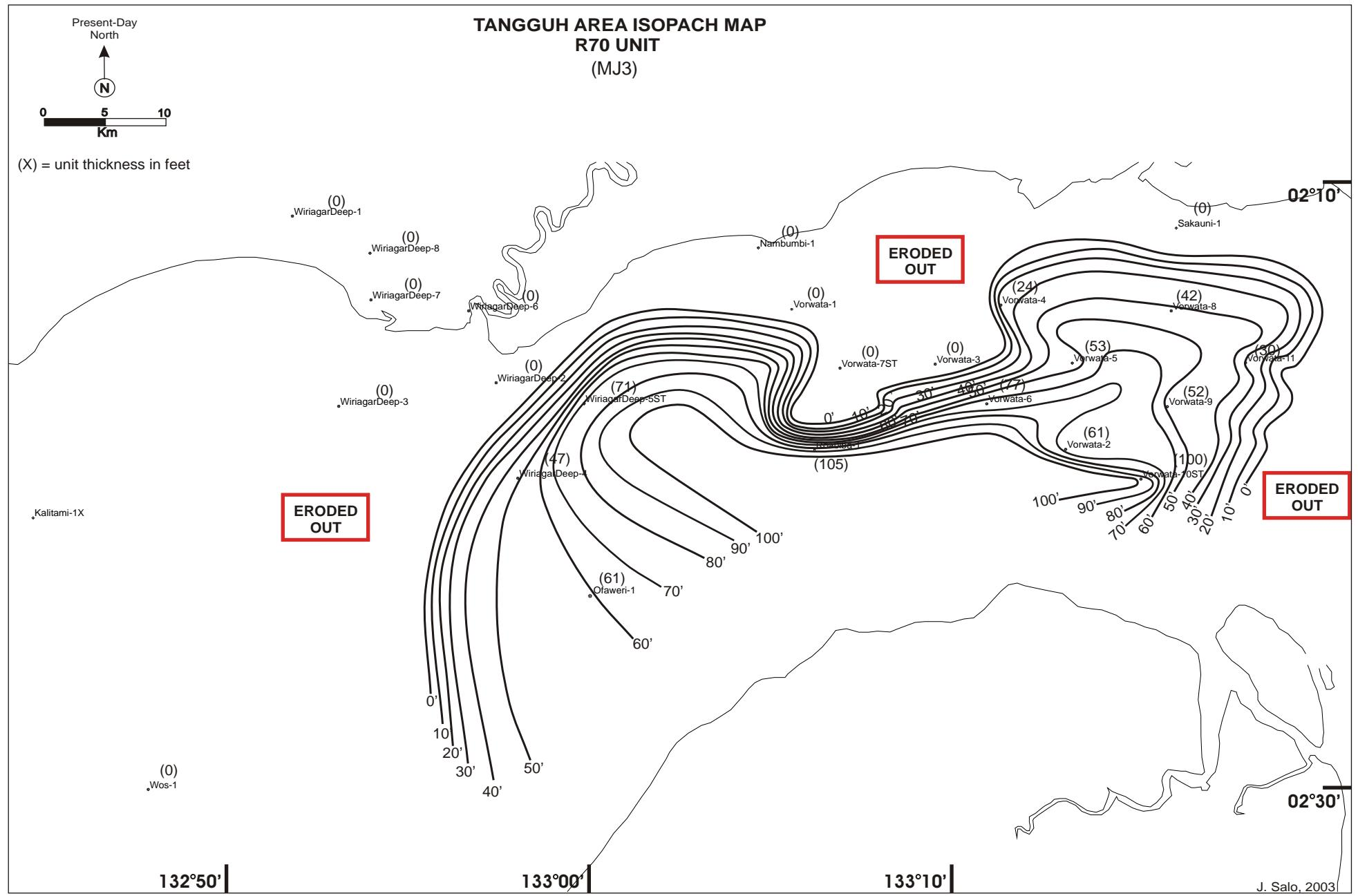


Figure 6.25: Isopach of the R70 zone. The angular unconformity overlying the R80 zone clearly has a significant impact on preservation of the R70 zone.

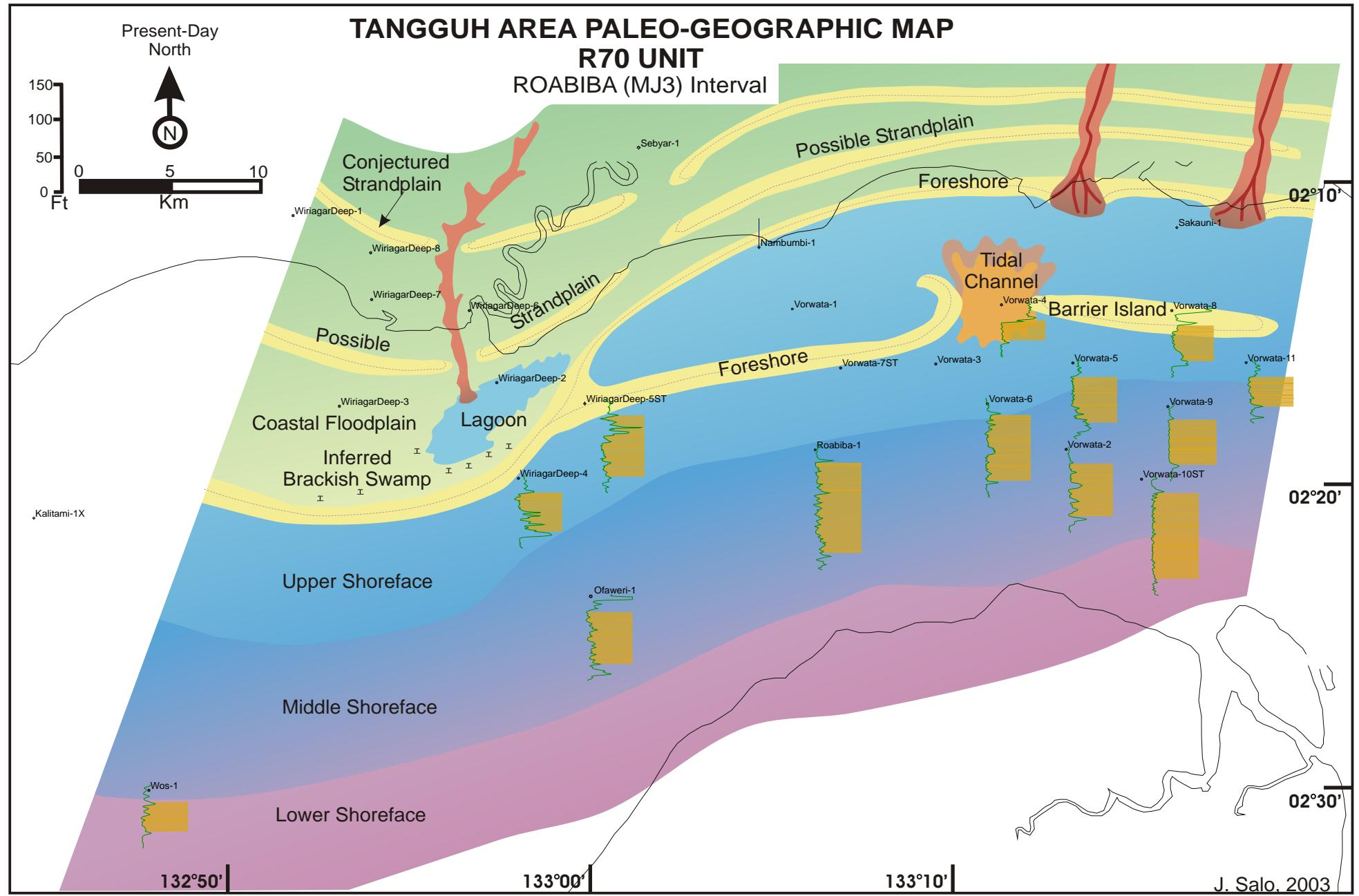


Figure 6.26: Paleogeographic map of the R70 zone. The paleo-coastline of the R70 trends roughly E-W.

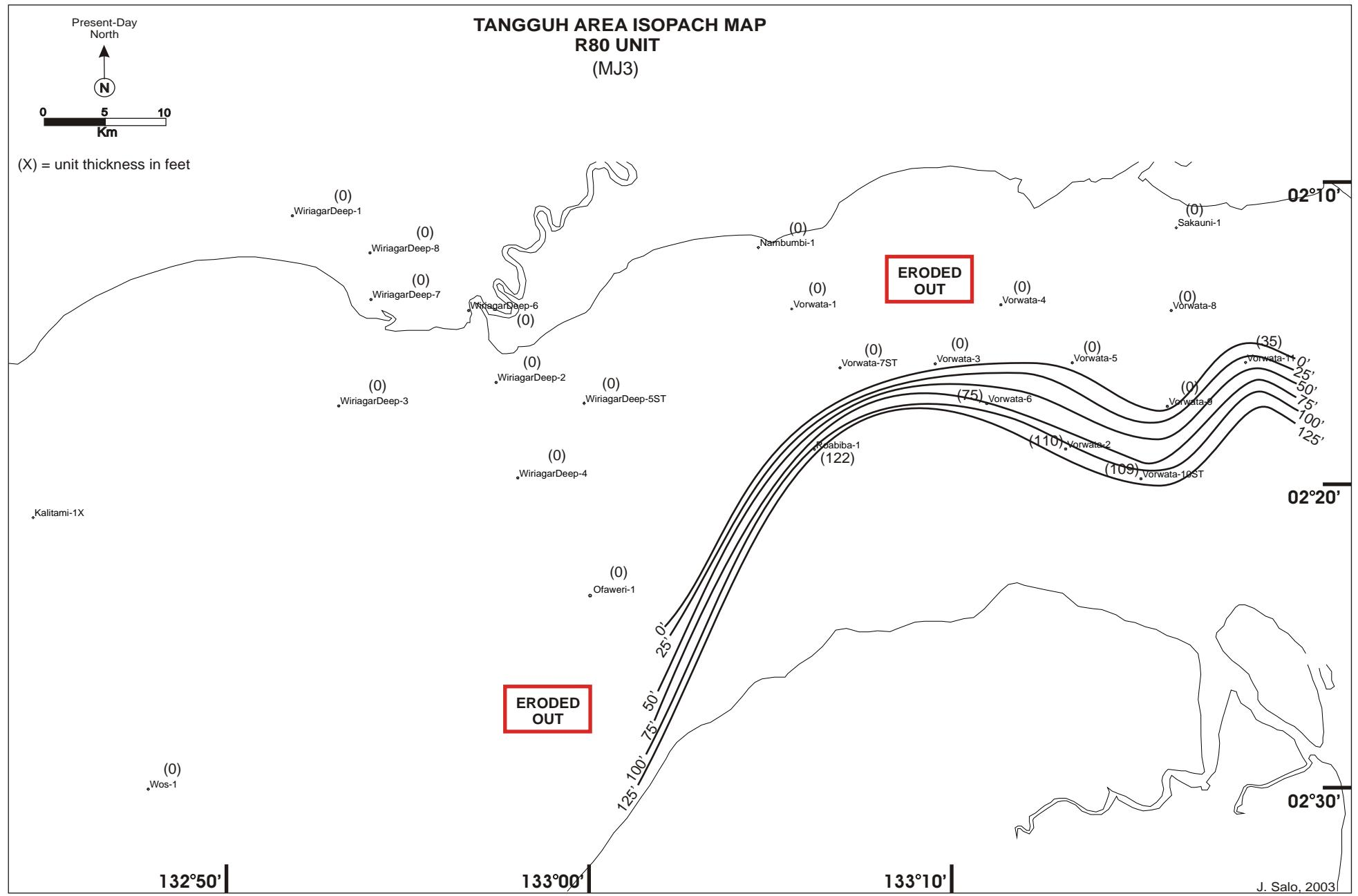


Figure 6.27: Isopach of the R80 zone, the top-most Bajocian/Bathonian Roabiba sequence stratigraphy unit preserved at the Tangguh area.

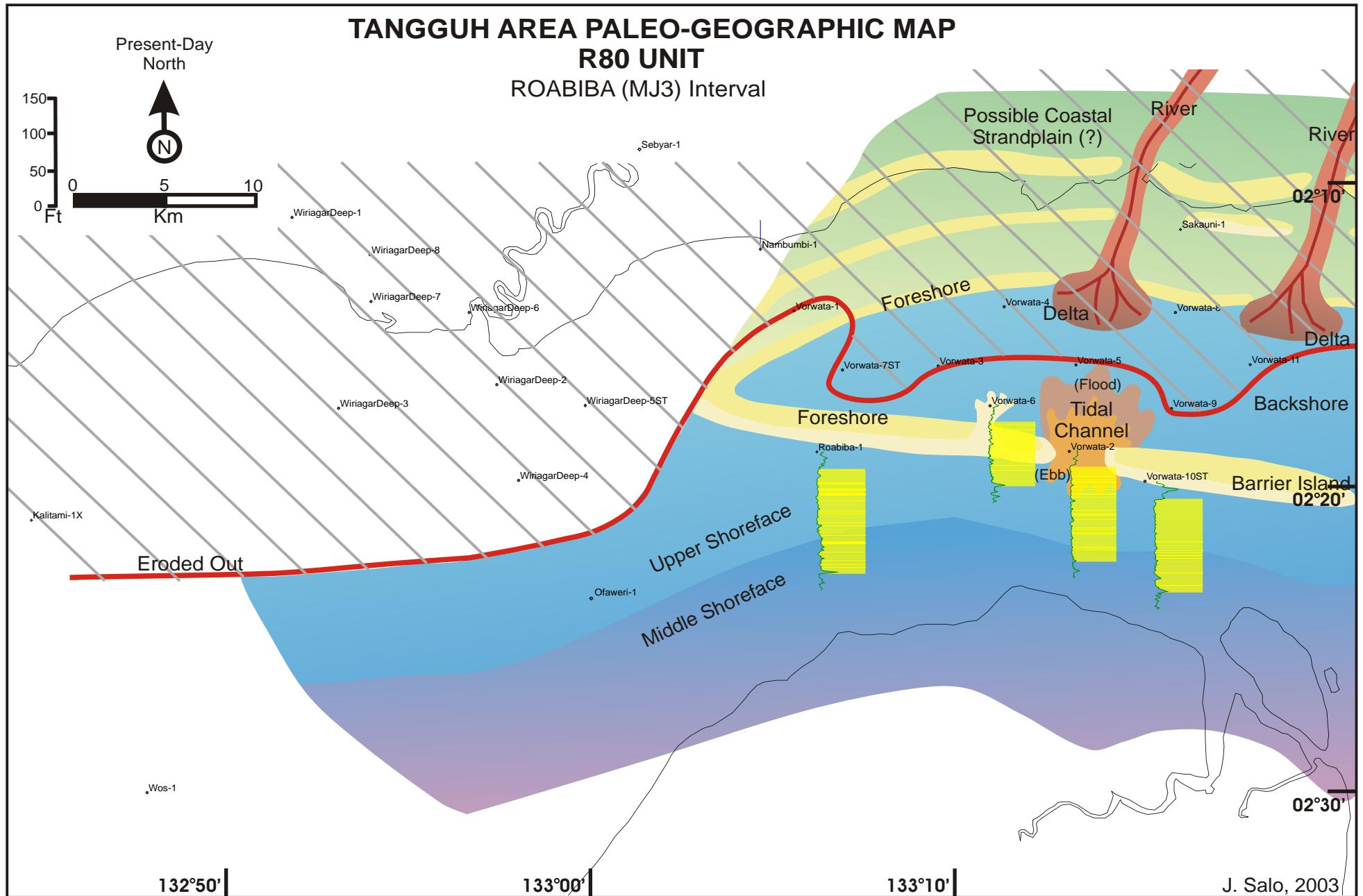


Figure 6.28: Paleogeographic map of the R80 zone. Sedimentological features (Tye and Hickey, 1999) and ichnological trace fossil fabric (Pemberton, 1997b-d) indicate a washover depositional facies at the V-6 well, a tidal channel facies at the V-2 well, and a barrier island beach facies at V-10 well.

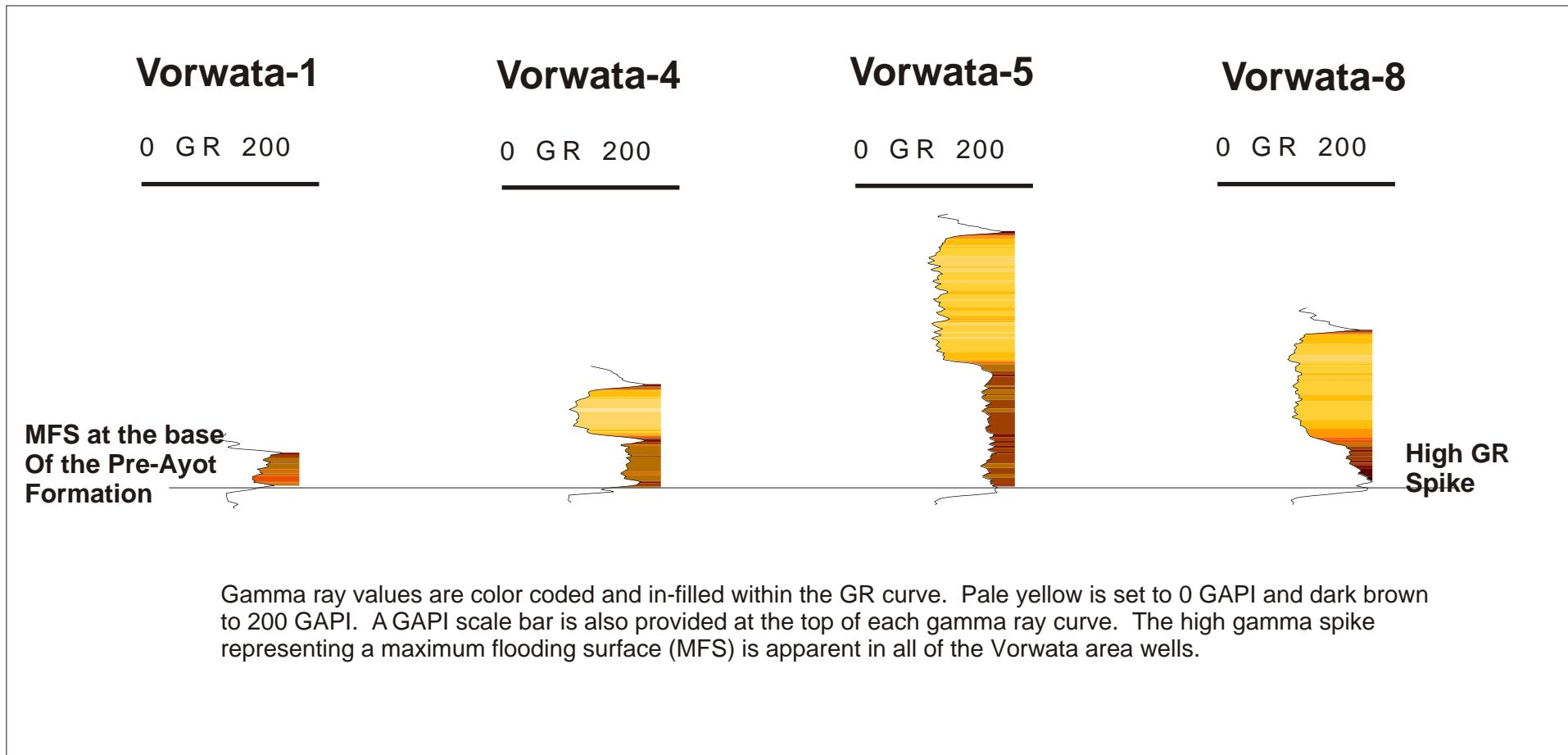


Figure 6.29: The top of the Callovian Sandstone Formation (CU50 zone) and the base of the Pre-Ayot Shales (PA10) sequence stratigraphic zone is based on a maximum flooding surface (MFS) sequence boundary, as shown from correlations of high GR spike on the V-1, V-4, V-5, and V-8 wells as examples.

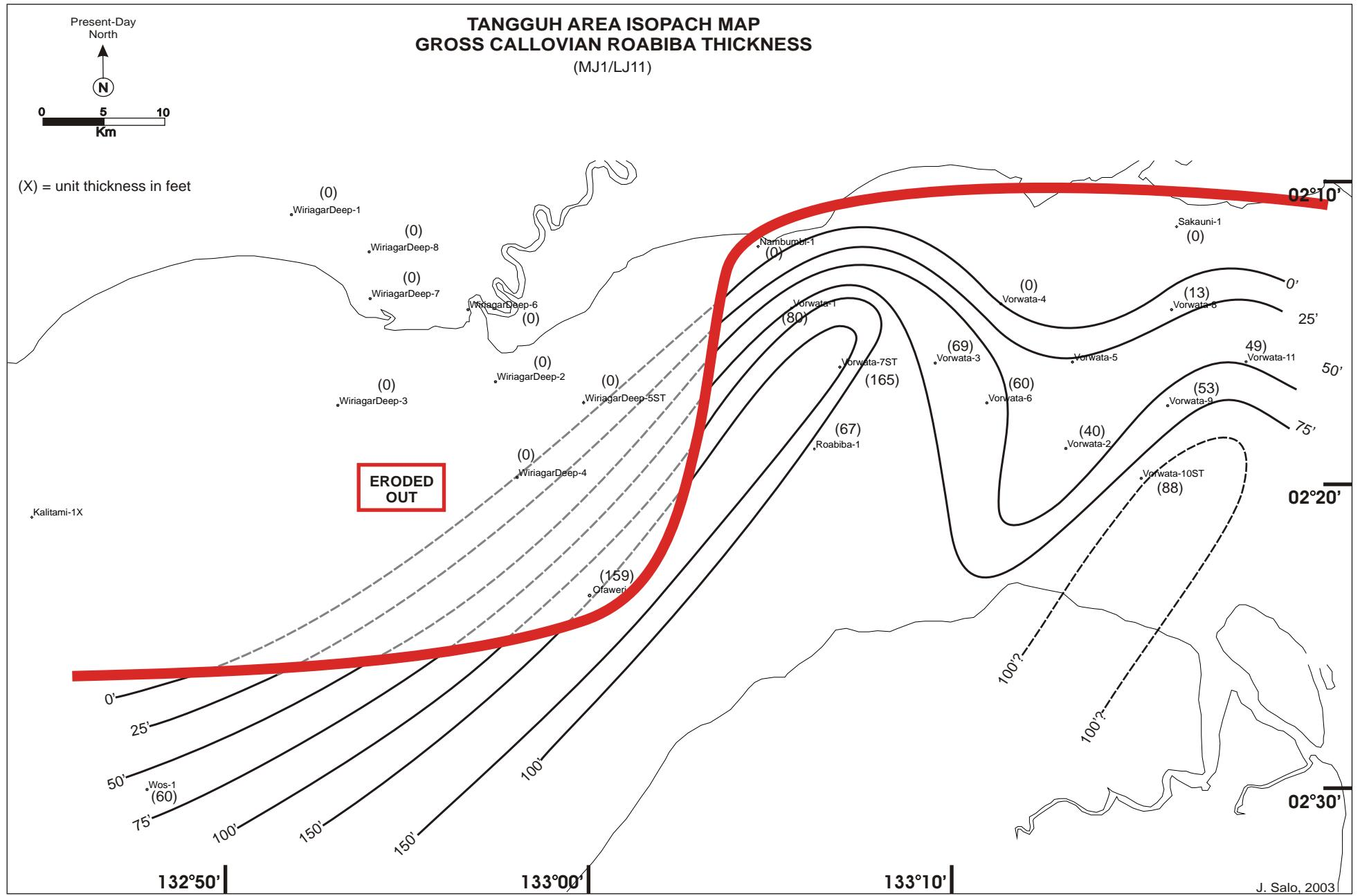


Figure 6.30: Isopach of the gross Callovian Roabiba sandstone interval. The interval is identified by an erosional unconformity SB at the base (MJ-2) and a maximum flood surface SB on the top.

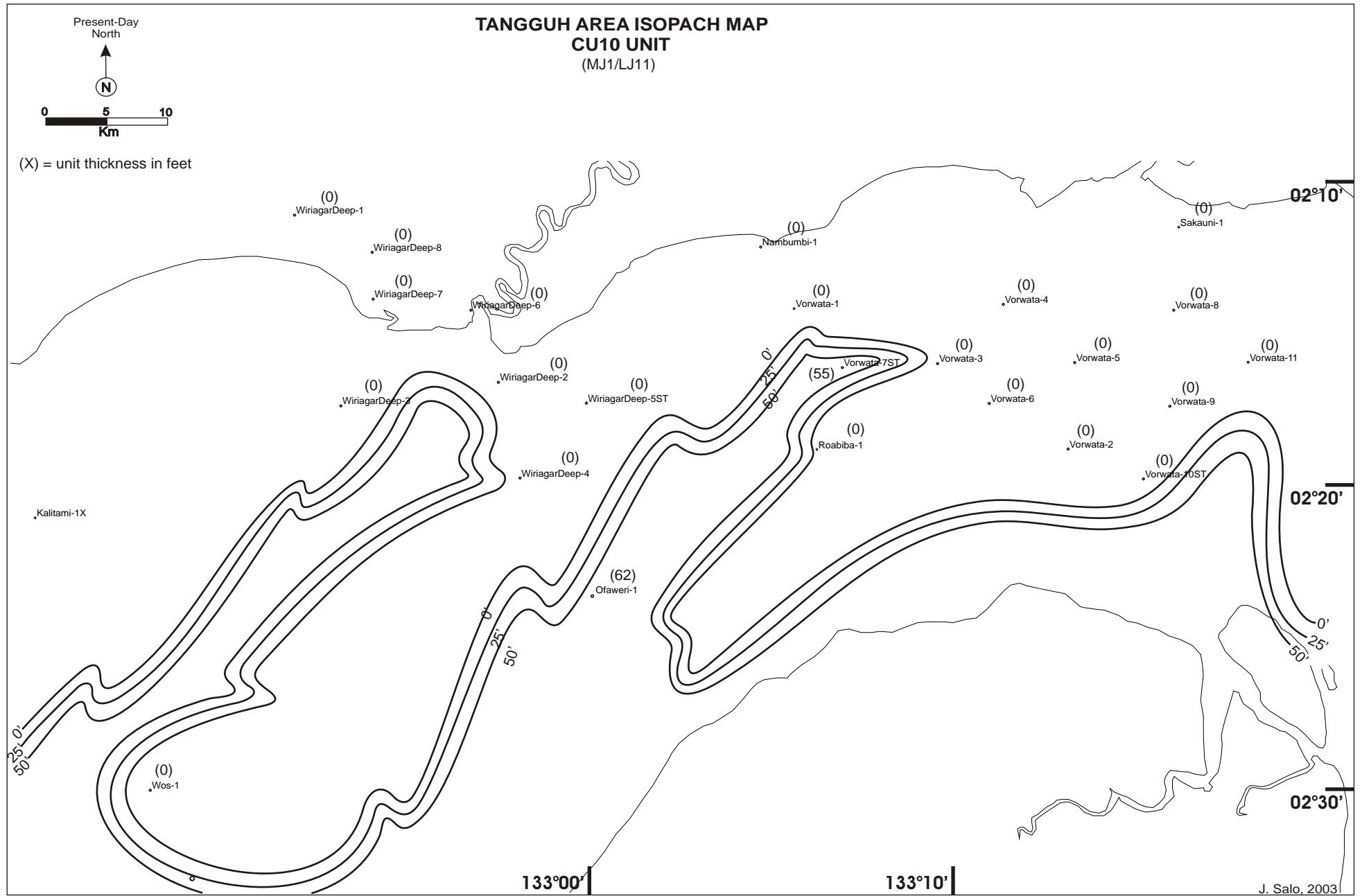


Figure 6.31: Isopach of the Callovian Roabiba CU10 zone. A thick marine sandstone comprises the renewed sedimentation at the O-1 and V-7 well locations. Identification of the erosional unconformity and isopach suggest that incised valley complexes developed during the MJ-2 (Late Bathonian) times.

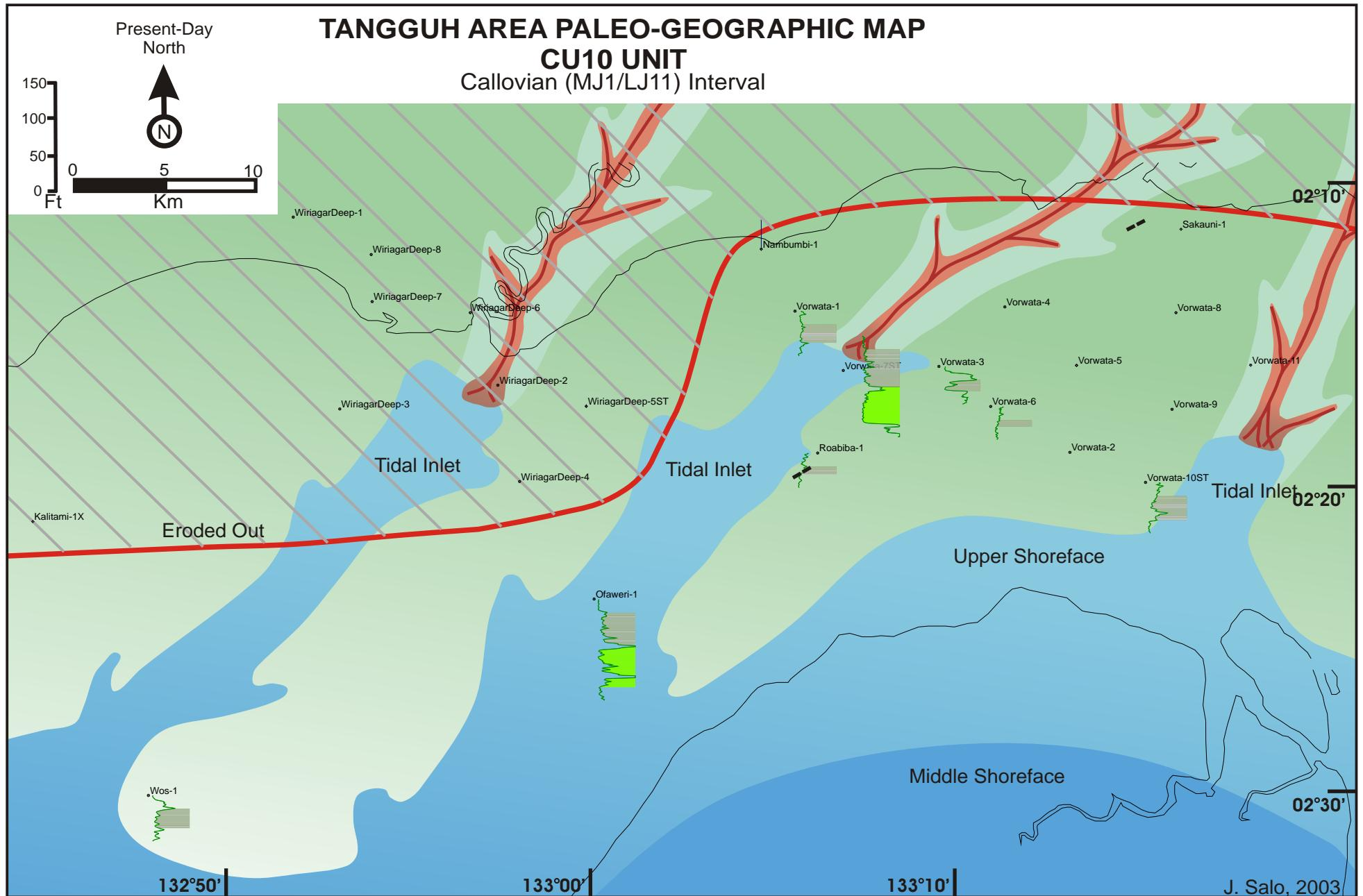


Figure 6.32: Paleogeographic map of the CU10 zone, showing topographic lows (e.g. incised valley complexes) receiving the renewed sedimentation.

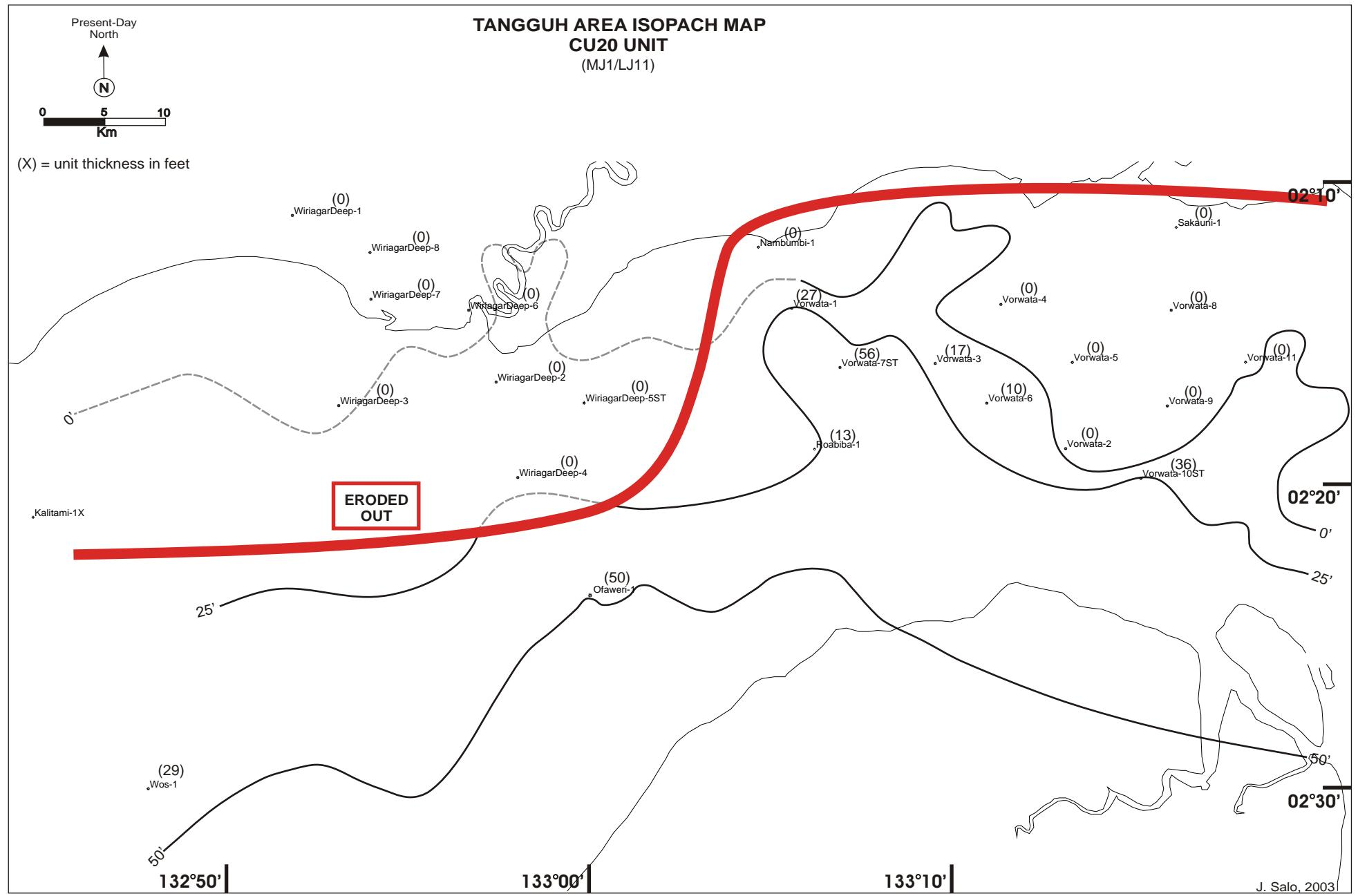


Figure 6.33: Isopach of the CU20 zone (part of the Callovian Roabiba Sandstone Formation).

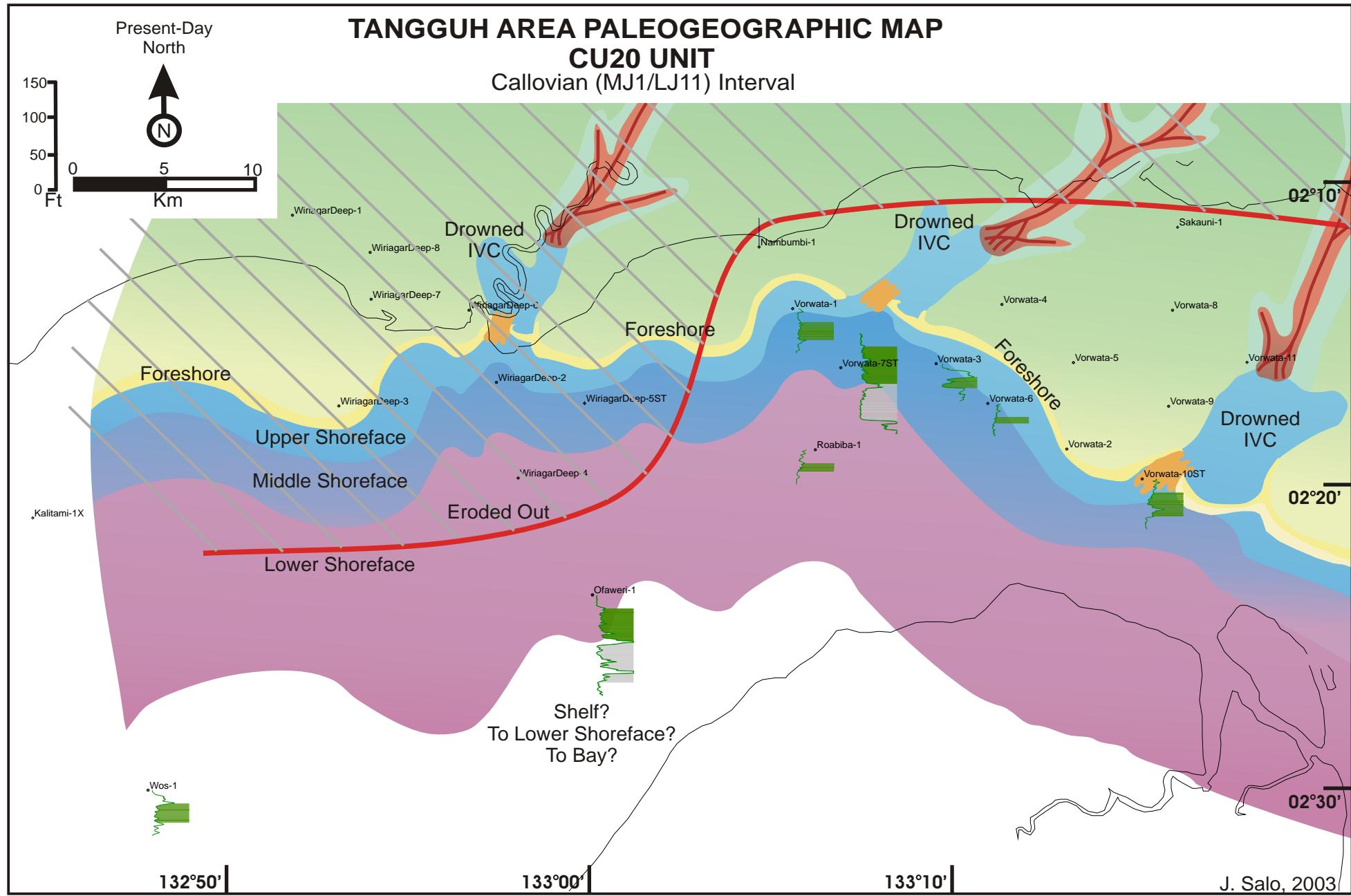


Figure 6.34: Paleogeographic map of CU20 zone. The renewed marine transgression is more areally widespread in the Tanggh area by the CU20 period.

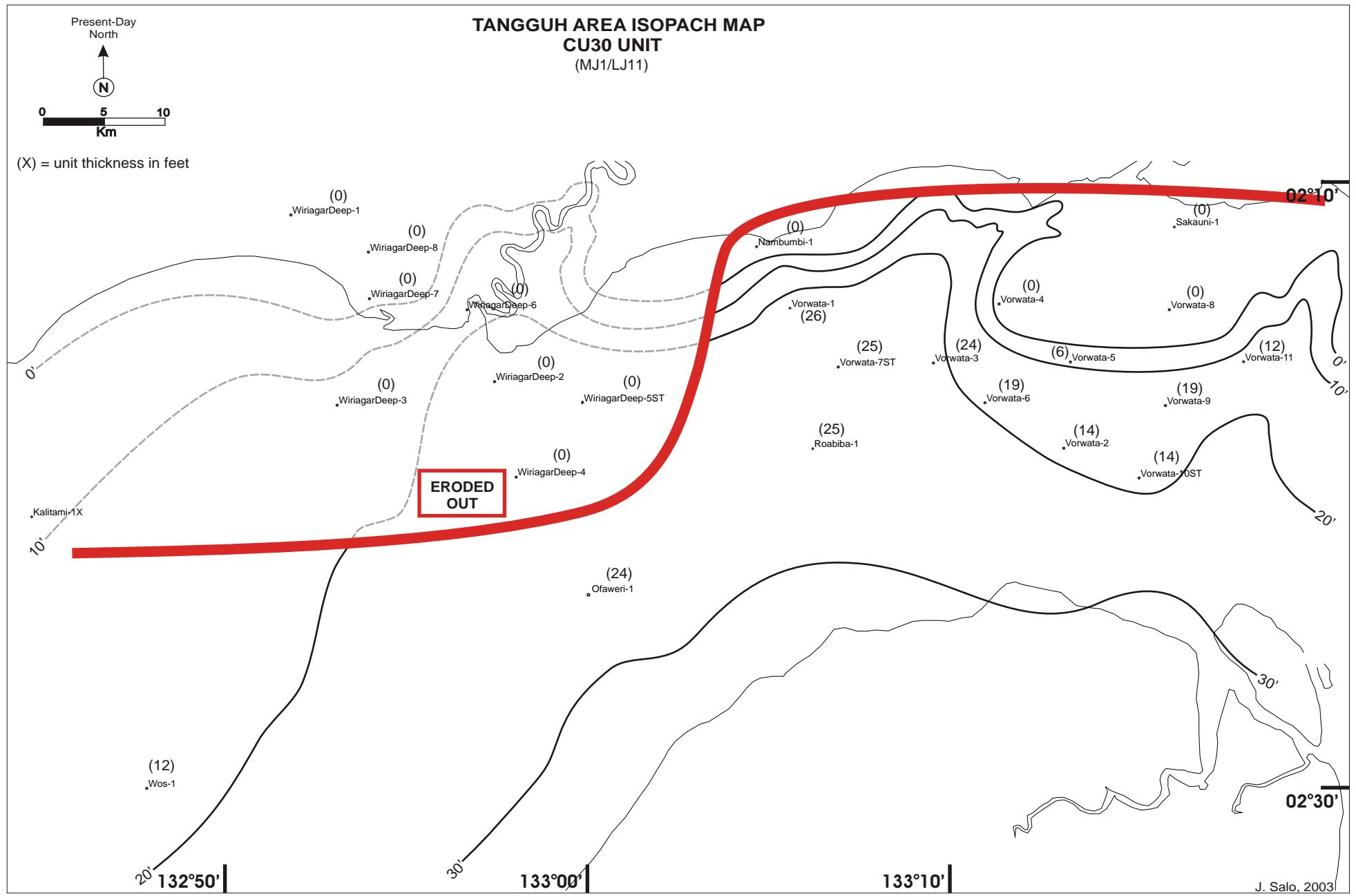


Figure 6.35: Isopach of the CU30 zone. CI = 10 ft.

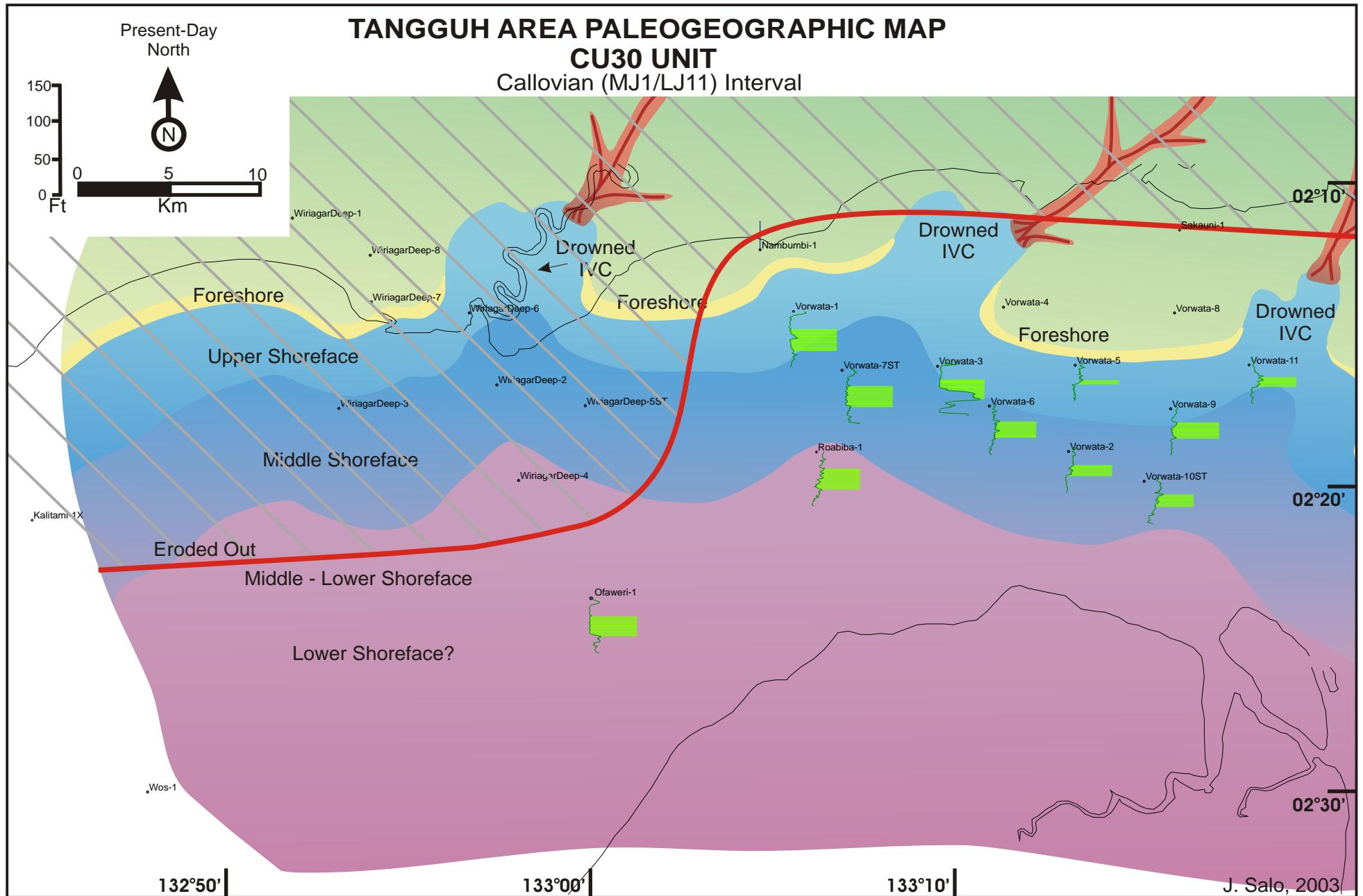


Figure 6.36: Paleogeographic map of the CU30 zone. Marine transgression (TST) has inundated most of the Vorwata area, and most-likely the Wiriagar Deep area, subsequently eroded out.

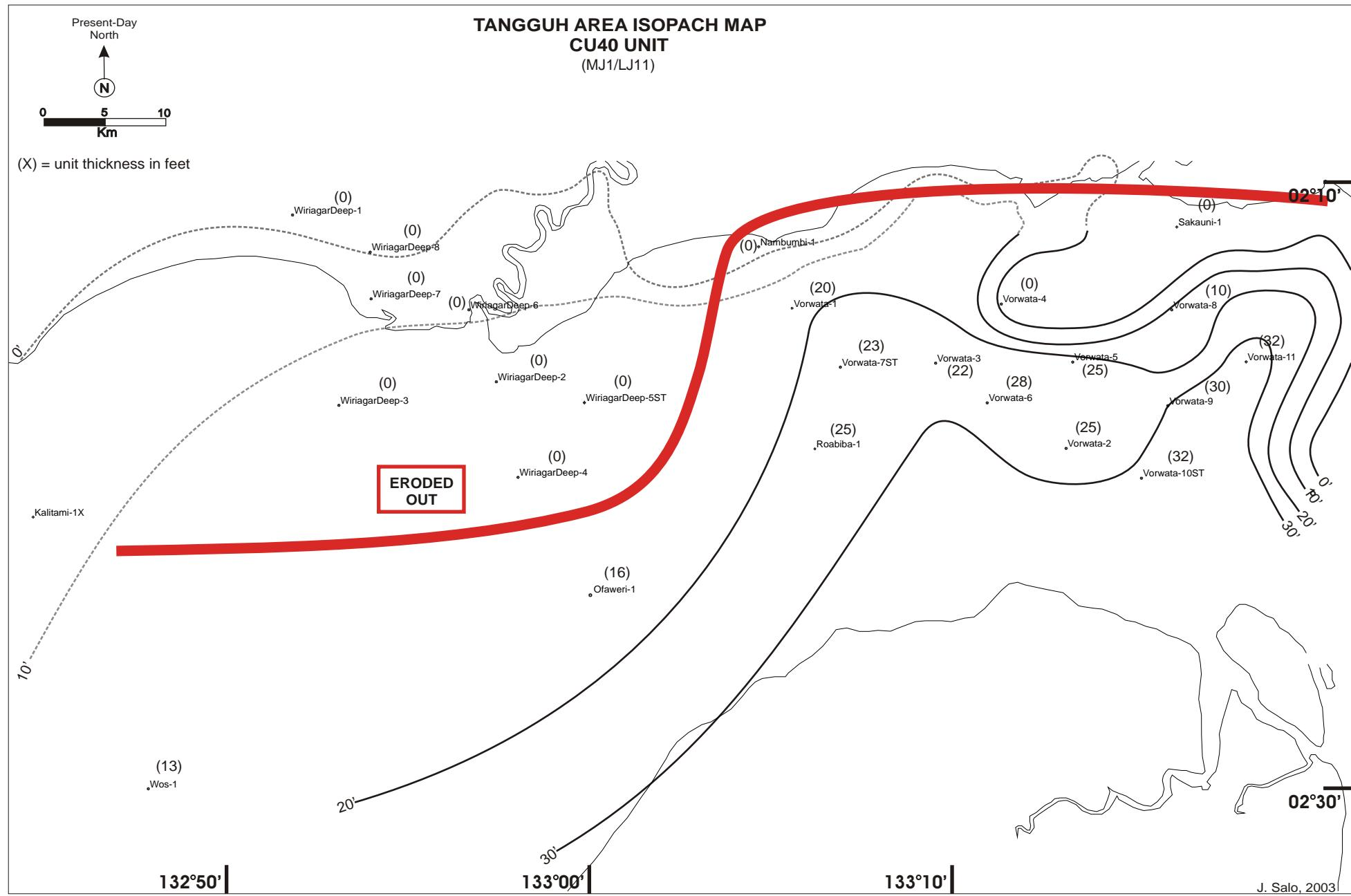


Figure 6.37: Isopach of the CU40 zone.

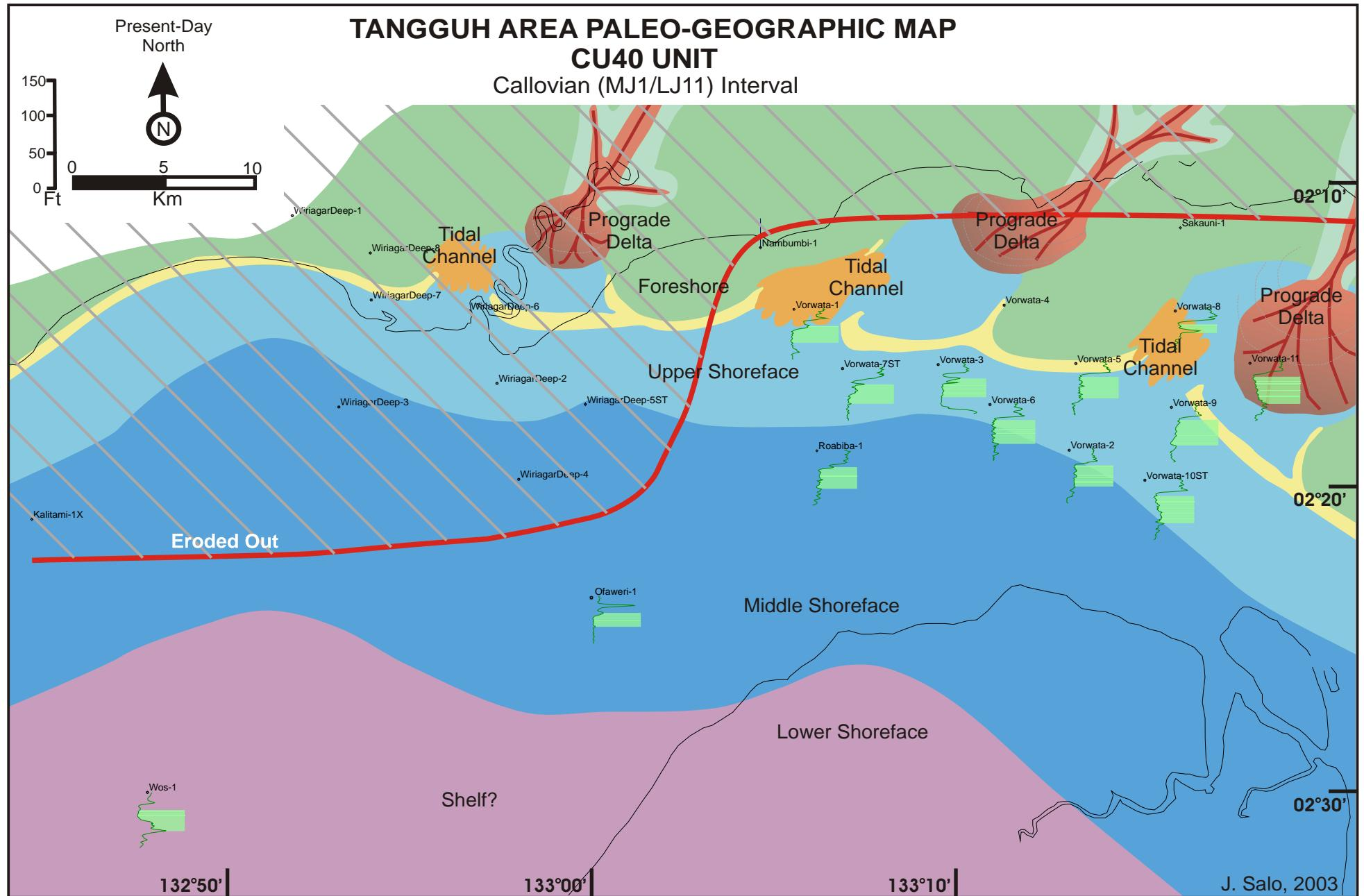


Figure 6.38: Paleogeographic map of the CU40 zone. Prograding coastline is indicative of a HST at Tangguh during the Callovian.

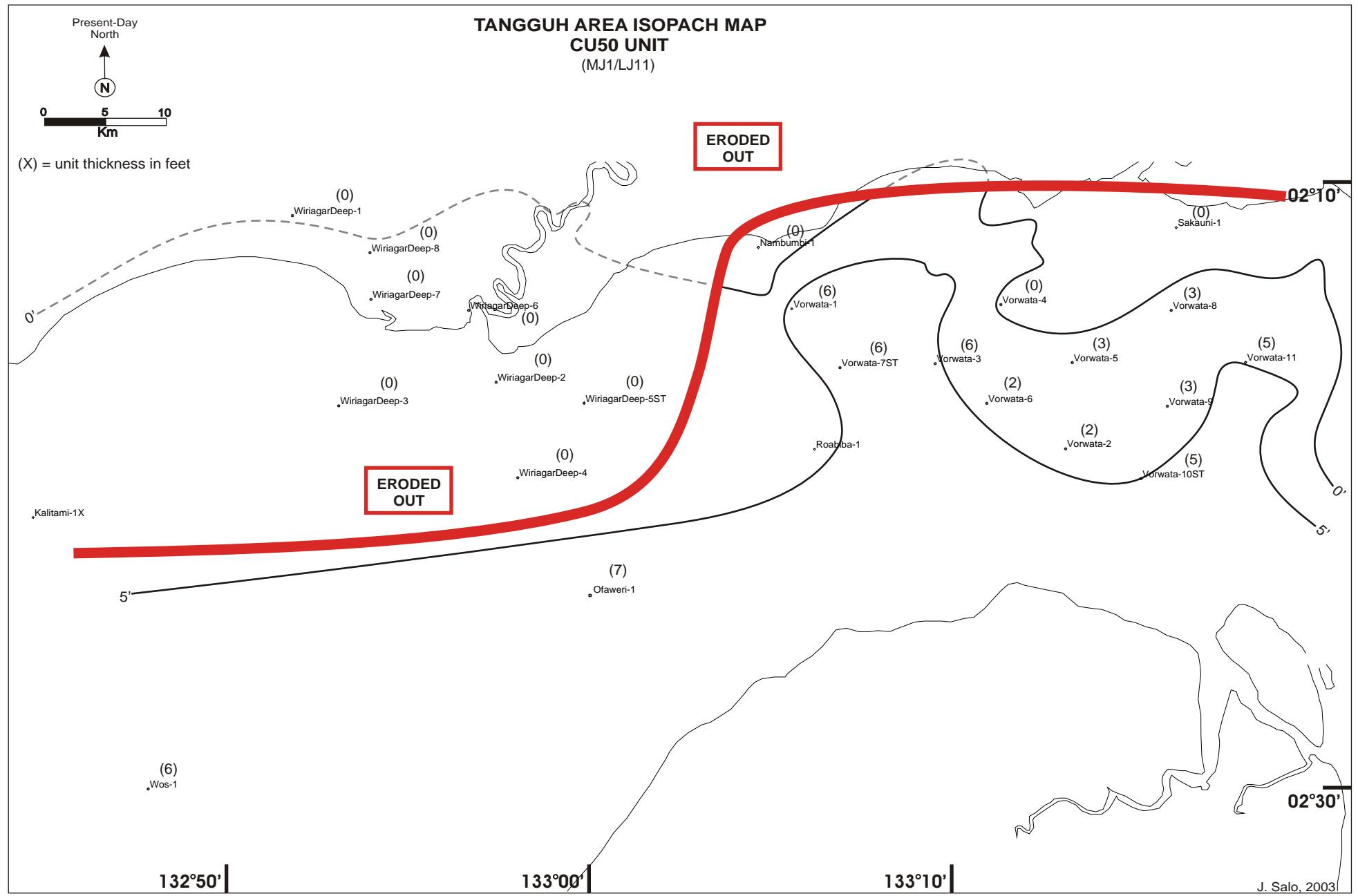


Figure 6.39: Isopach of the CU50 zone at Tangguh. The thin-bedded calcareous sandstone 'cap' on the Callovian Roabiba is correlatable on most Vorwata wells.

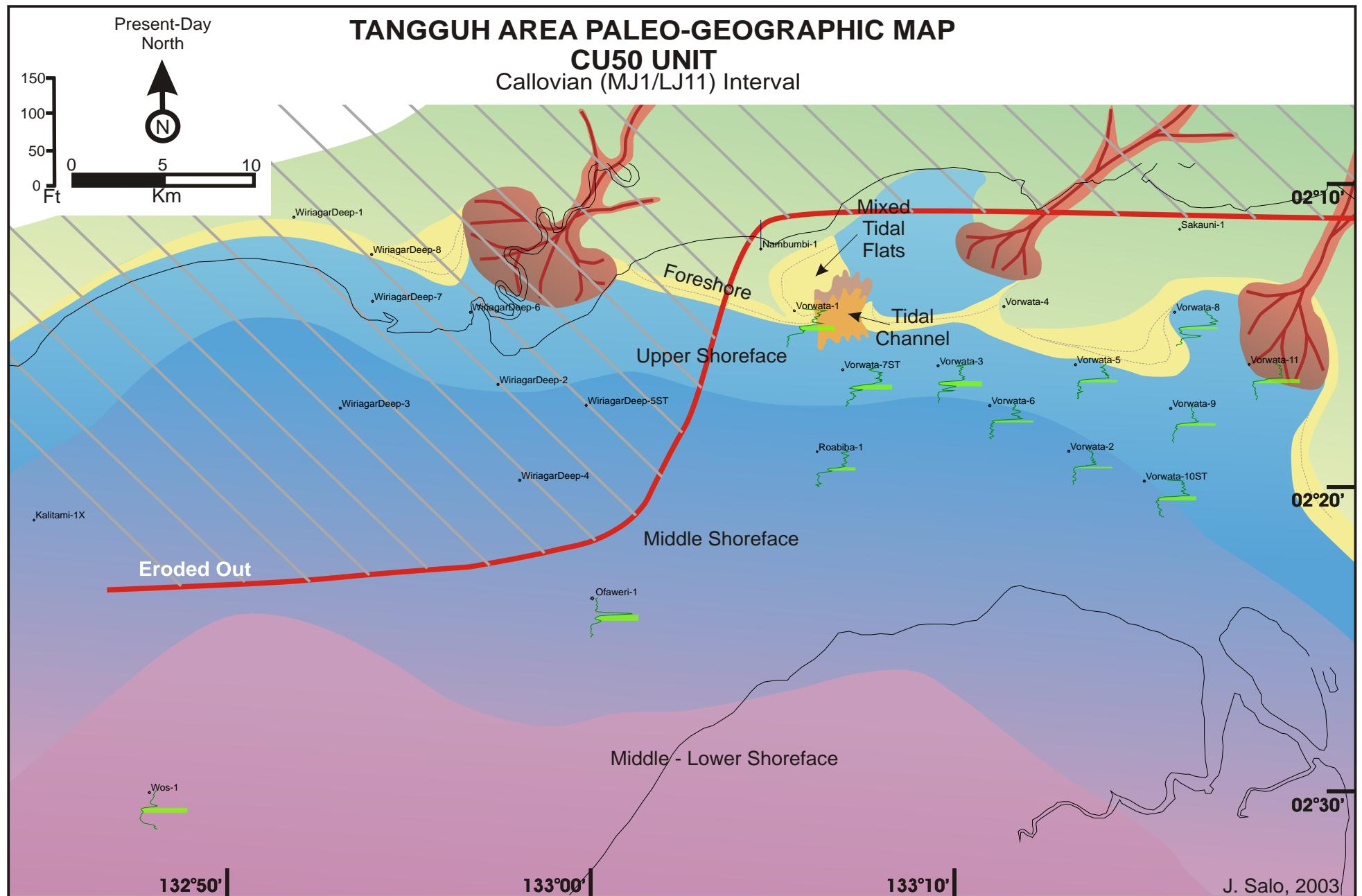


Figure 6.40: Paleogeographic map of the CU50 depositional facies at Tangguh.

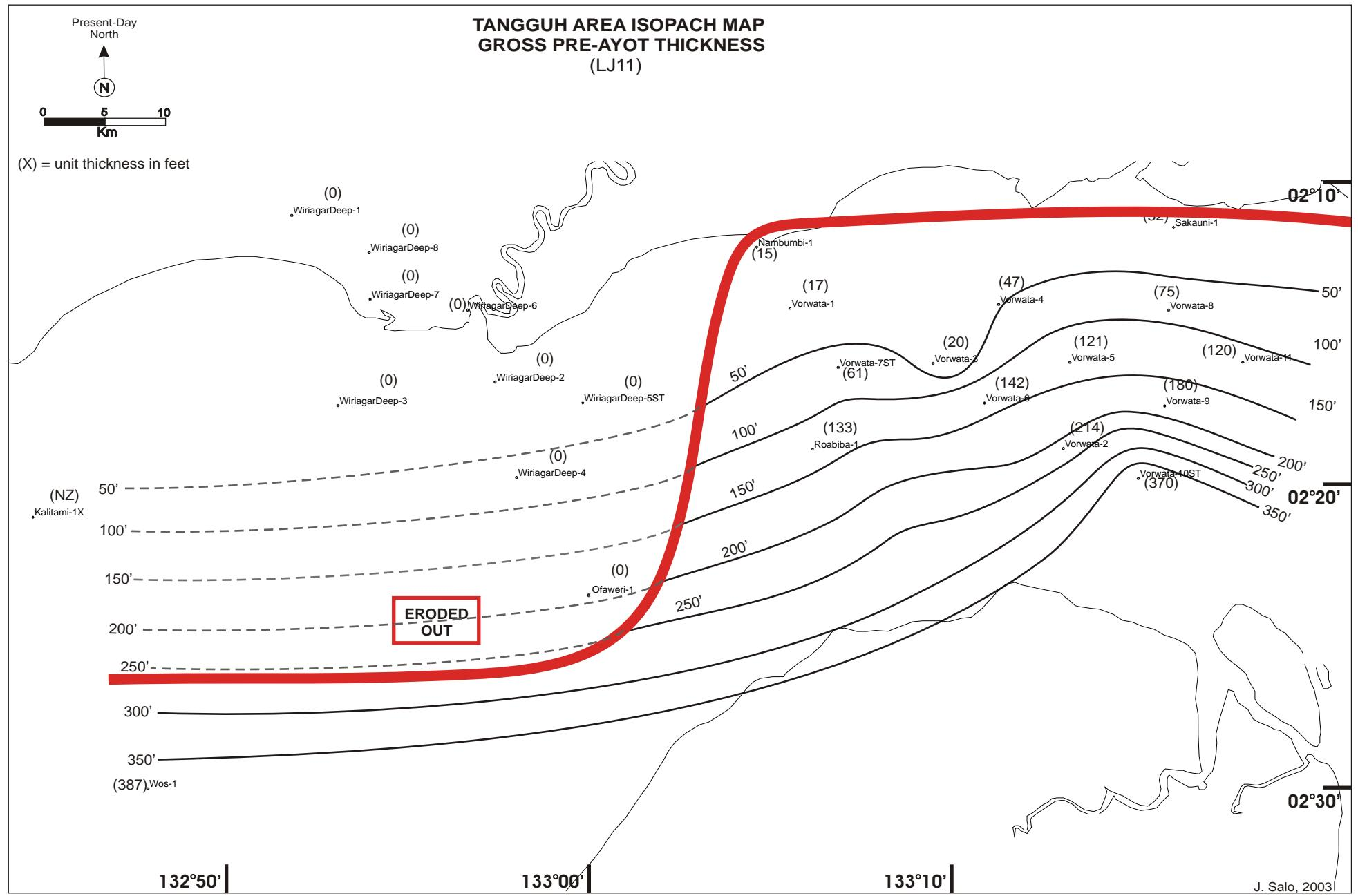


Figure 6.41: Isopach of the gross Pre-Ayot succession at Tangguh. CI = 50 ft.

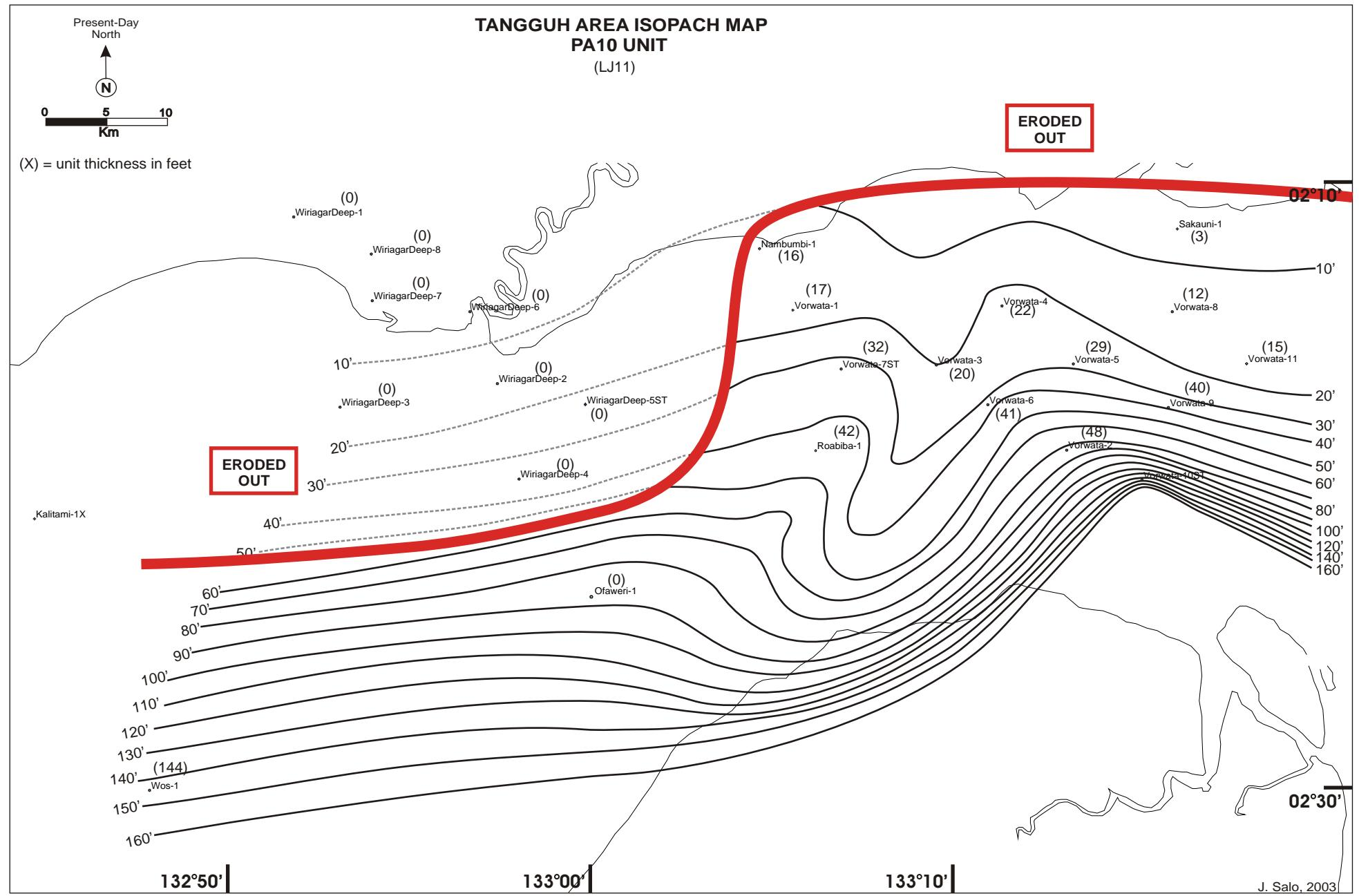


Figure 6.42: Isopach of the PA10 zone.

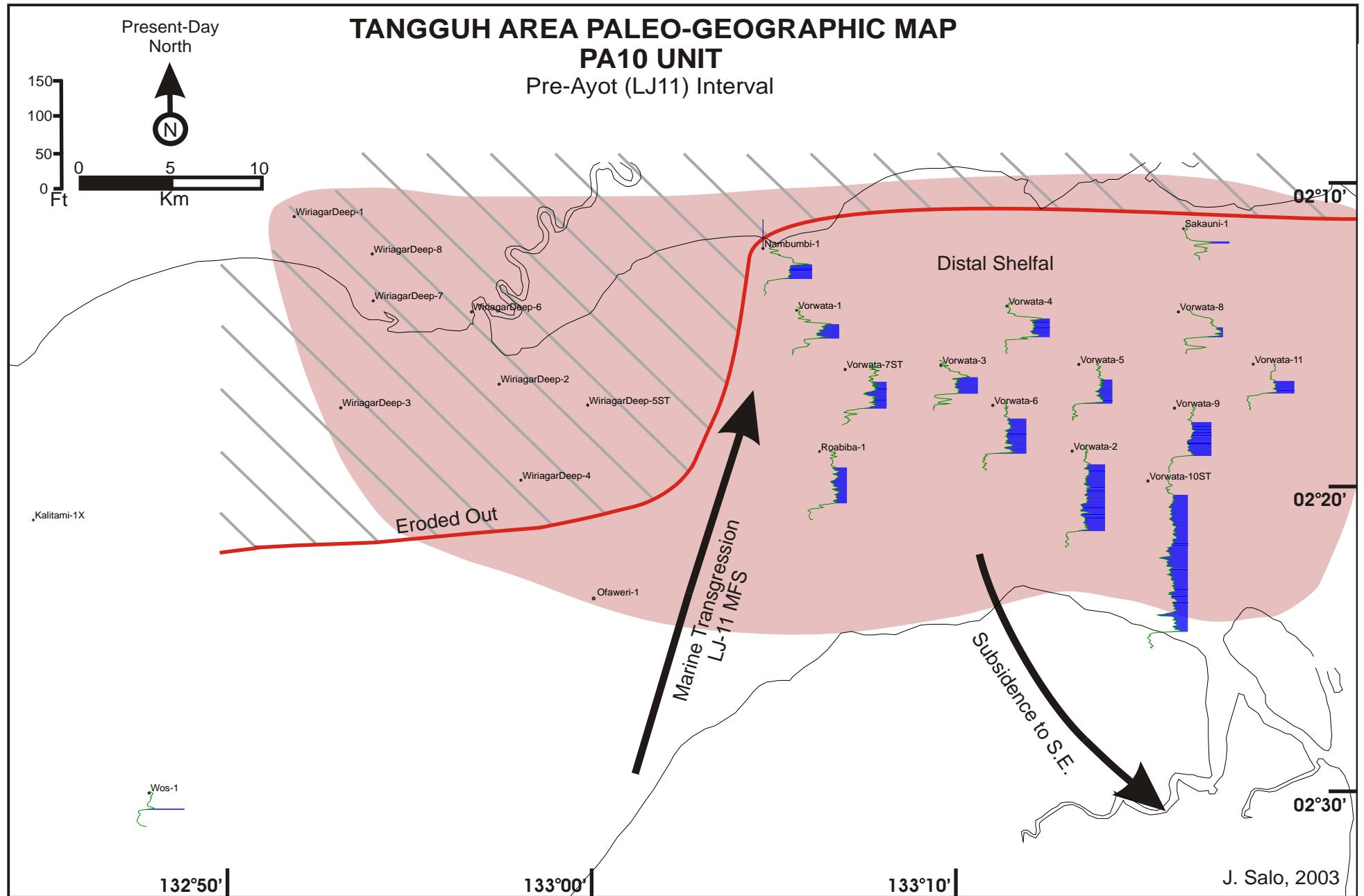


Figure 6.43: Paleogeographic map of the PA10 zone. Deepwater marine shales at the Vorwata area are interpreted as a major TST.

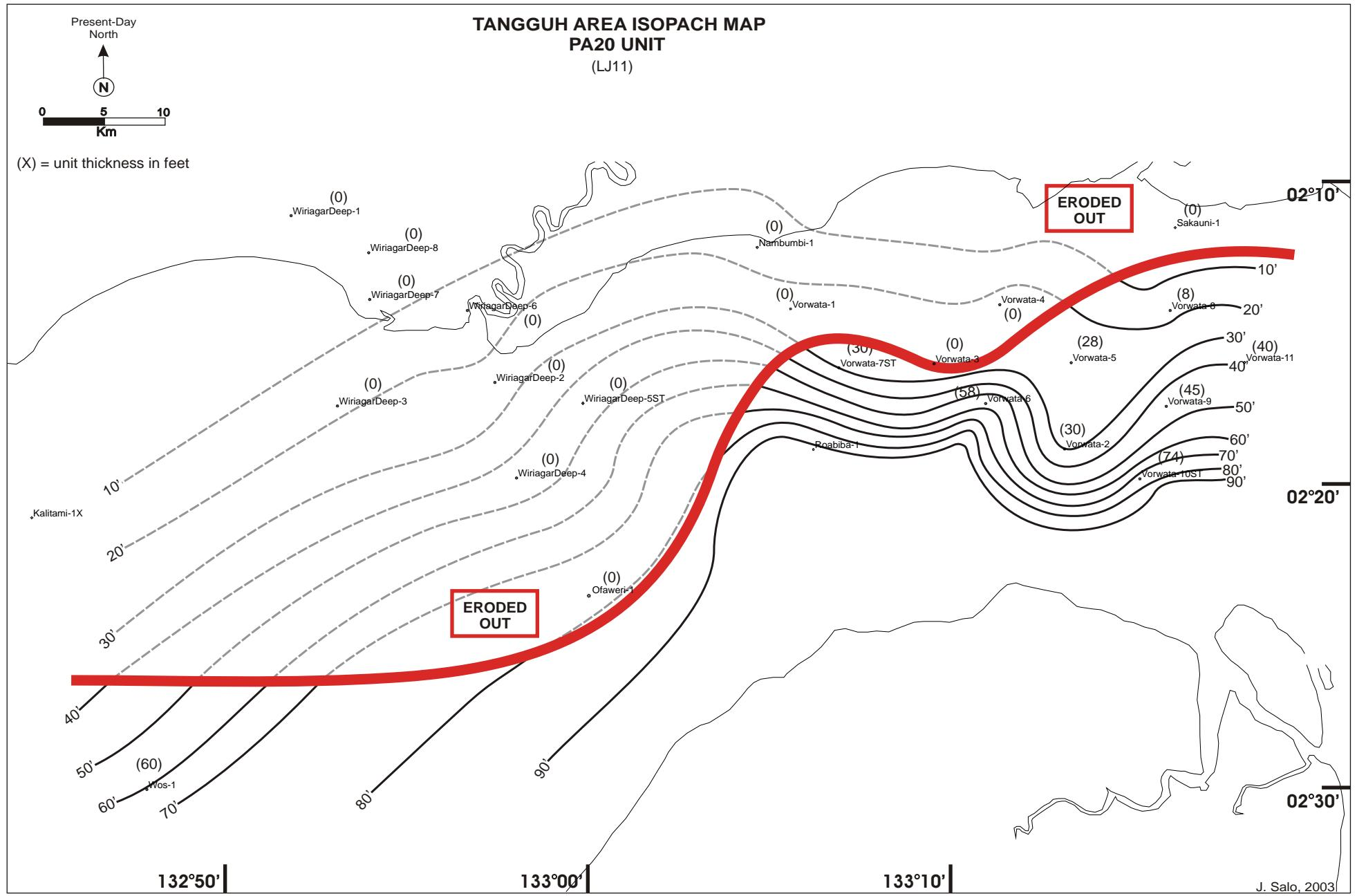


Figure 6.44: Isopach of the PA20 zone. CI = 10 ft.

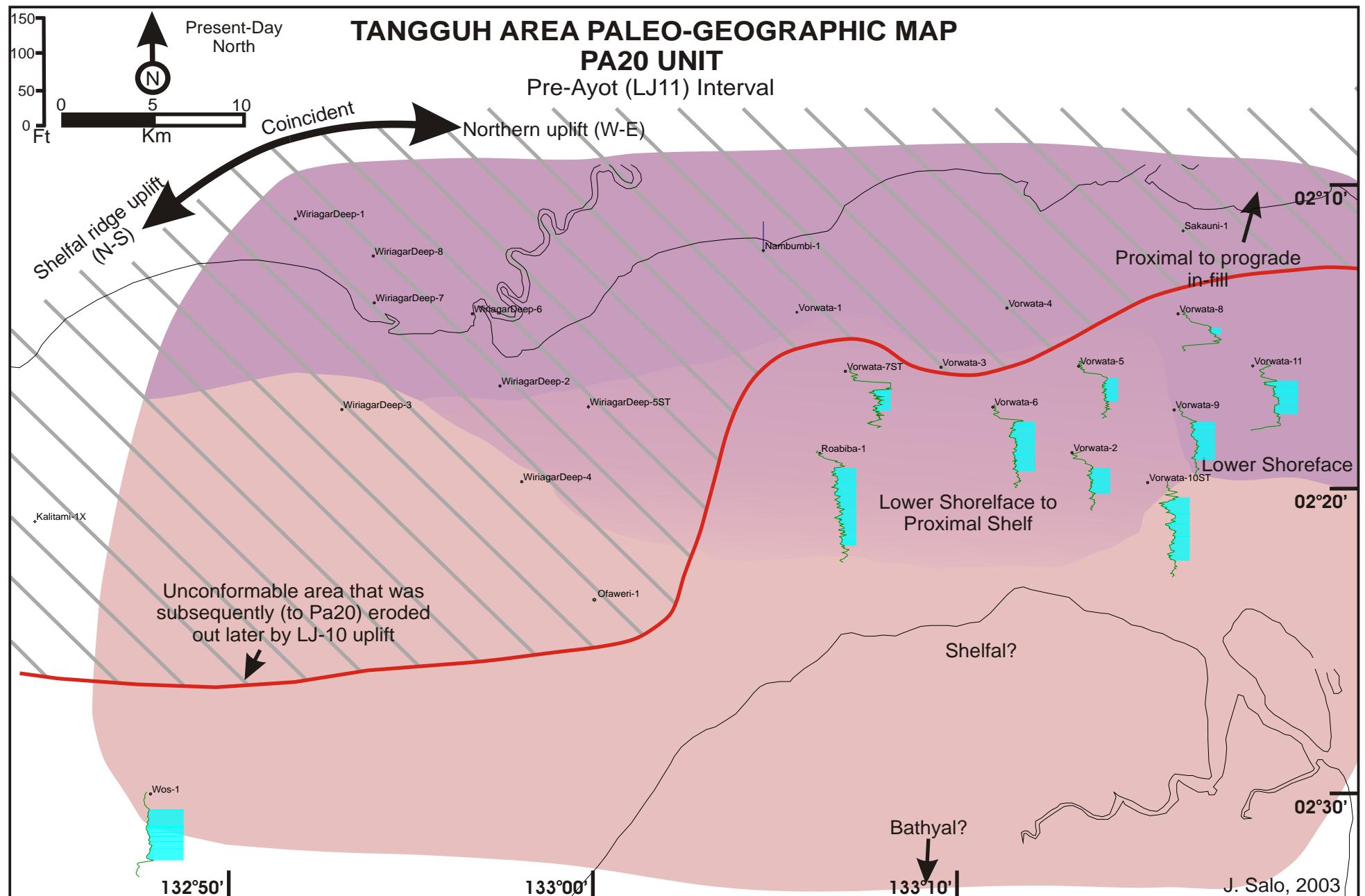


Figure 6.45: Paleogeographic map of the PA20 zone. Block tilting to the NW produces subsidence to the SE (and greater accommodation space).

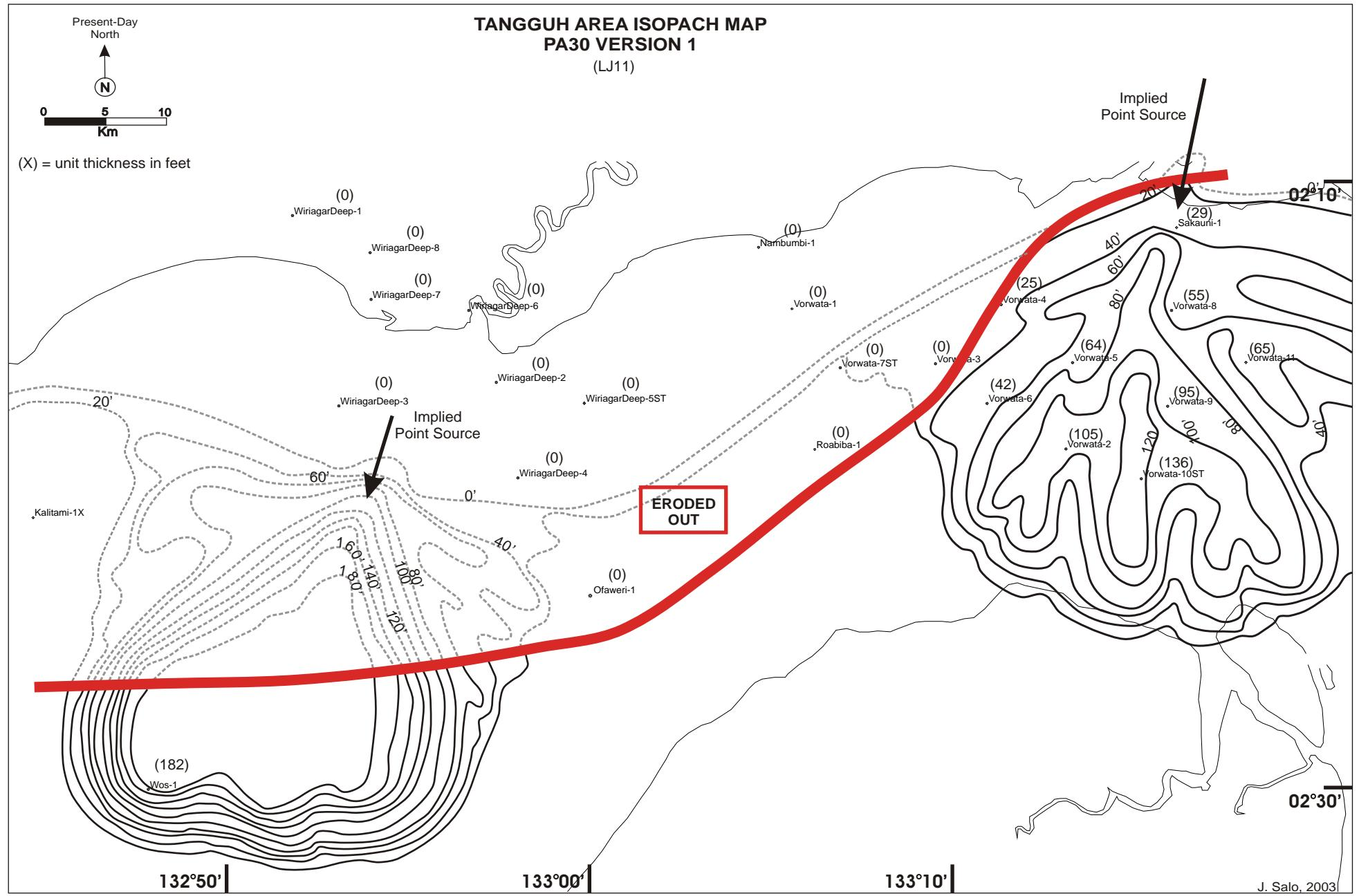


Figure 6.46: Isopach of the PA30 zone. This isopach version interpreted for PA30 sediments is based on two large prograde deltas (e.g. with the Mahakam River delta in Borneo as an analogue). 109

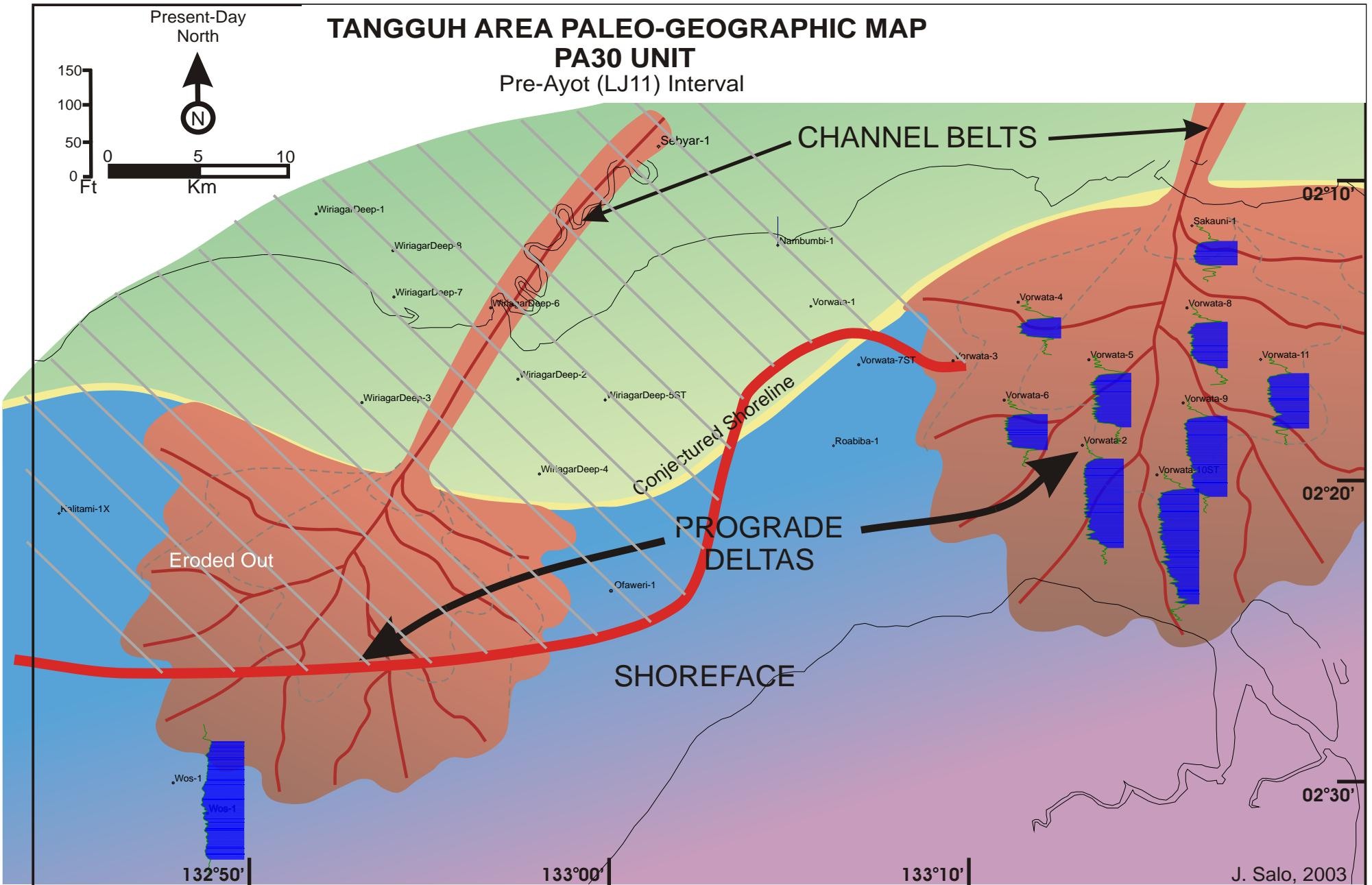


Figure 6.47: Paleogeographic map of the PA30 zone. Interpretation of the paleo-depositional facies is analogous to the Mahakam River delta in Borneo.

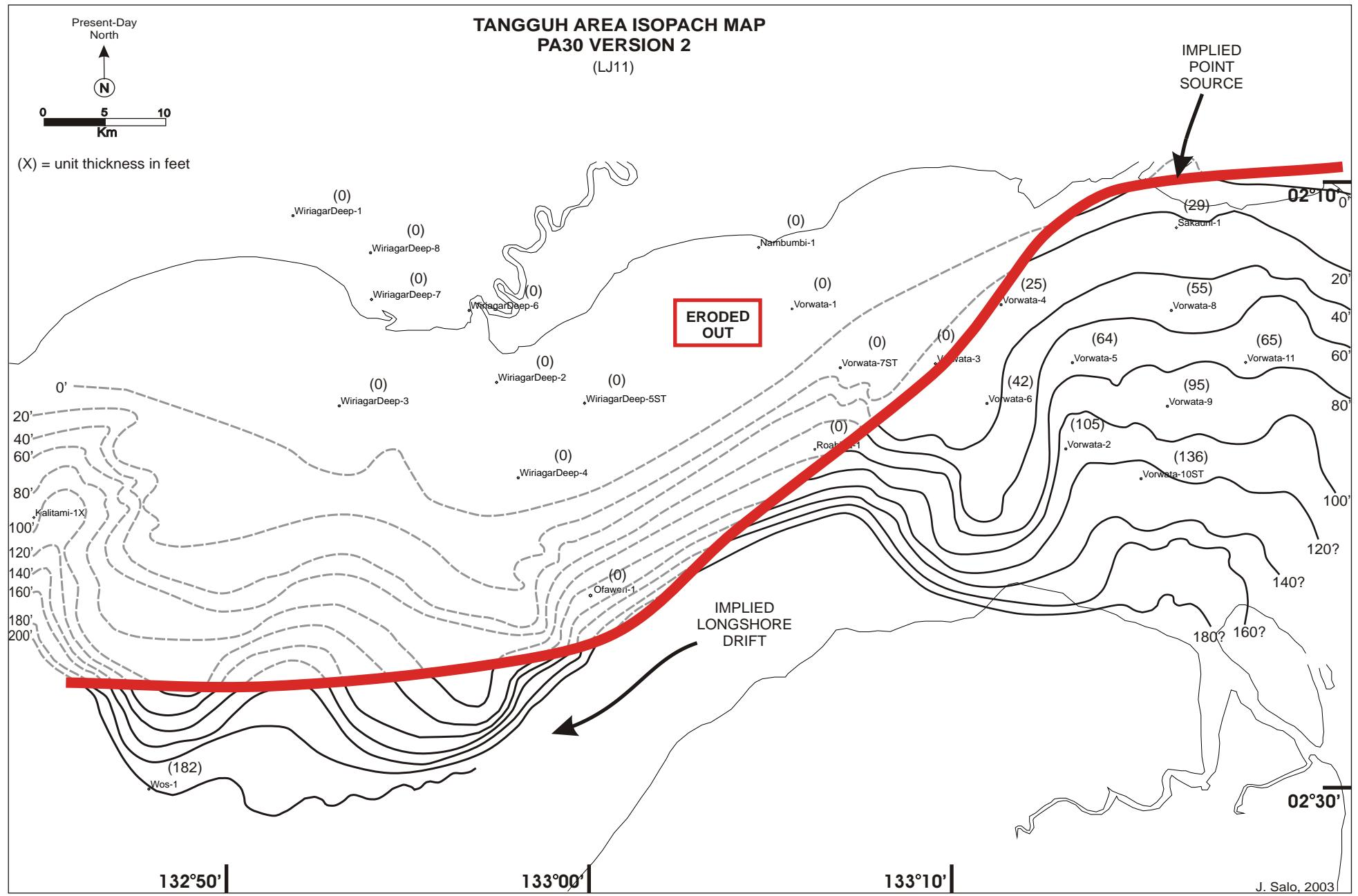


Figure 6.48: Isopach of the PA30 zone. Isopach style reflects a single areally widespread prograde delta, with deepwater currents moving large volumes of clastic sediments along the paleo-coastline towards the W-SW.

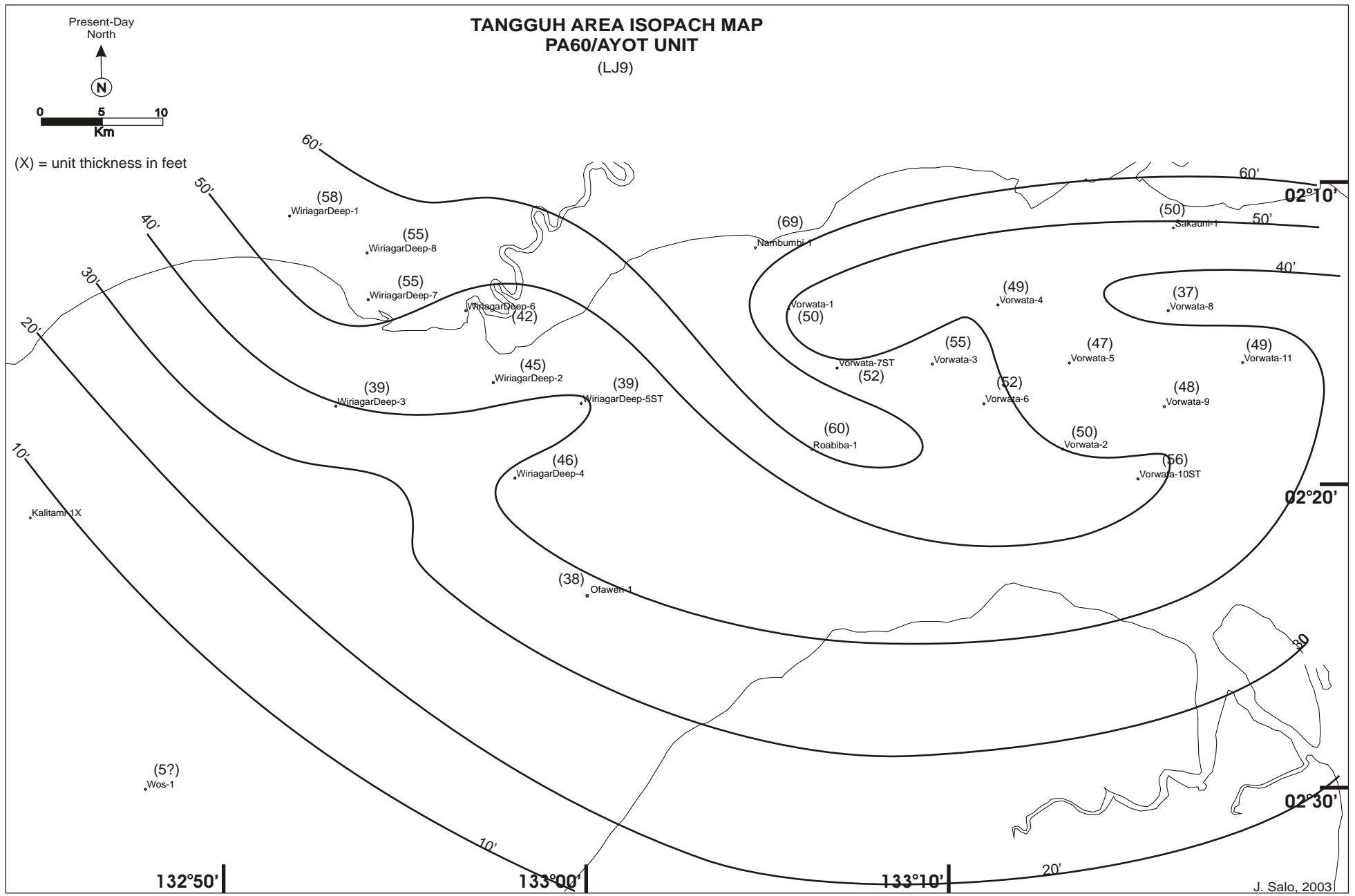


Figure 6.49: Isopach of the Ayot Limestone zone. CI = 10 ft.

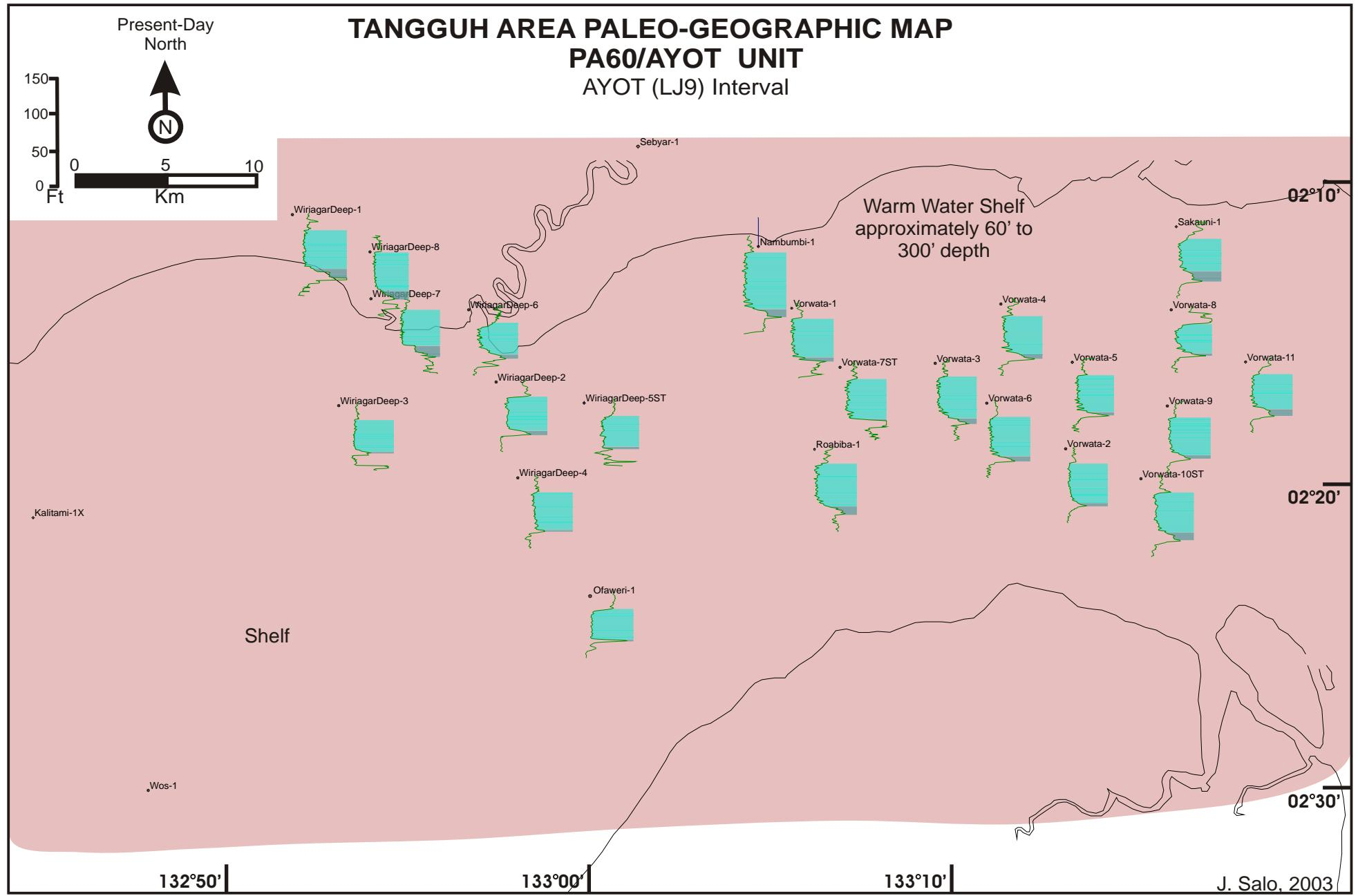


Figure 6.50: Paleogeographic map of the Ayot zone depositional facies at Tangguh. This stratigraphic unit overlies an erosional unconformity (LJ-10).

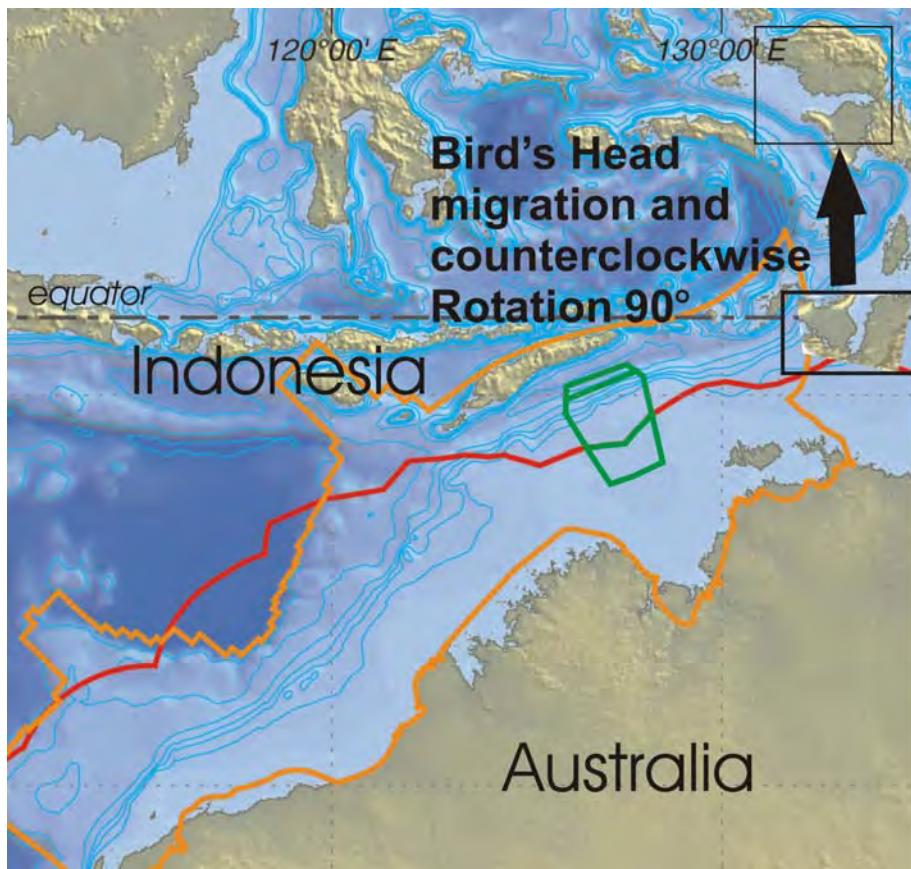


Figure 6.51: Simplified map showing areas of extensional rifting in the Jurassic and Cretaceous (outlined in orange) for the Lhasa, West Burma, and Argo blocks from the Australian-New Guinea Plate. Proposed migration and counterclockwise rotation of Bird's Head microplate during the Late Jurassic (Tithonian) to Miocene is outlined in black boxes with arrow (modified after Longley et al, 2002).

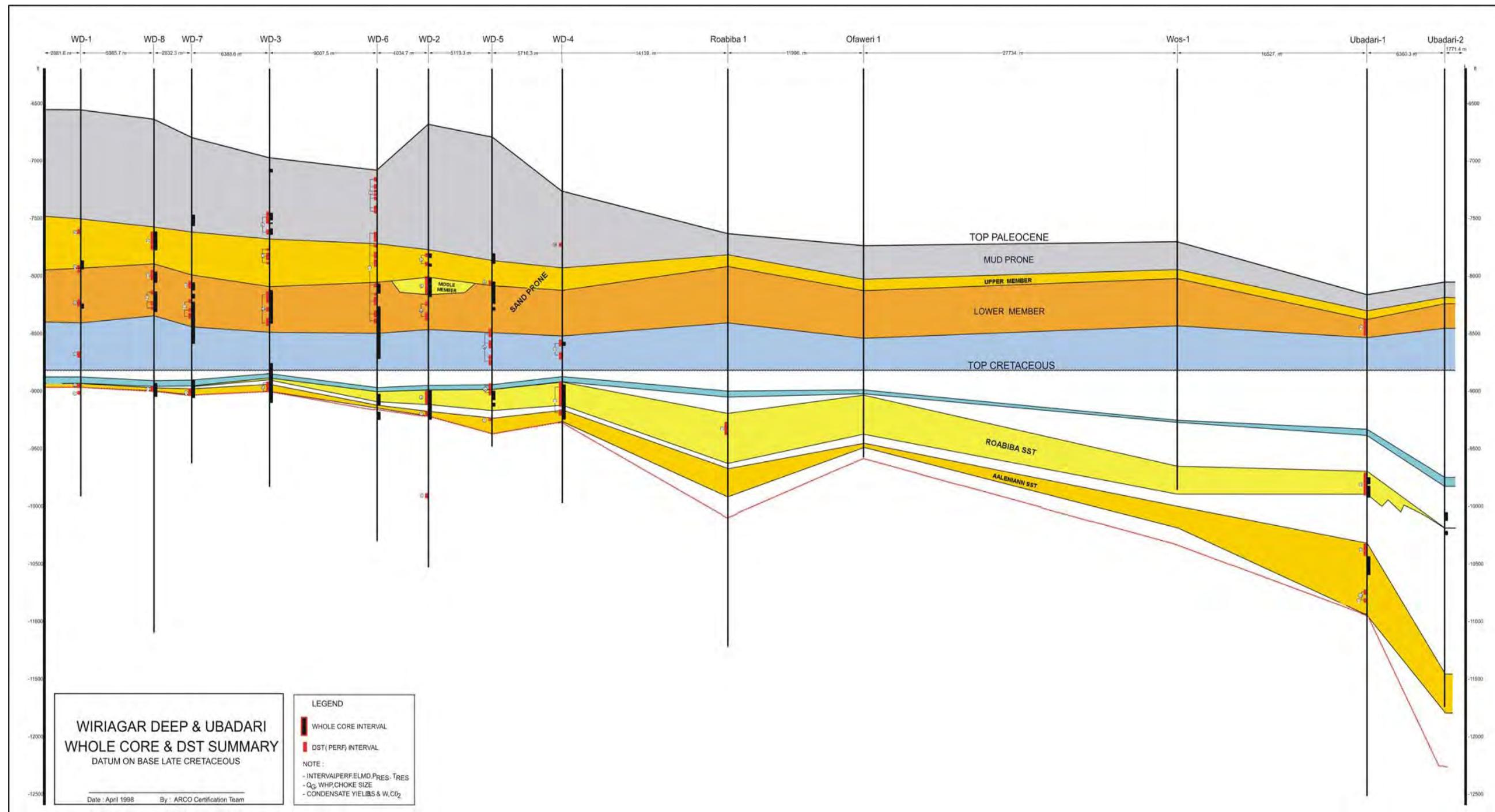


Figure 7.1: Cross-sectional schematic diagram of all Wiriagar Deep and Ubadari wells showing whole core and DST coverage through stratigraphic intervals and their relative positions within stratigraphic units (Bulling, et al., 1998). The cross-section is flattened on the Base Late Cretaceous. Whole core intervals are represented by black bars and DST intervals by red bars.

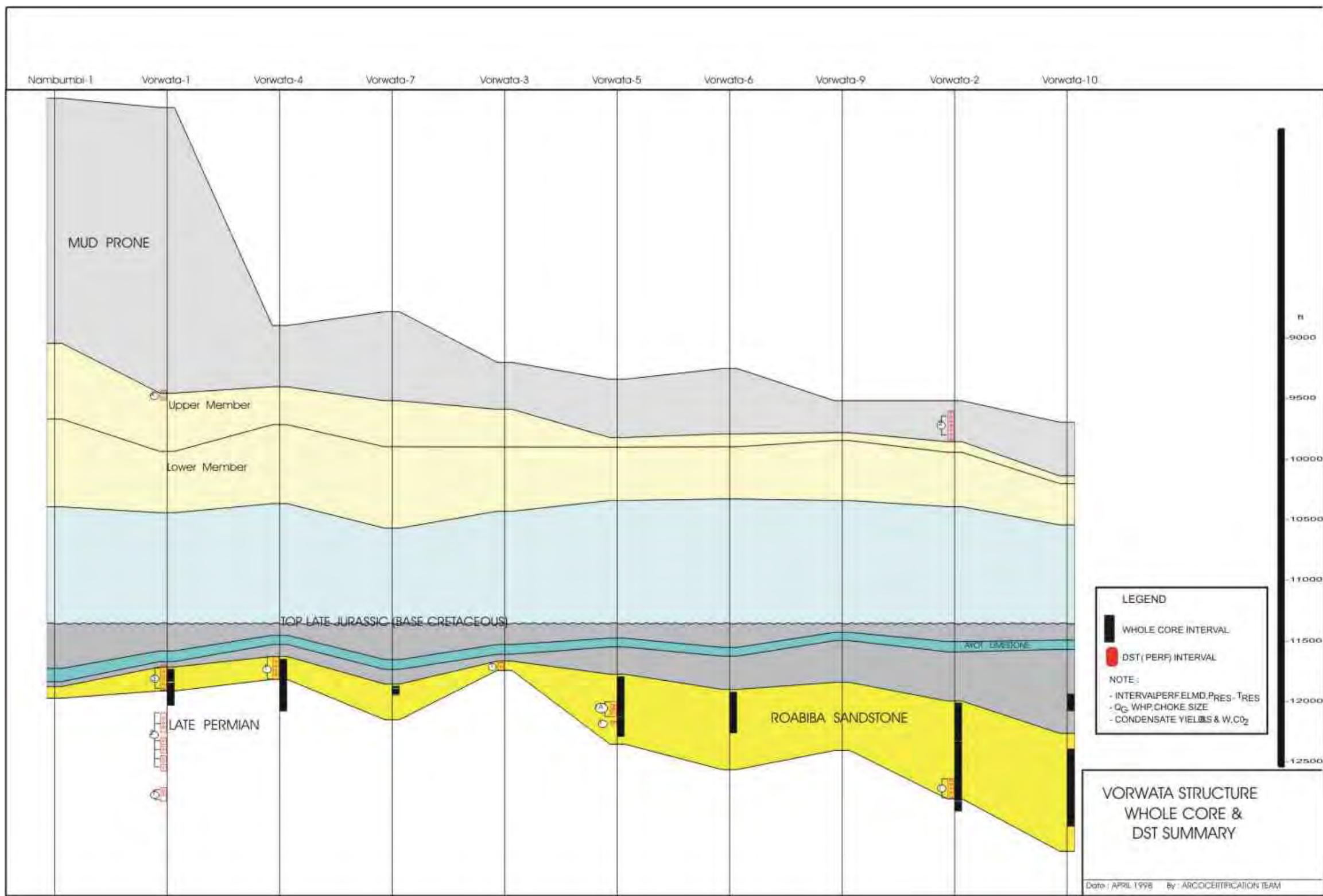


Figure 7.2: Cross-sectional schematic diagram of Vorwata wells showing whole core and DST coverage through stratigraphic intervals and their relative positions within the various stratigraphic units (Bulling, et al., 1998). The cross-section is flattened on the Base Late Cretaceous, with whole core intervals are represented by black bars and DST intervals by red bars.

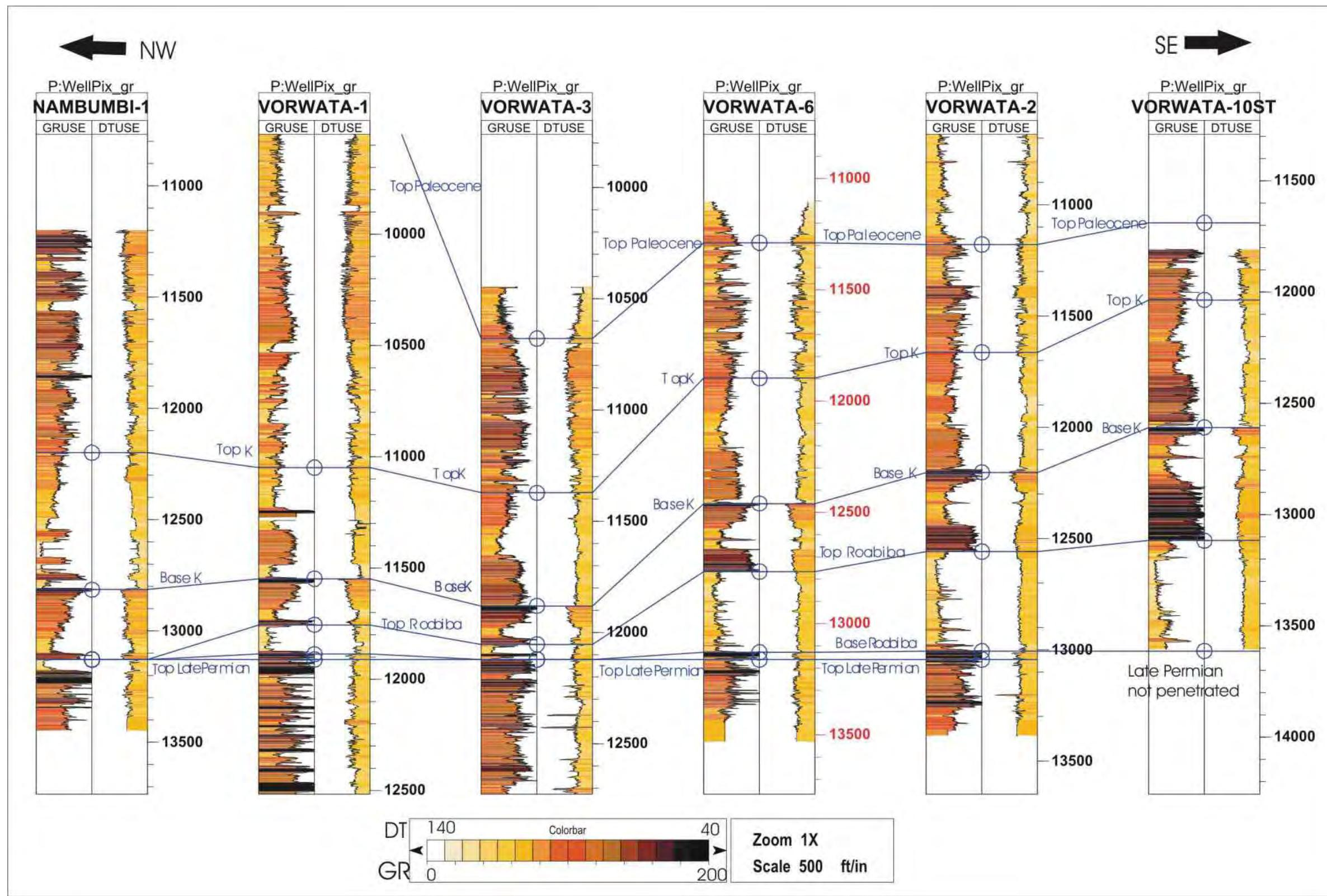


Figure 7.3: Wireline log correlation cross-section of selected wells from NW to SE over the Vorwata structure, flattened on the Top Permian as the datum. Cross-section shows thinly bedded fluvio-deltaic sandstone reservoirs of the Late Permian over Vorwata. DST testing showed the sandstone reservoirs to be relatively tight compared with the Jurassic reservoirs. Gamma-ray (GR) values in GAPI scaling and sonic (DT) in $\mu\text{s}/\text{ft}$ scaling are in-filled within the respective GR and DT curves (see colorbar above).

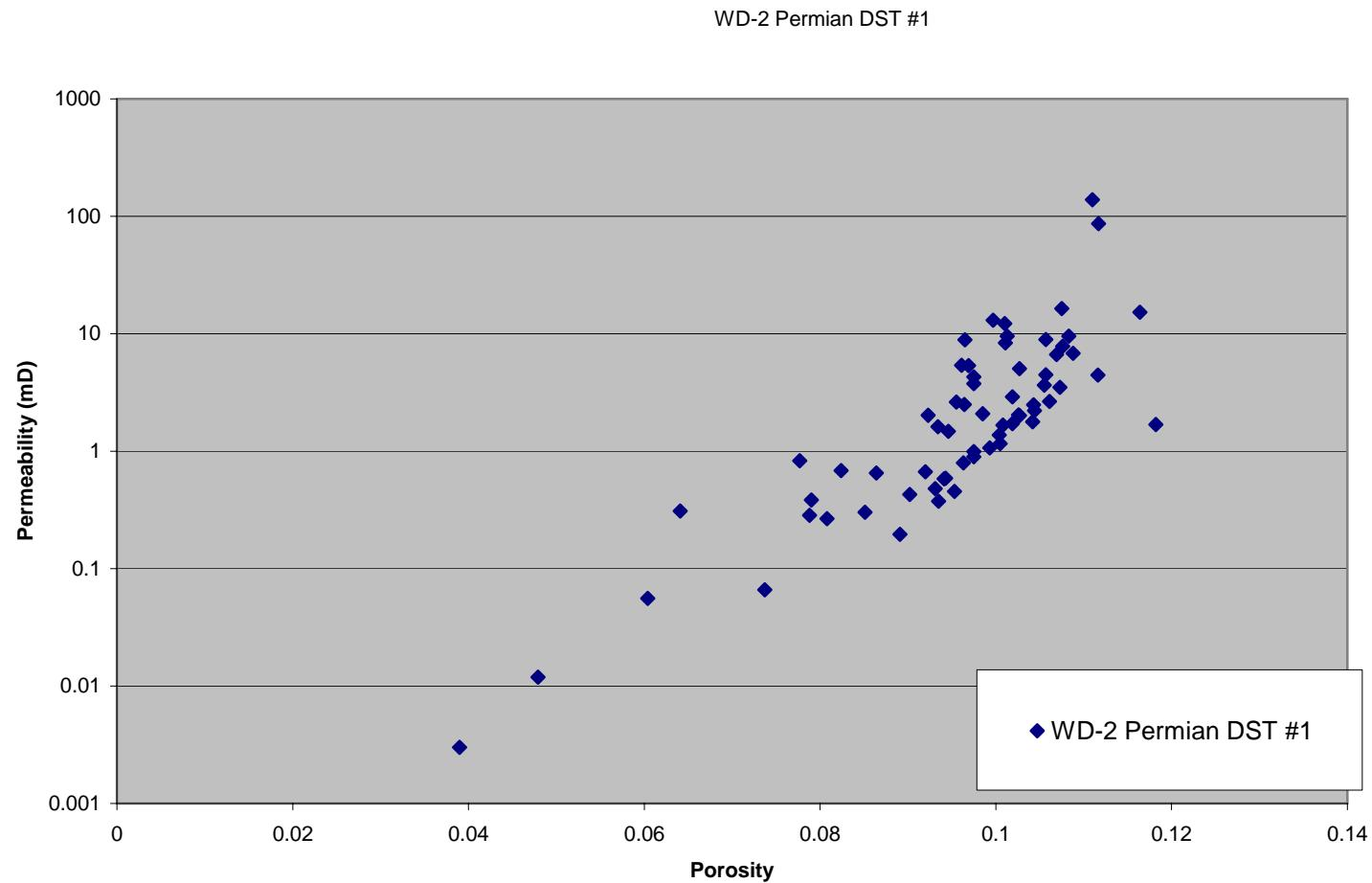


Figure 7.4: Crossplot of Late Permian Succession fluvial sandstone reservoir porosity and permeability from wireline logs, calibrated to core plugs taken in the WD-2 DST interval (DST #1: 9455 ft to 9487 ft).

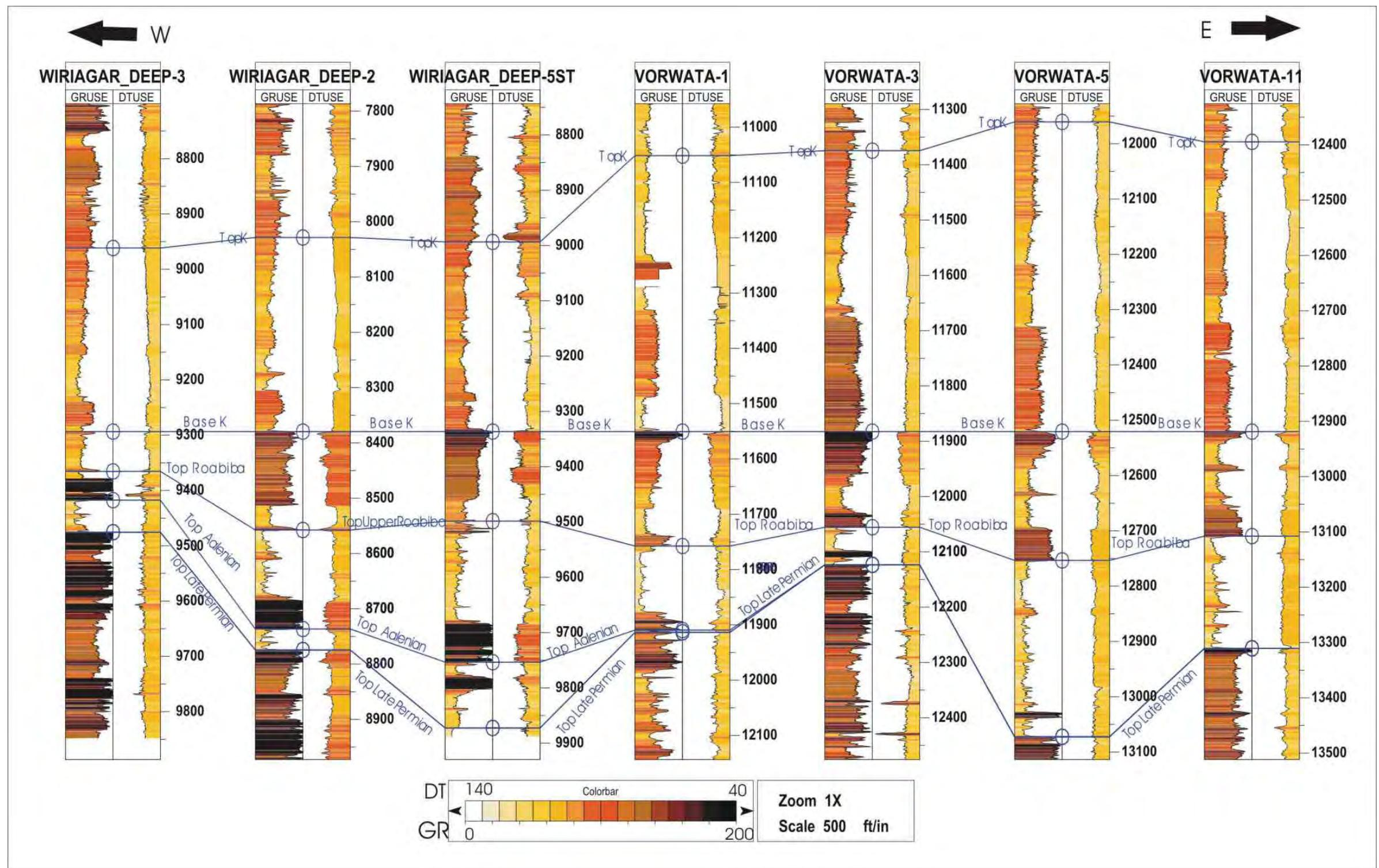


Figure 7.5: Wireline log correlation cross-section of selected wells from Wiriagar Deep to Vorwata structure, flattened on the Base Late Cretaceous as the datum. Cross-section runs from roughly west to east and showing both the Aalenian Sandstone Formation reservoir and the Roabiba Sandstone Formation reservoir at Wiriagar Deep wells, but only the Roabiba reservoir present at Vorwata. Gamma-ray (GR) values in GAPI scaling and sonic (DT) in $\mu\text{s}/\text{ft}$ scaling are in-filled within the respective GR and DT curves (see colorbar above).

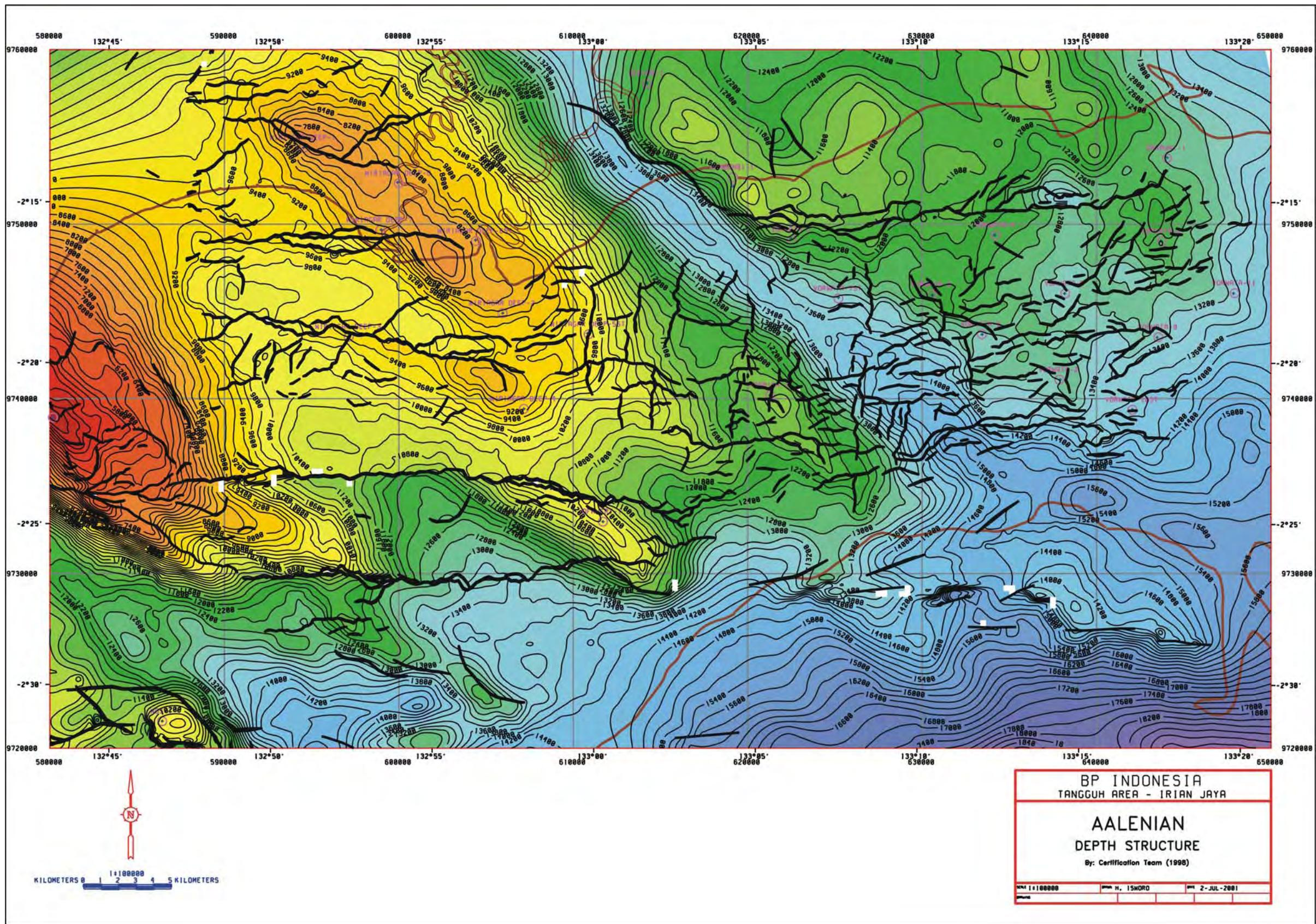


Figure 7.6: Top Aalenian Sandstone Formation reservoir depth structure map for Tangguh area (courtesy BP, 2001). Both coordinates (northing and easting) and latitude/longitude are displayed.

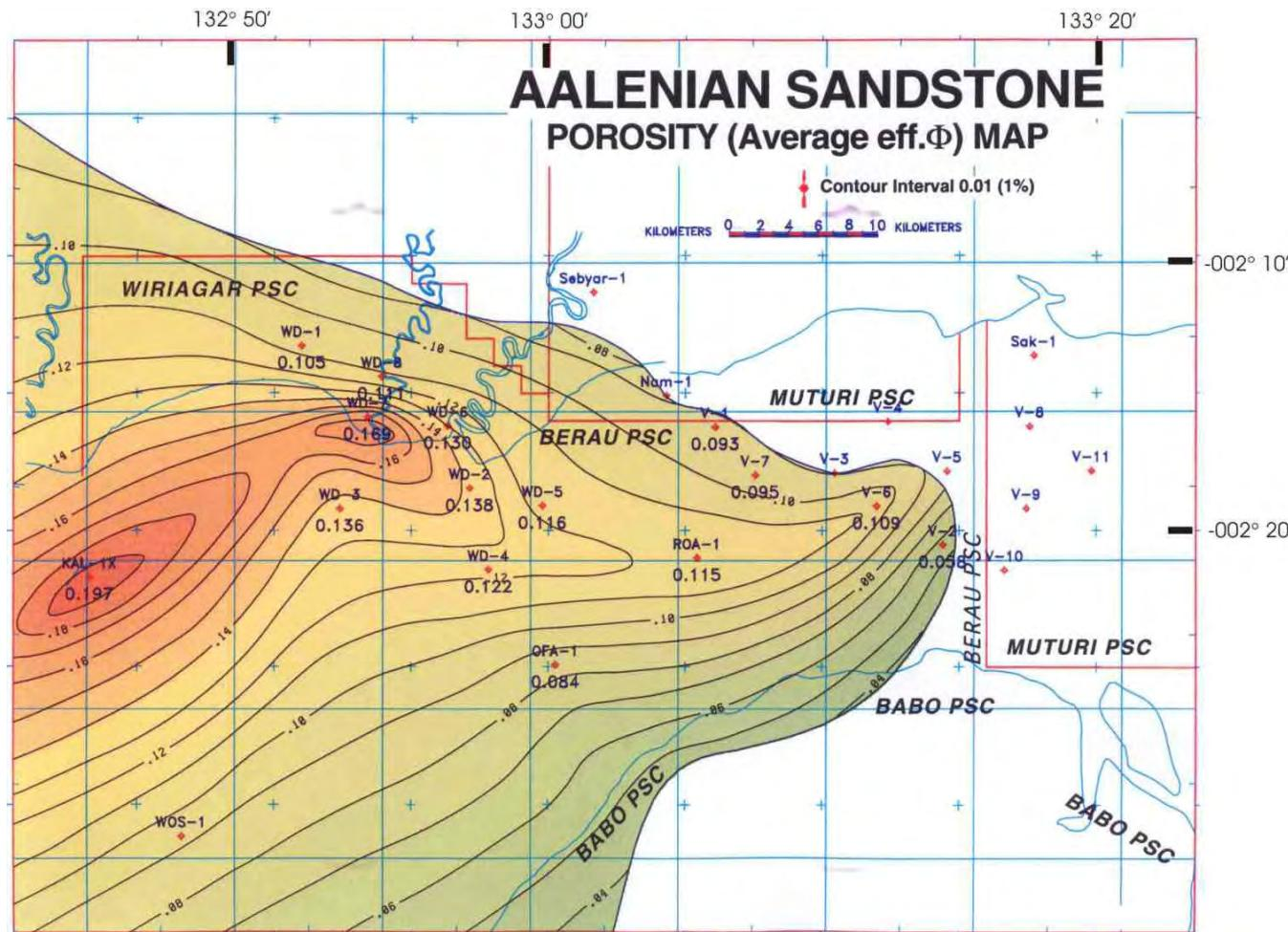


Figure 7.7: Aalenian Sandstone Formation reservoir effective porosity map based on results from petrophysical evaluation (Petcom) of wells (calibrated to whole core plugs). Note mapping of Aalenian at the V-1, V-7, and V-2 wells. Subsequent palynological analyses of these wells indicated no Aalenian sandstone present at their respective locations. This would have slightly changed the onlapping areal extent of the Aalenian at the northeastern pinch-out margin slightly, moving the zero pinch-out nose tapered at V-6 closer towards the Roabiba #1 (labelled ROA-1) well location (Bulling, et al., 1998).

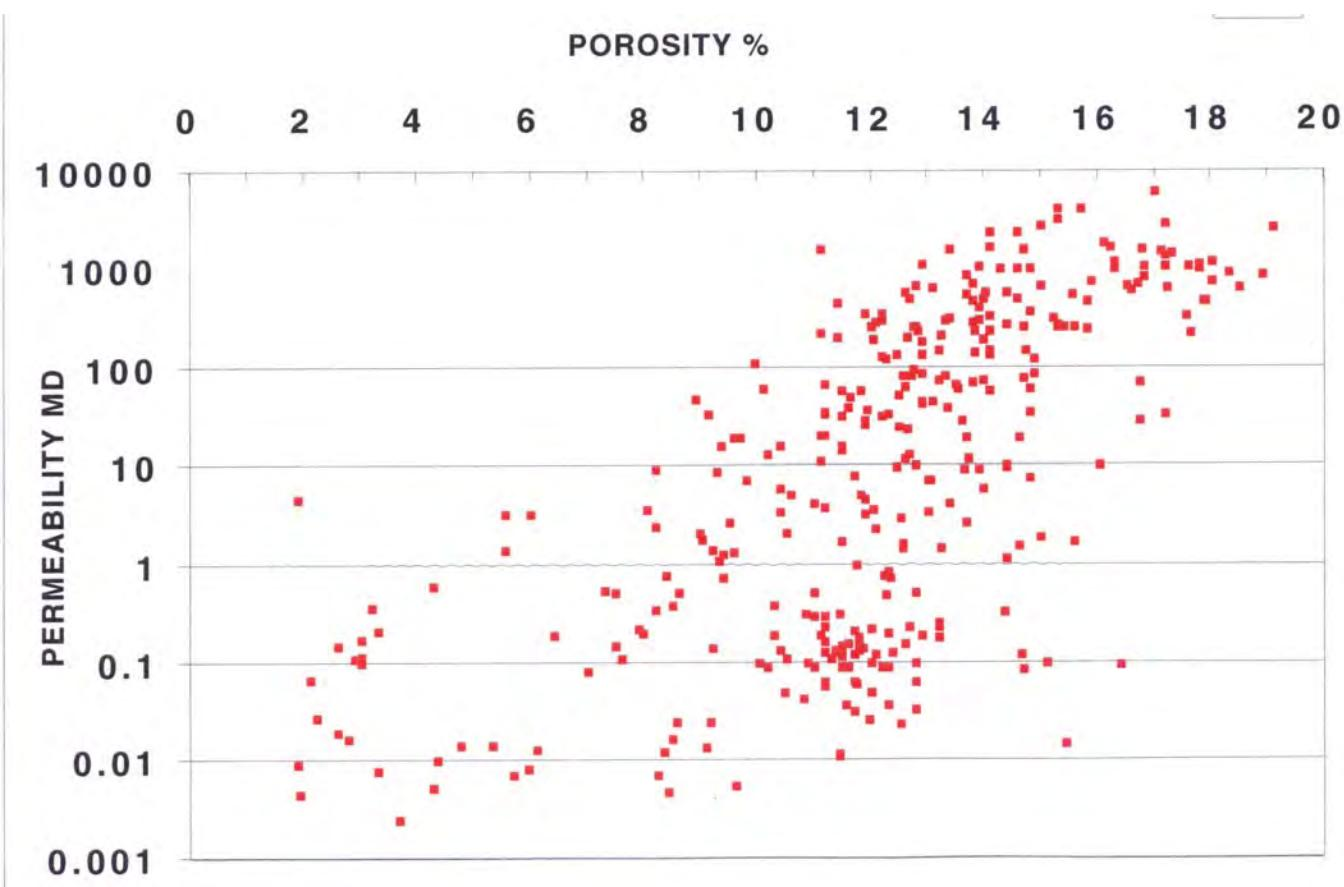


Figure 7.8: Aalenian Sandstone Formation reservoir porosity and permeability (corrected to NOB 800 psi) cross-plotted from whole core plugs on all Wiriagar Deep wells (Bulling, et. al., 1998).

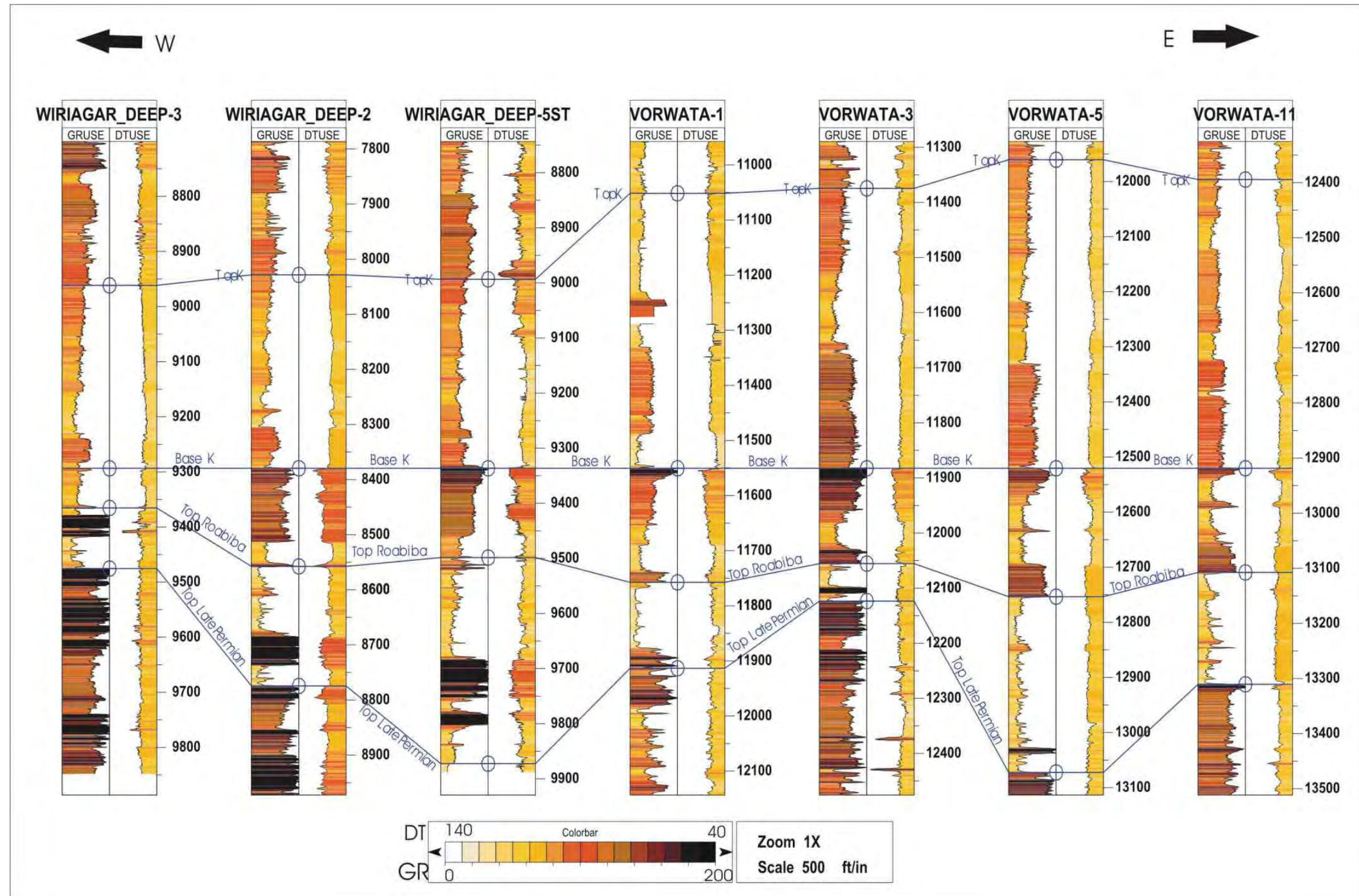


Figure 7.9: Wireline log correlation cross-section of selected wells from Wiriagar Deep to Vorwata structure, flattened on the Base Late Cretaceous as the datum. Cross-section runs from roughly west to east and shows a relatively massive Roabiba Sandstone Formation across the Wiriagar Deep and Vorwata structures, with thinning locally at Vorwata #3 (and V-7 and V-1) due to an MJ-2 erosional event. Gamma ray and sonic are presented for correlation purposes, with the scaling for the gamma-ray (GRUSE) and sonic (DTUSE) color infill shown in the key. The high gamma peaks below the top of the reservoir on some wells, such as WD-5, are not due to shales but rather to 'hot' sandstone streaks.

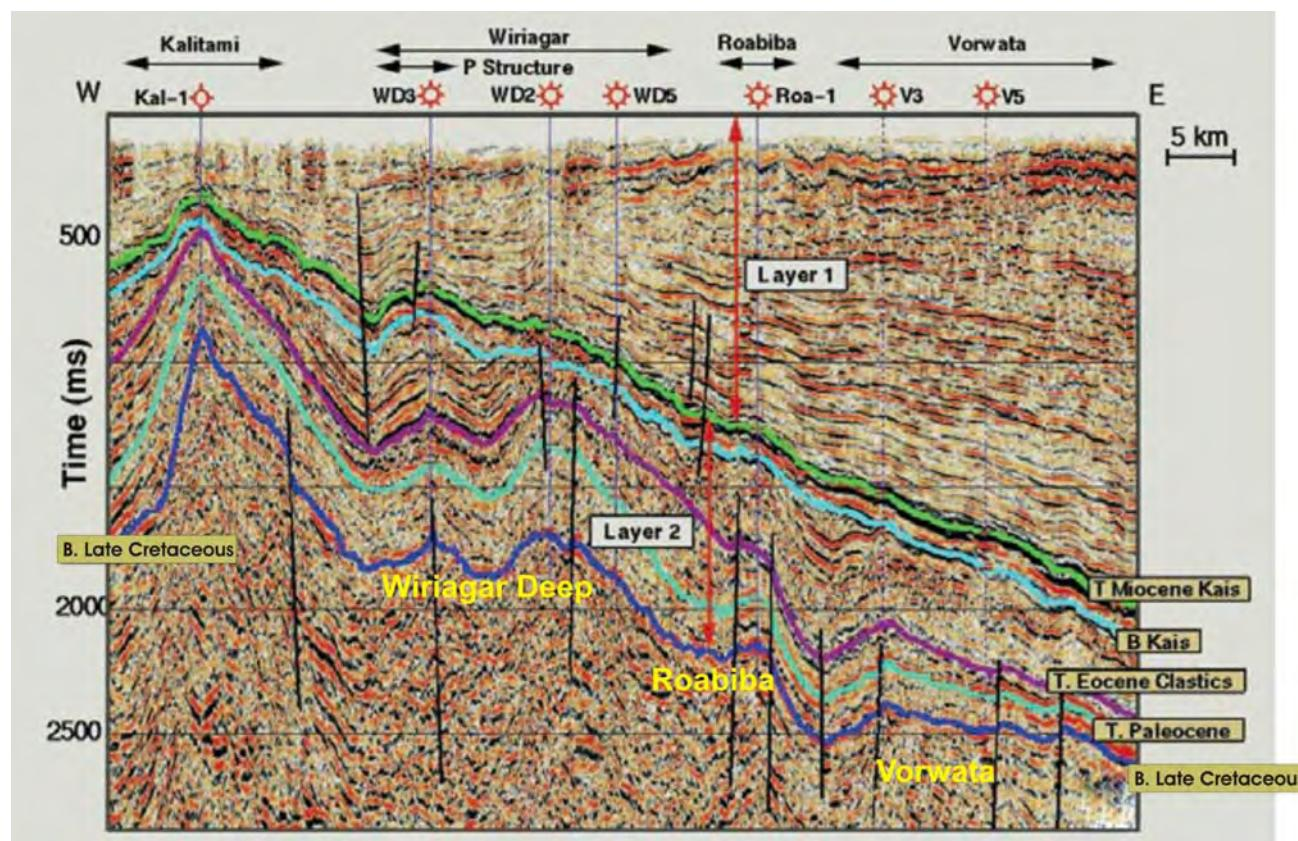


Figure 7.10: Interpreted seismic volume traverse from 3D seismic survey (1997-1998), W to E through Wiriagar Deep and Vorwata areas. Selected well locations intersected are indicated. See Figure 2.3 for map location of wells displayed on the seismic line above. Gas accumulations wells are indicated by star-burst well symbols. Poor resolution with depth due to scattering of seismic energy in thick near-surface NGLG yields poor resolution for interpretation of horizons below the NGLG. The Near-Top Late Permian, identifiable over part of the Tangguh area, is not interpreted here due to the poor resolution (Keho and Samsu, 2002).

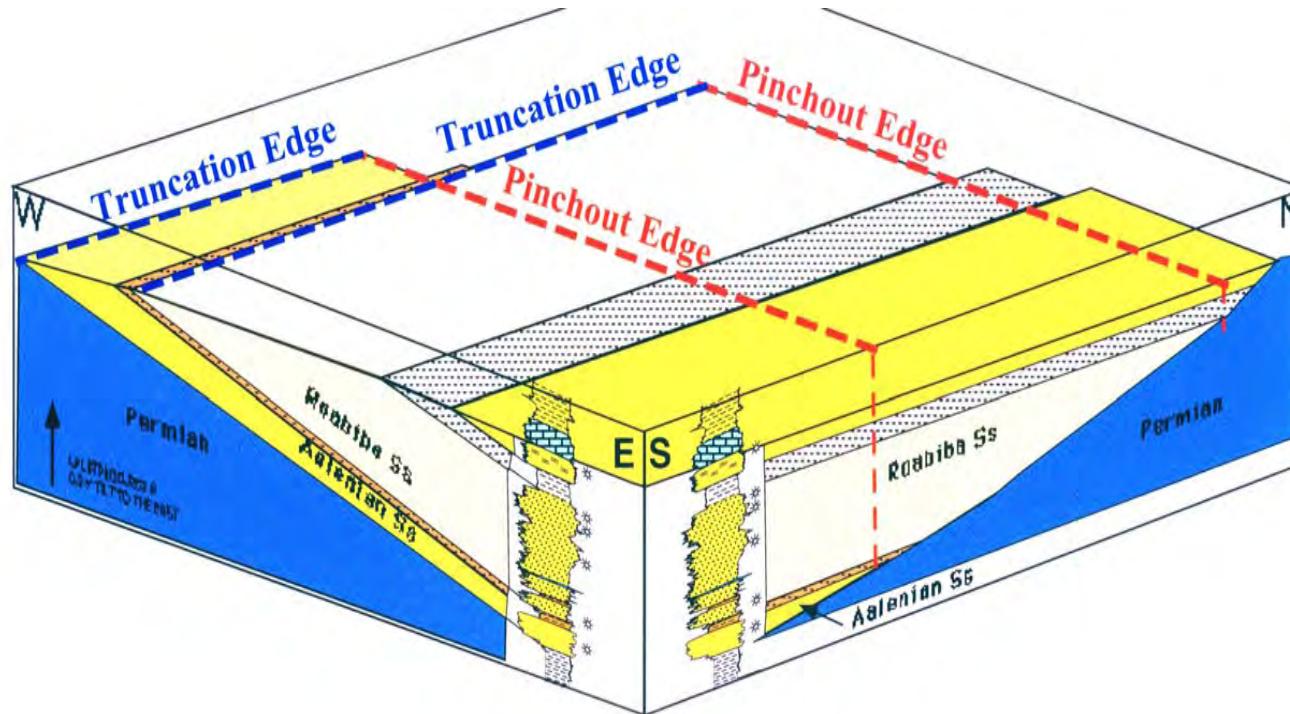


Figure 7.11: Geologic schematic diagram showing the relationship between simultaneous Jurassic sandstone unit onlap and erosional truncation to the north and the west (Bulling, et al., 1998).

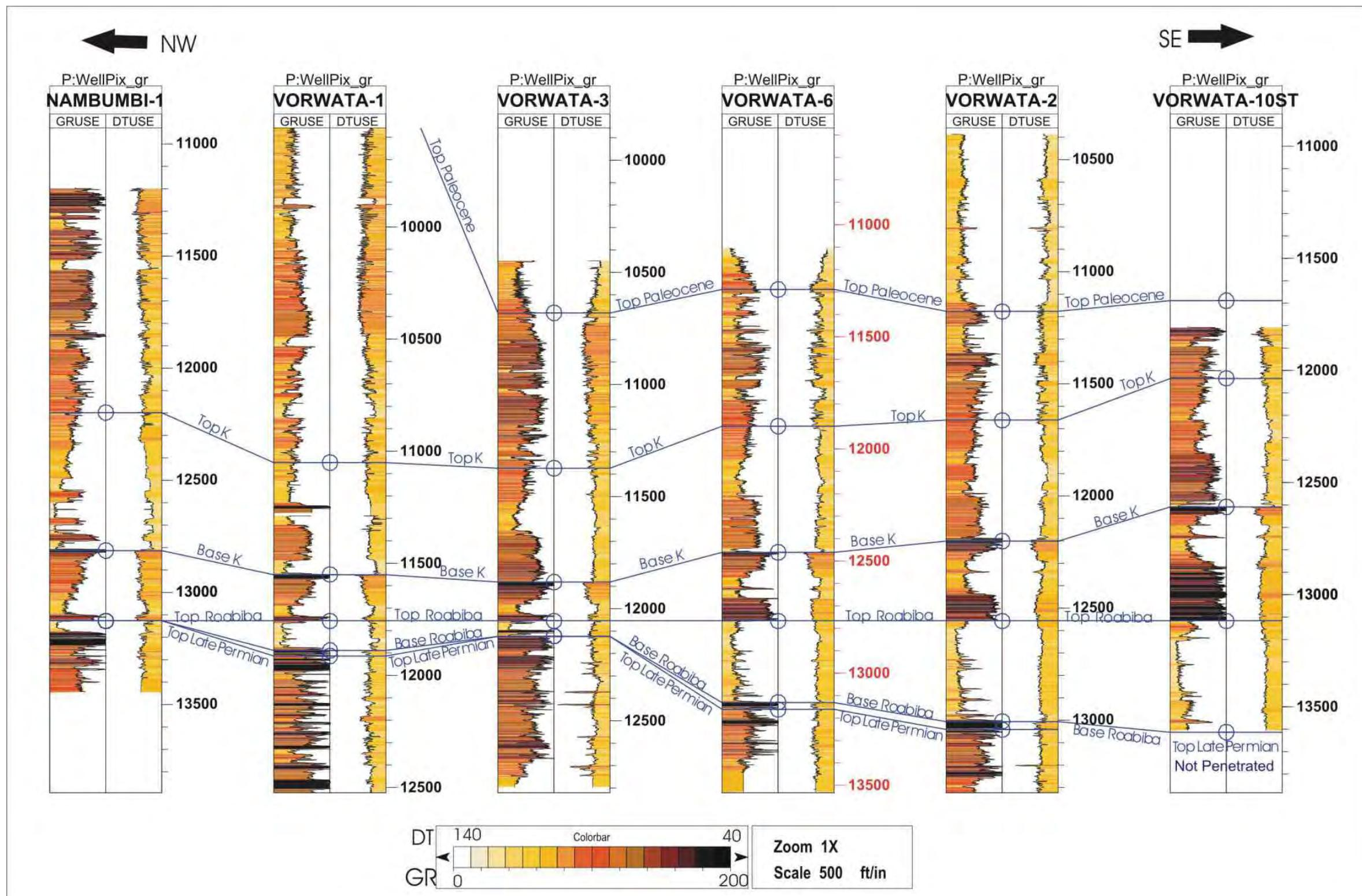


Figure 7.12: Wireline log correlation cross-section of selected wells from NW to SE across the Vorwata structure, flattened on the Top Roabiba Sandstone Formation as the datum. The thickening of the Roabiba Sandstone Formation reservoir towards the SE, with improving reservoir quality, is clear at the Vorwata #2 and Vorwata #10 well locations. Note that V-10 well did not drill through to the base of the Roabiba Sandstone Formation because the GWC had already been encountered. Gamma-ray (GRUSE) and sonic delta-T (DTUSE) curves are color-filled with the respective values (as per the legend scale).

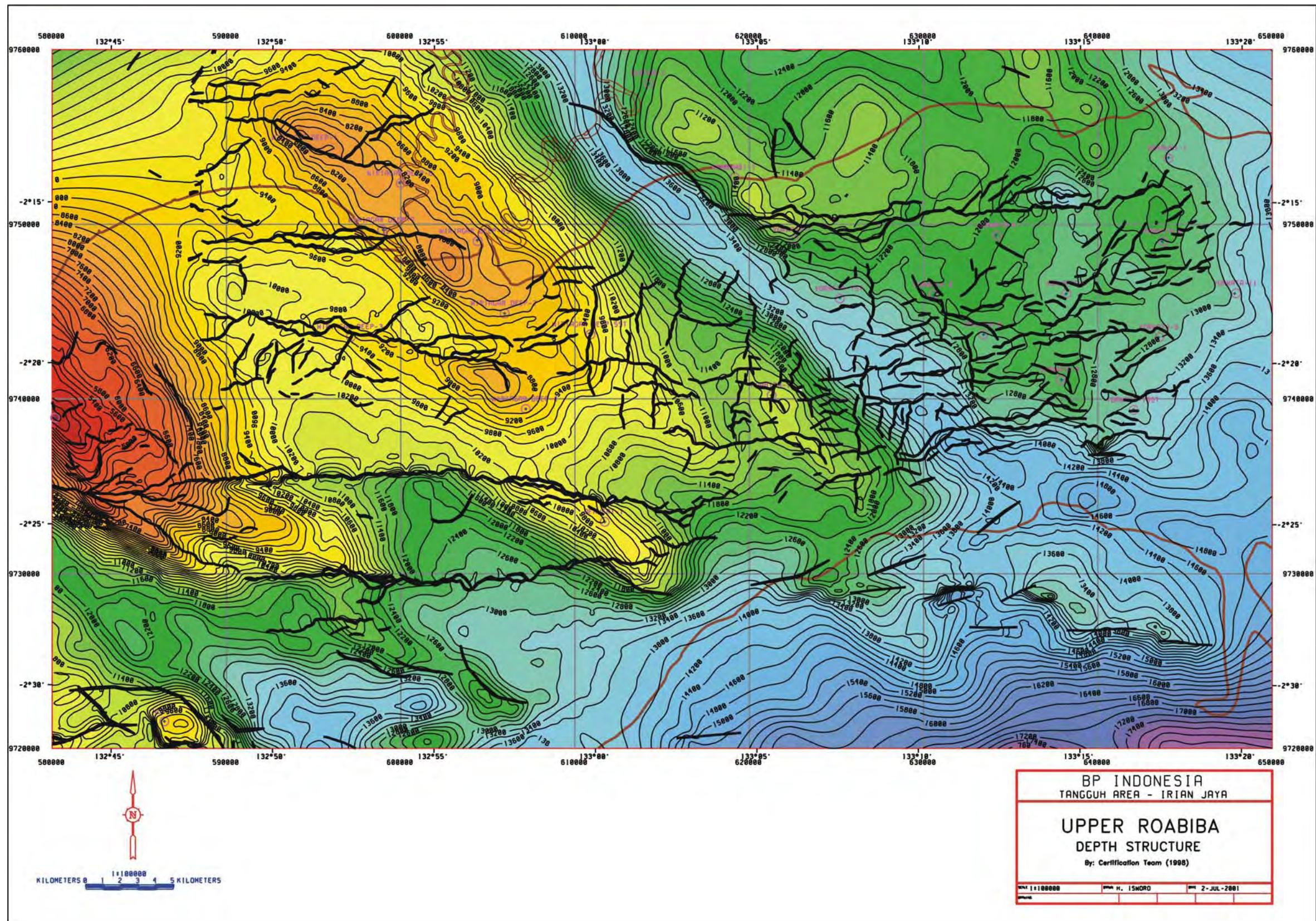


Figure 7.13: Top Roabiba Sandstone Formation depth structure map for the Tangguh area (courtesy of BP, 2001). The surface and faults have been phantomed down from the Base Late Cretaceous due to poor seismic resolution. Black line segments represent fault polygons, and Bintuni Bay coast is shown in red. CI = 200 ft. scaled from yellow for shallower depths to purple for deeper depths.

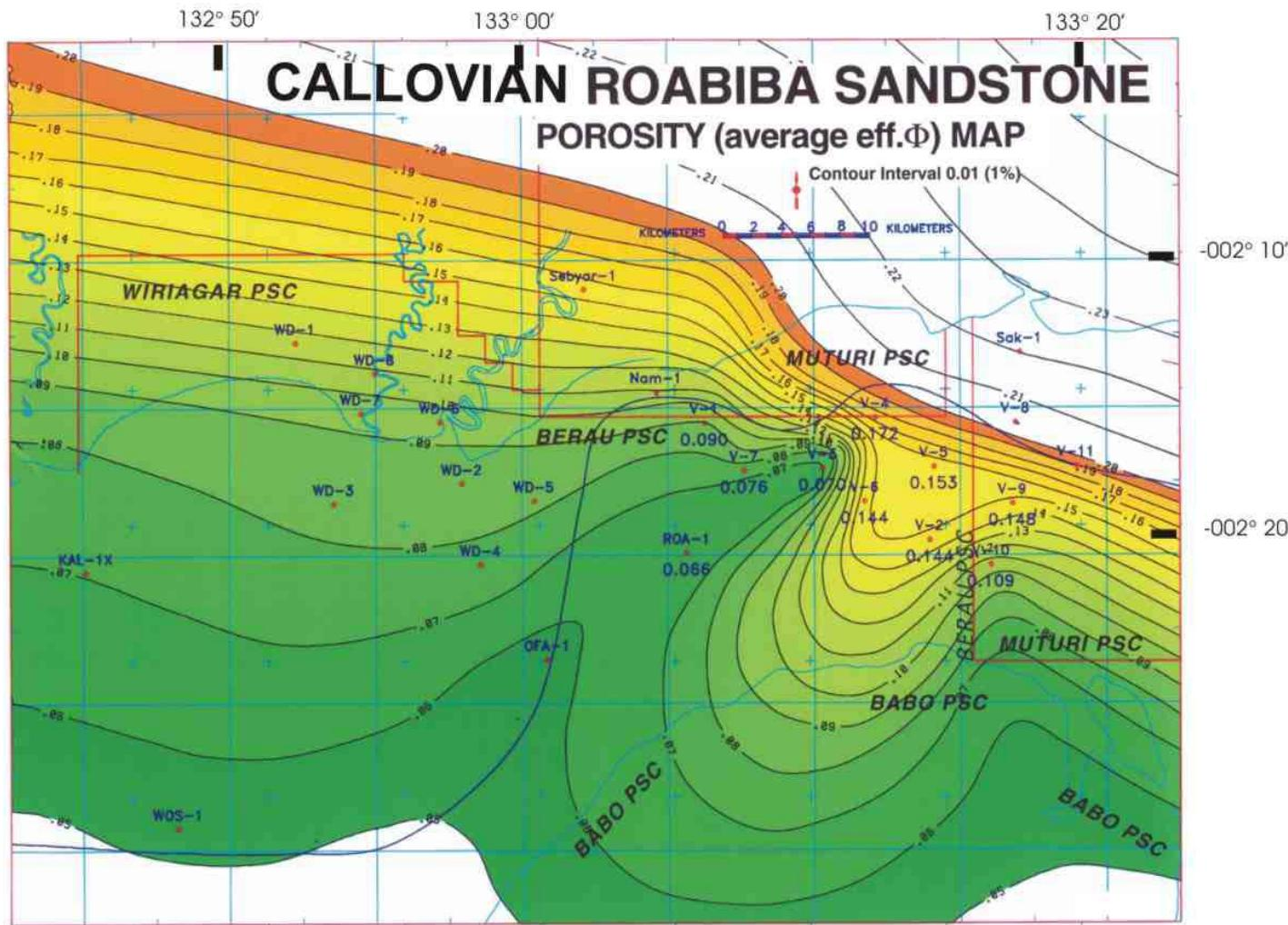


Figure 7.14: Map of effective porosity for the Callovian Roabiba Sandstone Formation in the Tangguh area (C.I. = 1% Average Effective Porosity). Rivers and coastlines are shown in blue, well locations and concession boundaries in red. Dark blue line shows the reservoir truncation limit cross-cutting the contour intervals in black, east of Ofaweri #1 (OFA-1). Actual average reservoir effective porosities are given at each well where the unit is present (Bulling, et al., 1998).

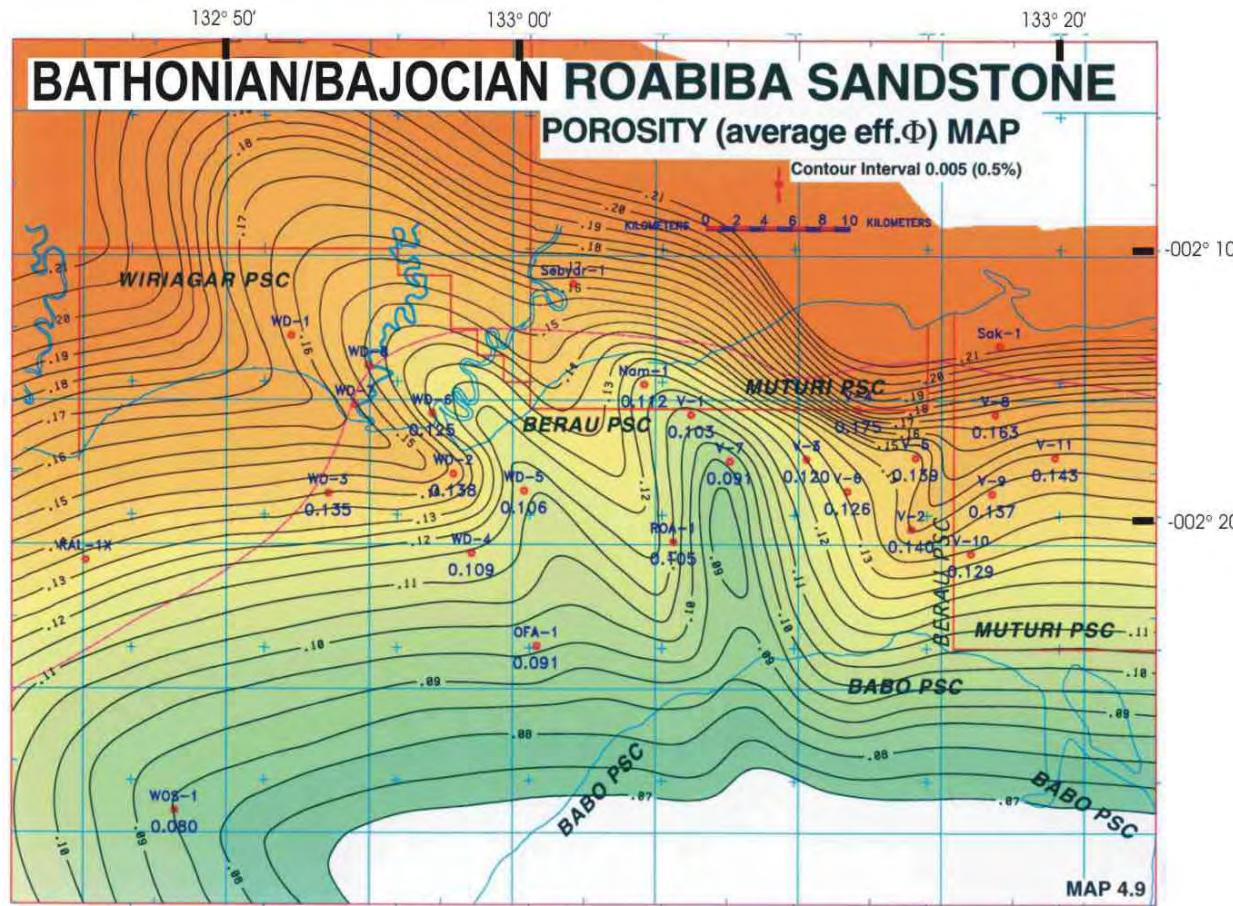


Figure 7.15: Map of average effective porosity for the Bathonian/Bajocian Roabiba Sandstone Formation in the Tangguh area (C.I. = 0.5% Average Effective Porosity). Rivers/coastlines are shown in blue, well locations/PSC boundaries in red. Dark red line shows the reservoir truncation limit cross-cutting the contour intervals in black (ie. west of WD-3 and WD-7). Average effective porosities are given at each well (in blue type) where the unit is present (Bulling, et al., 1998).

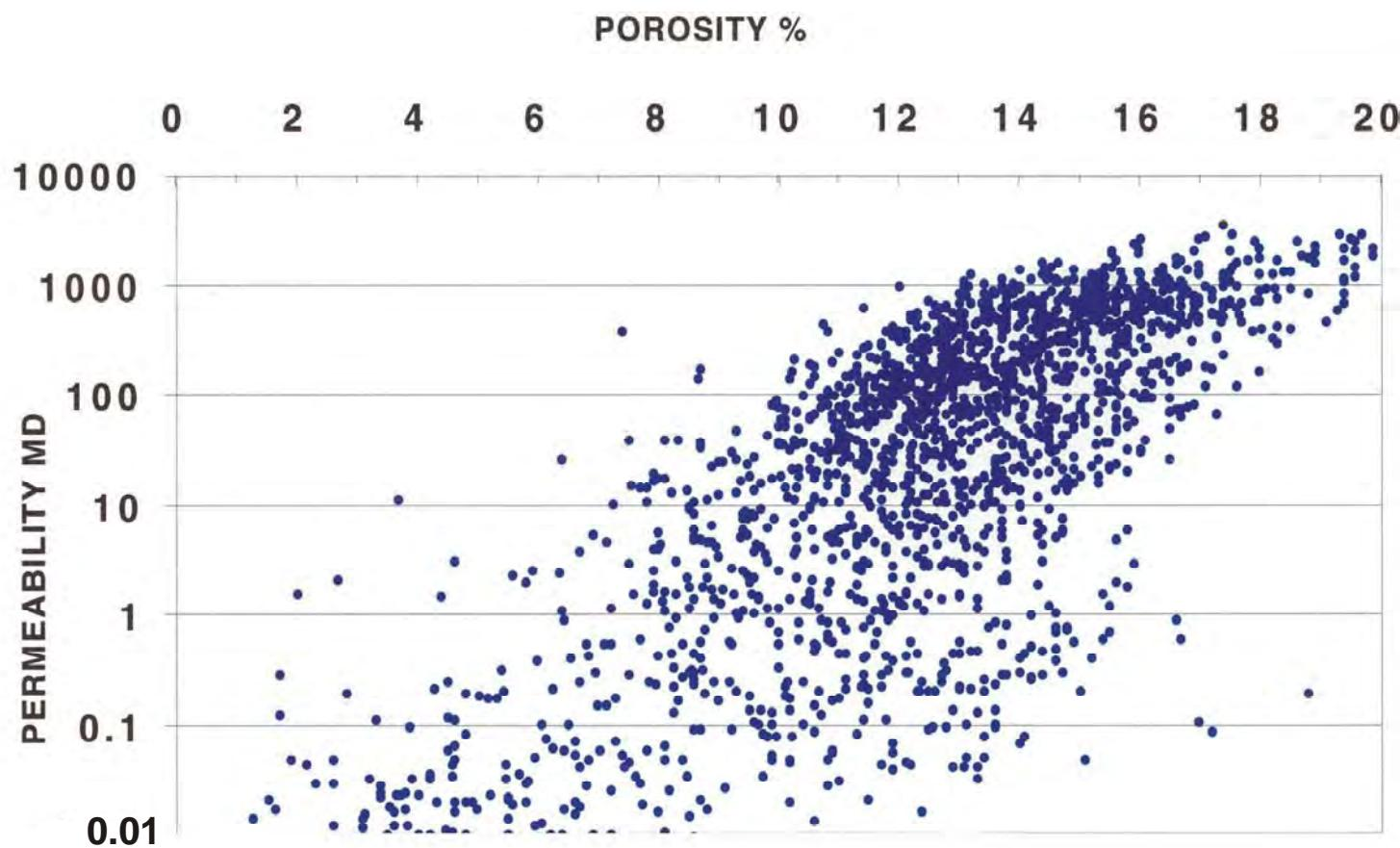


Figure 7.16: Cross-plot of Porosity versus Permeability for the Roabiba Sandstone Formation reservoir from whole core plugs on Wiriagar Deep and Vorwata wells. Plugs were sampled every 1 ft from cored reservoir intervals (tested at 800 psi NOB). Plot shows most reservoir values are greater than 11% porosity and 60 mD (Bulling, et. al., 1998).

Jurassic P-D Plot for all Structure

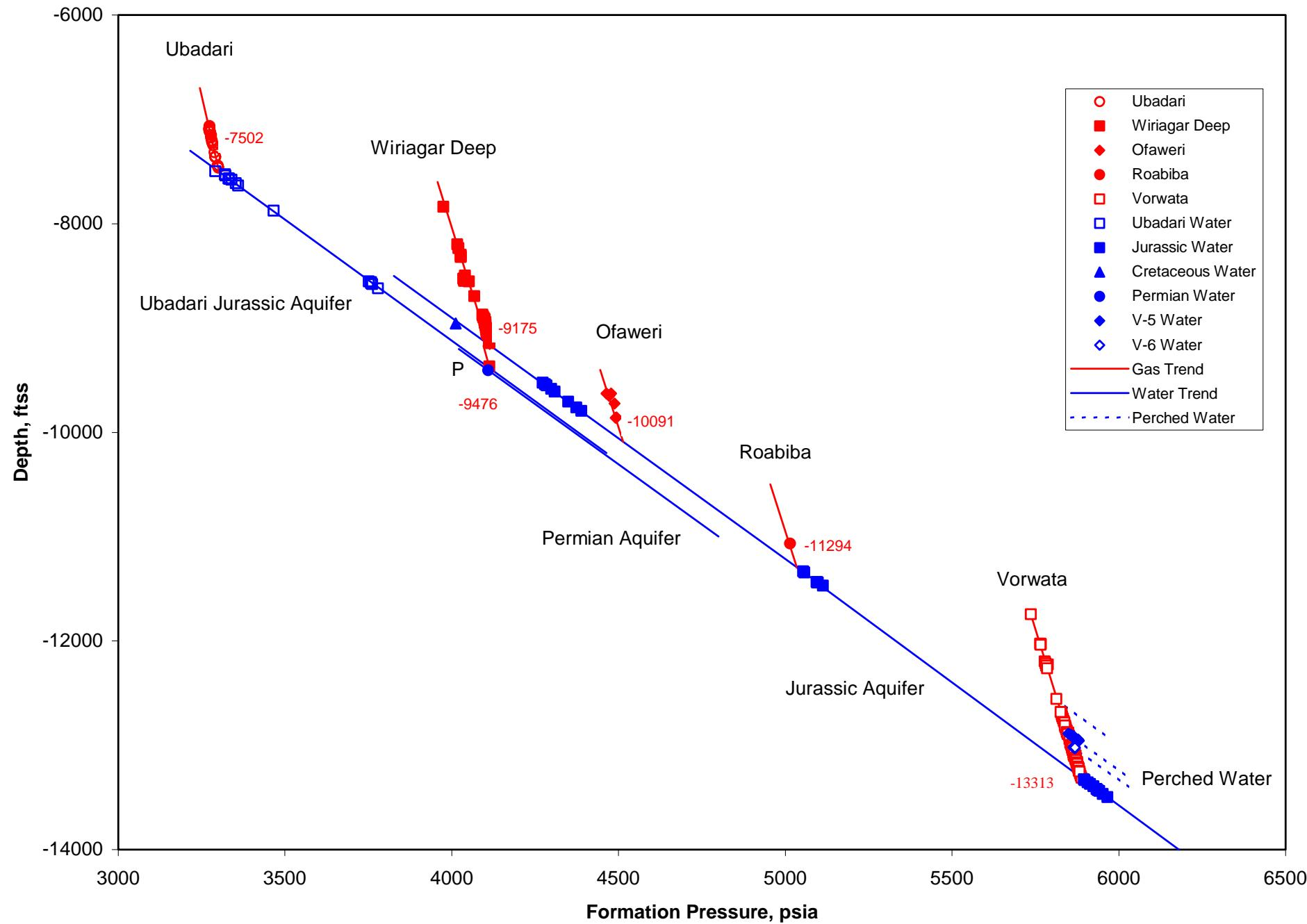


Figure 7.17: Plot of Jurassic pressures versus depths TVDss for MDT/DST points on all structures. Plot shows GWC contact for all structures including four GWC's for Vorwata, due to perched water. GWC for V-10 area is at -13,313ft TVDss (Yoshino, et al., 2003).

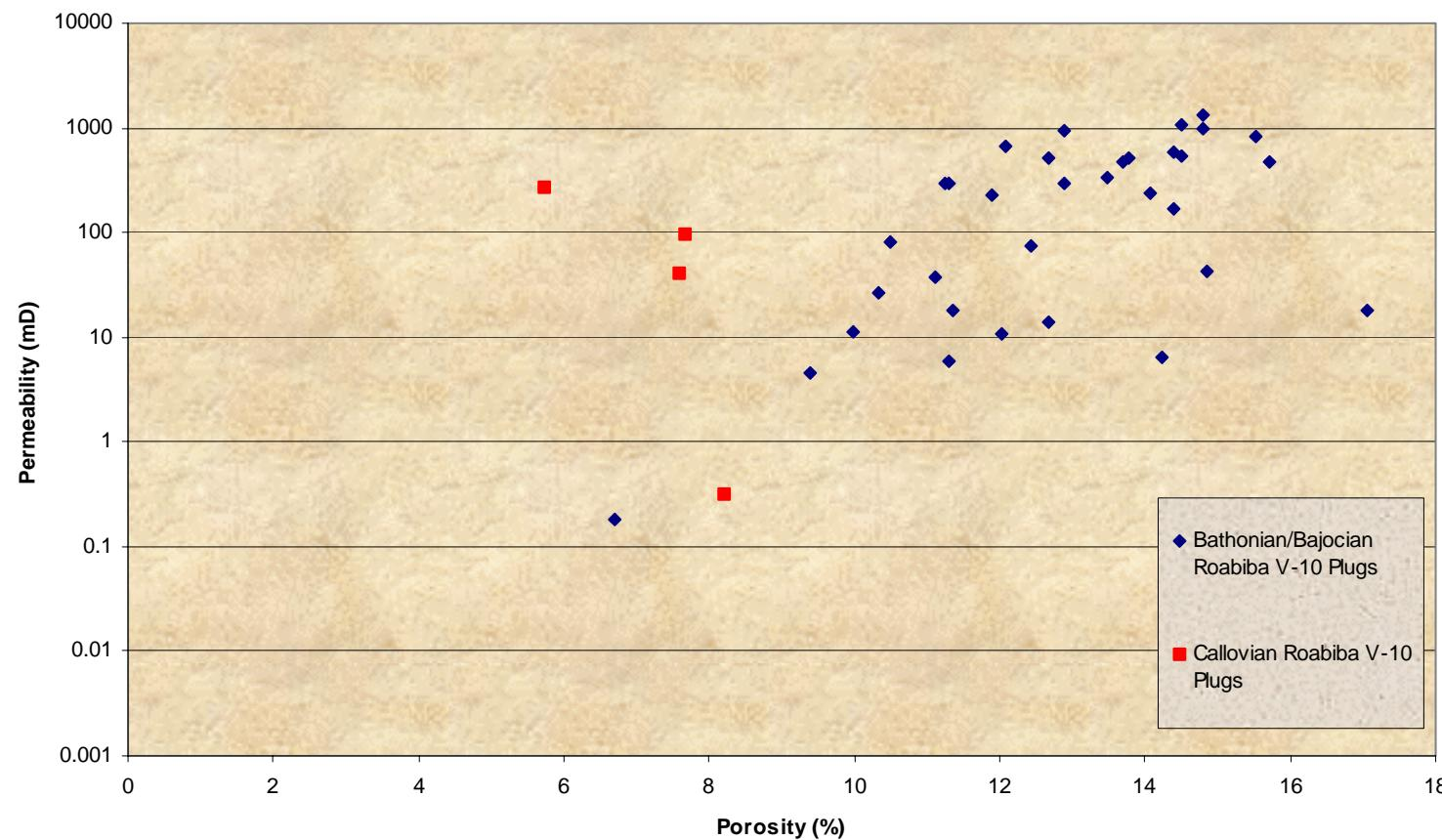


Figure 7.18: Cross-plot of porosity vs. permeability for newly re-sampled whole core plugs from the Vorwata-10 well. Callovian Roabiba Sandstone Formation samples have generally poorer porosity and permeability than Bathonian/Bajocian Roabiba plugs.

Vorwata #10 Roabiba Formation Porosity vs. Permeability for Whole Core Corrected Petrophysical Values and New Whole Core Plug Analyses in Gas and Water Zones

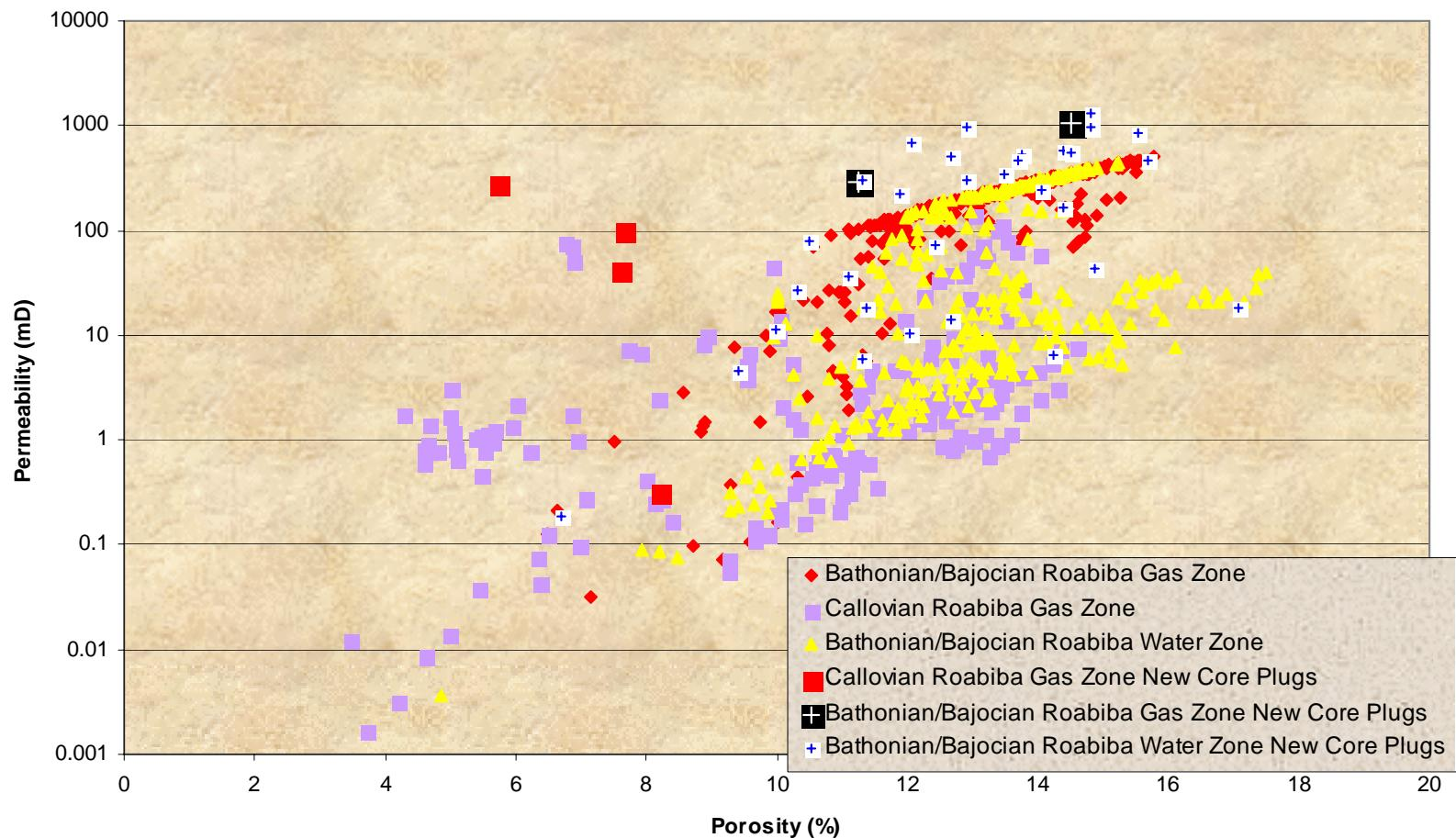


Figure 7.19: V-10 wireline porosity and calculated permeability corrected/calibrated to whole core analyses with petrophysics in 1998. New core plugs that were sampled and analyzed in 2002/2003 are potted also, and labelled as ‘new core plugs’. Bathonian/Bajocian Roabiba has the best reservoir quality, whether in the gas or water zones, compared to the overlying Callovian Roabiba reservoir quality.

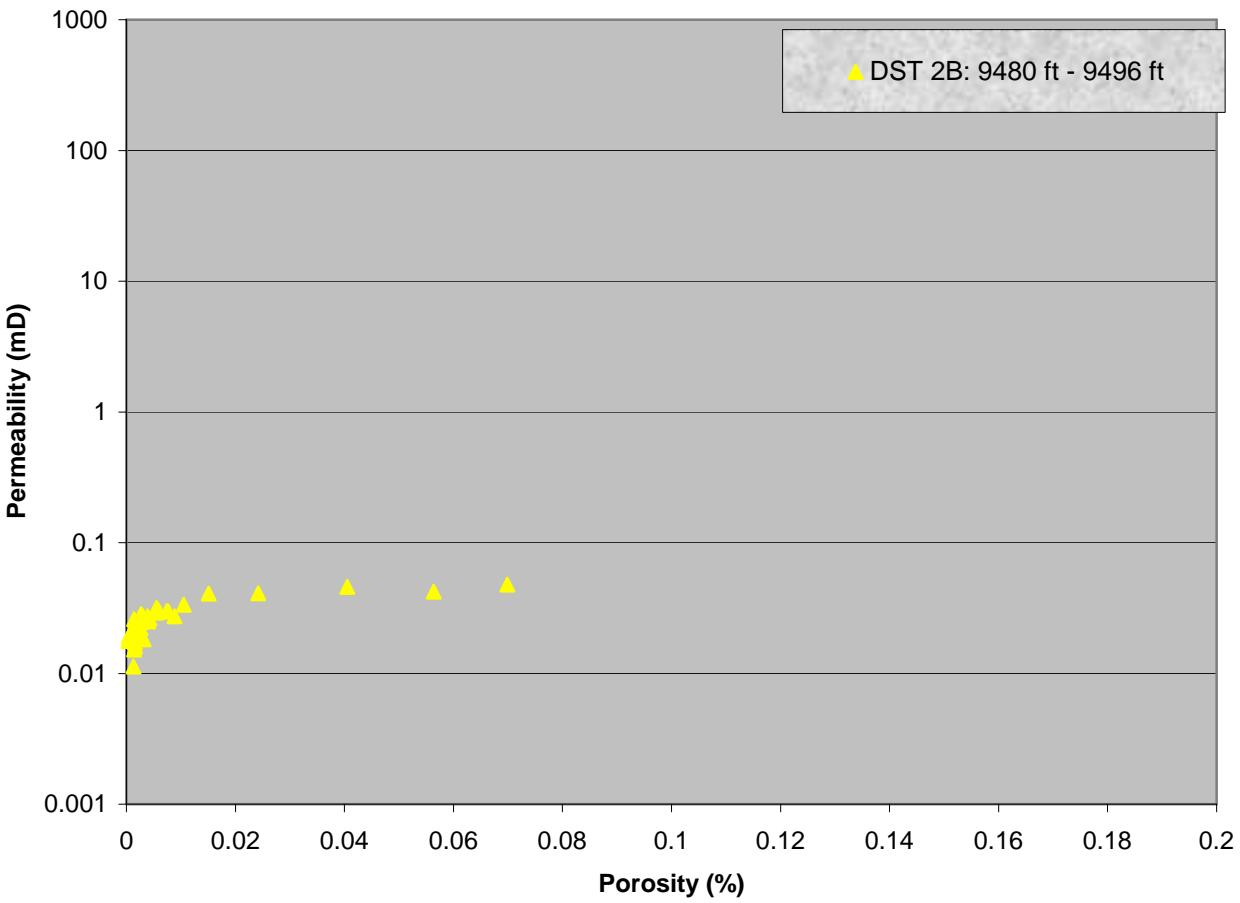


Figure 7.20: Porosity versus Permeability crossplot (from petrophysical analyses of wireline logs calibrated to whole cores) of the Ayot Limestone Formation interval that was tested on the WD-5, and flowed natural gas at a rate of only 0.02 MMscf/d.

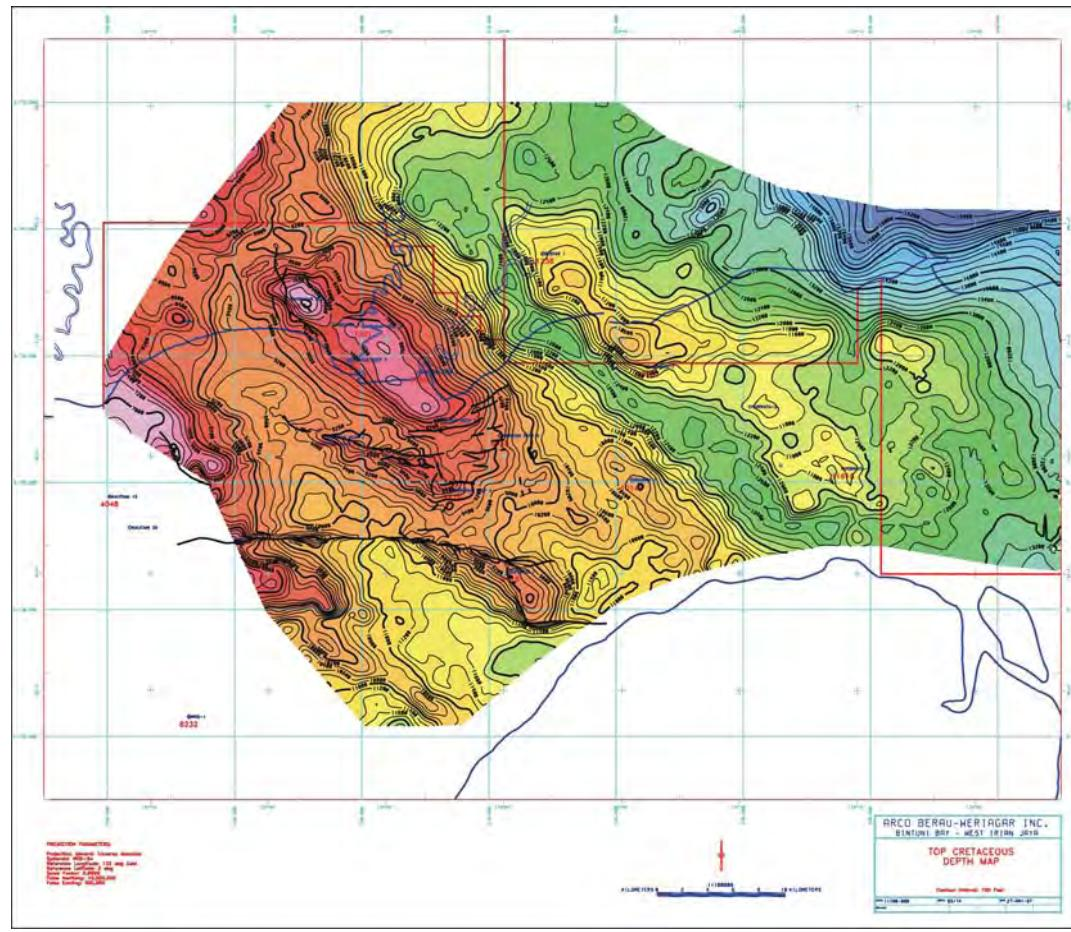


Figure 7.21: Depth structure map of the top Late Cretaceous Succession over the Tangguh area, as mapped from 3D seismic survey by ARCO 1997-1998 (courtesy of BP, 2002). Depth scaling is from shallowest to deepest, pink, red, orange, yellow, green, blue, and finally purple. Contour Interval (CI) = 200 vertical feet. The structure at left center with the pink contours is top Wiriagar Deep at 7560 ft (TVDss), and the top of the Vorwata structure (yellow contours to the east of Wiriagar Deep) is 10,400 ft (TVDss).

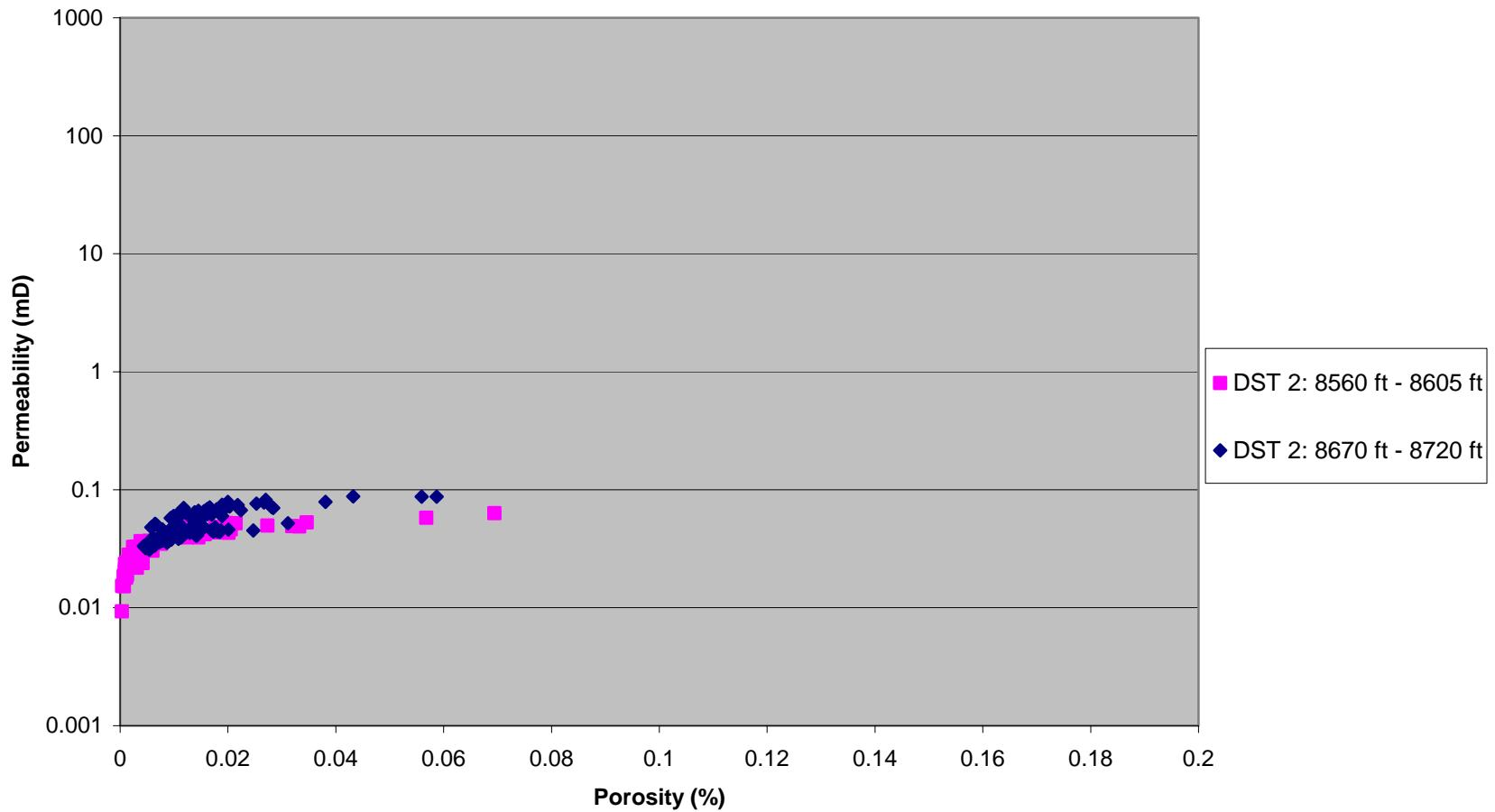


Figure 7.22: Porosity versus Permeability crossplot (from petrophysical analyses of wireline logs calibrated to whole cores) of two Late Cretaceous intervals that were comingled on the WD-4 DST, and flowed natural gas at a rate of 5.2 MMscf/d.

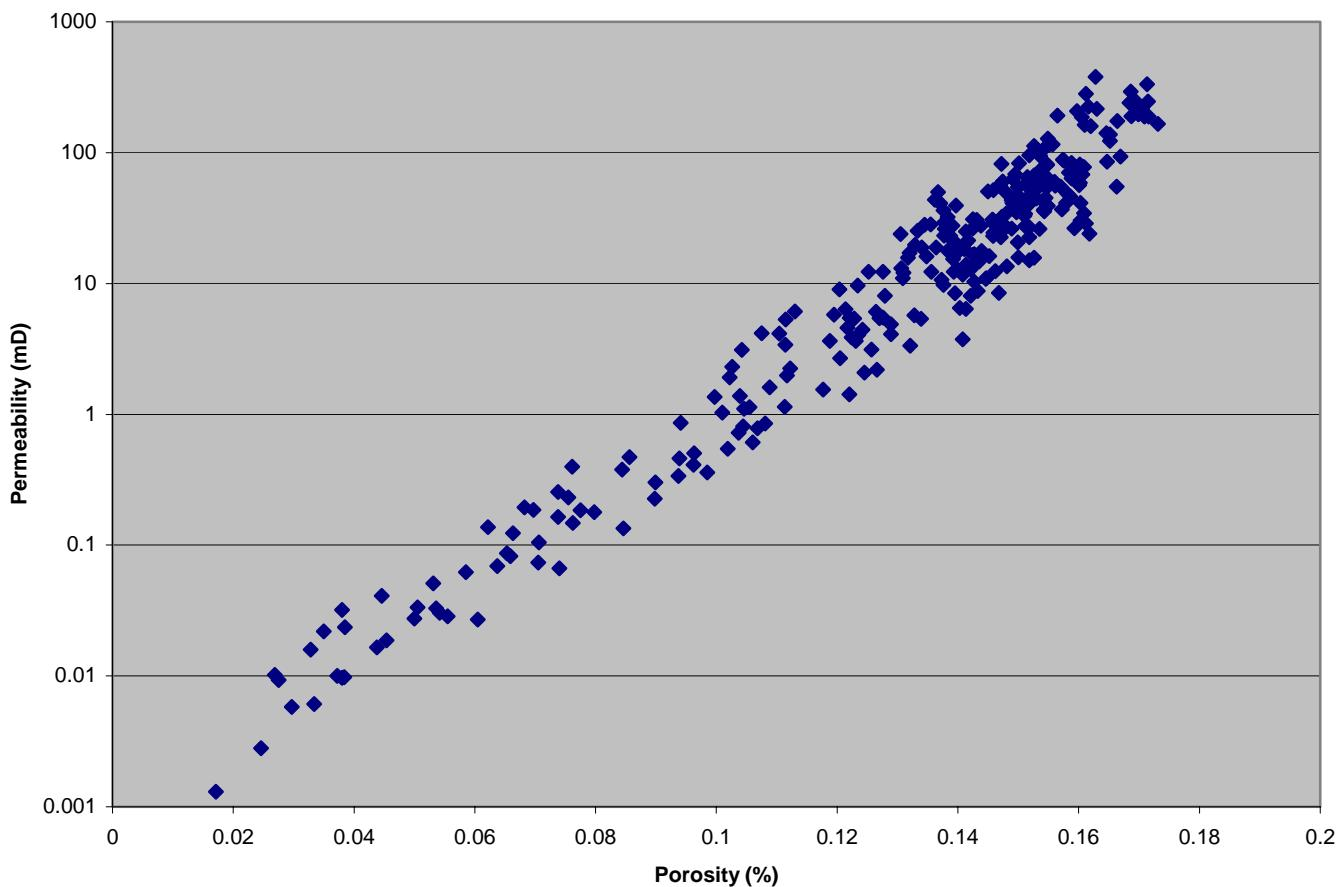


Figure 7.23: Porosity versus Permeability for Late Paleocene Sand-Prone Middle Member on the WD-2, a stacked turbidite channel at wireline depth 7568 ft to 7718 ft.

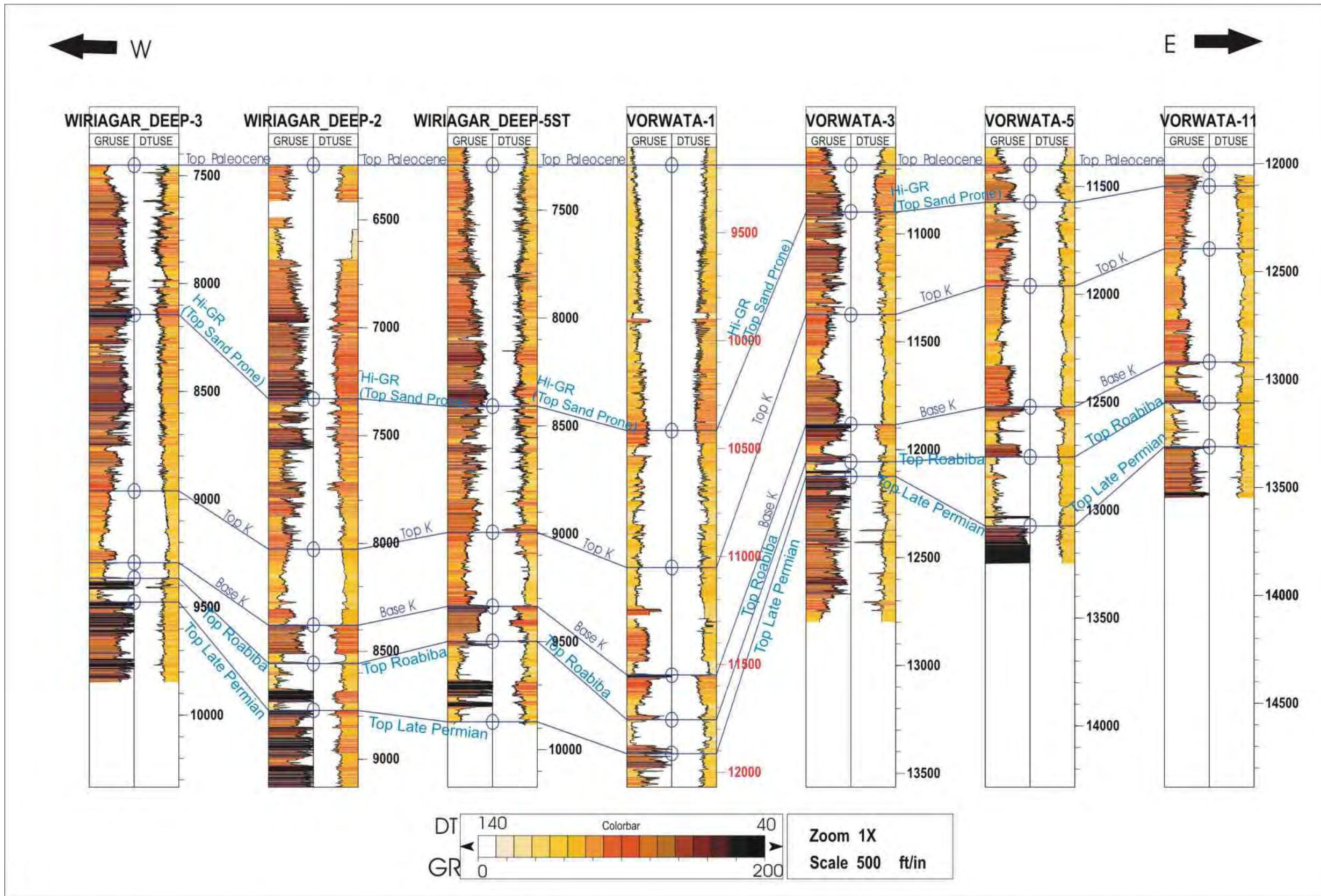


Figure 7.24: Wireline log correlation cross-section of selected wells from Wiriagar Deep to Vorwata structure, flattened on the Top Late Paleocene as the datum. Cross-section runs from roughly west to east and shows a thinning of the Paleocene over Vorwata, with less sandstone reservoirs in the 'Sand-prone Interval'. Gamma-ray (GRUSE) and sonic (DTUSE) curves are also color-filled with the respective values according to the legend scale shown.

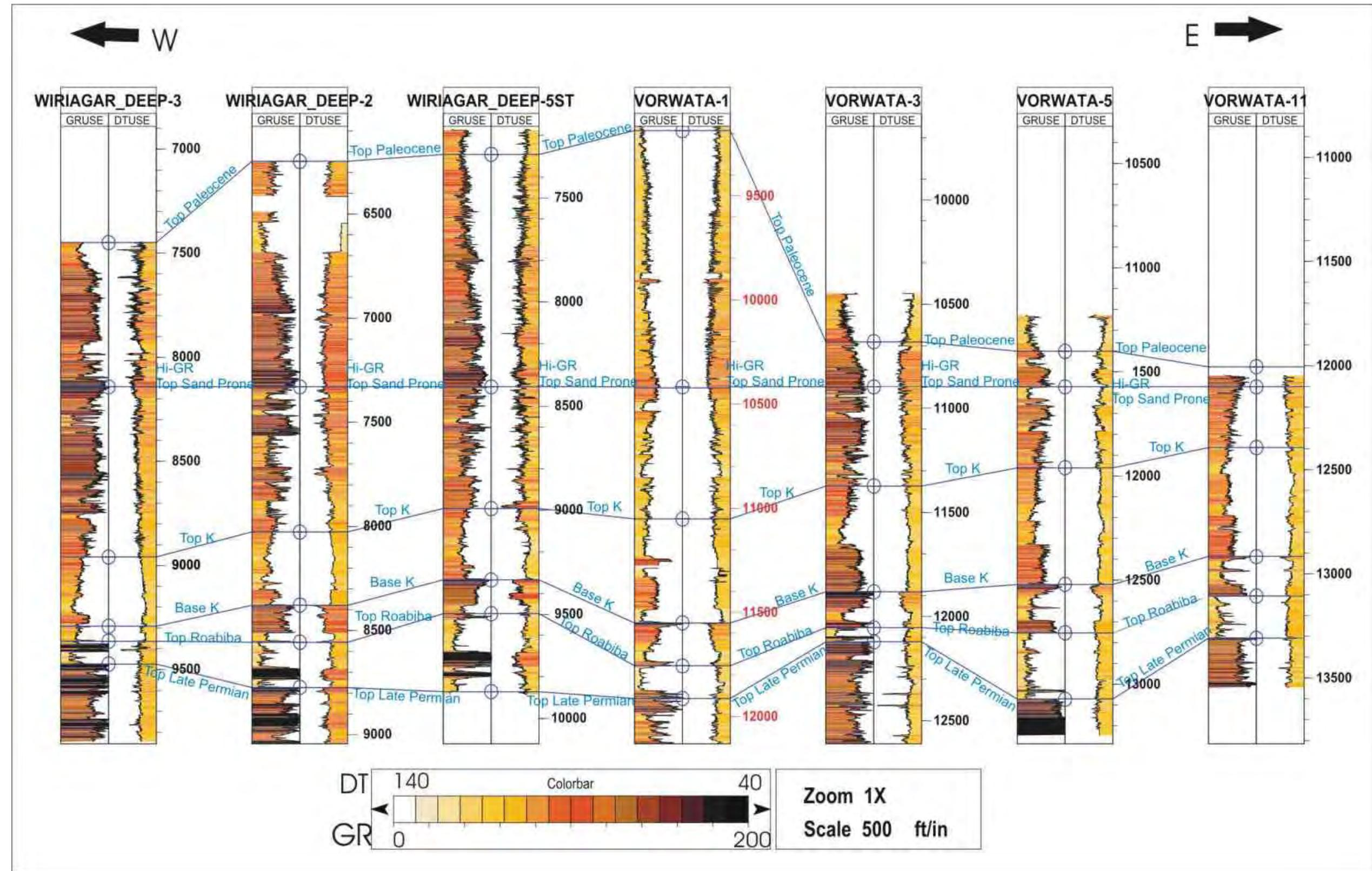


Figure 7.25: Wireline log correlation cross-section of selected wells from Wiriagar Deep to Vorwata structure, flattened on the Top Sand-Prone Interval as the datum. Cross-section runs from roughly west to east and shows a dramatic thinning of the Sand-Prone Interval over Vorwata, with less net sandstone at Vorwata. Gamma-ray (GRUSe) and sonic (DTUSE) curves are color-filled with the respective values according to legend scale.

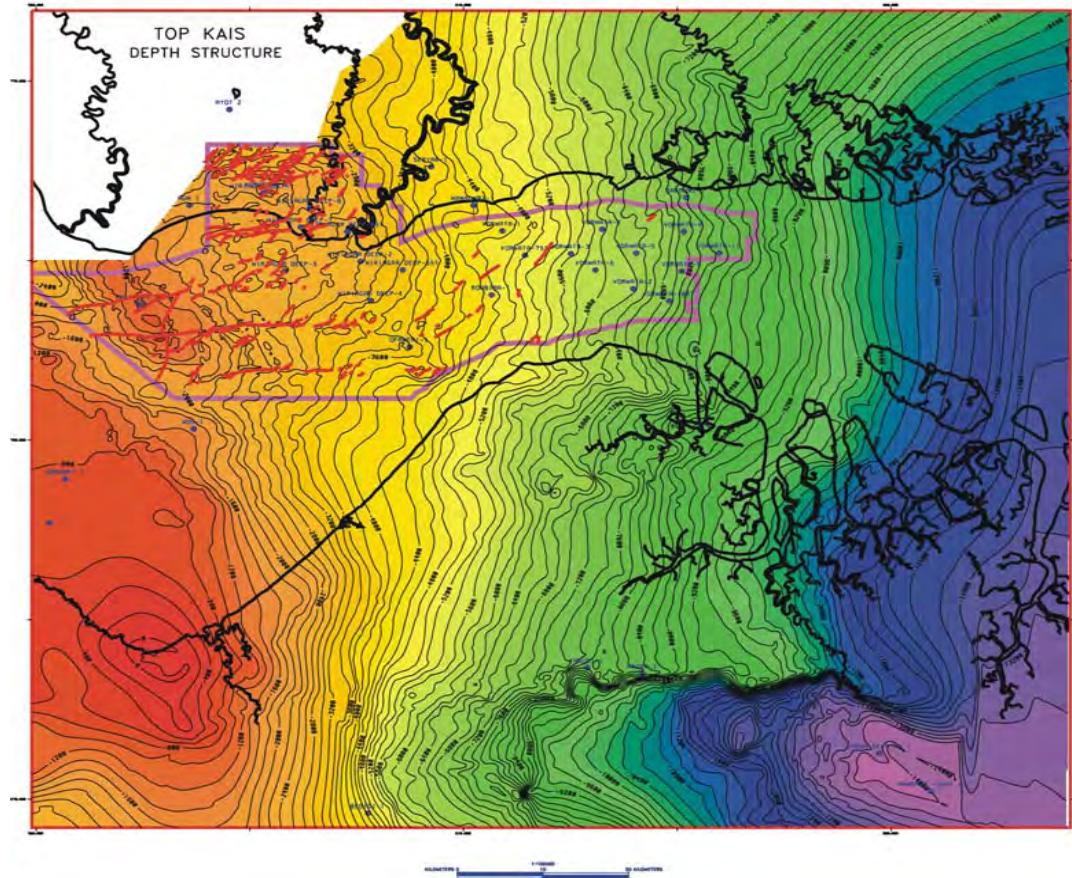


Figure 7.26: Top Kais Limestone Formation (NGLG) depth structure map of the Tangguh area. Color scale grades from red as shallowest depth of burial to blue as deepest depth. Contour intervals are 200 ft with the Kais outcropping at 0 ft contour on the south coast of the bay in the lower left corner of the map (top of deep red contours). Purple line shows outline of 3D seismic survey area. Red lines are interpreted faults in the Kais Limestone Formation. The top of the Kais Limestone Formation is buried at a depth of less than 2600 ft, particularly at the culminating crest of the Wiriagar Deep structure where CO₂ would be expected to migrate to if injected into the NGLG (Isworo, 2002).

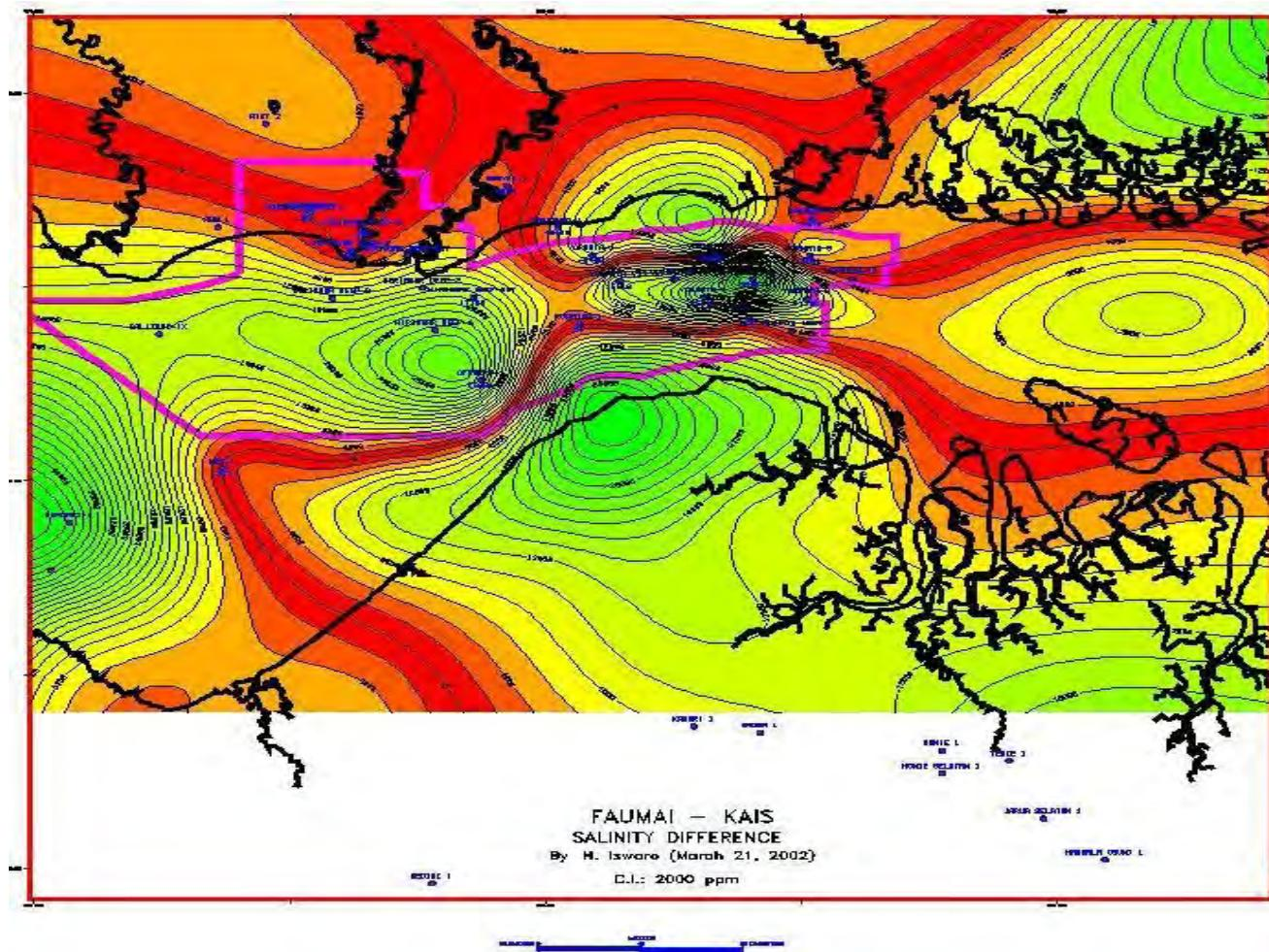


Figure 8.1: Salinity difference contour map between Faumai Formation and Kais Formation waters indicating good communication of fluids between the two formations. CI = 2000 ppm, with green indicating great contrast in salinity (in thousands ppm), and red indicating low contrast in salinity (in thousands ppm). Green bulls-eyes at Roabiba-1 and Ofaweri-1 suggest spurious data (Isworo, 2002).

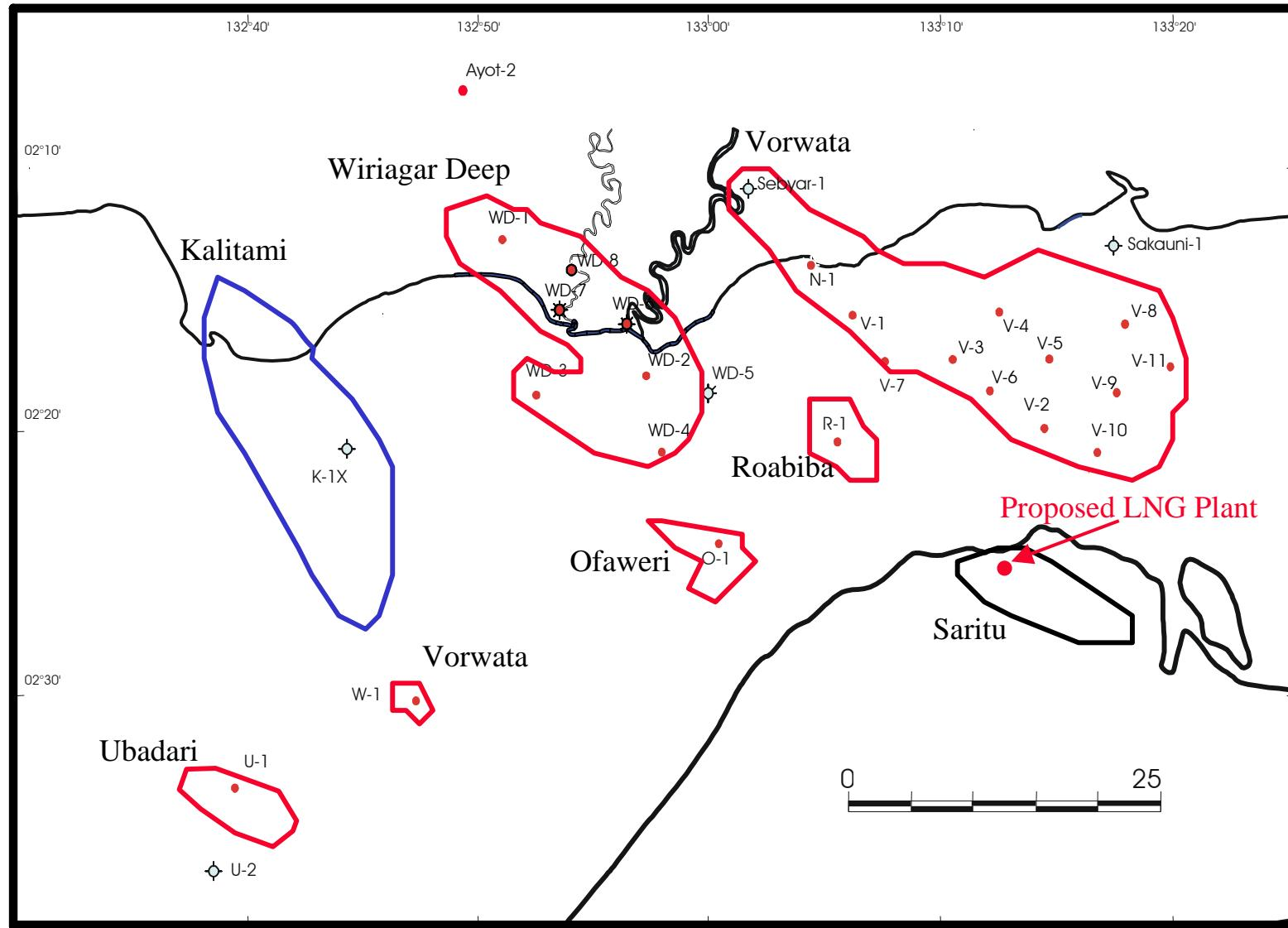


Figure 9.1: Map illustrating distances of potential sequestration structural traps from the proposed LNG plant location (red circle) on the south coast of Bintuni Bay. Structural closures containing natural gas accumulations are outlined in red. Kalitami structure is wet and is outlined in blue. Saritu structure at the proposed LNG plant location has not been drilled and is outlined in black.

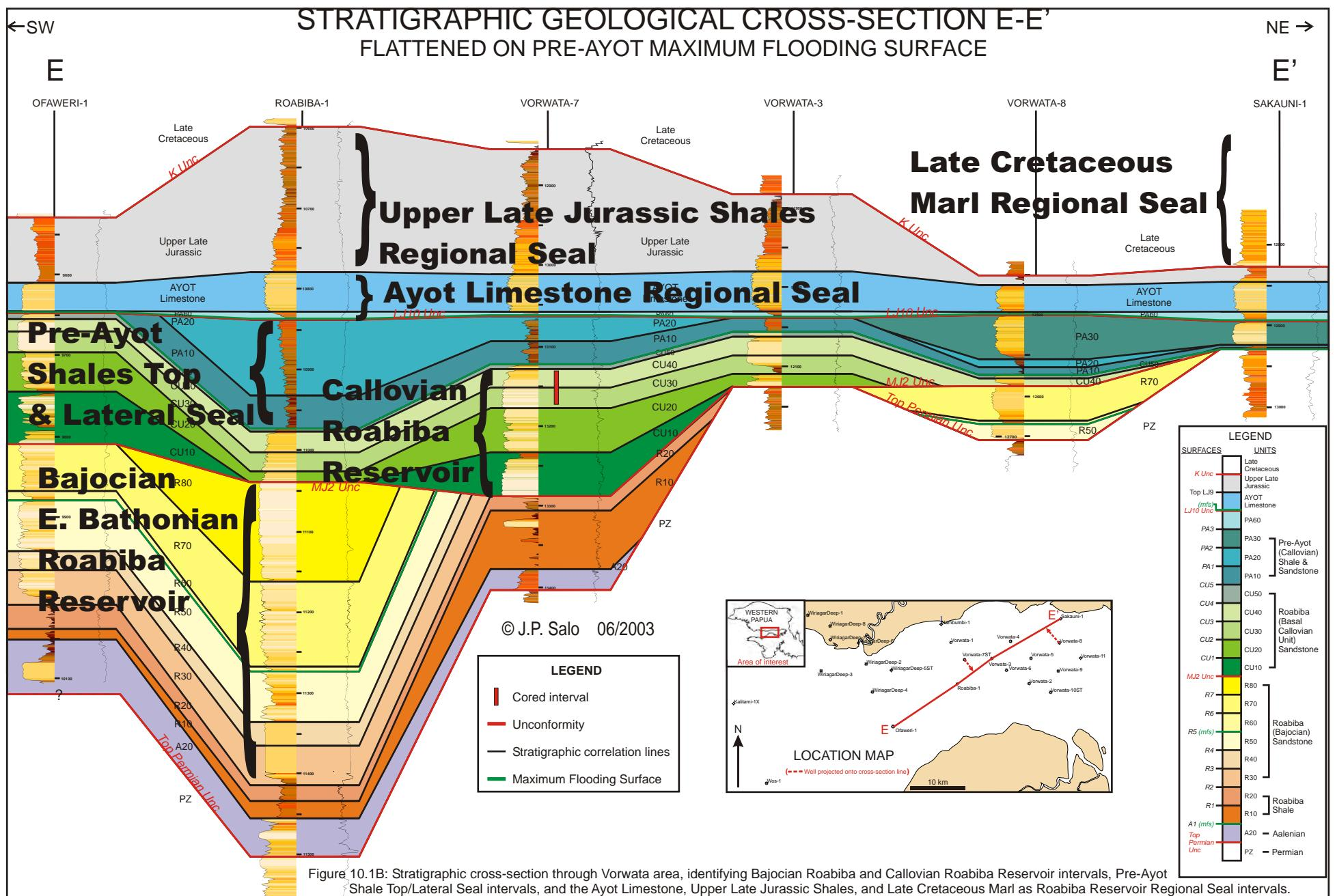
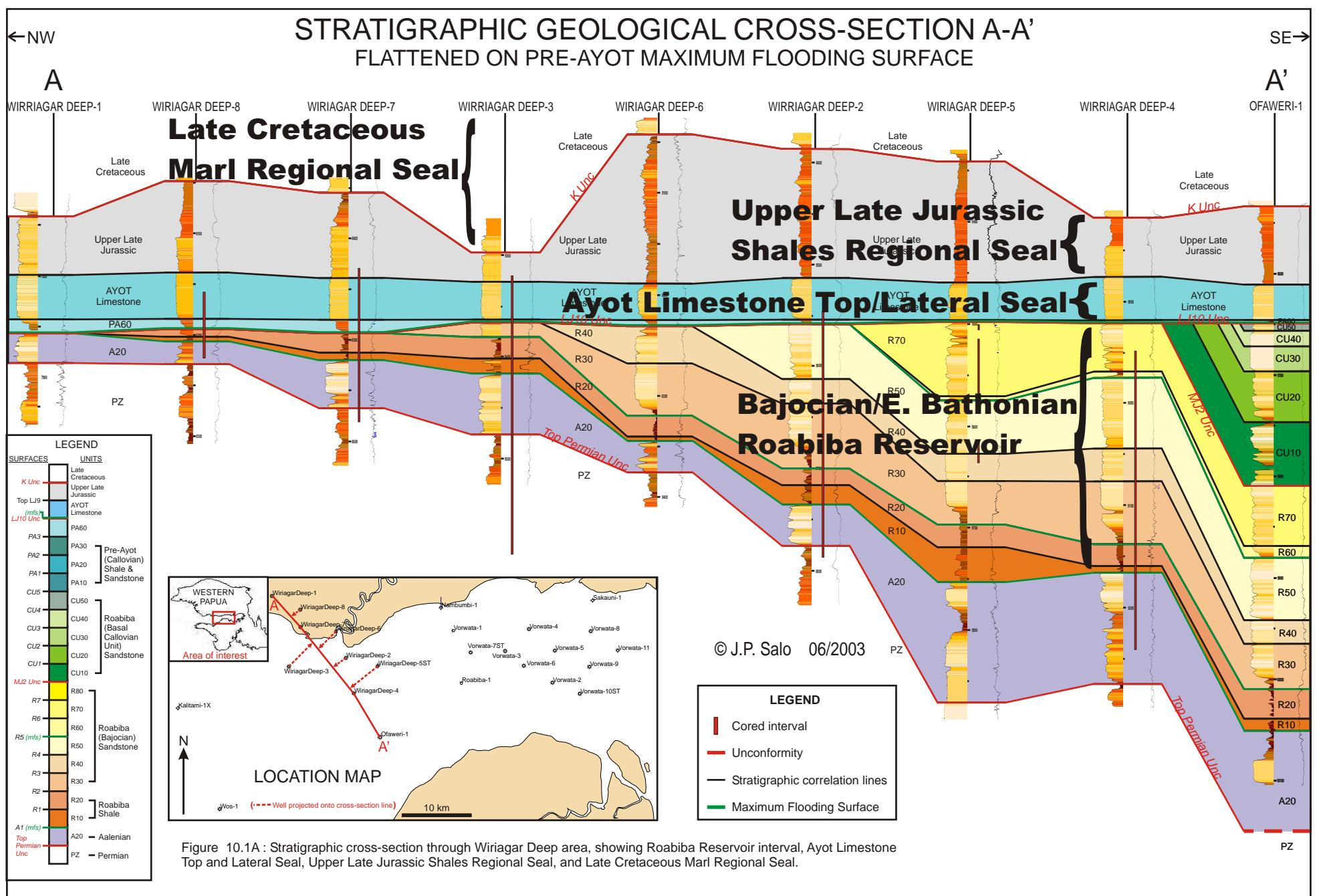


FIGURE 10.1A and 10.1B: Wiriagar Deep area and Vorwata area cross-sections showing various potential seals for the Roabiba Reservoir.

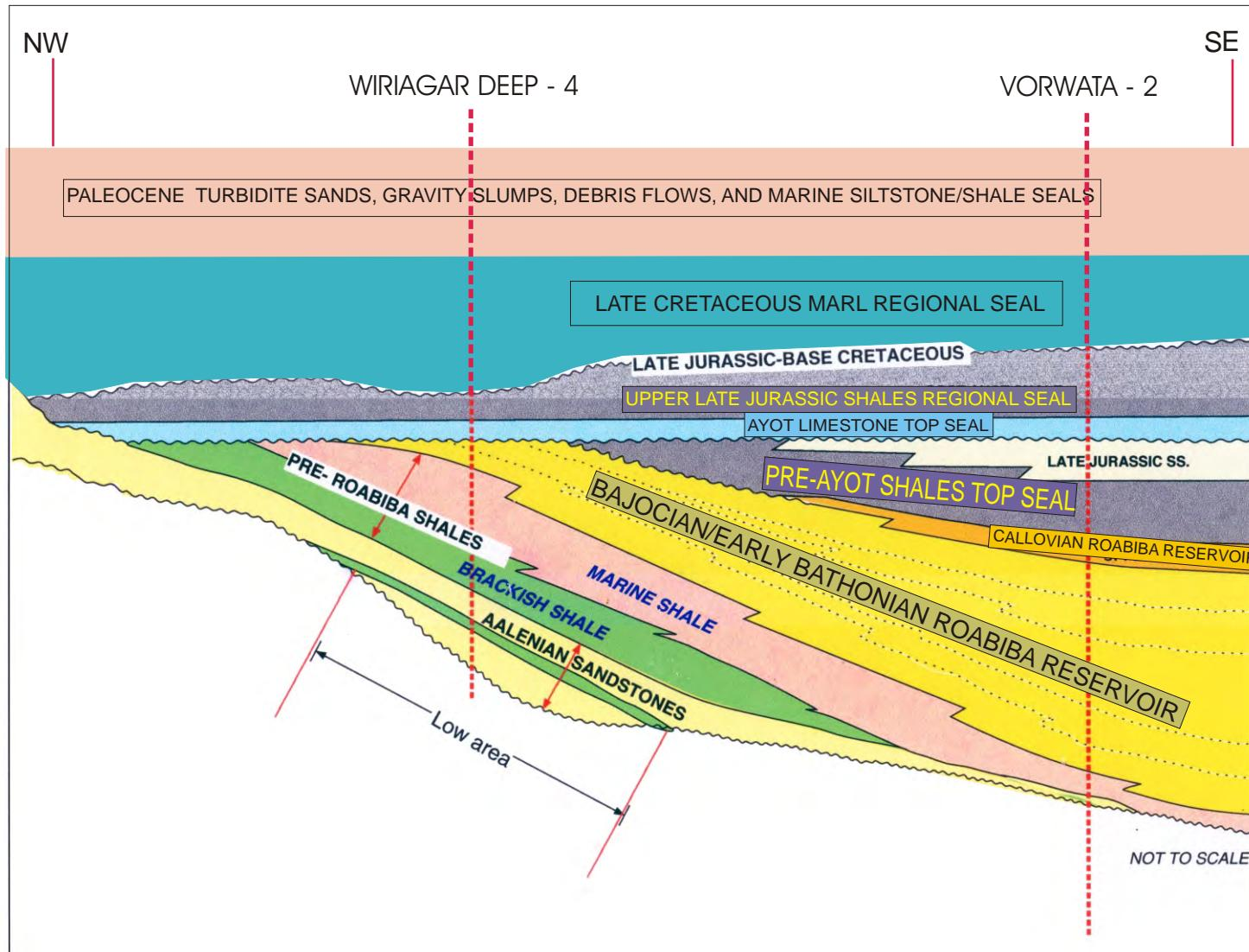


Figure 10.2: Geological schematic illustrating structural and stratigraphic position of top and regional seals relative to the Roabiba Reservoir at both the Wiriagar Deep and Vorwata anticlinoriums, with Wiriagar Deep-4 and Vorwata-2 wells used as references.

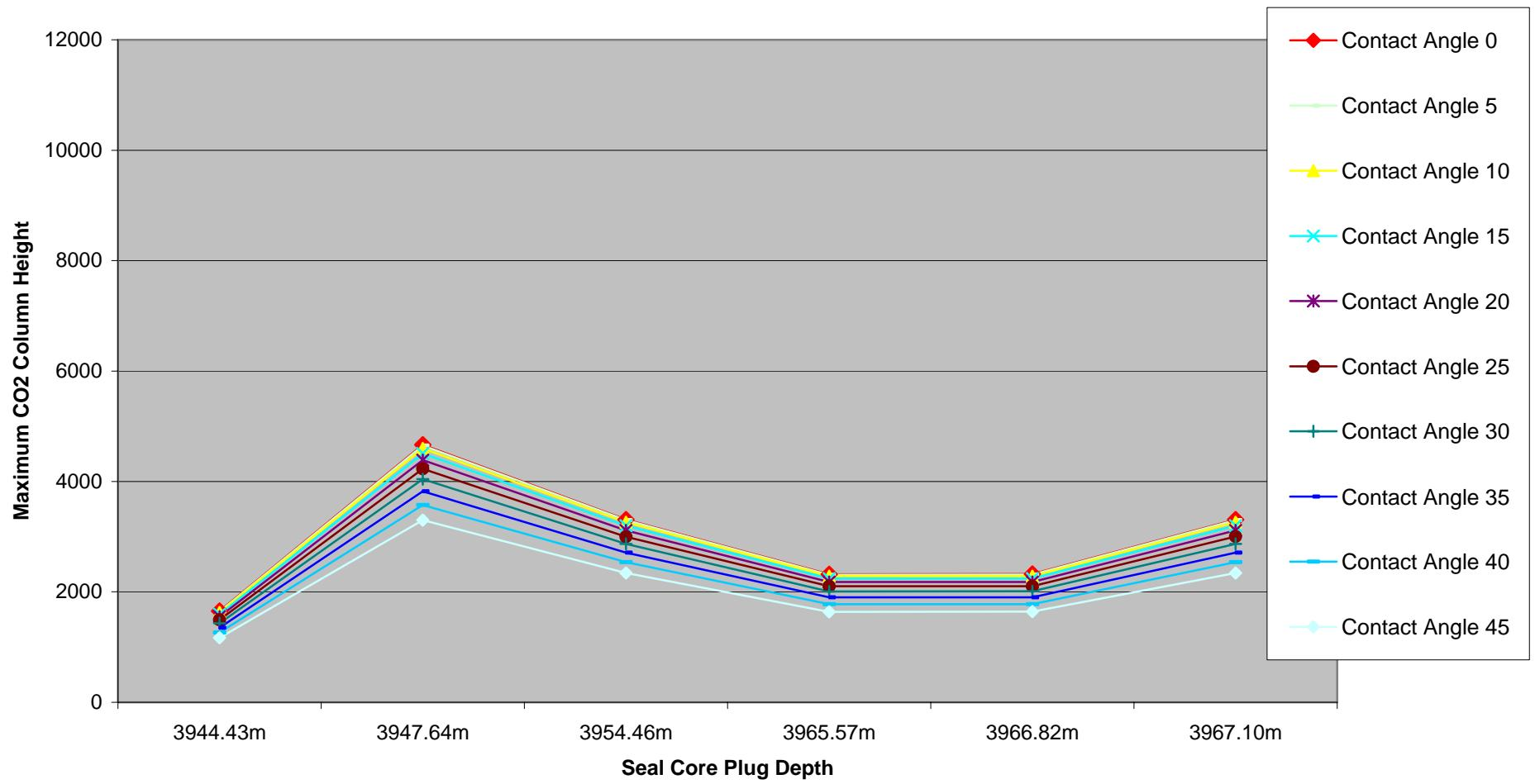


Figure 10.3: CO₂ Column Height sensitivities due to varied contact angle (with interfacial tension constant at 21.57 dynes/cm).

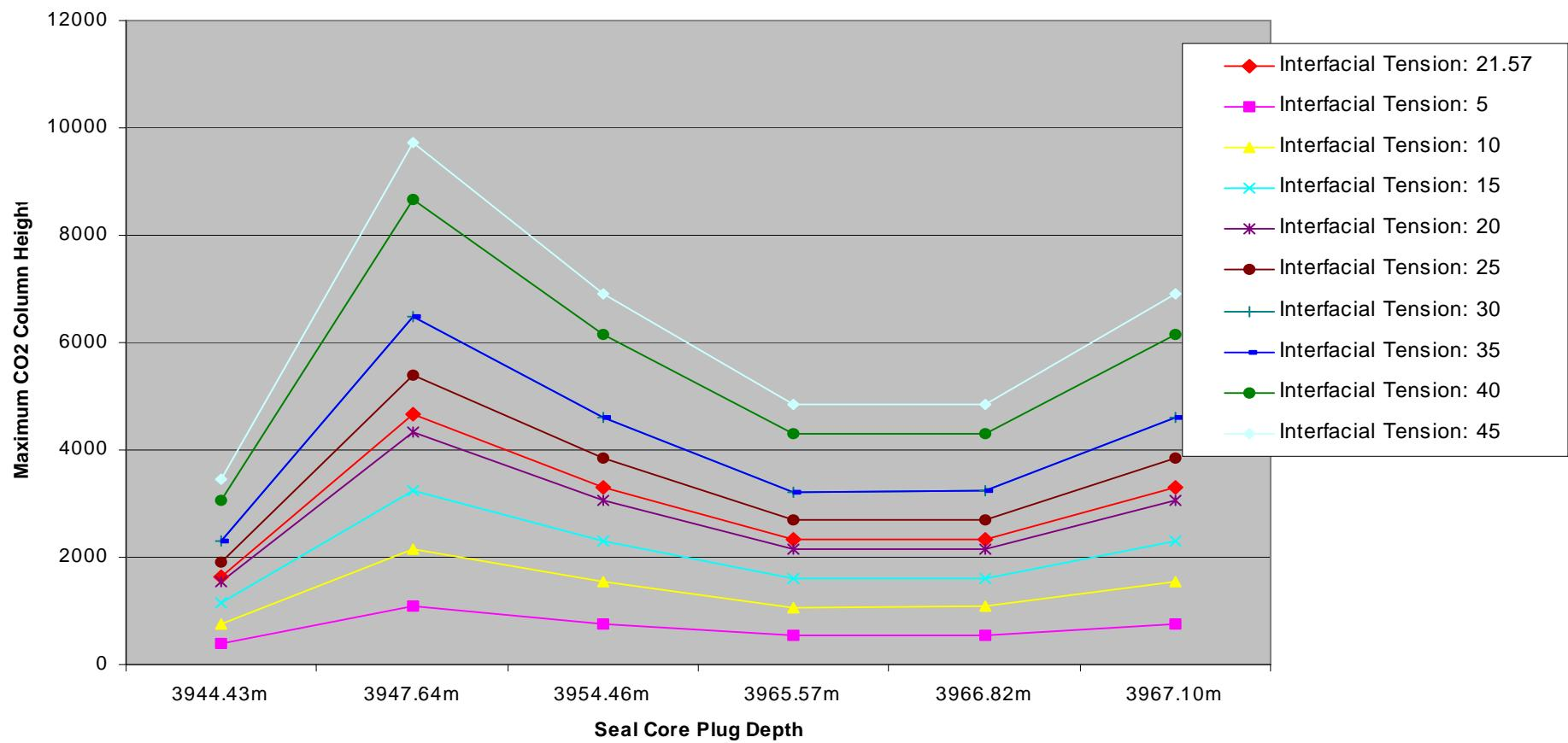


Figure 10.4: CO₂ Column Height sensitivities due to variations in interfacial tension.

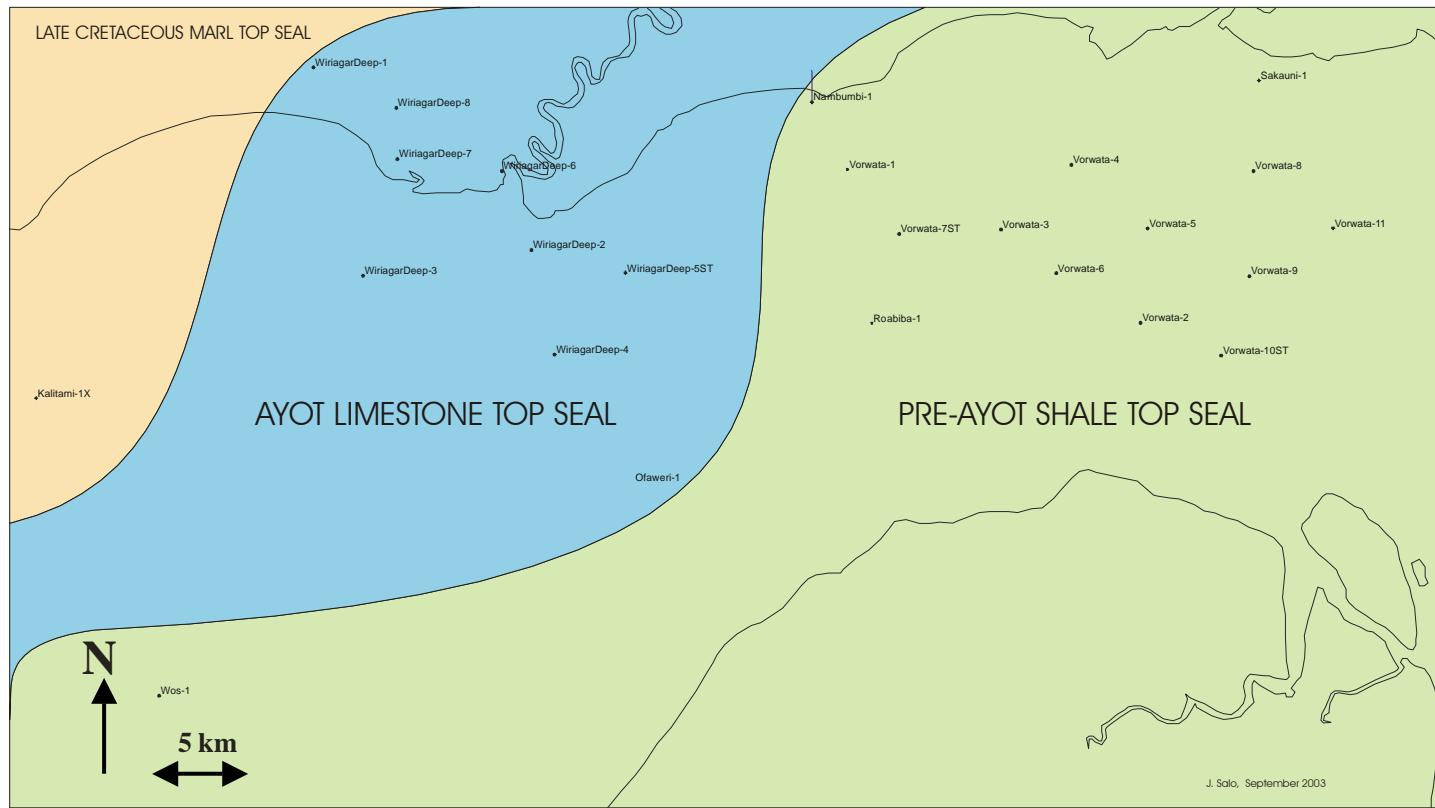


Figure 10.5: Map of the Tangguh area (with present-day coastline and well surface hole locations), showing the approximate areal extent of the Roabiba reservoir's top sealing units. Distribution of these units is due to an erosional unconformity truncating lithostratigraphic units, such as the Pre-Ayot Shales (sequence stratigraphic units PA10, PA20, and basal PA30), towards the NW. This erosional orientation towards the NW is the results of uplift along the N-S running Sekak Ridge just west of the Kalitami-1X well location, and contemporaneous W-E uplift just inland of the present-day northern coastline.



Figure 10.6: Example of Tangguh core illustrating massive alteration of the core from poor storage conditions. Post-coring diagenesis includes oxidation, hydration/swelling, stress relief at surface, and even growth of molds and fungus. The example is from WD-7 slabbed core, cut in early 1997, and digitally photographed in 2002. The author's core plug/chip sampling avoided visibly altered core intervals as pictured above.

Digital Whole Core Photograph:
(Massive Mineralogical Alteration
Due to Poor Storage Conditions.)

Potential Top Seals for Tangguh Reservoirs

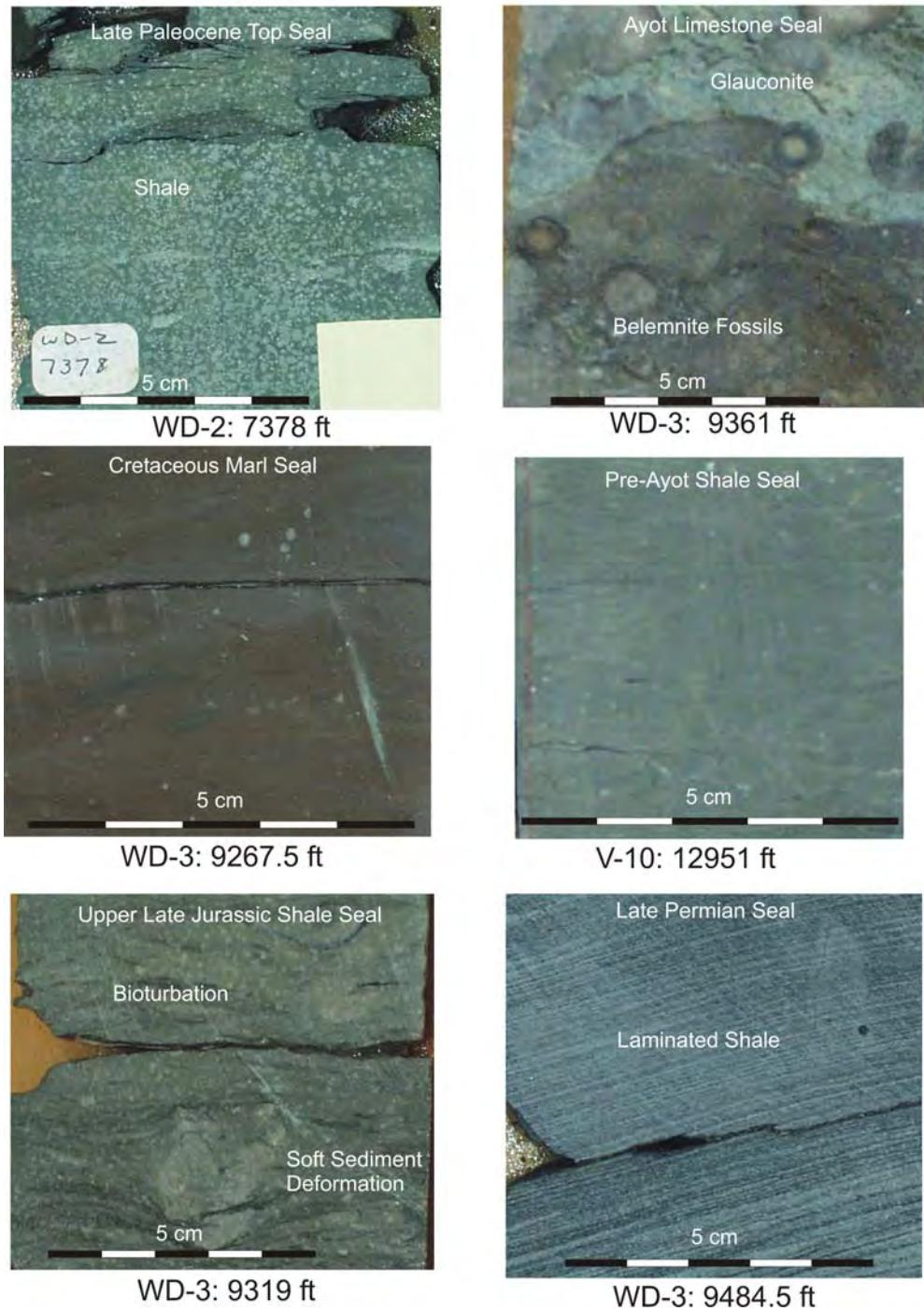


Figure 10.7: Close-up photographs of the various potential top seals in the Tangguh area from whole cores taken in Wiriagar Deep and Vorwata wells. The Upper Late Jurassic Shales are clearly siltier than the more homogeneous, clay-rich, Pre-Ayot Shales. Photographs are from slabbed cores after wetting.

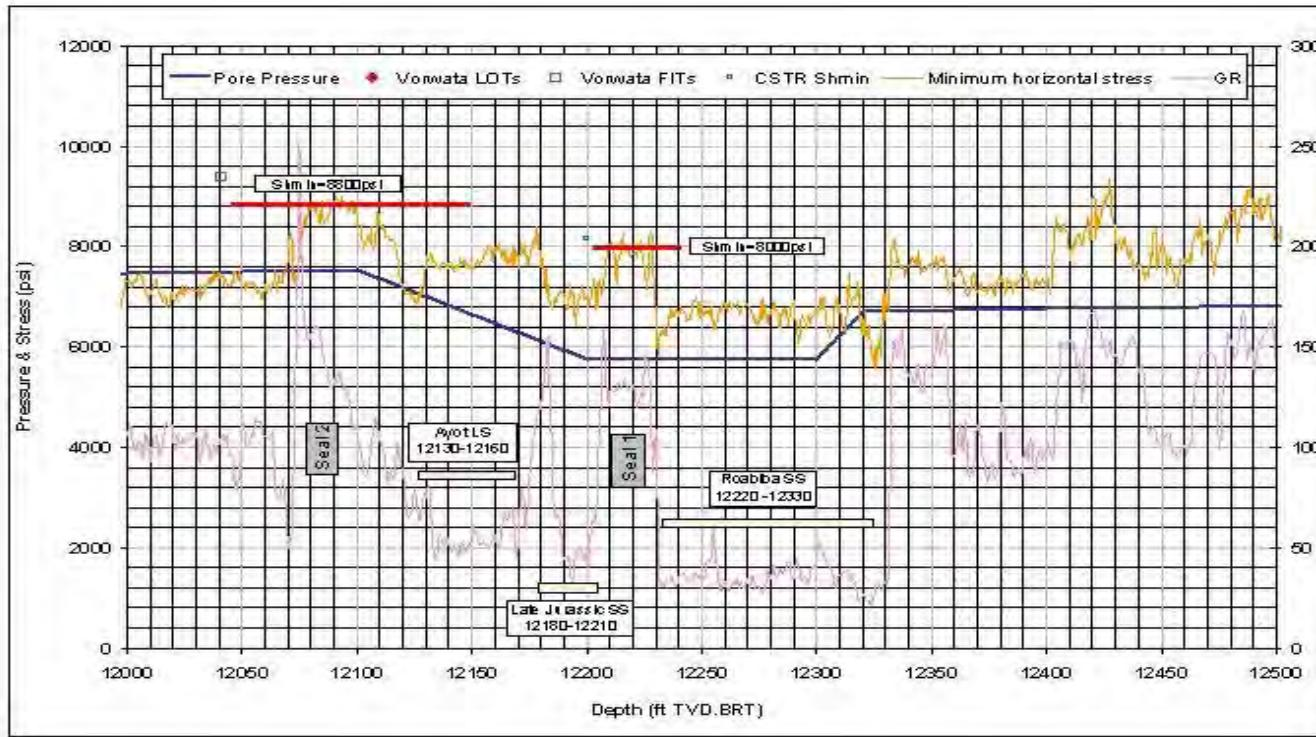


Figure 10.8: Calculated seal capacity at the Vorwata-4 well location based on evaluation of the sonic and gamma-ray wireline log from Vorwata #4. The reservoir pressure in the Roabiba reservoir at Vorwata #4 at mid-depth is approximately 5800 psi. It is calculated that the Pre-Ayot Shales top-seal immediately above the reservoir has a minimum horizontal stress of 8000 psi. It was estimated that if the injection pressure exceeds this value, then the seal could be breeched. Leaking CO₂ could charge the overlying Callovian sandstone (Upper LJ-11 Sandstone reservoir) above this seal, but a second shallower seal in the Upper Late Jurassic Shales, at approximately 12,075 ft, could retain pressure of 8800 psi (courtesy BP, 2002).

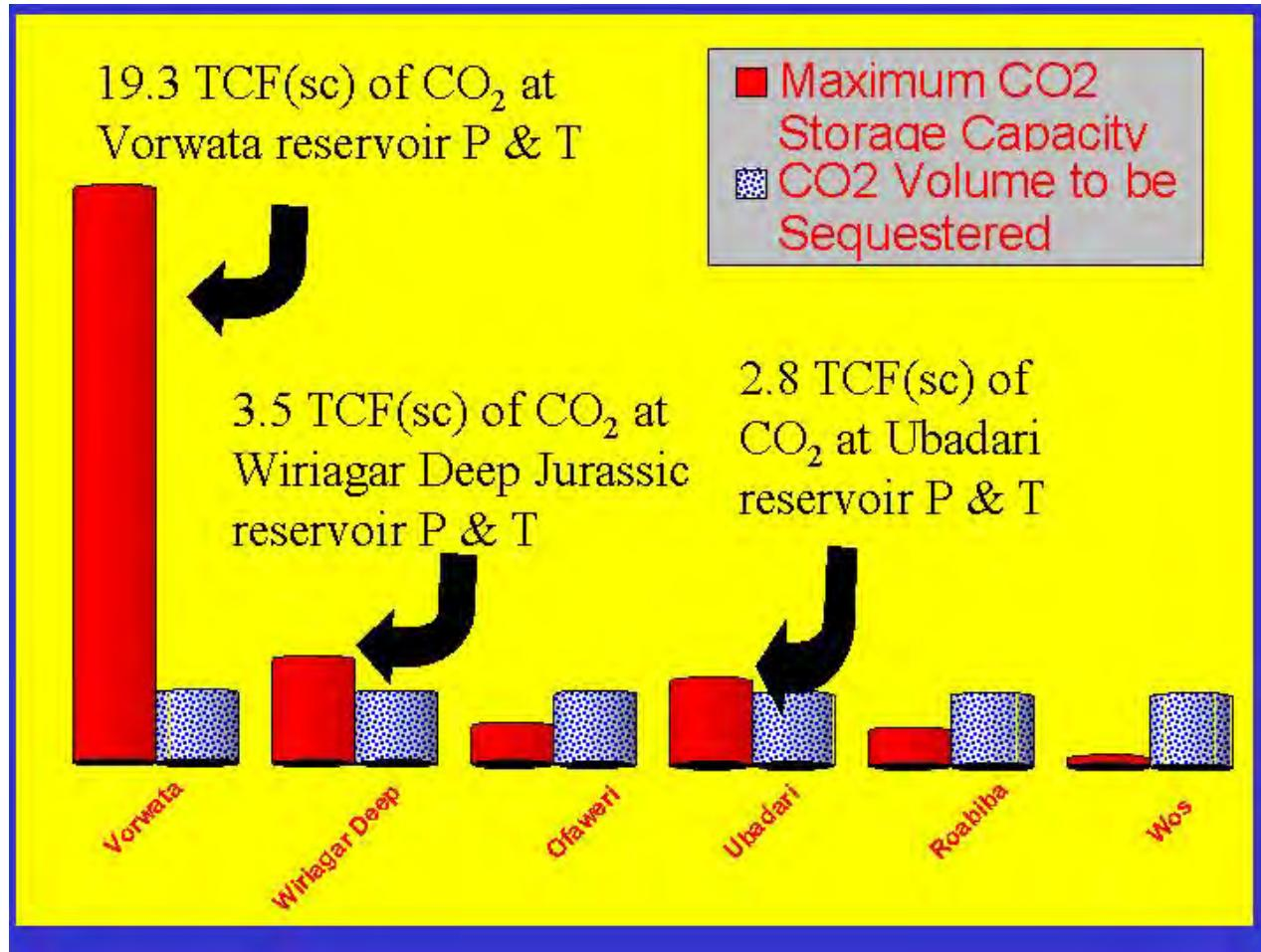


Figure 11.1: Potential supercritical CO₂ storage capacity in the Middle Jurassic reservoirs (Roabiba and/or Aalenian Sandstone Formations), per structure, calculated and shown (in red). Vorwata clearly has the largest excess potential capacity for storage. Blue shaded volume is the supercritical CO₂ to be sequestered at respective reservoir conditions (currently estimated at 2.4 TCFsc of CO₂ based on the 3P certified gas reserves).

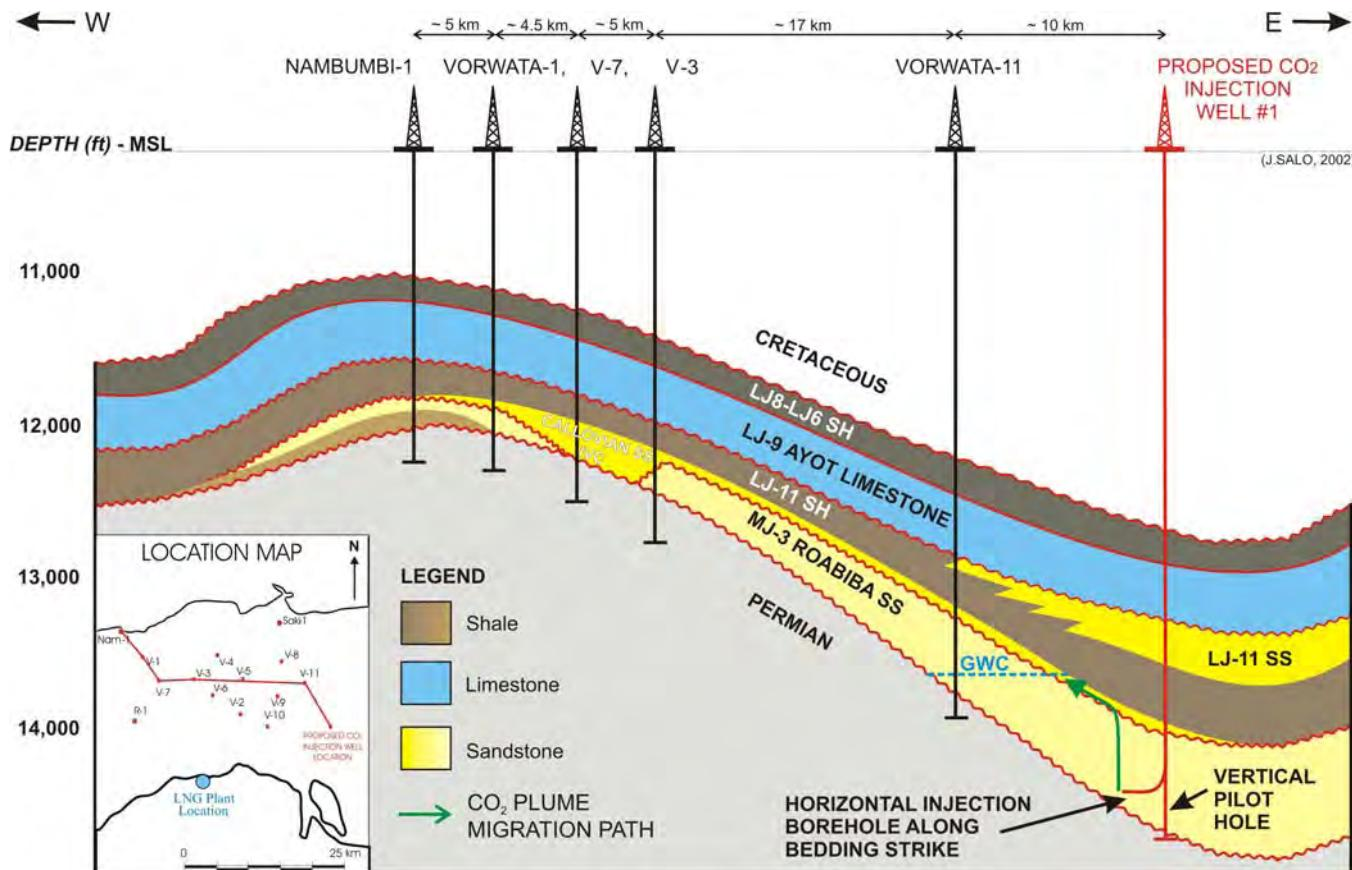


Figure 11.2: Geologic cross-sectional schematic of Vorwata anticlinorium Jurassic interval, along the plunging axial crest, illustrating the proposed injection location down-dip from, and to the east, of the GWC in the Middle Jurassic Roabiba Sandstone Formation.

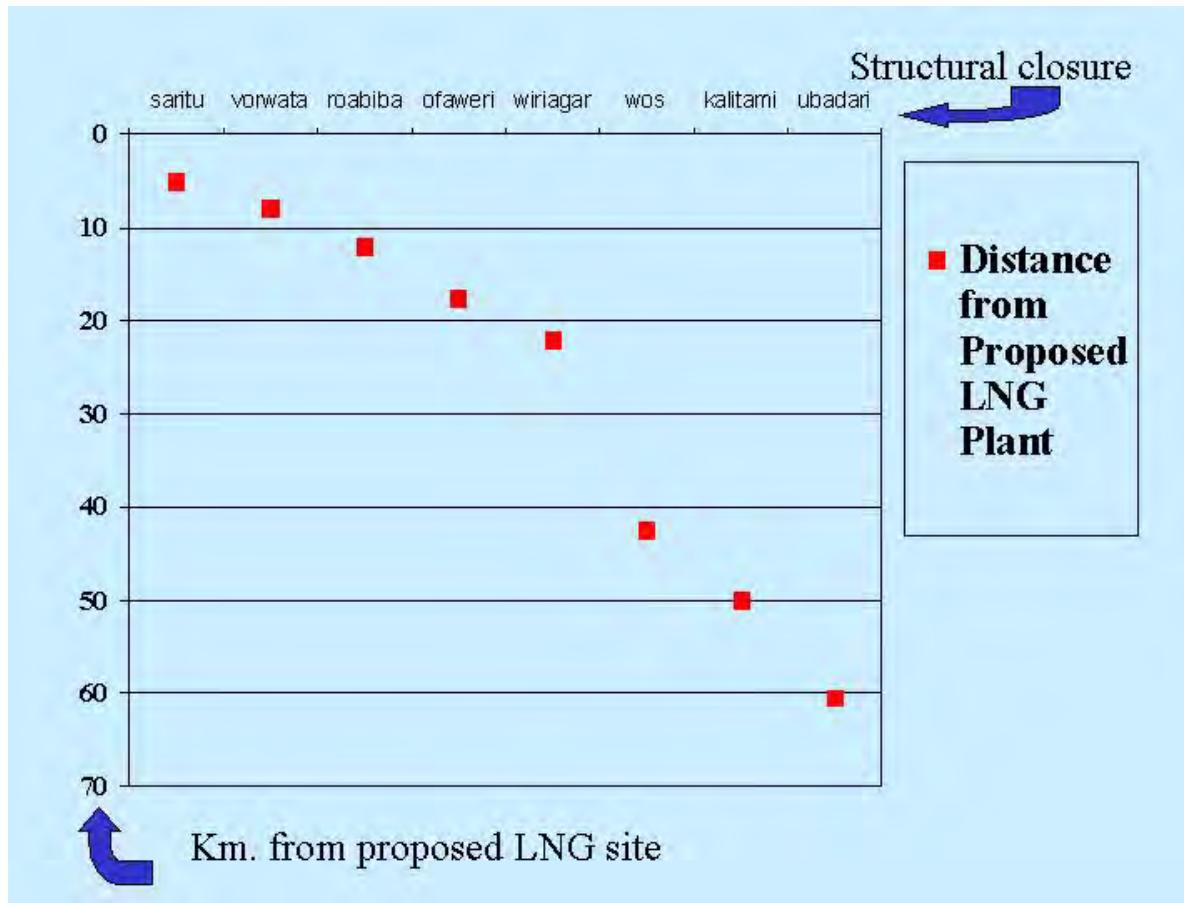


Figure 11.3: Chart of distances from proposed LNG Plant (CO₂ source) location to potential injection site structural trap closures in kilometers. If Saritu structure is discounted due to the present-day lack of data (and hence high risk), then Vorwata structure is the best ESSCI site if distance is considered as additional criteria for selecting the best potential ESSCI CO₂ injection location.

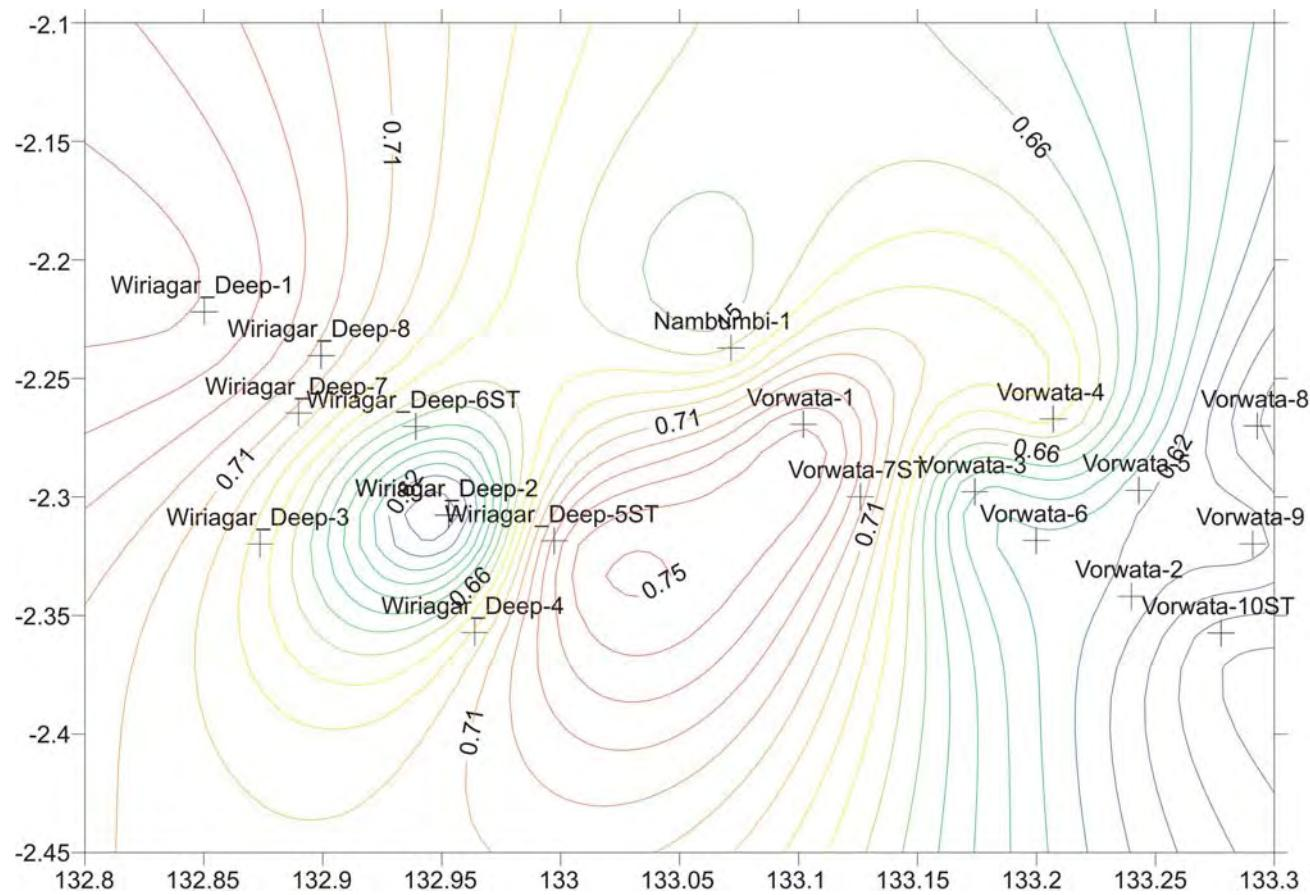


Figure 12.1: Leak-Off Test (LOT) gradient contour map of the Wiriagar Deep and Vorwata areas, based on drilling data from wells (Hillis and Meyer, 2002). Grid coordinates are latitude and longitude in degrees.

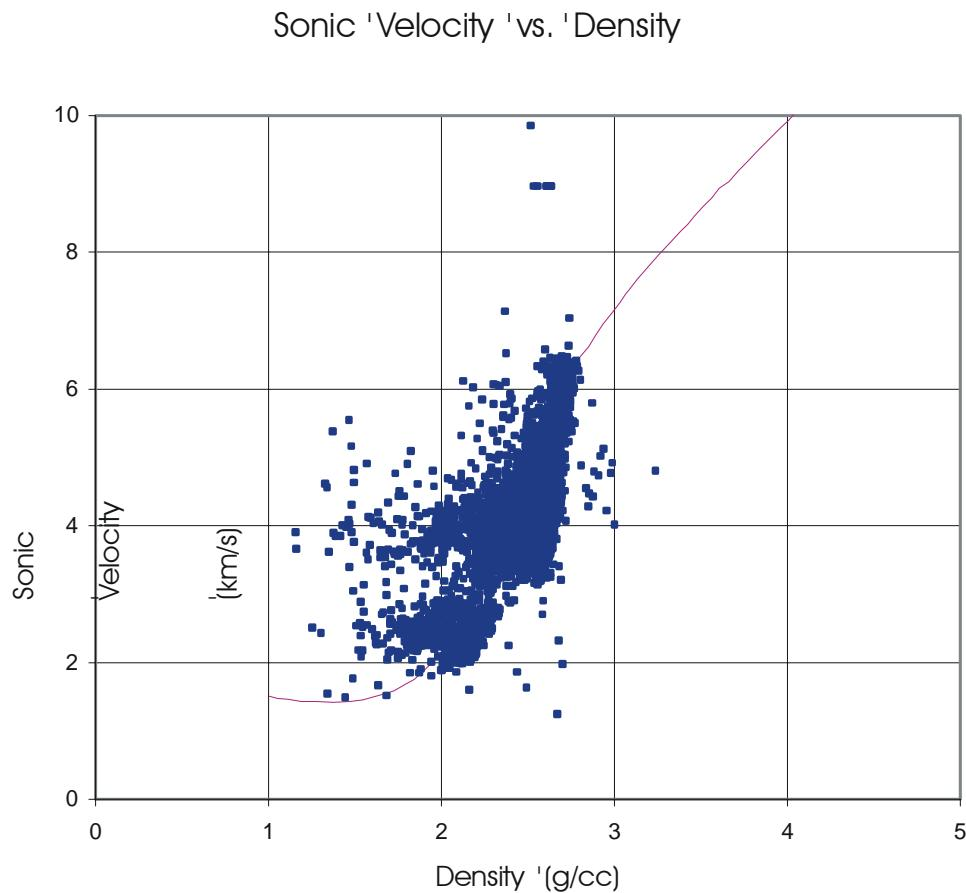


Figure 12.2: A Nafe-Drake velocity vs density transform (pink line), based on density and sonic data from Wiriagar Deep and Vorwata area wells (blue circles). The Nafe-Drake curve provides a ‘good fit’ to the data and was used to convert average velocities to the top of the density log to average densities and ultimately calculate vertical stress (Hillis and Meyer, 2002).

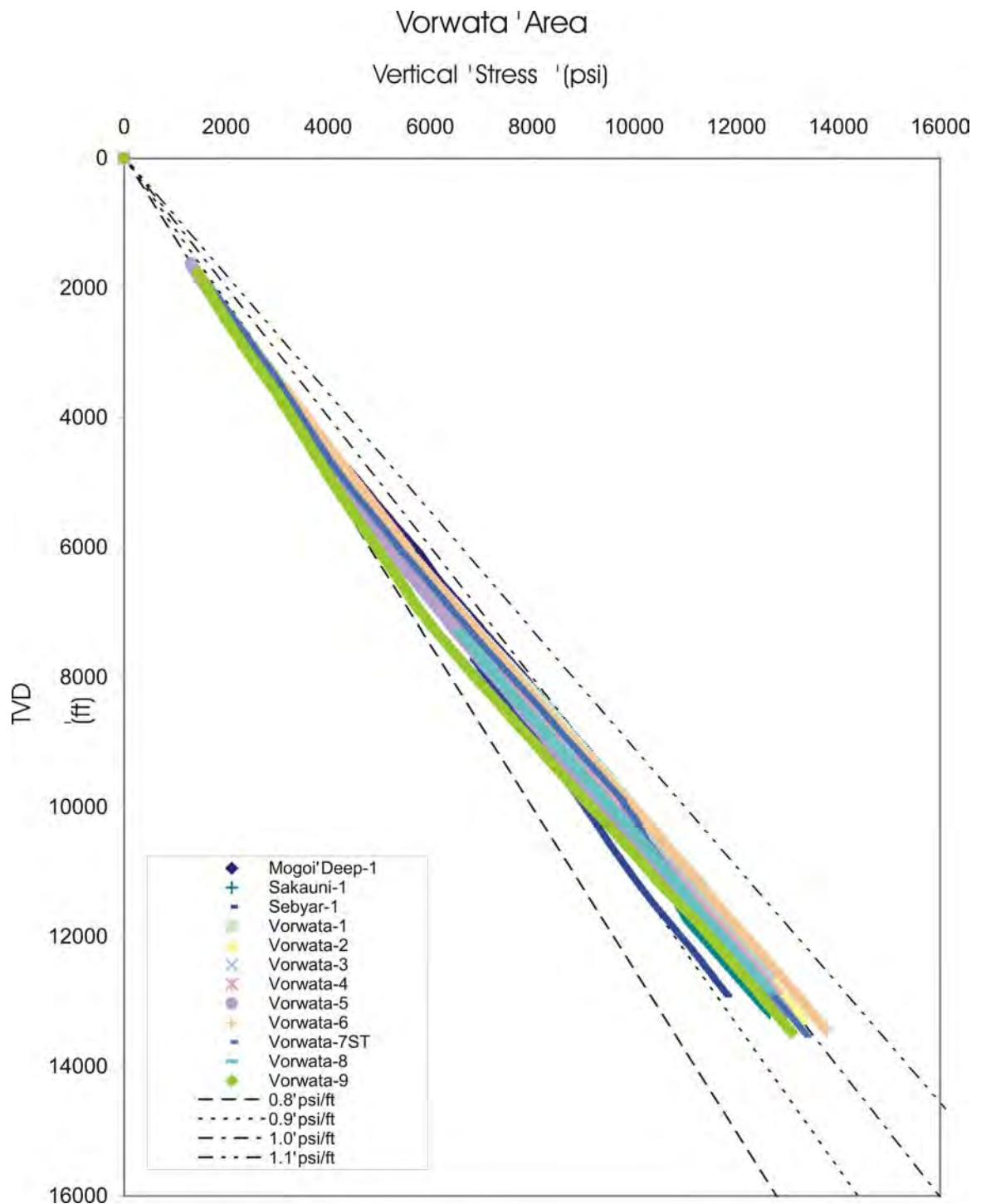


Figure 12.3: Vertical stress profile with depth for the Vorwata area (Hillis and Meyer, 2002).

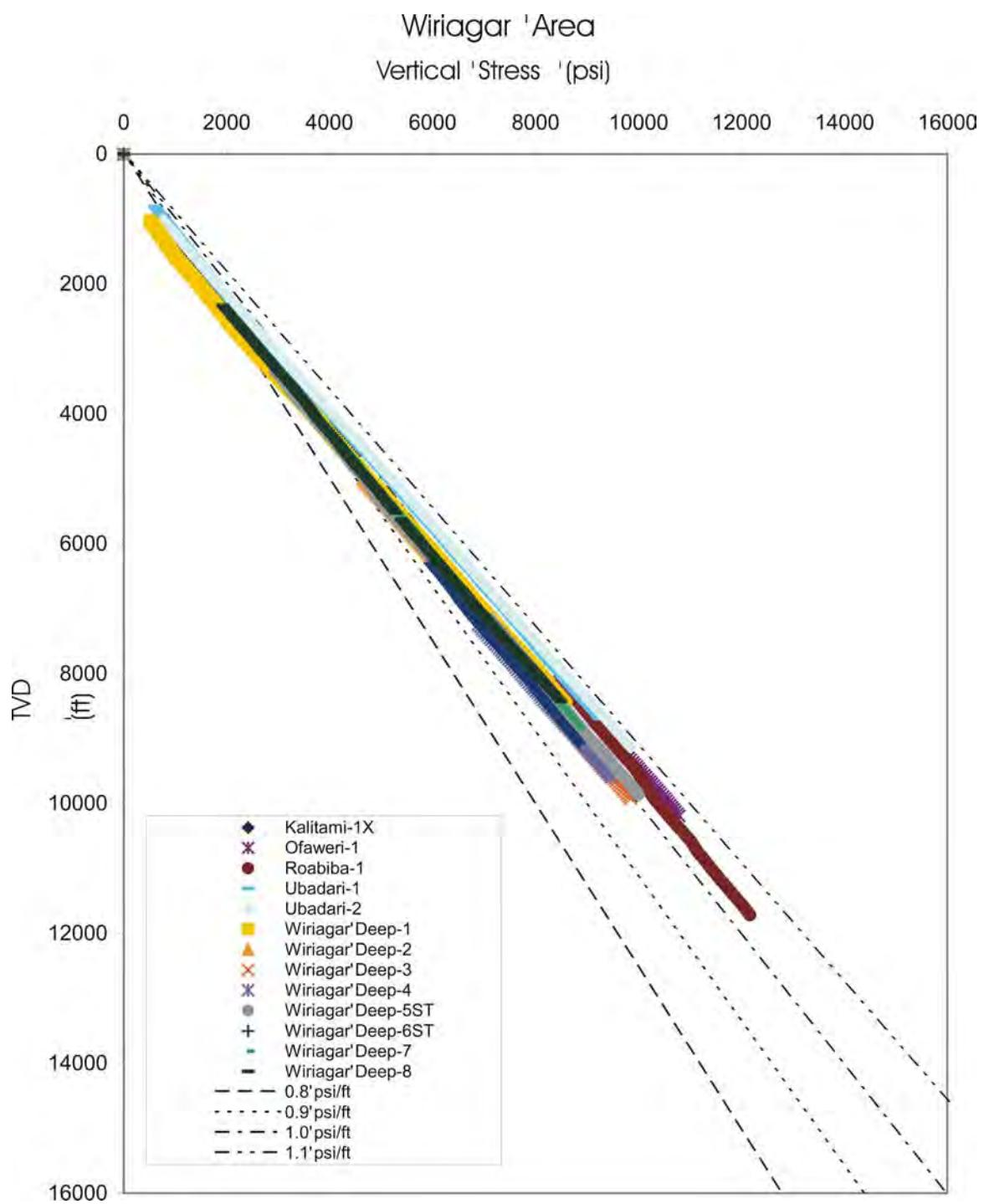


Figure 12.4: Vertical stress profile with depth for the Wiriagar Deep area (Hillis and Meyer, 2002).

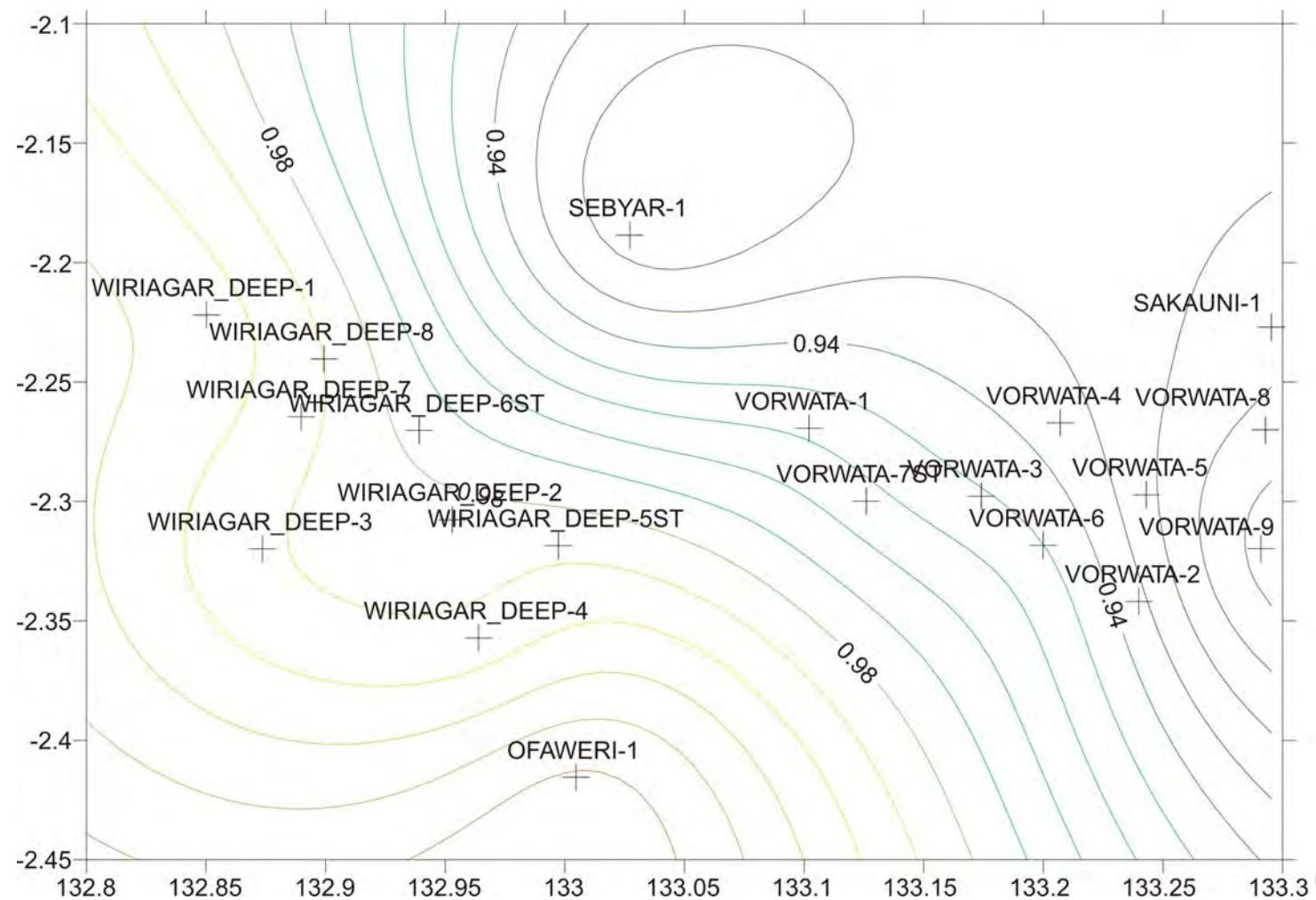


Figure 12.5: Vertical stress (Sv) gradient contour map of the Wiriagar Deep and Vorwata areas in psi/ft, for -8200 ft depth (Mesozoic interval generally) (Hillis and Meyer, 2002).

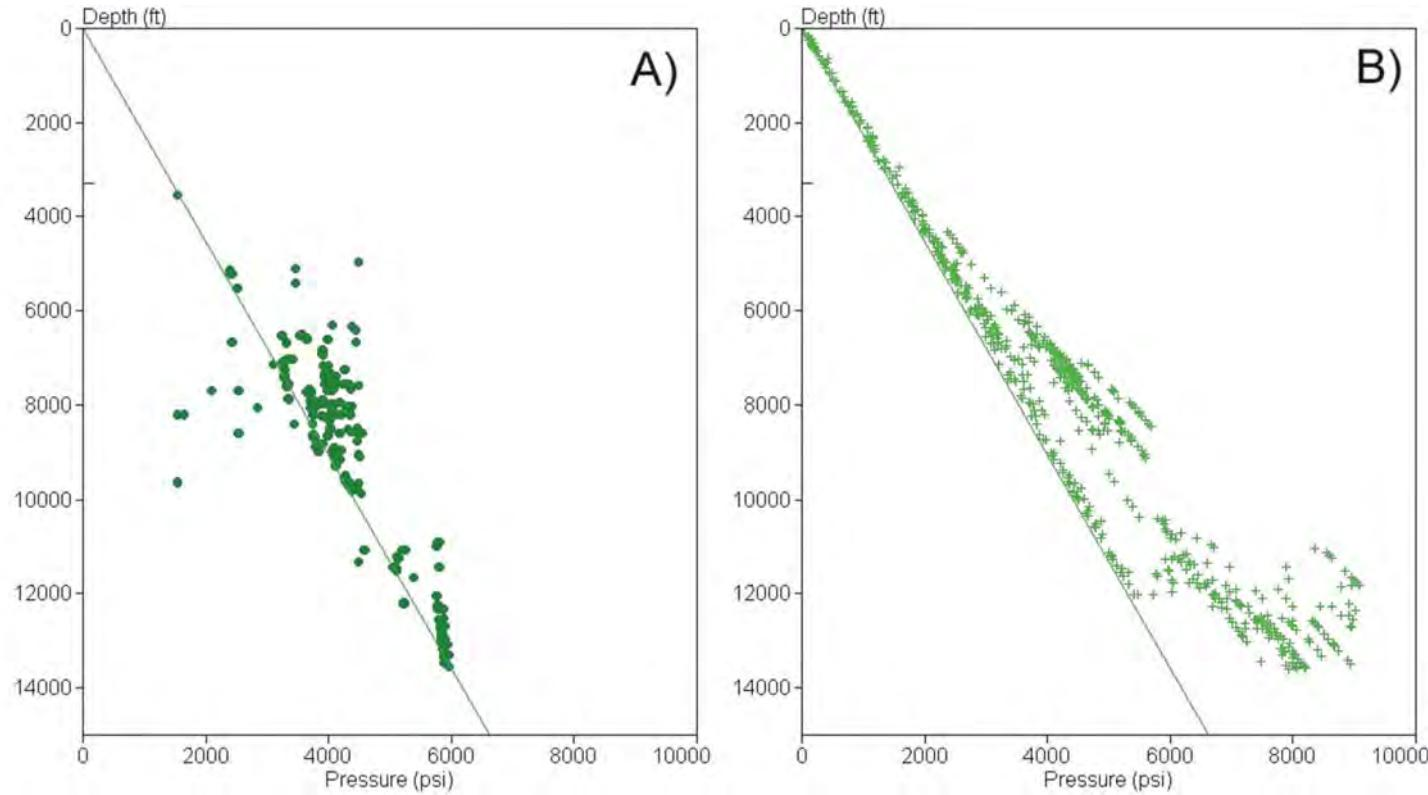


Figure 12.6: (A) Formation Pore Pressure distributions from 573 DST and MDT/RFT tests/runs on 23 wells in the Tangguh area; and (B) Estimated Formation Pressures extrapolated from 19 wells in the Tangguh area. Both show a ‘good fit’ for the datasets (Hillis and Meyer, 2002).

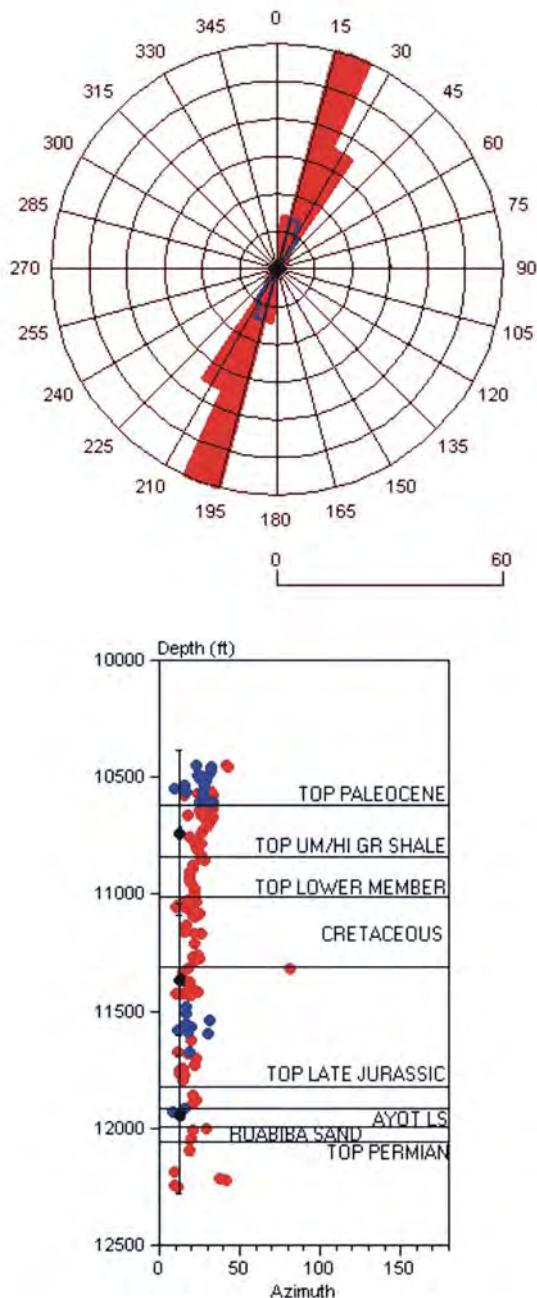


Figure 12.7: Data from Vorwata #3 well (as an example of methodology performed on all Tangguh area well data) displayed as a ‘Rose Diagram’ at top with borehole breakouts (red) and DITF’s (blue) plotted as planes to poles. Depth vs directional orientation graph at bottom, with borehole breakouts (red) and DITF’s (blue) plotted with corresponding depth with the various stratigraphic intervals labelled. Mean SH_{max} azimuth orientation inferred from breakouts: $023^\circ N$ ($SD=8^\circ$ $N=114$); and DITF’s: $022^\circ N$ ($SD=7^\circ$, $N=27$). (Hillis and Meyer, 2002).

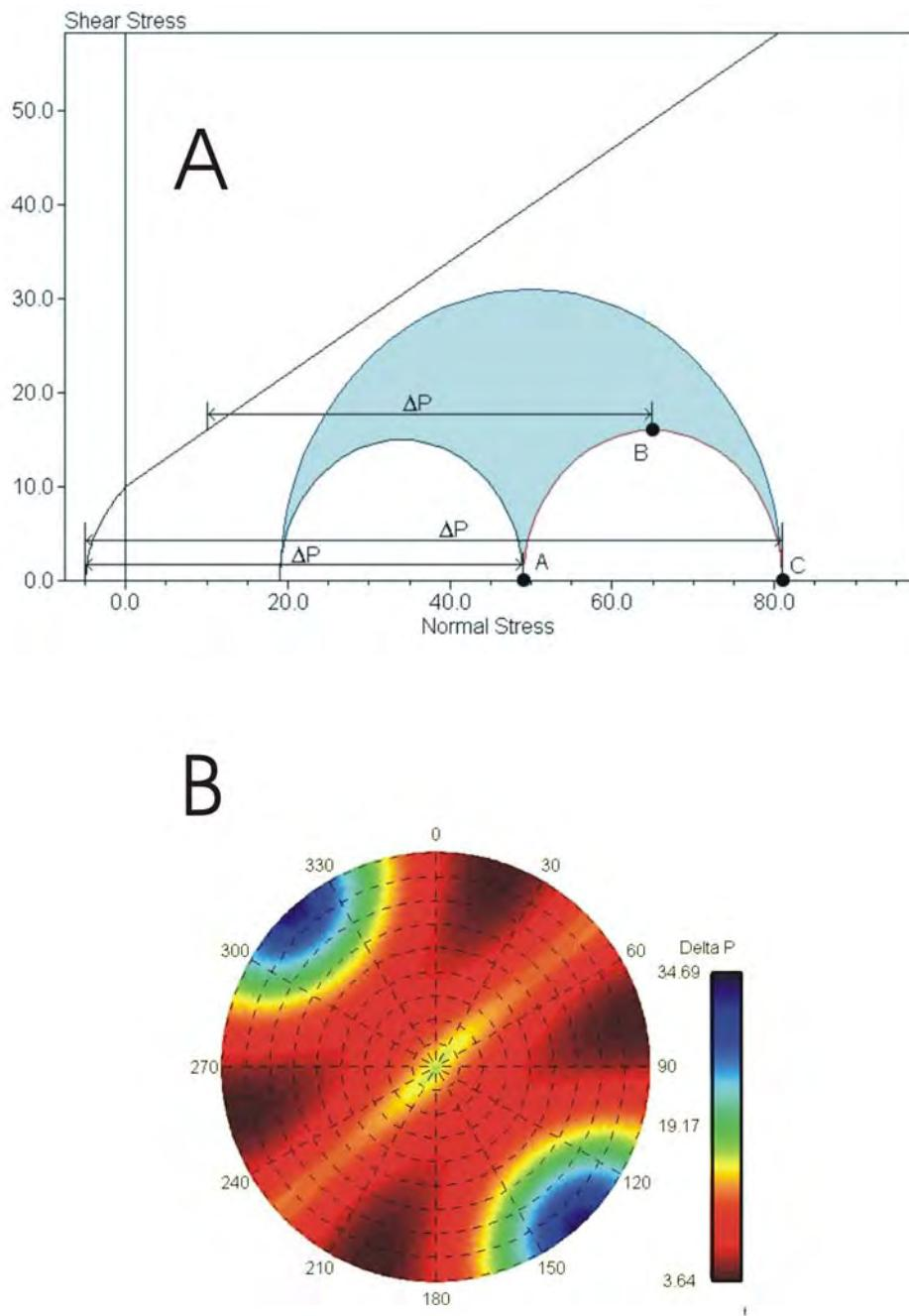


Figure 12.8: (A) At top is a 3D Mohr diagram as an example of in-situ stress field analysis, whereby all faults are in the blue shaded area. The diagonal line from lower left to upper right is the brittle failure point, and the horizontal distance (ΔP_p) between any orientation of fault and the failure envelope is used to assess the likelihood of fault re-activation. (B) At bottom is an example of a structural permeability diagram: the contoured polar diagram of normals to fault planes colored by ΔP change required to re-activate the fault. High ΔP implies low risk of re-activation (blue), and low ΔP implies high risk of re-activation (red) (Hillis and Meyer, 2002).

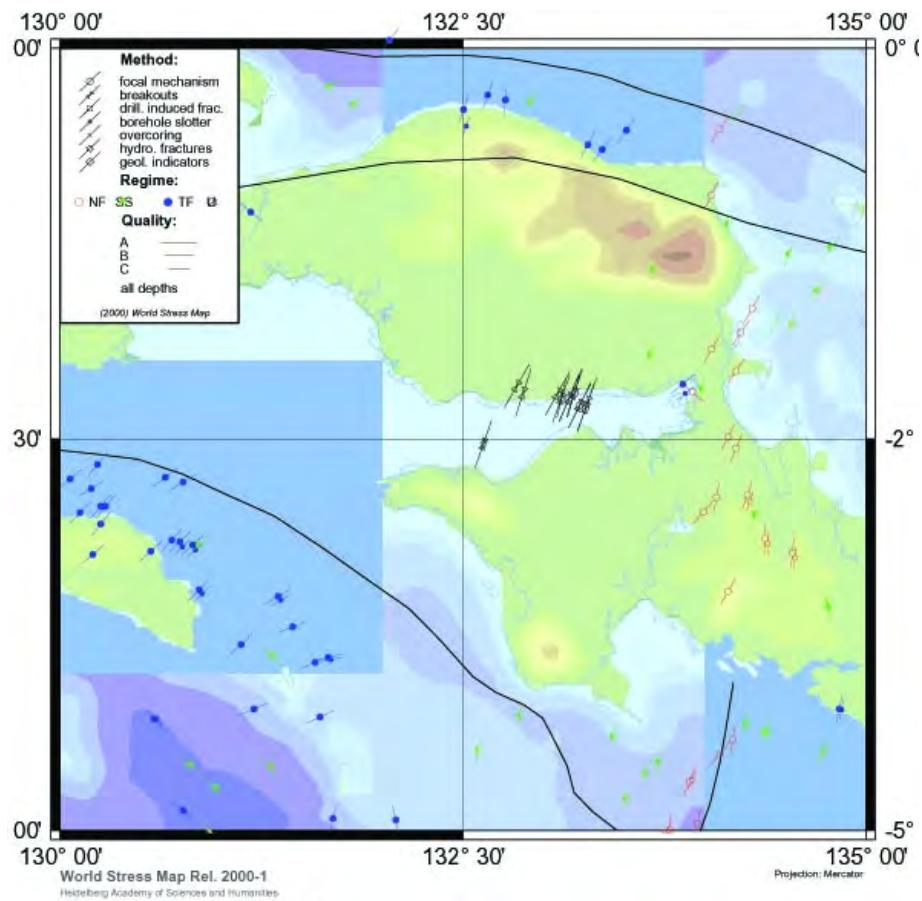


Figure 12.9: Map of the in-situ horizontal stress orientations for Berau/Bintuni Basins, at the Mesozoic depth of interest (Hillis and Meyer, 2002). Lines show direction of maximum stress at a given point (circles). Method key shows source of data and quality.

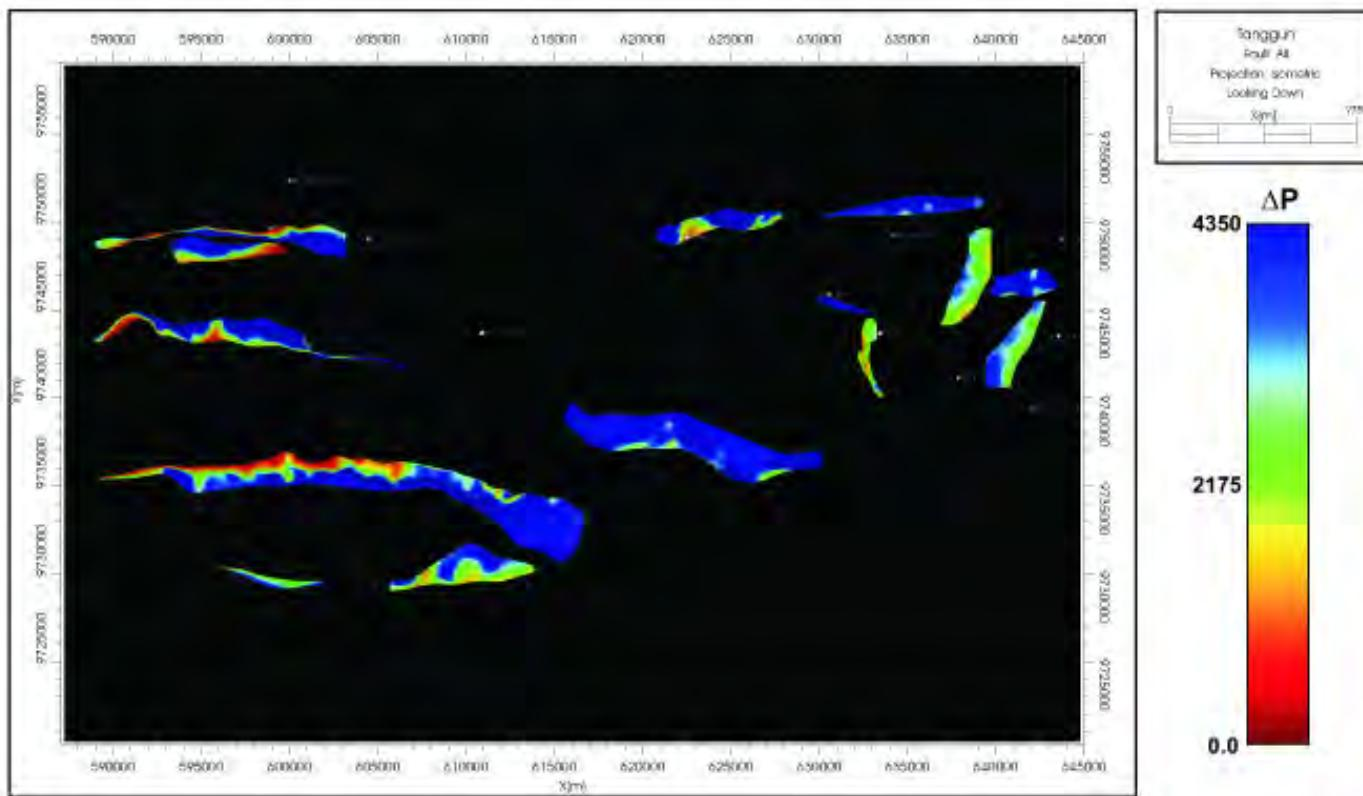


Figure 12.10: A ‘looking down’ view of all Tangguh area faults analyzed for this study. Almost 20 faults were selected based on significance of length and throw, variance of dips and strikes, and proximity to the southern and eastern flanks of the Vorwata structure. In some cases several interpreted faults that appeared to be continuations of the same planar surface were merged into a single larger fault plane, resulting in 14 faults displayed. Scaling on right indicates that red portions of faults are at the highest risk of re-activation with only slight increases in pore pressure required to re-activate them, and blue portions of faults are at the lowest risk of re-activation requiring up to 4350 psia increase in pressure over current hydrostatic pressures to re-active them (Hillis and Meyer, 2002).

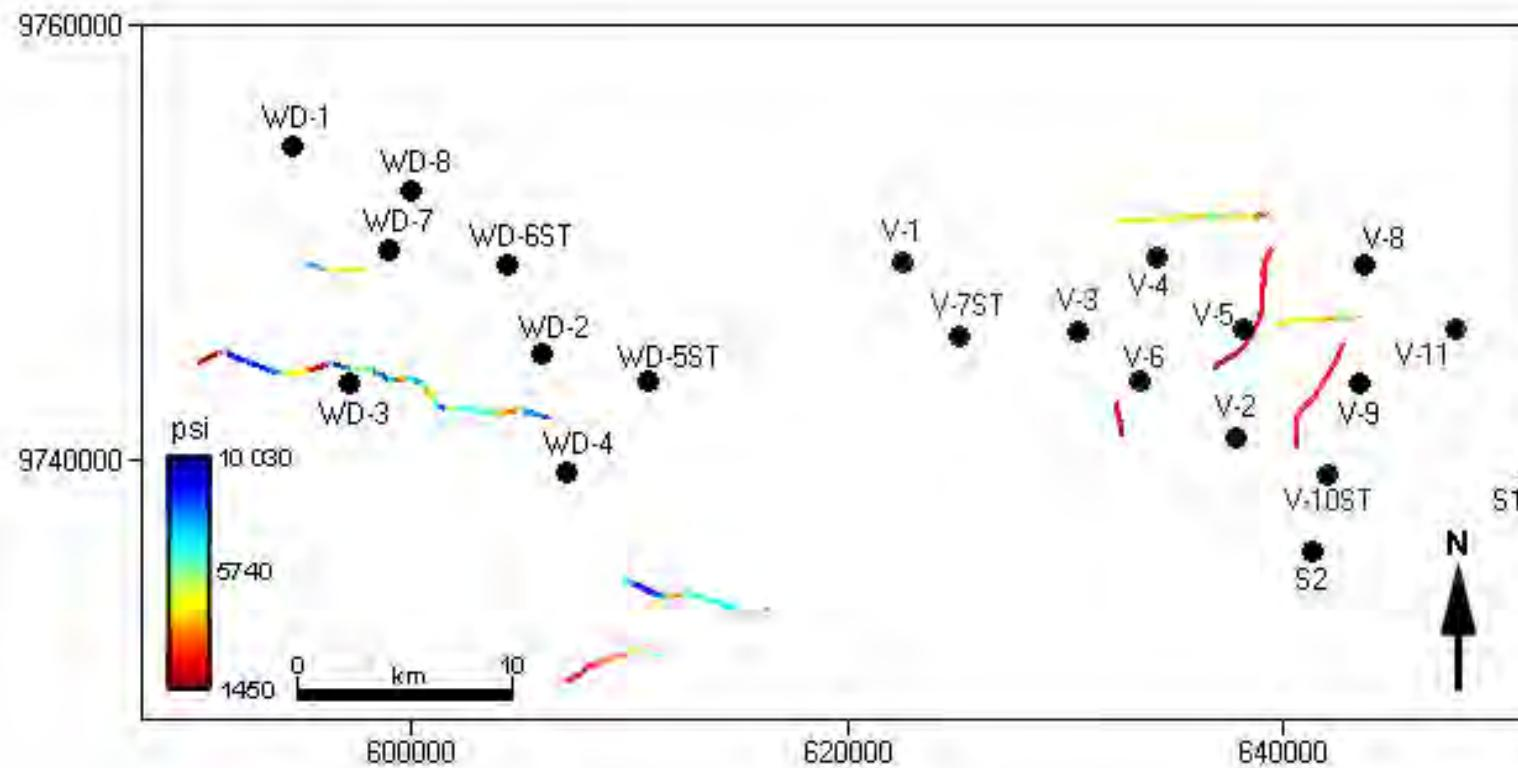


Figure 12.11: A depth-slice at ~14,000 ft TVDss of the Wiriagar Deep and Vorwata structure fault traces in the Tangguh area, showing the assessment of estimated fault re-activation pressure over hydrostatic in psia (see color-coded scale at left) processed in FAPS computer program. Nine faults are present at the -14,000 ft level (Roabiba Sandstone Formation at SE Vorwata structure) and they are color coded, as per psi scaling at lower left, for minimum pressure increase over hydrostatic to induce fault re-activation. Although two high risk faults are present between the V-5 and V-9 well locations, the fault locations are distant enough (>10 km) from CO₂ Injector Site #1 (S1) and Injector Site #2 (S2) that the supercritical CO₂ migration pressure at the faults should not increase formations pressure 1450 psi over the hydrostatic needed to cause re-activation. (J. Salo and J. Meyer 2003, after data presented in Hillis and Meyer 2002).

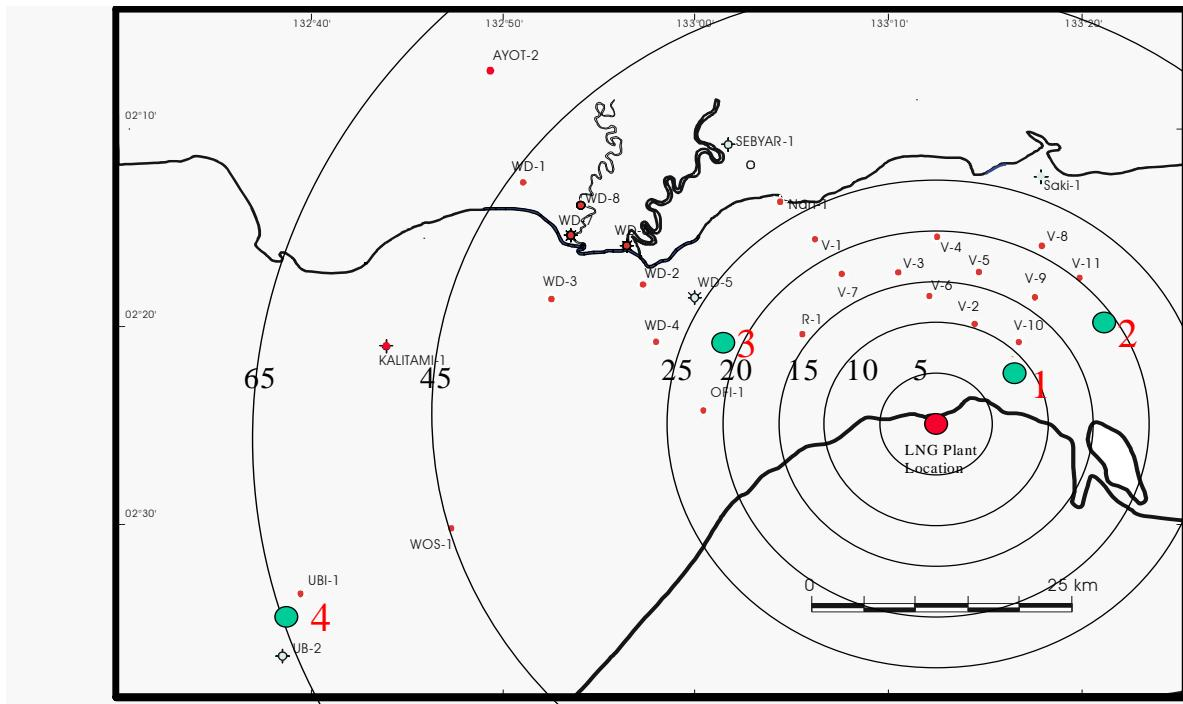


Figure 13.1: Bulls-eye distances are in kilometers from the proposed LNG plant location (in red), on the south coast of Bintuni Bay to the four proposed injection sites located in the downdip aquifer leg for each of the viable structures. Numbering (1 – 4) ranks closest proximity to LNG plant and not a ranking of sites based on geological evaluation.

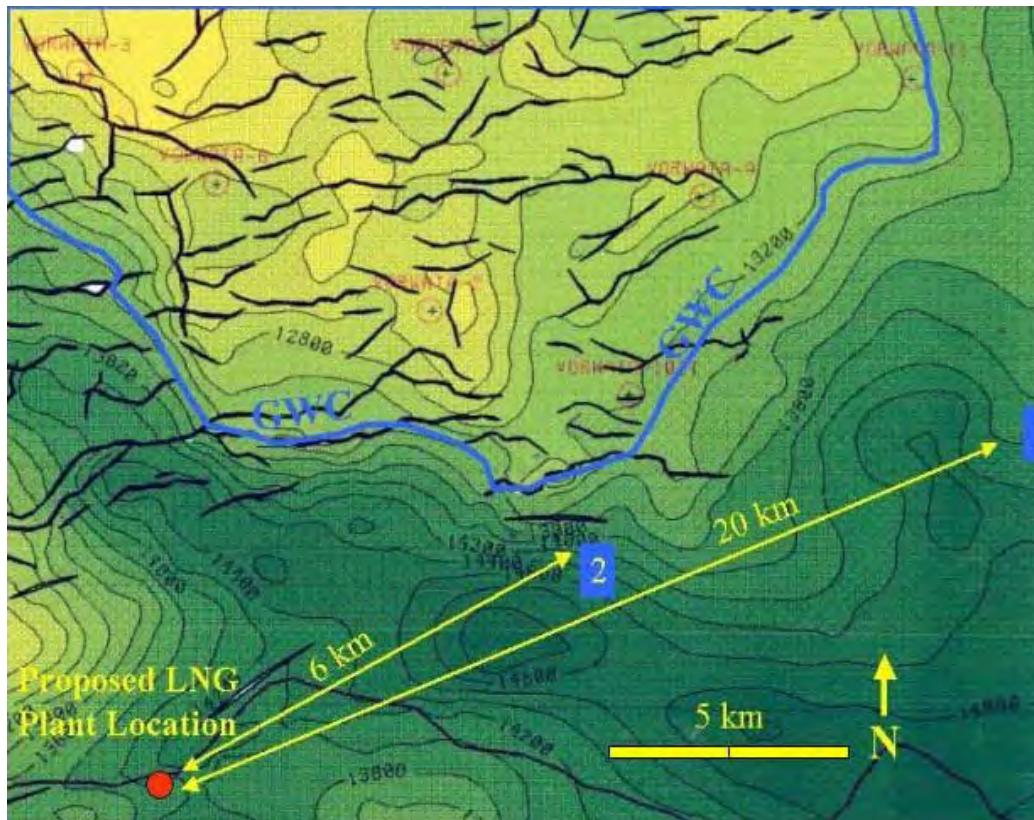


Figure 13.2: Subsurface location of the two recommended Vorwata injection sites, relative to the proposed LNG plant location. Base map is the Top Structure Depth Callovian/Bajocian/Bathonian Roabiba Sandstone contour map. Vorwata GWC is shown in blue, and well locations in red. CI = 200 ft.

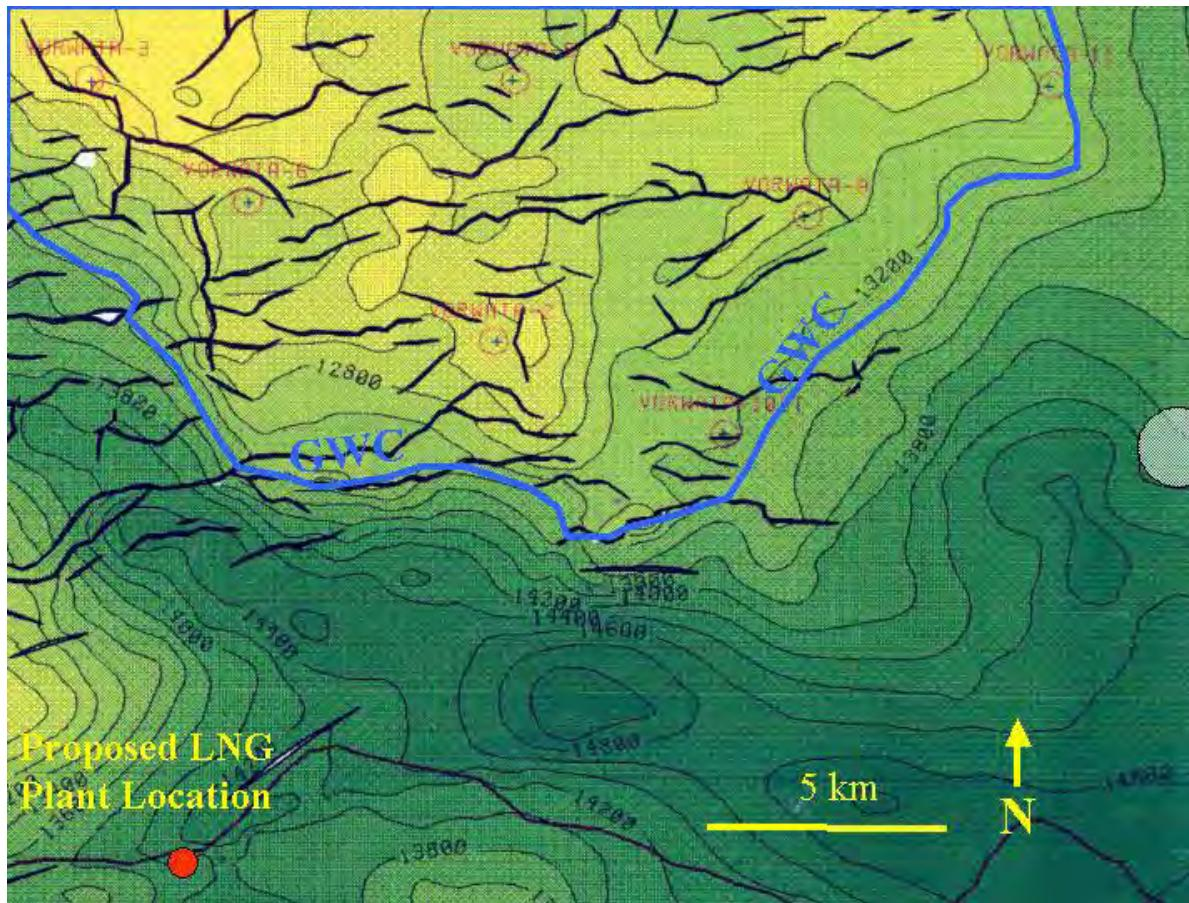


Figure 13.3: The aerial extent of 0.5 TCFsc CO₂ volume at reservoir pressure and temperature at the injector well proposed for the best ranked location, approximately 10 km east of the Vorwata-10st well. The injection location is in the Roabiba reservoir's downdip water-leg on Vorwata structure's eastern flank. The injected CO₂ volume has a diameter of 1.7 km assuming a reservoir thickness of 400 ft.

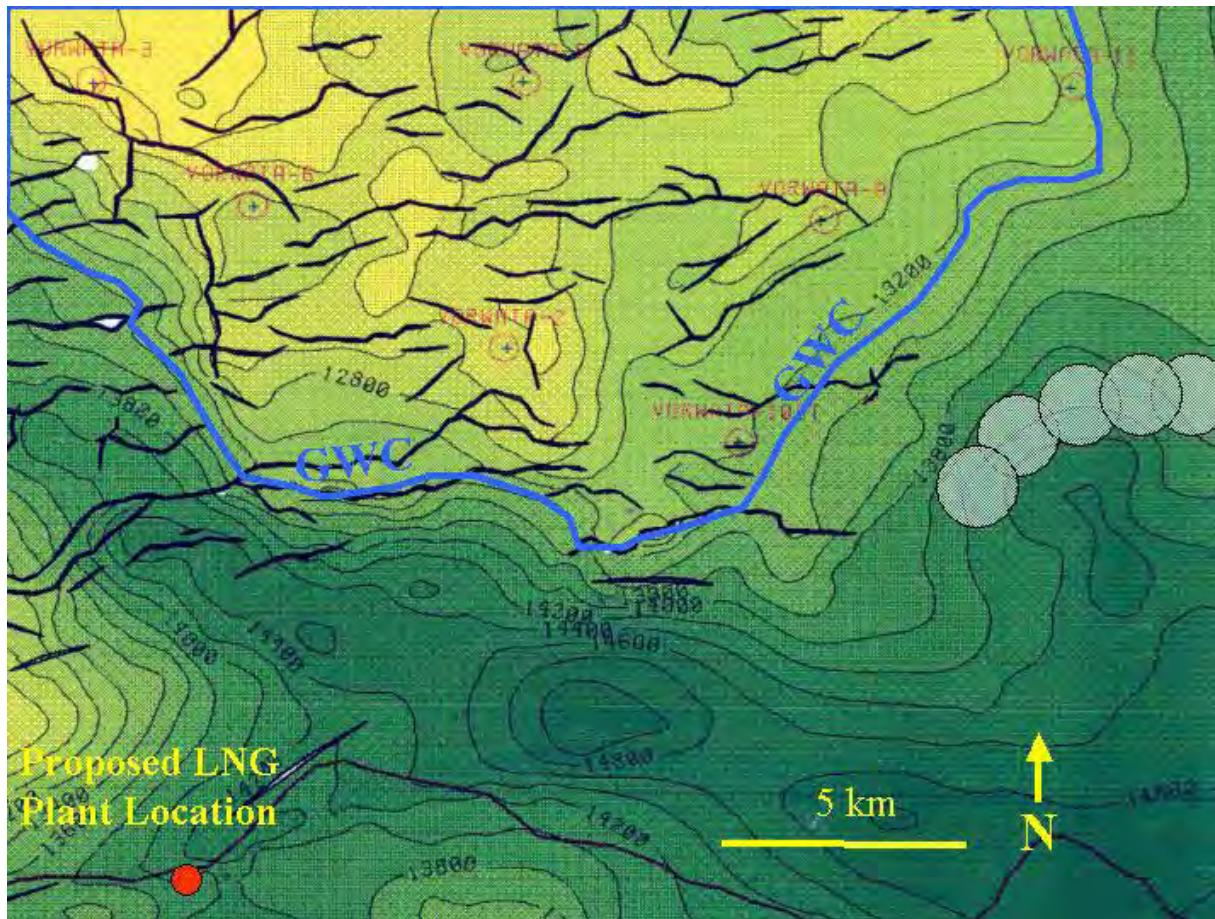


Figure 13.4: The projected areal extent for the total 2.4 TCFsc CO₂ supercritical volume at reservoir pressure and temperature, assuming a reservoir thickness of 400 ft. The areal extent depicts the volume occupied after injection of all the CO₂ to be sequestered into the subsurface Roabiba reservoir from five injector wells spaced equally apart at the best-ranked location (IS #1) without the effects of migration. Migration, volume, and areal extent with time are presented in reservoir simulation screen captures in Chapter 14.

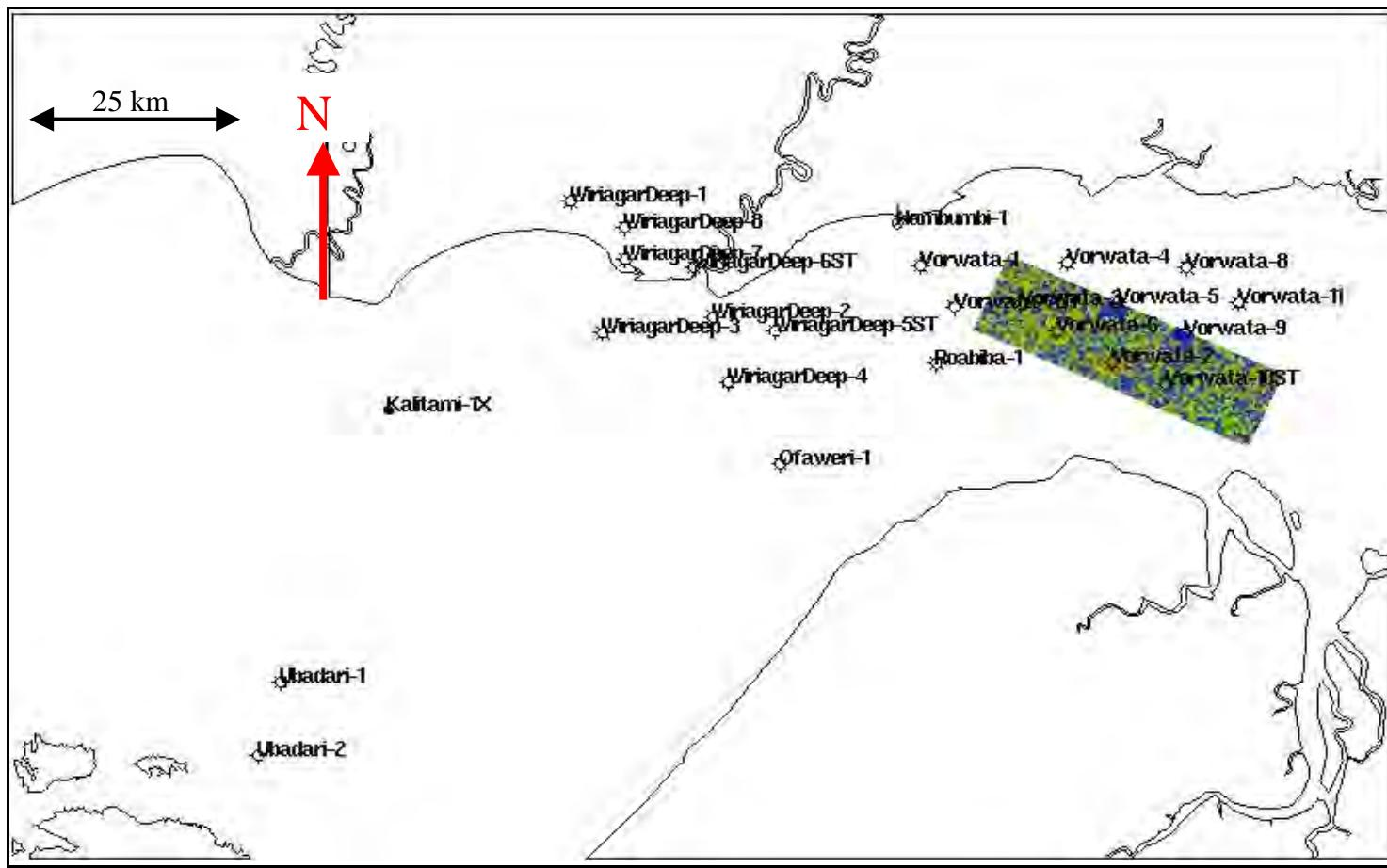


Figure 14.1: Test model area over a small portion of the Vorwata area only. Cells are colored by sonic values for DT as an example.

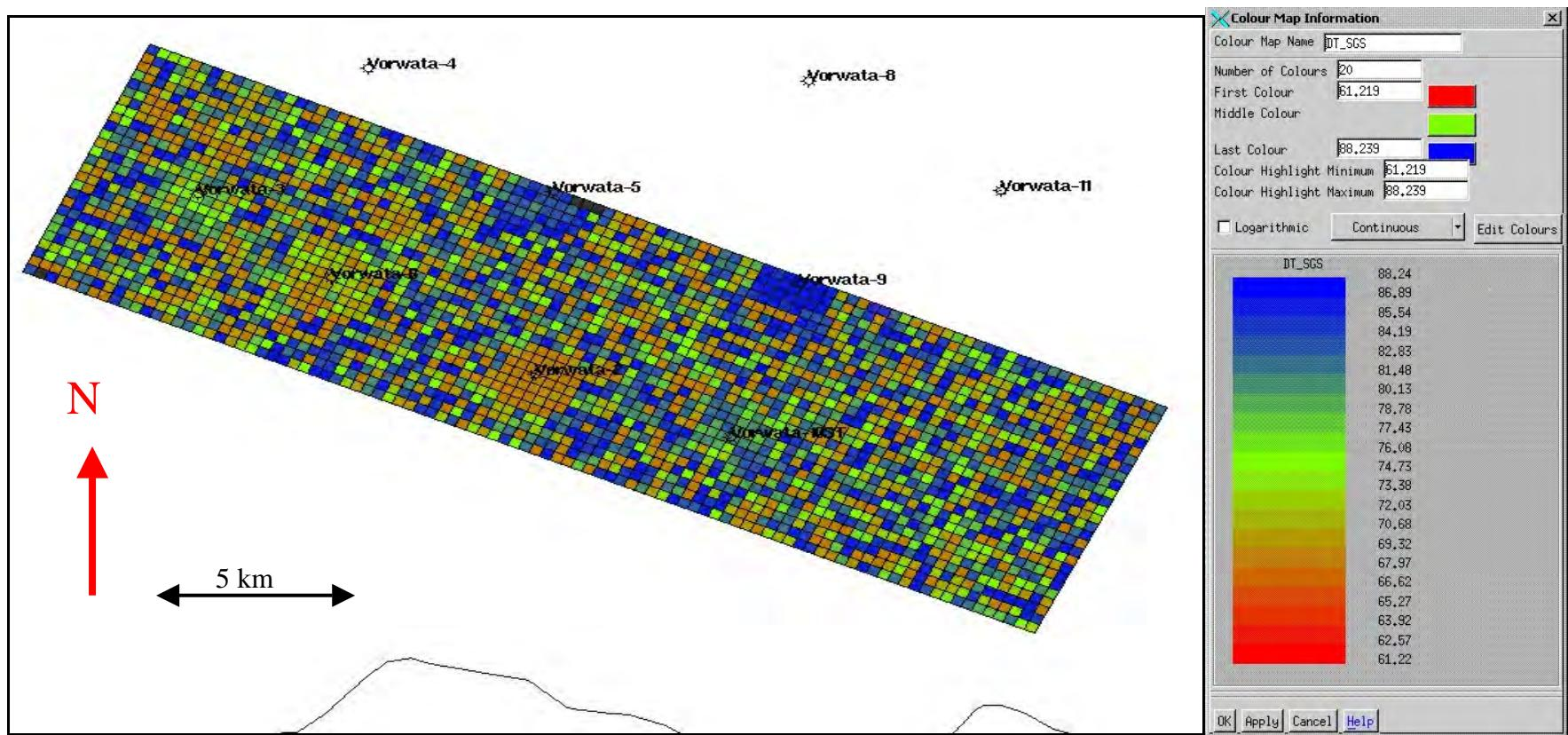


Figure 14.2: Close up of the test model area, with geo-cells of a single layer, color filled with values from sonic DT. Color scales for sonic values are shown on the right.

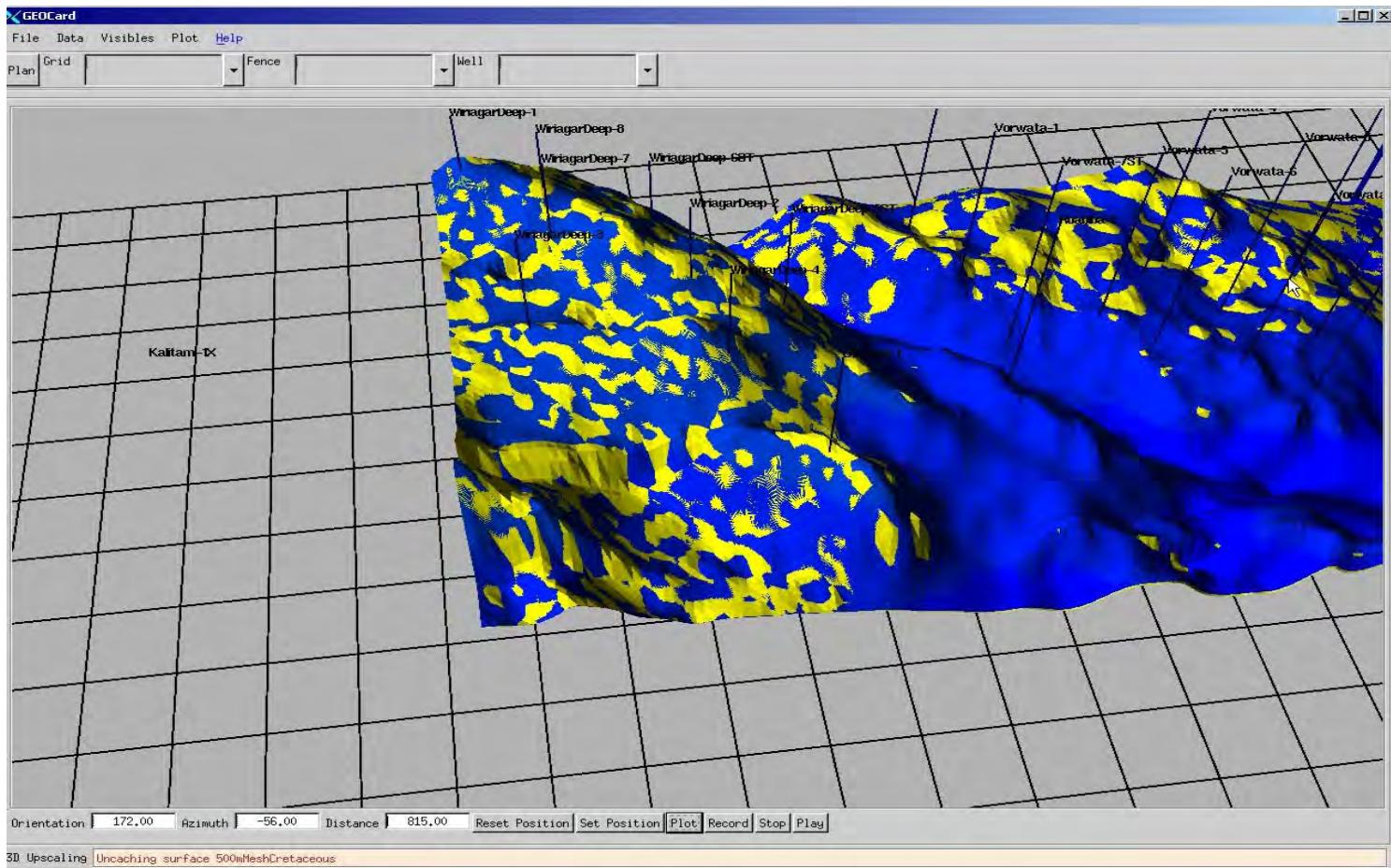


Figure 14.3: Base Late Cretaceous interpreted seismic surface with 'holes' in the surface apparent as yellow patches.

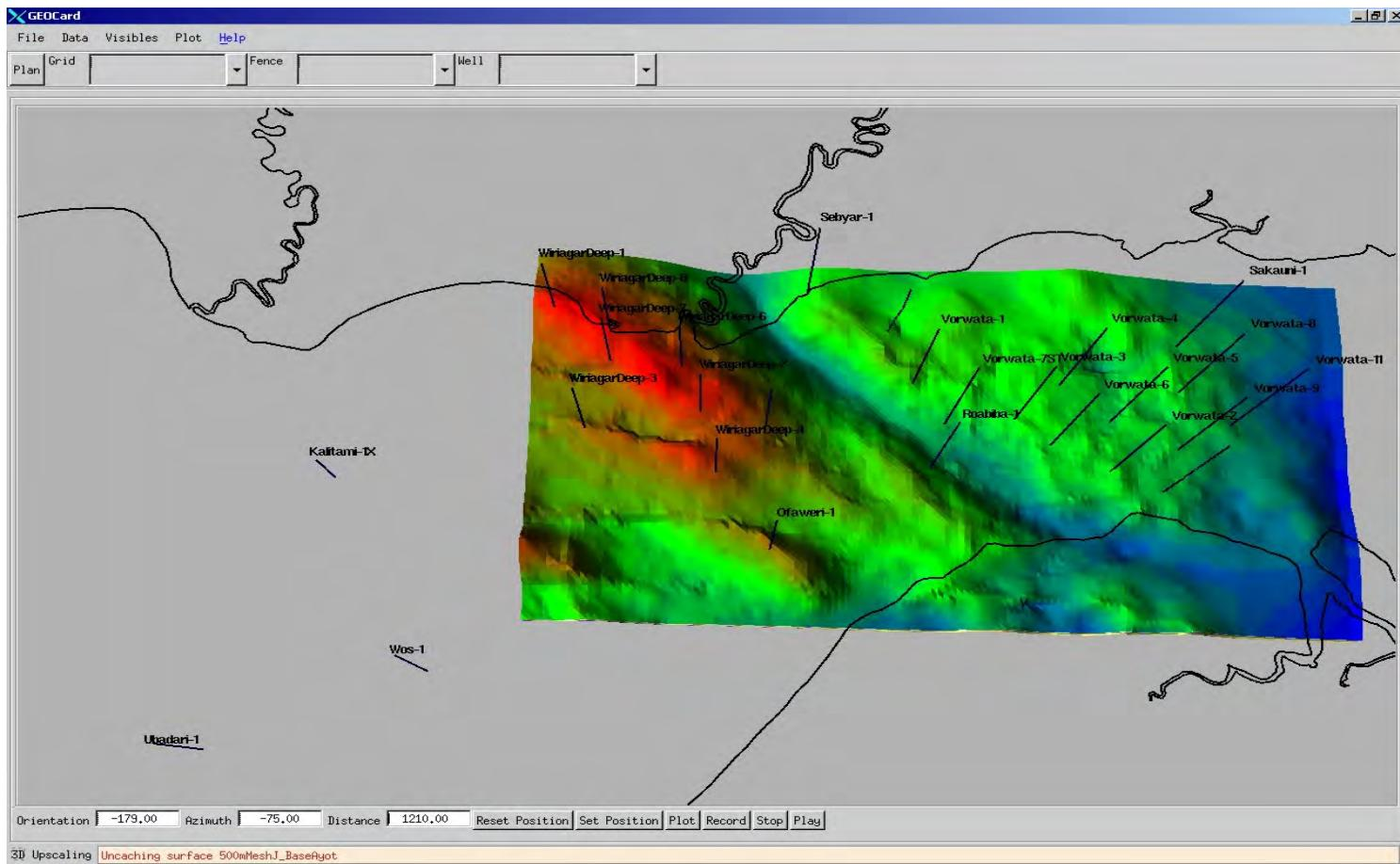


Figure 14.4: The area of the coarse grid 3D geo-cellular model encompassing both the Wiriagar Deep and Vorwata anticlinoriums, the smaller Roabiba and Ofaweri structures, the planned onshore LNG plant location on the south coast, and the 3 proposed CO₂ injection site locations.

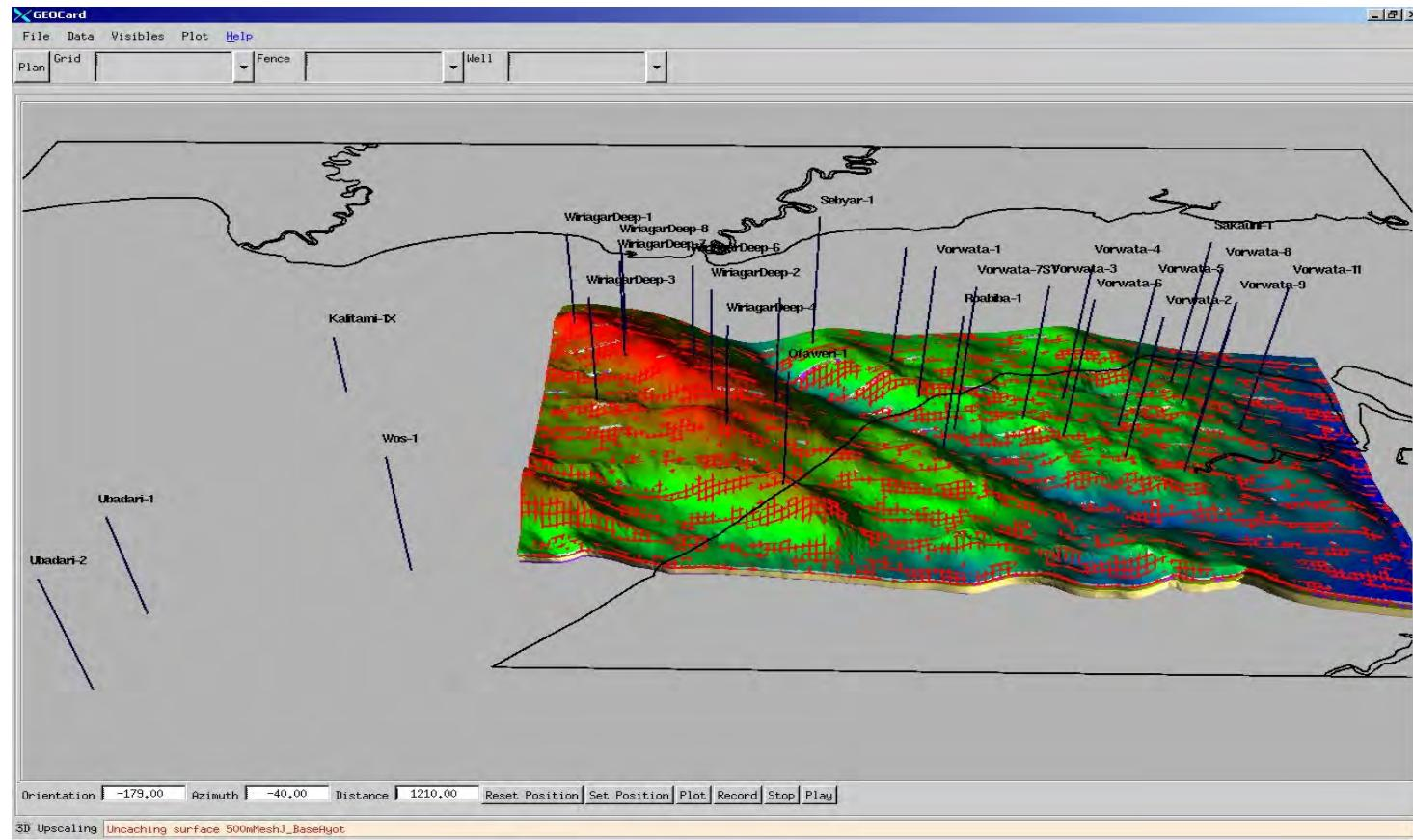


Figure 14.5: The 2D mesh (red ‘framework’) draped over the Base Late Cretaceous surface, and then registered.

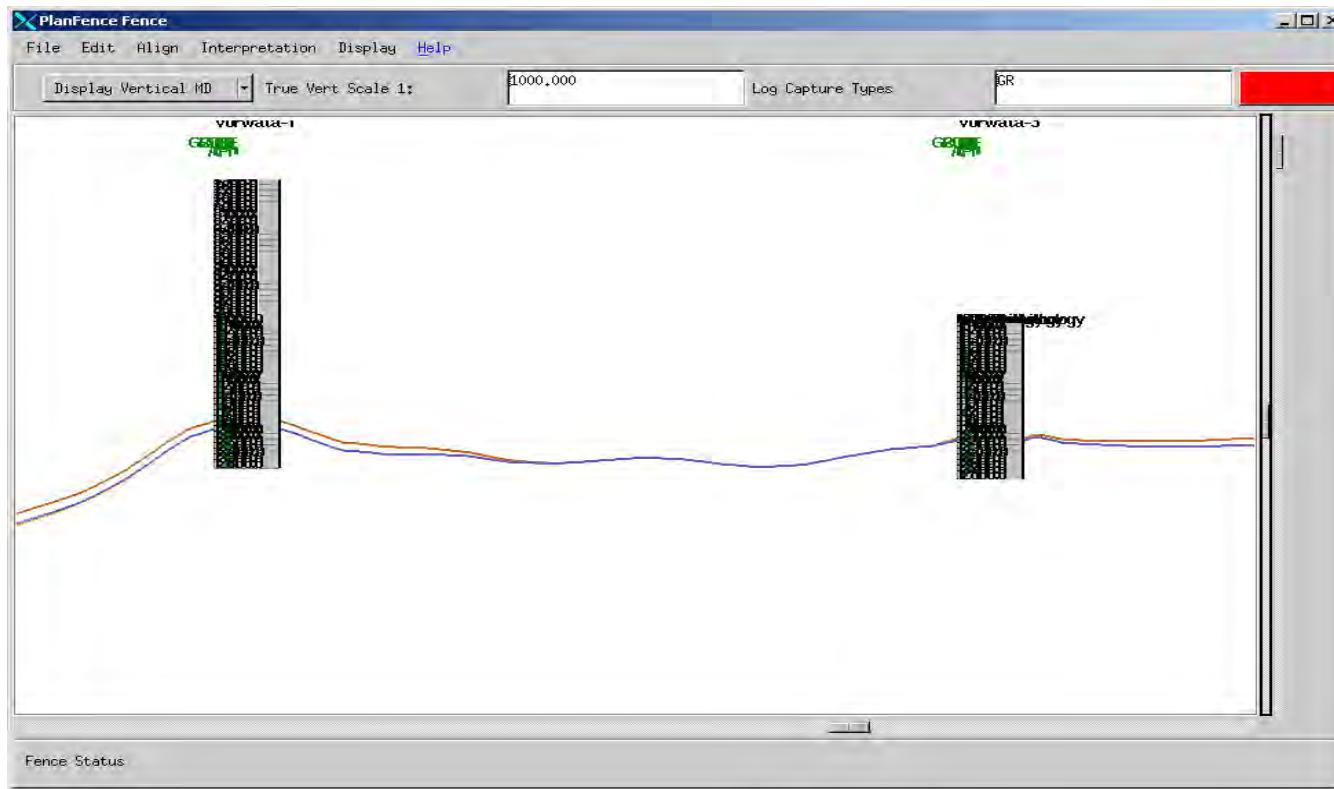


Figure 14.6: Surfaces are displayed in cross-sections, with wireline logs displayed at the appropriate well location along the surface (only Votwata-1 and Vorwata-3 wells are shown in this example). Close of fitting surfaces to wireline log picks to presented in Figure 14.7

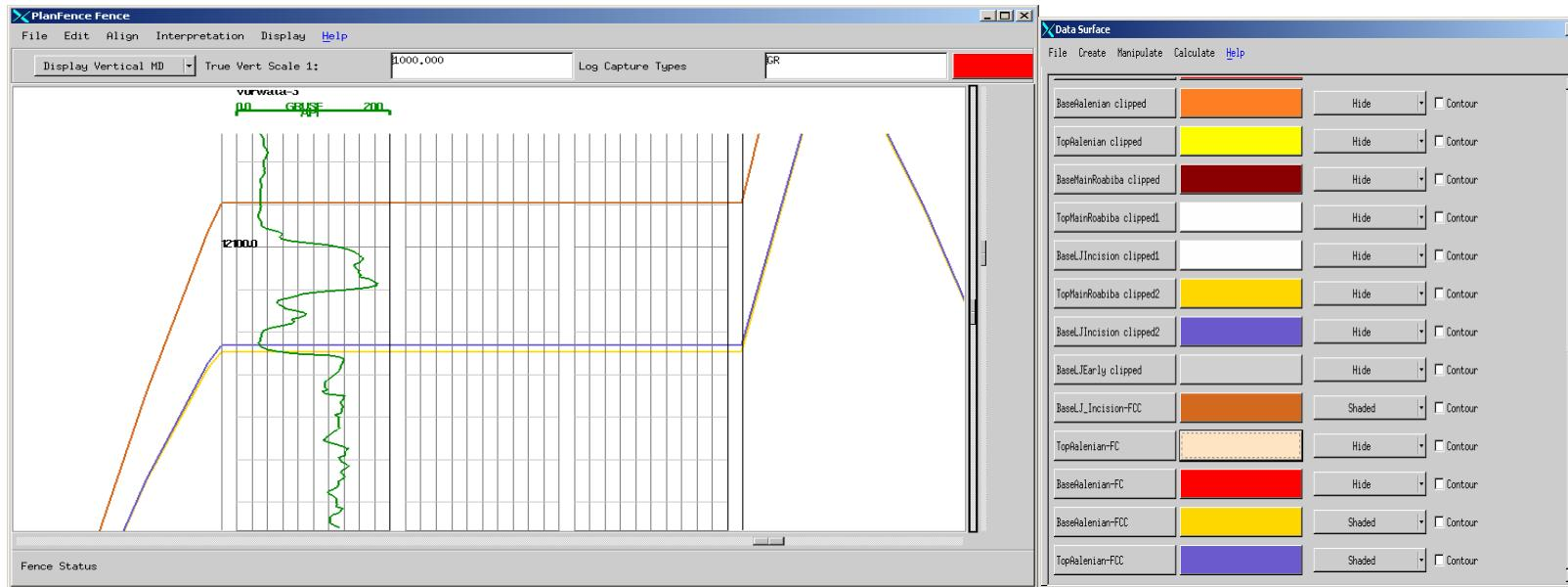


Figure 14.7: Close-up of the wireline log display for the Vorwata-1 well with gamma-ray (GR) displayed as the green curve in the left hand track for correlation of well log picks to surfaces. Surfaces are displayed as the color-coded horizontal lines with the surface identification legend displayed on the right. Individual surfaces are then shifted ('fitted') to the correct depth on the wireline log trace to match the well log pick for that surface at that well.

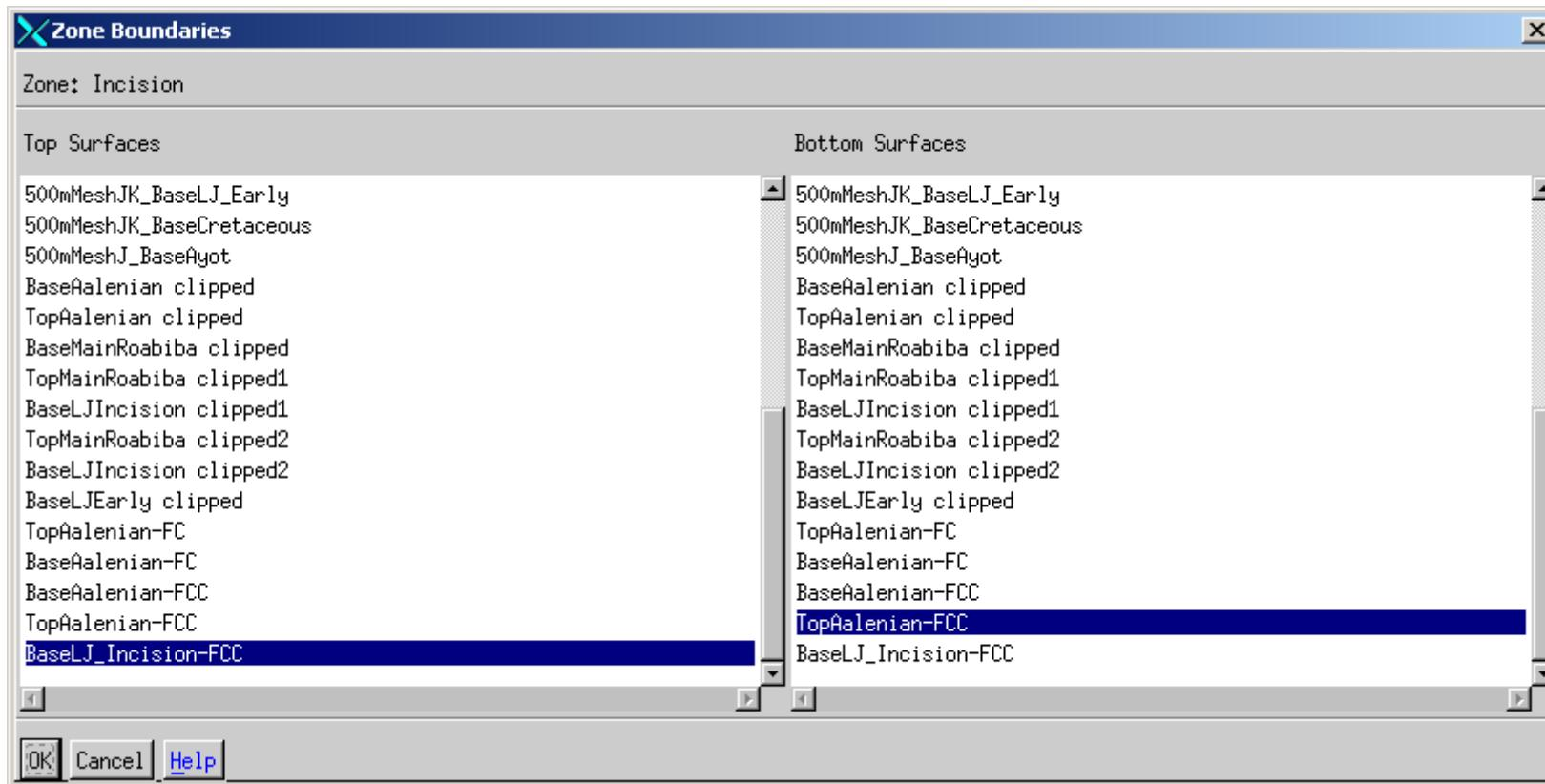


Figure 14.8: The zones in the 3D geo-cellular model are created by choosing upper and lower ‘bounding surfaces’, as shown in this screen capture from the GEOCARD ‘Zone Boundary’ creation panel.

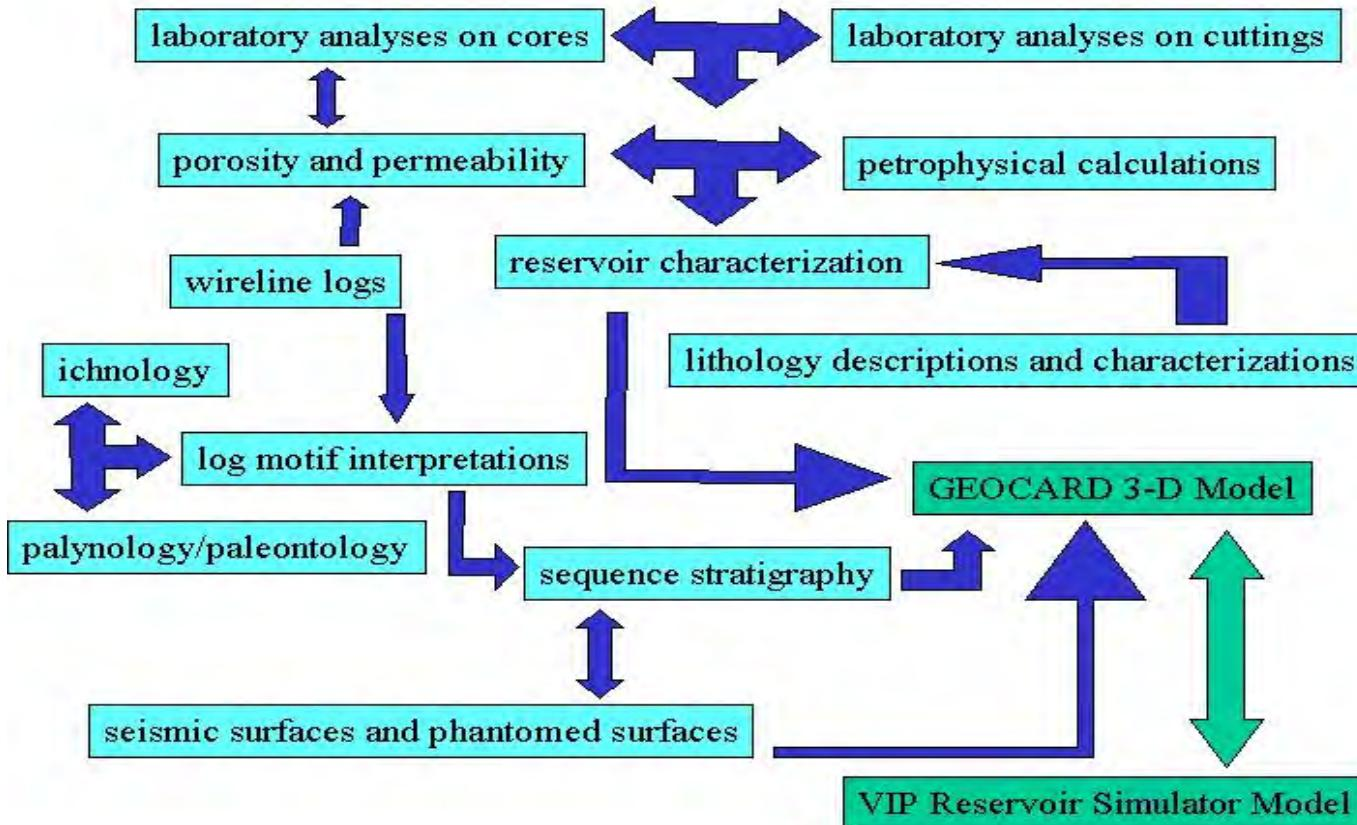


Figure 14.9: Work flow showing the various modules of the NCPGG study, and the relationship of the various study modules to the 3D geo-cellular model, and the export of it's grid and attributes to the VIP reservoir simulator.

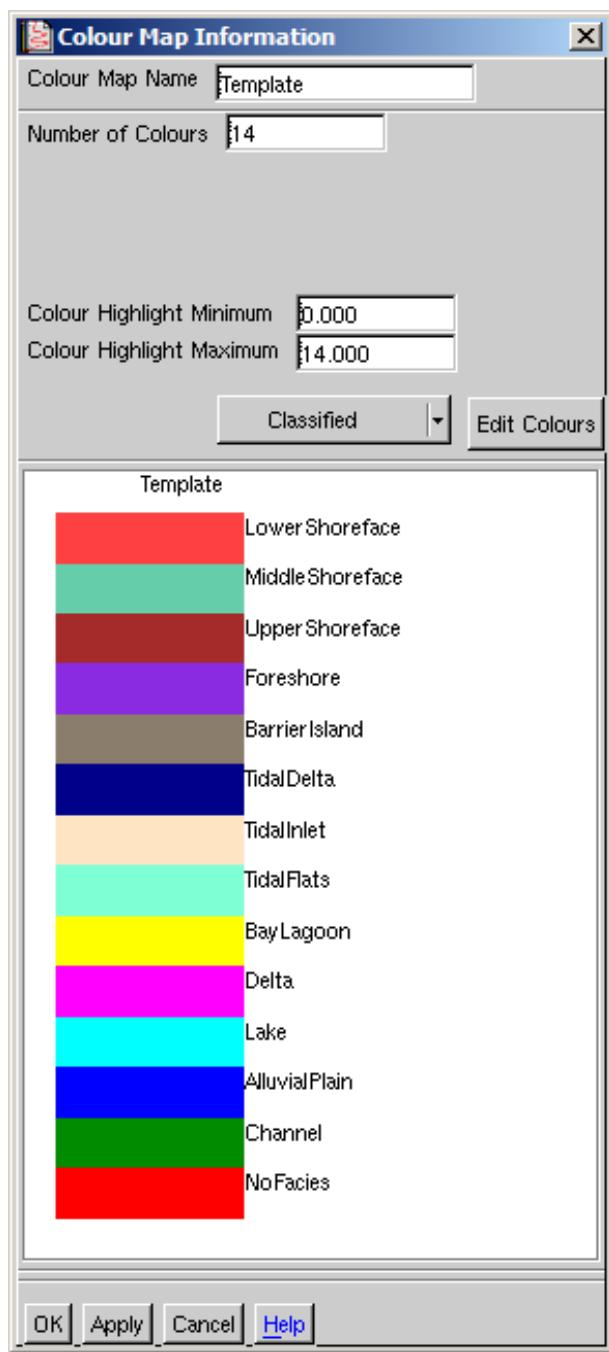


Figure 14.10: Color scheme and codes for facies shown above from a screen capture in GEOCARD for attribute “SimpleFacies_Use”. For example, SimpleFacies_Use=0 (on the bottom) represents no facies defined (i.e. continental or non-despositional), and the SimpleFacies_Use=13 is LowerShoreface (colored red at the top). Codes 2 (alluvial plain), 3 (Lake) and 6 (Tidal Flats) have been amalgamated with other facies and are not used in the model, though they had to be retained in the color map. Note that GEOCARD numbers attributes starting with zero (0) at the bottom and proceeding upwards.

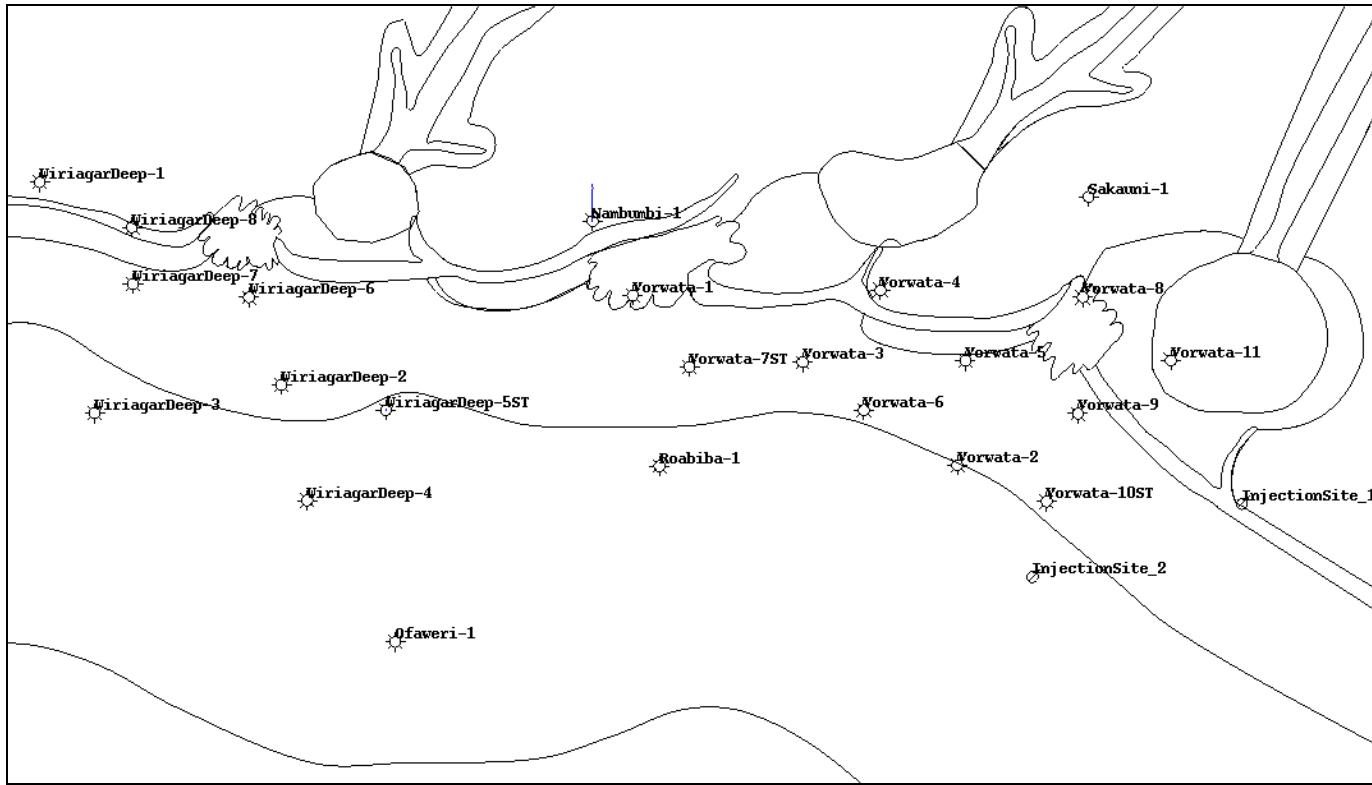


Figure 14.11: Example of digitized paleo-depositional facies polygons, created from the paleo-depositional geographical facies map series generated for the sequence stratigraphy module. The chronostratigraphic unit interval shown is the Callovian Roabiba Sandstone Reservoir Unit CU40; the model layer (k) is 21.

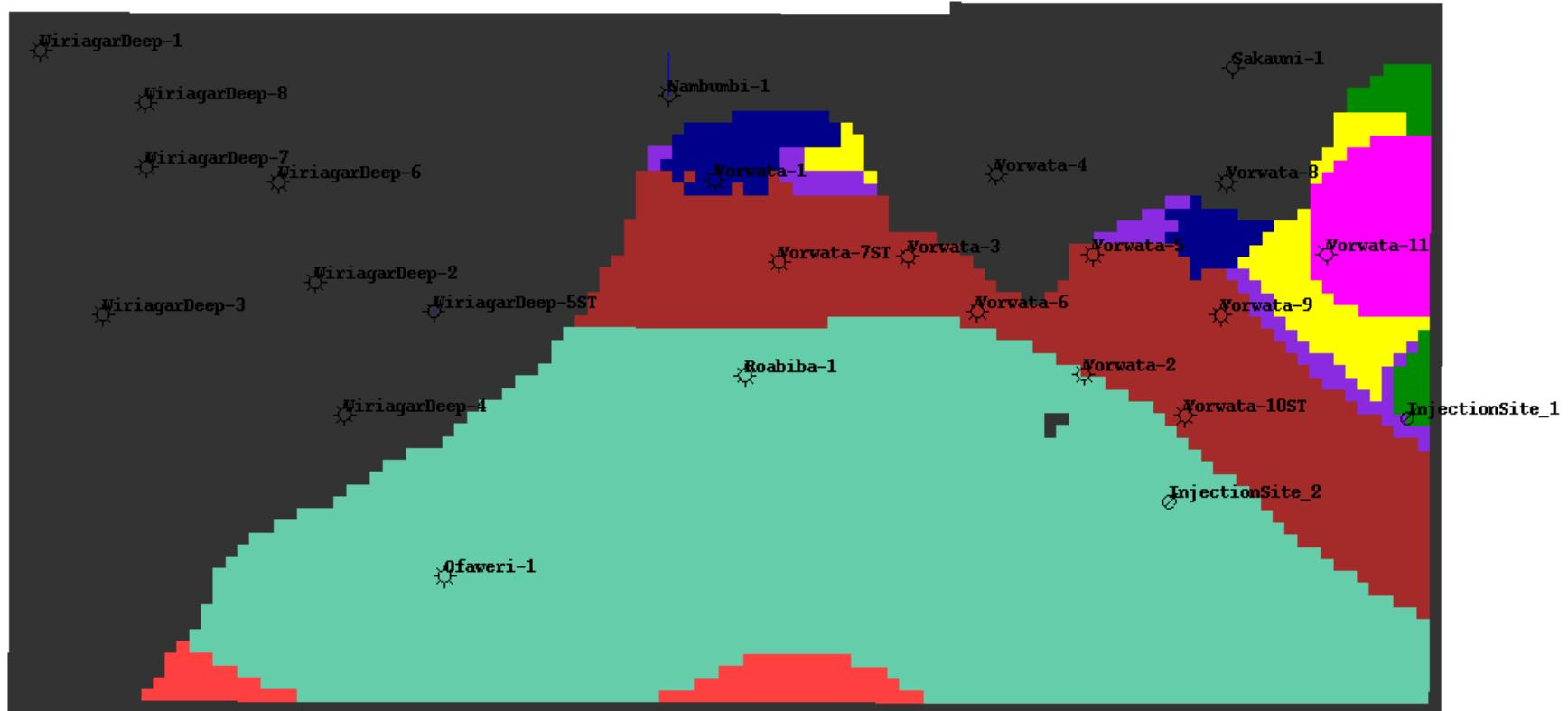


Figure 14.12: Example of facies polygons displayed in GEOCARD as attribute SimpleFacies_Use. Chronostratigraphic Interval shown is the CU40; and the GEOCARD model layer (k) is 21. Layering in Zone 4 (Callovian) is parallel to top. Grey cells are null-cells (inactive cells with null cell volume), due to truncation by overlying strata. Non-grey colors refer to reservoir paleo-depositional facies such as “floodplain/coastal plain” (green), “upper shoreface” (brown), “foreshore-spit” (purple), “lagoonal” (yellow), “tidal delta/inlet” (dark blue) and “bayhead delta” (magenta).

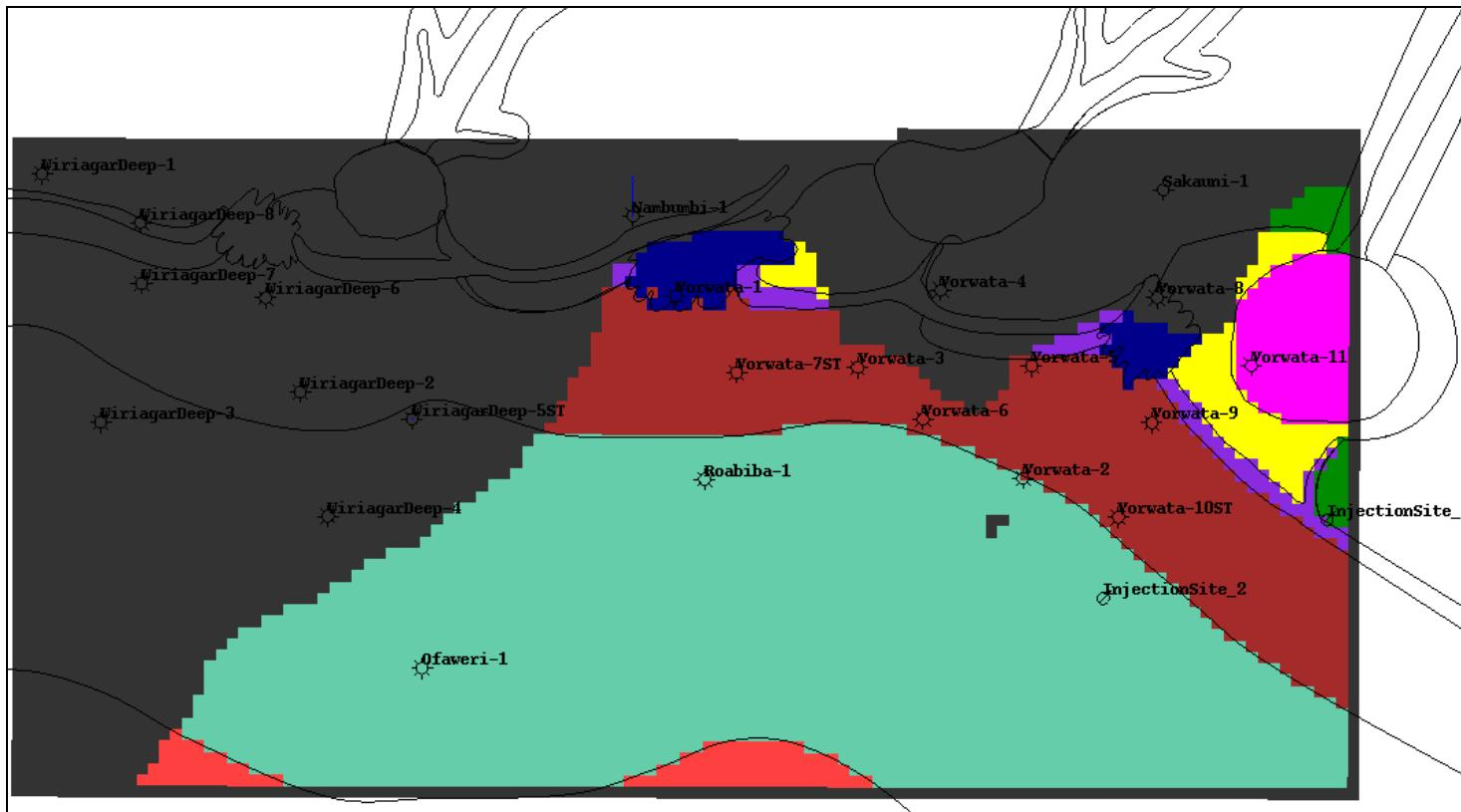


Figure 14.13: Example of paleo-facies polygons and attribute SimpleFacies_Use, showing the relationship between the digitized and then imported paleo-depositional polygon map, and the populating of GEOCARD 3D cells with the attribute SimpleFacies_Use.

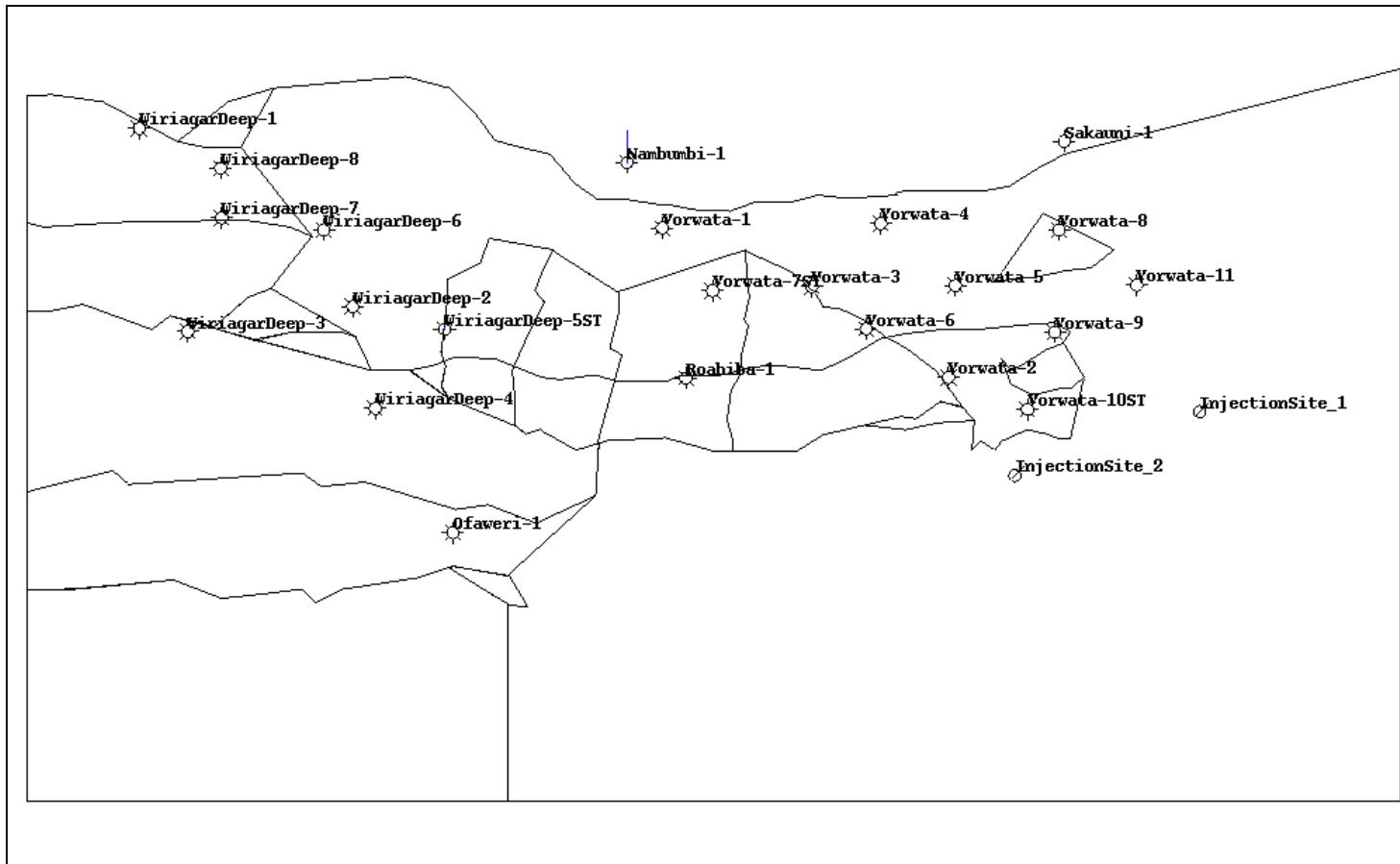


Figure 14.14: Fault compartment polygons. In a method similar to the imported paleo-depositional facies polygons, fault blocks were created by digitizing the major faults from the Top Structure Main Roabiba Depth map (provided by BP) and then creating fault bounded polygons. The polygons were then imported into GEOCARD as FaultCompartment_attribute.

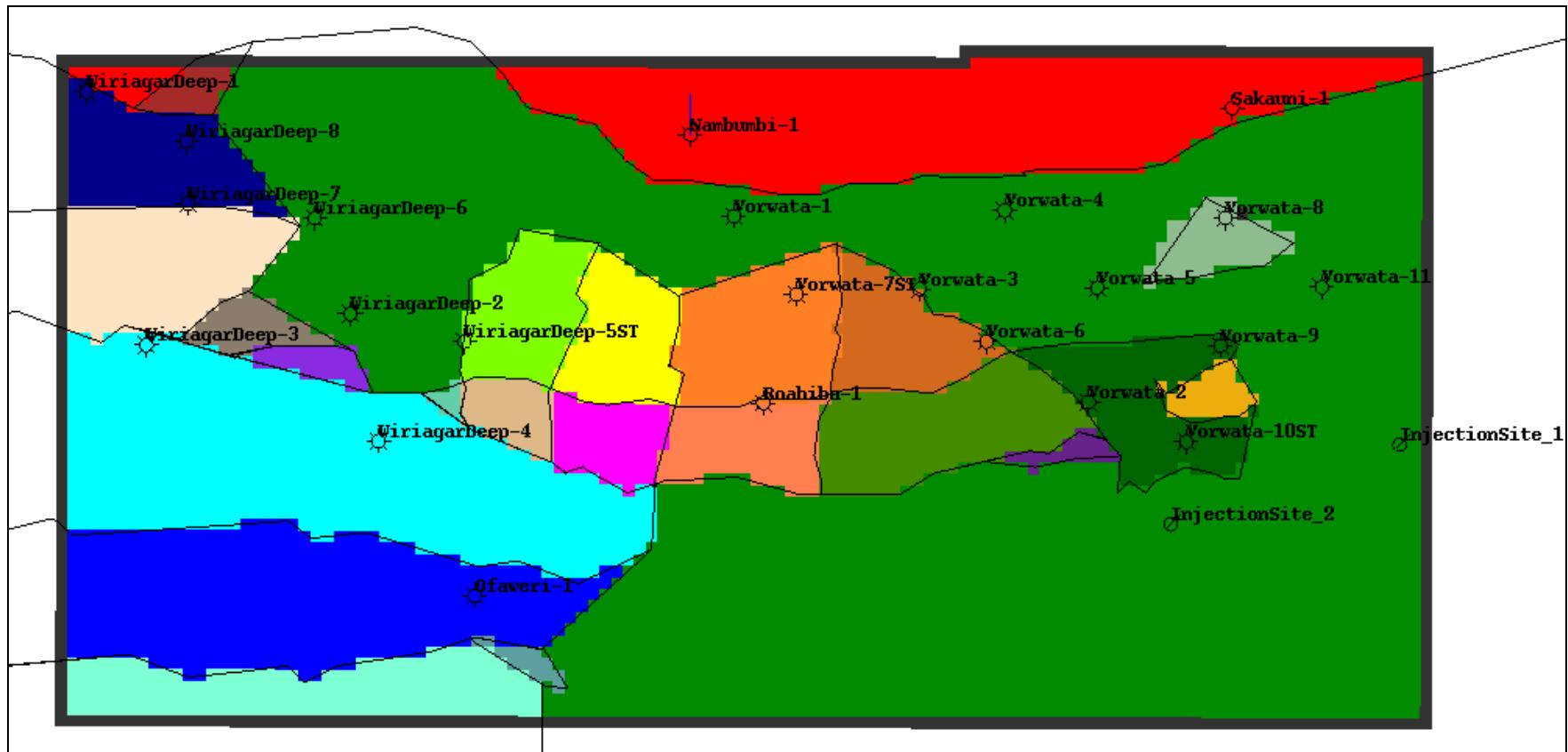


Figure 14.15: FaultCompartment_attribute as shown in a GEOCARD screen capture. The digitized fault boundaries are still visible as black lines, and the cells in the model are colored as an attribute dependent on which fault compartment polygon they are in. The faults are modelled as vertical strike-slip faults, therefore these polygons are present in all layers in the model.

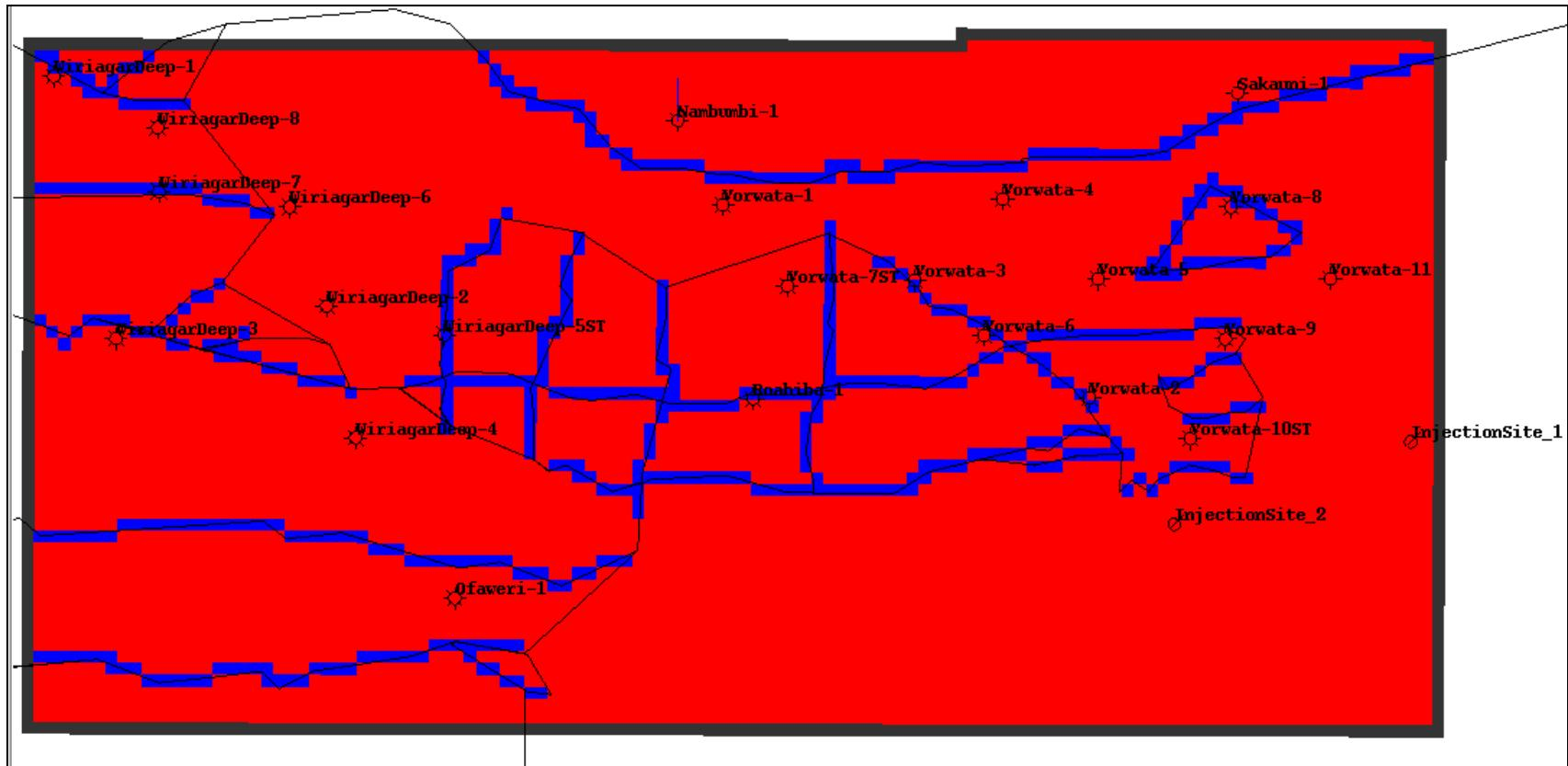


Figure 14.16: To simulate the effect of major faults as a barrier, the fault compartment boundaries were linked to “transmissibility multipliers” as an attribute for each of the directions in GEOCARD (i.e. the “i”, “j”, and “k” dimensions). The screen capture above shows an example of how the transmissibility multiplier for J-direction (TMULTJ_attribute) appears.

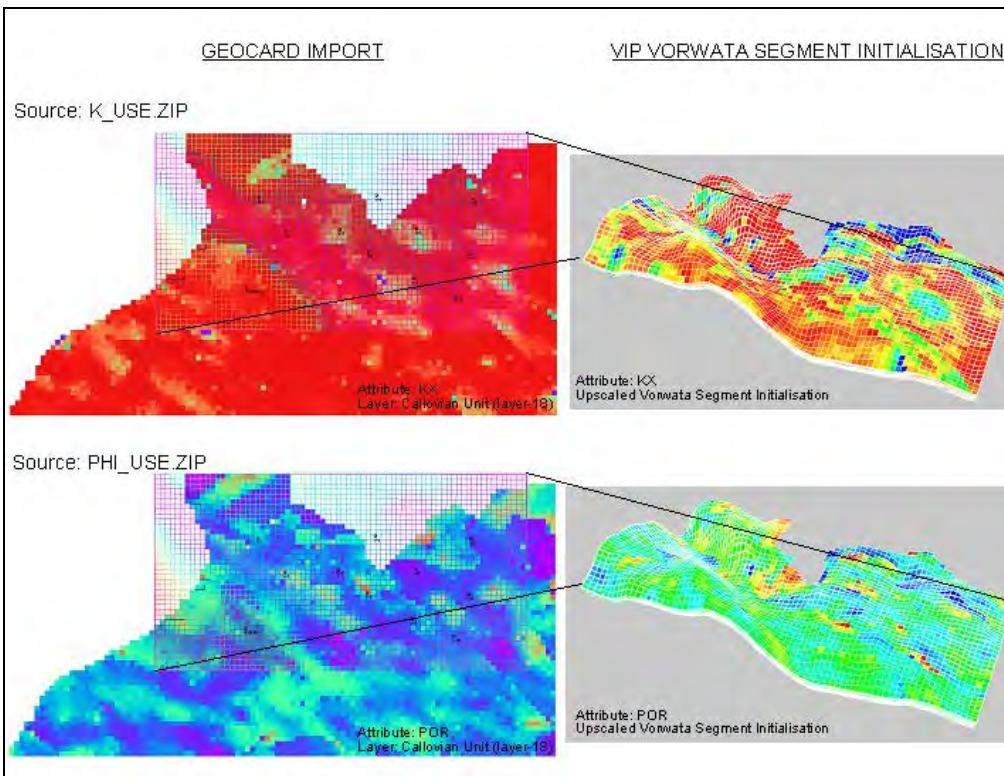


Figure 14.17: A screen capture of the VIP initialization for grids and attributes of the final GEOCARD 3D Tangguh Geologic Model. Shown here are the effective porosity and permeability results from Realization 1 for Roabiba Zone R50, layer 18. The effective porosity was determined by wireline logs (PHIE, FDC and sonic) which were calibrated to whole core plug analyses (PHIEC), ‘blocked’ into cells in the model that were intersected by wells, and then populated by SGS in all active cells of each layer. Permeability was then populated by CCS. There were 5 simulations run and the results from Realization 1 were exported to VIP as “PHI_USE.Zip” (effective porosity) and “K_USE.Zip” (effective permeability) attributes (BP, 2003).

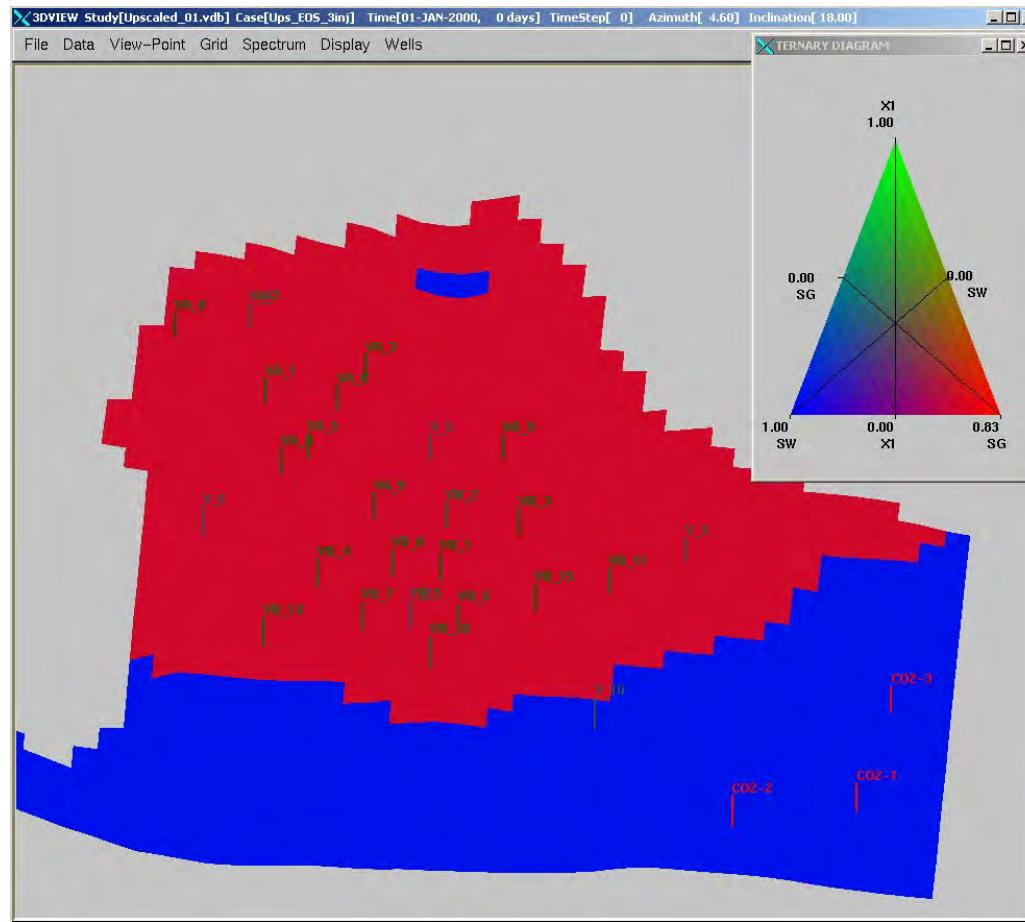


Figure 14.18: A screen capture from a ‘preliminary’ visualization of the VIP Reservoir Simulator at Year 0 - i.e. natural gas production wells and 3 injector wells have been drilled and platform/pipeline/compressor stations are present but LNG production and CO₂ injection have not yet commenced (BP, 2004).

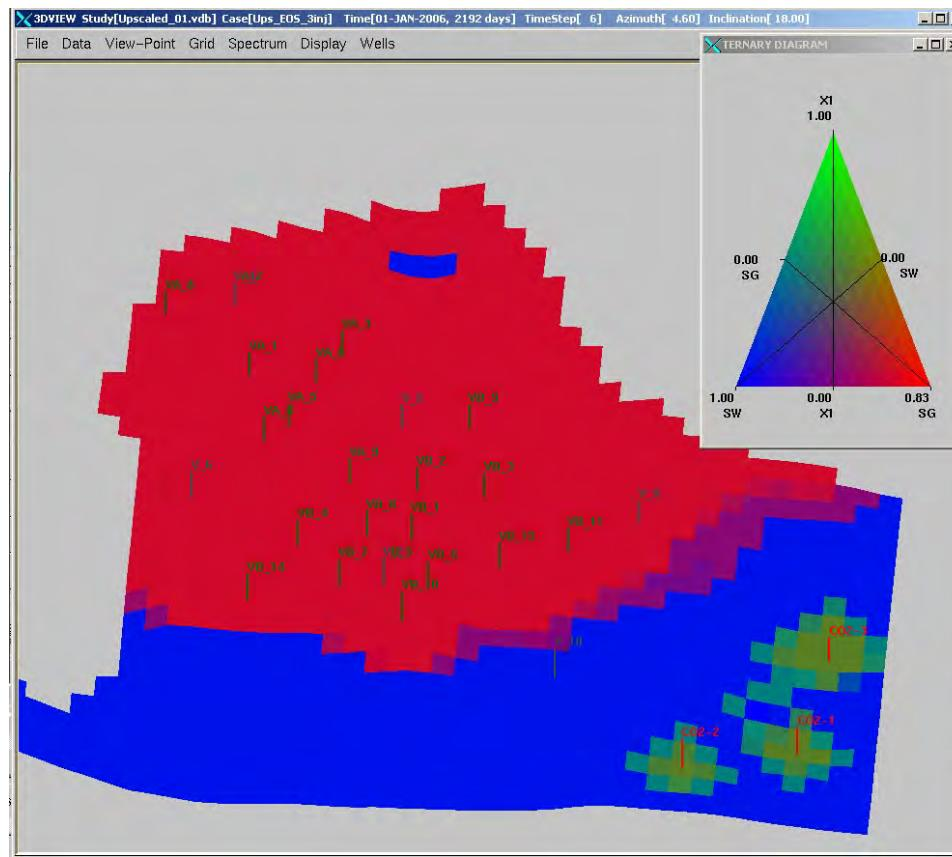


Figure 14.19: A screen capture from the VIP Reservoir Simulator at Year 5 - i.e. LNG production from Vorwata development wells and subsurface injection of CO₂ from 3 injector wells into the base of the Bajocian Roabiba Sandstone Reservoir has been continuous for 5 years (BP, 2004).

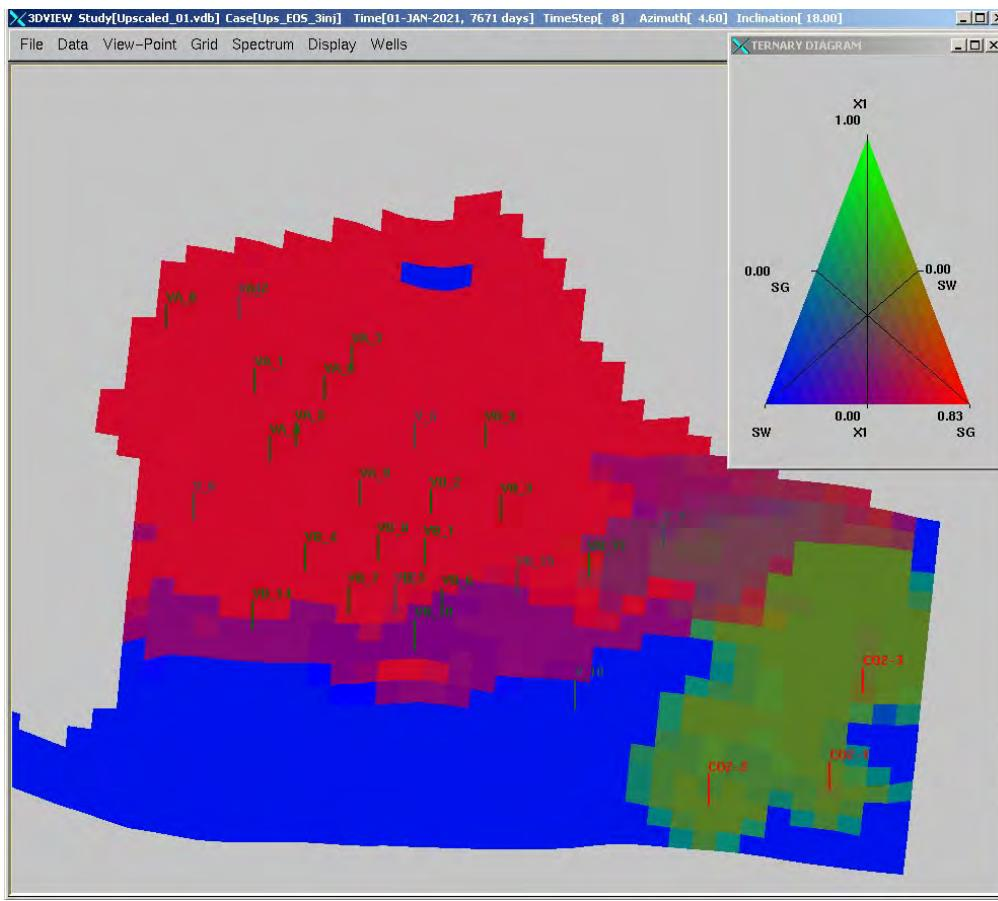


Figure 14.20: A screen capture from the VIP Reservoir Simulator at Year 20 (based on Realization 1 export of attributes and Grid from the GEOCARD 3D Geological Model for Tangguh). Note that the injected CO₂ plume (green) has just migrated to the edge of the original GWC, but the natural gas accumulation (bright red) has also migrated updip due to production (BP, 2004).

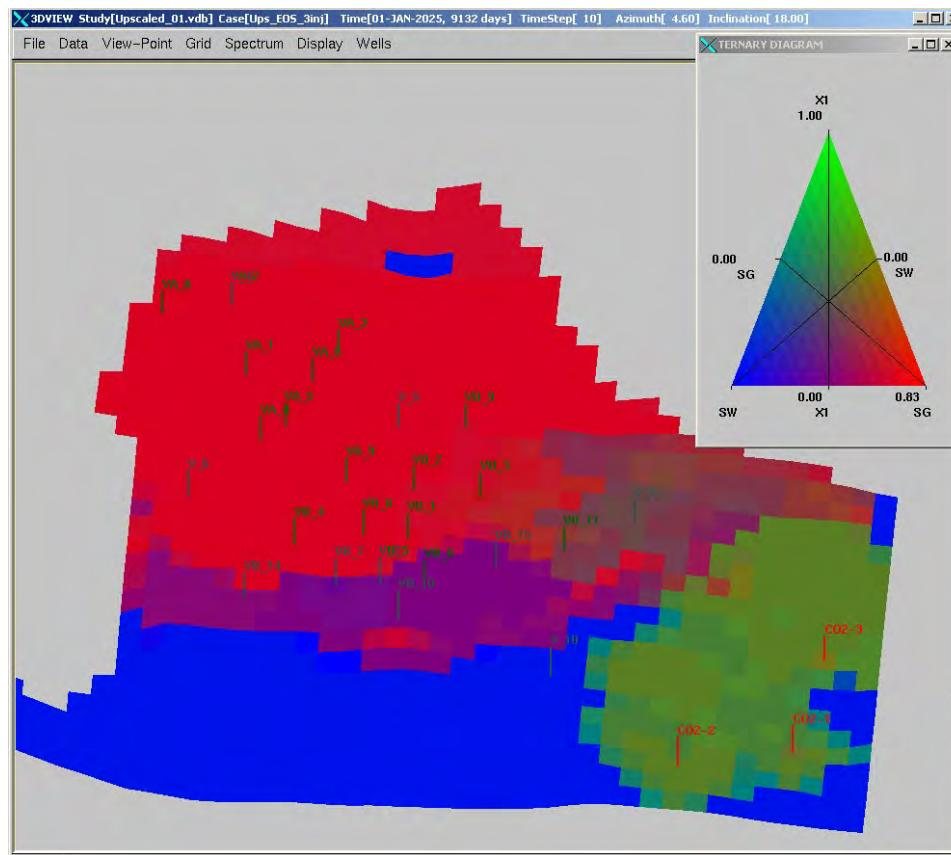


Figure 14.21: Another screen capture from the preliminary VIP Reservoir Simulator run at Year 25. Note that the injected CO₂ plume (green) has just migrated past the original GWC, but is still not in contact with the natural gas accumulation (bright red), which has continued to migrated updip due to production (BP, 2004).

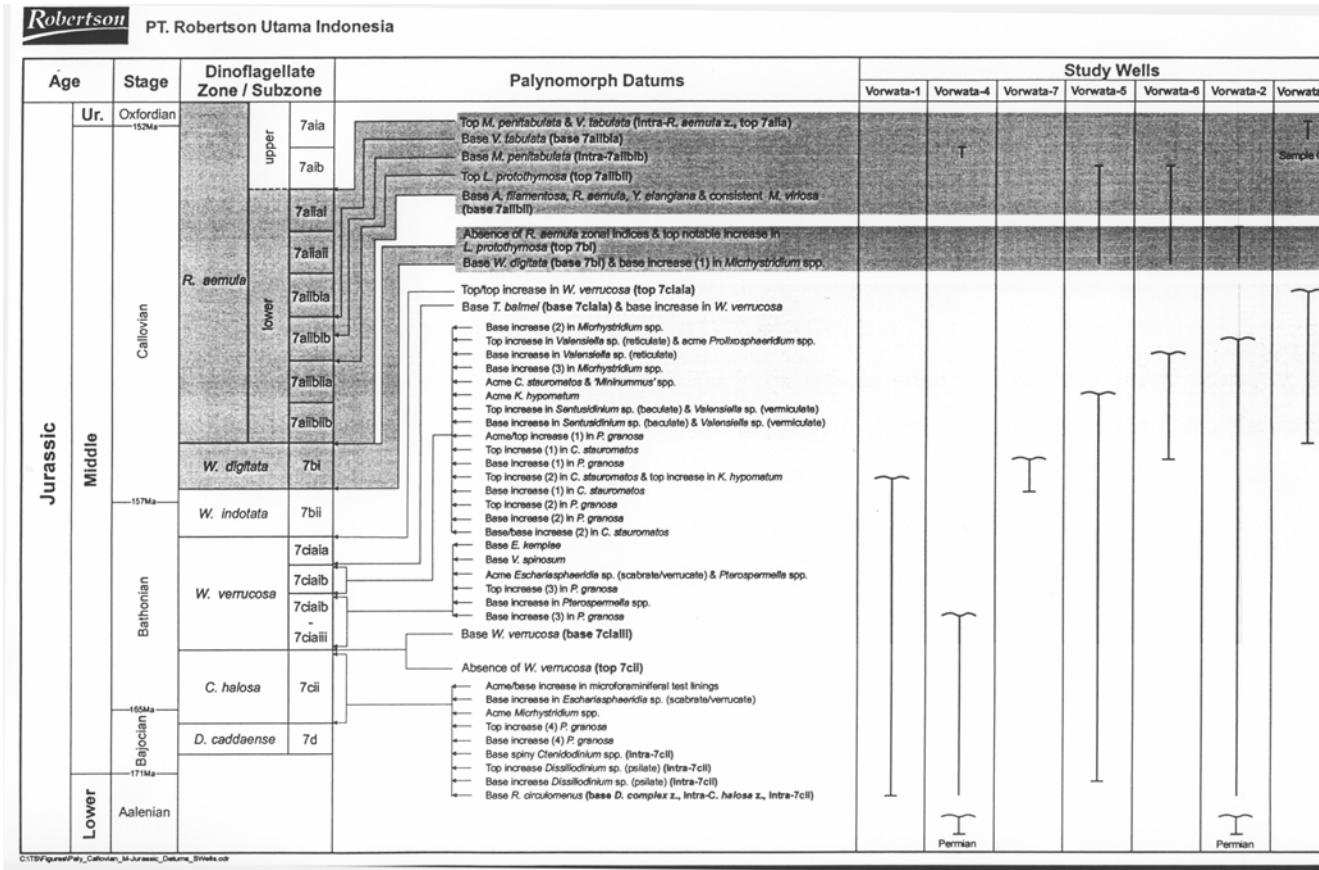


Figure 18.1: Chart showing results of high-resolution palynological/biostratigraphic study carried out for BP, by Chris Bates in 2002/2003, on cores from Vorwata wells. Note the massive amount of upper-most Bathonian/Bajocian Roabiba sandstone reservoir missing at V-7 location. The incised valley at V-3, V-7, V-5 resulted in unconformity at top of the Roabiba sandstone and erosional removal of the upper Bajocian/Bathonian Roabiba sandstone interval (C. Bates, courtesy of N. Davis and BP, 2004).

APPENDIX 1
PRESSURE TRANSIENT ANALYSIS (PTA) SUMMARIES
FOR WIRIAGAR DEEP, VORWATA, AND ROABIBA
DRILL-STEM TESTS (DST)

(ALL DST SUMMARIES COURTESY OF BP, 2002)

Wiriagar Deep #1 PTA Summary

Test	DST-1	DST-2	DST-3	DST-4A	DST-5	DST-6
Zone	Permian	Aaleniean	Cretaceous	Lo. Member	Up. Member	Up. Member
Produced Fluid	No Flow	Gas & Cond.	Gas & Cond.	Gas	Gas & Cond.	Gas & Cond.
Perf'd, ft	20	28	43	50	22	30
Pay (PTA), ft		28	43	50	22	30
Por.	20.5%	13.9%	13.4%	11.2%	13.9%	15.2%
Qmax, mmscf/d	Slug	3.73	9.51	0.84	11.7	3.8
Sep. Yield, b/mmcf	-	N/A	2.21	N/A	1.71	1.04
Water Cut, %	-		0.5	N/A	0.5	0.8
WHP, psig	-	121	128		2010	970
Homogeneous						
kh, md-ft	-	692	1731	35	1734	90
Perm., md	-	25	40	0.7	79	3
Rad. Inv., ft	-	217	2332	155	1562	555
Total skin	-	24	109	35	44	13
S	-	-	30	25	11.7	11
D	-	-	0.0085	0.0125	0.003	0.00054
P*, psia	-	3979.5	3941	3900	3811	3809
Pi , psia						
Composite						
k inner, md	-	-	-	-	-	-
M	-	-	-	-	-	-
w	-	-	-	-	-	-
Lrad, ft	-	-	-	-	-	-
Total skin						
S	-	-	-	-	-	-
D	-	-	-	-	-	-
Behavior	Slug Test	Radial Flow				
Cs, bbl/psi	-	-	-	-	-	-
Second Cs, bbl/psi	-	-	-	-	-	-
Time to Sec. Cs, hr	-	-	-	-	-	-
Boundaries	Inf. Act.	Infinitely acting				
L, ft	-	-	-	-	-	-

Wiriagar Deep #2 PTA Summary

Test	DST-1	DST-2	DST-3	DST-4A	DST-5	DST-6
Zone	Permian	Aaleniean	Roabiba	Lo. Member	Mid. Member	Up. Member
Produced Fluid	Water	Gas & Cond.	Gas & Cond.	Gas	Gas & Cond.	Gas & Cond.
Perf'd, ft	32	34	105	81	144	44
Pay (PTA), ft	3	34	106	50	131	44
Por.	20.5%	13.9%	13.4%	11.2%	13.9%	15.2%
Qmax, mmscf/d	Slug	30.4	36	0.18	29.9	13.8
Sep. Yield, b/mmcf	-	5.79	1.55	-	9.18	8.25
Water Cut, %	-	50	46	-	7	8.6
WHP, psig	-	1427	1475	16	1458	677
Homogeneous						
kh, md-ft	7	5018	88058	5	4603	361
Perm., md	0.2	147	830	0.1	35	8
Rad. Inv., ft	-	2965	6562	-	1619	659
Total skin	32	30	131	17.6	39	14
S	32	18	17	-	15	10
D	-	0.00040	0.0032	-	0.00078	0.0003
P*, psia	-	-	4025	3917	3948	3916
Pi , psia	4047	4056	4025	3917	3952	3919
Composite						
k inner, md	-	-	572.5	-	19.2	4.7
M	-	-	1.5	-	2.0	1.7
w	-	-	1.5	-	0.8	1.0
Lrad, ft	-	-	1335	-	234	87
Total skin			88		18	5.5
S	-	-	9.6	-	5.4	4.8
D	-	-	0.0022	-	0.00042	0.00005
Behavior	Slug Test	Homogeneous	Composite	Wb. Storage	Composite	Composite
Cs, bbl/psi	-	0.0267	0.0742	0.037	0.023	0.021
Second Cs, bbl/psi	-	-	-	0.013	-	0.0073
Time to Sec. Cs, hr	-	-	-	3.321	-	0.0569
Boundaries	Inf. Act.	Inters. Faults 120	Inf. Act.	Inf. Act.	Inf. Act.	Inf. Act.
L, ft	-	553.2	-	-	-	-

Wiriagar Deep #3 PTA Summary

Test	DST-1A	DST-2	DST-2A	DST-3	DST-4
Zone	Aal. - Roab.	Lo. Member	Lo. Member	Up. Member	Mud Prone
Produced Fluid	Gas & Cond.	Gas	Gas	Gas & Cond.	Gas & Cond.
Perf'd, ft	87	50	80	49	109
Pay (PTA), ft	67	34	73	32	99
Por.	13.3%	11.1%	11.1%	16.7%	11.0%
Qmax, mmscf/d	10.4	0.165	0.47	7.7	20.8
Sep. Yield, b/mmcf	0.58	-	-	3.38	2.44
Water Cut, %	73.7	-	-	72.5	36.6
WHP, psig	550	2	16	625	1046
Homogeneous					
kh, md-ft	645	3	8.76	119	520
Perm., md	10	0.09	0.12	3.7	5.3
Rad. Inv., ft	871	110	-	435	671
Total skin	51	12	12	2.3	6.1
S	48	-	-	1.52	1.8
D	0.00028	-	-	0.0001	0.0021
P*, psia	4106	3908	3909	3096	3745
Pi , psia	4106	3909	3909	3120	3745
Composite					
k inner, md	3.7	-	-	-	-
M	3.0	-	-	-	-
w	0.5	-	-	-	-
Lrad, ft	74	-	-	-	-
Total skin	16.23	-	-	-	-
S	15.12	-	-	-	-
D	0.00013	-	-	-	-
Behavior	Composite	Wb. Storage	Wb. Storage	Homogeneous	Homogeneous
Cs, bbl/psi	0.022	0.028	0.028	0.0378	0.024
Second Cs, bbl/psi	0.008	0.017	0.017		0.008
Time to Sec. Cs, hr	0.136	4.082	4.082		0.070
Boundaries	Inf. Act.	Inf. Act.	Inf. Act.	Trans. Reduc.	Trans. Reduc.
L, ft				177	137

Wiriagar Deep #4 PTA Summary

Test	DST-1	DST-2	DST-3A
Zone	Aal. - Roab.	Cretaceous	Mud Prone
Produced Fluid	Gas & Cond.	Gas & Cond.	Water
Perf'd, ft	249	95	20
Pay (PTA), ft	245	18	20
Por.	10.8%	11.8%	12.0%
Qmax, mmscf/d	32.6	5.2	209 bwpd
Sep. Yield, b/mmcf	2.27	2.2	
Water Cut, %	59.3	40	100
WHP, psig	1737	447	55
Homogeneous			
kh, md-ft	22614	10246	704
Perm., md	92	569	35
Rad. Inv., ft	2736	4607	654
Total skin	28	1936	9
S	16	14	9
D	0.00035	0.3682	-
P*, psia	4092	4058	3636
Pi , psia	4092	4058	3636
Composite			
k inner, md	46	-	-
M	2	-	-
w	0.99	-	-
Lrad, ft	450	-	-
Total skin	10	-	-
S	7	-	-
D	0.0001	-	-
Behavior	Composite	Homogeneous	Homogeneous
Cs, bbl/psi	0.100	0.040	0.0043
Second Cs, bbl/psi	0.010	0.018	0.0019
Time to Sec. Cs, hr	0.012	0.100	0.305
Boundaries	Inf. Act.	Inf. Act.	Inf. Act.

Wiriagar Deep #6 PTA Summary

Test	DST-1&1A	DST-2
Zone	Sand Prone	Mud Prone
Produced Fluid	Gas & Cond.	Gas & Cond.
Perf'd, ft	299	118
Pay (PTA), ft	299	118
Por.	10.0%	13.1%
Qmax, mmscfd	9.74	25.36
Sep. Yield, b/mmcft	5.64	5.48
Water Cut, %	25%	20%
WHP, psig	798	1117
Homogeneous		
kh, md-ft	138	889
Perm., md	0.5	7.5
Rad. Inv., ft	761	2108
Total skin	4	-0.6
S	3	-1
D	0.00014	0.00001
P*, psia	3794	3327
Composite		
k inner, md	-	-
M	-	-
w	-	-
Lrad, ft	-	-
Total skin	-	-
S	-	-
D	-	-
Behavior	Homogeneous	Homogeneous
Cs, bbl/psi	0.026	0.0294
Second Cs, bbl/psi	0.005	0.0115
Time to Sec. Cs, hr	0.080	0.0098
Boundaries	Inf. Act.	U Faults
L, ft		200;450;1200

Wiriagar Deep #7 PTA Summary

Test	DST-1	DST-2	DST-3
Zone	Aalenian	Lo. Member	Lo. Member
Produced Fluid	Gas & Cond.		
Perf'd, ft	48	71	50
Pay (PTA), ft	48	71	50
Por.	10.0%	11.2%	12.0%
Qmax, mmscf/d	34.4	Insuff. flow	weak blow
Sep. Yield, b/mmcf	0.99	-	-
Water Cut, %	49%	-	-
WHP, psig	1575	54	15
Homogeneous			
kh, md-ft	18085		
Perm., md	377		
Rad. Inv., ft	4094		
Total skin	9.4		
S	0.003		
D	0.00028		
P*, psia	4024		
Pi , psia	4024		
Composite			
k inner, md			
M			
w			
Lrad, ft			
Total skin			
S			
D			
Behavior	Homogeneous		
Cs, bbl/psi	0.015		
Second Cs, bbl/psi			
Time to Sec. Cs, hr			
Boundaries	Trans. Reduc.	Inf. Act.	Inf. Act.
L, ft	629		

Wiriagar Deep #8 PTA Summary

Test	DST-1	DST-2	DST-3A	DST-4
Zone	Aalenian	Lo. Member	Lo. Member	Up. Member
Produced Fluid	No Flow	Gas	Gas & Cond.	Gas & Cond.
Perf'd, ft	33	56	77	147
Pay (PTA), ft	33	56	77	147
Por.	14.0%	11.9%	11.9%	13.1%
Qmax, mmscf/d	No flow	1.67	1.74	30.45
Sep. Yield, b/mmcft		1.87	0.41	1.85
Water Cut, %		87%	85%	32%
WHP, psig		135	133	1338
Homogeneous				
kh, md-ft		42	17	1019
Perm., md		0.8	0.2	6.9
Rad. Inv., ft		270	128	541
Total skin		19	4.0	2.6
S			-1.5	1.1
D			0.00310	0.00005
P*, psia		3945	3939	3904
Pi , psia		3945	3940	3904
Composite/ Dual Perm.				
Perm., md		0.2	-	8.4
Lamda		4.10E-05	-	-
Kappa		0.2344	-	-
w		0.2	-	0.4
Lrad				155
M				0.8
Total skin		0.9	-	-
S		-	-	-
D		-	-	-
P*, psia		4256	-	-
Pi , psia		3945	-	-
Behavior		Dual Perm.	Homogeneous	Composite
Cs, bbl/psi		0.005	0.004	0.005
Second Cs, bbl/psi		0.004	0.002	0.000977
Time to Sec. Cs, hr		0.050	0.016	0.001
Boundaries		Inf. Act.	Trans. Reduc.	Inf. Act.
L, ft			49.0	

Vorwata #1 PTA Summary

Test	DST-1	DST-2	DST-3A	DST-4
Zone	Up. Permian	Permian	Roabiba	Up. Member
Produced Fluid	Gas	Gas	Gas & Cond.	No Flow
Perf'd, ft	64	210	119	42
Pay (PTA), ft	64	210	119	
Por.	9.6%	8.1%	11.0%	
Qmax, mmscf/d	0.11	0.95	29.3	No Flow
Sep. Yield, b/mmcf	-	-	7.41	
Water Cut, %	-	-	23%	
WHP, psig	24	47	1667	
Homogeneous				
kh, md-ft	0.25	0.33	7188	
Perm., md	0.0038	0.0016	61	
Rad. Inv., ft	28	20	2616	
Total skin			134	
S			60	
D			0.0025	
P*, psia	4750	4979	5731	
Composite				
k inner, md			-	
M			-	
w			-	
Lrad, ft			-	
Total skin			-	
S			-	
D			-	
Behavior			Homogeneous	
Cs, bbl/psi			0.024	
Second Cs, bbl/psi			-	
Time to Sec. Cs, hr			-	
Boundaries	Trans. Reduc.	Trans. Reduc.	Trans. Reduc.	
L, ft			625	

Vorwata #2 PTA Summary

Test	DST-1	DST-2
Zone	Roabiba	Paleocene
Produced Fluid	Gas & Cond.	Gas
Perf'd, ft	92	138
Pay (PTA), ft	92	-
Por.	13.0%	-
Qmax, mmscfd	33.8	Weak blow
Sep. Yield, b/mmcft	2.65	-
Water Cut, %	50	-
WHP, psig	1770	3
Homogeneous		
kh, md-ft	11379	-
Perm., md	124	-
Rad. Inv., ft	3442	-
Total skin	12	-
S	0	-
D	0.00035	-
P*, psia	5843	-
Composite		
k inner, md	-	-
M	-	-
w	-	-
Lrad, ft	-	-
Total skin	-	-
S	-	-
D	-	-
Behavior	Homogeneous	-
Cs, bbl/psi	0.142	-
Second Cs, bbl/psi	-	-
Time to Sec. Cs, hr	-	-
Boundaries	Trans. Reduc.	-
L, ft	592	

Vorwata #3 PTA Summary

Test	DST-1
Zone	Roabiba
Produced Fluid	Gas & Cond.
Perf'd, ft	35
Pay (PTA), ft	35
Por.	10.0%
Qmax, mmscf/d	29.2
Sep. Yield, b/mmcft	4.89
Water Cut, %	50
WHP, psig	1549
Homogeneous	
kh, md-ft	9708
Perm., md	277
Rad. Inv., ft	5613
Total skin	101.5
S	89.9
D	0.0004
P*, psia	5756
Composite	
k inner, md	88
M	3.15
w	0.6
Lrad, ft	507.3
Total skin	27
S	15
D	0.000403
Behavior	Composite
Cs, bbl/psi	0.026
Second Cs, bbl/psi	0.008
Time to Sec. Cs, hr	0.024
Boundaries	Inf. Act.
L, ft	

Vorwata #4 PTA Summary

Test	DST-1
Zone	Roabiba
Produced Fluid	Gas & Cond.
Perf'd, ft	102
Pay (PTA), ft	102
Por.	18.0%
Qmax, mmscf/d	36.3
Sep. Yield, b/mmcf	2.41
Water Cut, %	50%
WHP, psig	1458
Homogeneous	
kh, md-ft	54978
Perm., md	539
Rad. Inv., ft	5798
Total skin	15
S	1.3
D	0.00038
P*, psia	5769
Behavior	Homogeneous
Cs, bbl/psi	0.300
Second Cs, bbl/psi	-
Time to Sec. Cs, hr	-
Boundaries	Pll. Faults
L, ft	531
L, ft	1793

Analyses using PTA

Vorwata #5 PTA Summary

Test	DST-1	DST-1A
Zone	Roabiba	Roabiba
Produced Fluid	Water & Gas	Gas & Cond.
Perf'd, ft	15	85
Pay (PTA), ft	15	85
Por.	13.0%	13%
Qmax, mmscf/d	1233 bwpd	30.6
Sep. Yield, b/mmcft	3228	2.53
Water Cut, %	100%	90%
WHP, psig	310	1031
Homogeneous		
kh, md-ft	179	3315
Perm., md	12	39
Rad. Inv., ft	866	464
Total skin	-2.4	23
S	-2.4	-
D	n/a	-
P*, psia	5755	5831
Behavior	Homogeneous	Homogeneous
Cs, bbl/psi	0.0001	0.0008
Second Cs, bbl/psi	-	-
Time to Sec. Cs, hr	-	-
Boundaries	Trans. Reduc.	Infinitely acting
L, ft	176.4	

Analyses using PTA

Roabiba #1 PTA Summary

Test	DST-1
Zone	Roabiba
Produced Fluid	Gas & Cond.
Perf'd, ft	101
Pay (PTA), ft	101
Por.	12.0%
Qmax, mmscf/d	23
Sep. Yield, b/mmcf	4.53
Water Cut, %	60%
WHP, psig	2810
Homogeneous	
kh, md-ft	27270
Perm., md	270
Rad. Inv., ft	2559
Total skin	73
S	-
D	-
P*, psia	-
Pi , psia	5010
Composite	
k inner, md	97
M	-
w	-
Lrad, ft	150
Total skin	-
S	-
D	-
Behavior	Composite
Cs, bbl/psi	-
Second Cs, bbl/psi	-
Time to Sec. Cs, hr	-
Boundaries	Inf. Act.
L, ft	
* Based on revised OXY PTA	

APPENDIX 2

PETROPHYSICAL ANALYSIS RESULT SUMMARY OF WIRELINE LOGS FOR THE WIRIAGAR DEEP, VORWATA, OFAWERI, ROABIBA, AND WOS WELLS

**PETROPHYSICAL ANALYSES USING PETCOM PROGRAM BY T.
LAWRENCE, ARCO 1998, WITH WIRELINE LOG DATA CALIBRATED TO
EMPIRICAL LABORATORY CORE PLUG DATA WHERE AVAILABLE
(in Bulling, et al., 1998)**

Appendix 2 : Petrophysical analyses results for Late Paleocene to Late Permian reservoirs on Wiriagar Deep and Vorwata wells. Petrophysical analyses performed by T. Lawrence (ARCO 1998). Wireline log data calibrated to core plug data (Bulling, et al., 1998).

COMP : ATLANTIC RICHFIELD BERAU INC.											
WELL : VORWATA-1 (FINAL WELL REPORT)											
DATE : 9-JUN-98 @ 09:20:05											
ZONE : 4630.00 - 12620.00 FT											
<u>INPUT CURVES</u> :	POROSITY	=	PHIEC	<u>CUTOFFS</u> :						POROSITY MINIMUM =>	
.05				WATER SATURATION = SWCFWL						POROSITY MAXIMUM <=	
Not Used				CLAY VOLUME = VCLC						WATER SATURATION <=	
.99										CLAY VOLUME <=	
.50											
<u>DISCRIMINATORS</u> :	(None)										
NET	ZONE NAME	ZONE TOP (FT)	ZONE BASE (FT)	GROSS INTERVAL (FT)	NET PAY (FT)	HPVH (FT)	PHIH (FT)	PHI (FT)	Avg Sw	Avg VCL	Net RES ROCK (FT)
RES	PHIH	PHI	VCL								
-----	-----	-----	-----	-----	-----	-----	-----	-----	-----	-----	-----
EOCENE	8644.00	9189.00	545.50	1.00	.01	.14	.141	.899	.167	53.50	
5.08 .095 .208											
MUD PRONE PALEOC	9189.00	10419.00	1230.50	257.50	7.51	23.85	.093	.685	.281	357.50	
30.40 .085 .266											
UPPER MEMBER	10419.00	10713.00	294.50	64.00	3.32	6.96	.109	.523	.166	67.00	
7.13 .106 .166											
MIDDLE MEMBER	10713.00	10713.00	.50	.00	.00	.00	.000	1.000	1.000	.00	
.00 .000 1.000											
LOWER MEMBER	10713.00	11053.00	340.50	70.50	2.15	4.76	.068	.549	.137	72.00	
4.85 .067 .137											
CRETACEOUS	11053.00	11552.00	499.50	71.50	.93	6.34	.089	.853	.230	101.00	
9.67 .096 .220											
UP LATE JURASSIC	11552.00	11692.00	140.50	18.50	.63	1.60	.086	.608	.452	18.50	
1.60 .086 .452											
AYOT LIMESTONE	11692.00	11742.00	50.50	44.00	.92	2.96	.067	.689	.312	44.00	
2.96 .067 .312											
LATE JUR. SAND	11742.00	11742.00	.50	.00	.00	.00	.000	1.000	1.000	.00	
.00 .000 1.000											
UPPER ROABIBA	11759.00	11770.00	11.50	11.00	.62	1.00	.090	.376	.276	11.00	
1.00 .090 .276											
MAIN ROABIBA	11770.00	11891.00	121.50	100.50	8.23	10.34	.103	.205	.108	100.50	
10.34 .103 .108											
AALENIAN SAND	11911.00	11915.00	4.50	1.50	.09	.14	.093	.336	.328	1.50	
.14 .093 .328											
TOARCIAN	11915.00	11915.00	.50	.00	.00	.00	.000	1.000	1.000	.00	
.00 .000 1.000											
PERMIAN	11915.00	12404.00	489.50	184.00	10.31	17.50	.095	.411	.388	184.00	
17.50 .095 .388											
LOWER PERMIAN	12404.00	12620.00	216.50	.00	.00	.00	.000	1.000	1.000	.00	
.00 .000 1.000											

Appendix 2 : Petrophysical analyses results for Late Paleocene to Late Permian reservoirs on Wiriagar Deep and Vorwata wells. Petrophysical analyses performed by T. Lawrence (ARCO 1998). Wireline log data calibrated to core plug data (Bulling, et al., 1998).

COMP : ATLANTIC RICHFIELD BERAU, INC. WELL : VORWATA-2 (FINAL WELL REPORT) DATE : 9-JUN-98 @ 09:32:57 ZONE : 6380.00 - 13390.00 FT											
NET RES	ZONE NAME	ZONE TOP	ZONE BASE	GROSS INTERVAL	NET PAY	HPVH	PHIH	Avg PHI	Avg Sw	Avg VCL	NET RES ROCK
	AVG PHI	AVG VCL	(FT)	(FT)	(FT)	(FT)	(FT)				(FT)
	EOCENE	9998.00	11181.00	1183.50	5.00	.54	.86	.171	.372	.123	92.00
6.98	.076 .132										
	MUD PRONE PALEOC	11181.00	11370.00	189.50	138.00	6.74	13.22	.096	.490	.169	138.50
13.24	.096 .169										
	UPPER MEMBER	11370.00	11419.00	49.50	.00	.00	.00	.000	1.000	1.000	.00
.00	.000 1.000										
	MIDDLE MEMBER	11419.00	11419.00	.50	.00	.00	.00	.000	1.000	1.000	.00
.00	.000 1.000										
	LOWER MEMBER	11419.00	11666.00	247.50	55.00	1.33	3.59	.065	.630	.173	55.00
3.59	.065 .173										
	CRETACEOUS	11666.00	12205.00	539.50	69.50	.75	4.04	.058	.814	.231	76.00
4.39	.058 .227										
	UP LATE JURASSIC	12205.00	12294.00	89.50	28.00	.36	2.38	.085	.849	.256	33.50
2.73	.082 .253										
	AYOT LIMESTONE	12294.00	12345.00	51.50	1.00	.00	.06	.059	.975	.170	16.00
.86	.054 .180										
	LATE JUR. SAND	12345.00	12438.00	93.50	81.00	3.07	9.36	.116	.672	.139	88.00
9.82	.112 .150										
	UPPER ROABIBA	12561.00	12600.00	39.50	39.50	4.30	5.68	.144	.244	.101	39.50
5.68	.144 .101										
	MAIN ROABIBA	12600.00	13009.00	409.50	385.50	47.42	53.92	.140	.121	.060	385.50
53.92	.140 .060										
	AALENIAN SAND	13044.00	13046.00	2.50	1.50	.01	.09	.058	.852	.095	2.50
.15	.061 .116										
	TOARCIAN	13046.00	13046.00	.50	.00	.00	.00	.000	1.000	1.000	.50
.03	.063 .206										
	PERMO-TRIASSIC	13046.00	13046.00	.50	.00	.00	.00	.000	1.000	1.000	.50
.03	.063 .206										
	PERMIAN	13046.00	13365.00	319.50	28.50	.54	2.07	.073	.739	.352	39.50
2.68	.068 .320										

Appendix 2 : Petrophysical analyses results for Late Paleocene to Late Permian reservoirs on Wiriagar Deep and Vorwata wells. Petrophysical analyses performed by T. Lawrence (ARCO 1998). Wireline log data calibrated to core plug data (Bulling, et al., 1998).

COMP : ATLANTIC RICHFIELD BERAU, INC. WELL : VORWATA-3 (FINAL WELL REPORT) DATE : 9-JUN-98 @ 09:59:23 ZONE : 10450.00 - 12818.00 FT												
NET	ZONE NAME	ZONE TOP	ZONE BASE	GROSS INTERVAL	NET PAY	AVG HPVH	AVG PHIH	AVG PHI	AVG Sw	AVG VCL	NET RES	NET ROCK
	RES	PHI	PHI	VCL	(FT)	(FT)	(FT)	(FT)	(FT)	(FT)	(FT)	(FT)
EOCENE		10450.00	10683.00	233.50	12.00	.17	.92	.077	.813	.260	37.00	
2.37	.064	.250	MUD PRONE PALEOC	10683.00	10900.00	217.50	31.00	1.03	3.20	.103	.678	.297
3.41	.100	.298	UPPER MEMBER	10900.00	11073.00	173.50	37.50	2.44	4.90	.131	.502	.172
4.98	.128	.175	MIDDLE MEMBER	11073.00	11073.00	.50	.00	.00	.00	1.000	1.000	.00
.00	.000	1.000	LOWER MEMBER	11073.00	11376.00	303.50	70.00	2.05	5.31	.076	.614	.162
5.34	.076	.161	CRETACEOUS	11376.00	11884.00	508.50	75.50	1.18	5.84	.077	.797	.309
6.29	.077	.306	UP LATE JURASSIC	11884.00	11982.00	98.50	11.50	.12	.82	.072	.857	.334
.97	.069	.336	AYOT LIMESTONE	11982.00	12037.00	55.50	.50	.00	.03	.053	.815	.096
.03	.053	.096	LATE JUR. SAND	12037.00	12057.00	20.50	.00	.00	.00	1.000	1.000	.00
.00	.000	1.000	UPPER ROABIBA	12057.00	12068.00	11.50	6.50	.23	.45	.070	.485	.184
.45	.070	.184	MAIN ROABIBA	12068.00	12099.00	31.50	30.00	2.89	3.88	.129	.254	.039
3.88	.129	.039	AALENIAN SAND	12111.00	12125.00	14.50	13.00	.65	1.27	.098	.489	.145
1.27	.098	.145	TOARCIAN	12125.00	12125.00	.50	.50	.00	.03	.055	.921	.279
.03	.055	.279	PERMO-TRIASSIC	12125.00	12125.00	.50	.50	.00	.03	.055	.921	.279
.03	.055	.279	PERMIAN	12125.00	12818.00	693.50	41.50	.86	3.00	.072	.713	.332
3.17	.071	.327										44.50

Appendix 2 : Petrophysical analyses results for Late Paleocene to Late Permian reservoirs on Wiriagar Deep and Vorwata wells. Petrophysical analyses performed by T. Lawrence (ARCO 1998). Wireline log data calibrated to core plug data (Bulling, et al., 1998).

WELL : VORWATA-4 (GROUP 2)												
DATE : 9-JUN-98 @ 10:04:27												
ZONE : 10543.00 - 13007.00 FT												
<u>INPUT CURVES :</u>	POROSITY	=	PHIEC	<u>CUTOFFS :</u>						POROSITY MINIMUM	=>	
.05	WATER SATURATION	=	SWCFWL							POROSITY MAXIMUM	<=	
Not Used	CLAY VOLUME	=	VCLC							WATER SATURATION	<=	
.99										CLAY VOLUME	<=	
.50												
<u>DISCRIMINATORS :</u>	(None)											
NET	ZONE	ZONE	ZONE	GROSS	NET			Avg	Avg	Avg	Net	
RES	PHIH	PHI	VCL	TOP	BASE	INTERVAL	PAY	HPVH	PHIH	PHI	Sw	VCL
	(FT)			(FT)	(FT)	(FT)	(FT)	(FT)				(FT)
-----	-----	-----	-----	-----	-----	-----	-----	-----	-----	-----	-----	-----
EOCENE	10543.00	10709.00		166.50	39.00		.85	3.37	.086	.749	.129	75.50
5.55 .074 .162												
MUD PRONE PALEOC	10709.00	10989.00		280.50	34.50		.60	3.32	.096	.819	.368	96.50
7.38 .077 .323												
UPPER MEMBER	10989.00	11163.00		174.50	125.00		8.13	14.47	.116	.438	.162	125.00
14.47 .116 .162												
MIDDLE MEMBER	11163.00	11163.00		.50	.00		.00	.00	.000	1.000	1.000	.00
.00 .000 1.000												
LOWER MEMBER	11163.00	11522.00		359.50	100.50		3.35	8.32	.083	.598	.151	100.50
8.32 .083 .151												
CRETACEOUS	11522.00	12076.00		554.50	161.50		2.46	13.30	.082	.815	.257	218.00
16.68 .076 .253												
UP LATE JURASSIC	12076.00	12132.00		56.50	9.50		.21	1.11	.116	.806	.198	14.50
1.45 .100 .217												
AYOT LIMESTONE	12132.00	12183.00		51.50	.00		.00	.00	.000	1.000	1.000	11.50
.66 .057 .104												
LATE JUR. SAND	12183.00	12207.00		24.50	19.50		.79	2.68	.138	.705	.080	20.00
2.73 .137 .080												
UPPER ROABIBA	12228.00	12256.00		28.50	25.50		3.73	4.38	.172	.149	.023	25.50
4.38 .172 .023												
MAIN ROABIBA	12256.00	12332.00		76.50	74.50		10.90	13.07	.175	.166	.013	74.50
13.07 .175 .013												
AALENIAN SAND	12332.00	12332.00		.50	.00		.00	.00	.000	1.000	1.000	.00
.00 .000 1.000												
TOARCIAN	12332.00	12332.00		.50	.00		.00	.00	.000	1.000	1.000	.00
.00 .000 1.000												
PERMO-TRIASSIC	12332.00	12332.00		.50	.00		.00	.00	.000	1.000	1.000	.00
.00 .000 1.000												
PERMIAN	12332.00	12970.00		638.50	64.00		1.88	6.55	.102	.713	.333	64.50
6.58 .102 .334												

Appendix 2 : Petrophysical analyses results for Late Paleocene to Late Permian reservoirs on Wiriagar Deep and Vorwata wells. Petrophysical analyses performed by T. Lawrence (ARCO 1998). Wireline log data calibrated to core plug data (Bulling, et al., 1998).

COMP : ATLANTIC RICHFIELD BERAU, INC. WELL : VORWATA-5 DATE : 9-JUN-98 @ 10:10:14 ZONE : 10564.00 - 13268.00 FT												
NET	ZONE NAME	ZONE TOP	ZONE BASE	GROSS INTERVAL	NET PAY	HPVH	PHIH	PHI	Avg Sw	Avg VCL	Avg RES	NET ROCK
RES	PHIH	PHI	VCL	(FT)	(FT)	(FT)	(FT)	(FT)				(FT)
EOCENE		11240.00	11403.00	163.50	6.50	.12	.46	.070	.744	.230	8.00	
.54	.068	.207										
MUD PRONE PALEOC		11403.00	11574.00	171.50	44.00	1.66	3.33	.076	.501	.179	44.00	
3.33	.076	.179										
UPPER MEMBER		11574.00	11713.00	139.50	71.50	3.14	6.28	.088	.500	.101	73.00	
6.38	.087	.100										
MIDDLE MEMBER		11713.00	11713.00	.50	.00	.00	.00	.000	1.000	1.000	.00	
.00	.000	1.000										
LOWER MEMBER		11713.00	11962.00	249.50	59.50	1.32	3.66	.061	.640	.196	59.50	
3.66	.061	.196										
CRETACEOUS		11962.00	12522.00	560.50	130.00	1.21	7.73	.059	.844	.267	130.00	
7.73	.059	.267										
UP LATE JURASSIC		12522.00	12588.00	66.50	15.00	.30	1.18	.079	.747	.268	15.50	
1.21	.078	.271										
AYOT LIMESTONE		12588.00	12636.00	48.50	.00	.00	.00	.000	1.000	1.000	.00	
.00	.000	1.000										
LATE JUR SAND		12636.00	12696.00	60.50	54.50	2.40	5.00	.092	.519	.128	54.50	
5.00	.092	.128										
UPPER ROABIBA		12755.00	12790.00	35.50	33.50	4.14	5.11	.153	.190	.087	33.50	
5.11	.153	.087										
MAIN ROABIBA		12790.00	13074.00	284.50	140.50	15.82	19.54	.139	.190	.068	266.00	
36.66	.138	.075										
AALENIAN SAND		13074.00	13074.00	.50	.00	.00	.00	.000	1.000	1.000	.00	
.00	.000	1.000										
TOARCIAN		13074.00	13074.00	.50	.00	.00	.00	.000	1.000	1.000	.00	
.00	.000	1.000										
PERMO-TRIASSIC		13074.00	13074.00	.50	.00	.00	.00	.000	1.000	1.000	.00	
.00	.000	1.000										
PERMIAN		13074.00	13185.00	111.50	.00	.00	.00	.000	1.000	1.000	.00	
.00	.000	1.000										

Appendix 2 : Petrophysical analyses results for Late Paleocene to Late Permian reservoirs on Wiriagar Deep and Vorwata wells. Petrophysical analyses performed by T. Lawrence (ARCO 1998). Wireline log data calibrated to core plug data (Bulling, et al., 1998).

COMP : ATLANTIC RICHFIELD BERAU, INC. WELL : VORWATA-6 DATE : 9-JUN-98 @ 10:17:38 ZONE : 11105.00 - 13534.00 FT												
NET	ZONE NAME	ZONE TOP	ZONE BASE	GROSS INTERVAL	NET PAY	HPVH	PHIH	PHI	Avg Sw	Avg VCL	Avg RES	NET ROCK
RES	PHIH	PHI	VCL	(FT)	(FT)	(FT)	(FT)	(FT)				(FT)
(FT)												
EOCENE		11150.00	11291.00	141.50	10.00	.26	.76	.076	.658	.238	10.00	
.76	.076	.238										
MUD PRONE PALEOC		11291.00	11483.00	192.50	69.50	2.15	4.98	.072	.568	.136	69.50	
4.98	.072	.136										
UPPER MEMBER		11483.00	11648.00	165.50	35.00	1.35	3.04	.087	.554	.165	35.00	
3.04	.087	.165										
MIDDLE MEMBER		11648.00	11648.00	.50	.00	.00	.00	.000	1.000	1.000	.00	
.00	.000	1.000										
LOWER MEMBER		11648.00	11900.00	252.50	6.00	.11	.32	.054	.657	.156	6.00	
.32	.054	.156										
CRETACEOUS		11900.00	12463.00	563.50	.00	.00	.00	.000	1.000	1.000	.00	
.00	.000	1.000										
UP LATE JURASSIC		12463.00	12575.00	112.50	15.00	.23	1.27	.085	.821	.335	21.00	
1.61	.077	.348										
AYOT LIMESTONE		12575.00	12627.00	52.50	.00	.00	.00	.000	1.000	1.000	1.50	
.08	.051	.112										
LATE JUR SAND		12627.00	12670.00	43.50	35.50	1.26	3.75	.106	.664	.125	36.50	
3.83	.105	.125										
UPPER ROABIBA		12769.00	12800.00	31.50	31.00	3.61	4.47	.144	.192	.090	31.00	
4.47	.144	.090										
MAIN ROABIBA		12800.00	13132.00	332.50	293.50	31.16	36.97	.126	.157	.085	325.50	
40.71	.125	.087										
AALENIAN SAND		13152.00	13164.00	12.50	.00	.00	.00	.000	1.000	1.000	6.50	
.71	.109	.186										
TOARCIAN		13164.00	13164.00	.50	.00	.00	.00	.000	1.000	1.000	.50	
.04	.083	.320										
PERMO-TRIASSIC		13164.00	13164.00	.50	.00	.00	.00	.000	1.000	1.000	.50	
.04	.083	.320										
PERMIAN		13164.00	13450.00	286.50	.00	.00	.00	.000	1.000	1.000	143.00	
14.26	.100	.287										

Appendix 2 : Petrophysical analyses results for Late Paleocene to Late Permian reservoirs on Wiriagar Deep and Vorwata wells. Petrophysical analyses performed by T. Lawrence (ARCO 1998). Wireline log data calibrated to core plug data (Bulling, et al., 1998).

WELL :	VORWATA-7										
DATE :	11-JUN-98 @ 14:29:59										
ZONE :	11270.00 - 13548.00 FT										
<u>INPUT CURVES</u> :	POROSITY	=	PHIEC	<u>CUTOFFS</u> :						POROSITY MINIMUM =>	
.05				WATER SATURATION	=	SWCFWL				POROSITY MAXIMUM <=	
Not Used				CLAY VOLUME	=	VCLC				WATER SATURATION <=	
.99										CLAY VOLUME <=	
.50											
<u>DISCRIMINATORS</u> :	(None)										
NET	ZONE NAME	ZONE TOP (FT)	ZONE BASE (FT)	GROSS INTERVAL (FT)	NET PAY (FT)	HPVH	PHIH	PHI	AVG	AVG	NET RES ROCK (FT)
RES	PHIH	PHI	VCL								
-----	-----	-----	-----	-----	-----	-----	-----	-----	-----	-----	-----
EOCENE		11300.00	11408.00	108.50	22.50	.43	1.57	.070	.729	.286	26.00
1.77 .068 .269											
MUD PRONE PALEOC		11408.00	11753.00	345.50	39.00	.77	2.57	.066	.700	.313	39.50
2.59 .066 .313											
UPPER MEMBER		11753.00	12004.00	251.50	19.00	.39	1.25	.066	.687	.153	19.50
1.28 .065 .154											
MIDDLE MEMBER		12004.00	12004.00	.50	.00	.00	.00	.000	1.000	1.000	.00
.00 .000 1.000											
LOWER MEMBER		12004.00	12355.00	351.50	44.00	1.26	2.82	.064	.554	.209	45.50
2.90 .064 .204											
CRETACEOUS		12355.00	12848.00	493.50	49.50	.47	3.46	.070	.865	.290	56.50
3.91 .069 .276											
UP LATE JURASSIC		12848.00	13012.00	164.50	21.00	.21	1.32	.063	.843	.286	24.50
1.50 .061 .289											
AYOT LIMESTONE		13012.00	13061.00	49.50	.00	.00	.00	.000	1.000	1.000	.00
.00 .000 1.000											
LATE JUR. SAND		13061.00	13061.00	.50	.00	.00	.00	.000	1.000	1.000	.00
.00 .000 1.000											
UPPER ROABIBA		13122.00	13148.00	26.50	21.00	.87	1.59	.076	.457	.079	21.00
1.59 .076 .079											
MAIN ROABIBA		13148.00	13290.00	142.50	120.50	8.47	10.97	.091	.228	.059	120.50
10.97 .091 .059											
AALENIAN SAND		13318.00	13328.00	10.50	8.50	.39	.81	.095	.516	.066	8.50
.81 .095 .066											
TOARCIAN		13328.00	13328.00	.50	.50	.01	.04	.089	.704	.120	.50
.04 .089 .120											
PERMO-TRIASSIC		13328.00	13328.00	.50	.50	.01	.04	.089	.704	.120	.50
.04 .089 .120											
PERMIAN		13328.00	13440.00	112.50	7.50	.17	.55	.074	.697	.222	7.50
.55 .074 .222											

Appendix 2 : Petrophysical analyses results for Late Paleocene to Late Permian reservoirs on Wiriagar Deep and Vorwata wells. Petrophysical analyses performed by T. Lawrence (ARCO 1998). Wireline log data calibrated to core plug data (Bulling, et al., 1998).

Petrophysical analyses results for Late Paleocene to Late Permian reservoirs on Wiriagar Deep and Vorwata wells. Petrophysical analyses performed by T. Lawrence (ARCO 1998). Wireline log data calibrated to core plug data (Bulling, et al., 1998).												
COMP : British Gas, Cairns		WELL : Vorwata-8		DATE : 10-JUN-98 @ 15:30:29		ZONE : 11170.00 - 12888.50 FT						
NET	ZONE	ZONE	ZONE	GROSS	NET			Avg	Avg	Avg	Net	
RES	PHIH	PHI	VCL	TOP	BASE	INTERVAL	PAY	HPVH	PHIH	PHI	Sw	VCL RES ROCK
(FT)	(FT)	(FT)	(FT)	(FT)	(FT)	(FT)	(FT)	(FT)	(FT)	(FT)		(FT)
MUD PRONE PALEOC	11500.00	11569.00		69.50	4.50	.31	.67	.149	.541	.298		4.50
.67 .149 .298												
UPPER MEMBER	11569.00	11702.00		133.50	24.00	.77	2.07	.086	.626	.097		24.50
2.09 .085 .100												
MIDDLE MEMBER	11702.00	11702.00		.50	.00	.00	.00	.000	1.000	1.000		.00
.00 .000 1.000												
LOWER MEMBER	11702.00	11920.00		218.50	45.50	1.59	3.63	.080	.562	.199		45.50
3.63 .080 .199												
CRETACEOUS	11920.00	12458.00		538.50	216.50	2.13	14.41	.067	.852	.291		227.00
15.03 .066 .293												
UP LATE JURASSIC	12458.00	12462.00		4.50	.00	.00	.00	.000	1.000	1.000		.00
.00 .000 1.000												
AYOT LIMESTONE	12462.00	12501.00		39.50	.00	.00	.00	.000	1.000	1.000		1.00
.05 .052 .275												
LATE JUR. SAND	12501.00	12552.00		51.50	45.00	1.30	5.14	.114	.747	.111		46.50
5.24 .113 .115												
UPPER ROABIBA	12574.00	12574.00		.50	.00	.00	.00	.000	1.000	1.000		.00
.00 .000 1.000												
MAIN ROABIBA	12574.00	12654.00		80.50	45.50	5.25	8.00	.176	.344	.075		75.50
12.28 .163 .102												
AALENIAN SAND	12654.00	12654.00		.50	.00	.00	.00	.000	1.000	1.000		.00
.00 .000 1.000												
TOARCIAN	12654.00	12654.00		.50	.00	.00	.00	.000	1.000	1.000		.00
.00 .000 1.000												
PERMO-TRIASSIC	12654.00	12654.00		.50	.00	.00	.00	.000	1.000	1.000		.00
.00 .000 1.000												
PERMIAN	12654.00	12820.00		166.50	5.00	.12	.44	.088	.730	.413		5.00
.44 .088 .413												

Appendix 2 : Petrophysical analyses results for Late Paleocene to Late Permian reservoirs on Wiriagar Deep and Vorwata wells. Petrophysical analyses performed by T. Lawrence (ARCO 1998). Wireline log data calibrated to core plug data (Bulling, et al., 1998).

COMP : Atlantic Richfield Berau, Inc.												
WELL : Vorwata-9												
DATE : 9-JUN-98 @ 10:34:31												
ZONE : 11748.50 - 13584.00 FT												
NET	ZONE NAME	ZONE TOP	ZONE BASE	GROSS INTERVAL	NET PAY	HPVH	PHIH	PHI	Avg Sw	Avg VCL	Avg RES	NET ROCK
RES	PHIH	PHI	VCL	(FT)	(FT)	(FT)	(FT)	(FT)				(FT)
	LOWER MEMBER	11810.00	12010.00	200.50	10.50	.44	.98	.093	.552	.168	10.50	
.98	.093	.168										
	CRETACEOUS	12010.00	12579.00	569.50	242.50	4.47	19.62	.081	.772	.257	290.00	
22.29	.077	.242										
	UP LATE JURASSIC	12579.00	12618.00	39.50	10.00	.07	.93	.093	.922	.243	16.00	
1.36	.085	.248										
	AYOT LIMESTONE	12618.00	12666.00	48.50	4.00	.03	.27	.068	.907	.131	34.50	
2.00	.058	.110										
	LATE JUR. SAND	12666.00	12758.00	92.50	75.00	2.34	8.72	.116	.731	.145	86.00	
9.40	.109	.168										
	UPPER ROABIBA	12845.00	12878.00	33.50	31.50	3.32	4.67	.148	.288	.075	31.50	
4.67	.148	.075										
	MAIN ROABIBA	12878.00	13155.00	277.50	254.00	26.26	34.75	.137	.245	.058	254.00	
34.75	.137	.058										
	AALENIAN SAND	13155.00	13155.00	.50	.00	.00	.00	.000	1.000	1.000	.00	
.00	.000	1.000										
	TOARCIAN	13155.00	13155.00	.50	.00	.00	.00	.000	1.000	1.000	.00	
.00	.000	1.000										
	PERMO-TRIASSIC	13155.00	13155.00	.50	.00	.00	.00	.000	1.000	1.000	.00	
.00	.000	1.000										
	PERMIAN	13155.00	13480.00	325.50	6.00	.39	.66	.110	.415	.374	6.00	
.66	.110	.374										

Appendix 2 : Petrophysical analyses results for Late Paleocene to Late Permian reservoirs on Wiriagar Deep and Vorwata wells. Petrophysical analyses performed by T. Lawrence (ARCO 1998). Wireline log data calibrated to core plug data (Bulling, et al., 1998).

COMP : BRITISH GAS

WELL :	VORWATA-10 SIDETRACK										
DATE :	9-JUN-98 @ 10:39:47										
ZONE :	11581.00 - 13648.00 FT										
<u>INPUT CURVES</u> :	<u>CUTOFFS</u> :										
.05	POROSITY	=	PHIEC								
Not Used	WATER SATURATION	=	SWCFWL								
.99	CLAY VOLUME	=	VCLC								
.50											
<u>DISCRIMINATORS</u> :	(None)										
NET	ZONE NAME	ZONE TOP	ZONE BASE	GROSS INTERVAL	NET PAY	AVG HPVH	AVG PHIH	AVG PHI	AVG Sw	AVG VCL	NET RES ROCK
RES	PHIH	PHI	VCL	(FT)	(FT)	(FT)	(FT)	(FT)			(FT)
-----	-----	-----	-----	-----	-----	-----	-----	-----	-----	-----	-----
00 .000 1.000	UPPER MEMBER	11811.00	11841.00	30.50	.00	.00	.00	.000	1.000	1.000	.00
00 .000 1.000	MIDDLE MEMBER	11841.00	11841.00	.50	.00	.00	.00	.000	1.000	1.000	.00
05 .052 .251	LOWER MEMBER	11841.00	12038.00	197.50	1.00	.01	.05	.052	.715	.251	1.00
.21 .069 .131	CRETACEOUS	12038.00	12611.00	573.50	3.00	.07	.21	.069	.650	.131	3.00
1.93 .060 .323	UP LATE JURASSIC	12611.00	12693.00	82.50	27.00	.16	1.65	.061	.900	.322	32.00
00 .000 1.000	AYOT LIMESTONE	12693.00	12749.00	56.50	.00	.00	.00	.000	1.000	1.000	.00
7.85 .099 .180	LATE JUR. SAND	12749.00	12874.00	125.50	79.50	1.81	7.85	.099	.769	.180	79.50
8.75 .109 .175	UPPER ROABIBA	13120.00	13209.00	89.50	80.50	5.52	8.75	.109	.369	.175	80.50
50.49 .129 .072	MAIN ROABIBA	13209.00	13622.00	413.50	194.00	21.70	25.11	.129	.136	.022	390.50
00 .000 1.000	AALENIAN SAND	13622.00	13622.00	.50	.00	.00	.00	.000	1.000	1.000	.00

Appendix 2 : Petrophysical analyses results for Late Paleocene to Late Permian reservoirs on Wiriagar Deep and Vorwata wells. Petrophysical analyses performed by T. Lawrence (ARCO 1998). Wireline log data calibrated to core plug data (Bulling, et al., 1998).

COMP : British Gas, Cairns, SPW WELL : Vorwata 11 DATE : 9-JUN-98 @ 10:44:16 ZONE : 11412.50 - 13641.00 FT											
NET	ZONE NAME	ZONE TOP	ZONE BASE	GROSS INTERVAL	NET PAY	HPVH	PHIH	Avg PHI	Avg Sw	Avg VCL	NET RES ROCK
		(FT)	(FT)	(FT)	(FT)						(FT)
	MUD PRONE PALEOC	12050.00	12105.00	55.50	2.00	.10	.22	.111	.530	.422	2.00
.22	.111	.422									
	UPPER MEMBER	12105.00	12180.00	75.50	4.00	.19	.28	.071	.340	.102	4.00
.28	.071	.102									
	MIDDLE MEMBER	12180.00	12180.00	.50	.00	.00	.00	.000	1.000	1.000	.00
.00	.000	1.000									
	LOWER MEMBER	12180.00	12396.00	216.50	13.50	.43	.98	.072	.559	.215	13.50
.98	.072	.215									
	CRETACEOUS	12396.00	12920.00	524.50	178.00	3.05	12.21	.069	.750	.265	184.50
12.58	.068	.265									
	UP LATE JURASSIC	12920.00	12941.00	21.50	.00	.00	.00	.000	1.000	1.000	.00
.00	.000	1.000									
	AYOT LIMESTONE	12941.00	12990.00	49.50	.00	.00	.00	.000	1.000	1.000	1.50
.10	.067	.173									
	LATE JUR. SAND	12990.00	13062.00	72.50	35.00	.94	3.52	.101	.732	.121	40.50
3.83	.094	.136									
	UPPER ROABIBA	13109.00	13109.00	.50	.00	.00	.00	.000	1.000	1.000	.00
.00	.000	1.000									
	MAIN ROABIBA	13109.00	13312.00	203.50	189.50	17.77	27.14	.143	.345	.103	190.50
27.25	.143	.102									
	AALENIAN SAND	13312.00	13312.00	.50	.00	.00	.00	.000	1.000	1.000	.00
.00	.000	1.000									
	TOARCIAN	13312.00	13312.00	.50	.00	.00	.00	.000	1.000	1.000	.00
.00	.000	1.000									
	PERMO-TRIASSIC	13312.00	13312.00	.50	.00	.00	.00	.000	1.000	1.000	.00
.00	.000	1.000									
	PERMIAN	13312.00	13575.00	263.50	1.00	.01	.05	.051	.852	.432	1.00
.05	.051	.432									

Appendix 2 : Petrophysical analyses results for Late Paleocene to Late Permian reservoirs on Wiriagar Deep and Vorwata wells. Petrophysical analyses performed by T. Lawrence (ARCO 1998). Wireline log data calibrated to core plug data (Bulling, et al., 1998).

COMP : BRITISH GAS WELL : NAMBUMBI-1 CORRECTED DATA IN FT DATE : 9-JUN-98 @ 14:05:26 ZONE : 9842.50 - 13484.00 FT											
NET	ZONE NAME	ZONE TOP	ZONE BASE	GROSS INTERVAL	NET PAY	HPVH	PHIH	Avg PHI	Avg Sw	Avg VCL	NET RES ROCK
		(FT)	(FT)	(FT)	(FT)	(FT)	(FT)				(FT)
	MUD PRONE PALEOC	11200.00	11308.00	108.50	1.50	.03	.10	.068	.705	.282	2.00
.17	.086	.283									
13.37	.123	.128	UPPER MEMBER	11308.00	11719.00	411.50	105.00	5.42	13.12	.125	.587
.00	.000	1.000	MIDDLE MEMBER	11719.00	11719.00	.50	.00	.00	.000	1.000	1.000
8.03	.077	.196	LOWER MEMBER	11719.00	12201.00	482.50	104.50	3.83	8.03	.077	.523
12.70	.110	.170	CRETACEOUS	12201.00	12815.00	614.50	98.00	1.95	11.63	.119	.833
5.17	.075	.227	UP LATE JURASSIC	12815.00	13035.00	220.50	2.00	.04	.24	.118	.815
1.23	.059	.107	AYOT LIMESTONE	13035.00	13112.00	77.50	.00	.00	.00	.000	1.000
.00	.000	1.000	LATE JUR. SAND	13112.00	13112.00	.50	.00	.00	.00	.000	1.000
4.75	.112	.035	UPPER ROABIBA	13130.00	13130.00	.50	.00	.00	.00	.000	1.000
.00	.000	1.000	MAIN ROABIBA	13130.00	13181.00	51.50	42.50	2.44	4.75	.112	.486
AALENIAN SAND	13181.00	13181.00	.50	.00	.00	.00	.00	.000	1.000	1.000	.00
.00	.000	1.000	TOARCIAN	13181.00	13181.00	.50	.00	.00	.00	.000	1.000
.00	.000	1.000	PERMO-TRIASSIC	13181.00	13181.00	.50	.00	.00	.00	.000	1.000
PERMIAN	13181.00	13450.00	269.50	138.50	5.05	14.12	.102	.643	.313	141.00	
14.28	.101	.313									

Appendix 2 : Petrophysical analyses results for Late Paleocene to Late Permian reservoirs on Wiriagar Deep and Vorwata wells. Petrophysical analyses performed by T. Lawrence (ARCO 1998). Wireline log data calibrated to core plug data (Bulling, et al., 1998).

COMP : ATLANTIC RICHFIELD

WELL : WIRIAGAR DEEP NO. 1
 DATE : 9-JUN-98 @ 10:56:22
 ZONE : 5400.00 - 8510.00 FT

<u>INPUT CURVES :</u>			POROSITY	=	PHIEC	<u>CUTOFFS :</u>			POROSITY MINIMUM =>			
.05												
Not Used												
.99												
.50												
<u>DISCRIMINATORS :</u>			(None)									
NET	ZONE NAME	AVG TOP	ZONE BASE	GROSS INTERVAL	NET PAY	HPVH	PHIH	PHI	Avg Sw	Avg VCL	Avg RES	NET ROCK
RES	PHIH	PHI	VCL	(FT)	(FT)	(FT)	(FT)	(FT)				(FT)
-----	-----	-----	-----	-----	-----	-----	-----	-----	-----	-----	-----	-----
EOCENE		5400.00	5477.00	77.50	.00	.00	.00	.00	.000	1.000	1.000	.00
.00	.000	1.000										
MUD PRONE PALEOC		5477.00	6404.00	927.50	9.00	.38	.81	.090	.526	.282		9.00
.81	.090	.282										
UPPER MEMBER		6404.00	6855.00	451.50	28.50	2.82	3.91	.137	.279	.147		33.00
4.16	.126	.163										
MIDDLE MEMBER		6855.00	6855.00	.50	.00	.00	.00	.000	1.000	1.000		.00
.00	.000	1.000										
LOWER MEMBER		6855.00	7320.00	465.50	80.00	4.23	7.91	.099	.465	.228		81.50
8.01	.098	.229										
CRETACEOUS		7320.00	7743.00	423.50	38.50	1.41	3.12	.081	.547	.047		46.00
3.56	.077	.061										
UP LATE JURASSIC		7743.00	7800.00	57.50	18.50	.25	1.25	.068	.797	.173		22.50
1.48	.066	.171										
AYOT LIMESTONE		7800.00	7856.00	56.50	8.00	.08	.55	.069	.857	.080		14.00
.90	.064	.085										
LATE JUR. SAND		7856.00	7856.00	.50	.00	.00	.00	.000	1.000	1.000		.00
.00	.000	1.000										
UPPER ROABIBA		7856.00	7856.00	.50	.00	.00	.00	.000	1.000	1.000		.00
.00	.000	1.000										
MAIN ROABIBA		7856.00	7856.00	.50	.00	.00	.00	.000	1.000	1.000		.00
.00	.000	1.000										
AALENIAN SAND		7856.00	7886.00	30.50	20.50	1.49	2.16	.105	.309	.051		20.50
2.16	.105	.051										
TOARCIAN		7886.00	7886.00	.50	.50	.07	.10	.202	.305	.091		.50
.10	.202	.091										
PERMO-TRIASSIC		7886.00	7886.00	.50	.50	.07	.10	.202	.305	.091		.50
.10	.202	.091										
PERMIAN		7886.00	8500.00	614.50	21.00	.94	2.03	.096	.538	.407		27.00
2.36	.087	.382										

Appendix 2 : Petrophysical analyses results for Late Paleocene to Late Permian reservoirs on Wiriagar Deep and Vorwata wells. Petrophysical analyses performed by T. Lawrence (ARCO 1998). Wireline log data calibrated to core plug data (Bulling, et al., 1998).

COMP : ATLANTIC RICHFIELD WIRIAGAR INC. WELL : WIRIAGAR DEEP NO. 6 DATE : 9-JUN-98 @ 13:47:22 ZONE : 5230.00 - 9194.00 FT												
NET	ZONE NAME	ZONE TOP	ZONE BASE	GROSS INTERVAL	NET PAY	AVG HPVH	AVG PHIH	AVG PHI	AVG Sw	AVG VCL	NET RES ROCK	
	RES PHIH (FT)	PHI (FT)	VCL (FT)									
MUD PRONE PALEOC		6296.00	6940.00	644.50	91.00	6.64	11.36	.125	.416	.256	92.00	
11.43 .124 .254												
UPPER MEMBER		6940.00	7283.00	343.50	60.00	1.60	5.44	.091	.705	.325	74.50	
6.35 .085 .324												
MIDDLE MEMBER		7283.00	7283.00	.50	.50	.01	.03	.067	.664	.260	.50	
.03 .067 .260												
LOWER MEMBER		7283.00	7714.00	431.50	209.50	9.12	18.80	.090	.515	.212	212.50	
18.96 .089 .211												
CRETACEOUS		7714.00	8041.00	327.50	7.00	.09	.60	.086	.847	.247	70.50	
4.37 .062 .110												
UP LATE JURASSIC		8041.00	8194.00	153.50	.00	.00	.00	.000	1.000	1.000	.50	
.03 .056 .304												
AYOT LIMESTONE		8194.00	8234.00	40.50	1.00	.00	.06	.063	.970	.173	12.00	
.65 .054 .116												
LATE JUR. SAND		8234.00	8234.00	.50	.00	.00	.00	.000	1.000	1.000	.00	
.00 .000 1.000												
UPPER ROABIBA		8234.00	8234.00	.50	.00	.00	.00	.000	1.000	1.000	.00	
.00 .000 1.000												
MAIN ROABIBA		8234.00	8313.00	79.50	70.00	7.36	8.78	.125	.161	.031	70.00	
8.78 .125 .031												
AALENIAN SAND		8345.00	8377.00	32.50	14.50	1.05	1.88	.130	.442	.212	14.50	
1.88 .130 .212												
TOARCIAN		8377.00	8377.00	.50	.00	.00	.00	.000	1.000	1.000	.00	
.00 .000 1.000												
PERMO-TRIASSIC		8377.00	8377.00	.50	.00	.00	.00	.000	1.000	1.000	.00	
.00 .000 1.000												
PERMIAN		8377.00	9080.00	703.50	31.00	.60	2.09	.067	.712	.439	33.50	
2.22 .066 .437												

Appendix 2 : Petrophysical analyses results for Late Paleocene to Late Permian reservoirs on Wiriagar Deep and Vorwata wells. Petrophysical analyses performed by T. Lawrence (ARCO 1998). Wireline log data calibrated to core plug data (Bulling, et al., 1998).

COMP : ATLANTIC RICHFIELD WIRIAGAR INC.												
WELL : WIRIAGAR DEEP NO. 7												
DATE : 9-JUN-98 @ 13:52:37												
ZONE : 5872.00 - 8913.00 FT												
NET RES	ZONE NAME	ZONE TOP	ZONE BASE	GROSS INTERVAL	NET PAY	HPVH	PHIH	PHI	Avg Sw	Avg VCL	Avg RES	Net ROCK
NET (FT)	AVG PHIH	AVG PHI	AVG VCL	(FT)	(FT)	(FT)	(FT)	(FT)				(FT)
-----	-----	-----	-----	-----	-----	-----	-----	-----	-----	-----	-----	-----
EOCENE		6140.00	6336.00	196.50	17.50	.48	1.26	.072	.616	.384		17.50
1.26	.072	.384										
MUD PRONE PALEOC		6336.00	7141.00	805.50	73.50	2.93	7.97	.108	.632	.284		76.00
8.17	.108	.280										
UPPER MEMBER		7141.00	7525.00	384.50	33.50	1.13	3.17	.095	.644	.295		34.00
3.20	.094	.296										
MIDDLE MEMBER		7525.00	7525.00	.50	.00	.00	.00	.000	1.000	1.000		.00
.00	.000	1.000										
LOWER MEMBER		7525.00	7977.00	452.50	125.50	5.33	13.03	.104	.591	.243		131.50
13.41	.102	.241										
CRETACEOUS		7977.00	8354.00	377.50	4.00	.03	.26	.066	.897	.219		61.50
3.77	.061	.101										
UP LATE JURASSIC		8354.00	8439.00	85.50	27.50	.61	2.84	.103	.783	.205		50.50
4.52	.090	.224										
AYOT LIMESTONE		8439.00	8494.00	55.50	.00	.00	.00	.000	1.000	1.000		25.50
1.47	.058	.130										
LATE JUR. SAND		8494.00	8494.00	.50	.00	.00	.00	.000	1.000	1.000		.00
.00	.000	1.000										
UPPER ROABIBA		8494.00	8494.00	.50	.00	.00	.00	.000	1.000	1.000		.00
.00	.000	1.000										
MAIN ROABIBA		8494.00	8494.50	1.00	.00	.00	.00	.000	1.000	1.000		.00
.00	.000	1.000										
AALENIAN SAND		8522.00	8566.00	44.50	38.00	5.03	6.42	.169	.216	.073		38.00
6.42	.169	.073										
TOARCIAN		8566.00	8566.00	.50	.50	.04	.07	.143	.458	.165		.50
.07	.143	.165										
PERMO-TRIASSIC		8566.00	8566.00	.50	.50	.04	.07	.143	.458	.165		.50
.07	.143	.165										
PERMIAN		8566.00	8815.00	249.50	19.50	.46	1.79	.092	.745	.365		20.00
1.82	.091	.368										

Appendix 2 : Petrophysical analyses results for Late Paleocene to Late Permian reservoirs on Wiriagar Deep and Vorwata wells. Petrophysical analyses performed by T. Lawrence (ARCO 1998). Wireline log data calibrated to core plug data (Bulling, et al., 1998).

COMP : ATLANTIC RICHFIELD WIRIAGAR, INC.

WELL :	WIRIAGAR DEEP NO. 8										
DATE :	9-JUN-98 @ 13:55:37										
ZONE :	5296.00 - 8617.00 FT										
<u>INPUT CURVES</u> :	POROSITY	=	PHIEC	<u>CUTOFFS</u> :					POROSITY MINIMUM	=>	
.05	WATER SATURATION	=	SWCFWL						POROSITY MAXIMUM	<=	
Not Used	CLAY VOLUME	=	VCLC						WATER SATURATION	<=	
.99											
.50											
<u>DISCRIMINATORS</u> :	(None)										
NET	ZONE NAME	ZONE TOP (FT)	ZONE BASE (FT)	GROSS INTERVAL (FT)	NET PAY (FT)	HPVH (FT)	PHIH (FT)	PHI (FT)	AVG Sw	AVG VCL	AVG RES ROCK (FT)
RES	PHIH	PHI	VCL								
-----	-----	-----	-----	-----	-----	-----	-----	-----	-----	-----	-----
EOCENE		5640.00	5835.00	195.50	7.50	.21	.62	.082	.663	.387	7.50
.62 .082 .387											
MUD PRONE PALEOC		5835.00	6731.00	896.50	24.00	.41	2.02	.084	.795	.296	50.50
3.71 .074 .276											
UPPER MEMBER		6731.00	7136.00	405.50	104.50	7.62	12.69	.121	.400	.210	104.50
12.69 .121 .210											
MIDDLE MEMBER		7136.00	7136.00	.50	.00	.00	.00	.000	1.000	1.000	.00
.00 .000 1.000											
LOWER MEMBER		7136.00	7576.00	440.50	127.00	5.16	12.31	.097	.581	.184	129.50
12.45 .096 .182											
CRETACEOUS		7576.00	8050.00	474.50	1.50	.03	.14	.094	.767	.069	20.00
1.23 .062 .051											
UP LATE JURASSIC		8050.00	8140.00	90.50	11.00	.10	1.05	.096	.905	.164	46.00
3.85 .084 .190											
AYOT LIMESTONE		8140.00	8195.00	55.50	11.00	.12	1.05	.095	.889	.058	39.00
2.69 .069 .095											
LATE JUR. SAND		8195.00	8195.00	.50	.00	.00	.00	.000	1.000	1.000	.00
.00 .000 1.000											
UPPER ROABIBA		8195.00	8195.00	.50	.00	.00	.00	.000	1.000	1.000	.00
.00 .000 1.000											
MAIN ROABIBA		8195.00	8195.00	.50	.00	.00	.00	.000	1.000	1.000	.00
.00 .000 1.000											
AALENIAN SAND		8195.00	8230.00	35.50	17.00	.86	1.89	.111	.542	.203	17.00
1.89 .111 .203											
TOARCIAN		8230.00	8230.00	.50	.50	.02	.07	.137	.715	.194	.50
.07 .137 .194											
PERMIAN		8230.00	8230.00	.50	.50	.02	.07	.137	.715	.194	.50
.07 .137 .194											
LOWER PERMIAN		8230.00	8452.00	222.50	45.00	.67	3.96	.088	.830	.278	55.00
4.67 .085 .281											

Appendix 2 : Petrophysical analyses results for Late Paleocene to Late Permian reservoirs on Wiriagar Deep and Vorwata wells. Petrophysical analyses performed by T. Lawrence (ARCO 1998). Wireline log data calibrated to core plug data (Bulling, et al., 1998).

COMP : ARCO BERAU INC.

WELL :	WIRIAGAR DEEP NO. 2										
DATE :	9-JUN-98 @ 11:01:11										
ZONE :	6200.00 - 9765.00 FT										
<u>INPUT CURVES</u> :	POROSITY	=	PHIEC	<u>CUTOFFS</u> :						POROSITY MINIMUM =>	
.05				WATER SATURATION	=	SWCFWL				POROSITY MAXIMUM <=	
Not Used				CLAY VOLUME	=	VCLC				WATER SATURATION <=	
.99										CLAY VOLUME <=	
.50											
<u>DISCRIMINATORS</u> :	(None)										
NET	ZONE NAME	ZONE TOP (FT)	ZONE BASE (FT)	GROSS INTERVAL (FT)	NET PAY (FT)	HPVH	PHIH	PHI	AVG	AVG	NET RES ROCK (FT)
RES	PHIH	PHI	VCL								
MUD PRONE PALEOC	6690.00	7333.00	643.50	40.50	1.18	3.62	.089	.674	.332	.332	63.50
4.91 .077 .324											
UPPER MEMBER	7333.00	7568.00	235.50	62.00	5.46	8.28	.134	.340	.153	.153	63.00
8.34 .132 .156											
MIDDLE MEMBER	7568.00	7718.00	150.50	135.00	12.56	18.35	.136	.315	.184	.184	135.50
18.38 .136 .184											
LOWER MEMBER	7718.00	8030.00	312.50	76.00	2.91	6.98	.092	.583	.165	.165	80.50
7.24 .090 .169											
CRETACEOUS	8030.00	8381.00	351.50	.00	.00	.00	.000	1.000	1.000	1.000	18.00
.98 .055 .065											
UP LATE JURASSIC	8381.00	8514.00	133.50	.00	.00	.00	.000	1.000	1.000	1.000	.00
.00 .000 1.000											
AYOT LIMESTONE	8514.00	8559.00	45.50	1.00	.01	.08	.081	.886	.121	.121	10.00
.57 .057 .118											
LATE JUR. SAND	8559.00	8559.00	.50	.00	.00	.00	.000	1.000	1.000	1.000	.00
.00 .000 1.000											
UPPER ROABIBA	8559.00	8559.00	.50	.00	.00	.00	.000	1.000	1.000	1.000	.00
.00 .000 1.000											
MAIN ROABIBA	8559.00	8680.00	121.50	117.00	13.47	16.14	.138	.165	.063	.063	117.00
16.14 .138 .063											
AALENIAN SAND	8738.00	8776.00	38.50	37.00	3.61	5.11	.138	.294	.067	.067	37.00
5.11 .138 .067											
TOARCIAN	8776.00	8776.00	.50	.00	.00	.00	.000	1.000	1.000	1.000	.00
.00 .000 1.000											
PERMO-TRIASSIC	8776.00	8776.00	.50	.00	.00	.00	.000	1.000	1.000	1.000	.00
.00 .000 1.000											
PERMIAN	8776.00	9670.00	894.50	79.50	2.54	7.90	.099	.678	.256	.256	82.00
8.06 .098 .255											

Appendix 2 : Petrophysical analyses results for Late Paleocene to Late Permian reservoirs on Wiriagar Deep and Vorwata wells. Petrophysical analyses performed by T. Lawrence (ARCO 1998). Wireline log data calibrated to core plug data (Bulling, et al., 1998).

COMP : ATLANTIC RICHFIELD BERAU, INC. WELL : WIRIAGAR DEEP NO. 3 DATE : 9-JUN-98 @ 11:05:50 ZONE : 7304.00 - 9986.00 FT												
NET	ZONE NAME	ZONE TOP	ZONE BASE	GROSS INTERVAL	NET PAY	HPVH	PHIH	PHI	Avg Sw	Avg VCL	Avg RES	NET ROCK
RES	PHIH	PHI	VCL	(FT)	(FT)	(FT)	(FT)	(FT)				(FT)
MUD PRONE PALEOC		7453.00	8146.00	693.50	190.00	11.62	20.64	.109	.437	.241	190.50	
20.66 .108 .241												
UPPER MEMBER		8146.00	8561.00	415.50	58.00	4.49	8.60	.148	.478	.154	58.00	
8.60 .148 .154												
MIDDLE MEMBER		8561.00	8561.00	.50	.00	.00	.00	.000	1.000	1.000	.00	
.00 .000 1.000												
LOWER MEMBER		8561.00	8963.00	402.50	107.50	4.80	10.11	.094	.525	.232	107.50	
10.11 .094 .232												
CRETACEOUS		8963.00	9295.00	332.50	10.00	.23	.86	.086	.729	.102	21.50	
1.49 .070 .061												
UP LATE JURASSIC		9295.00	9326.00	31.50	27.00	.62	2.24	.083	.724	.150	29.50	
2.39 .081 .150												
AYOT LIMESTONE		9326.00	9367.00	41.50	8.00	.32	.75	.094	.572	.148	14.00	
1.07 .076 .115												
LATE JUR. SAND		9367.00	9367.00	.50	.50	.05	.07	.144	.347	.126	.50	
.07 .144 .126												
UPPER ROABIBA		9367.00	9367.00	.50	.50	.05	.07	.144	.347	.126	.50	
.07 .144 .126												
MAIN ROABIBA		9367.00	9380.00	13.50	13.00	1.03	1.75	.135	.410	.064	13.00	
1.75 .135 .064												
AALENIAN SAND		9419.00	9477.00	58.50	57.00	5.03	7.73	.136	.350	.054	57.00	
7.73 .136 .054												
TOARCIAN		9477.00	9477.00	.50	.00	.00	.00	.000	1.000	1.000	.00	
.00 .000 1.000												
PERMO-TRIASSIC		9477.00	9477.00	.50	.00	.00	.00	.000	1.000	1.000	.00	
.00 .000 1.000												
PERMIAN		9477.00	9850.00	373.50	25.00	.58	2.03	.081	.713	.437	26.50	
2.12 .080 .437												

Appendix 2 : Petrophysical analyses results for Late Paleocene to Late Permian reservoirs on Wiriagar Deep and Vorwata wells. Petrophysical analyses performed by T. Lawrence (ARCO 1998). Wireline log data calibrated to core plug data (Bulling, et al., 1998).

COMP : ARCO BERAU INC. WELL : WIRIAGAR DEEP NO. 4 DATE : 9-JUN-98 @ 11:25:00 ZONE : 6950.00 - 9660.00 FT												
NET	ZONE NAME	ZONE TOP	ZONE BASE	GROSS INTERVAL	NET PAY	HPVH	PHIH	PHI	Avg Sw	Avg VCL	Avg RES	NET ROCK
RES	PHIH	PHI	VCL	(FT)	(FT)	(FT)	(FT)	(FT)				(FT)
				-----	-----	-----	-----	-----	-----	-----	-----	-----
MUD PRONE PALEOC		7256.00	7932.00	676.50	.00	.00	.00	.000	1.000	1.000	110.00	
10.65 .097 .238												
UPPER MEMBER		7932.00	7973.00	41.50	.00	.00	.00	.000	1.000	1.000	.00	
.00 .000 1.000												
MIDDLE MEMBER		7973.00	8124.00	151.50	79.00	3.57	7.84	.099	.545	.237	84.00	
8.17 .097 .229												
LOWER MEMBER		8124.00	8528.00	404.50	42.00	1.22	3.59	.086	.659	.318	44.00	
3.70 .084 .316												
CRETACEOUS		8528.00	8819.00	291.50	44.50	.61	2.92	.066	.792	.147	52.50	
3.34 .064 .152												
UP LATE JURASSIC		8819.00	8876.00	57.50	28.50	.71	2.57	.090	.723	.250	30.50	
2.69 .088 .254												
AYOT LIMESTONE		8876.00	8921.00	45.50	8.00	.10	.48	.060	.793	.194	10.00	
.59 .059 .180												
LATE JUR. SAND		8921.00	8921.00	.50	.00	.00	.00	.000	1.000	1.000	.00	
.00 .000 1.000												
UPPER ROABIBA		8921.00	8921.00	.50	.00	.00	.00	.000	1.000	1.000	.00	
.00 .000 1.000												
MAIN ROABIBA		8921.00	9122.00	201.50	198.50	16.90	21.70	.109	.221	.105	198.50	
21.70 .109 .105												
AALENIAN SAND		9167.00	9272.00	105.50	40.50	3.52	4.92	.122	.285	.109	72.00	
8.15 .113 .200												
TOARCIAN		9272.00	9272.00	.50	.00	.00	.00	.000	1.000	1.000	.00	
.00 .000 1.000												
PERMO-TRIASSIC		9272.00	9272.00	.50	.00	.00	.00	.000	1.000	1.000	.00	
.00 .000 1.000												
PERMIAN		9272.00	9520.00	248.50	60.00	1.06	4.97	.083	.788	.359	72.50	
5.63 .078 .357												

Appendix 2 : Petrophysical analyses results for Late Paleocene to Late Permian reservoirs on Wiriagar Deep and Vorwata wells. Petrophysical analyses performed by T. Lawrence (ARCO 1998). Wireline log data calibrated to core plug data (Bulling, et al., 1998).

COMP : ATLANTIC RICHFIELD BERAU INC.

WELL :	WIRIAGAR DEEP NO.5												
DATE :	9-JUN-98 @ 13:29:59												
ZONE :	7175.00 - 9978.50 FT												
<u>INPUT CURVES</u> :	POROSITY = PHIEC						<u>CUTOFFS</u> :	POROSITY MINIMUM =>					
.05	WATER SATURATION = SWCFWL							POROSITY MAXIMUM <=					
Not Used	CLAY VOLUME = VCLC							WATER SATURATION <=					
.99								CLAY VOLUME <=					
.50													
<u>DISCRIMINATORS</u> :	(None)												
NET	ZONE NAME	ZONE TOP (FT)	ZONE BASE (FT)	GROSS INTERVAL (FT)	NET PAY (FT)	HPVH	PHIH	PHI	AVG Sw	AVG VCL	AVG RES	NET ROCK (FT)	
RES	PHIH	PHI	VCL										
-----	-----	-----	-----	-----	-----	-----	-----	-----	-----	-----	-----	-----	-----
EOCENE		7200.00	7294.00	94.50	1.00	.01	.05	.052	.715	.148	1.00		
.05 .052	.148												
MUD PRONE PALEOC		7294.00	8411.00	1117.50	122.50	2.49	8.60	.070	.710	.281	126.00		
8.92 .071	.277												
UPPER MEMBER		8411.00	8590.00	179.50	13.00	.50	1.22	.094	.592	.239	44.00		
4.41 .100	.220												
MIDDLE MEMBER		8590.00	8590.00	.50	.00	.00	.00	.000	1.000	1.000	.00		
.00 .000	1.000												
LOWER MEMBER		8590.00	8995.00	405.50	.00	.00	.00	.000	1.000	1.000	117.50		
9.70 .083	.279												
CRETACEOUS		8995.00	9338.00	343.50	.50	.00	.03	.057	.980	.292	2.50		
.14 .055	.265												
UP LATE JURASSIC		9338.00	9464.00	126.50	.00	.00	.00	.000	1.000	1.000	.00		
.00 .000	1.000												
AYOT LIMESTONE		9464.00	9500.00	36.50	.00	.00	.00	.000	1.000	1.000	2.50		
.16 .064	.233												
LATE JUR. SAND		9500.00	9500.00	.50	.00	.00	.00	.000	1.000	1.000	.00		
.00 .000	1.000												
UPPER ROABIBA		9500.00	9500.00	.50	.00	.00	.00	.000	1.000	1.000	.00		
.00 .000	1.000												
MAIN ROABIBA		9500.00	9685.00	185.50	.00	.00	.00	.000	1.000	1.000	167.50		
17.67 .106	.115												
AALENIAN SAND		9755.00	9874.00	119.50	.00	.00	.00	.000	1.000	1.000	84.00		
9.71 .116	.107												
TOARCIAN		9874.00	9874.00	.50	.00	.00	.00	.000	1.000	1.000	.00		
.00 .000	1.000												
PERMO-TRIASSIC		9874.00	9874.00	.50	.00	.00	.00	.000	1.000	1.000	.00		
.00 .000	1.000												
PERMIAN		9874.00	9880.00	6.50	3.00	.07	.25	.084	.723	.000	3.00		
.25 .084	.000												

Appendix 2 : Petrophysical analyses results for Late Paleocene to Late Permian reservoirs on Wiriagar Deep and Vorwata wells. Petrophysical analyses performed by T. Lawrence (ARCO 1998). Wireline log data calibrated to core plug data (Bulling, et al., 1998).

COMP : OCCIDENTAL WELL : OFAWERI-1 DATE : 9-JUN-98 @ 14:22:09 ZONE : 8000.00 - 10201.00 FT											
NET RES	ZONE NAME	ZONE TOP	ZONE BASE	GROSS INTERVAL	NET PAY	HPVH	PHIH	Avg PHI	Avg Sw	Avg VCL	NET RES ROCK
	AVG PHI	AVG VCL	(FT)	(FT)	(FT)	(FT)	(FT)				(FT)
	EOCENE	8000.00	8355.00	355.50	39.00	1.15	2.93	.075	.609	.052	139.00
8.65	.062 .156										
MUD PRONE PALEOC	8355.00	8653.00	298.50	89.50	3.71	7.83	.087	.525	.253	.253	90.00
7.85	.087 .253										
UPPER MEMBER	8653.00	8678.00	25.50	1.00	.03	.08	.079	.557	.429	.429	1.00
.08	.079 .429										
MIDDLE MEMBER	8678.00	8678.00	.50	.50	.02	.04	.081	.581	.364	.364	.50
.04	.081 .364										
LOWER MEMBER	8678.00	9158.00	480.50	171.50	6.33	14.09	.082	.551	.276	.276	172.00
14.12	.082 .276										
CRETACEOUS	9158.00	9440.00	282.50	31.00	.76	2.32	.075	.671	.149	.149	36.50
2.61	.071 .160										
UP LATE JURASSIC	9440.00	9611.00	171.50	1.50	.04	.16	.105	.757	.166	.166	3.00
.26	.087 .191										
AYOT LIMESTONE	9611.00	9648.00	37.50	1.00	.04	.10	.096	.547	.186	.186	1.00
.10	.096 .186										
LATE JUR. SAND	9649.00	9649.00	.50	.50	.03	.05	.100	.315	.158	.158	.50
.05	.100 .158										
UPPER ROABIBA	9649.00	9649.00	.50	.50	.03	.05	.100	.315	.158	.158	.50
.05	.100 .158										
MAIN ROABIBA	9649.00	10005.00	356.50	317.00	22.49	28.99	.091	.224	.082	.082	317.00
28.99	.091 .082										
AALENIAN SAND	10080.00	10103.00	23.50	23.00	1.32	1.93	.084	.316	.134	.134	23.00
1.93	.084 .134										
TOARCIAN	10103.00	10103.00	.50	.00	.00	.00	.000	1.000	1.000	.00	
.00	.000 1.000										
PERMO-TRIASSIC	10103.00	10103.00	.50	.00	.00	.00	.000	1.000	1.000	.00	
.00	.000 1.000										
PERMIAN	10201.00	10201.00	.50	.00	.00	.00	.000	1.000	1.000	.00	
.00	.000 1.000										

Appendix 2 : Petrophysical analyses results for Late Paleocene to Late Permian reservoirs on Wiriagar Deep and Vorwata wells. Petrophysical analyses performed by T. Lawrence (ARCO 1998). Wireline log data calibrated to core plug data (Bulling, et al., 1998).

COMP : OCCIDENTAL WELL : ROABIBA-1 DATE : 9-JUN-98 @ 14:17:10 ZONE : 9100.00 - 12007.00 FT												
NET RES	ZONE NAME	ZONE TOP	ZONE BASE	GROSS INTERVAL	NET PAY	HPVH	PHIH	PHI	Avg Sw	Avg VCL	Avg RES	NET ROCK
	AVG (FT)	AVG (FT)	AVG (FT)	AVG (FT)	AVG (FT)	AVG (FT)	AVG (FT)	AVG (FT)	NET (FT)			
	EOCENE	9100.00	9417.00	317.50	144.50	5.35	15.68	.109	.659	.210	195.50	
18.64	.095 .200											
	MUD PRONE PALEOC	9417.00	9689.00	272.50	95.00	4.10	11.26	.118	.636	.345	96.00	
11.31	.118 .343											
	UPPER MEMBER	9689.00	9706.00	17.50	.00	.00	.00	.000	1.000	1.000	.00	
.00	.000 1.000											
	MIDDLE MEMBER	9706.00	9706.00	.50	.00	.00	.00	.000	1.000	1.000	.00	
.00	.000 1.000											
	LOWER MEMBER	9706.00	10186.00	480.50	176.50	6.65	16.50	.093	.597	.232	177.50	
16.55	.093 .232											
	CRETACEOUS	10186.00	10598.00	412.50	138.00	5.86	14.05	.102	.583	.092	180.50	
16.53	.092 .091											
	UP LATE JURASSIC	10598.00	10780.00	182.50	3.00	.01	.18	.059	.944	.394	14.00	
.79	.056 .405											
	AYOT LIMESTONE	10780.00	10840.00	60.50	5.00	.06	.37	.073	.823	.183	24.00	
1.42	.059 .139											
	LATE JUR. SAND	10840.00	10840.00	.50	.50	.01	.04	.075	.788	.388	.50	
.04	.075 .388											
	UPPER ROABIBA	10975.00	11030.00	55.50	53.50	3.86	6.04	.113	.361	.150	53.50	
6.04	.113 .150											
	MAIN ROABIBA	11030.00	11408.00	378.50	288.00	22.86	30.17	.105	.242	.038	348.50	
34.52	.099 .041											
	AALENIAN SAND	11458.00	11485.00	27.50	.00	.00	.00	.000	1.000	1.000	23.50	
2.70	.115 .146											
	TOARCIAN	11485.00	11485.00	.50	.00	.00	.00	.000	1.000	1.000	.50	
.07	.133 .261											
	PERMO-TRIASSIC	11485.00	11485.00	.50	.00	.00	.00	.000	1.000	1.000	.50	
.07	.133 .261											
	PERMIAN	11507.00	11700.00	193.50	96.00	4.84	10.85	.113	.553	.247	96.50	
10.92	.113 .246											

Appendix 2 : Petrophysical analyses results for Late Paleocene to Late Permian reservoirs on Wiriagar Deep and Vorwata wells. Petrophysical analyses performed by T. Lawrence (ARCO 1998). Wireline log data calibrated to core plug data (Bulling, et al., 1998).

COMP : OCCIDENTAL

WELL :	WOS-1										
DATE :	9-JUN-98 @ 16:57:48										
ZONE :	4700.00 - 9700.00 FT										
<u>INPUT CURVES</u> :	POROSITY	=	PHIEC	<u>CUTOFFS</u> :						POROSITY MINIMUM =>	
.05				WATER SATURATION	=	SWCFWL				POROSITY MAXIMUM <=	
Not Used				CLAY VOLUME	=	VCLC				WATER SATURATION <=	
.99										CLAY VOLUME <=	
.50											
<u>DISCRIMINATORS</u> :	(None)										
NET	ZONE NAME	ZONE TOP (FT)	ZONE BASE (FT)	GROSS INTERVAL (FT)	NET PAY (FT)	HPVH (FT)	PHIH (FT)	PHI (FT)	AVG Sw	AVG VCL	NET RES ROCK (FT)
RES	PHIH	PHI	VCL								
EOCENE		7308.00	7549.00	241.50	15.00	.72	1.14	.076	.370	.061	15.00
1.14 .076 .061											
MUD PRONE PALEOC		7549.00	7860.00	311.50	51.00	1.69	3.49	.068	.516	.268	51.50
3.52 .068 .266											
UPPER MEMBER		7860.00	7990.00	130.50	49.50	1.42	3.42	.069	.585	.286	49.50
3.42 .069 .286											
MIDDLE MEMBER		7990.00	7990.00	.50	.50	.01	.03	.054	.611	.496	.50
.03 .054 .496											
LOWER MEMBER		7990.00	8271.00	281.50	82.50	2.26	5.08	.062	.555	.331	82.50
5.08 .062 .331											
CRETACEOUS		8271.00	8674.00	403.50	68.50	3.18	5.08	.074	.374	.141	68.50
5.08 .074 .141											
UP LATE JURASSIC		8674.00	9070.00	396.50	15.00	.86	1.19	.079	.278	.326	15.00
1.19 .079 .326											
AYOT LIMESTONE		9070.00	9114.00	44.50	14.00	.30	1.01	.072	.707	.406	14.00
1.01 .072 .406											
LATE JUR. SAND		9114.00	9325.00	211.50	210.00	7.66	16.66	.079	.540	.165	210.00
16.66 .079 .165											
UPPER ROABIBA		9365.00	9365.00	.50	.00	.00	.00	.000	1.000	1.000	.00
.00 .000 1.000											
MAIN ROABIBA		9365.00	9650.00	285.50	267.50	10.16	21.11	.079	.519	.166	267.50
21.11 .079 .166											
AALENIAN SAND		9700.00	9700.00	.50	.00	.00	.00	.000	1.000	1.000	.00
.00 .000 1.000											
TOARCIAN		9700.00	9700.00	.50	.00	.00	.00	.000	1.000	1.000	.00
.00 .000 1.000											
PERMO-TRIASSIC		9700.00	9700.00	.50	.00	.00	.00	.000	1.000	1.000	.00
.00 .000 1.000											
PERMIAN		9700.00	9700.00	.50	.00	.00	.00	.000	1.000	1.000	.00
.00 .000 1.000											

APPENDIX 3

POROSITY AND PERMEABILITY MEASUREMENTS FROM VORWATA #10 CORE PLUGS

CORE PLUG ANALYSIS PERFORMED AT CORE LABORATORIES, JAKARTA
INDONESIA BY BG, AT 800 PSI NET OVERBURDEN PRESSURE (NOB 800)
(COURTESEY OF BP, 2002)

CORE LABORATORIES

Company: British Gas International
Well: Vorwata #10

File: JCA-98045

**CORE ANALYSIS RESULTS
(HYDROSTATIC CONFINEMENT)**

Sample number	Depth (M.)	Confining Pressure 800psi.		Porosity (%)	Confining Pressure 3300psi.		Porosity (%)	Grain Density (gm/cc)	REMARKS
		Permeability KI (md)	Kair (md)		Permeability KI (md)	Kair (md)			

Core # 1 (Interval : 3944.00 - 3967.33 m.)

Shale : No analysis

Core # 2 (Interval : 4021.00 - 4043.24m.)

201	4021.05	33.6	37.4	13.1	29.1	32.1	12.5	2.645	
202	4021.30	0.033	0.067	5.2	0.005	0.014	4.5	2.671	
203	4021.60	0.028	0.061	8.0	0.008	0.020	7.3	2.672	
204	4021.90	0.033	0.066	6.5	0.007	0.019	5.9	2.683	
205	4022.20	0.026	0.054	9.0	0.010	0.023	8.6	2.738	
206	4022.48	0.044	0.078	5.7	0.006	0.017	5.1	2.673	
207	4022.78	0.059	0.107	8.3	0.009	0.023	7.5	2.672	
208	4023.10	0.151	0.256	14.5	0.071	0.139	14.0	2.669	
209	4023.40	0.208	0.324	14.0	0.080	0.149	13.4	2.663	
210	4023.71	0.115	0.205	13.9	0.052	0.108	13.4	2.665	
211	4024.02	0.224	0.344	13.9	0.133	0.213	13.3	2.666	
212	4042.30	0.095	0.175	13.4	0.042	0.090	12.9	2.669	
213	4024.65	0.045	0.084	8.8	0.009	0.028	8.2	2.671	
214	4024.90	0.098	0.180	13.6	0.042	0.094	13.1	2.666	
215	4025.19	127	135	13.1	122	129	12.8	2.628	
216	4025.47	74.1	76.2	10.6	71.5	73.5	10.3	2.639	
217	4025.80	94.3	97.4	11.0	90.8	93.8	10.7	2.639	
218	4026.10	464	473	14.8	430	432.0	14.5	2.652	
219	4026.31	1020	1040	13.8	990	1000	13.1	2.662	
220	4026.75	744	757	12.9	723	735	12.5	2.652	
221	4027.03	1320	1590	14.9	1270	1590	14.4	2.663	
222	4027.30								Fractured
223	4027.52	1390	1460	15.5	1150	1170	14.9	2.650	
224	4027.90	70.9	76.0	11.2	66.7	71.6	10.9	2.634	
225	4028.20	923	939	15.6	894	909	15.1	2.645	
226	4028.50	785	799	14.2	759	772	13.8	2.648	
227	4028.80	331	339	12.4	317	325	12.0	2.639	
228	4029.11	356	365	12.2	340	348	11.9	2.641	
229	4029.40	257	264	11.3	245	252	11.0	2.642	
230	4029.70	1110	1120	15.2	1070	1090	14.8	2.652	
231	4030.05	41.4	41.8	8.4	39.6	40.0	8.1	2.648	
232	4030.29	703	716	14.2	682	694	13.8	2.650	
233	4030.67	705	717	13.8	682	695	13.5	2.649	
234	4030.92	624	636	13.7	604	616	13.4	2.648	
235	4031.20	530	541	13.7	515	526	13.4	2.650	
236	4031.50	306	313	12.5	297	304	12.3	2.650	
237	4031.83	426	436	13.0	414	423	12.8	2.647	
238	4031.10	432	441	12.9	418	427	12.7	2.643	
239	4032.40	384	392	12.3	371	379	12.0	2.648	
240	4032.70	440	449	12.6	424	433	12.3	2.649	
241	4033.02	797	810	13.8	772	785	13.5	2.648	

CORE LABORATORIES

Company: British Gas International
Well: Vorwata #10

File: JCA-98045

**CORE ANALYSIS RESULTS
(HYDROSTATIC CONFINEMENT)**

Sample number	Depth (M.)	Confining Pressure 800psi.			Confining Pressure 3300psi.			Grain Density (gm/cc)	REMARKS
		Permeability KI (md)	Kair (md)	Porosity (%)	Permeability KI (md)	Kair (md)	Porosity (%)		
242	4033.30	500	510	12.5	482	491	12.2	2.648	
243	4033.60	440	449	12.2	425	434	11.9	2.649	
244	4033.90	697	709	12.9	675	687	12.6	2.649	
245	4034.20	550	560	12.6	531	541	12.2	2.650	
246	4034.51	709	722	13.3	686	698	13.0	2.648	
247	4034.80	580	591	13.4	560	571	13.1	2.646	
248	4035.10	195	197	11.7	185	187	11.3	2.645	
249	4035.40	274	281	13.0	265	272	12.7	2.644	
250	4035.70	243	250	12.1	234	240	11.8	2.647	
251	4036.02	284	292	12.7	273	281	12.4	2.648	
252	4036.47	232	233	12.1	223	224	11.8	2.653	
253	4036.69	81.2	82.3	11.7	77.8	78.8	11.3	2.643	
254	4036.92	166	169	11.5	152	154	11.2	2.645	
255	4037.18	82.9	83.8	11.0	79.3	80.1	10.7	2.648	
256	4037.48	252	259	12.7	242	249	12.3	2.647	
257	4037.84	302	310	12.7	293	301	12.5	2.647	
258	4038.15	318	325	12.2	309	316	12.0	2.649	
259	4038.42	1420	1440	13.5	1070	1180	13.1	2.651	
260	4038.74	88.7	96.8	12.9	69.9	75.2	12.6	2.647	
261	4039.10	81.2	82.4	12.8	72.4	73.6	12.3	2.647	
262	4039.31	86.2	86.8	12.1	82.9	83.4	11.8	2.649	
263	4039.62	141	146	13.3	135	140	13.0	2.650	
264	4039.92	31.5	32.6	11.1	29.3	30.2	10.8	2.647	
265	4040.20	74.5	76.2	14.1	70.9	72.5	13.8	2.651	
266	4040.53	55.2	58.7	14.5	51.0	54.2	14.1	2.648	
267	4040.85	34.1	35.8	13.6	31.9	33.3	13.2	2.671	
268	4041.12	66.5	70.6	14.3	61.7	65.1	14.0	2.646	
269	4041.40	16.7	20.1	13.4	12.6	15.5	13.0	2.649	
270	4041.70	95.2	98.8	13.7	89.3	92.3	13.3	2.649	
271	4042.03	138	143	14.4	129	134	13.9	2.651	
272	4042.29	39.3	50.6	13.4	31.6	40.4	12.9	2.651	
273	4042.62	40.9	44.2	12.9	34.4	37.2	12.4	2.647	
274	4042.90								Rubble
275	4043.20								Rubble
Core # 3 (Interval : 4044.00 - 4056.72 m.)									
301	4044.03	36.0	38.3	12.8	27.9	29.7	12.4	2.655	
302	4044.35	103	105	12.9	97	98.4	12.4	2.649	
303	4044.61	236	243	13.0	227	233	12.7	2.649	
304	4044.90	51.4	54.3	12.8	42.9	46.1	12.4	2.652	
305	4045.20	70.2	71.9	13.1	67.4	69.0	12.8	2.654	
306	4045.53	182	188	14.1	174	180	13.8	2.652	
307	4045.80	215	216	14.4	208	209	14.1	2.653	
308	4046.10	186	188	14.4	180	181	14.1	2.650	
309	4046.40	329	337	13.9	316	324	13.5	2.649	
310	4046.70	301	312	14.7	285	295	14.2	2.649	

CORE LABORATORIES

Company: British Gas International
Well: Vorwata #10

File: JCA-98045

**CORE ANALYSIS RESULTS
(HYDROSTATIC CONFINEMENT)**

Sample number	Depth (M.)	Confining Pressure 800psi.		Porosity (%)	Confining Pressure 3300psi.		Porosity (%)	Grain Density (gm/cc)	REMARKS
		KI (md)	Permeability Kair (md)		KI (md)	Permeability Kair (md)			
311	4047.02	157	159	12.5	150	152	12.0	2.646	
312	4047.35	5.25	8.43	12.9	2.84	4.60	12.5	2.647	
313	4047.65	142	142	13.3	137	137	13.0	2.647	
314	4047.90	99	100	13.8	95	95.8	13.5	2.646	
315	4048.21	113	115	12.9	100	103	12.5	2.653	
316	4048.50	118	119	13.4	113.0	114	13.0	2.652	
317	4048.84	82.3	83.6	11.3	77.5	78.6	11.0	2.653	
318	4049.10	16.5	17.8	9.7	13.2	14.2	9.3	2.652	
319	4049.40	18.4	19.7	10.1	16.1	17.1	9.7	2.651	
320	4049.70	40.3	41.4	10.2	37.4	38.4	10.0	2.652	
321	4050.02	38.1	39.1	10.3	36.1	36.8	10.0	2.651	
322	4050.32	46.6	47.8	11.3	44.3	45.4	11.0	2.648	
323	4050.62	233	240	12.1	227	234	11.8	2.648	
324	4050.90	144	149	11.8	140	145	11.6	2.651	
325	4051.25	190	200	10.9	181	188	10.6	2.649	
326	4051.50	302	310	12.1	287	296	11.7	2.650	
327	4051.81	181	182	9.2	171	173	8.7	2.649	
328	4052.13	665	676	11.6	640	651	11.4	2.650	
329	4052.46	1010	1030	14.5	948	963	14.0	2.658	
330	4052.75	0.141	0.218	3.8	0.033	0.062	3.2	2.659	
331	4053.02	4.54	5.27	9.6	2.77	3.34	9.2	2.654	
332	4053.30	10.20	11.6	13.3	7.95	9.04	12.9	2.652	
333	4053.65	0.334	0.471	13.0	0.211	0.311	12.6	2.651	
334	4053.93	5.79	6.91	12.9	3.06	3.38	12.4	2.651	
335	4052.26	1.47	1.70	5.9	0.327	0.391	5.4	2.657	
336	4054.52	7.78	8.76	12.5	6.54	7.36	12.0	2.651	
337	4054.80	146	147	10.9	131	136	10.5	2.649	
338	4055.10	275	282	11.8	265	272	11.4	2.650	
339	4055.40	2690	2720	20.1	2560	2590	19.6	2.651	
340	4055.70	29.2	30.8	9.4	25.0	26.3	8.9	2.652	
341	4056.02	1630	1650	17.5	1560	1580	17.0	2.652	
342	4056.31	553	564	14.1	536	547	13.8	2.651	
343	4056.62	180	186	13.2	170	176	12.8	2.651	
Core # 4 (Interval : 4057.00 - 4062.75 m.)									
401	4057.02	105	106	12.6	99.8	101	12.3	2.650	
402	4057.32	89.8	91.6	12.6	84.6	86.4	12.2	2.649	
403	4057.62	15.3	16.4	9.9	14.2	15.1	9.6	2.651	
404	4057.91	2.63	3.15	10.6	2.24	2.67	10.3	2.658	
405	4058.27	35.9	43.1	14.3	9.06	10.4	13.1	2.654	
406	4058.52	0.123	0.203	5.9	0.023	0.052	5.2	2.659	
407	4058.81	0.094	0.154	6.2	0.014	0.035	5.5	2.668	
408	4059.10	0.085	0.137	3.6	0.012	0.026	3.1	2.707	
409	4059.40	11.5	12.6	8.9	9.28	10.1	8.5	2.659	
410	4059.72	27.3	29.0	11.6	23.7	25.1	11.3	2.650	
411	4060.02	7.01	7.90	12.8	6.23	7.01	12.4	2.652	

CORE LABORATORIES

Company: British Gas International
Well: Vorwata #10

File: JCA-98045

**CORE ANALYSIS RESULTS
(HYDROSTATIC CONFINEMENT)**

Sample number	Depth (M.)	Confining Pressure 800psi.		Porosity (%)	Confining Pressure 3300psi.		Porosity (%)	Grain Density (gm/cc)	REMARKS
		KI (md)	Kair (md)		KI (md)	Kair (md)			
412	4060.37							2.660	
413	4060.61	156	161	11.4	150	155	11.1	2.650	
414	4060.90	120	125	12.0	115	119	11.7	2.652	
415	4061.17	12.8	14.3	12.6	10.8	12.2	12.3	2.648	
416	4061.50	15.0	16.2	12.0	13.8	14.8	11.5	2.652	
417	4061.80	70.7	71.7	11.9	67.4	68.2	11.6	2.651	
418	4062.09	40.1	41.7	11.8	36.5	38.0	11.4	2.669	
419	4062.38	184	185	12.8	176	177	12.5	2.645	
420	4062.70	221	223	13.0	210	211	12.4	2.652	
Core # 5 (Interval : 4063.00 - 4064.40 m.)									
501	4063.02	81.5	85.0	13.4	76.4	79.5	13.1	2.651	
502	4063.32	176	182	13.1	168	174	12.6	2.657	
503	4063.60	255	264	14.5	232	236	14.1	2.653	
504	4063.91	291	293	13.5	261	262	13.0	2.661	
505	4064.20	350	358	14.8	327	331	14.4	2.650	
Core # 6 (Interval : 4064.50 - 4089.77m.)									
601	4064.60	181	187	13.2	173	179	12.9	2.649	
602	4064.91	257	264	13.1	246	253	12.8	2.652	
603	4065.21	167	172	12.1	160	165	11.8	2.650	
604	4065.52	55.6	58.4	11.3	50.5	53.0	11.0	2.648	
605	4065.81	2.06	2.46	8.0	1.55	1.85	7.6	2.651	
606	4066.11	52.9	55.3	13.0	49.5	51.7	12.6	2.649	
607	4066.46	2.36	2.90	8.7	1.58	1.97	8.3	2.656	
608	4066.75	121	122	13.1	115	116	12.7	2.651	
609	4067.04	44.5	46.3	12.3	40.9	42.4	11.9	2.652	
610	4067.92	3.87	4.66	9.8	2.56	3.17	9.4	2.657	
611	4067.60	5.82	6.94	10.0	3.89	4.66	9.6	2.650	
612	4067.89	41.9	43.7	13.0	38.6	40.1	12.6	2.650	
613	4068.20	453	463	13.4	434	443	13.0	2.653	
614	4068.50	204	208	14.0	194	197	13.6	2.652	
615	4068.79	708	722	16.7	664	677	16.2	2.651	
616	4069.12	510	521	15.7	477	487	15.3	2.655	
617	4069.42	457	468	15.5	453	455	15.1	2.653	
618	4069.71	360	369	13.6	346	354	13.2	2.652	
619	4070.02	587	599	14.9	569	581	14.6	2.653	
620	4070.30	85.0	89.4	13.4	77.4	81.1	13.0	2.651	
621	4070.69	518	529	13.8	495	505	13.4	2.651	
622	4070.90	602	615	16.4	577	589	16.0	2.649	
623	4071.21	194	200	12.4	184	190	12.0	2.650	
624	4071.52	327	336	15.2	312	320	14.8	2.649	
625	4071.84	176	177	14.2	169	169	13.8	2.648	
626	4072.10	142	142	13.7	135	136	13.4	2.649	
627	4072.41	139	142	14.8	129	132	14.4	2.656	
628	4072.71	74.7	76.9	13.5	68.4	70.4	13.1	2.656	
629	4072.03	50.6	52.3	12.7	46.3	47.8	12.3	2.656	

CORE LABORATORIES

Company: British Gas International
Well: Vorwata #10

File: JCA-98045

**CORE ANALYSIS RESULTS
(HYDROSTATIC CONFINEMENT)**

Sample number	Depth (M.)	Confining Pressure 800psi.			Confining Pressure 3300psi.			Grain Density (gm/cc)	REMARKS
		KI (md)	Permeability Kair (md)	Porosity (%)	KI (md)	Permeability Kair (md)	Porosity (%)		
630	4073.32	33.1	35.9	12.2	30.3	32.9	11.9	2.651	
631	4073.52	135	136	13.9	130	130	13.5	2.651	
632	4073.93	107	108	12.9	102	103	12.6	2.651	
633	4074.20	179	181	13.4	170	172	13.1	2.654	
634	4074.51	204	211	13.3	194	200	13.0	2.650	
635	4074.80	67.9	70.2	10.8	63.3	65.2	10.5	2.661	
636	4075.10	300	308	13.2	299	300	12.9	2.653	
637	4075.40	201	205	12.7	190	193	12.4	2.656	
638	4075.70	159	161	11.9	150	151	11.5	2.651	
639	4076.02	435	445	14.0	418	428	13.7	2.651	
640	4076.30	412	422	14.5	397	406	14.2	2.651	
641	4076.60	154	155	12.6	145	145	12.2	2.658	
642	4076.90	290	298	14.3	279	287	14.0	2.650	
643	4077.20	88.1	89.2	11.2	82.9	83.8	10.8	2.652	
644	4077.50	188	194	13.5	180	186	13.2	2.652	
645	4077.87	382	391	14.7	367	377	14.3	2.647	
646	4078.10	264	272	13.6	250	257	13.2	2.653	
647	4078.41	718	732	16.0	691	705	15.6	2.650	
648	4078.71	483	494	15.0	463	474	14.7	2.650	
649	4079.05	608	620	14.6	583	595	14.1	2.650	
650	4079.31	725	739	15.6	695	708	15.1	2.650	
651	4079.60	856	871	16.2	820	835	15.8	2.650	
652	4079.93	928	944	16.1	891	907	15.6	2.652	
653	4080.20	620	632	14.8	596	608	14.4	2.651	
654	4080.50	33.4	49.4	14.0	17.7	27.6	13.6	2.652	
655	4080.80	18.6	28.8	13.8	9.9	16.7	13.4	2.653	
656	4081.10	32.6	45.6	14.1	20.5	29.5	13.7	2.654	
657	4081.40	470	480	14.2	449	459	13.8	2.650	
658	4081.69	711	725	15.3	683	696	14.9	2.649	
659	4081.02	529	541	14.9	505	516	14.5	2.653	
660	4082.30	1050	1070	16.0	1010	1030	15.7	2.650	
661	4082.60	137	144	11.5	125	130	11.0	2.652	
662	4082.93	1140	1160	15.5	1100	1110	15.1	2.654	
663	4083.19	764	778	15.5	732	745	15.1	2.652	
664	4083.49	438	442	14.6	399	704	14.0	2.655	
665	4083.80	417	424	15.7	374	382	15.1	2.655	
666	4084.09	370	380	14.9	353	362	14.5	2.648	
667	4084.40	310	318	14.1	281	289	13.6	2.655	
668	4084.70	88.8	95.6	14.2	64.7	71.8	13.7	2.655	
669	4085.03	162	166	15.0	155	158	14.6	2.653	
670	4085.30	212	218	15.5	196	201	15.0	2.656	
671	4085.60	262	265	15.5	246	248	14.7	2.648	
672	4085.89	352	353	15.9	336	337	15.4	2.649	
673	4086.19	316	325	15.2	303	312	14.8	2.650	
674	4086.50	42.3	44.8	13.5	38.1	40.4	13.0	2.652	

CORE LABORATORIES

Company: British Gas International
Well: Vorwata #10

File: JCA-98045

**CORE ANALYSIS RESULTS
(HYDROSTATIC CONFINEMENT)**

Sample number	Depth (M.)	Confining Pressure 800psi.		Porosity (%)	Confining Pressure 3300psi.		Porosity (%)	Grain Density (gm/cc)	REMARKS
		KI (md)	Permeability Kair (md)		KI (md)	Permeability Kair (md)			
675	4086.79	502	513	14.3	484	494	14.1	2.651	
676	4087.10	274	275	13.5	246	248	13.0	2.651	
677	4087.38	300	308	14.2	287	295	13.8	2.651	
678	4087.69	212	213	12.1	200	200	11.7	2.650	
679	4088.03	493	504	15.3	472	482	15.0	2.649	
680	4088.30	414	424	14.2	398	408	13.4	2.650	
681	4088.54	43.7	46.0	12.1	38.3	40.4	11.6	2.649	
682	4088.90	97.0	98.5	13.5	92.4	93.9	13.1	2.652	
683	4089.31	35.6	37.2	12.8	33.5	35.0	12.5	2.650	
684	4089.54	51.9	53.5	12.2	49.1	50.7	11.8	2.650	
Core # 7 (Interval : 4090.50 - 4118.50 m.)									
701	4090.54	78.0	80.2	13.4	73.6	75.5	12.9	2.656	
702	4090.80	69.9	76.1	14.2	59.4	64.4	13.6	2.655	
703	4091.11	82.6	85.7	15.0	77.4	80.6	14.5	2.654	
704	4091.40	99.1	102.0	11.8	94.3	97.1	11.4	2.652	
705	4091.70	46.2	48.3	12.8	44.6	46.5	12.5	2.658	
706	4092.06	33.9	37.1	13.4	30.7	33.5	12.9	2.656	
707	4092.32	257	261	13.0	244	247	12.6	2.657	
708	4092.60	103	120	13.7	87.6	99.8	12.9	2.659	
709	4092.87	72.4	106.0	15.4	65.2	90.2	15.0	2.656	
710	4093.20	248	276	14.7	207	232	14.3	2.655	
711	4093.50	413	415	14.6	381	382	14.1	2.657	
712	4093.80	4.22	5.14	11.2	2.88	3.6	10.7	2.658	
713	4094.10	19.2	21.5	13.8	15.0	17.0	13.3	2.663	
714	4094.40	322	331	14.9	311	320	14.6	2.647	
715	4094.74	308	309	15.7	293	294	15.4	2.649	
716	4095.06	225	231	15.6	210	215	15.2	2.655	
717	4095.36	226	227	15.0	216	217	14.6	2.652	
718	4095.60	393	415	15.6	354	372	15.2	2.652	
719	4095.93	236	238	15.2	226	228	14.7	2.659	
720	4096.21	275	277	16.1	265	266	15.8	2.654	
721	4096.50	496	498	14.5	474	477	14.2	2.650	
722	4096.80	1.75	2.28	10.8	1.00	1.4	10.4	2.660	
723	4097.10	17.2	18.3	11.6	15.5	16.5	11.1	2.665	
724	4097.42	116	119	14.7	110	113	14.4	2.653	
725	4097.70	14.2	15.8	14.5	12.3	13.6	14.1	2.659	
726	4098.02	121	123	19.1	115	117	18.6	2.649	
727	4098.32	2.41	3.13	14.7	1.50	2.1	14.2	2.653	
728	4098.60	25.0	26.7	13.6	22.6	24.1	13.1	2.651	
729	4098.90	56.0	58.7	15.0	52.4	55.0	14.6	2.648	
730	4099.20	84.4	86.5	14.0	80.2	82.3	13.7	2.647	
731	4099.50	208	210	14.6	199	201	14.0	2.652	
732	4099.80	113	117	14.3	106	110	13.9	2.651	
733	4100.08	112	115	13.5	106	109	13.2	2.650	
734	4100.40	149	152	14.3	140	143	14.0	2.650	

CORE LABORATORIES

Company: British Gas International
Well: Vorwata #10

File: JCA-98045

**CORE ANALYSIS RESULTS
(HYDROSTATIC CONFINEMENT)**

Sample number	Depth (M.)	Confining Pressure 800psi.			Confining Pressure 3300psi.			Grain Density (gm/cc)	REMARKS
		KI (md)	Permeability Kair (md)	Porosity (%)	KI (md)	Permeability Kair (md)	Porosity (%)		
735	4100.75	111	114	15.4	104	107	14.9	2.650	
736	4101.03	72.8	74.3	12.4	69.6	71.1	12.1	2.673	
737	4101.30	10.4	11.3	12.1	9.6	10.4	11.8	2.712	
738	4101.62	37.4	40.4	13.8	27.5	29.4	13.4	2.678	
739	4101.90	80.3	83.1	15.9	75.1	77.8	15.5	2.649	
740	4102.19	48.4	51.2	16.0	41.6	44.0	15.6	2.653	
741	4102.49	13.6	15.2	15.4	11.5	13.1	14.9	2.664	
742	4102.80	19.9	21.0	10.7	18.9	19.8	10.4	2.686	
743	4103.10	15.1	16.6	13.8	14.0	15.4	13.4	2.684	
744	4113.25	285	287	17.2	271	273	16.4	2.648	
745	4113.50	69.2	71.6	15.3	64.8	67.0	14.8	2.656	
746	4113.80	21.6	24.2	14.3	17.7	19.9	13.8	2.665	
747	4114.13	0.174	0.268	7.8	0.059	0.110	7.2	2.678	
748	4114.40	27.3	29.8	18.5	24.6	26.9	17.9	2.652	
749	4114.70	15.3	17.2	14.6	13.5	15.2	14.2	2.653	
750	4115.03	16.0	17.8	15.1	14.3	16.0	14.6	2.658	
751	4115.30	11.2	12.8	15.5	9.7	11.0	15.1	2.653	
752	4115.60	11.6	13.2	15.3	10.3	11.8	14.9	2.657	
753	4115.93	9.88	11.4	14.7	8.29	9.68	14.2	2.650	
754	4116.19	19.8	21.8	14.7	17.7	19.5	14.3	2.654	
755	4116.50	19.9	22.0	15.2	17.5	19.5	14.7	2.664	
756	4116.80	23.5	25.8	15.0	22.0	24.2	14.6	2.667	
757	4117.10	12.1	13.8	14.7	10.7	12.3	14.3	2.664	
758	4117.40	14.0	15.8	14.4	13.1	14.8	14.1	2.667	
759	4117.70	23.2	25.6	15.6	21.5	23.8	15.2	2.664	
760	4118.00	20.4	22.5	14.7	19.0	21.0	14.4	2.662	
761	4118.30	29.1	31.6	15.0	27.5	29.9	14.7	2.667	
Core # 8 (Interval : 4118.50 - 4129.00 m.)									
801	4118.50	9.57	11.1	14.7	7.95	9.3	14.2	2.669	
802	4118.80	21.3	23.3	14.9	19.7	21.5	14.3	2.664	
803	4119.10	20.7	22.9	15.7	19.2	21.3	15.3	2.666	
804	4119.39	29.3	31.9	15.4	27.8	30.2	15.0	2.670	
805	4119.68	24.6	27.2	16.1	22.5	25.0	15.7	2.663	
806	4120.03	23.7	26.4	15.5	19.7	22.2	15.1	2.661	
807	4120.32	3.65	4.47	13.1	2.83	3.44	12.5	2.671	
808	4120.61	42.9	46.2	15.5	40.2	43.3	15.2	2.673	
809	4120.93	19.4	21.7	16.1	18.0	20.1	15.7	2.665	
810	4121.22	39.0	42.0	15.4	36.3	39.0	15.0	2.682	
811	4121.50	0.859	1.21	14.8	0.170	0.326	14.5	2.692	
812	4121.80	20.3	22.6	14.9	18.2	20.4	14.4	2.681	
813	4122.11	25.5	28.0	14.2	23.2	25.5	13.7	2.669	
814	4122.40	20.0	22.2	13.8	17.2	19.1	13.3	2.720	
815	4122.70	8.81	10.4	15.2	7.92	9.38	14.7	2.693	
816	4123.02	29.9	32.8	16.6	28.0	30.8	16.2	2.669	
817	4123.29	6.83	8.10	14.7	5.61	6.73	14.2	2.699	

CORE LABORATORIES

Company: British Gas International
Well: Vorwata #10

File: JCA-98045

**CORE ANALYSIS RESULTS
(HYDROSTATIC CONFINEMENT)**

Sample number	Depth (M.)	Confining Pressure 800psi.		Porosity (%)	Confining Pressure 3300psi.		Porosity (%)	Grain Density (gm/cc)	REMARKS
		KI (md)	Permeability Kair (md)		KI (md)	Permeability Kair (md)			
818	4123.60	61.4	64.3	17.0	58.6	61.4	16.5	2.667	
819	4123.94	113	118	16.6	108	113	16.2	2.661	
820	4124.20	168	171	16.9	161	165	16.4	2.662	
821	4124.53	728	888	17.4	610	717	16.8	2.652	
822	4124.81	364	392	16.6	331	355	16.2	2.653	
823	4125.10	481	526	15.6	446	482	15.1	2.656	
824	4125.38	229	237	14.7	219	226	14.2	2.654	
825	4125.71	218	222	14.8	207	210	14.4	2.653	
826	4126.03	115	122	14.5	101	108	14.0	2.660	
827	4126.30	597	608	15.6	568	579	14.9	2.654	
828	4126.69	361	395	13.8	276	320	13.3	2.653	
829	4126.95	52.4	61.0	13.8	38.9	46.5	13.4	2.651	
830	4127.30	519	530	15.0	505	516	14.7	2.652	
831	4127.62	190	200	14.2	179	189	13.8	2.650	
832	4127.78	192	195	14.5	182	185	14.0	2.651	
833	4128.10	470	471	15.6	451	452	15.1	2.650	
834	4128.40	381	383	15.2	367	368	14.8	2.652	
835	4128.75	165	171	14.1	156	162	13.7	2.650	

APPENDIX 4

CORE PLUG/CHIP ATLAS SUMMARY OF ANALYSES RESULTS FOR WIRIAGAR DEEP AND VORWATA CORE (2002-2003)

**CORE PLUGS/CHIPS OBTAINED 2002 AND ANALYSES PERFORMED 2003
BY THE AUTHOR UNLESS OTHERWISE NOTED**

**Whole Core
Digital
Photographs**

(Photography by
J. Salo)

**Core Plug/Chip
Digital
Photographs**

(Photography by
J. Salo)

**Petrographic
Photomicrograph
Images**

(Petrography by
S.E.Phillips)

Bulk XRD

(XRD analysis by
J. Salo)

**MICP Pressure
Plots**

(MICP interpretation
by J.Salo)

**SEM
Photomicrograph
Images**

(SEM preparation,
analysis, and images
by J.Salo, Figure 55C
by J. Salo and P. Uwins)

SEM EDX

(SEM EDX analysis and
interpretation by J.Salo,
Figure 55C by J. Salo
and P. Uwins)

**He Porosity and
Air Permeability
Data**

(Poro-perm analysis
by Amdel or Core
Laboratories)

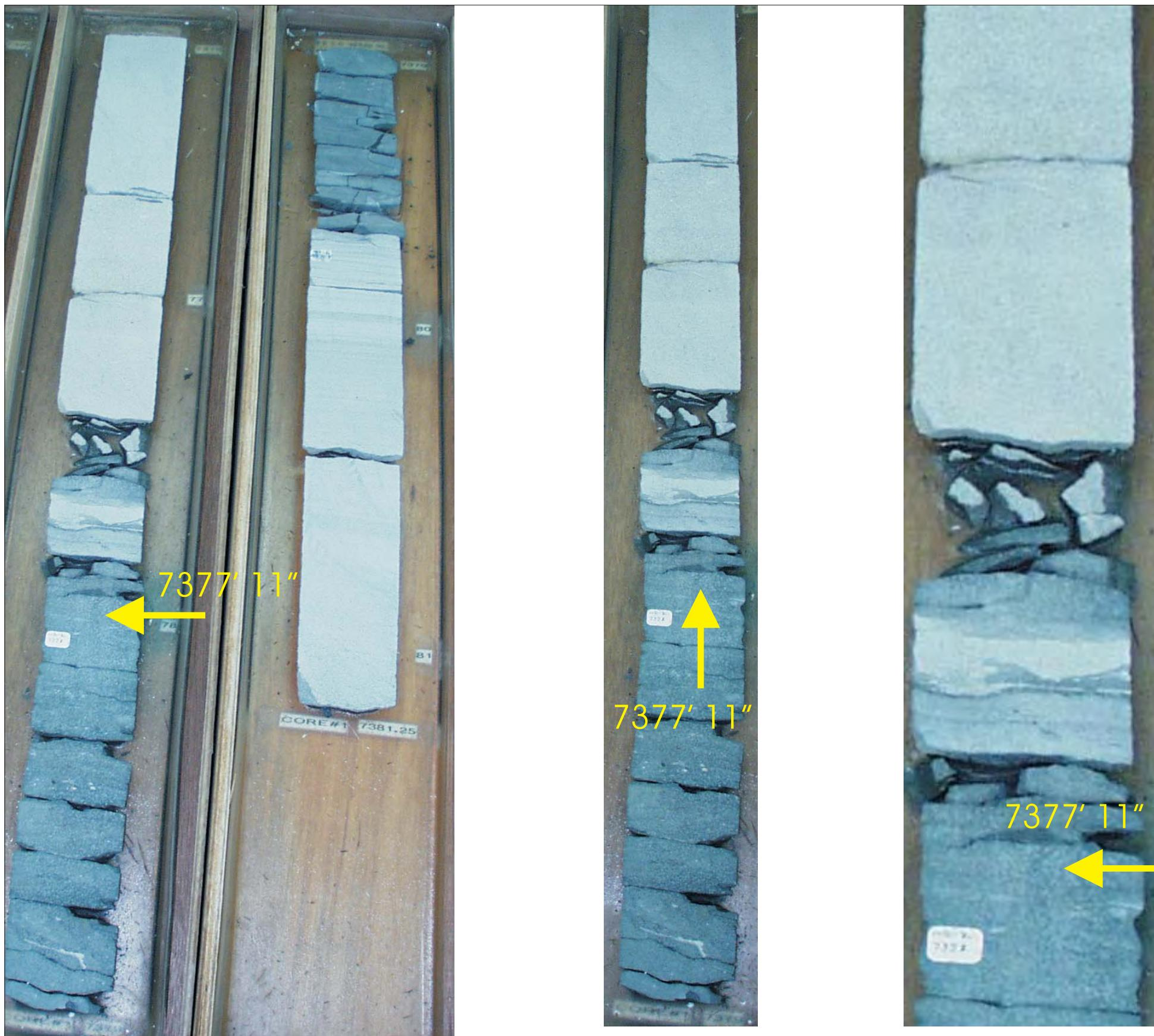
Core Plug/Chip Atlas Guide

(Some or all of the analyses listed in this guide were carried out on
the whole core plugs/chips presented in this "Core Plug/Chip Atlas").

Figure Number 1

Core Plug Atlas Guide

**Core Plug/Chip
Sample and Analyses
Information Legend**

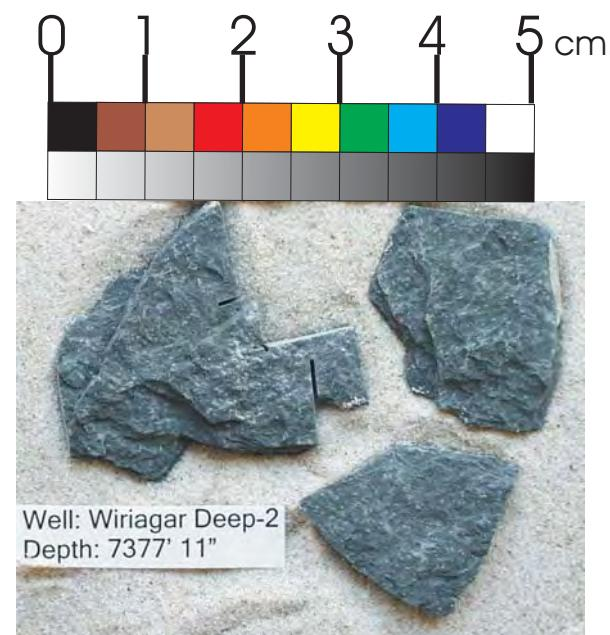
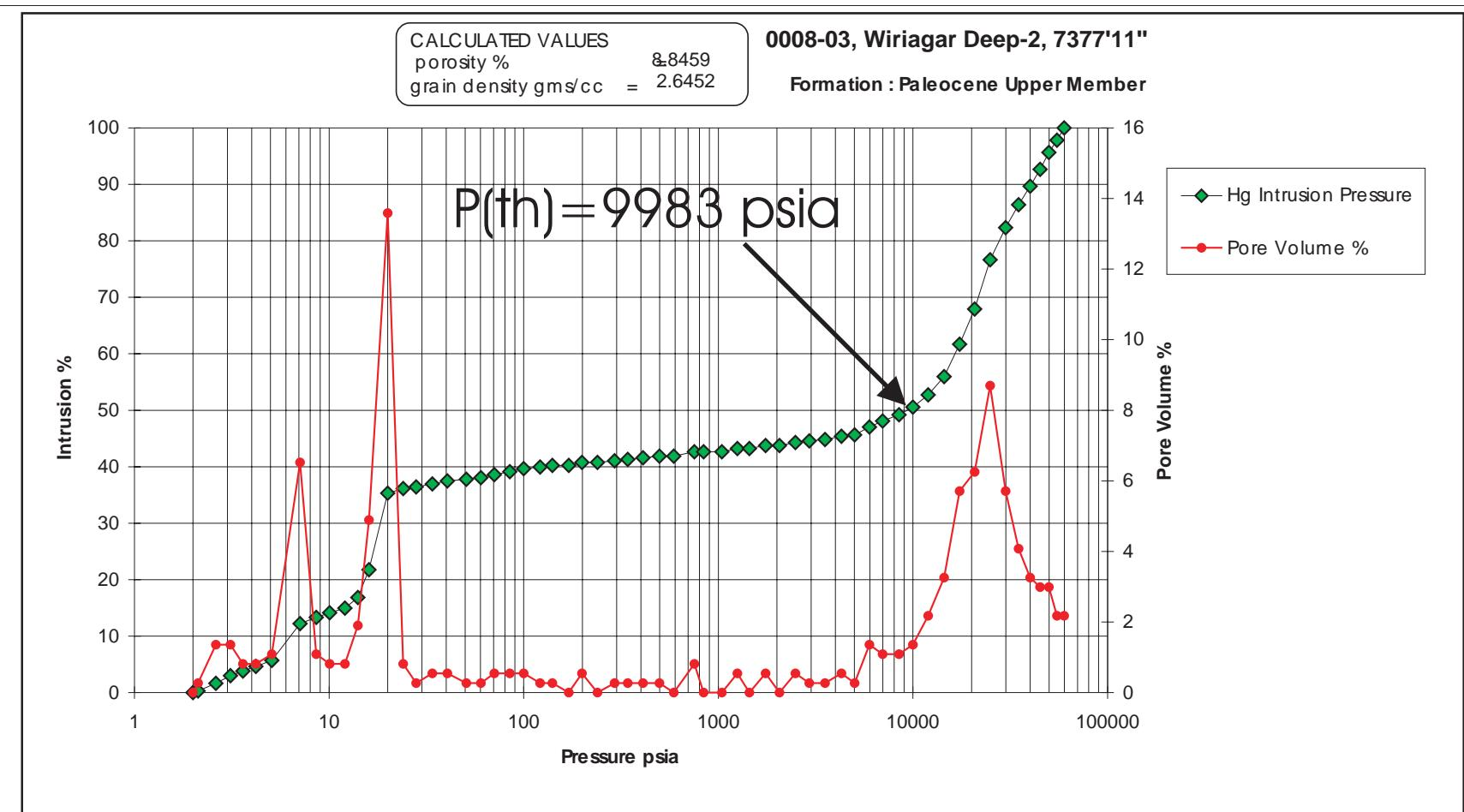


WHOLE CORE PLUG ANALYSES
WELL: WIRIAGAR DEEP - 2
DEPTH: 7377' 11"

PLATE A:

Digital Whole Core Photographs

Figure 2A: Core Plug/Chip Atlas for sample 7377' 11" from Wiriagar Deep-2.



Sample Depth: 7377' 11"
Shifted Depth: 7395' 11"
MICP Entry Pressure: 752 psia
MICP Threshold Pressure: 9983 psia
Lithology: Shale

WHOLE CORE PLUG ANALYSES
WELL: WIRIAGAR DEEP - 2
DEPTH: 7377' 11"

PLATE B:
Digital Whole Core Photographs
Digital Core Chip/Plug Photograph
Mercury Injection Capillary Pressure

Figure 2B: Core Plug/Chip Atlas for sample 7377' 11" from Wiriagar Deep-2.

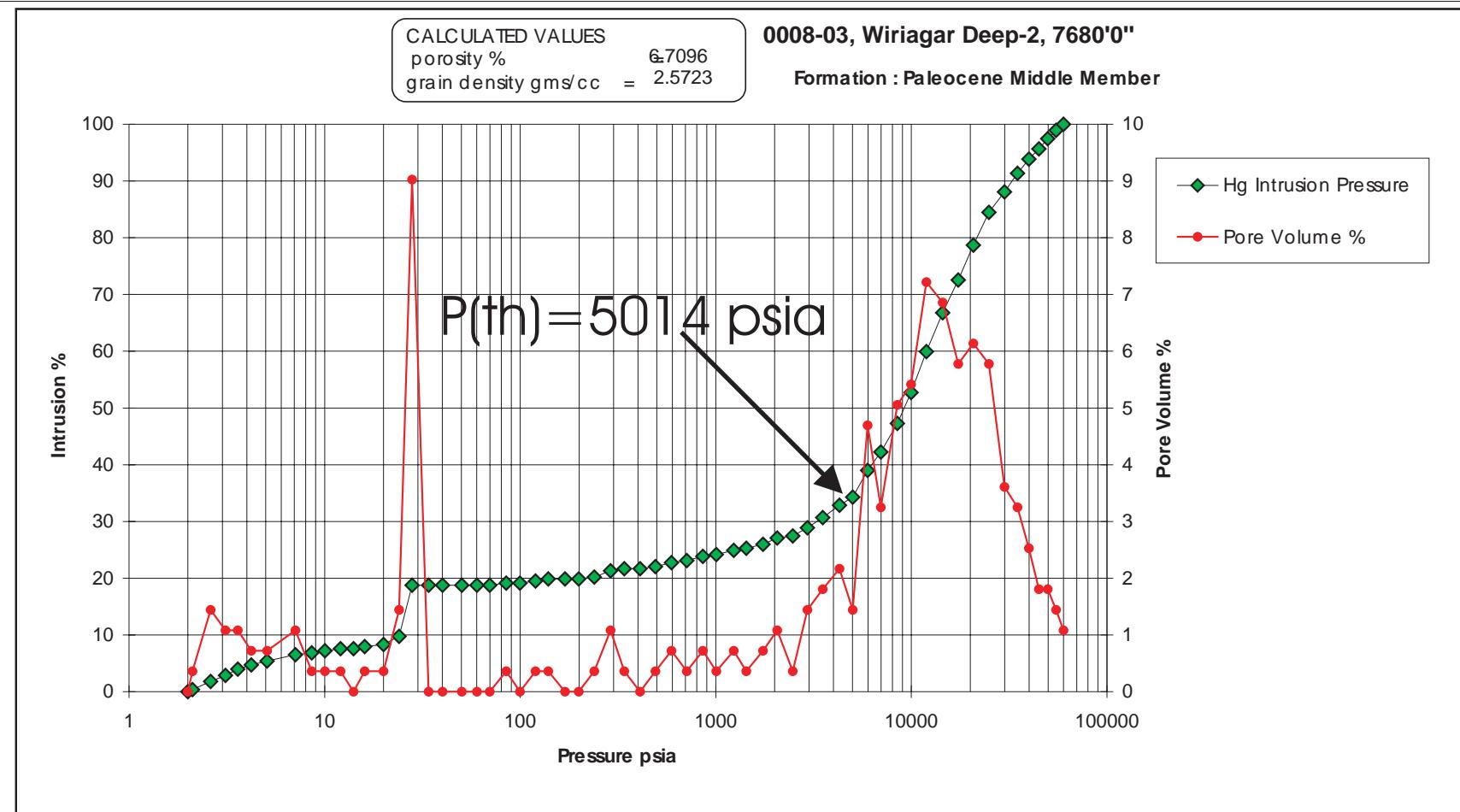
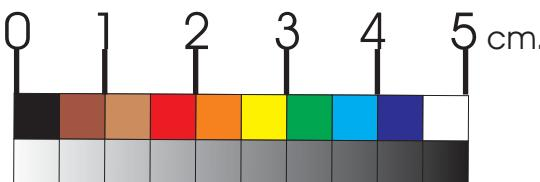


Figure 3A: Core Plug/Chip Atlas for sample 7380' 0" from Wiriagar Deep-2.

WHOLE CORE PLUG ANALYSES
WELL: WIRIAGAR DEEP - 2
DEPTH: 7380' 0"

PLATE A:

Digital Whole Core Photographs

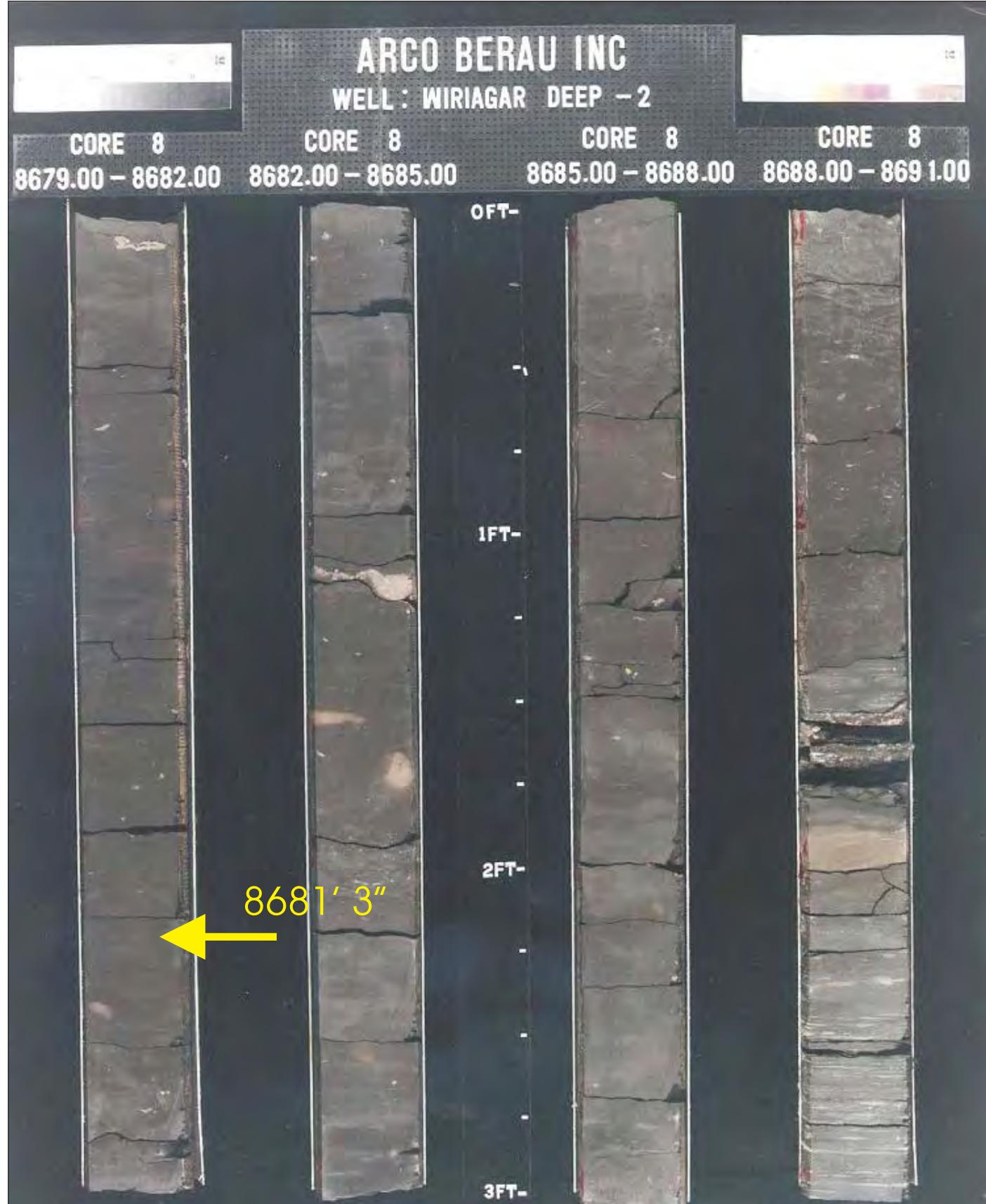


Sample Depth: 7380' 0"
Shifted Depth: 7398' 0"
MICP Entry Pressure: 239 psia
MICP Threshold Pressure: 5014 psia
Lithology: Shale

WHOLE CORE PLUG ANALYSES
WELL: WIRIAGAR DEEP - 2
DEPTH: 7380' 0"

PLATE B
Digital Whole Core Photographs
Digital Core Chip/Plug Photograph
Mercury Injection Capillary Pressure

Figure 3B: Core Plug/Chip Atlas for sample 7380' 0" from Wiriagar Deep-2.



WHOLE CORE PLUG ANALYSES

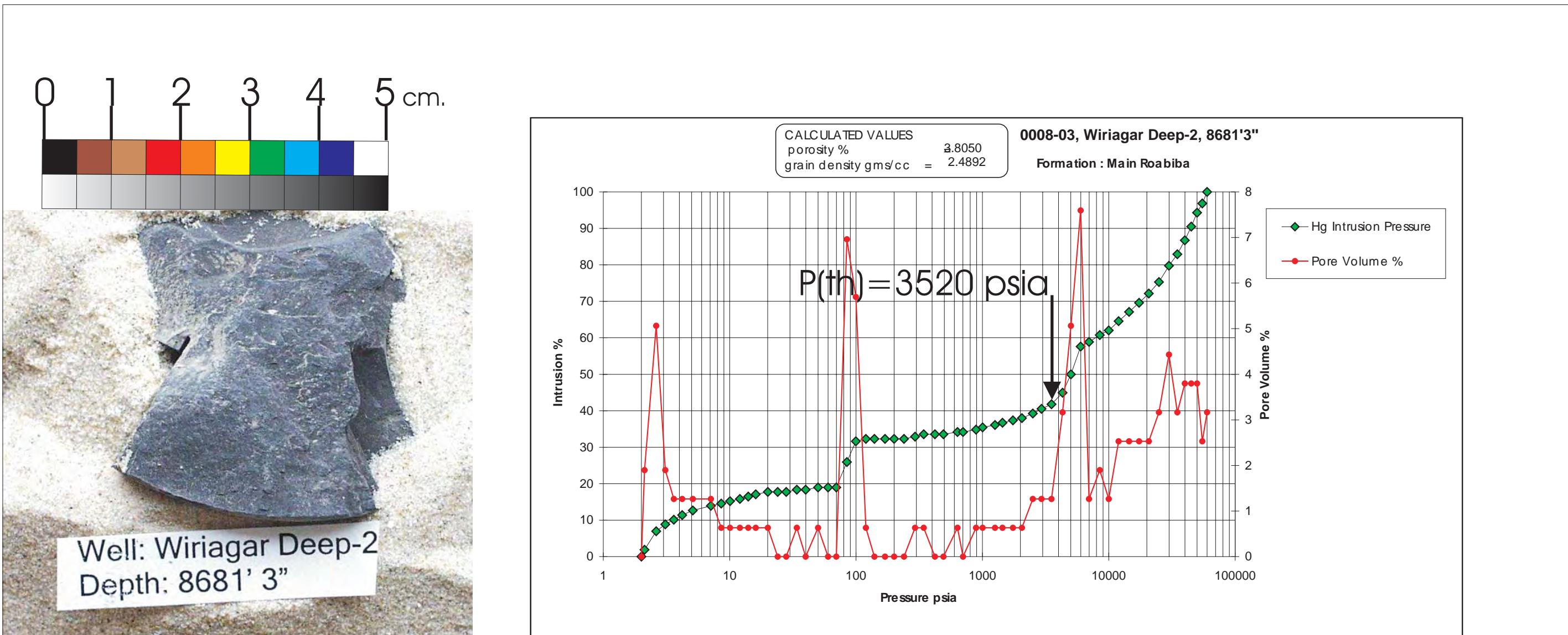
WELL: WIRIAGAR DEEP - 2

DEPTH: 8681' 3"

PLATE A:

Digital Whole Core Photographs

Figure 4A: Core Plug/Chip Atlas for sample 8681' 3" from Wiriagar Deep-2.



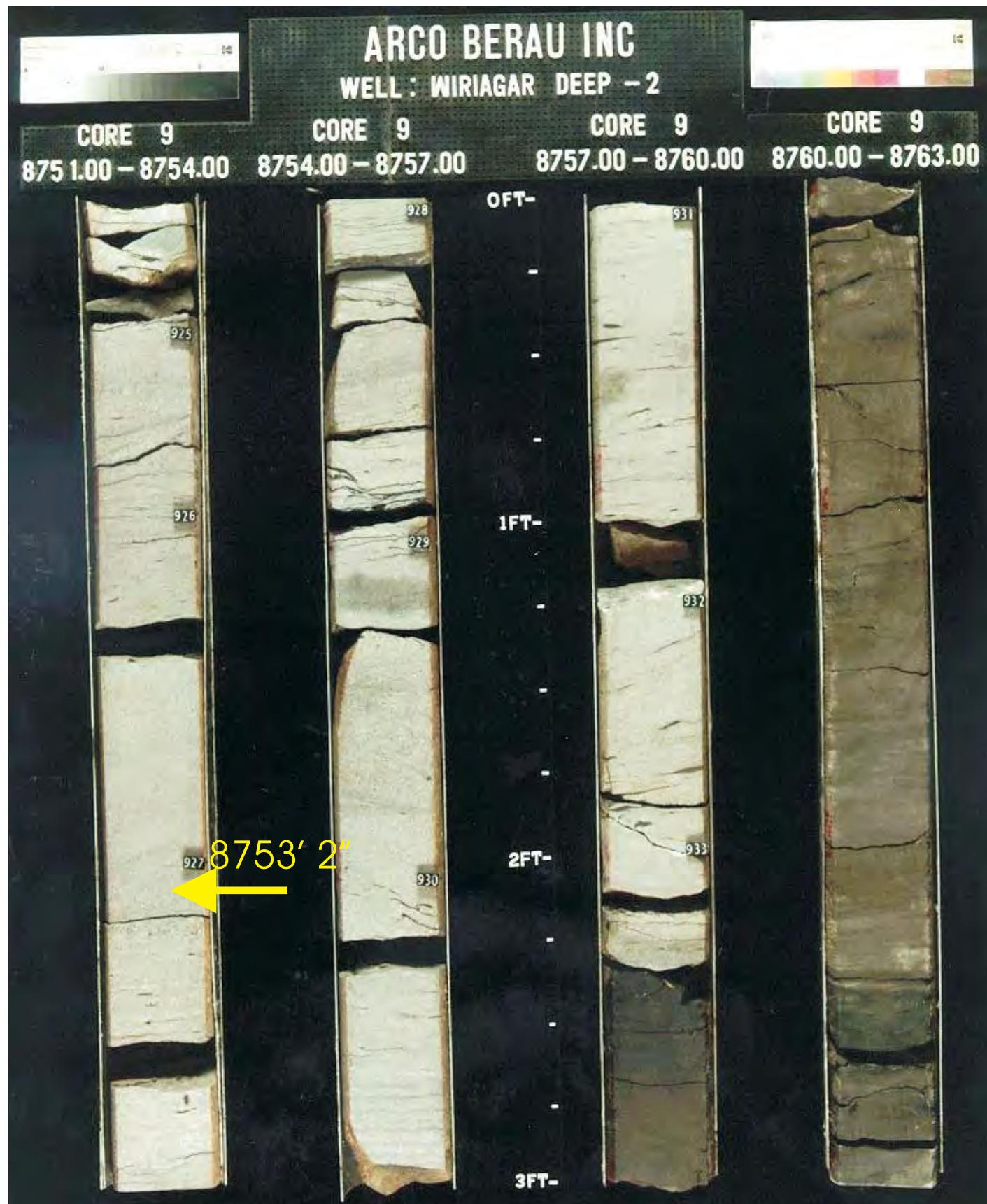
Sample Depth: 8681' 3"
 Shifted Depth: 8699' 3"
 MICP Entry Pressure: 889 psia
 MICP Threshold Pressure: 3520 psia
 Lithology: Shale

WHOLE CORE PLUG ANALYSES
 WELL: WIRIAGAR DEEP - 2
 DEPTH: 8681' 3"

PLATE B:

Digital Core Chip/Plug Photograph
 Mercury Injection Capillary Pressure

Figure 4B: Core Plug/Chip Atlas for sample 8681' 3" from Wiriagar Deep-2.



Sample Depth: 8753' 2"
Shifted Depth: 8771' 2"
He-Ø: 14.8%
k air: 529 mD (NOB 800 psia)

WHOLE CORE PLUG ANALYSES
WELL: WIRIAGAR DEEP - 2
DEPTH: 8753' 2"

PLATE A:

Digital Whole Core Photographs
Digital Core Chip/Plug Photograph

Figure 5: Core Plug/Chip Atlas for sample 8753' 2" from Wiriagar Deep-2.

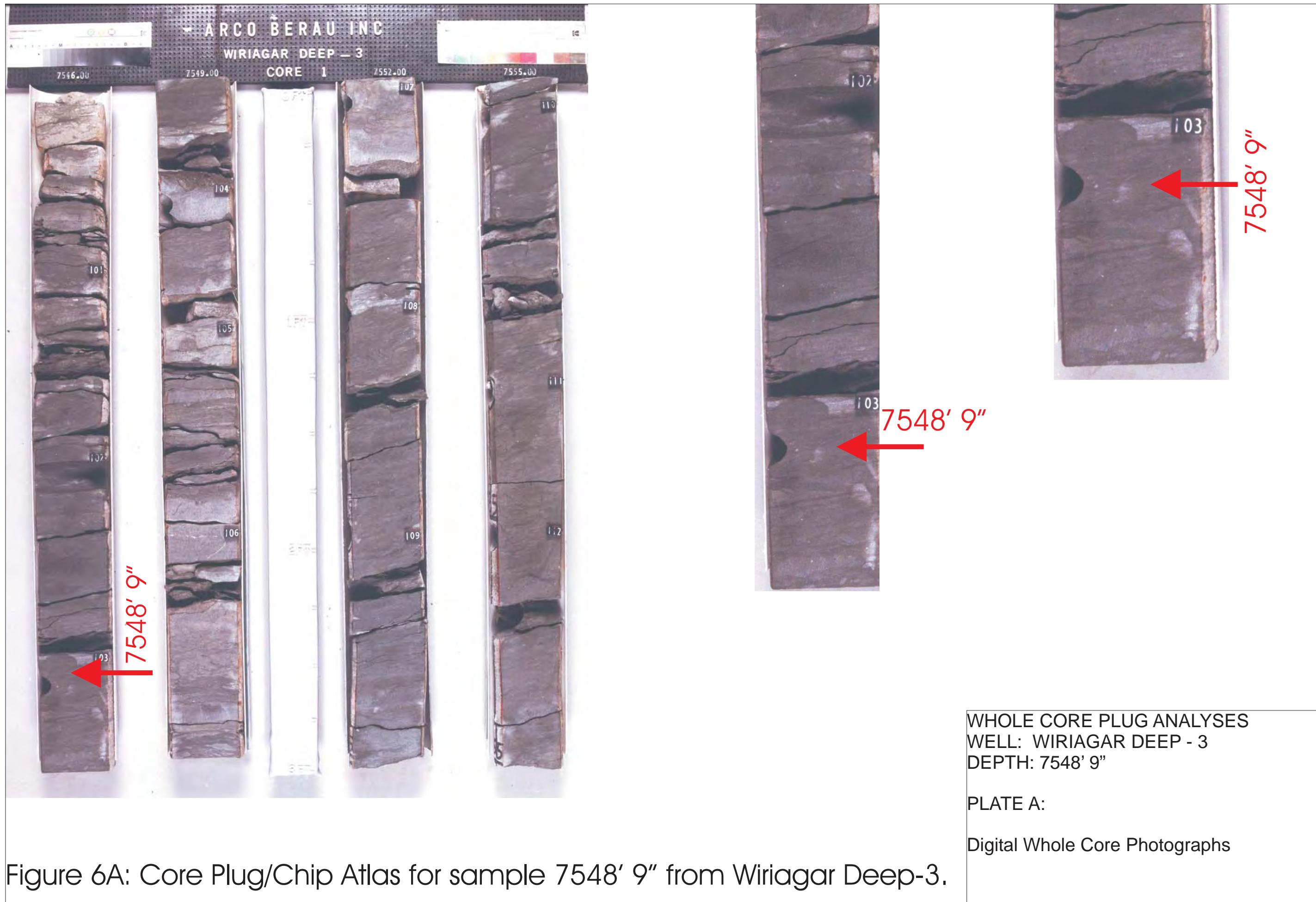
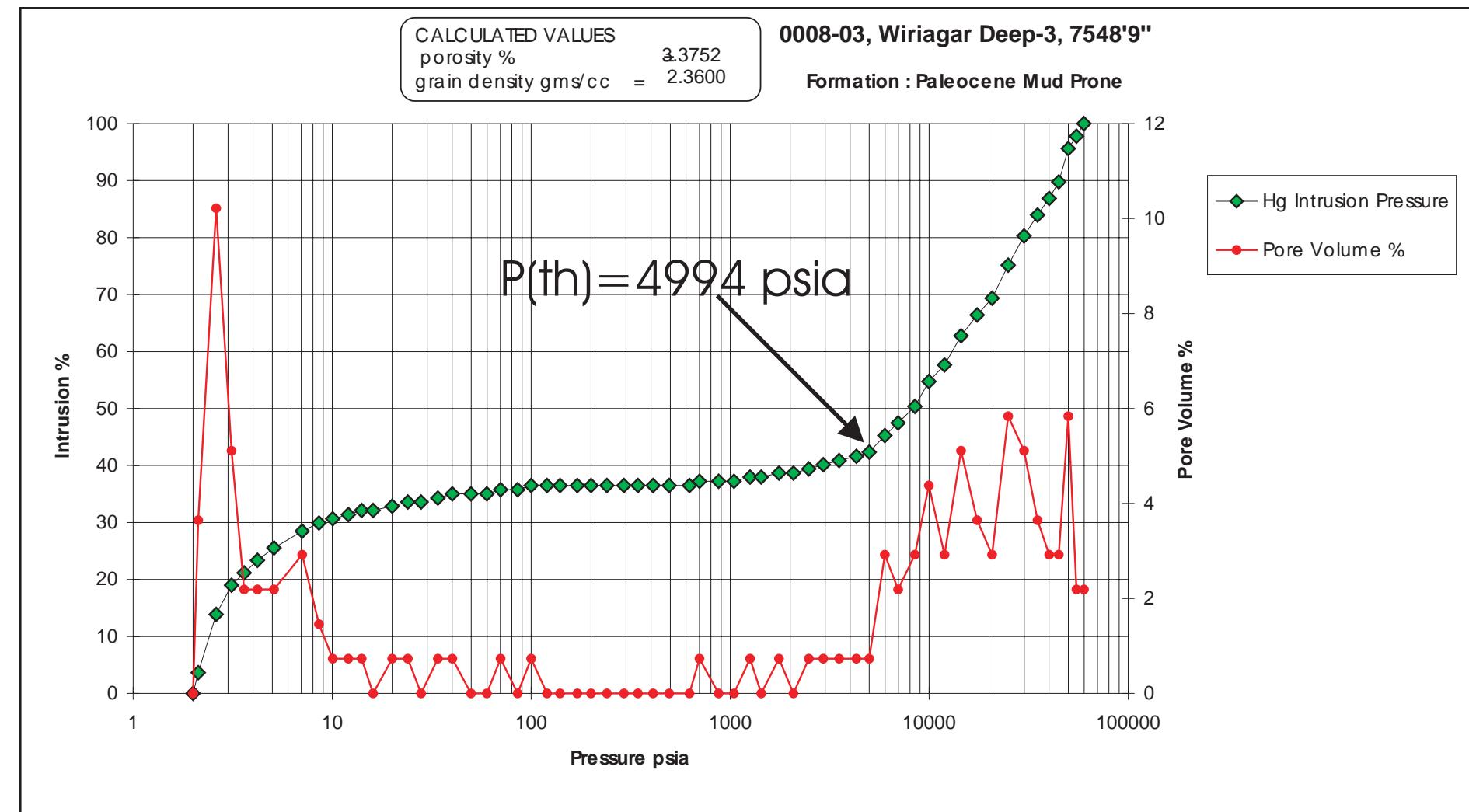


Figure 6A: Core Plug/Chip Atlas for sample 7548' 9" from Wiriagar Deep-3.



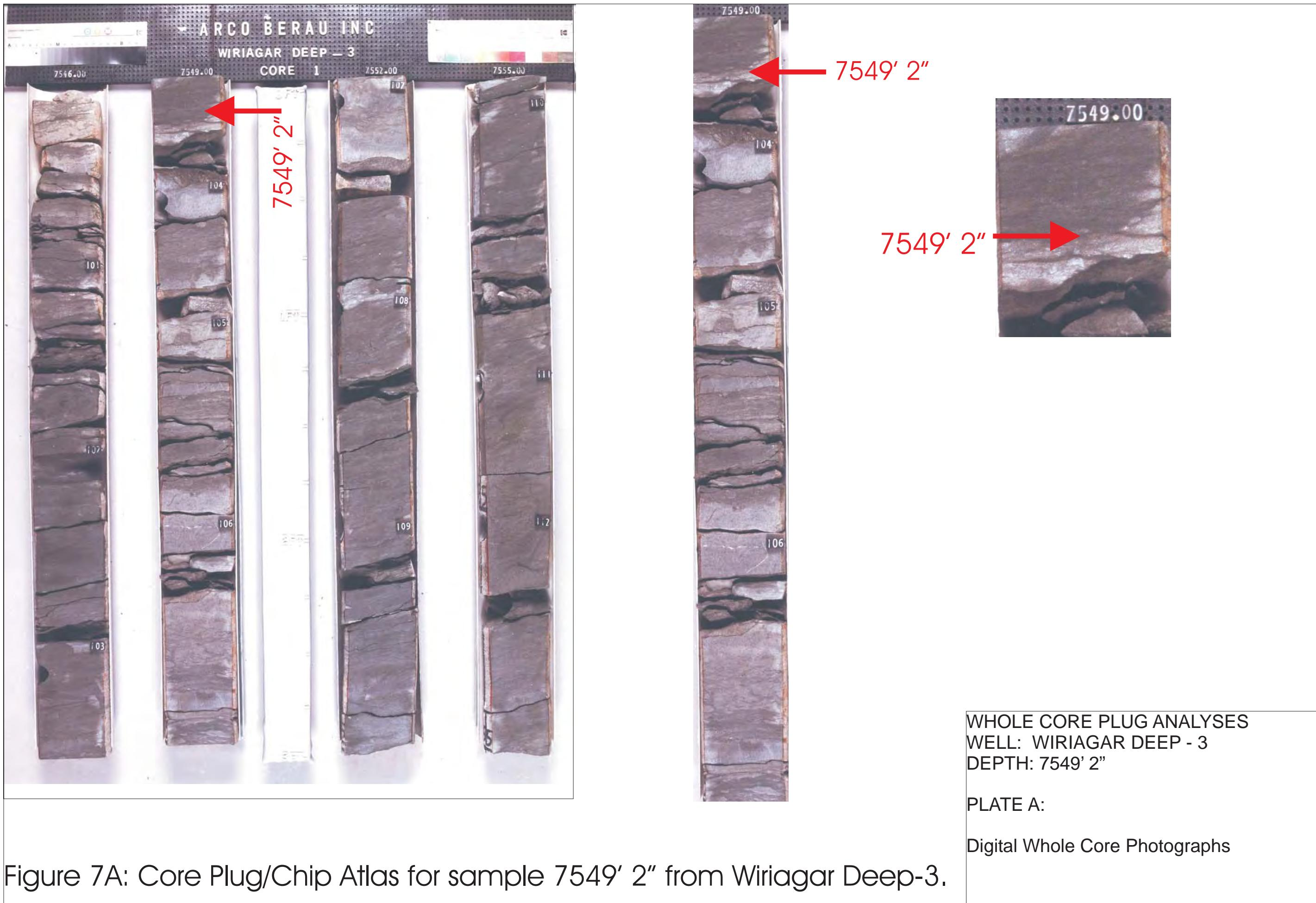
Sample Depth: 7548' 9"
 Shifted Depth: 7556' 9"
 MICP Entry Pressure: 701 psia
 MICP Threshold Pressure: 4994 psia
 Lithology: Shale

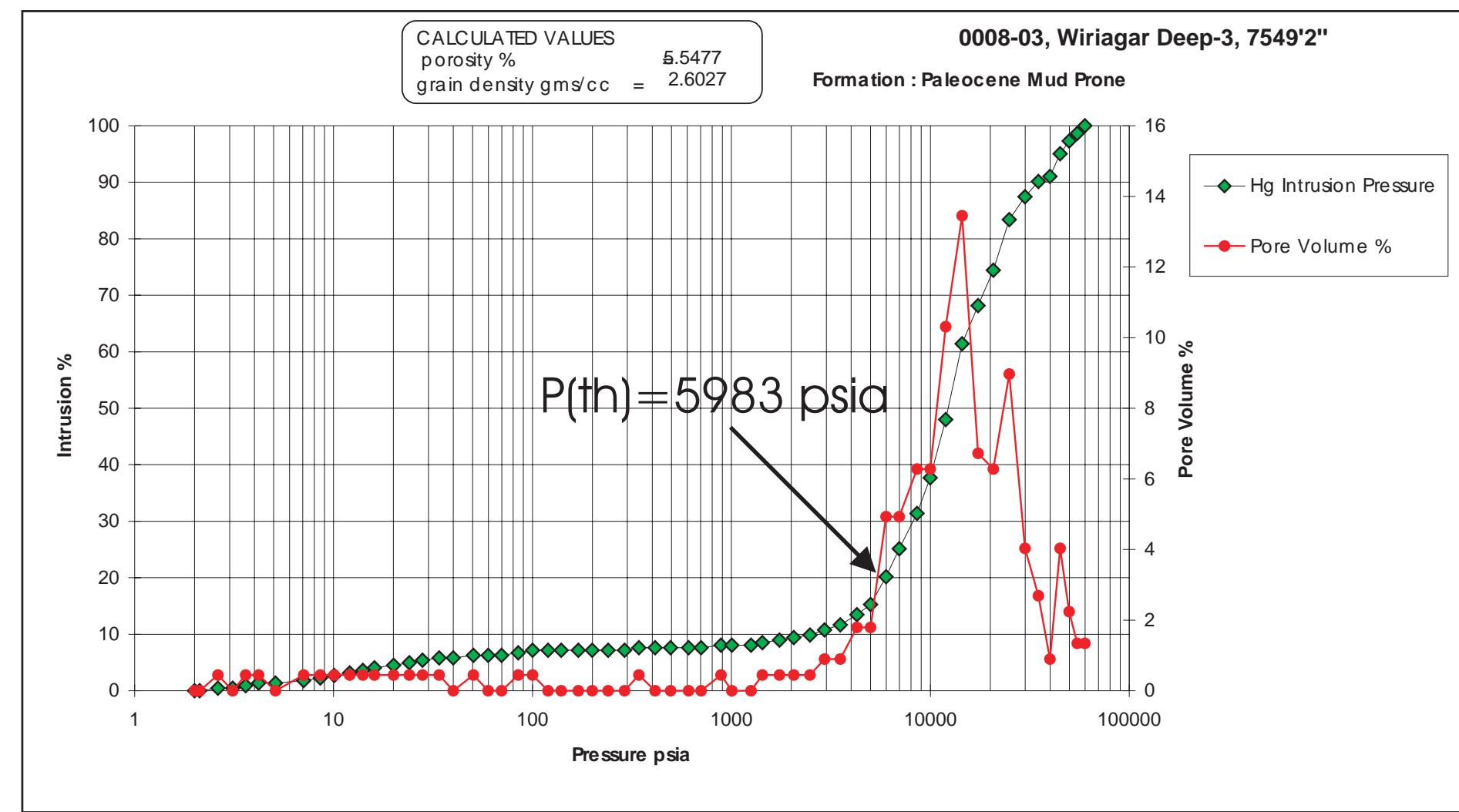
WHOLE CORE PLUG ANALYSES
 WELL: WIRIAGAR DEEP - 3
 DEPTH: 7548' 9"

PLATE B:

Digital Core Chip/Plug Photograph
 Mercury Injection Capillary Pressure

Figure 6B: Core Plug/Chip Atlas for sample 7548' 9" from Wiriagar Deep-3.





Sample Depth: 7549' 2"
 Shifted Depth: 7557' 2"
 MICP Entry Pressure: 342 psia
 MICP Threshold Pressure: 5983 psia
 Lithology: Shale

WHOLE CORE PLUG ANALYSES
 WELL: WIRIAGAR DEEP - 3
 DEPTH: 7549' 2"

PLATE B:

Digital Core Chip/Plug Photograph
 Mercury Injection Capillary Pressure

Figure 7B: Core Plug/Chip Atlas for sample 7549' 2" from Wiriagar Deep-3.

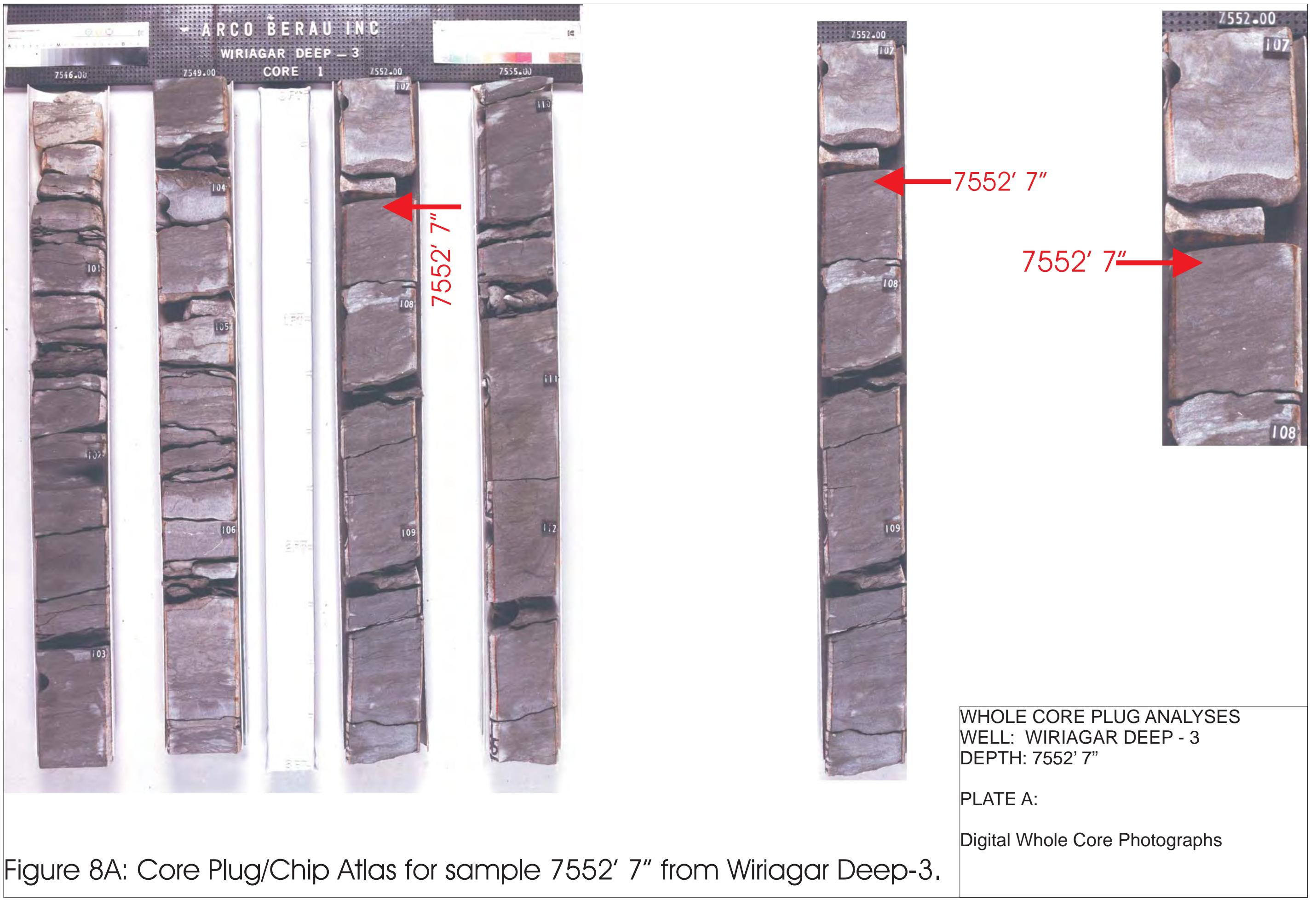
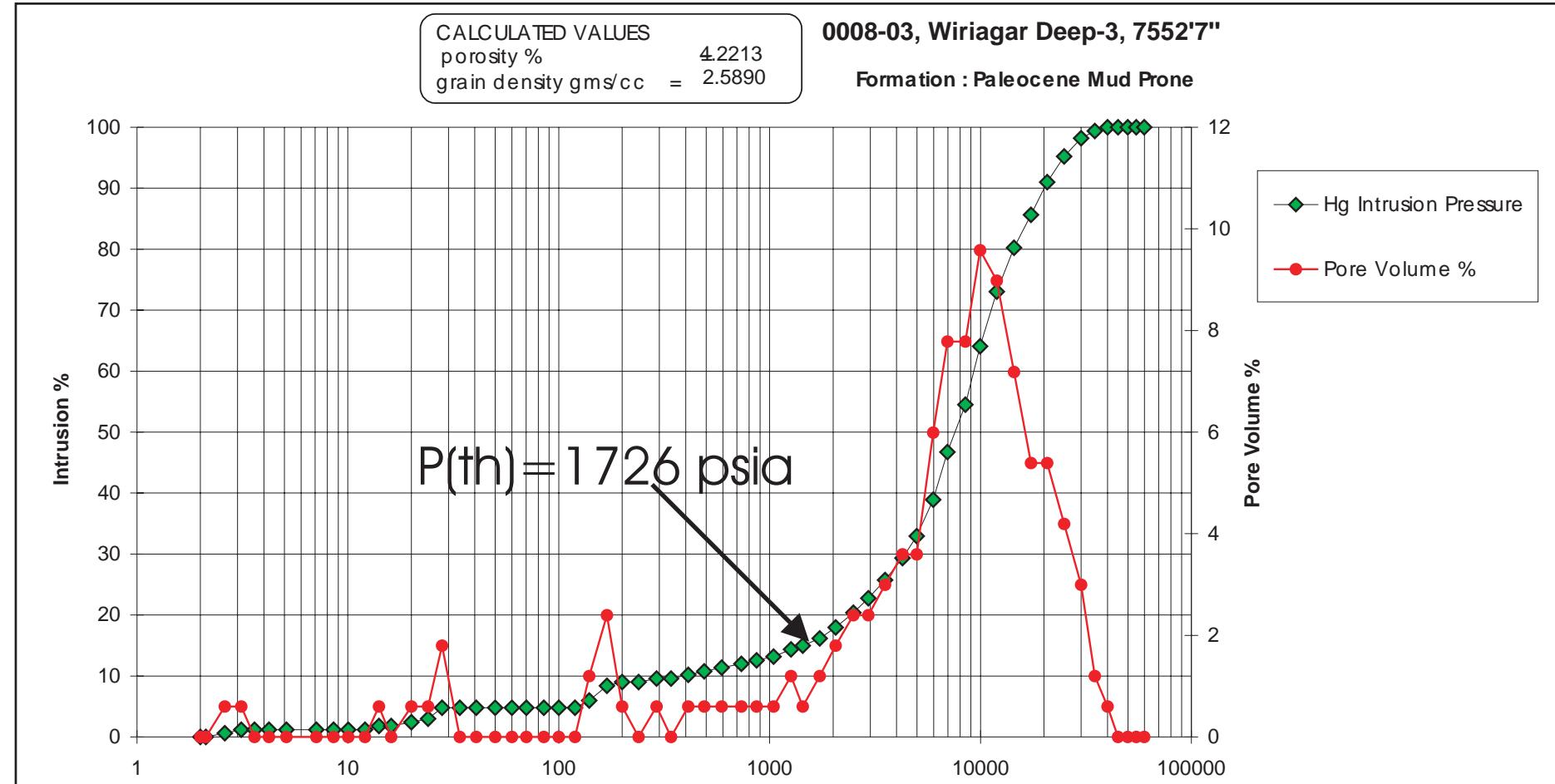


Figure 8A: Core Plug/Chip Atlas for sample 7552' 7" from Wiriagar Deep-3.



Sample Depth: 7552' 7"
 Shifted Depth: 7560' 7"
 MICP Entry Pressure: 170 psia
 MICP Threshold Pressure: 1726 psia
 Lithology: Shale

WHOLE CORE PLUG ANALYSES
 WELL: WIRIAGAR DEEP - 3
 DEPTH: 7552' 7"

PLATE B:

Digital Core Chip/Plug Photograph
 MICP Graph

Figure 8B: Core Plug/Chip Atlas for sample 7552' 7" from Wiriagar Deep-3.

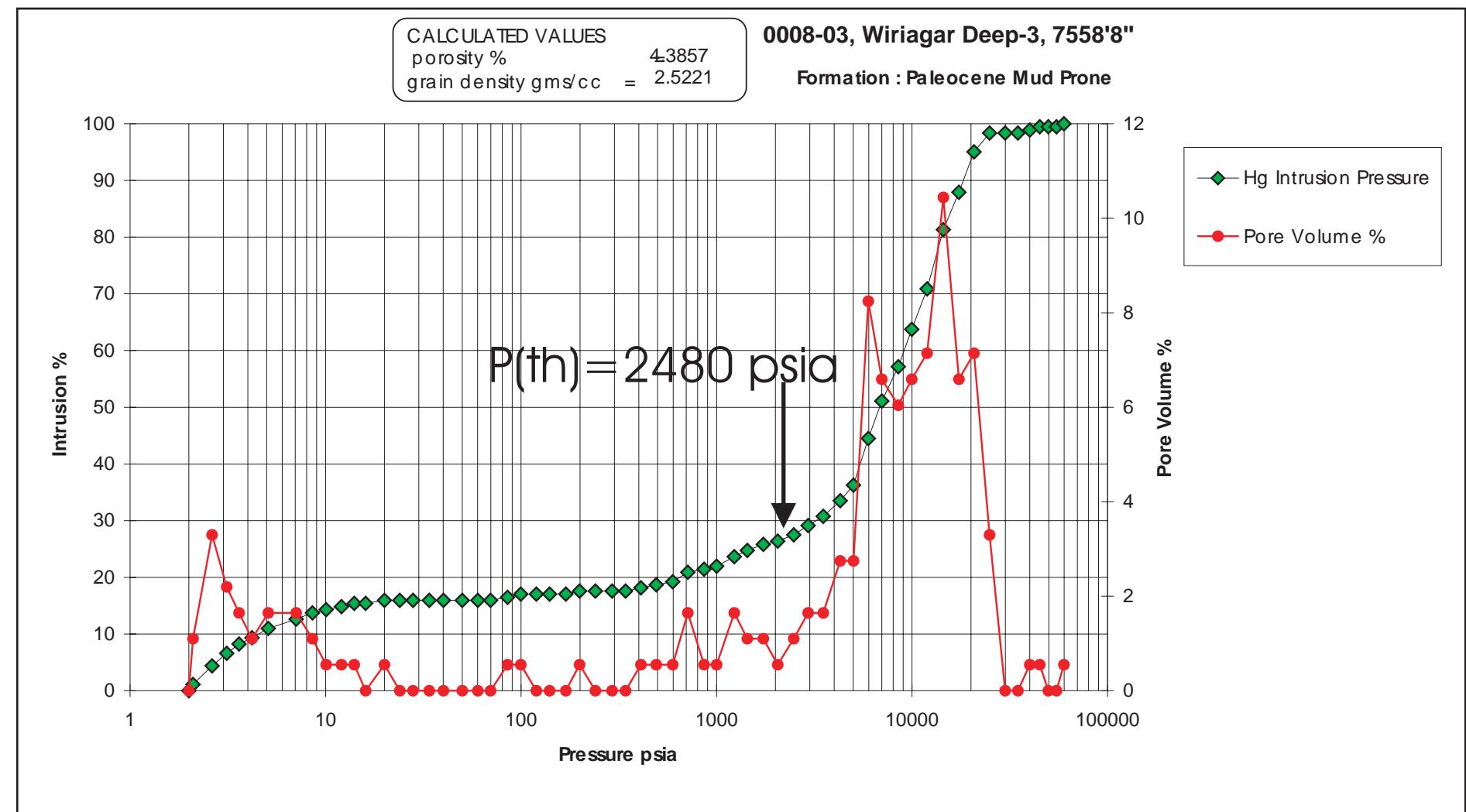


WHOLE CORE PLUG ANALYSES
WELL: WIRIAGAR DEEP - 3
DEPTH: 7558' 8"

PLATE A:

Digital Whole Core Photographs

Figure 9A: Core Plug/Chip Atlas for sample 7558' 8" from Wiriagar Deep-3.



Sample Depth: 7558' 8"
Shifted Depth: 7566' 8"
MICP Entry Pressure: 99 psia
MICP Threshold Pressure: 2480 psia
Lithology: Shale

WHOLE CORE PLUG ANALYSES
WELL: WIRIAGAR DEEP - 3
DEPTH: 7558' 8"

PLATE B:

Digital Core Chip/Plug Photograph
Mercury Injection Capillary Pressure

Figure 9B: Core Plug/Chip Atlas for sample 7558' 8" from Wiriagar Deep-3.



Well: Wiriagar Deep-3
Depth: 7956' 3"

Sample Depth: 7956' 3"
Shifted Depth: 7964' 3"
He-Ø: 12.3%
k air: 19.7 mD (NOB 800 psia)

WHOLE CORE PLUG ANALYSES
WELL: WIRIAGAR DEEP - 3
DEPTH: 7956' 3"

PLATE A
Digital Whole Core Photographs
Digital Core Chip/Plug Photograph

Figure 10: Core Plug/Chip Atlas for sample 7956' 3" from Wiriagar Deep-3.

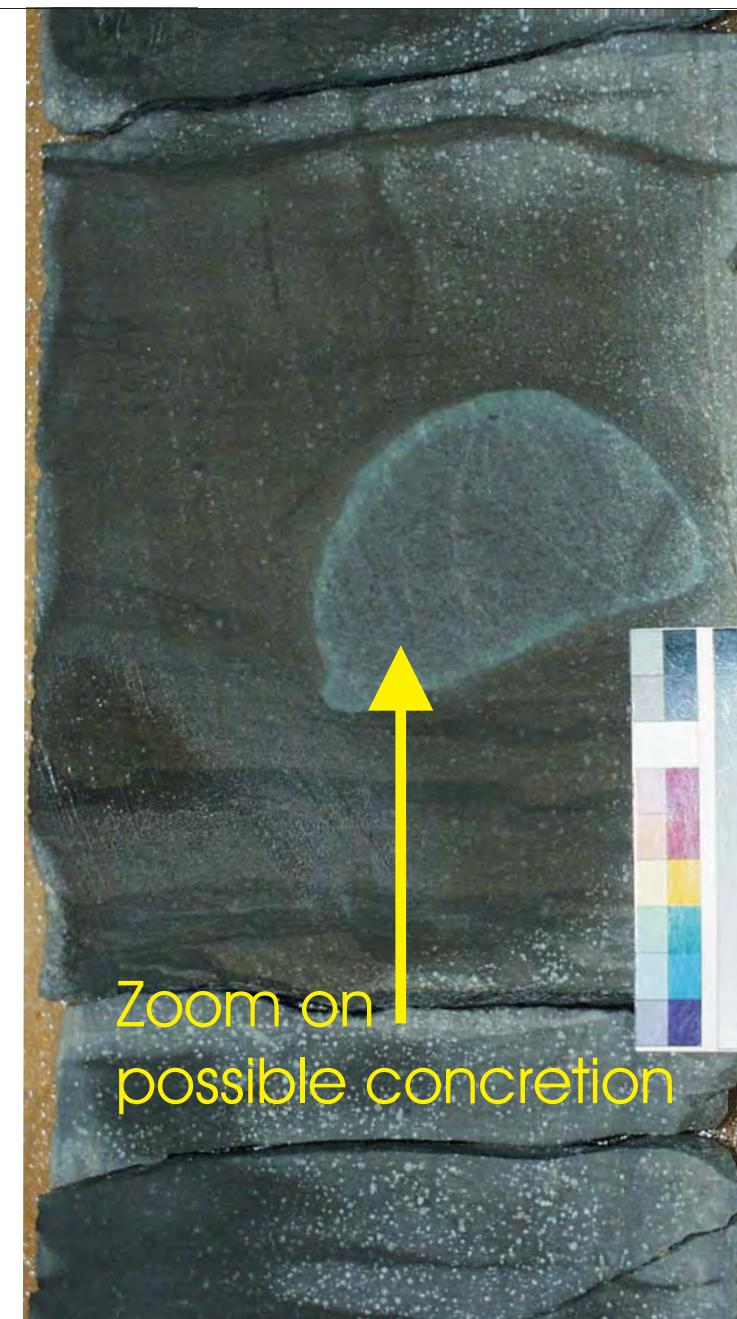
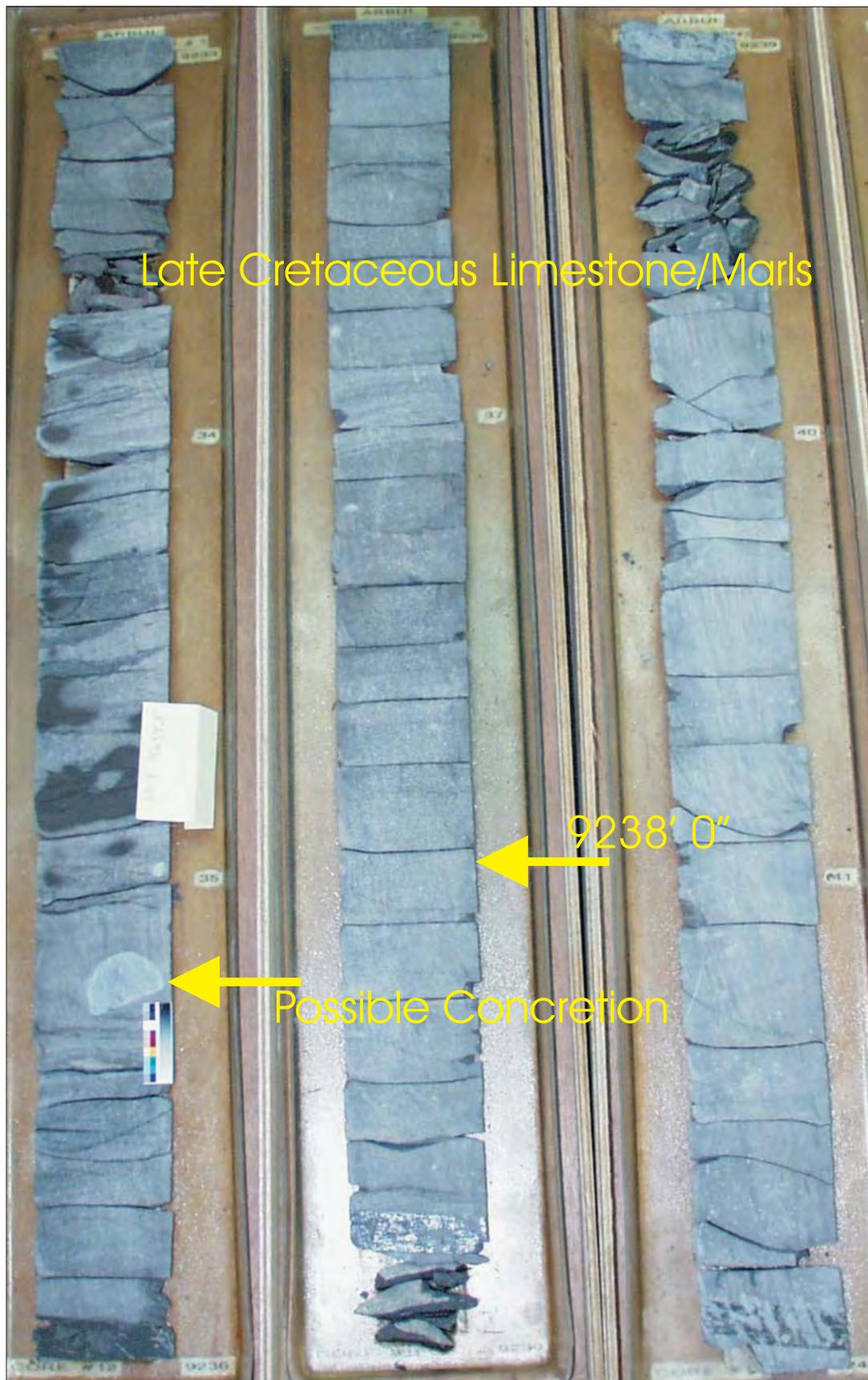
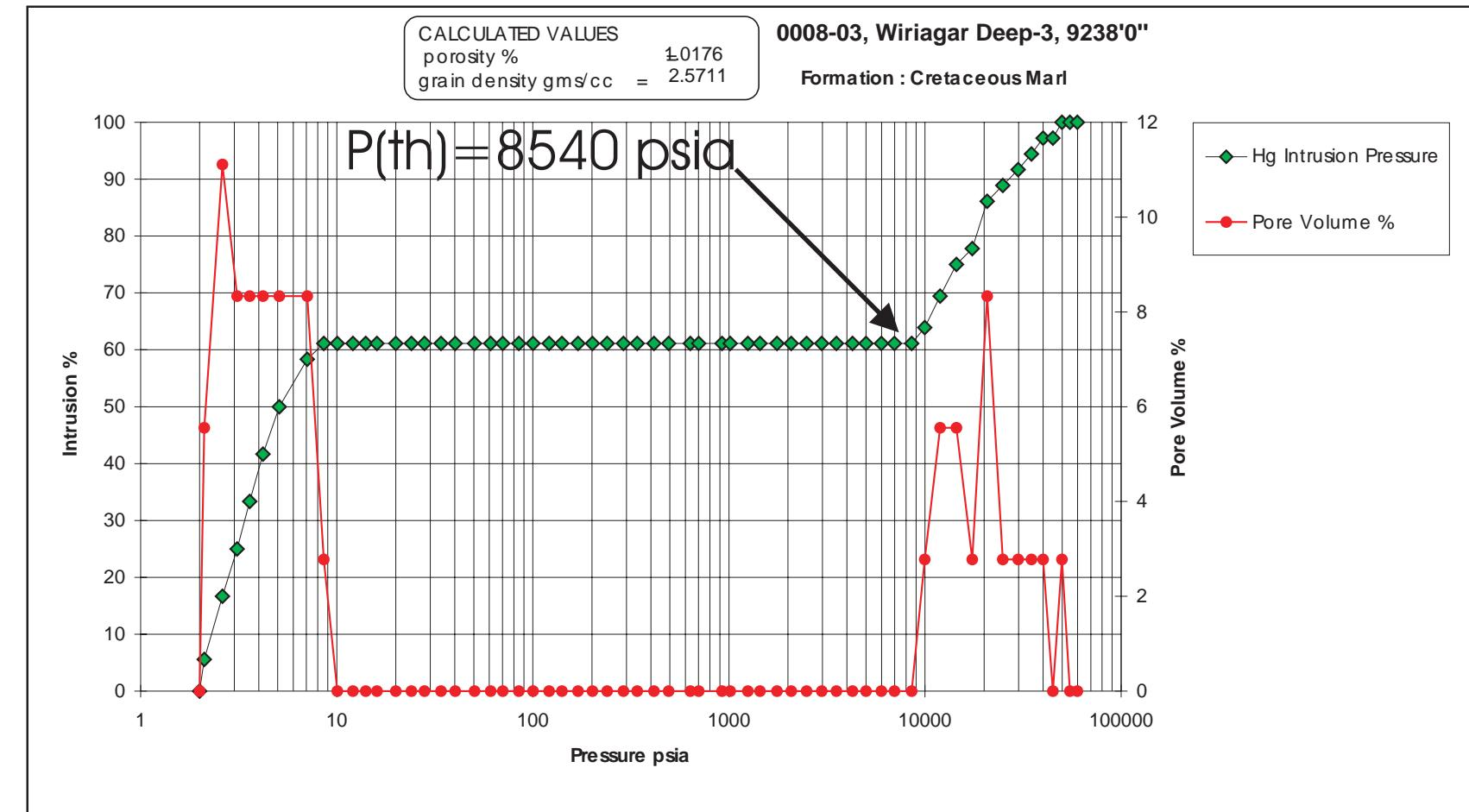
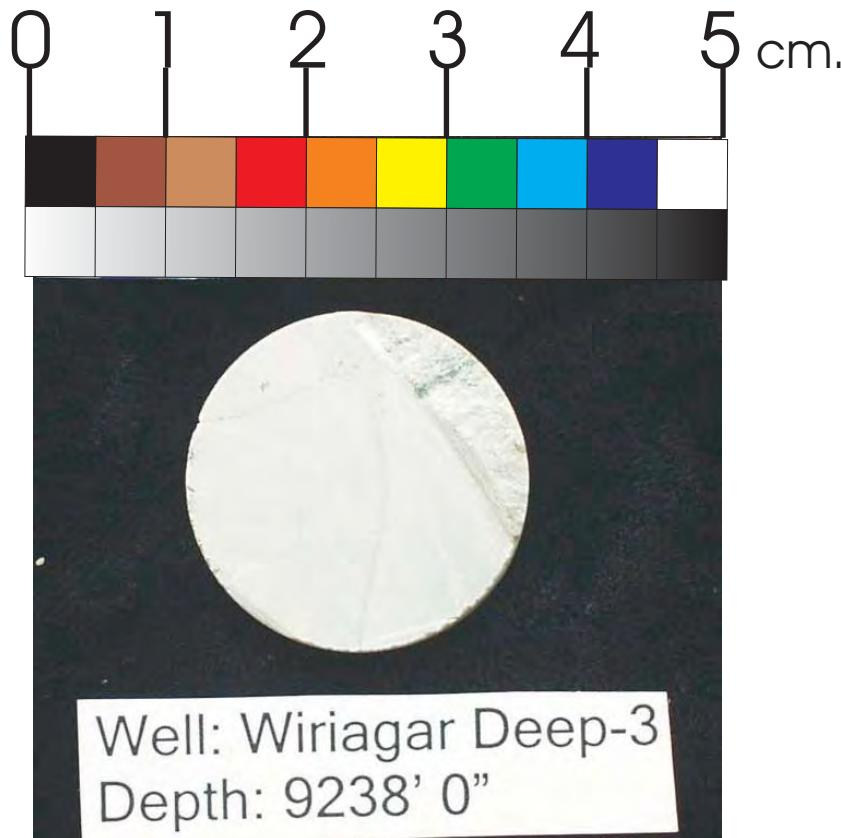


Figure 11A: Core Plug/Chip Atlas for sample 9238' 0" from Wiriagar Deep-3.

WHOLE CORE PLUG ANALYSES
WELL: WIRIAGAR DEEP - 3
DEPTH: 9238' 0"

PLATE A:

Digital Whole Core Photographs



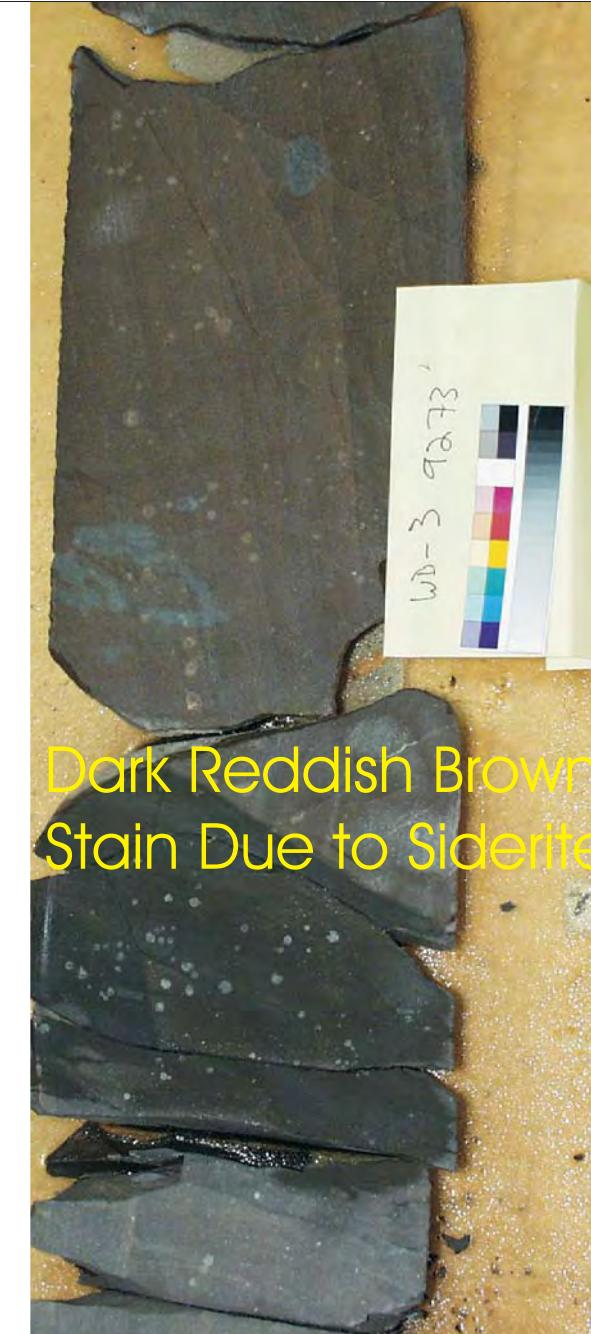
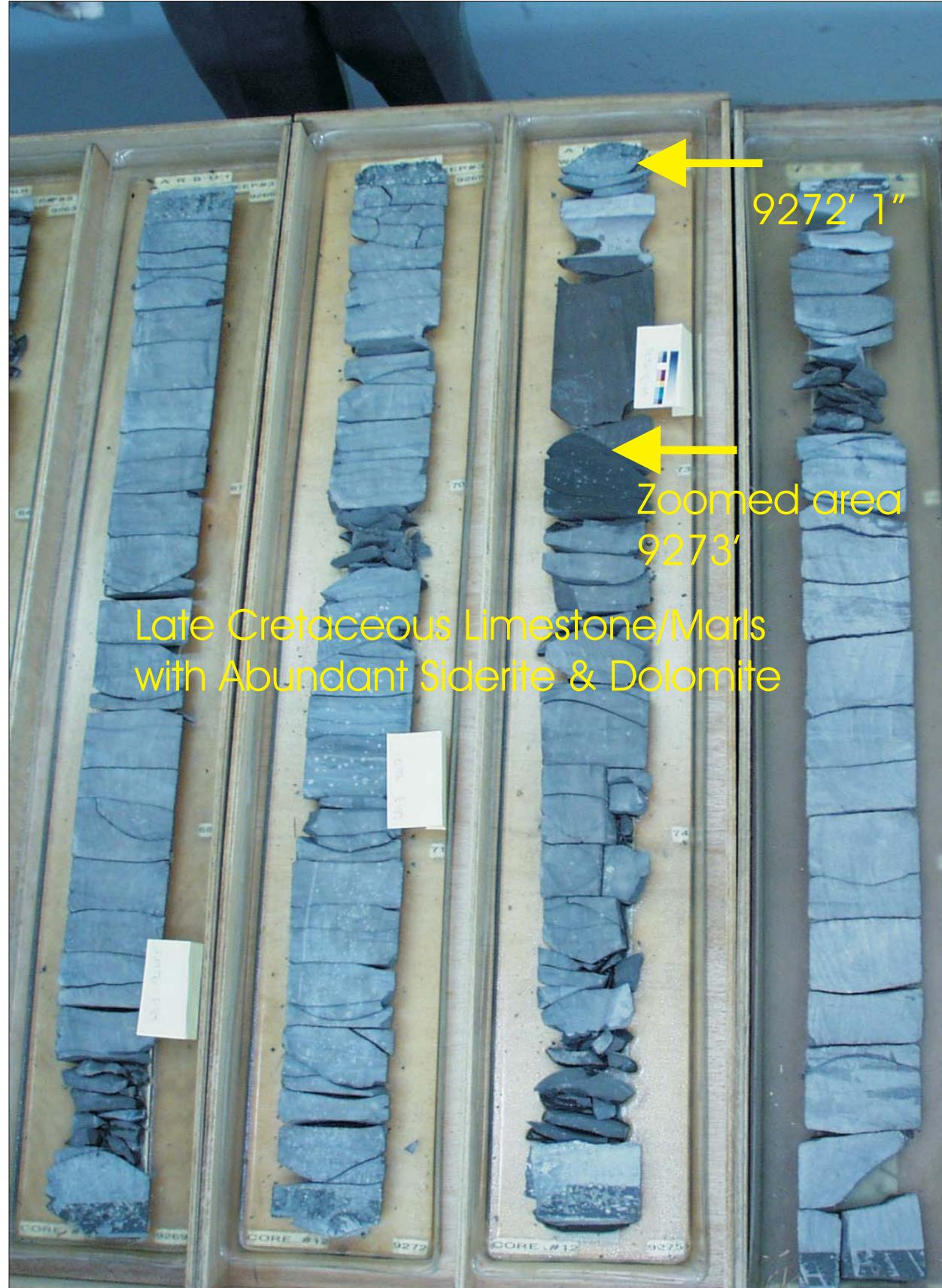
Sample Depth: 9238' 0"
Shifted Depth: 9248' 0"
MICP Entry Pressure: 8 psia
MICP Threshold Pressure: 8540 psia
Lithology: Limestone/Marl

WHOLE CORE PLUG ANALYSES
WELL: WIRIAGAR DEEP - 3
DEPTH: 9238' 0"

PLATE B:

Digital Core Chip/Plug Photograph
Mercury Injection Capillary Pressure

Figure 11B: Core Plug/Chip Atlas for sample 9238' 0" from Wiriagar Deep-3.

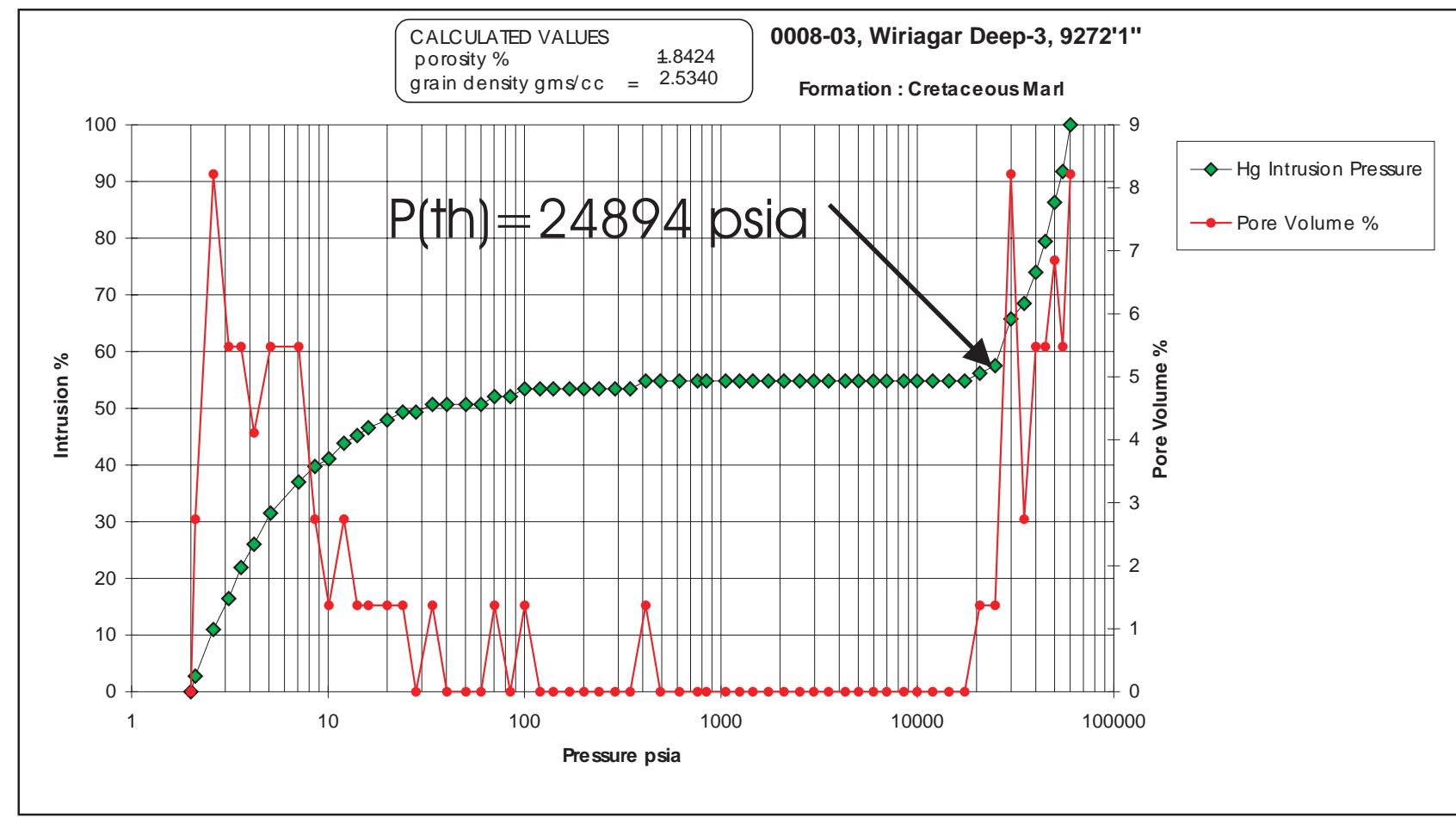
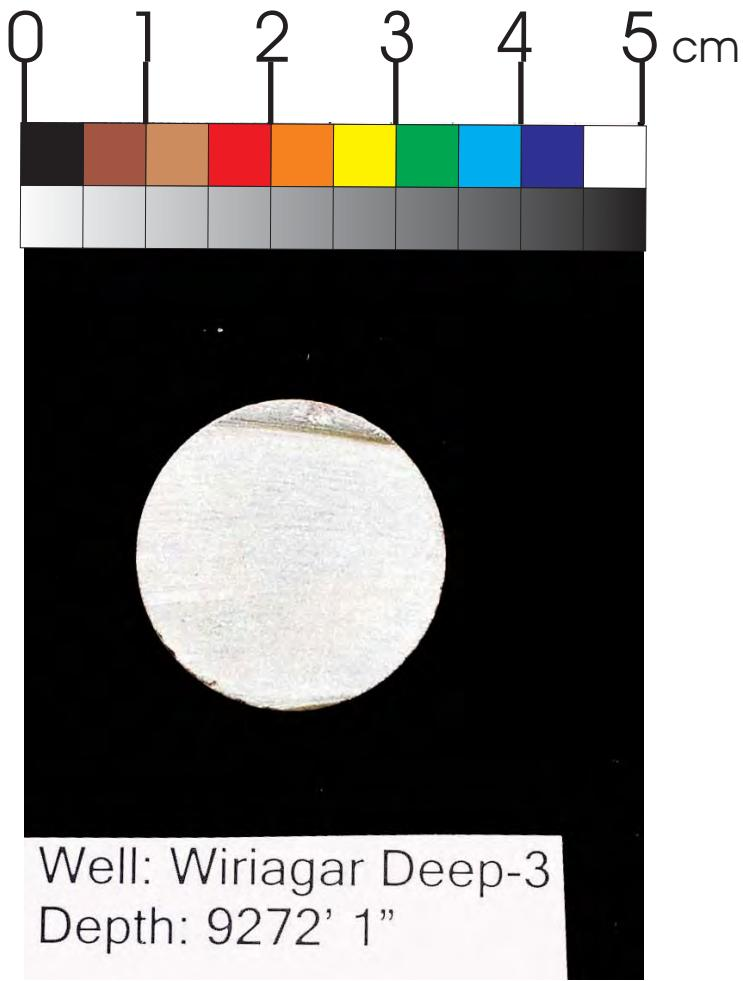


WHOLE CORE PLUG ANALYSES
WELL: WIRIAGAR DEEP - 3
DEPTH: 9272' 1"

PLATE A:

Digital Whole Core Photographs

Figure 12A: Core Plug/Chip Atlas for sample 9272' 1" from Wiriagar Deep-3.



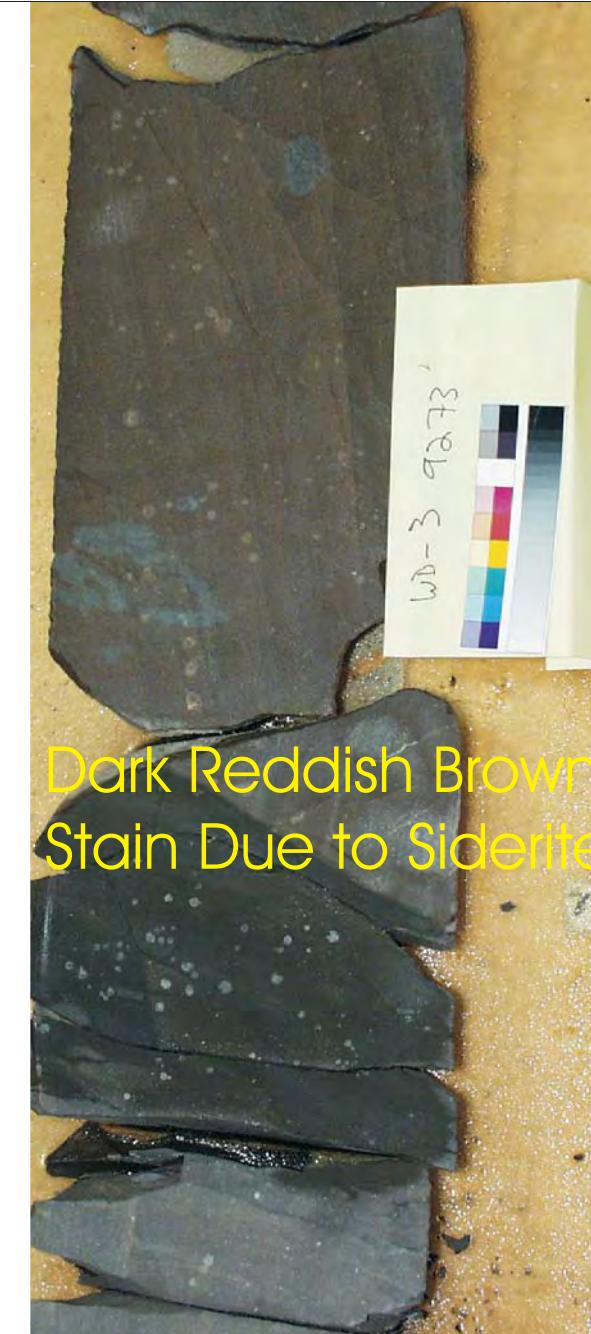
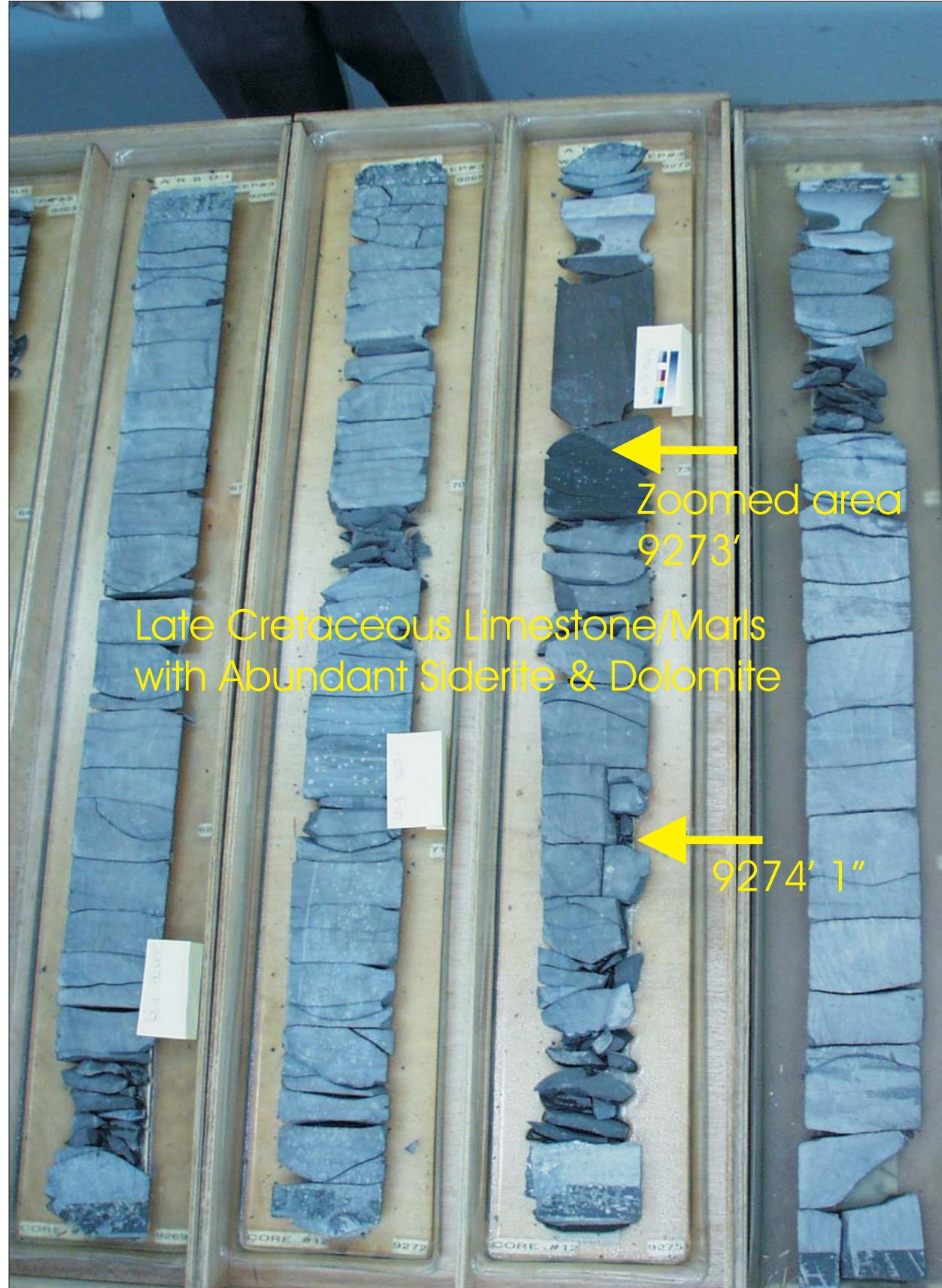
Sample Depth: 9272' 1"
 Shifted Depth: 9282' 1"
 MICP Entry Pressure: 414 psia
 MICP Threshold Pressure: 24894 psia
 Lithology: Limestone/Marl

WHOLE CORE PLUG ANALYSES
 WELL: WIRIAGAR DEEP - 3
 DEPTH: 9272' 1"

PLATE B:

Digital Core Chip/Plug Photograph
 Mercury Injection capillary Pressure

Figure 12B: Core Plug/Chip Atlas for sample 9272' 1" from Wiriagar Deep-3.

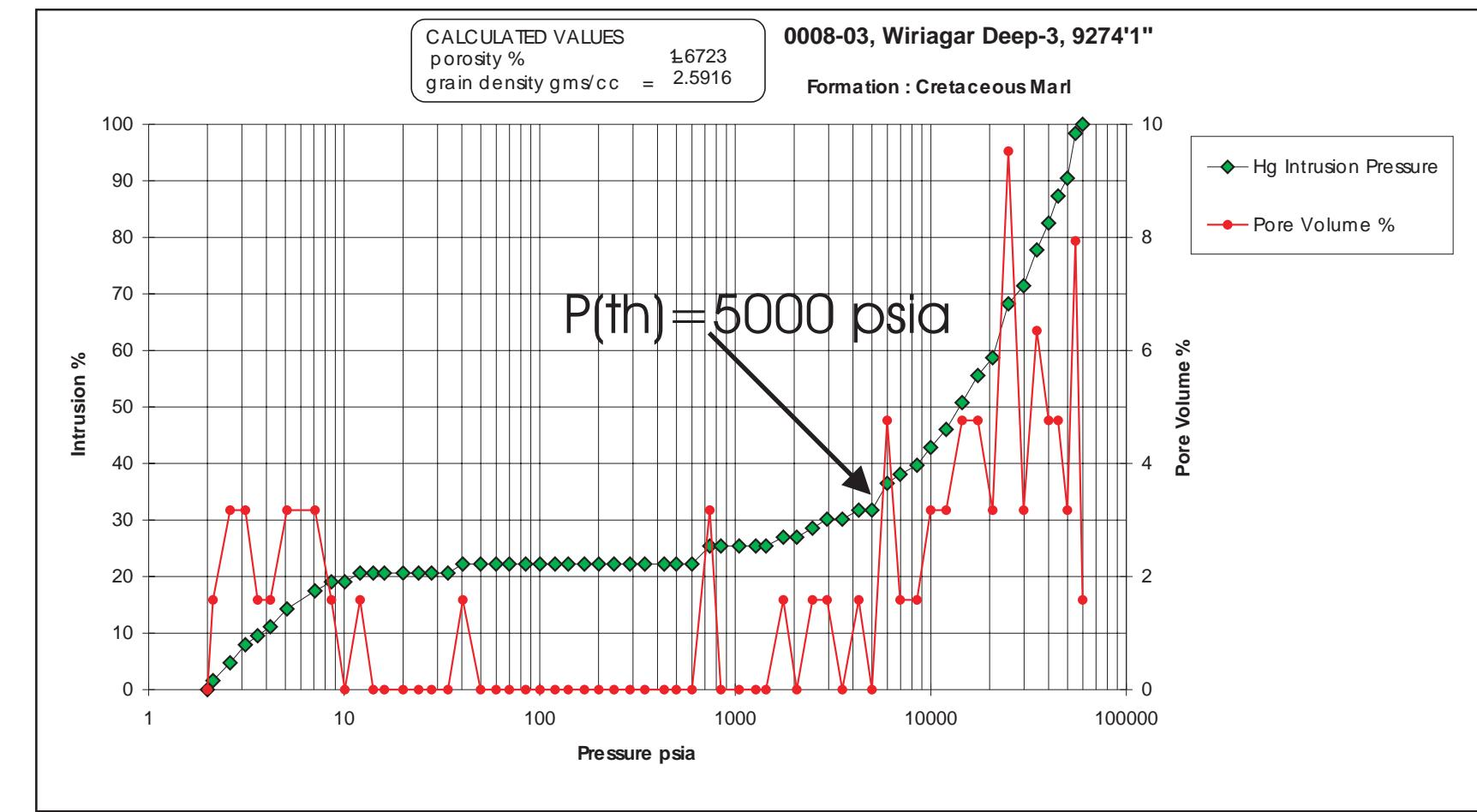
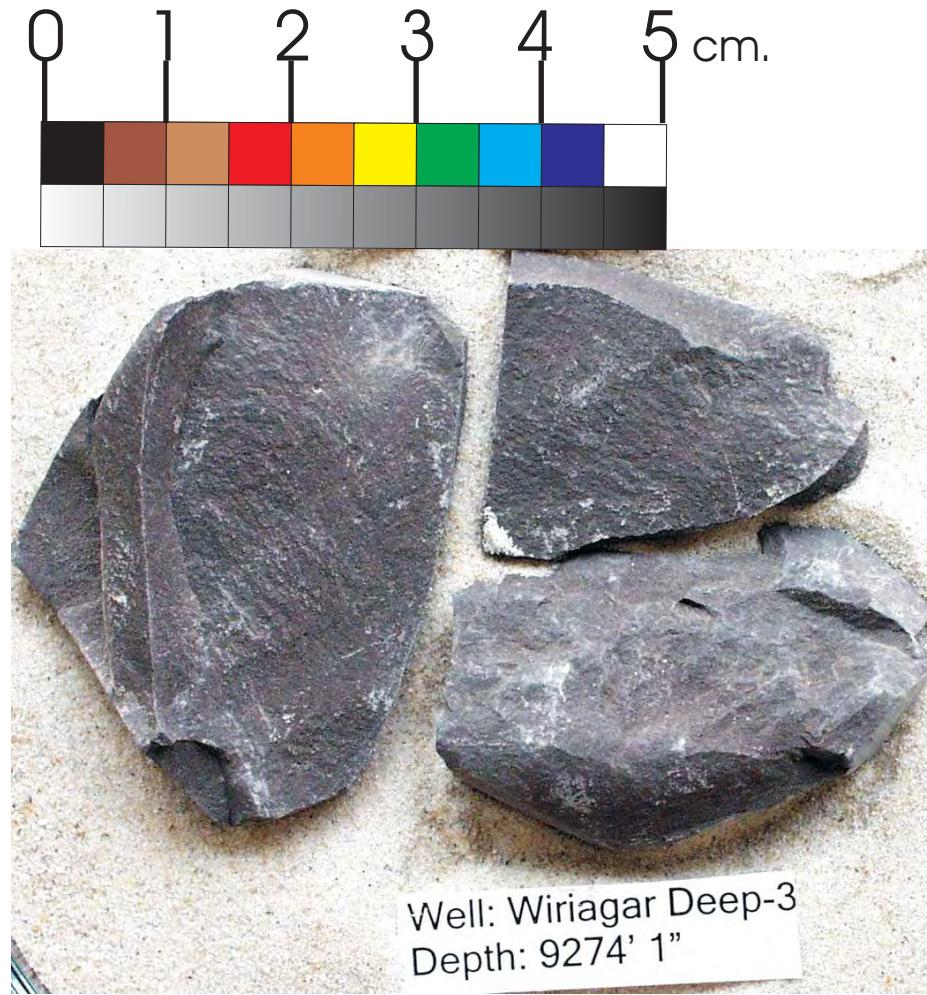


WHOLE CORE PLUG ANALYSES
WELL: WIRIAGAR DEEP - 3
DEPTH: 9274' 1"

PLATE A:

Digital Whole Core Photographs

Figure 13A: Core Plug/Chip Atlas for sample 9274' 1" from Wiriagar Deep-3.



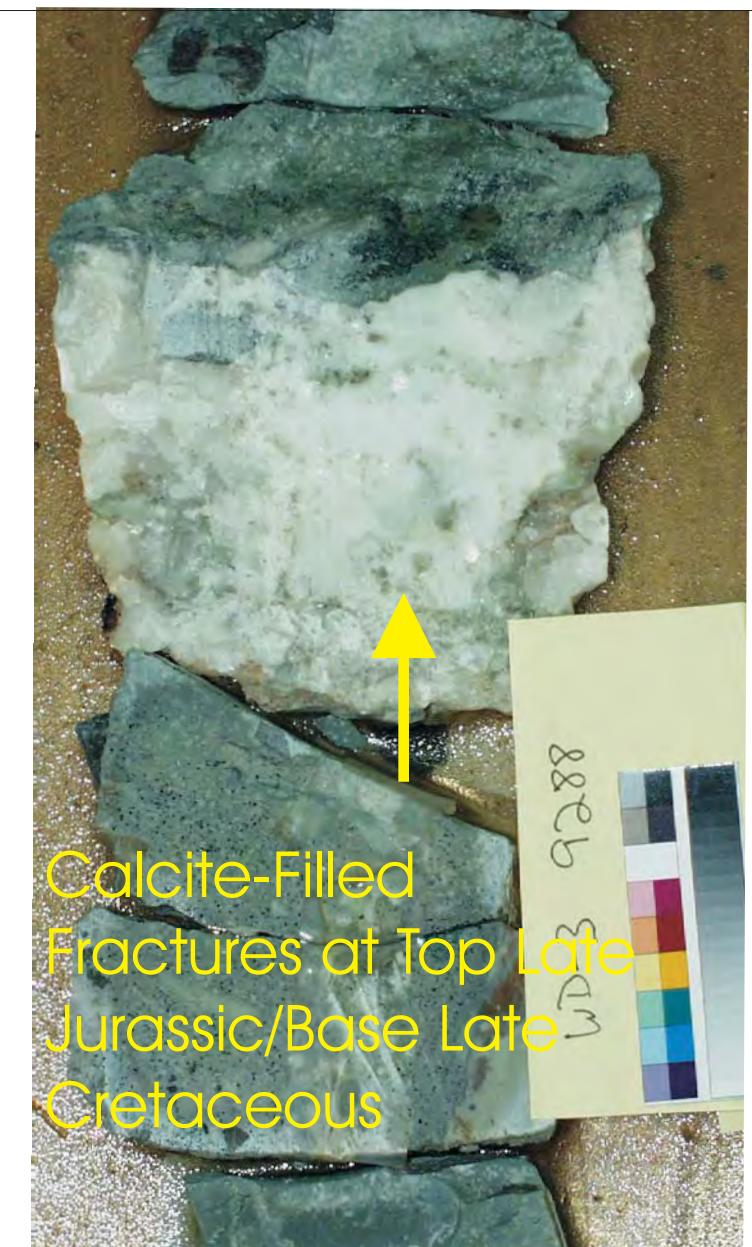
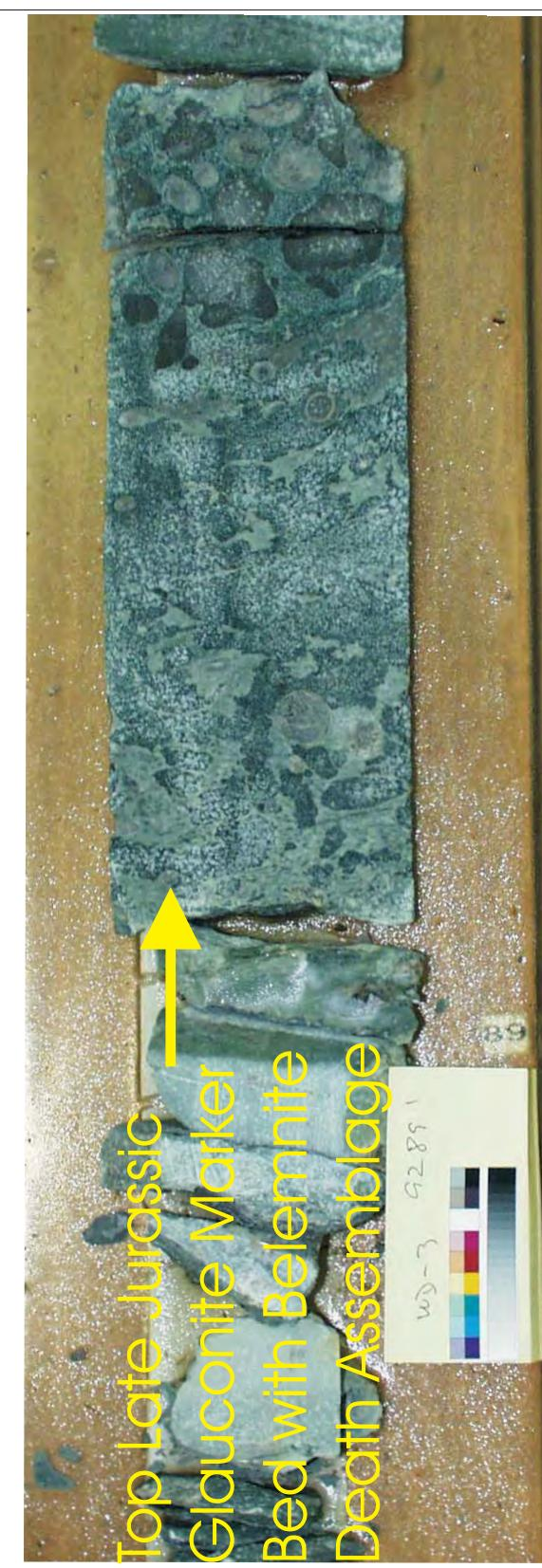
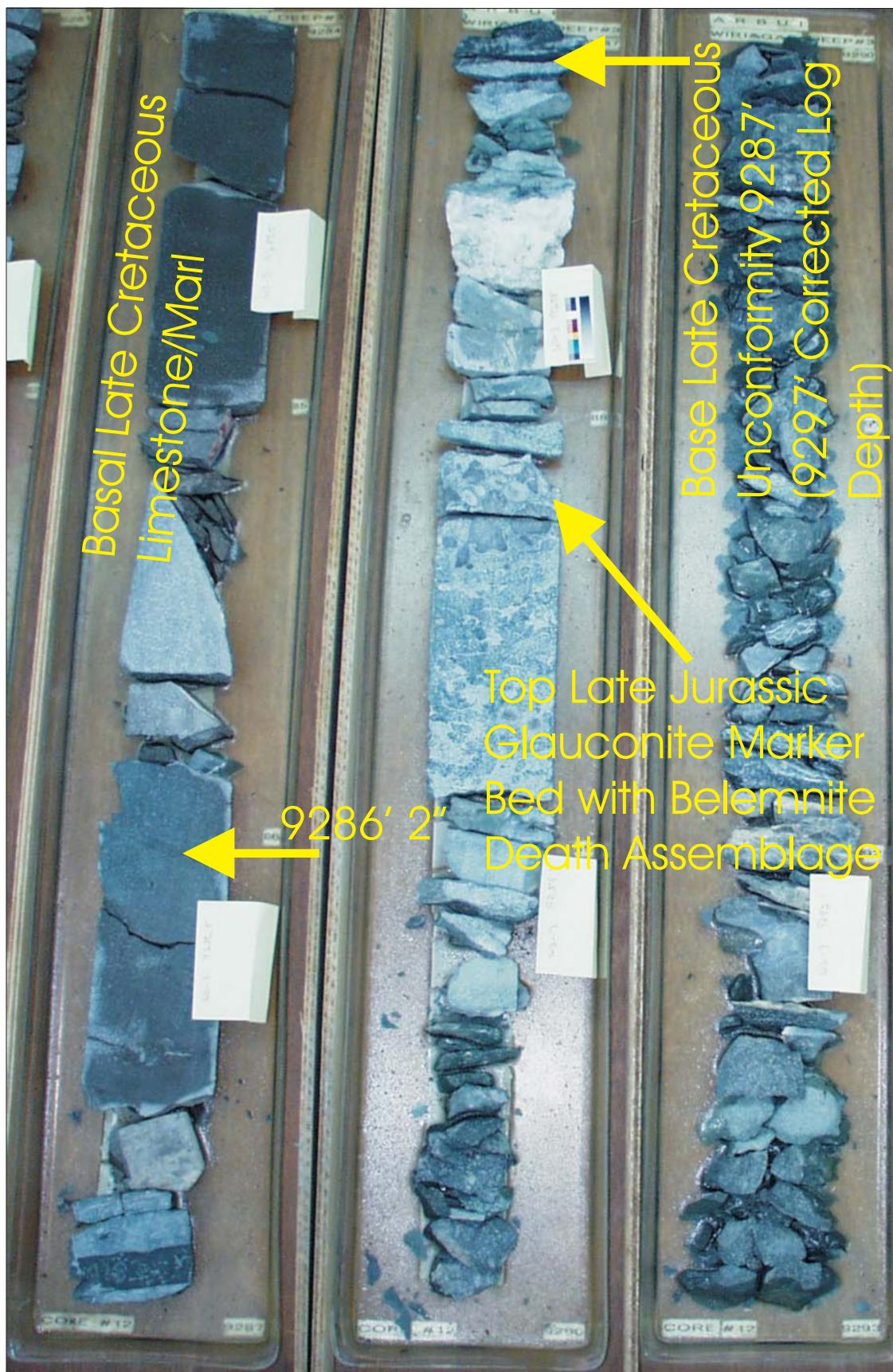
Sample Depth: 9274' 1"
Shifted Depth: 9284' 1"
MICP Entry Pressure: 601 psia
MICP Threshold Pressure: 5000 psia
Lithology: Limestone/Marl

WHOLE CORE PLUG ANALYSES
WELL: WIRIAGAR DEEP - 3
DEPTH: 9274' 1"

PLATE B:

Digital Core Chip/Plug Photograph
Mercury Injection Capillary Pressure

Figure 13B: Core Plug/Chip Atlas for sample 9274' 1" from Wiriagar Deep-3.

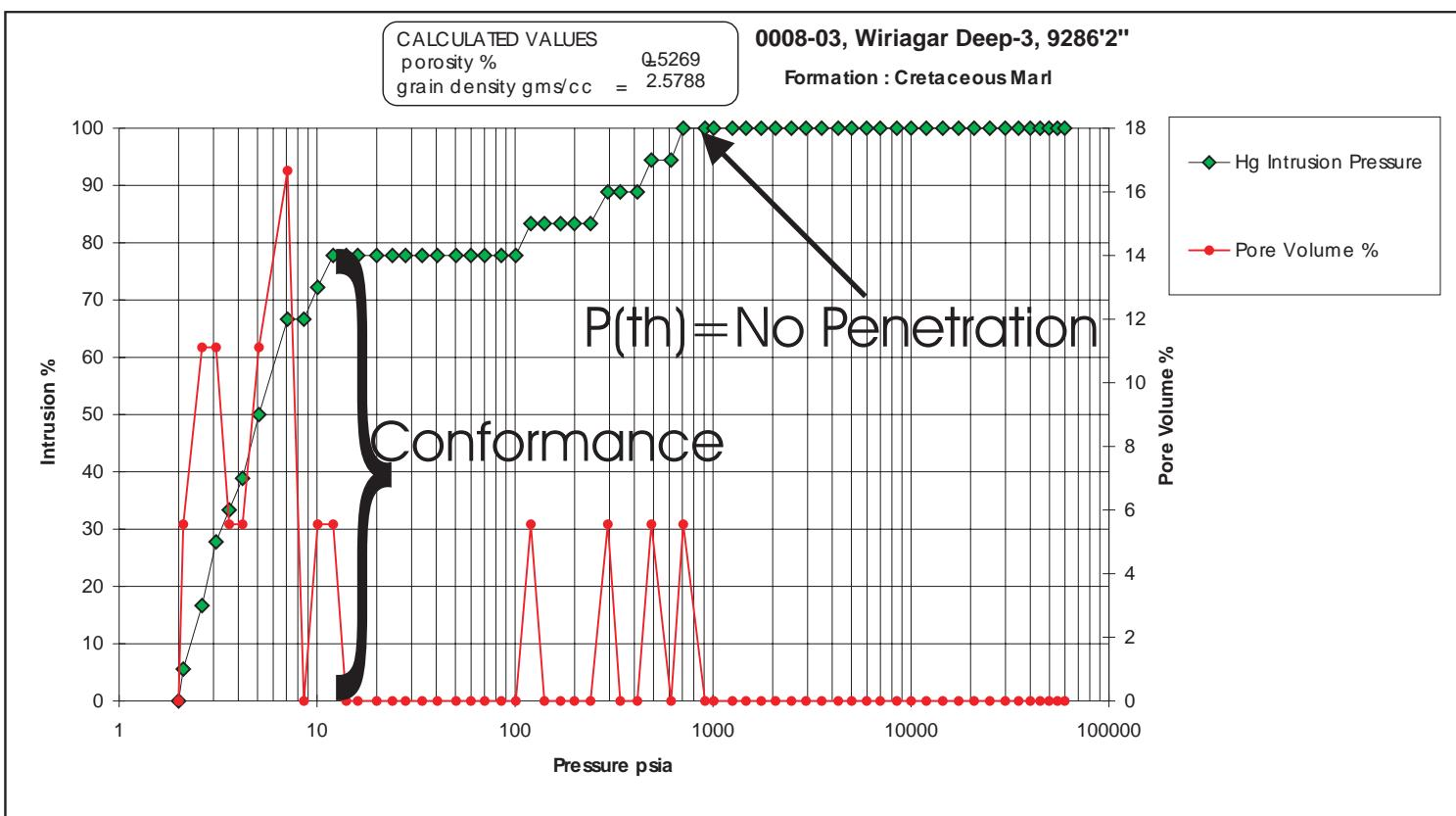
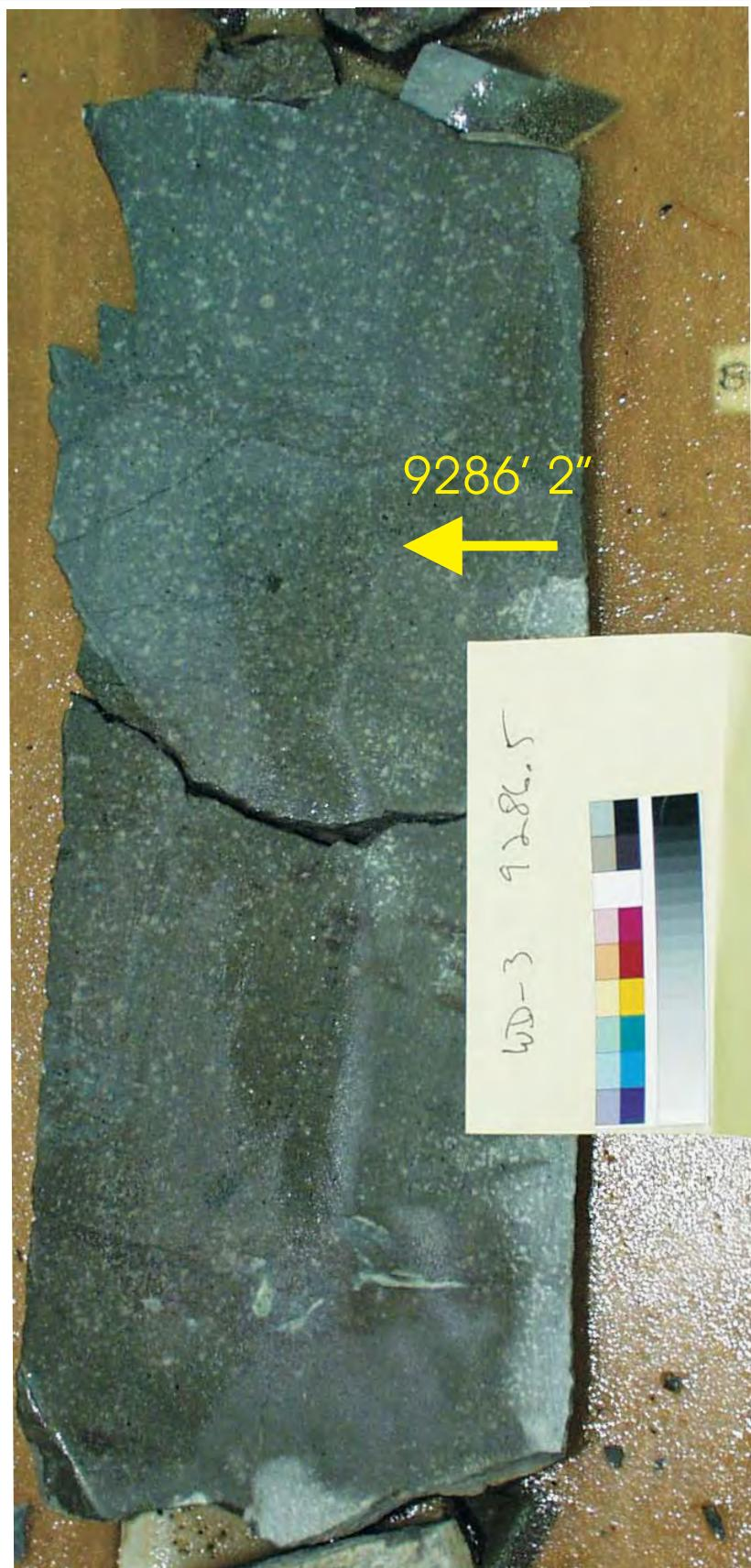


WHOLE CORE PLUG ANALYSES
WELL: WIRIAGAR DEEP - 3
DEPTH: 9286' 2"

PLATE A:

Digital Whole Core Photographs

Figure 14A: Core Plug/Chip Atlas for sample 9286' 2" from Wiriagar Deep-3.

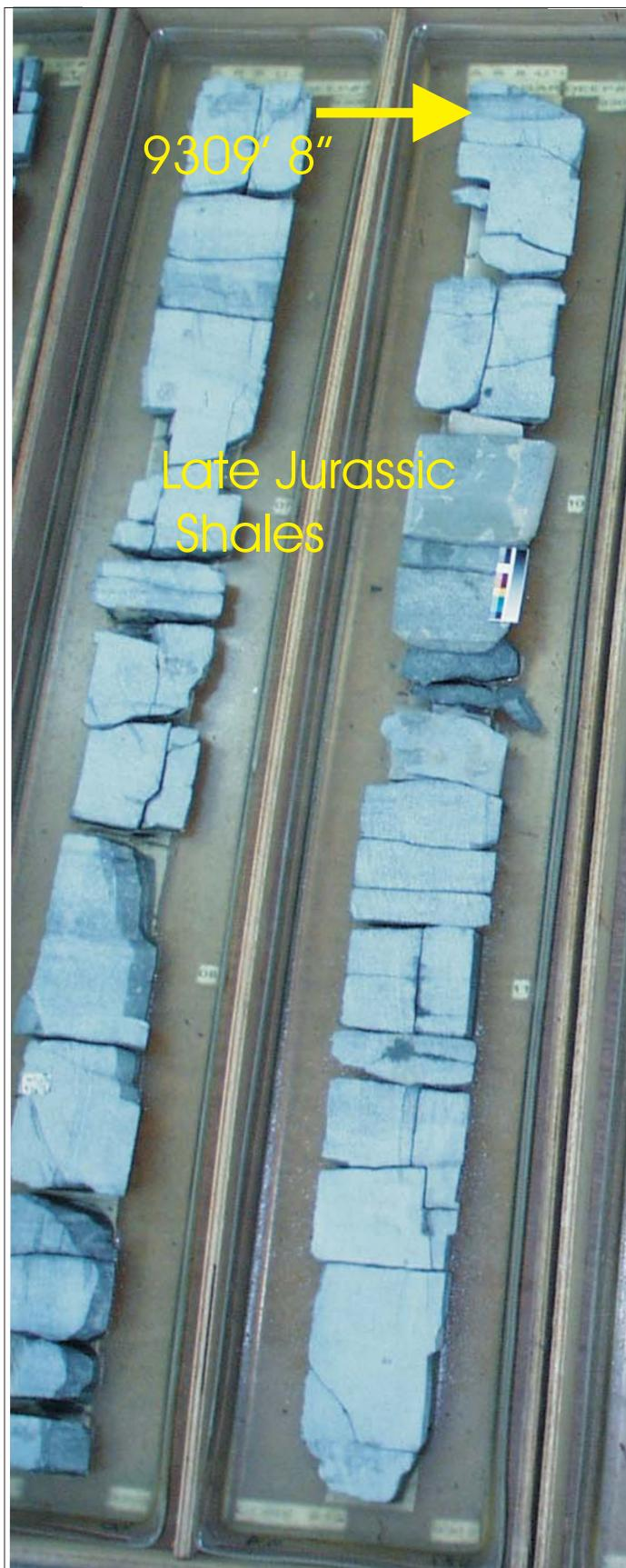


Sample Depth: 9286' 2"
Shifted Depth: 9296' 2"
MICP Entry Pressure: No Penetration
MICP Threshold Pressure: No Pene.
Lithology: Limestone/Marl

WHOLE CORE PLUG ANALYSES
WELL: WIRIAGAR DEEP - 3
DEPTH: 9286' 2"

PLATE B:
Digital Whole Core Photographs
Digital Core Chip/Plug Photograph
Mercury Injection Capillary Pressure

Figure 14B: Core Plug/Chip Atlas for sample 9286' 2" from Wiriagar Deep-3.

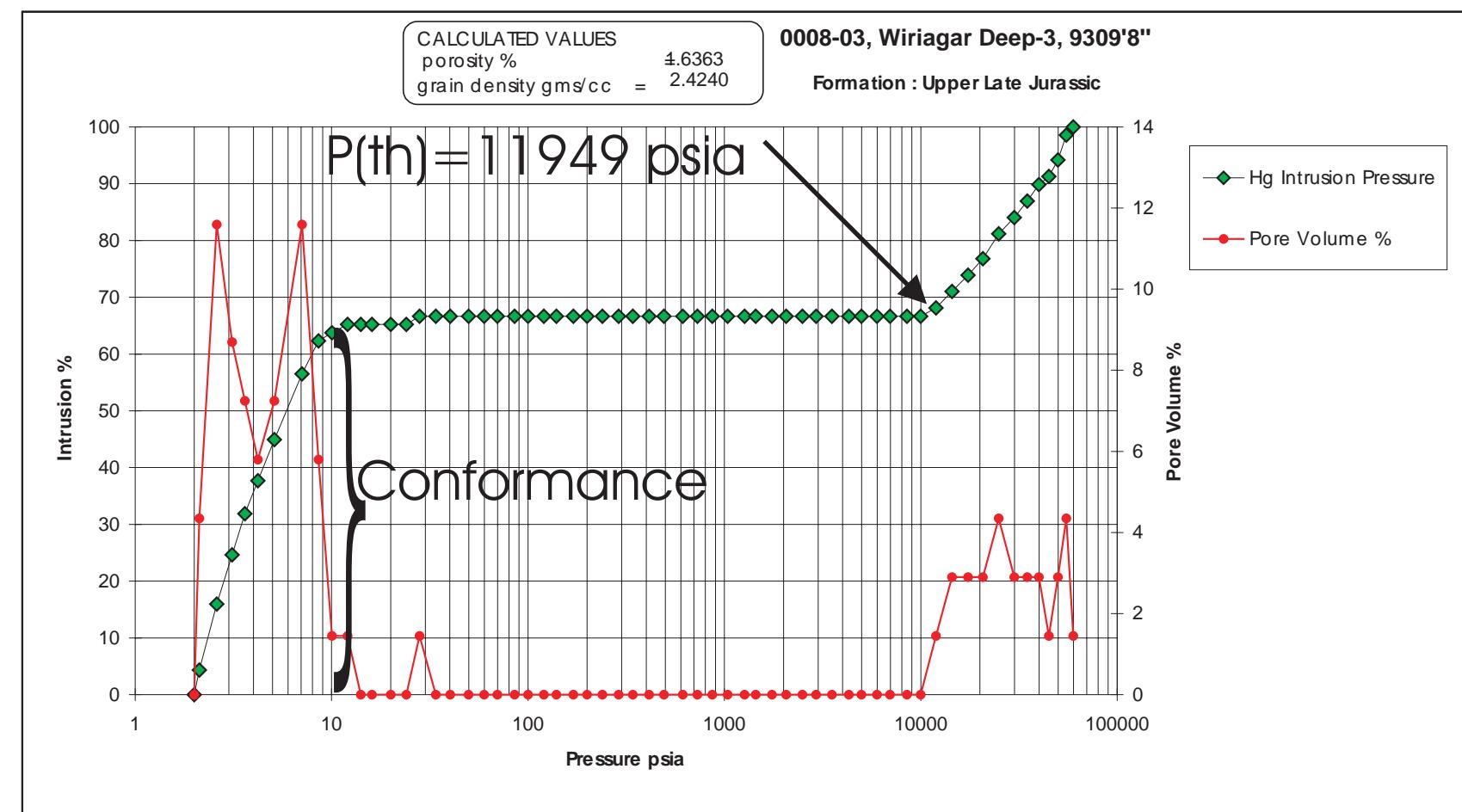
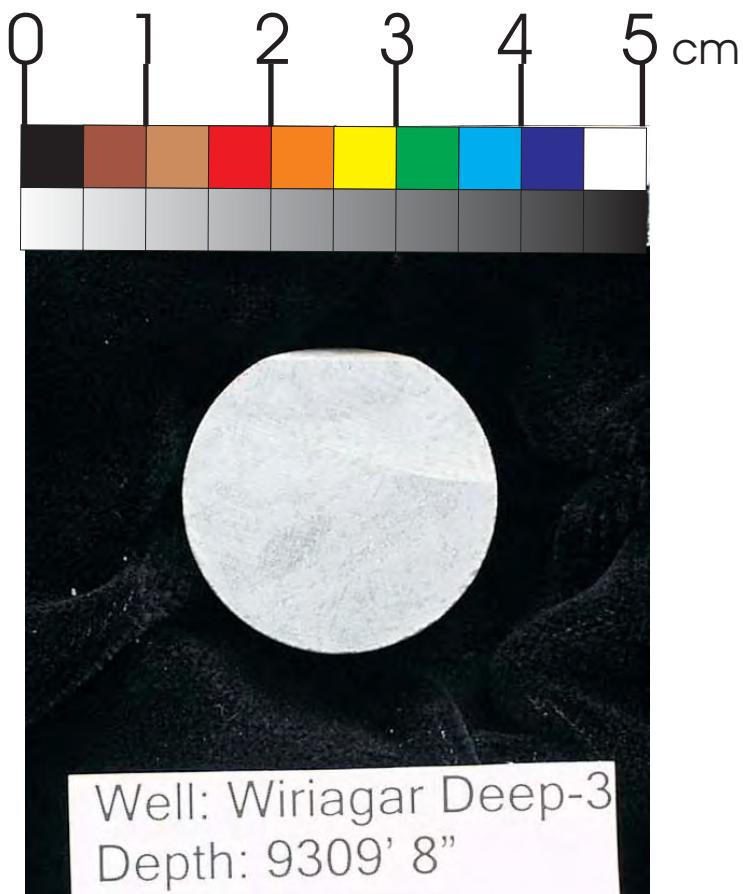


WHOLE CORE PLUG ANALYSES
WELL: WIRIAGAR DEEP - 3
DEPTH: 9309' 8"

PLATE A:

Digital Whole Core Photographs

Figure 15A: Core Plug/Chip Atlas for sample 9309' 8" from Wiriagar Deep-3.



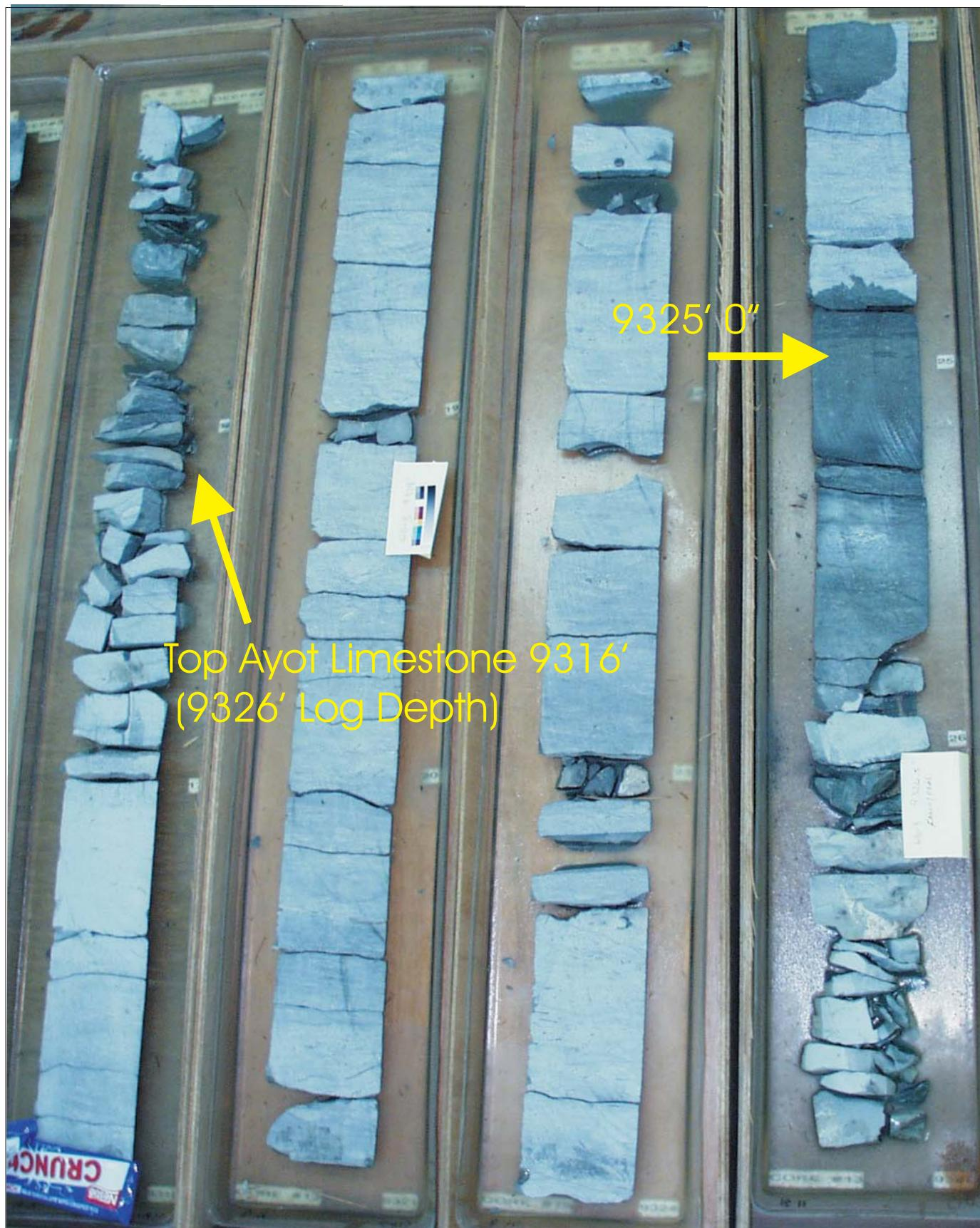
Sample Depth: 9309' 8"
 Shifted Depth: 9319' 8"
 MICP Entry Pressure: 28 psia
 MICP Threshold Pressure: 11949 psia
 Lithology: Shale

WHOLE CORE PLUG ANALYSES
WELL: WIRIAGAR DEEP - 3
DEPTH: 9309' 8"

PLATE B:

Digital Core Chip/Plug Photograph
Mercury Injection Capillary Pressure

Figure 15B: Core Plug/Chip Atlas for sample 9309' 8" from Wiriagar Deep-3.

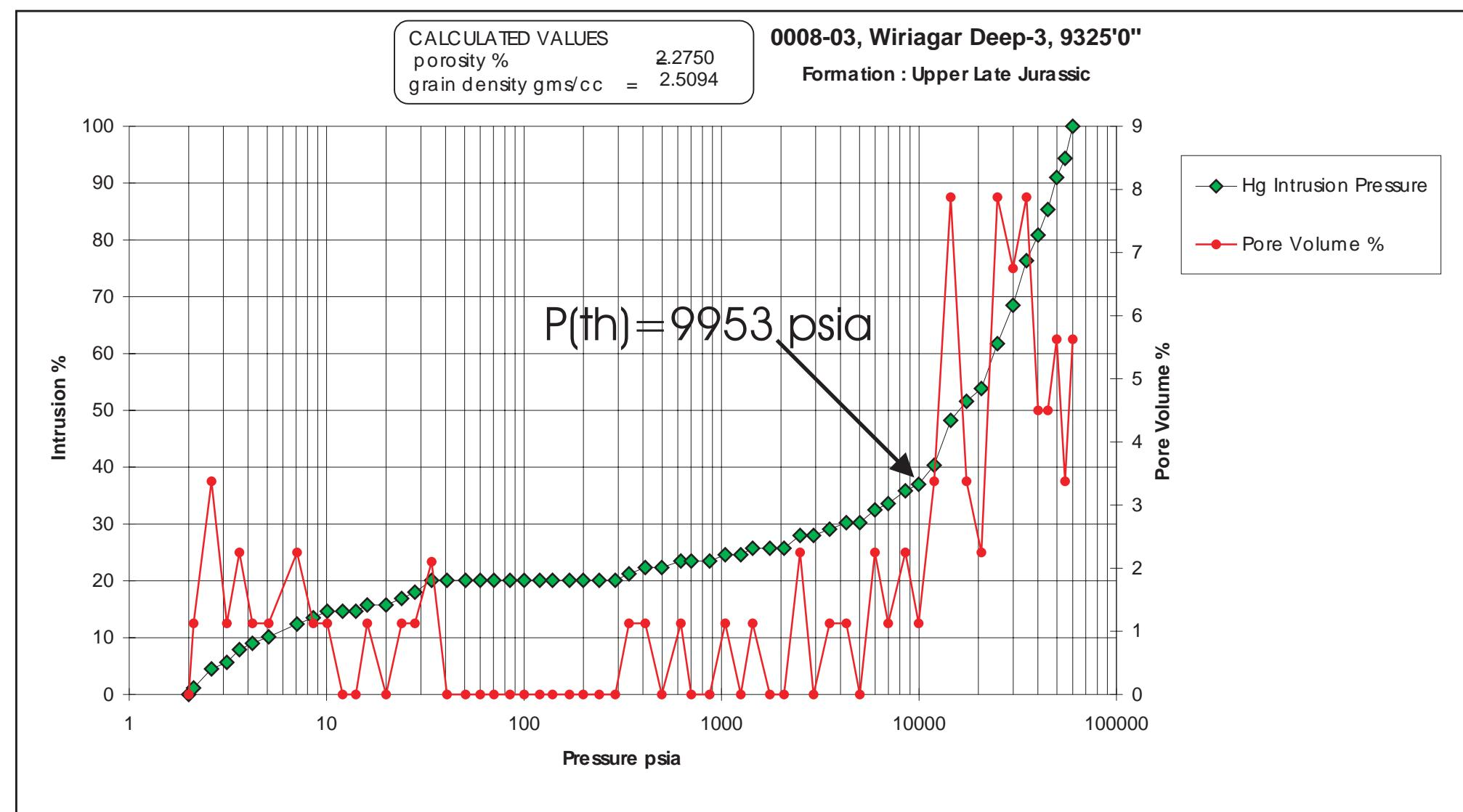
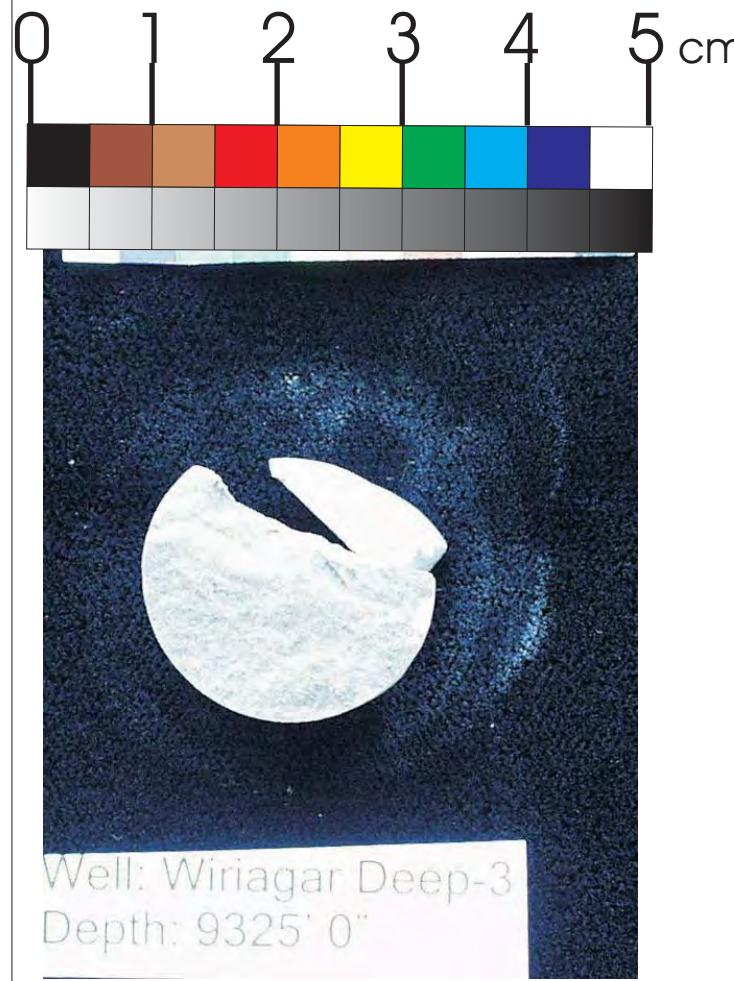


WHOLE CORE PLUG ANALYSES
WELL: WIRIAGAR DEEP - 3
DEPTH: 9325' 0"

PLATE A:

Digital Whole Core Photographs

Figure 16A: Core Plug/Chip Atlas for sample 9325' 0" from Wiriagar Deep-3.



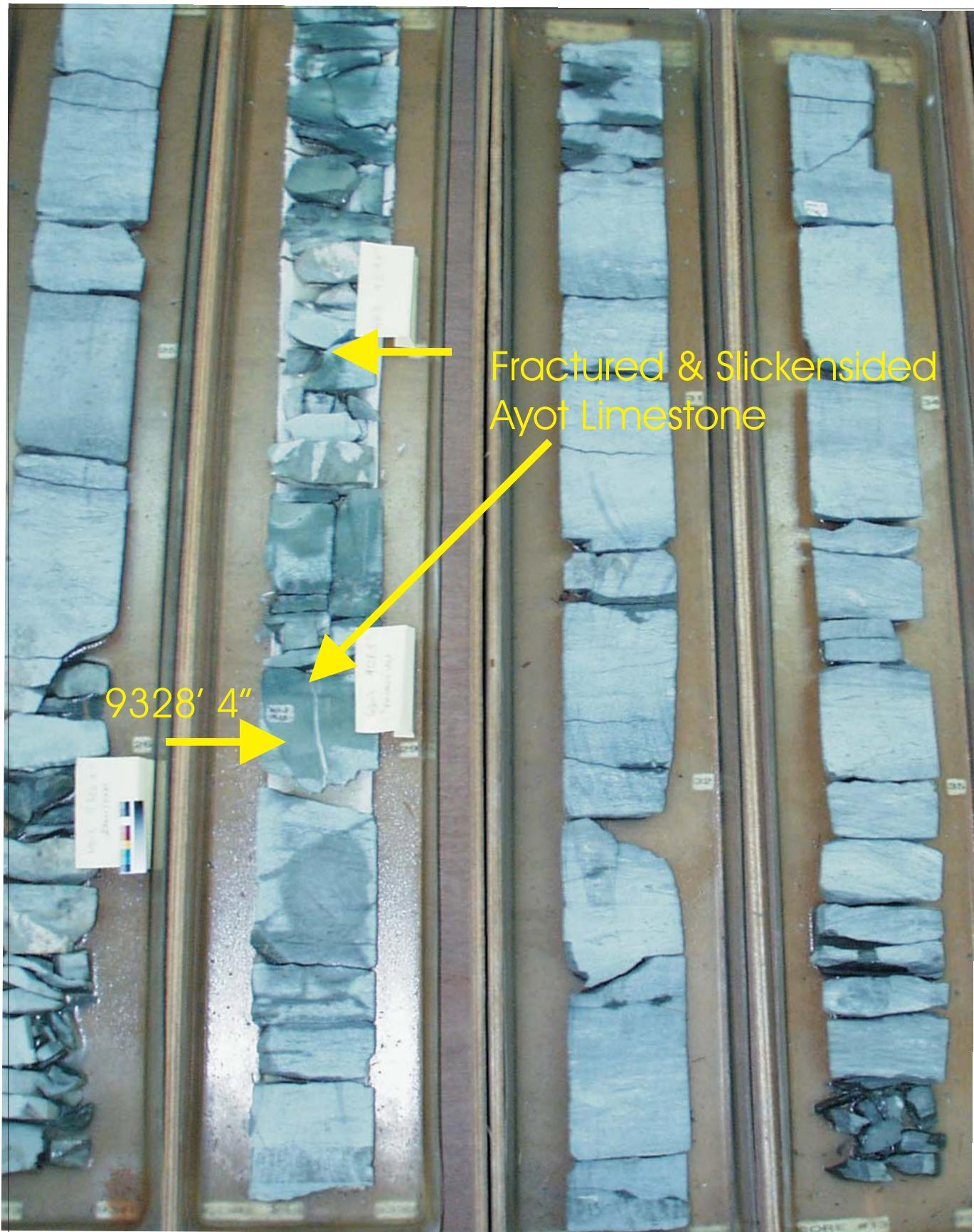
Sample Depth: 9325' 0"
Shifted Depth: 9335' 0"
MICP Entry Pressure: 339 psia
MICP Threshold Pressure: 9953 psia
Lithology: Shale

WHOLE CORE PLUG ANALYSES
WELL: WIRIAGAR DEEP - 3
DEPTH: 9325' 0"

PLATE B:

Digital Core Chip/Plug Photograph
Mercury Injection Capillary Pressure

Figure 16B: Core Plug/Chip Atlas for sample 9325' 0" from Wiriagar Deep-3.



WHOLE CORE PLUG ANALYSES
WELL: WIRIAGAR DEEP - 3
DEPTH: 9328' 4"

PLATE A:

Digital Whole Core Photographs

Figure 17A: Core Plug/Chip Atlas for sample 9328' 4" from Wiriagar Deep-3.

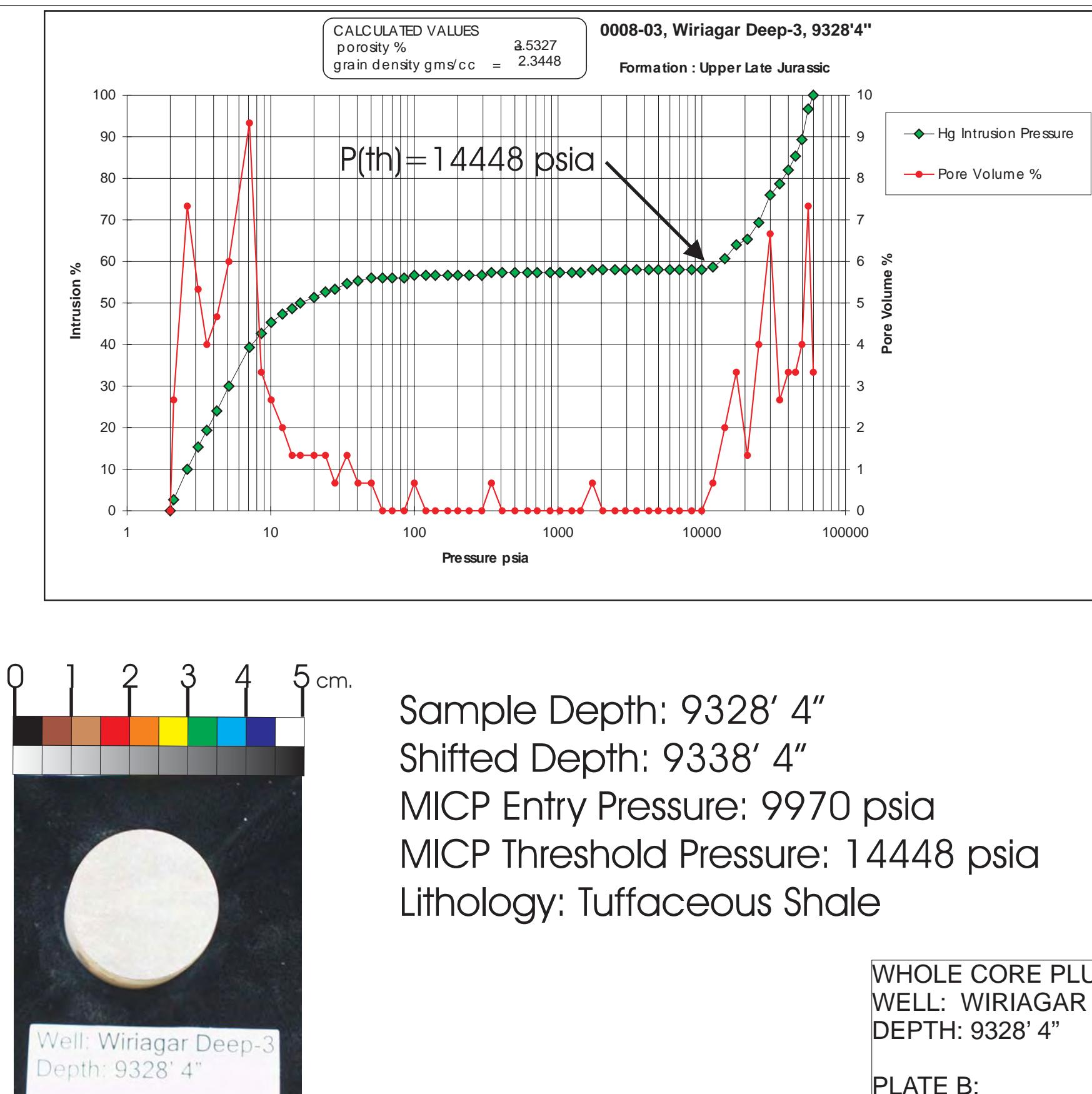
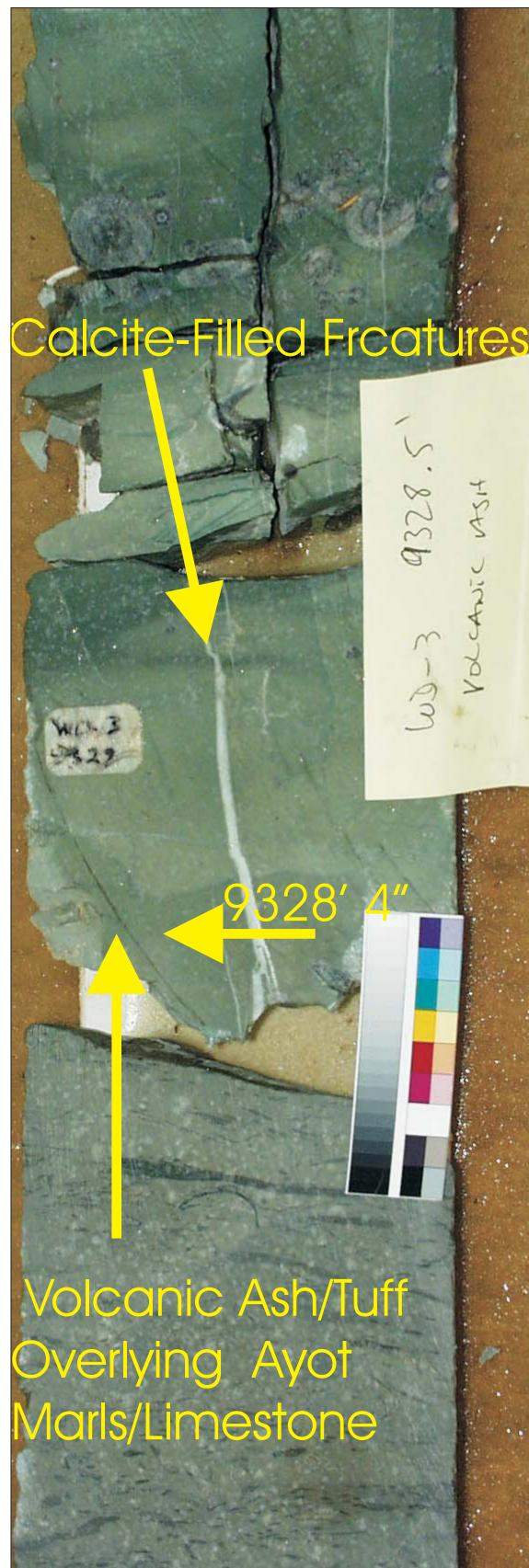
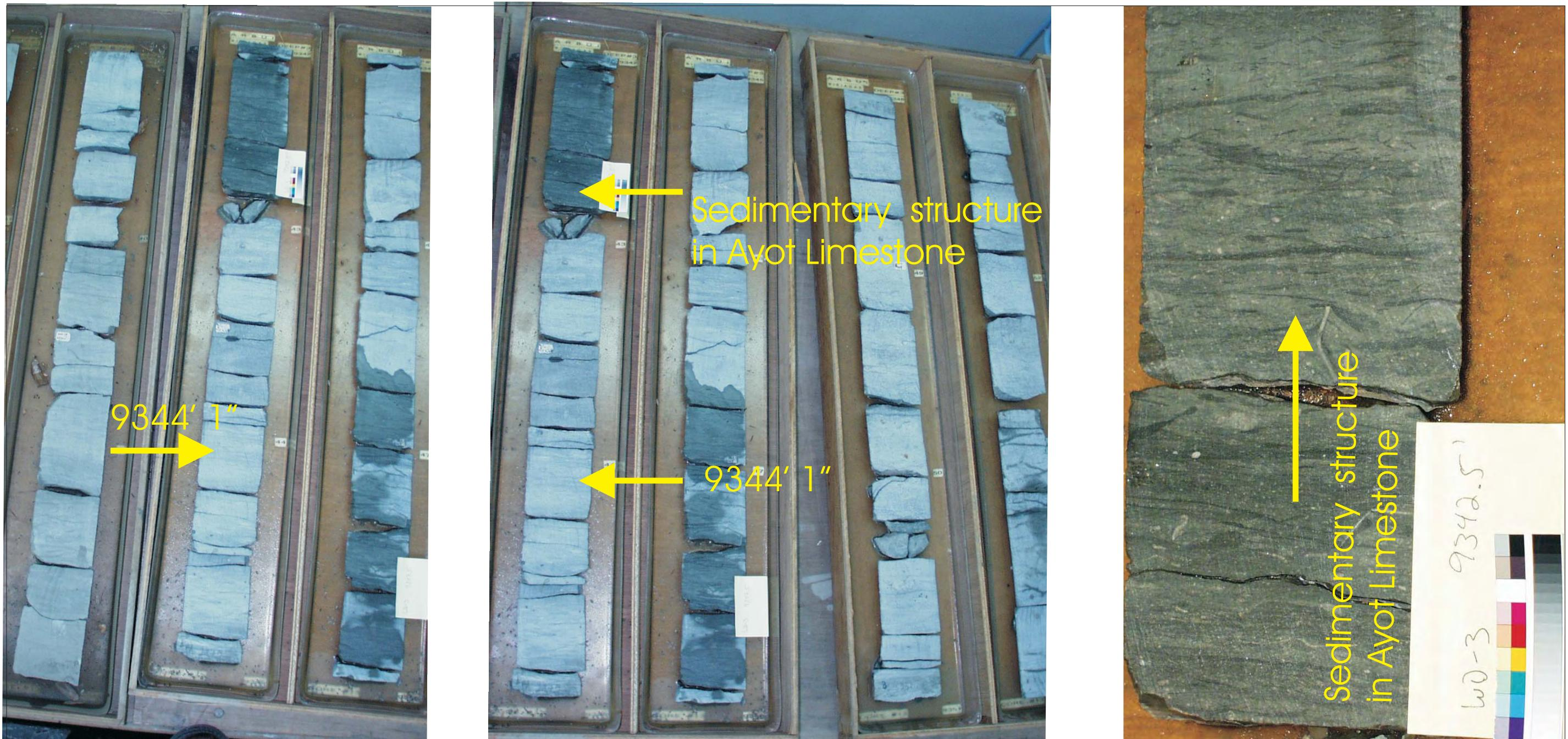


Figure 17B: Core Plug/Chip Atlas for sample 9328' 4" from Wiriagar Deep-3.

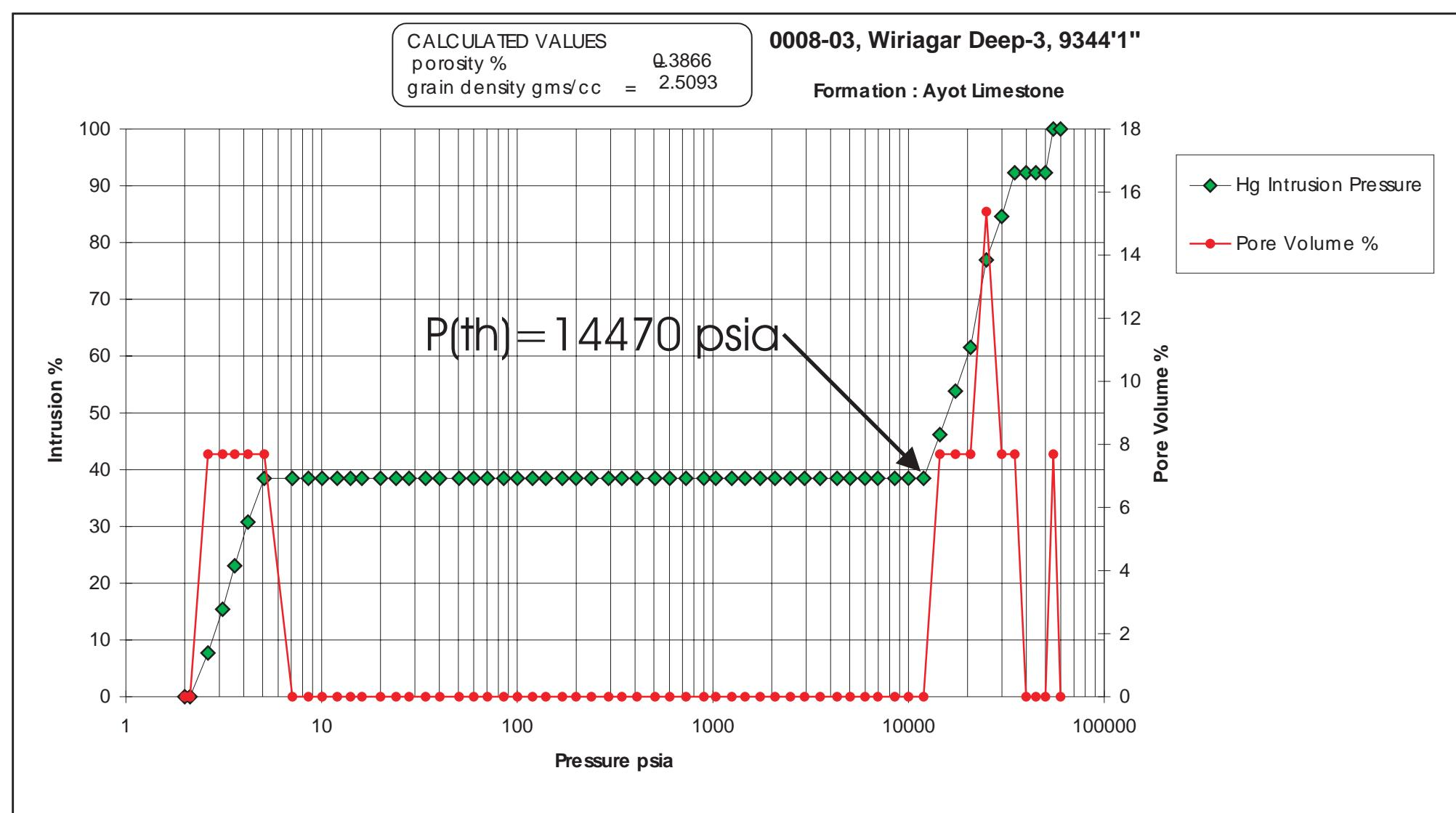


WHOLE CORE PLUG ANALYSES
WELL: WIRIAGAR DEEP - 3
DEPTH: 9344' 1"

PLATE A:

Digital Whole Core Photographs

Figure 18A: Core Plug/Chip Atlas for sample 9344' 1" from Wiriagar Deep-3.



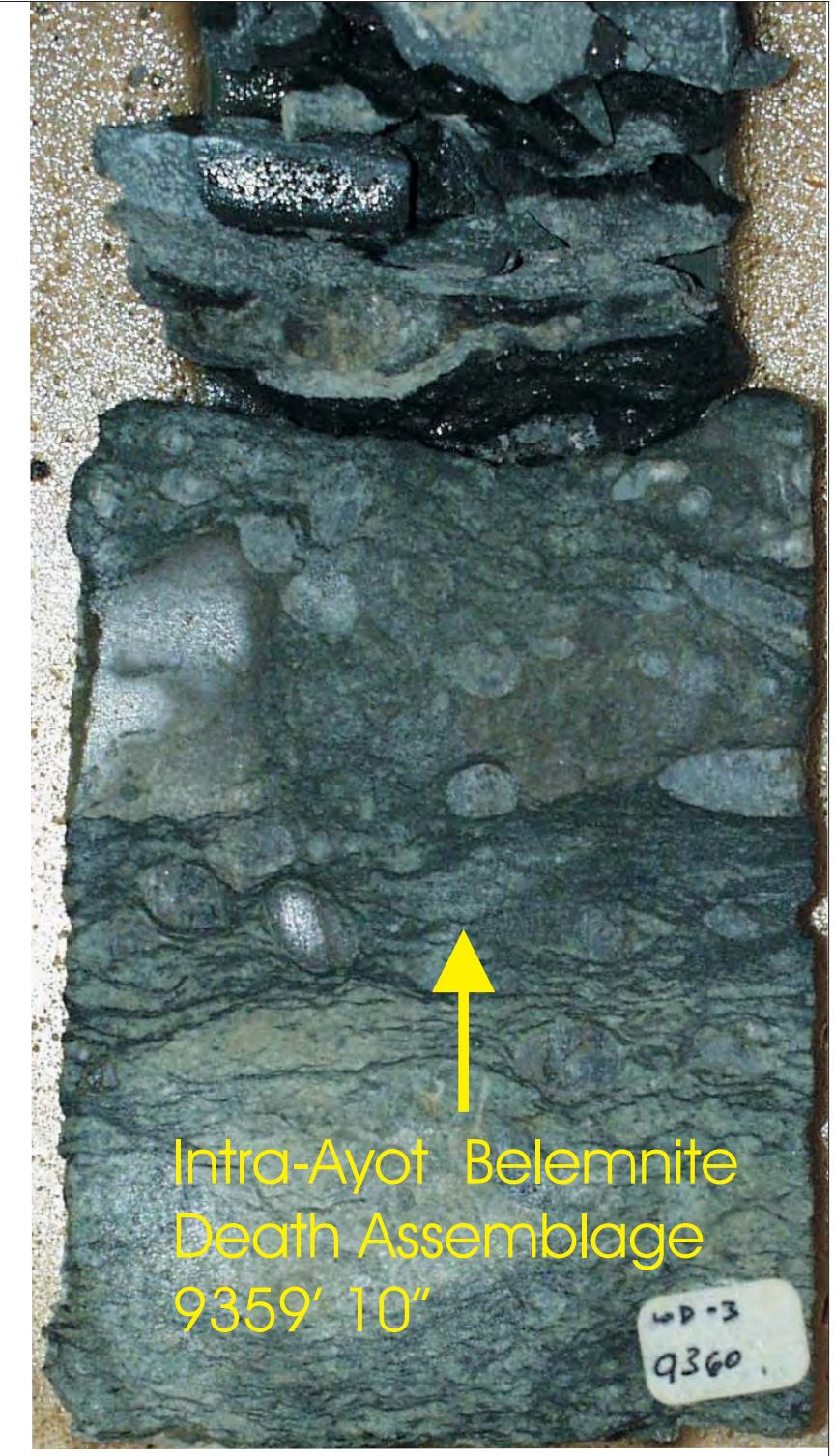
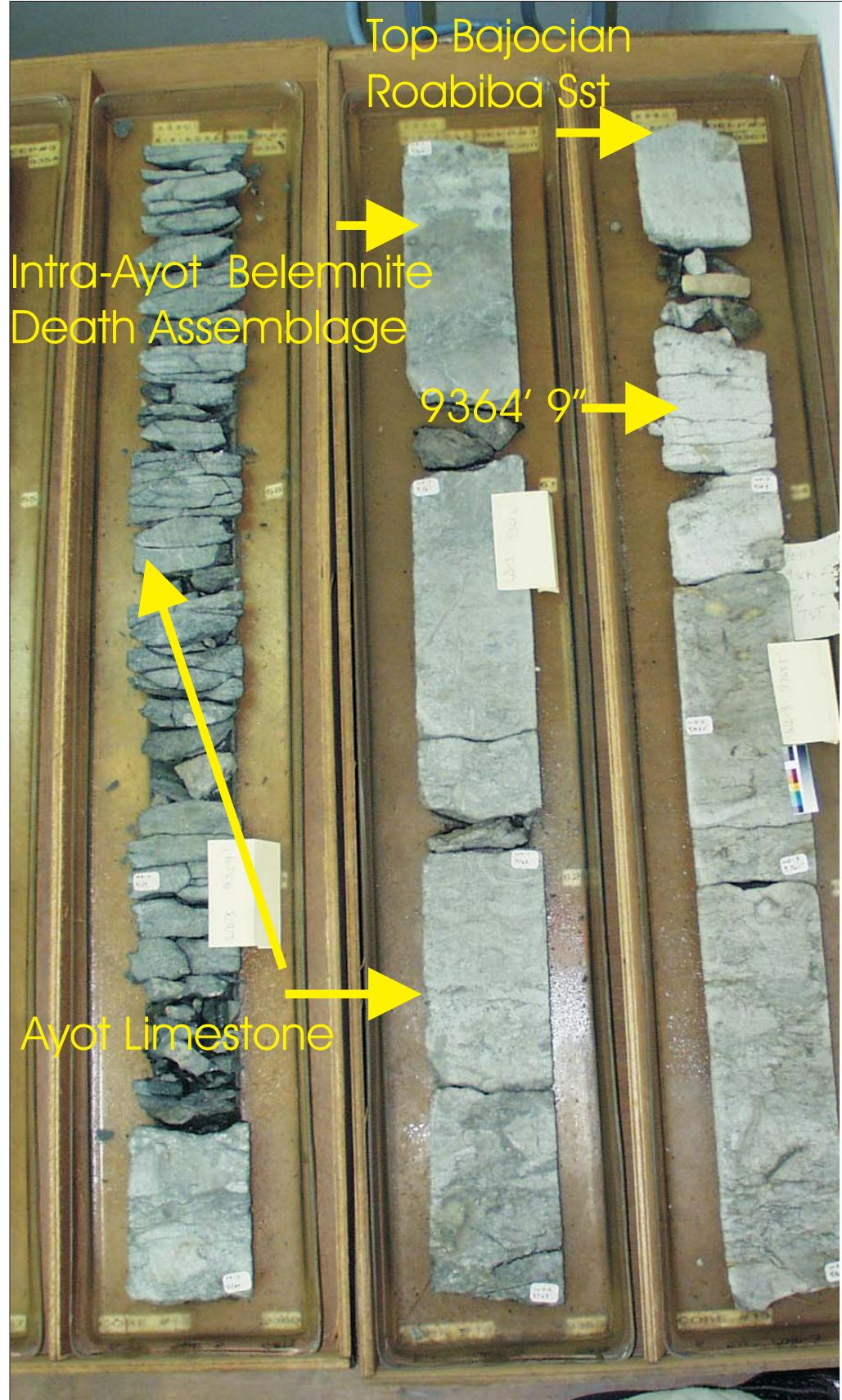
Sample Depth: 9344' 1"
 Shifted Depth: 9354' 1"
 MICP Entry Pressure: 11950 psia
 MICP Threshold Pressure: 14470 psia
 Lithology: Limestone

WHOLE CORE PLUG ANALYSES
 WELL: WIRIAGAR DEEP - 3
 DEPTH: 9344' 1"

PLATE B:

Digital Core Chip/Plug Photograph
 Mercury Injection capillary Pressure

Figure 18B: Core Plug/Chip Atlas for sample 9344' 1" from Wiriagar Deep-3.



WHOLE CORE PLUG ANALYSES
WELL: WIRIAGAR DEEP - 3
DEPTH: 9364' 9"

PLATE A:

Digital Whole Core Photographs

Figure 19A: Core Plug/Chip Atlas for sample 9364' 9" from Wiriagar Deep-3.



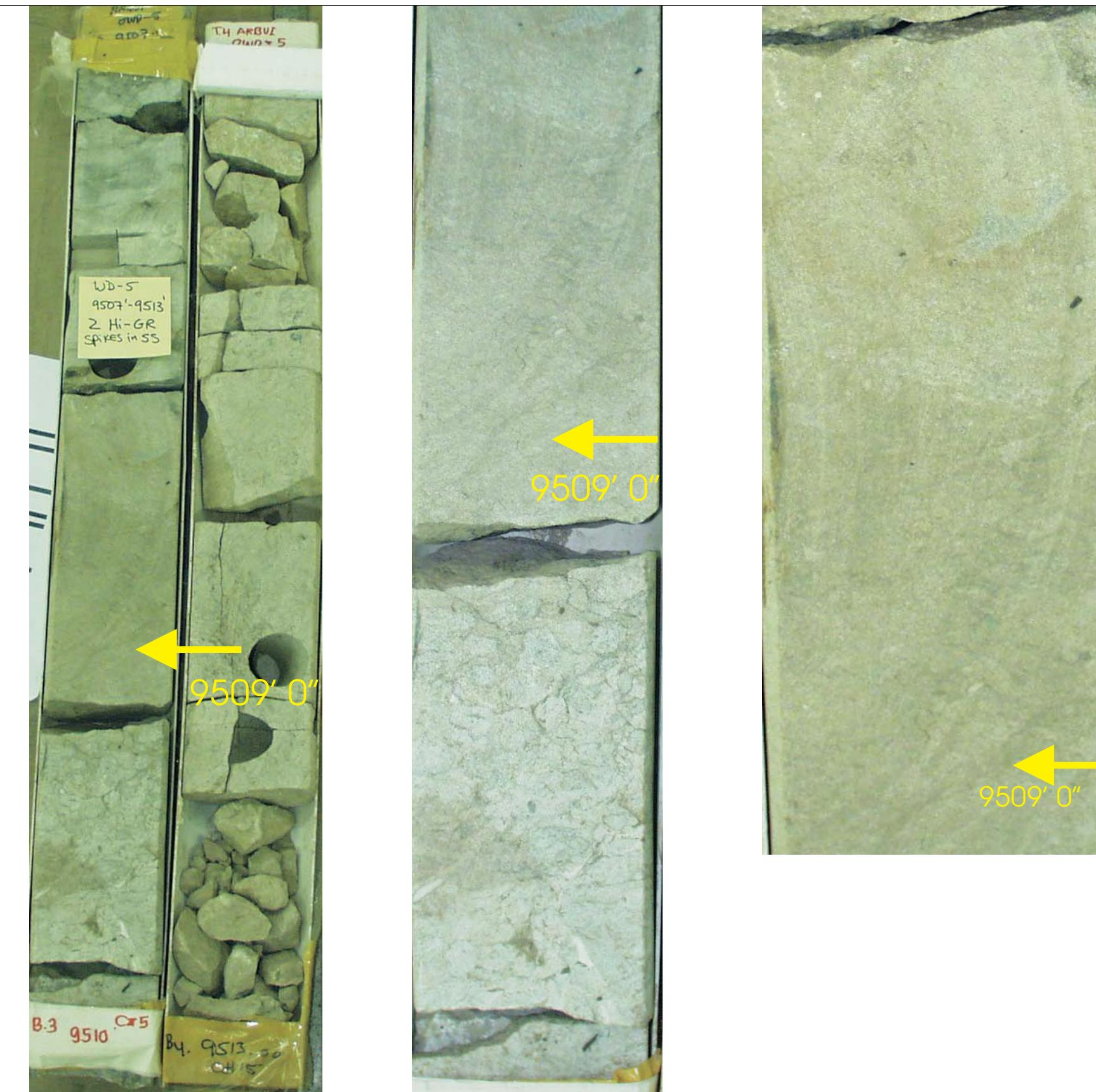
Sample Depth: 9364' 9"
Shifted Depth: 9374' 9"
He-Ø: 13.2%
k air: 0.74 mD (NOB 800 psia)

WHOLE CORE PLUG ANALYSES
WELL: WIRIAGAR DEEP - 3
DEPTH: 9364' 9"

PLATE B:

Digital Whole Core Photographs
Digital Core Chip/Plug Photograph

Figure 19B: Core Plug/Chip Atlas for sample 9364' 9" from Wiriagar Deep-3.



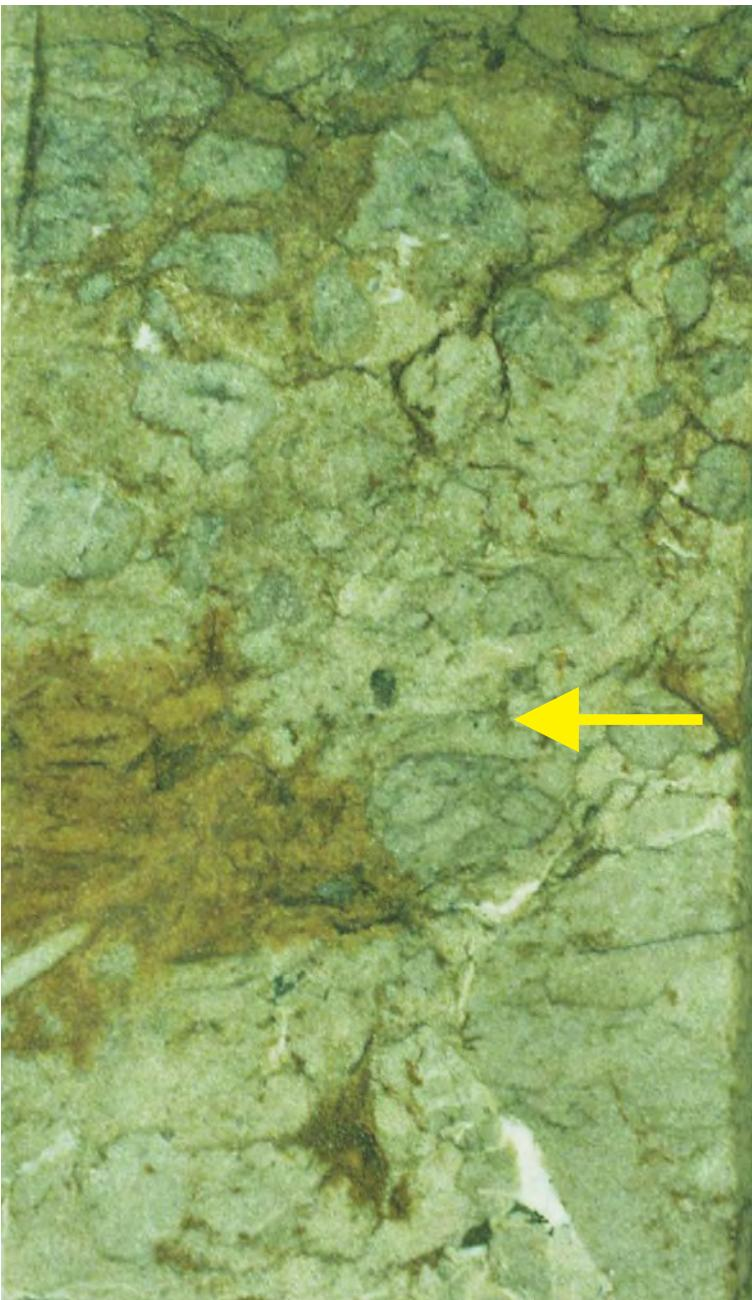
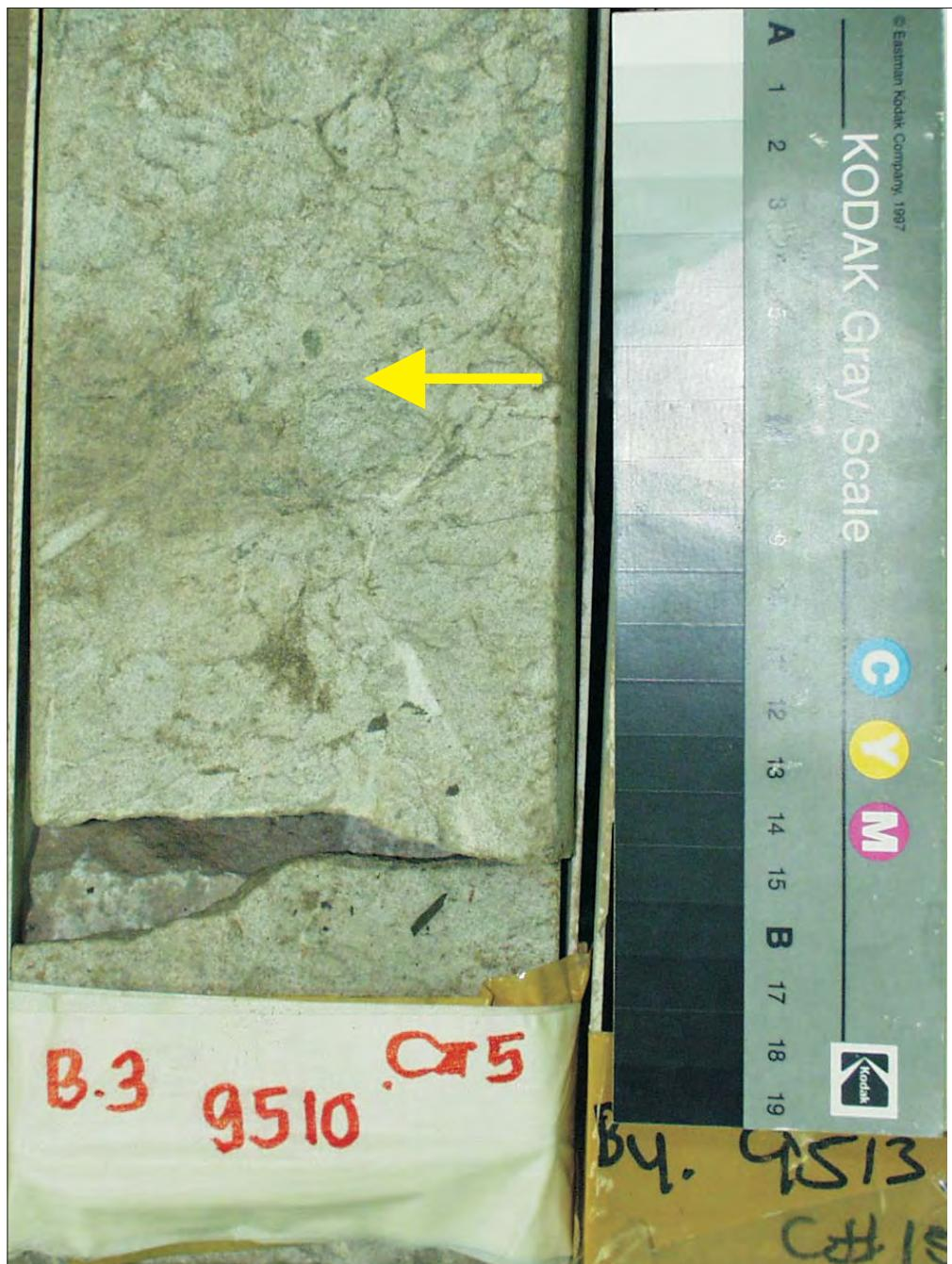
Sample Depth: 9509' 0"
Shifted Depth: 9519' 0"
He-Ø: 4.4%
k air: 0.008 mD (NOB 800 psia)

WHOLE CORE PLUG ANALYSES
WELL: WIRIAGAR DEEP - 5
DEPTH: 9509' 0"

PLATE A:

Digital Whole Core Photographs
Digital Core Chip/Plug Photograph

Figure 20: Core Plug/Chip Atlas for sample 9509' 0" from Wiriagar Deep-5st.



Sample Depth: 9509' 5"
Shifted Depth: 9519' 5"
He- \varnothing : 2.2%
k air: 0.016 mD (NOB 800 psia)

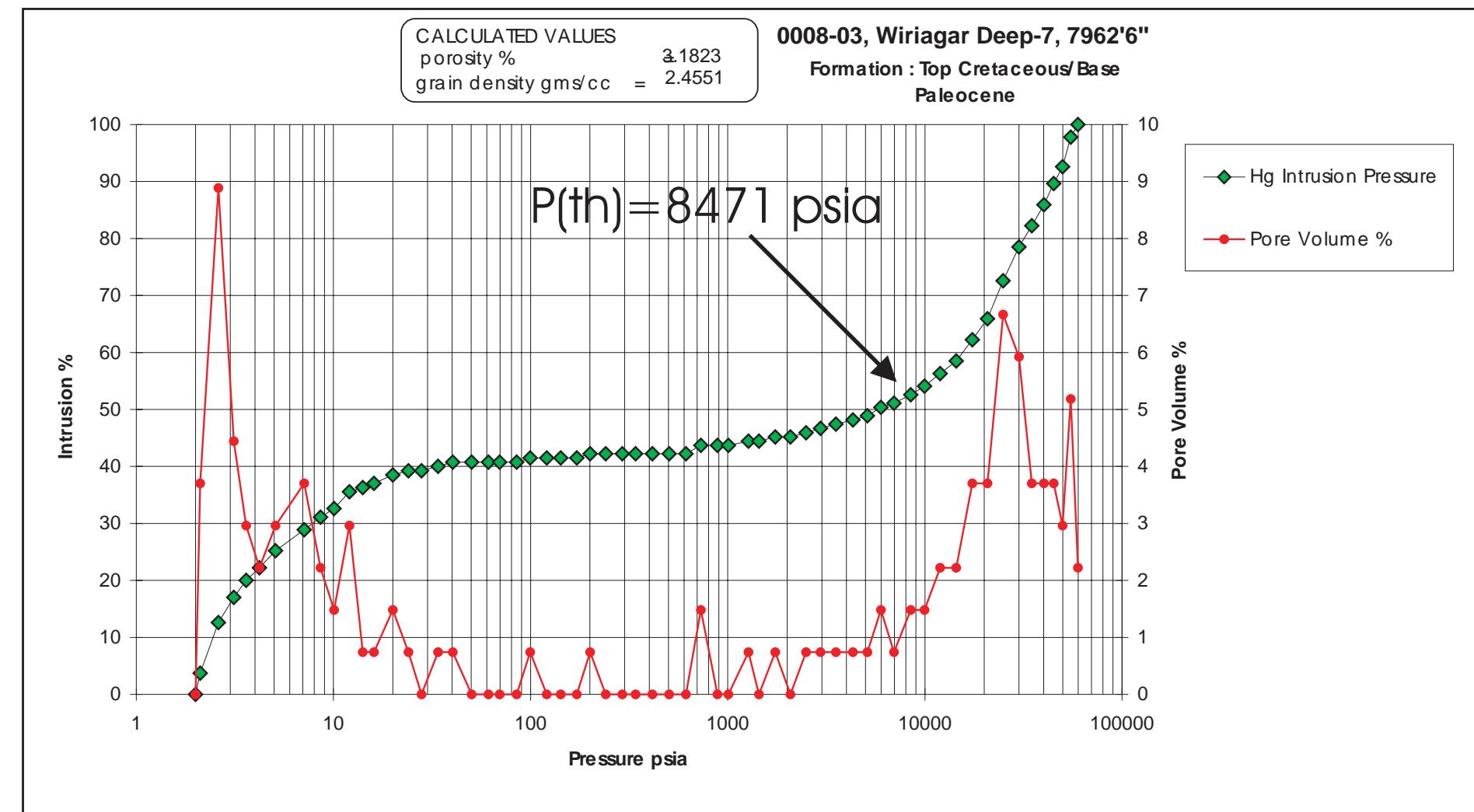
WHOLE CORE PLUG ANALYSES
WELL: WIRIAGAR DEEP - 5
DEPTH: 9509' 5"

PLATE B:

Digital Whole Core Photographs
Digital Core Chip/Plug Photograph

Figure 21B: Core Plug/Chip Atlas for sample 9509' 5" from Wiriagar Deep-5st.





Sample Depth: 7962' 6"
Shifted Depth: 7972' 6"
MICP Entry Pressure: 730 psia
MICP Threshold Pressure: 8471 psia
Lithology: Shale

WHOLE CORE PLUG ANALYSES
WELL: WIRIAGAR DEEP - 7
DEPTH: 7962' 6"

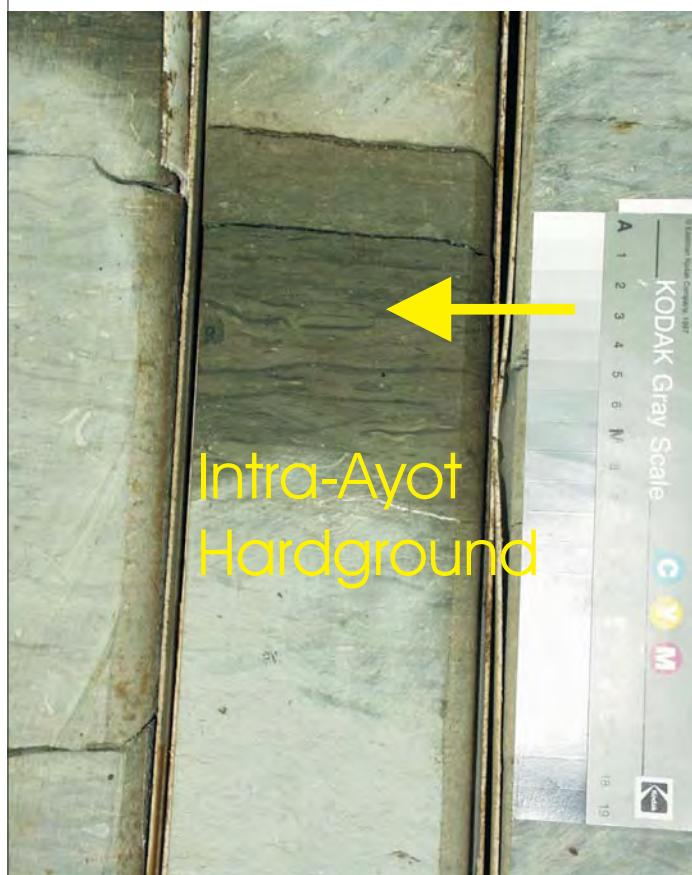
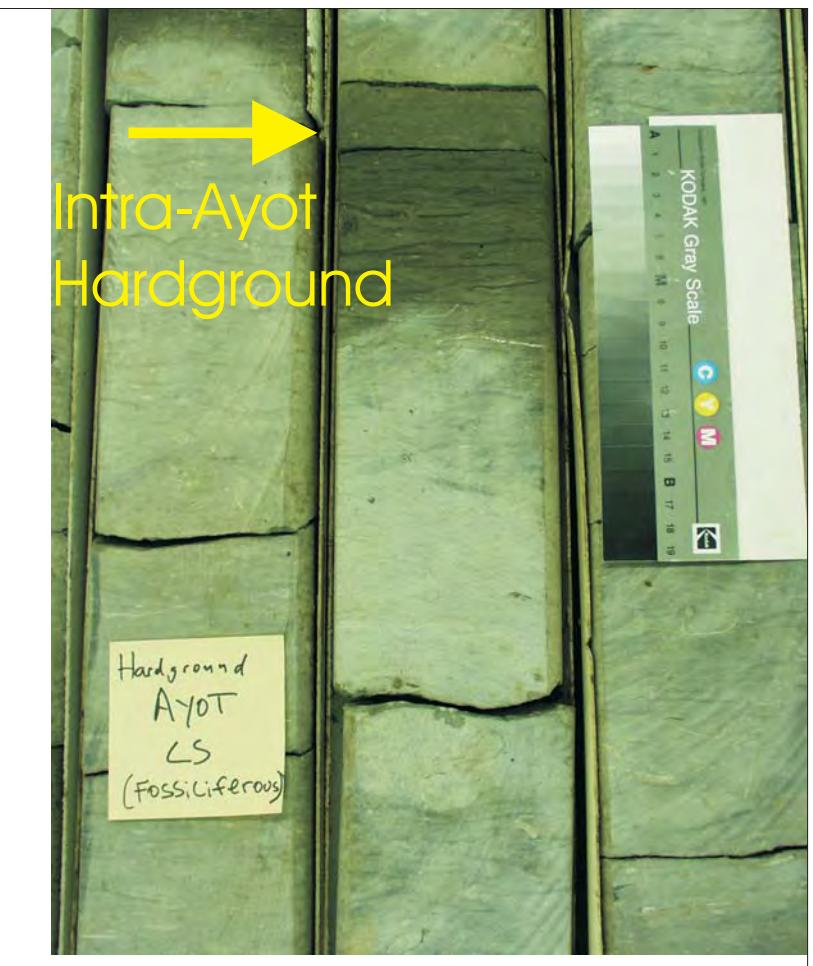
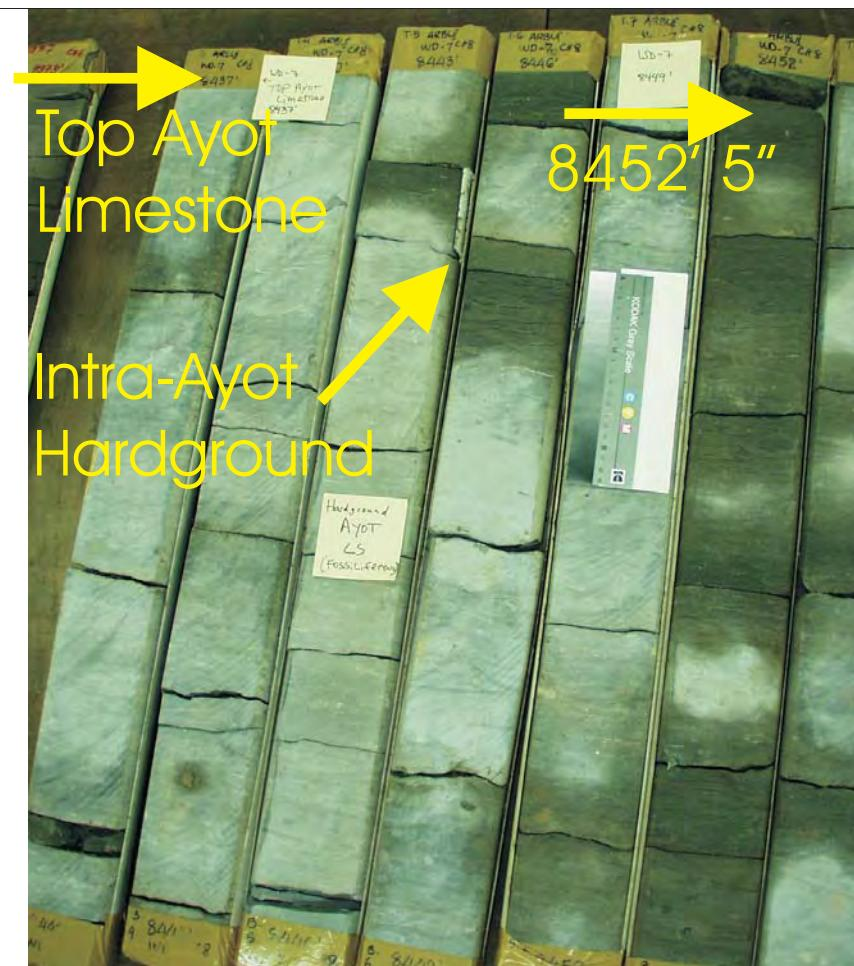
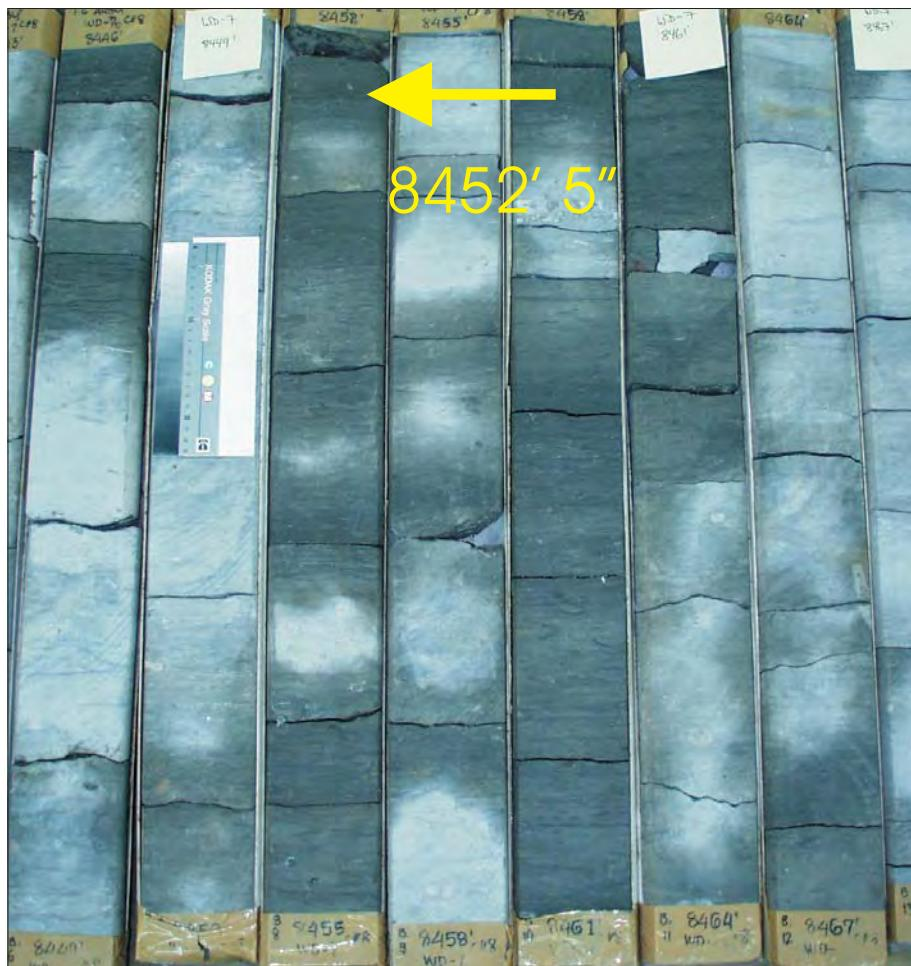
PLATE B:

Digital Core Chip/Plug Photograph
Mercury Injection Capillary Pressure

Figure 22B: Core Plug/Chip Atlas for sample 7962' 6" from Wiriagar Deep-7.



Figure 23A: Core Plug/Chip Atlas for sample 7981' 6" from Wiriagar Deep-7.

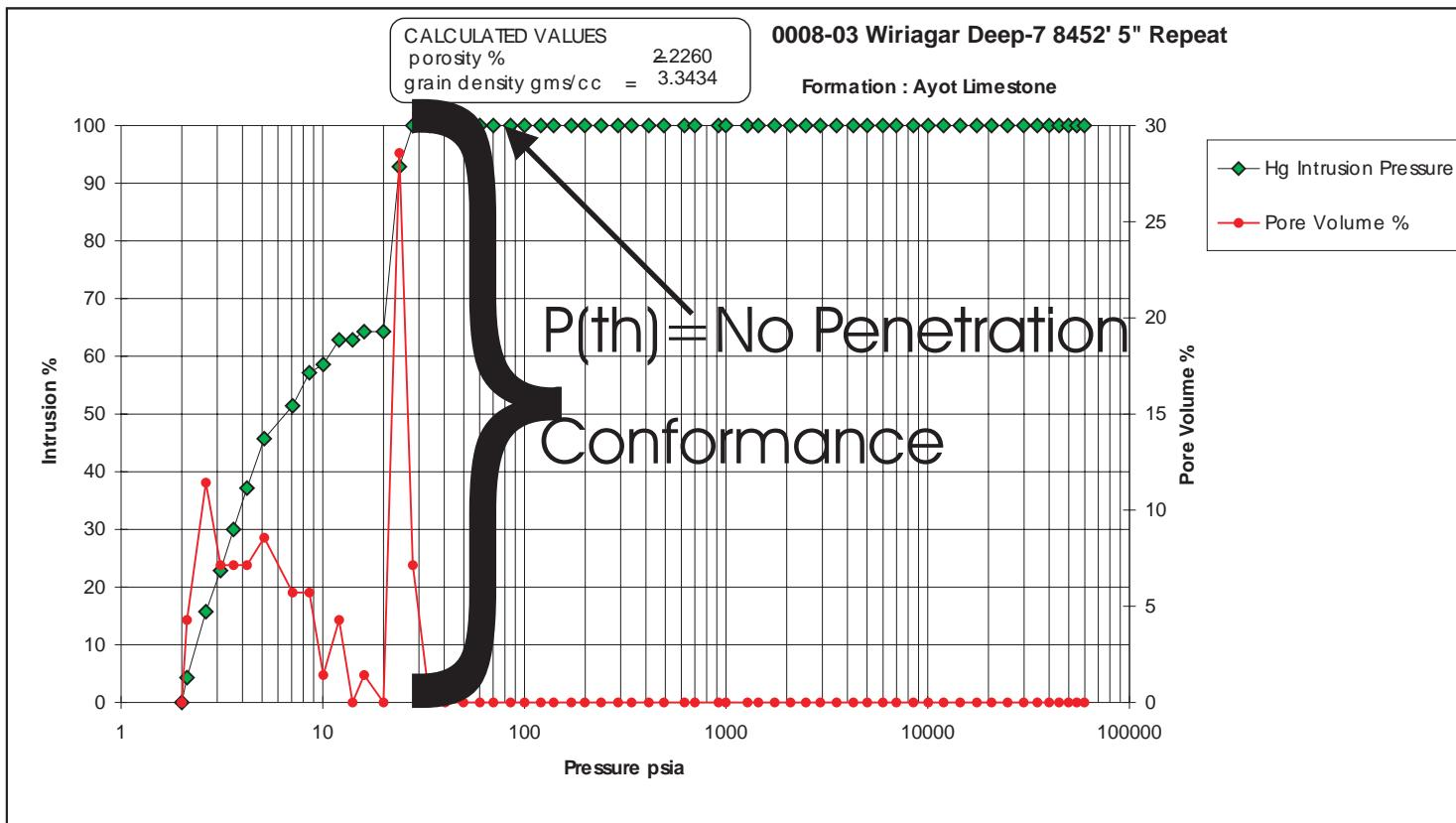
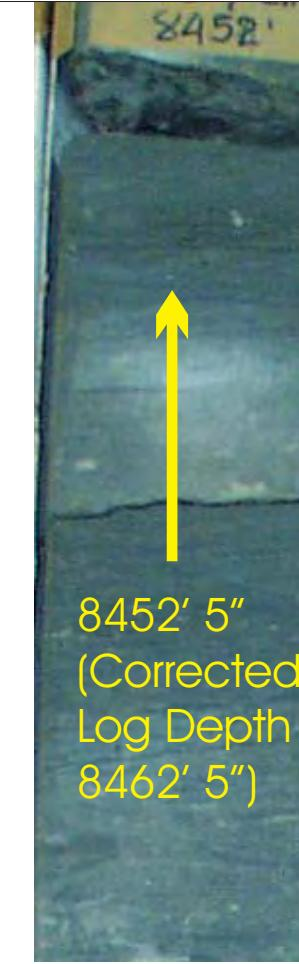
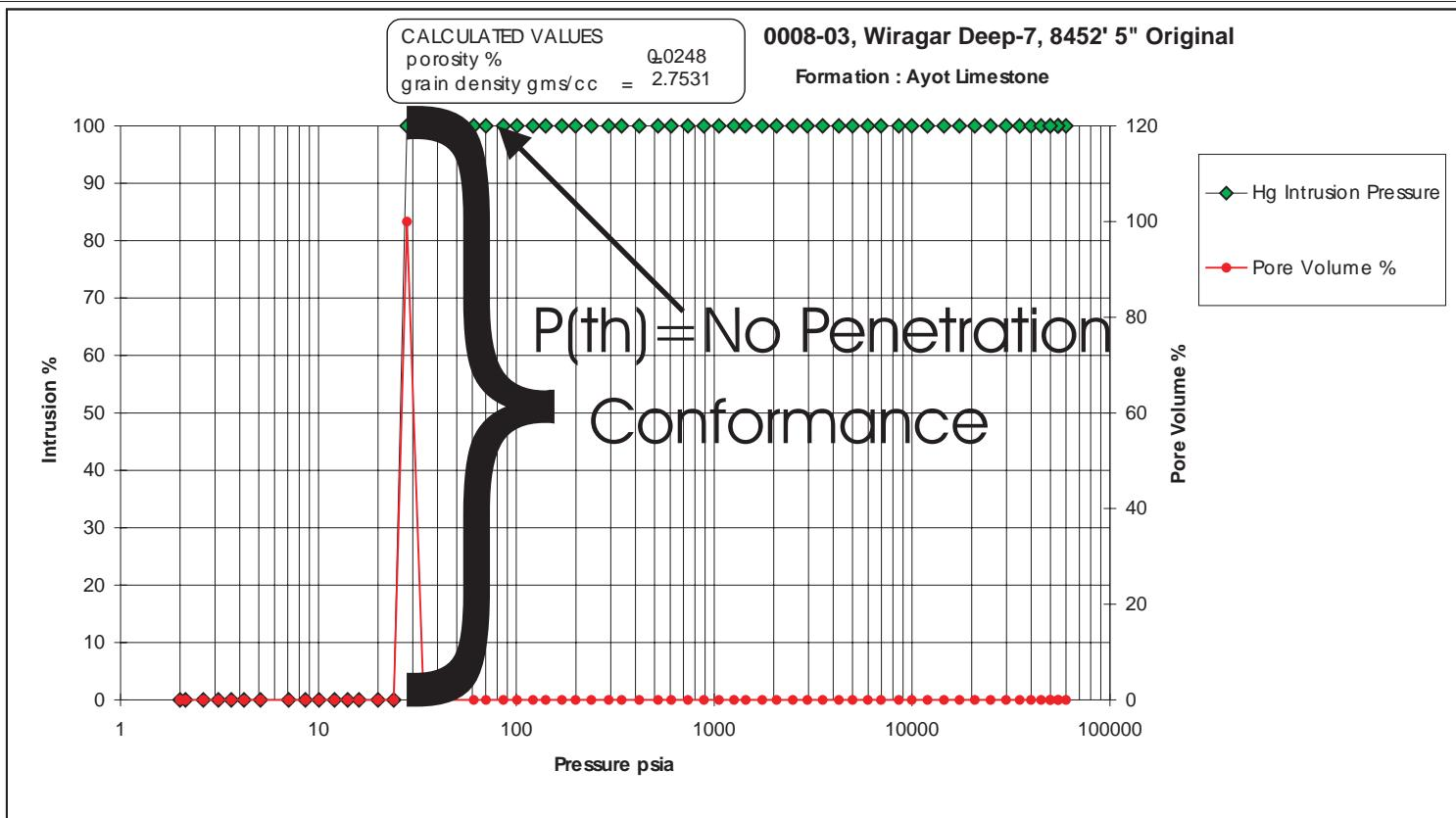


WHOLE CORE PLUG ANALYSES
WELL: WIRIAGAR DEEP - 7
DEPTH: 8452' 5"

PLATE A:

Digital Whole Core Photographs

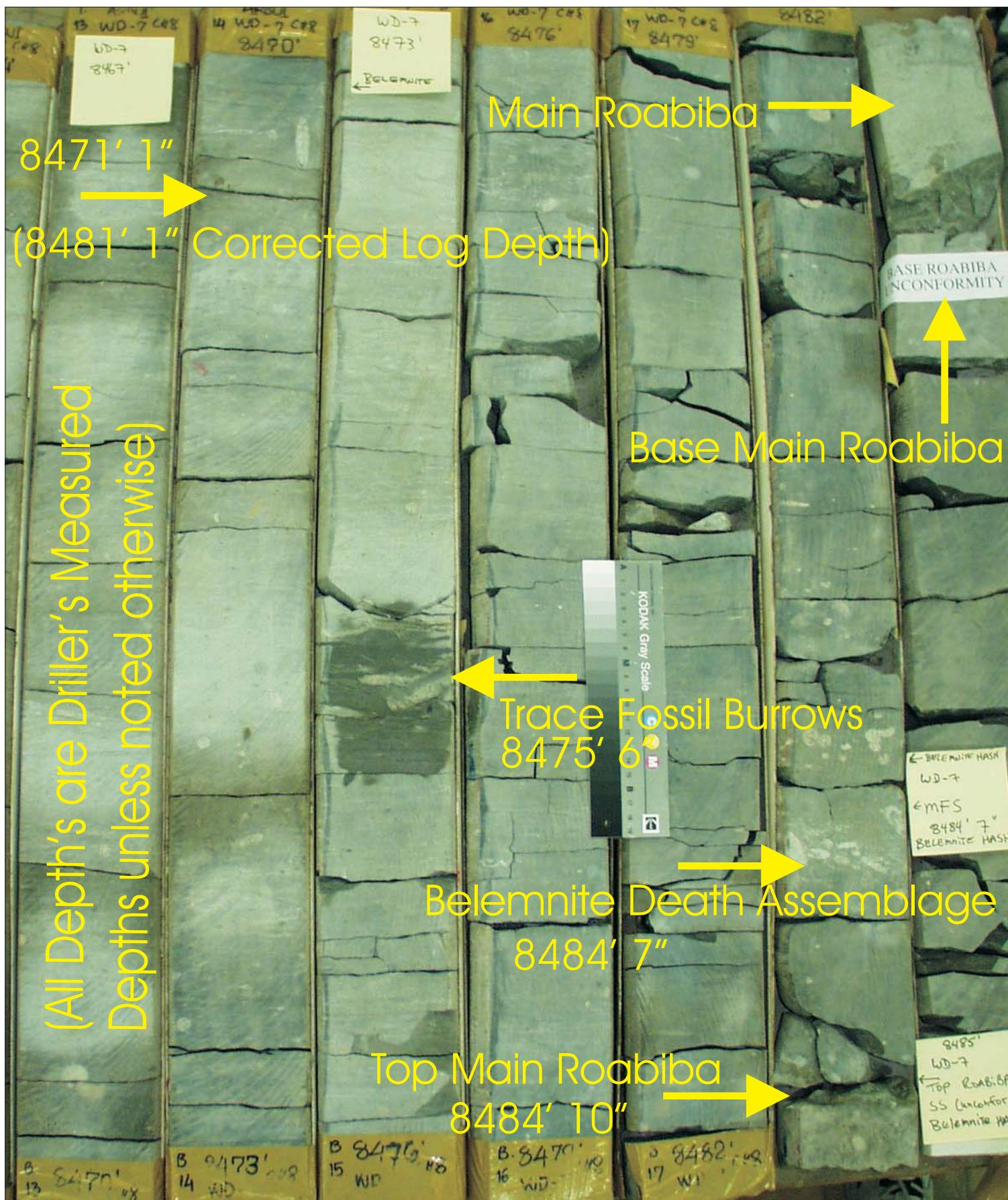
Figure 24A: Core Plug/Chip Atlas for sample 8452' 5" from Wiriagar Deep-7.



Sample Depth: 8452' 5"
Shifted Depth: 8462' 5"
MICP Entry Pressure: No Penetration
MICP Threshold Pressure: No Penetration
Lithology: Limestone

WHOLE CORE PLUG ANALYSES
WELL: WIRIAGAR DEEP - 7
DEPTH: 8452' 5"
PLATE B:
Digital Whole Core Photographs
Digital Core Chip/Plug Photograph
Mercury Injection Capillary Pressure
Mercury Injection Capillary Pr. Rerun

Figure 24B: Core Plug/Chip Atlas for sample 8452' 5" from Wiriagar Deep-7.



WHOLE CORE PLUG ANALYSES
WELL: WIRIAGAR DEEP - 7
DEPTH: 8471' 1"

PLATE A:

Digital Whole Core Photographs

Figure 25A: Core Plug/Chip Atlas for sample 8471' 1" from Wiriagar Deep-7.

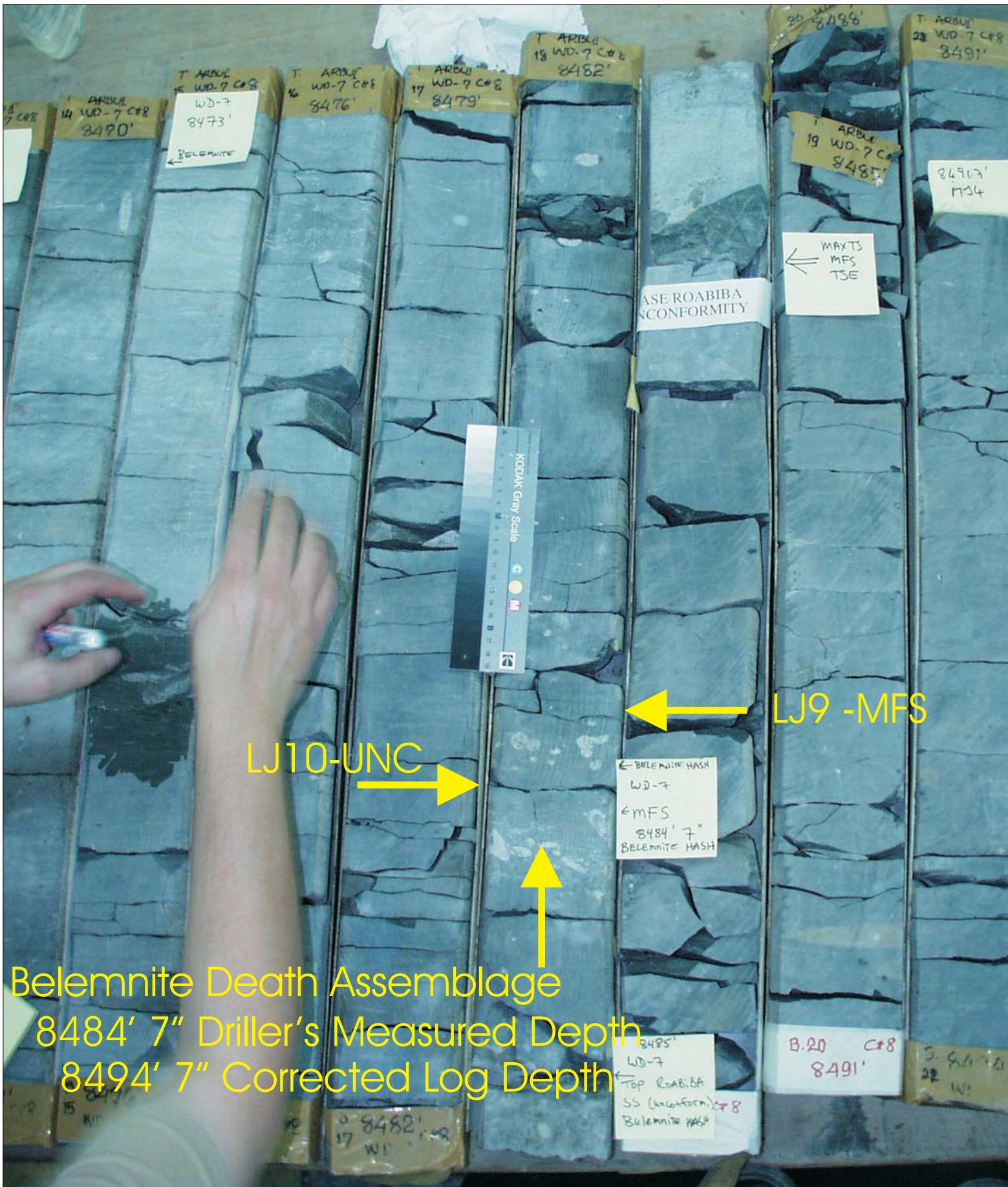
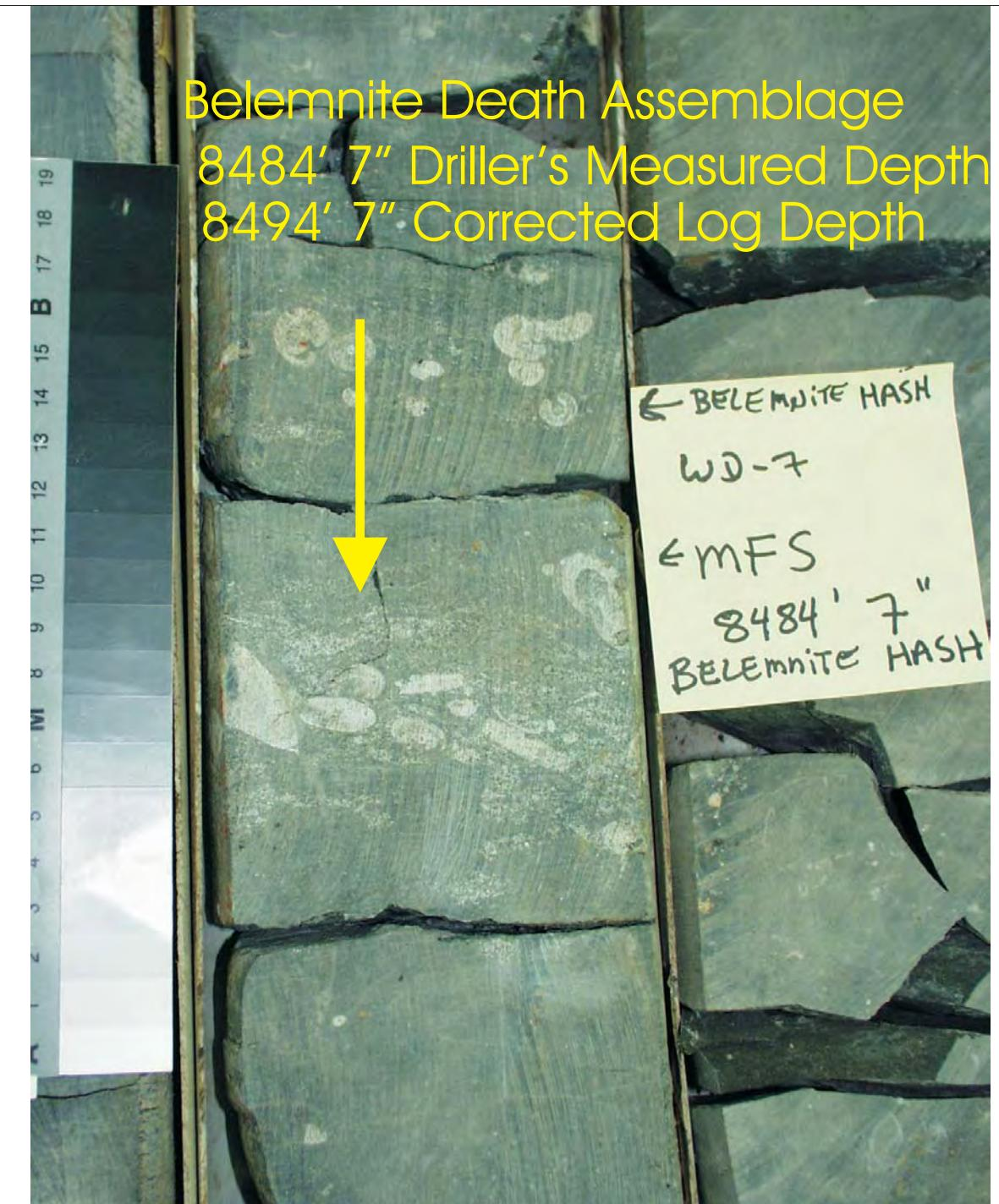


Figure 25B: Core Plug/Chip Atlas for sample 8471' 1" from Wiriagar Deep-7.

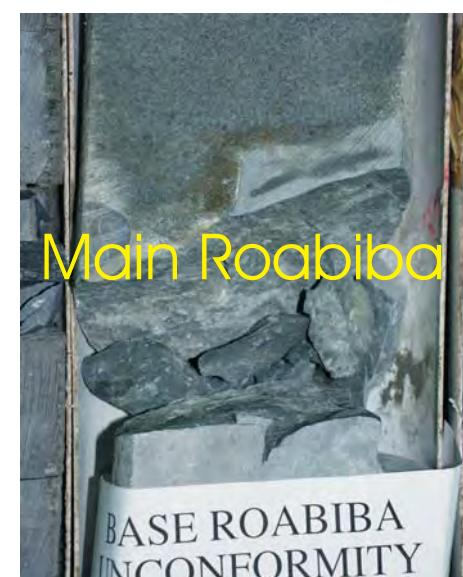
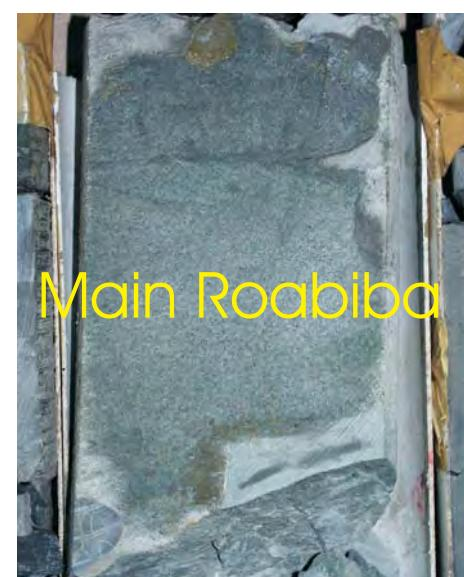
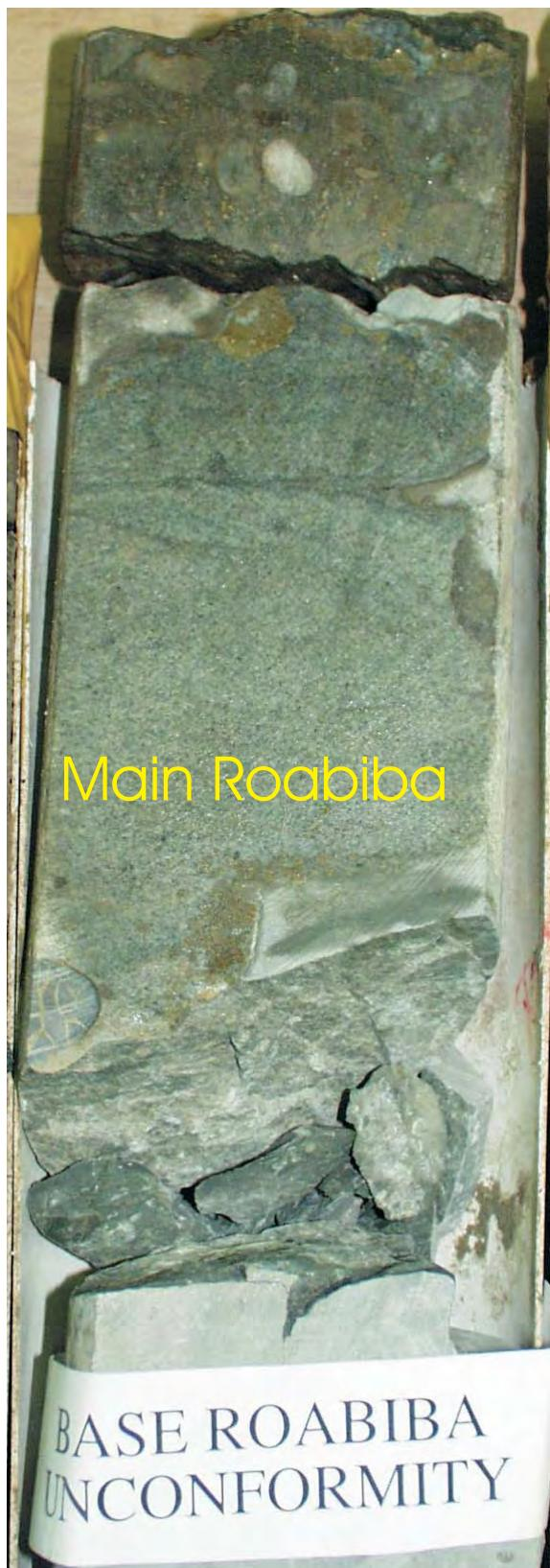
Belemnite Death Assemblage
8484' 7" Driller's Measured Depth
8494' 7" Corrected Log Depth



WHOLE CORE PLUG ANALYSES
WELL: WIRIAGAR DEEP - 7
DEPTH: 8471' 1"

PLATE B:

Digital Whole Core Photographs

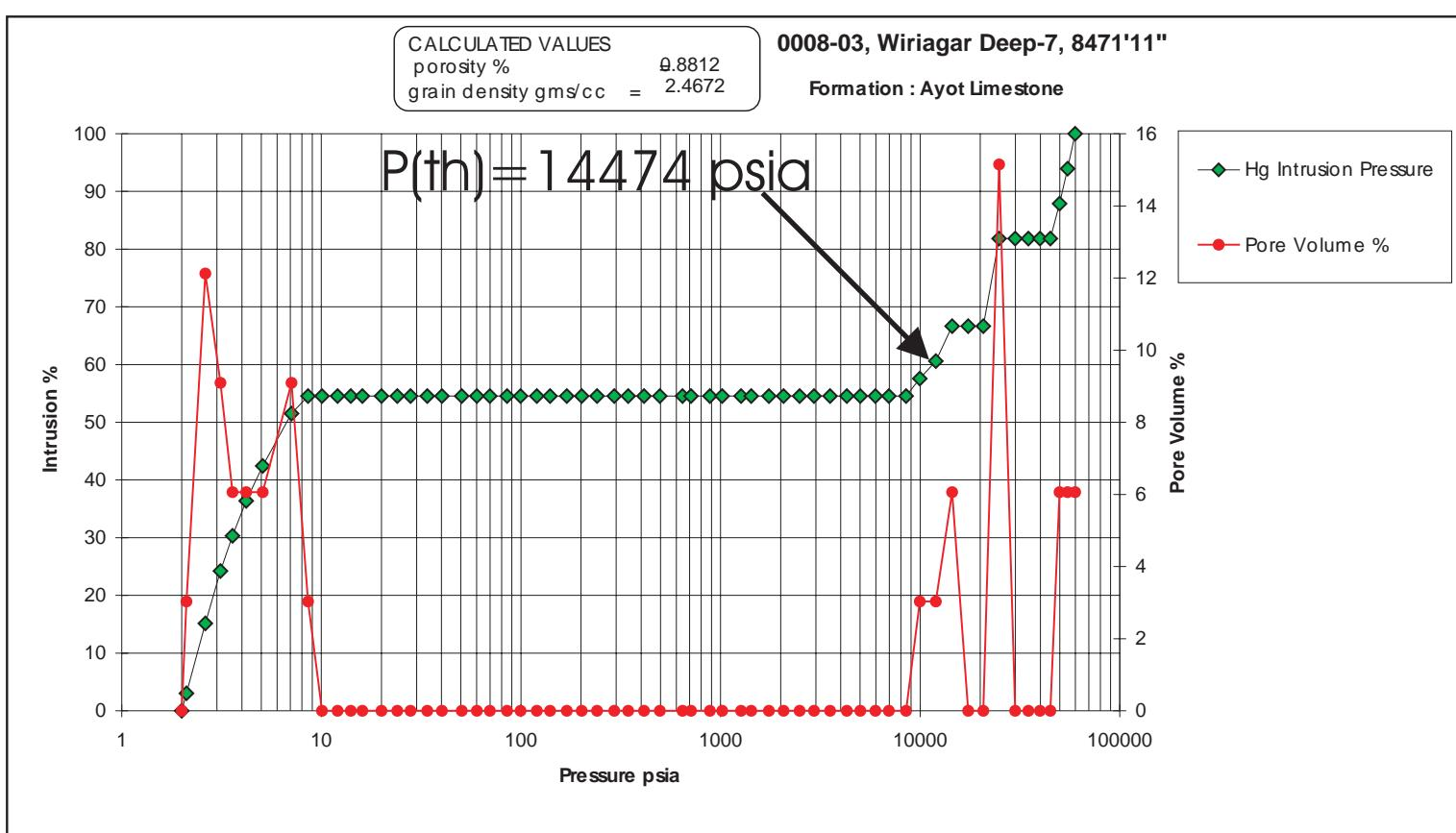
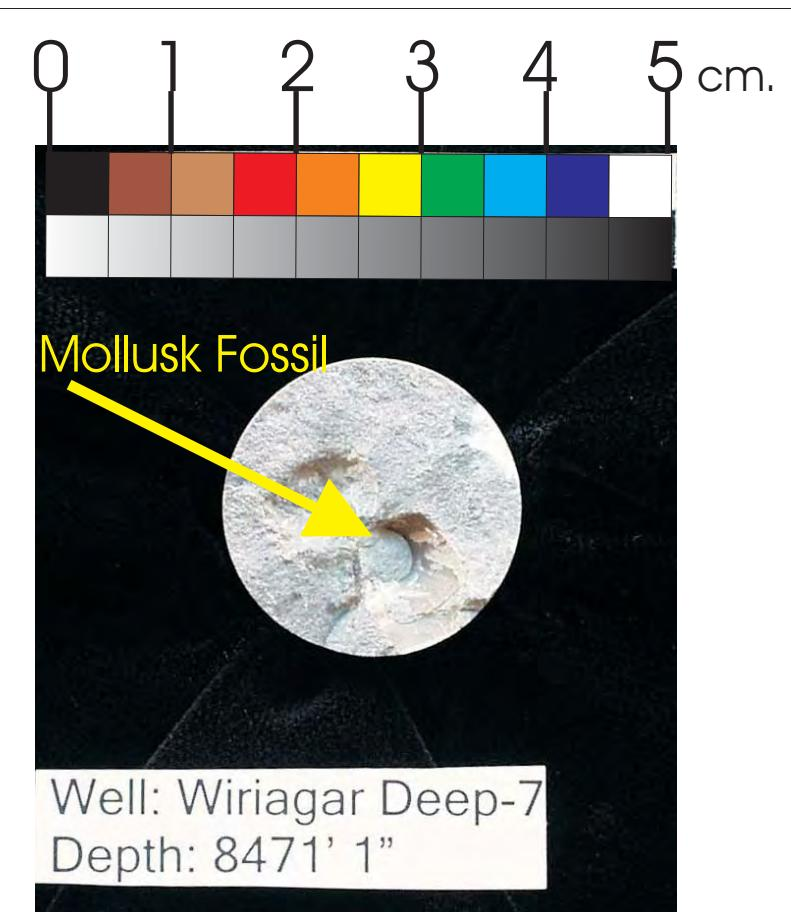
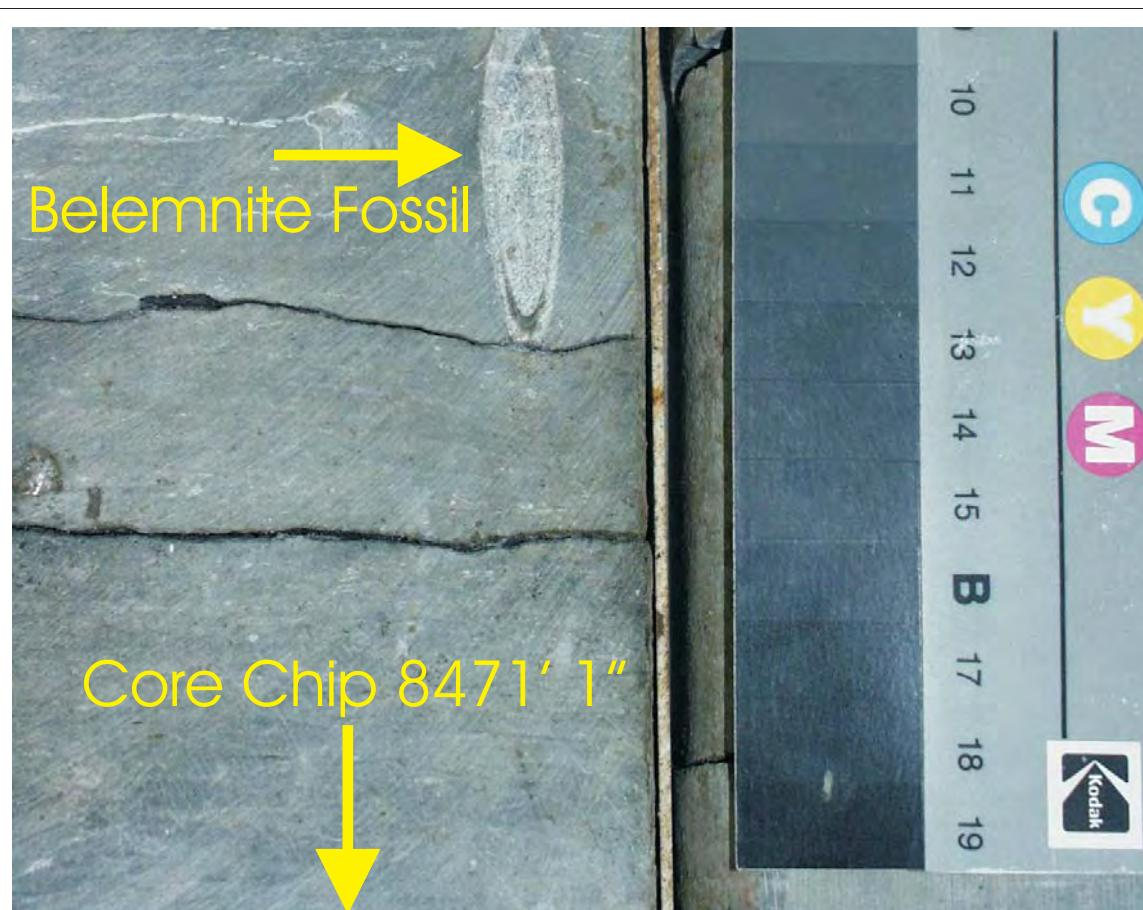


WHOLE CORE PLUG ANALYSES
WELL: WIRIAGAR DEEP - 7
DEPTH: 8471' 1"

PLATE C:

Digital Whole Core Photographs

Figure 25C: Core Plug/Chip Atlas for sample 8471' 1" from Wiriagar Deep-7.

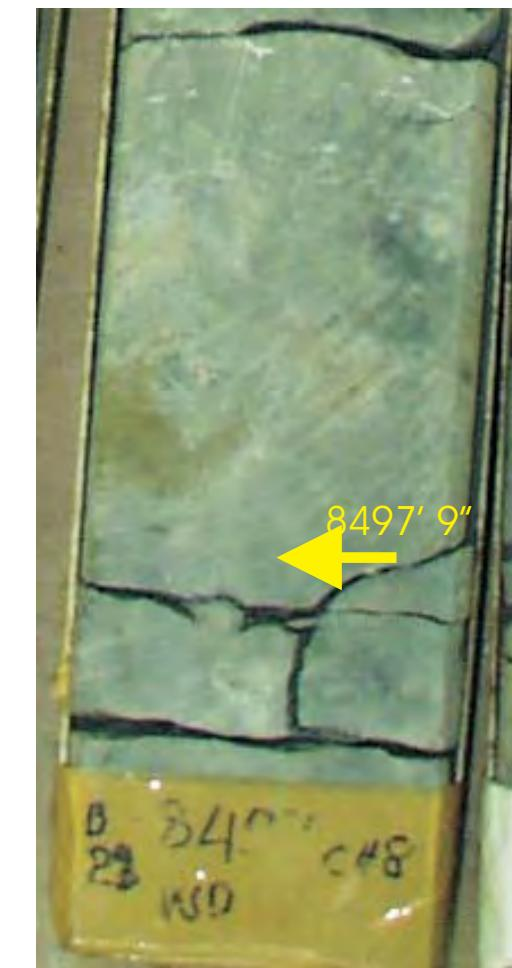
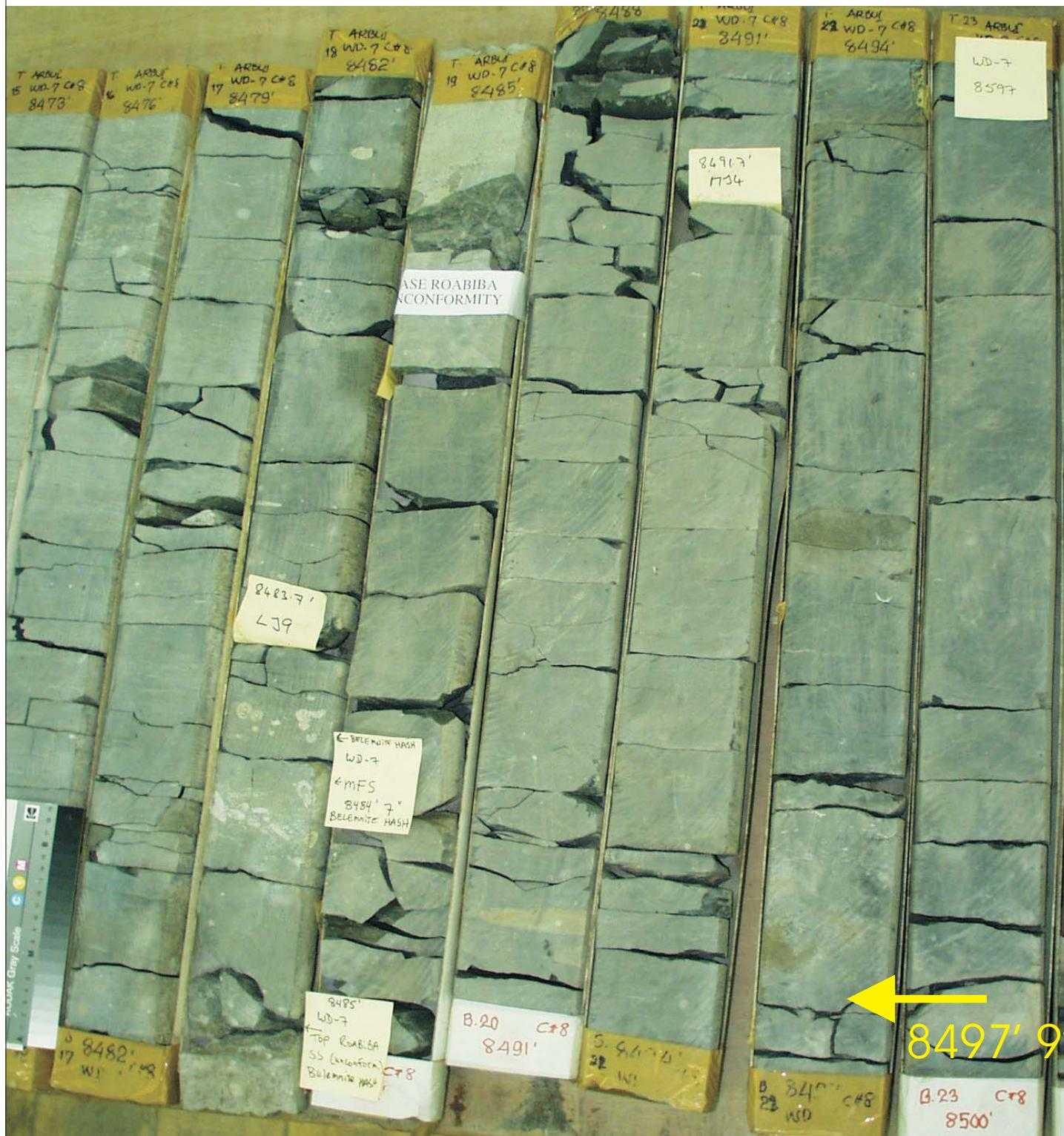


Sample Depth: 8471' 1"
Shifted Depth: 8481' 1"
MICP Entry Pressure: 8507 psia
MICP Threshold Pressure: 14474 psia
Lithology: Limestone/Marl

WHOLE CORE PLUG ANALYSES
WELL: WIRIAGAR DEEP - 7
DEPTH: 8471' 1"

PLATE D:
Digital Whole Core Photographs
Digital Core Chip/Plug Photograph
Mercury Capillary Pressure

Figure 25D: Core Plug/Chip Atlas for sample 8471' 1" from Wiriagar Deep-7.

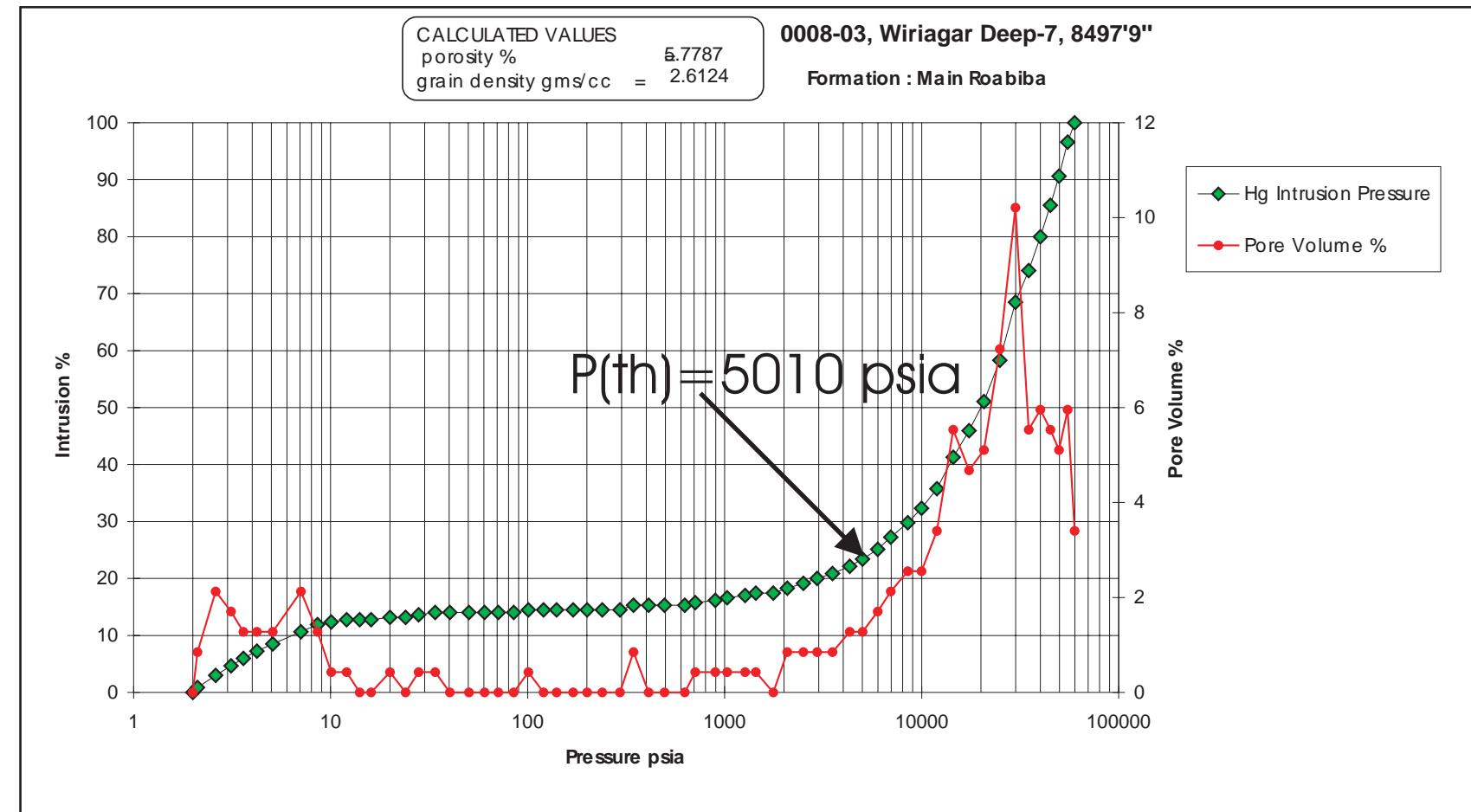
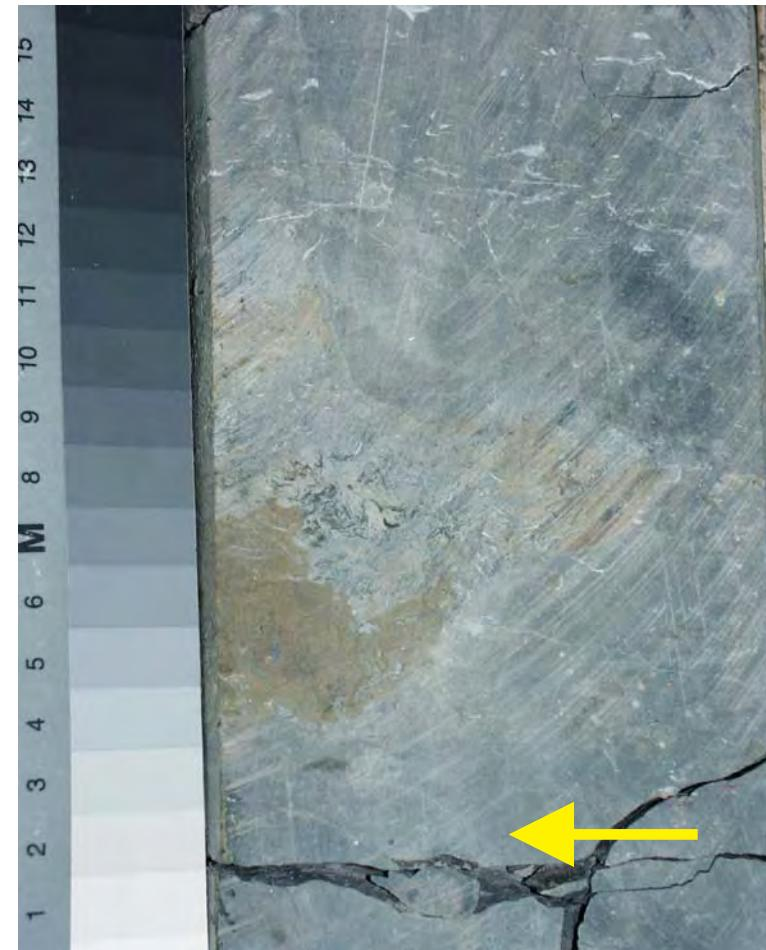


WHOLE CORE PLUG ANALYSES
WELL: WIRIAGAR DEEP - 7
DEPTH: 8497' 9"

PLATE A:

Digital Whole Core Photographs

Figure 26A: Core Plug/Chip Atlas for sample 8497' 9" from Wiriagar Deep-7.



Sample Depth: 8497' 9"
Shifted Depth: 8507' 9"
MICP Entry Pressure: 1029 psia
MICP Threshold Pressure: 5010 psia
Lithology: Shale

WHOLE CORE PLUG ANALYSES
WELL: WIRIAGAR DEEP - 7
DEPTH: 8497' 9"

PLATE B:
Digital Whole Core Photographs
Digital Core Chip/Plug Photograph
Mercury Injection Capillary Pressure

Figure 26B: Core Plug/Chip Atlas for sample 8497' 9" from Wiriagar Deep-7.



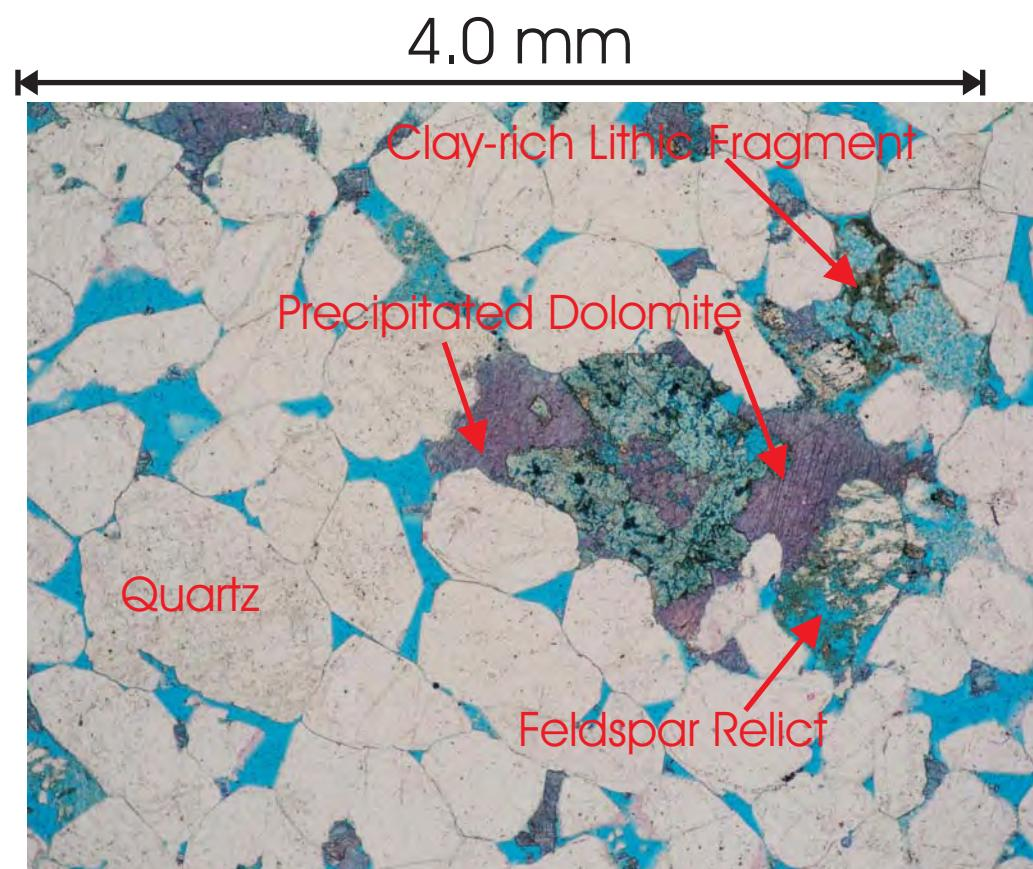
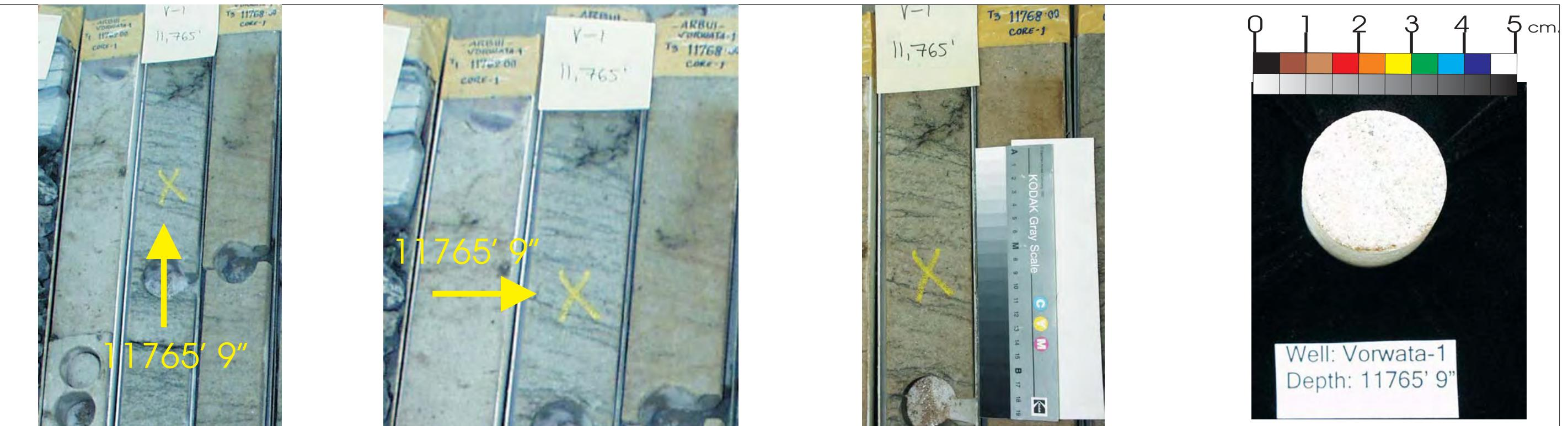
Sample Depth: 8524' 7"
Shifted Depth: 8534' 7"
He-Ø: 19%
k air: 2264 mD (sc)

WHOLE CORE PLUG ANALYSES
WELL: WIRIAGAR DEEP - 7
DEPTH: 8524' 7"

PLATE A:

Digital Whole Core Photographs
Digital Core Chip/Plug Photograph

Figure 27A: Core Plug/Chip Atlas for sample 8524' 7" from Wiriagar Deep-7.

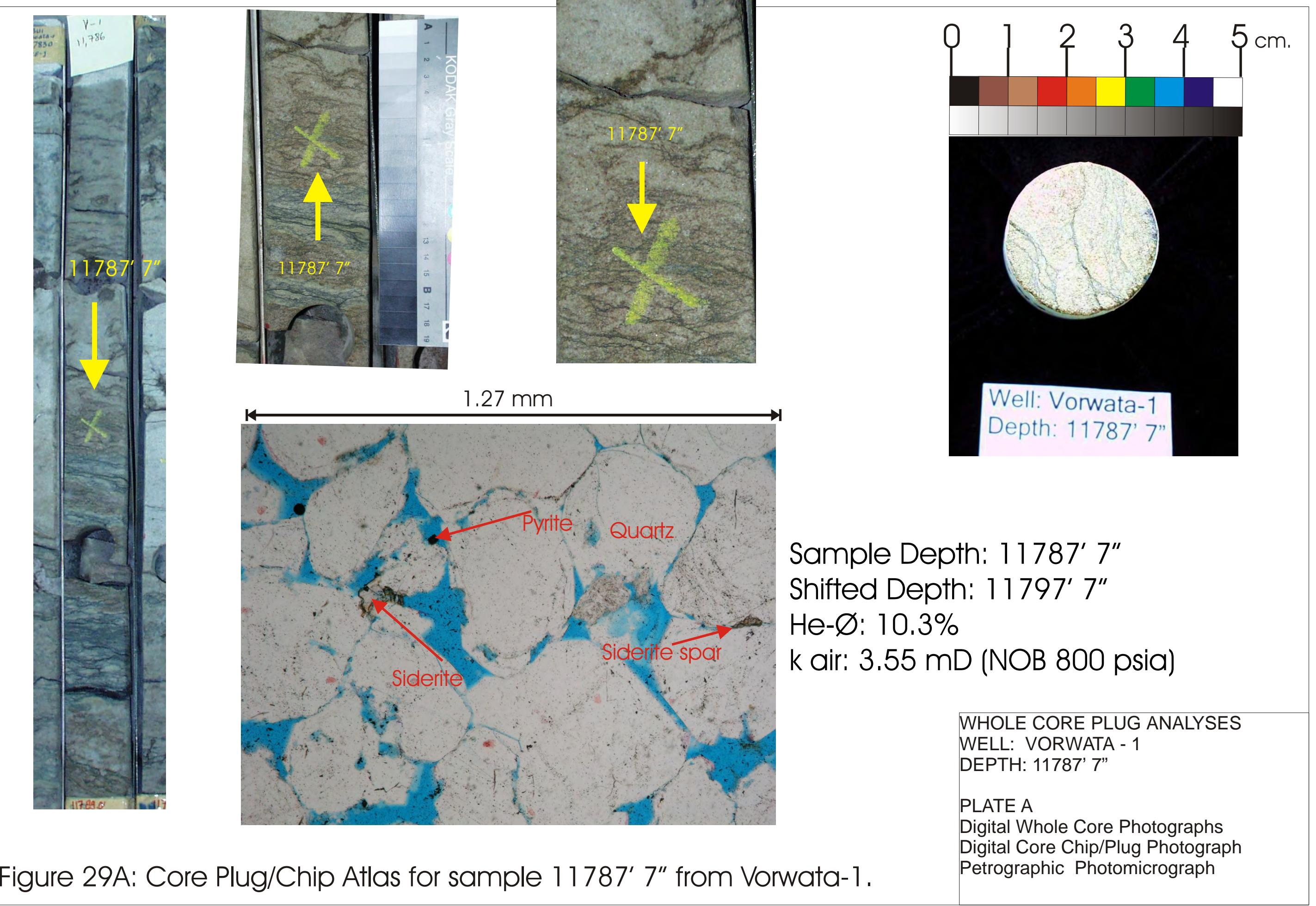


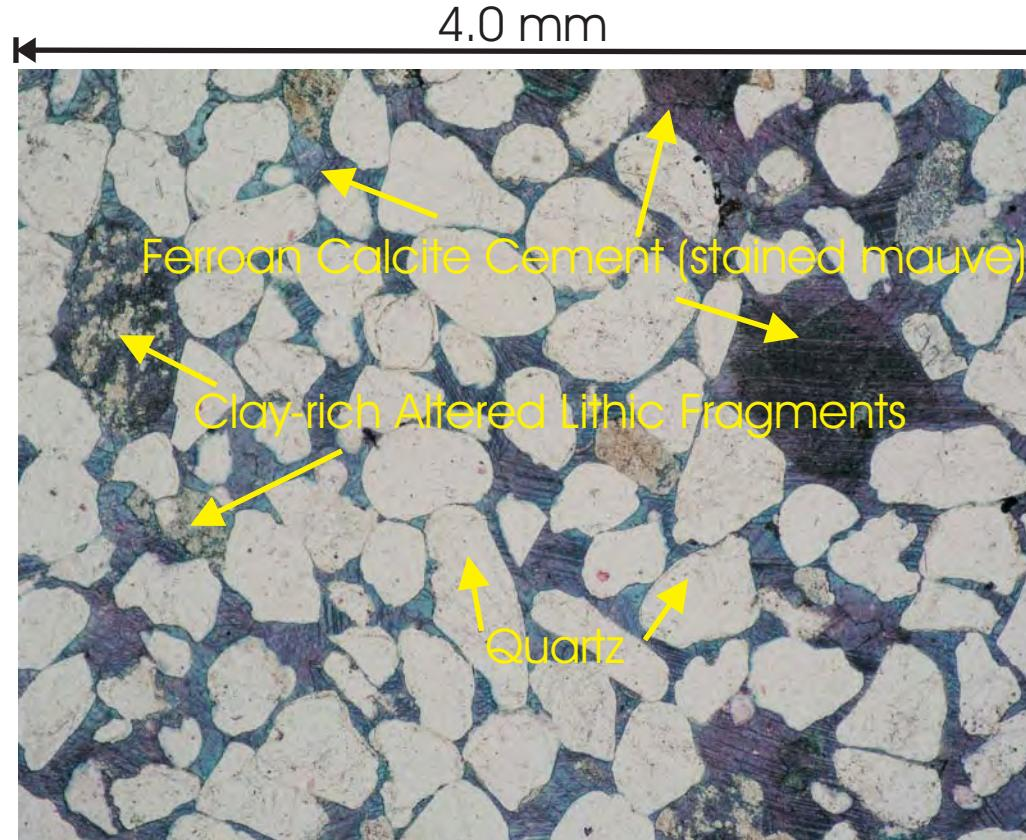
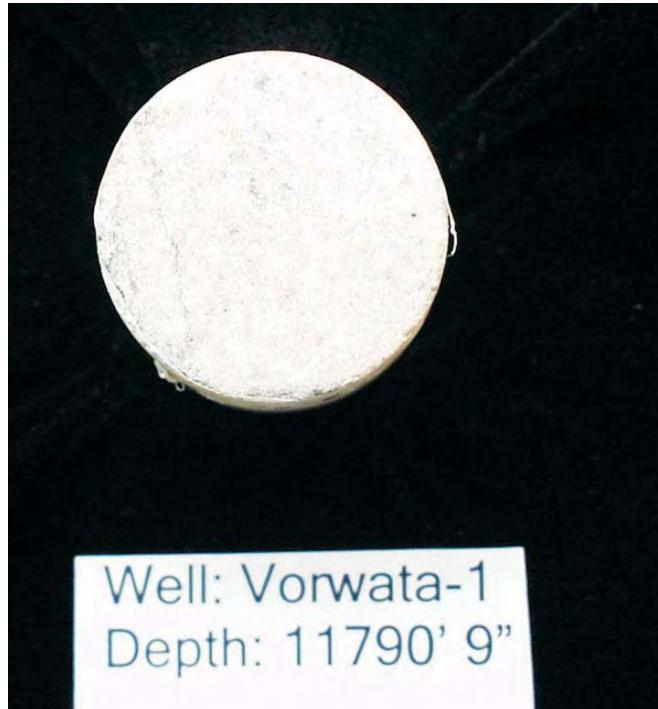
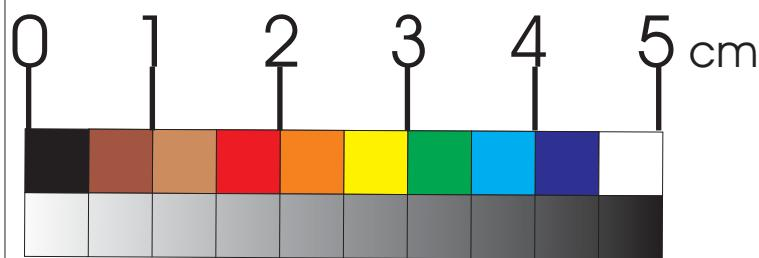
Sample Depth: 11765' 9"
Shifted Depth: 11775' 9"
He-Ø: 11.2%
k air: 150 mD (NOB 800 psia)

WHOLE CORE PLUG ANALYSES
WELL: VORWATA - 1
DEPTH: 11765' 9"

PLATE A
Digital Whole Core Photographs
Digital Core Chip/Plug Photograph
Petrographic Photomicrograph

Figure 28A: Core Plug/Chip Atlas for sample 11765' 9" from Vorwata-1.





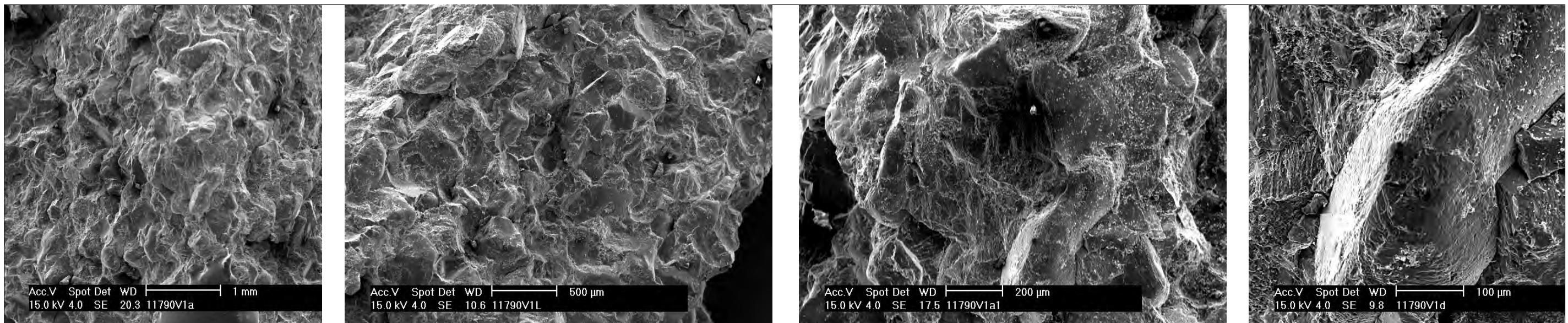
11790' 9"

Sample Depth: 11790' 9"
Shifted Depth: 11800' 9"
He-Ø: 2.5%
k air: 0.05 mD (NOB 800 psia)

WHOLE CORE PLUG ANALYSES
WELL: VORWATA - 1
DEPTH: 11790' 9"

PLATE A:
Digital Whole Core Photographs
Digital Core Chip/Plug Photograph
Petrographic Photomicrograph

Figure 30A: Core Plug/Chip Atlas for sample 11790' 9" from Vorwata-1.



SEM images showing poikilotopic Ferroan Calcite grains precipitated between Quartz grains, and occasionally replacing Clays/Feldspars.

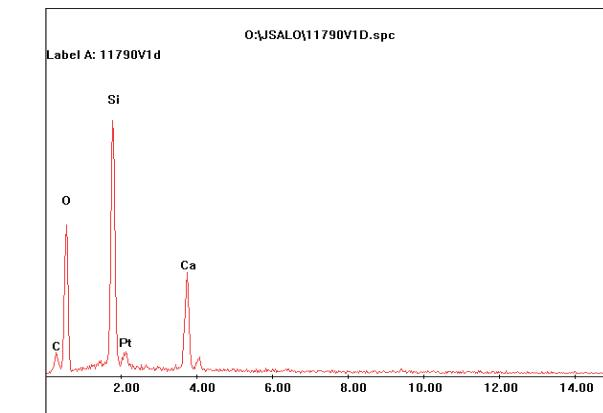
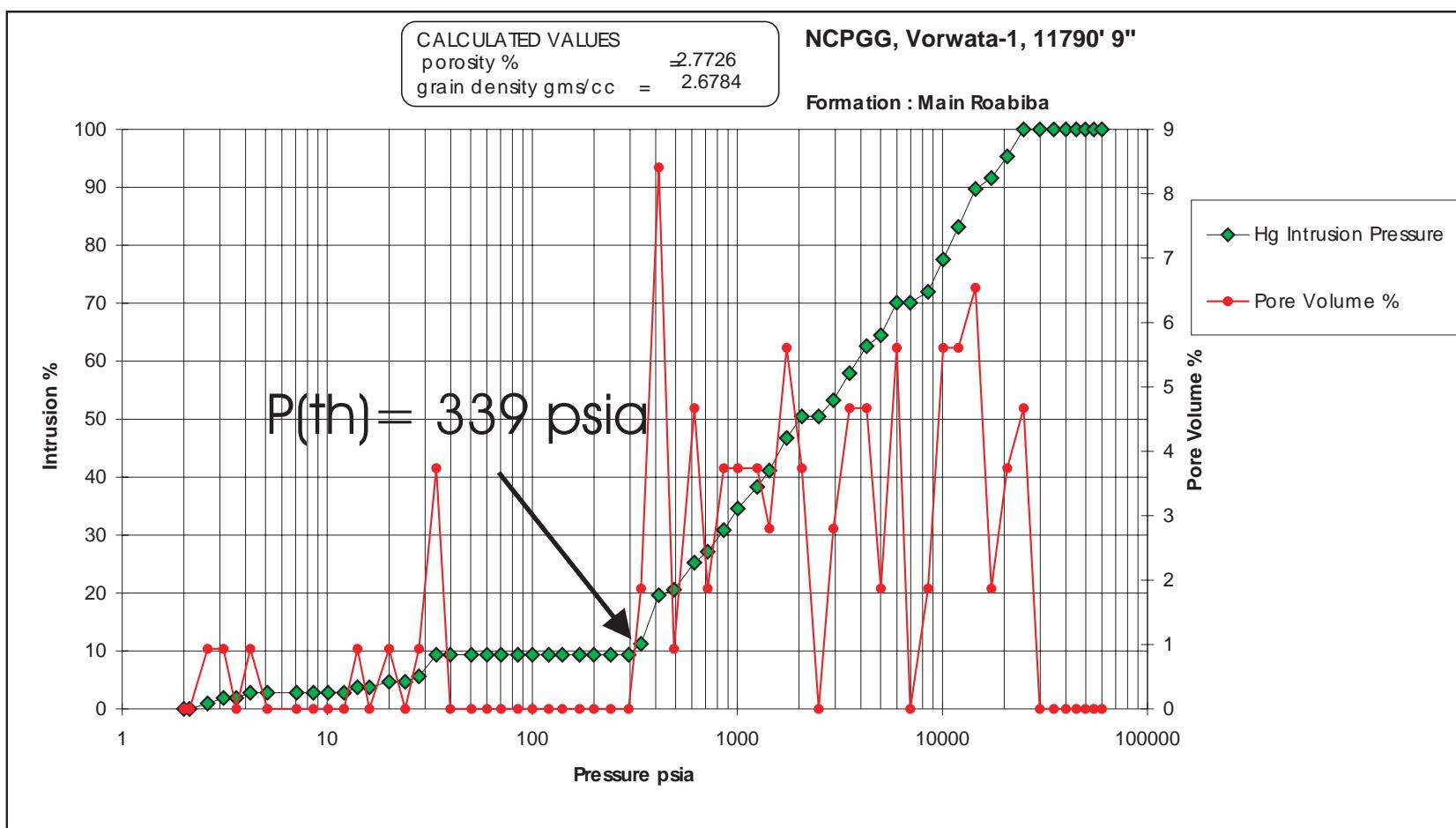
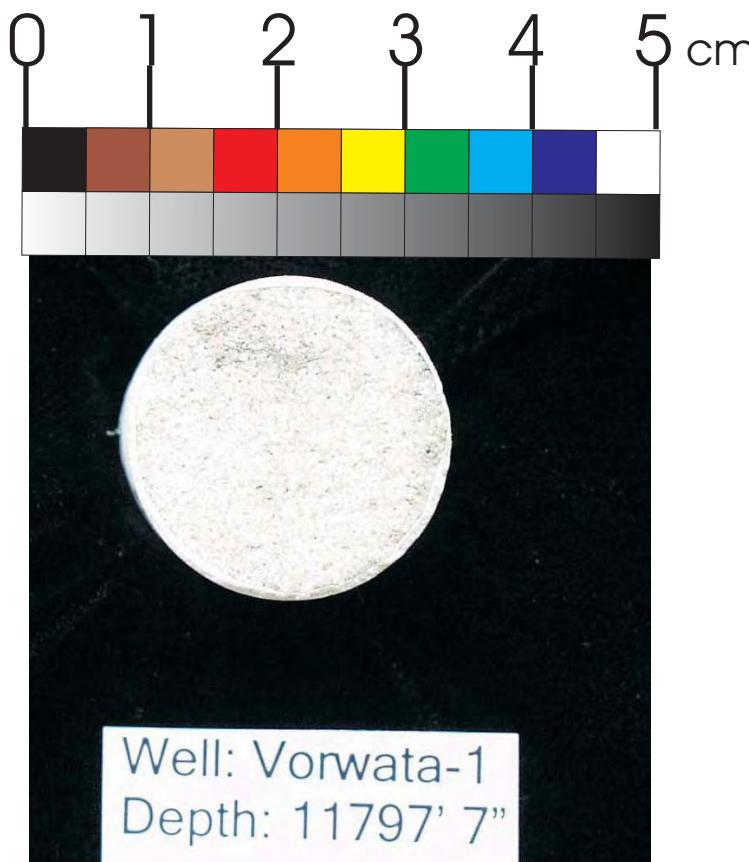
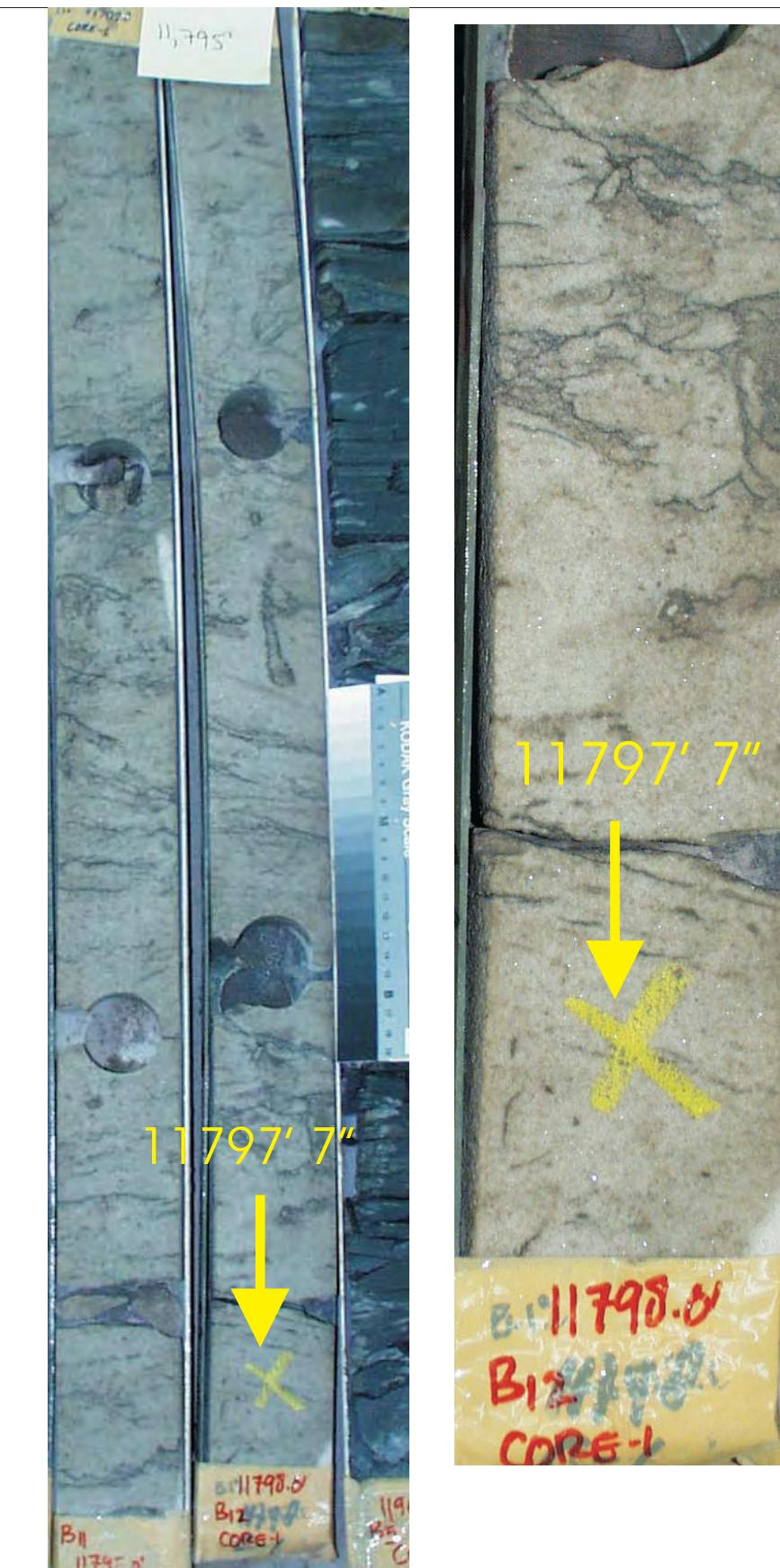
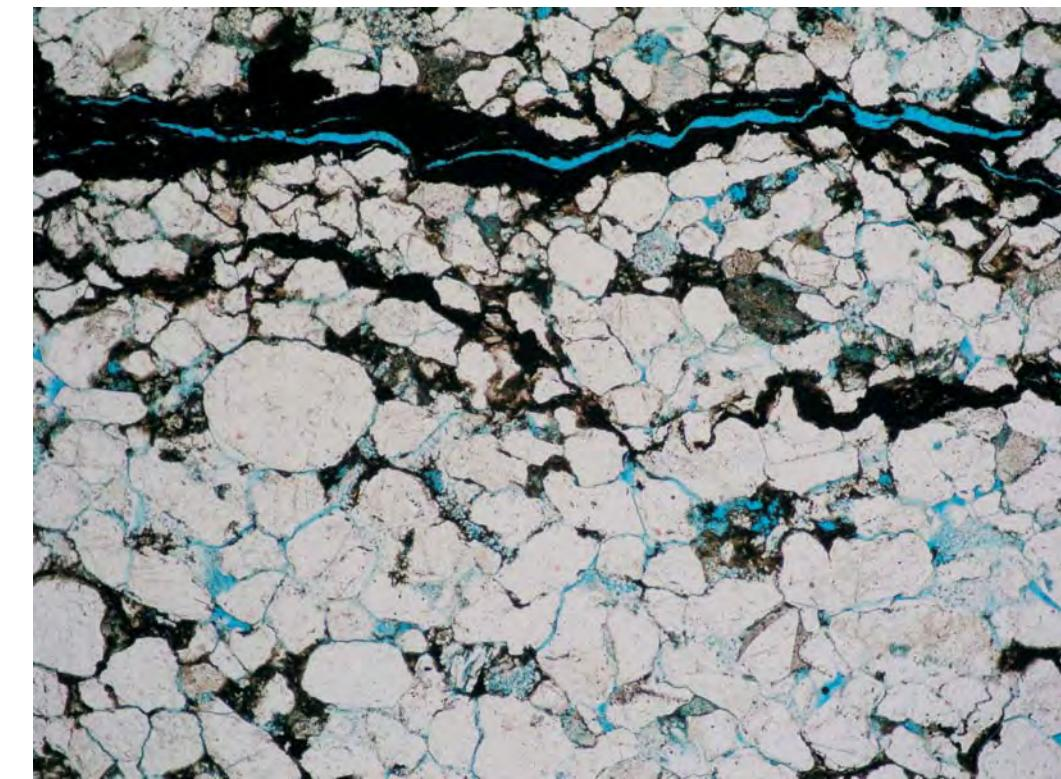


Figure 30B: Core Plug/Chip Atlas for sample 11790' 9" from Vorwata-1.



Sample Depth: 11797' 7"
 Shifted Depth: 11807' 7"
 $\text{He-}\emptyset$: 13.5%
 k_{air} : 137 mD (NOB 800 psia)



Sublitharenite from the Roabiba Reservoir composed of Quartz, K-Feldspar, and lithic fragments including chalcedony, chert, granite, volcanics, siltsone, quartzite, and micaceous schist. Bent/ altered muscovite and biotite, plus tourmaline and zircons are also present. Clays and micrite have in-filled burrows and pores, with large burrow in-fill visible at top of image. Open fracture was probably induced during sampling.

WHOLE CORE PLUG ANALYSES

WELL: VORWATA - 1

DEPTH: 11797' 7"

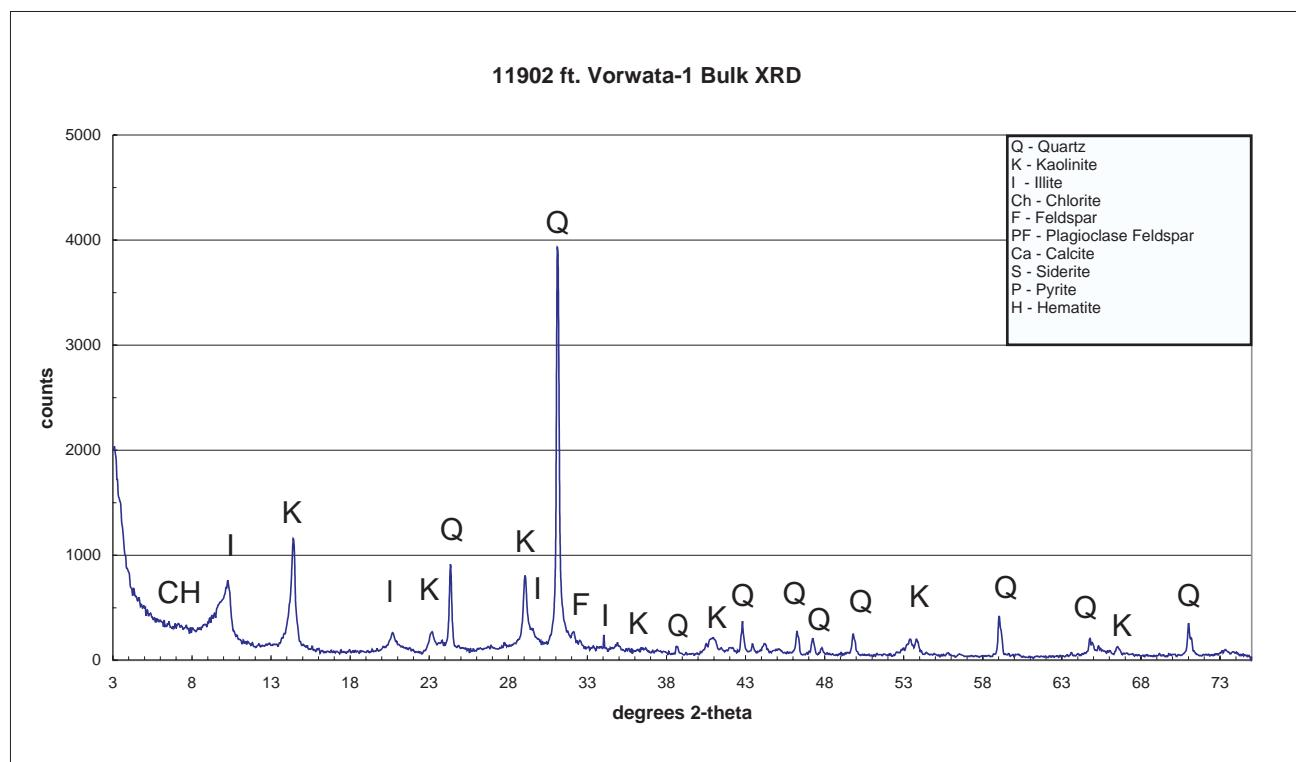
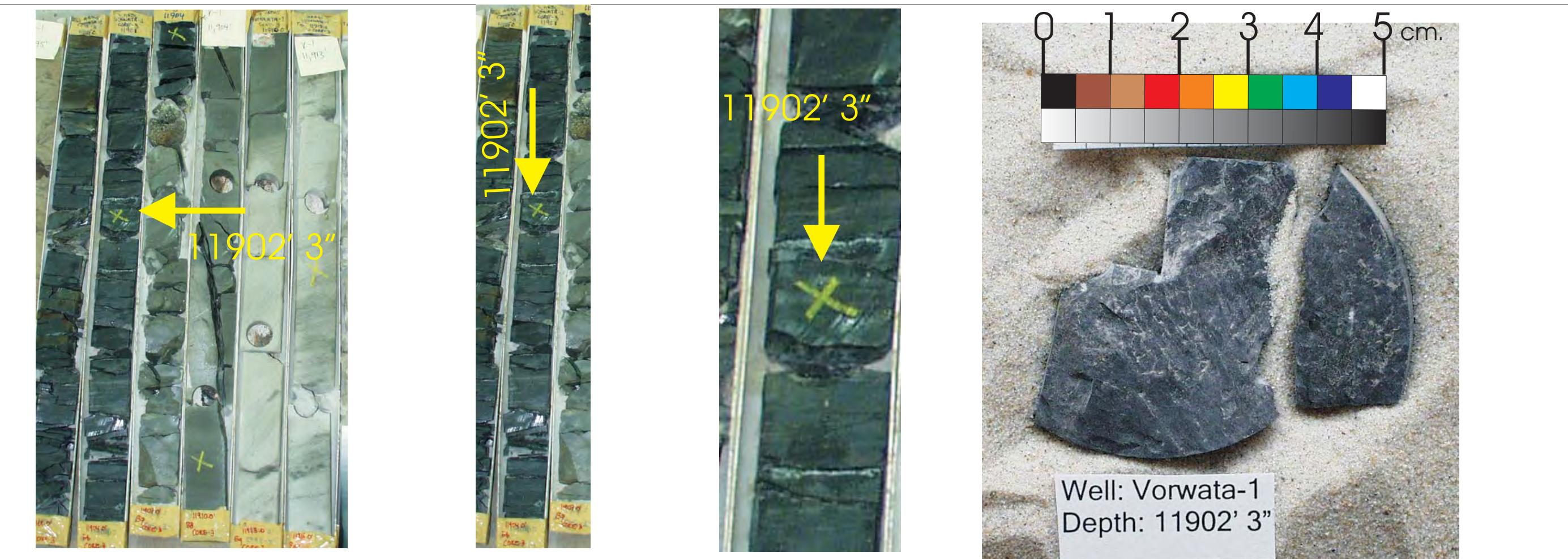
PLATE A:

Digital Whole Core Photographs

Digital Core Chip/Plug Photograph

Petrographic Photomicrograph

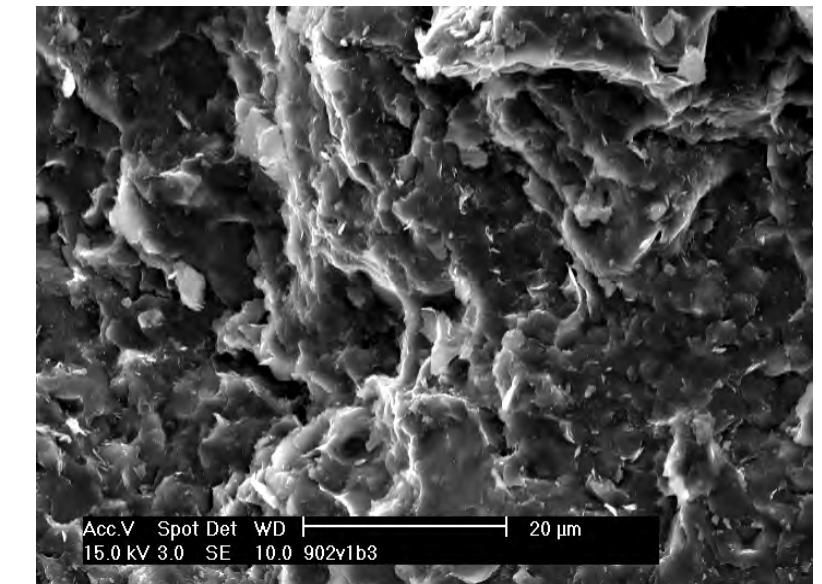
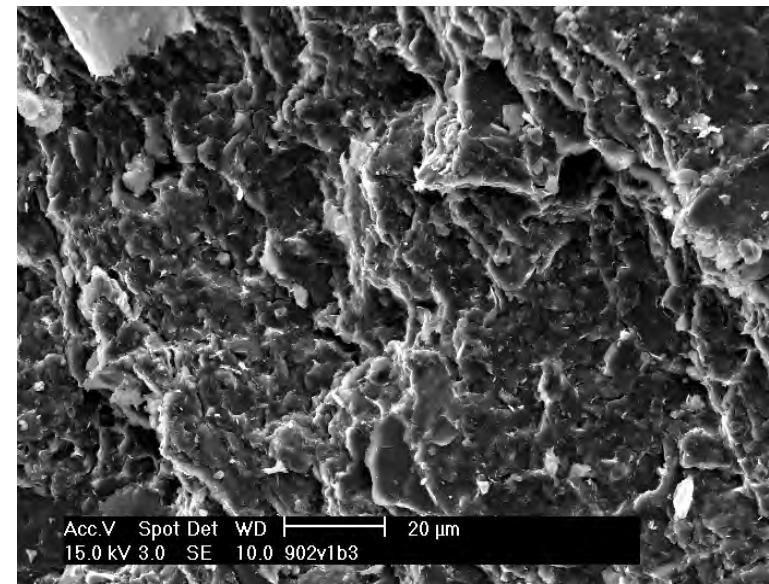
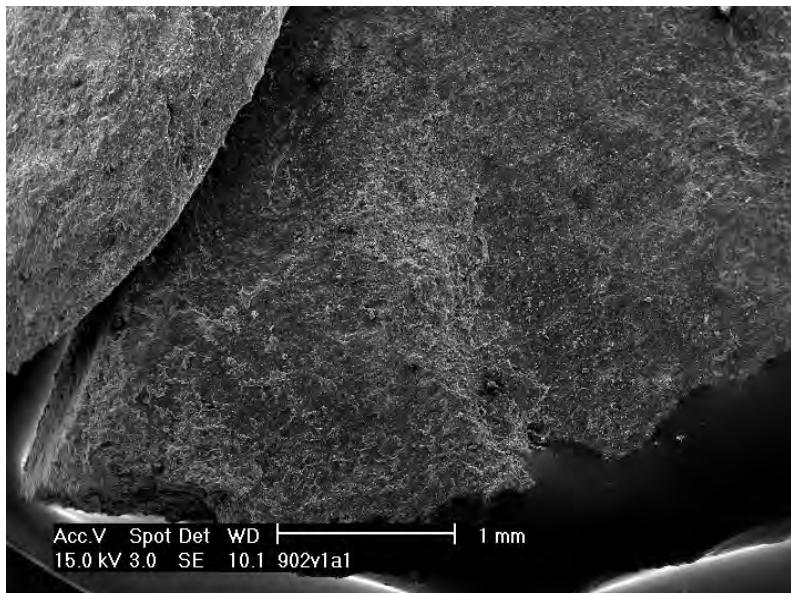
Figure 31A: Core Plug/Chip Atlas for sample 11797' 7" from Vorwata-1.



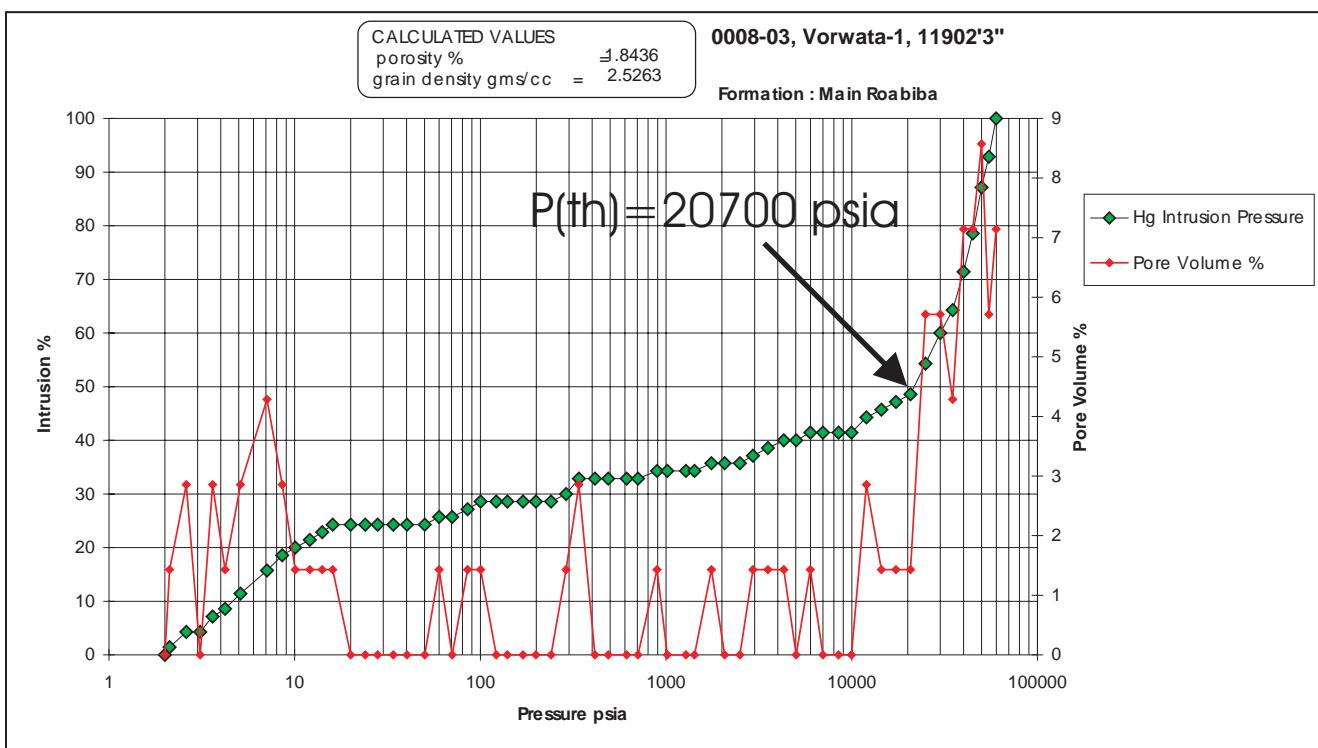
WHOLE CORE PLUG ANALYSES
WELL: VORWATA - 1
DEPTH: 11902' 3"

PLATE A
Digital Whole Core Photographs
Digital Core Chip/Plug Photograph
Bulk X-Ray Diffraction (XRD)

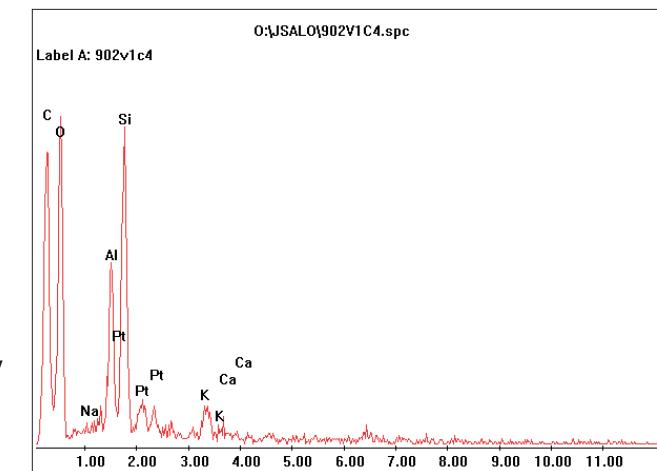
Figure 32A: Core Plug/Chip Atlas for sample 11902' 3" from Vorwata-1.



SEM images and EDX analysis show the shale core sample composed primarily of illitic and smectitic clays, quartz silts, and carbonate minerals. No porosity is visible under SEM magnification.



Sample Depth: 11902' 3"
Shifted Depth: 11912' 3"
MICP Entry Pressure: 339 psia
MICP Threshold Pressure: 20700 psia
Lithology: Shale



WHOLE CORE PLUG ANALYSES
WELL: VORWATA - 1
DEPTH: 11902' 3"

PLATE B
FESEM Photomicrograph
FESEM EDX (SEM XRD)
Mercury Injection Capillary Pressure

Figure 32B: Core Plug/Chip Atlas for sample 11902' 3" from Vorwata-1.

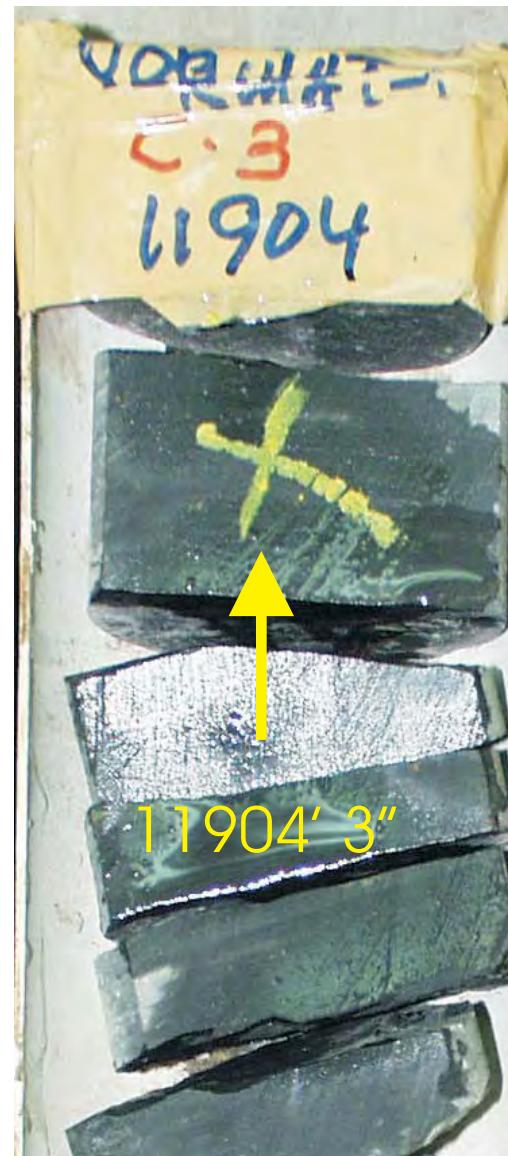
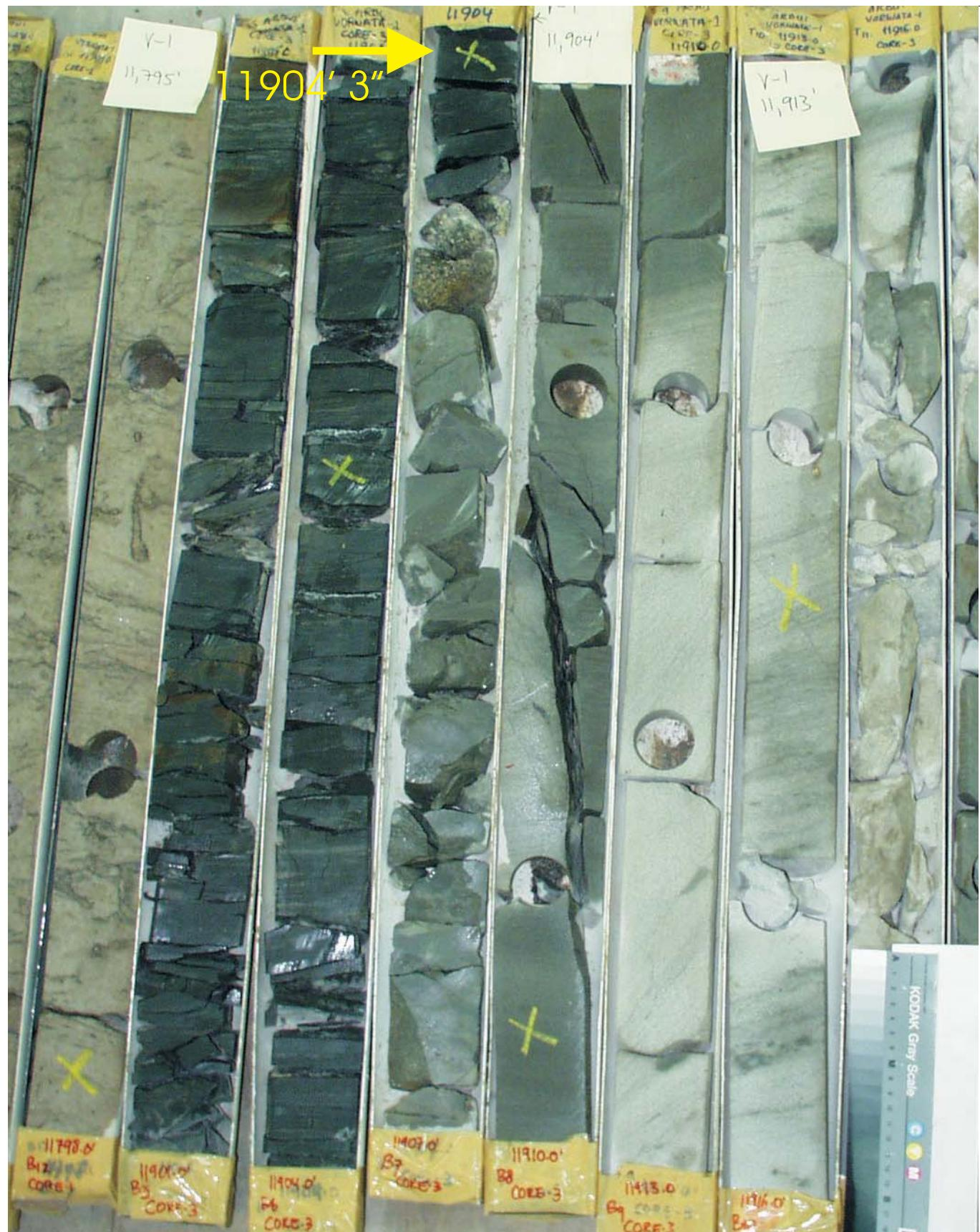


Figure 33A: Core Plug/Chip Atlas for sample 11904' 3" from Vorwata-1.

WHOLE CORE PLUG ANALYSES

WELL: VORWATA - 1

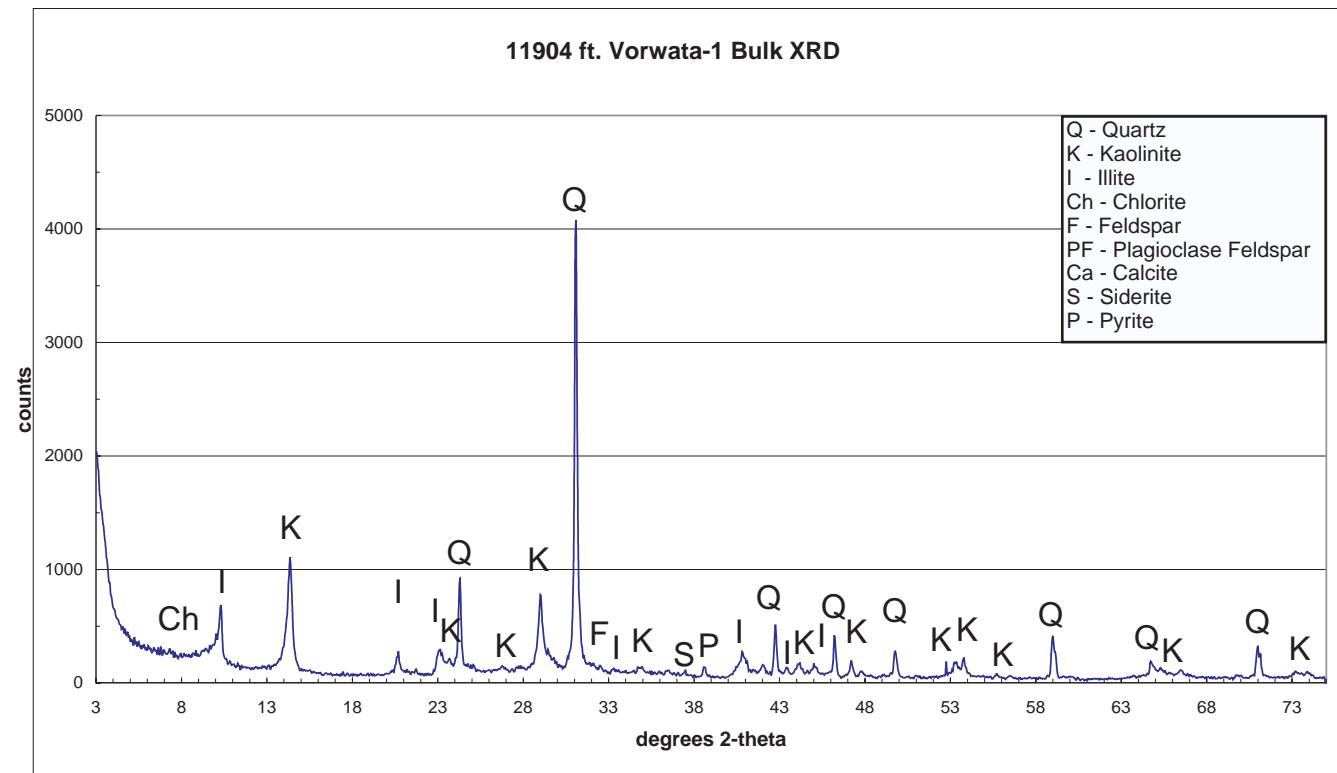
DEPTH: 11904' 3"

PLATE A

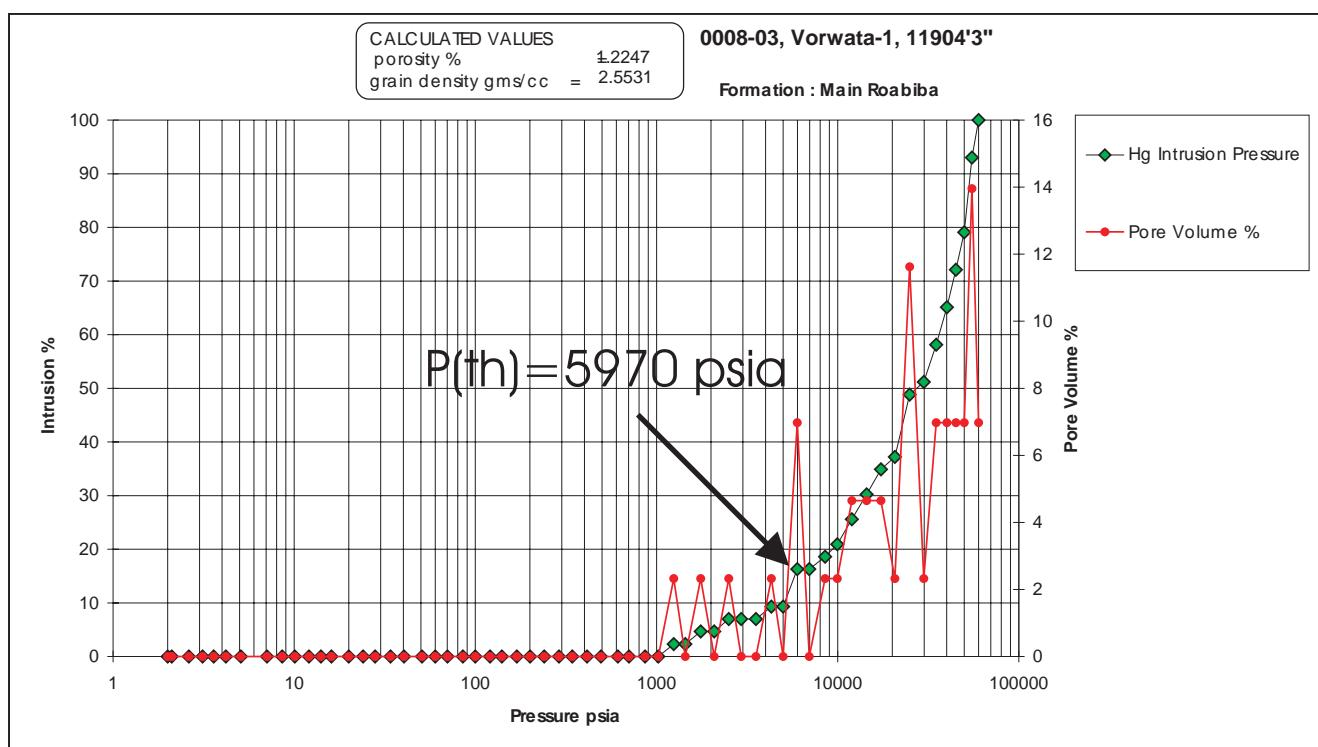
Digital Whole Core Photographs

Digital Core Chip/Plug Photograph

SEM Photomicrograph



Bulk XRD indicates a composition of primarily illite, kaolinite, quartz, and chlorite.



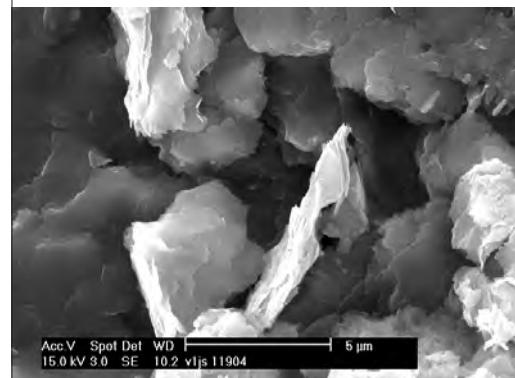
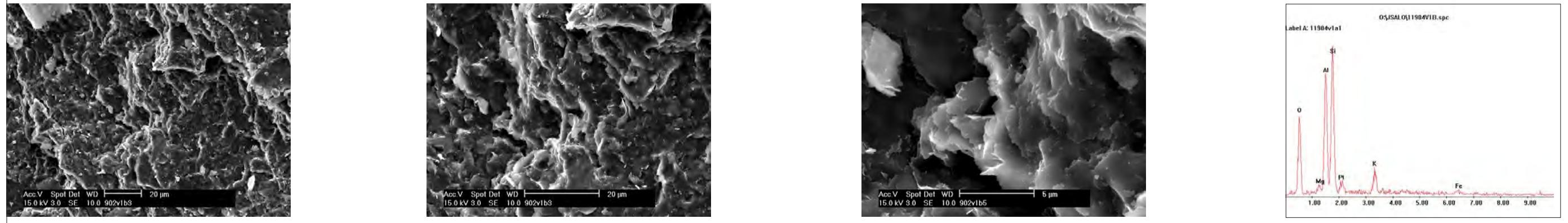
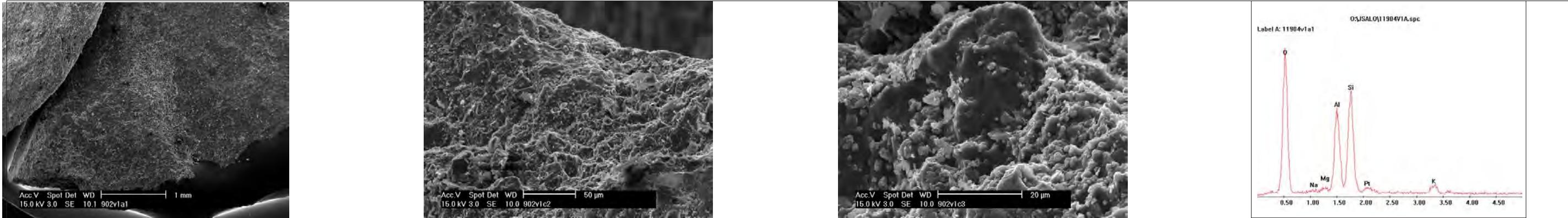
Sample Depth: 11904' 3"
Shifted Depth: 11914' 3"
MICP Entry Pressure: 1000 psia
MICP Threshold Pressure: 5970 psia
Lithology: Shale

Figure 33B: Core Plug/Chip Atlas for sample 11904' 3" from Vorwata-1.

WHOLE CORE PLUG ANALYSES
WELL: VORWATA - 1
DEPTH: 11904' 3"

PLATE B:

BULK XRD
Mercury Injection Capillary Pressure



The composition of this shale core sample was examined by Bulk XRD, SEM examination, and EDX (dispersive x-ray analysis). These analyses all confirm a composition primarily of illite, kaolinite, chlorite, and quartz.

Figure 33C: Core Plug/Chip Atlas for sample 11904' 3" from Vorwata-1.

WHOLE CORE PLUG ANALYSES

WELL: VORWATA - 1

DEPTH: 11904' 3"

PLATE C:

FESEM Photomicrographs

FESEM EDX (SEM XRD)

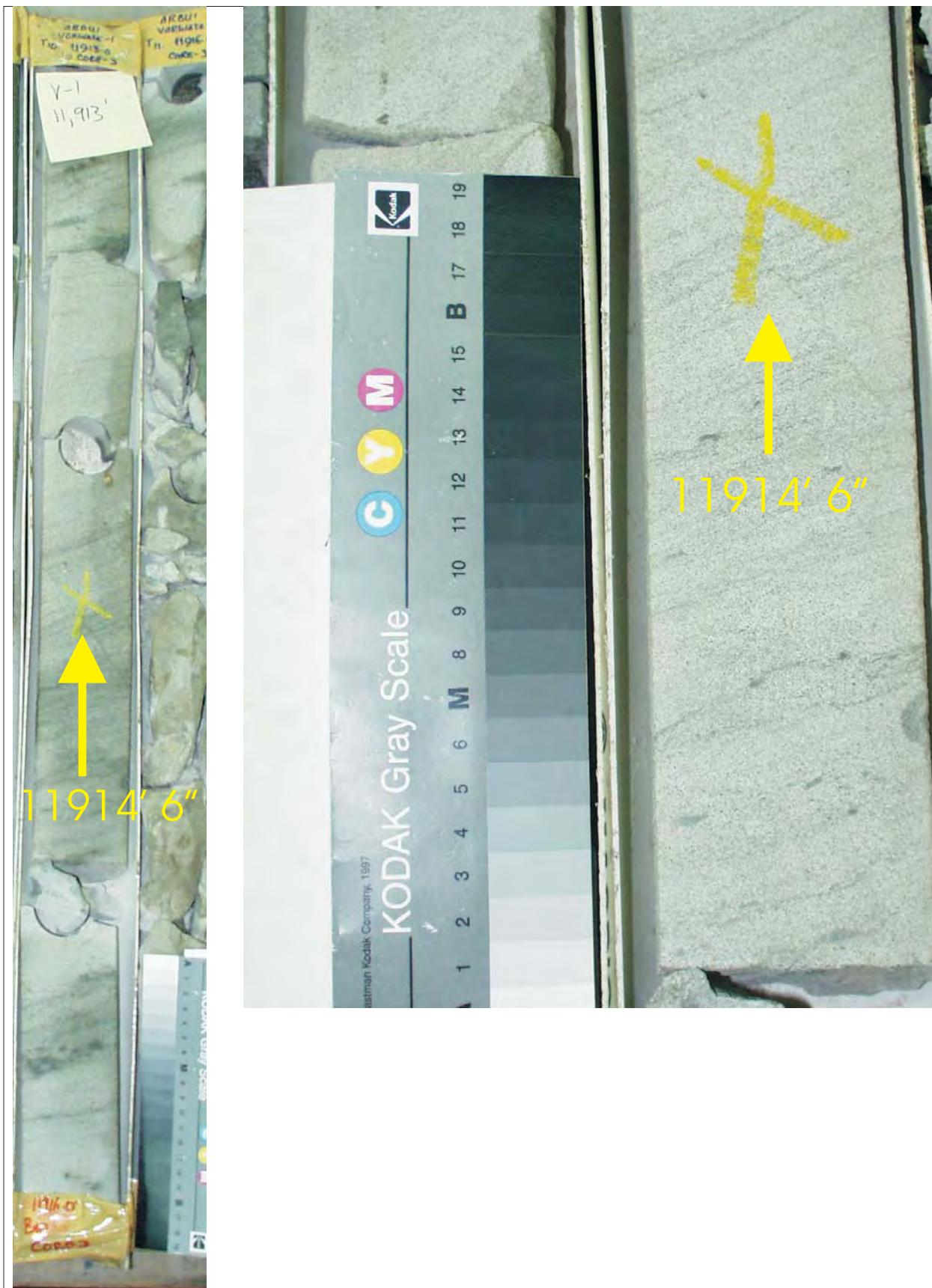


Sample Depth: 11909' 7"
Shifted Depth: 11919' 7"
He-Ø: 3.5%
k air: 0.052 mD (NOB 800 psia)

WHOLE CORE PLUG ANALYSES
WELL: VORWATA - 1
DEPTH: 11909' 7"

PLATE A
Digital Whole Core Photographs
Digital Core Chip/Plug Photograph

Figure 34A: Core Plug/Chip Atlas for sample 11909' 7" from Vorwata-1.



Sample Depth: 11914' 6"
 Shifted Depth: 11924' 6"
 He-∅: 6.9%
 k air: 1.0 mD (NOB 800 psia)

WHOLE CORE PLUG ANALYSES
 WELL: VORWATA - 1
 DEPTH: 11914' 6"
 PLATE A
 Digital Whole Core Photographs
 Digital Core Chip/Plug Photograph

Figure 35A: Core Plug/Chip Atlas for sample 11914' 6" from Vorwata-1.

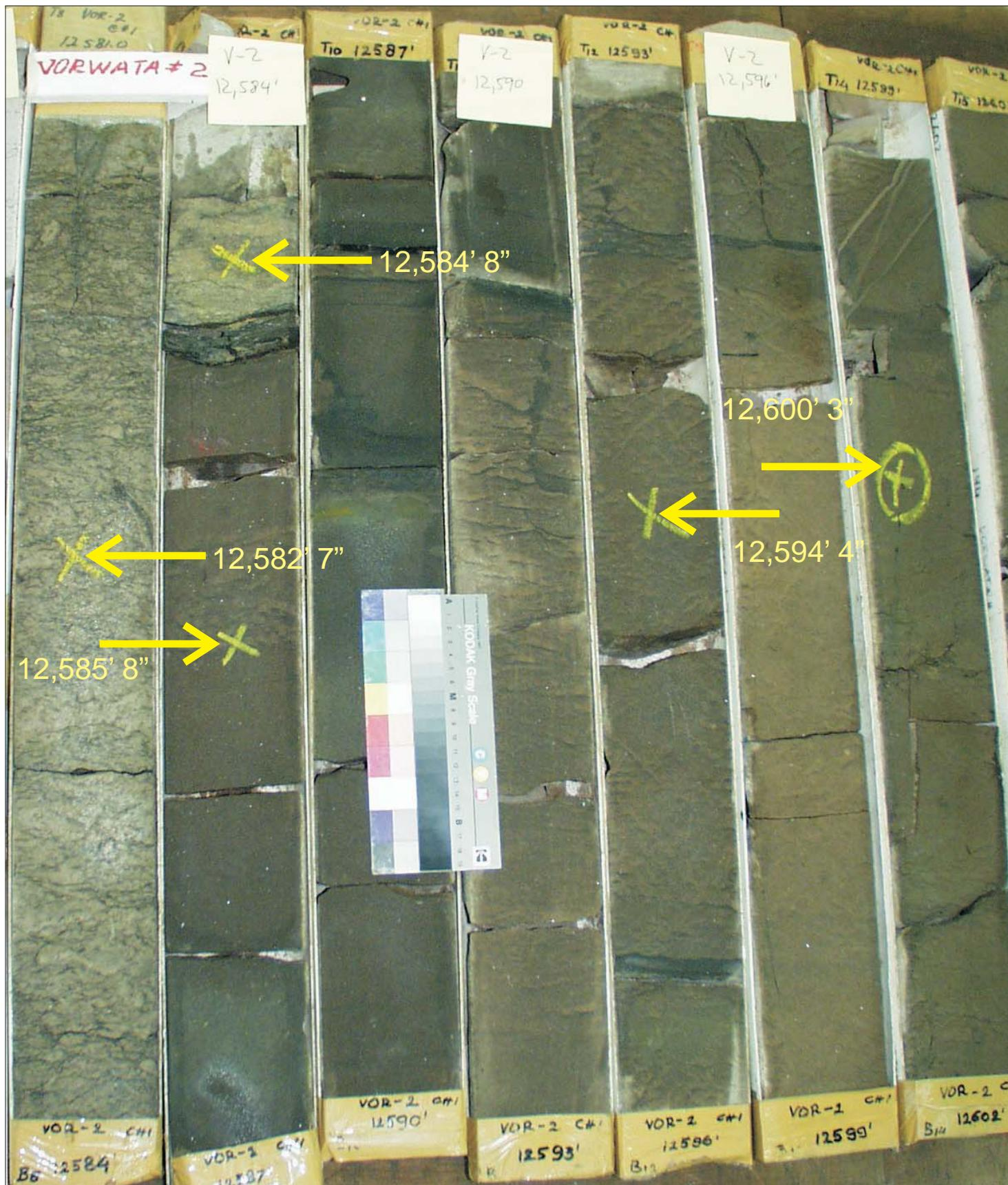
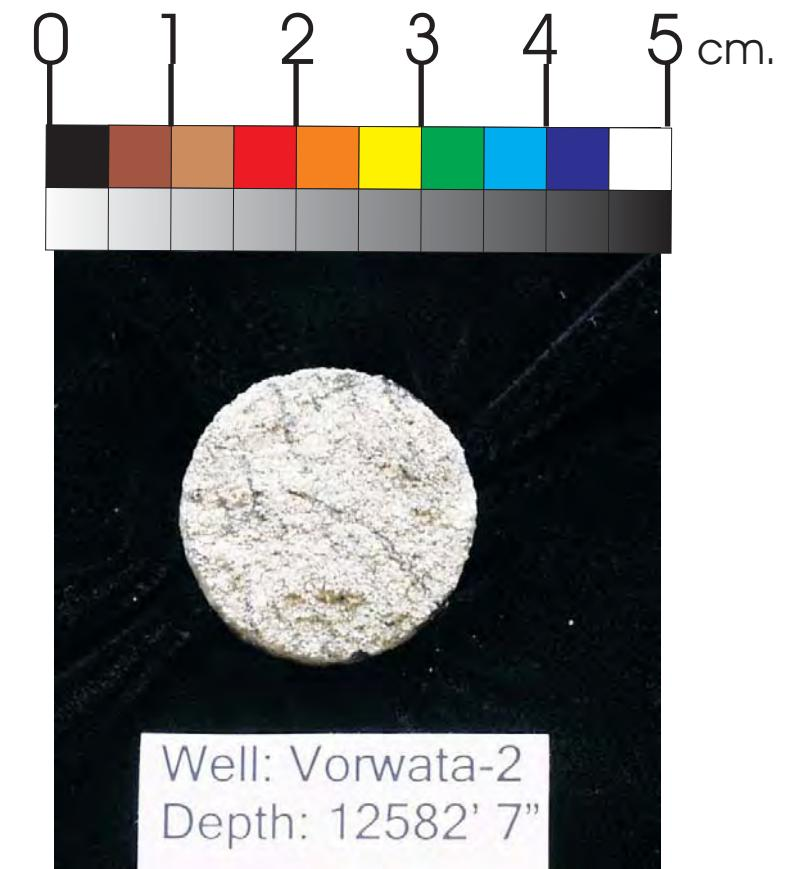
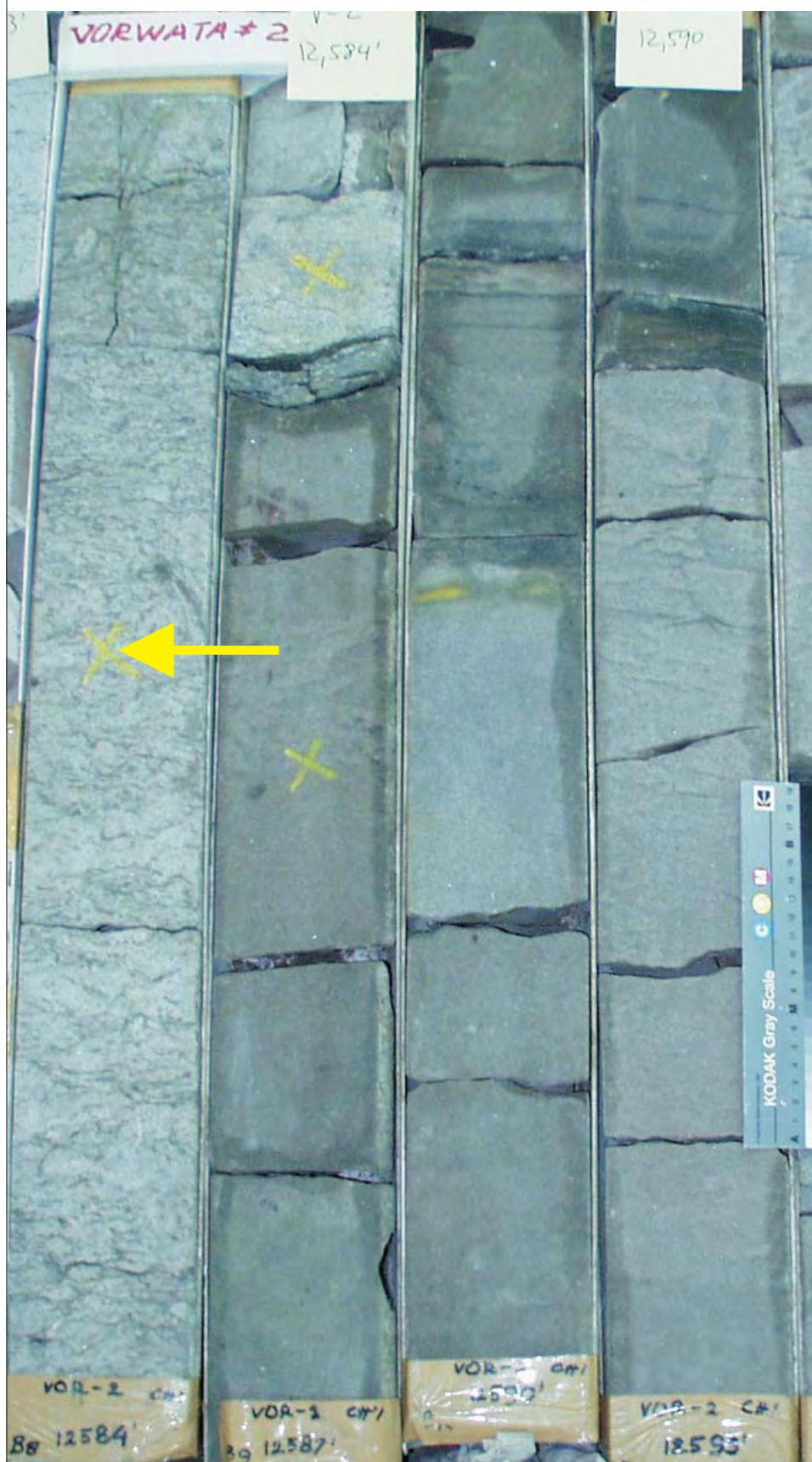


Figure 36A: Core Plug/Chip Atlas for sample 12582' 7" from Vorwata-2.

WHOLE CORE PLUG ANALYSES
WELL: VORWATA - 2
DEPTH: 12582' 7"

PLATE A:

Digital Whole Core Photographs



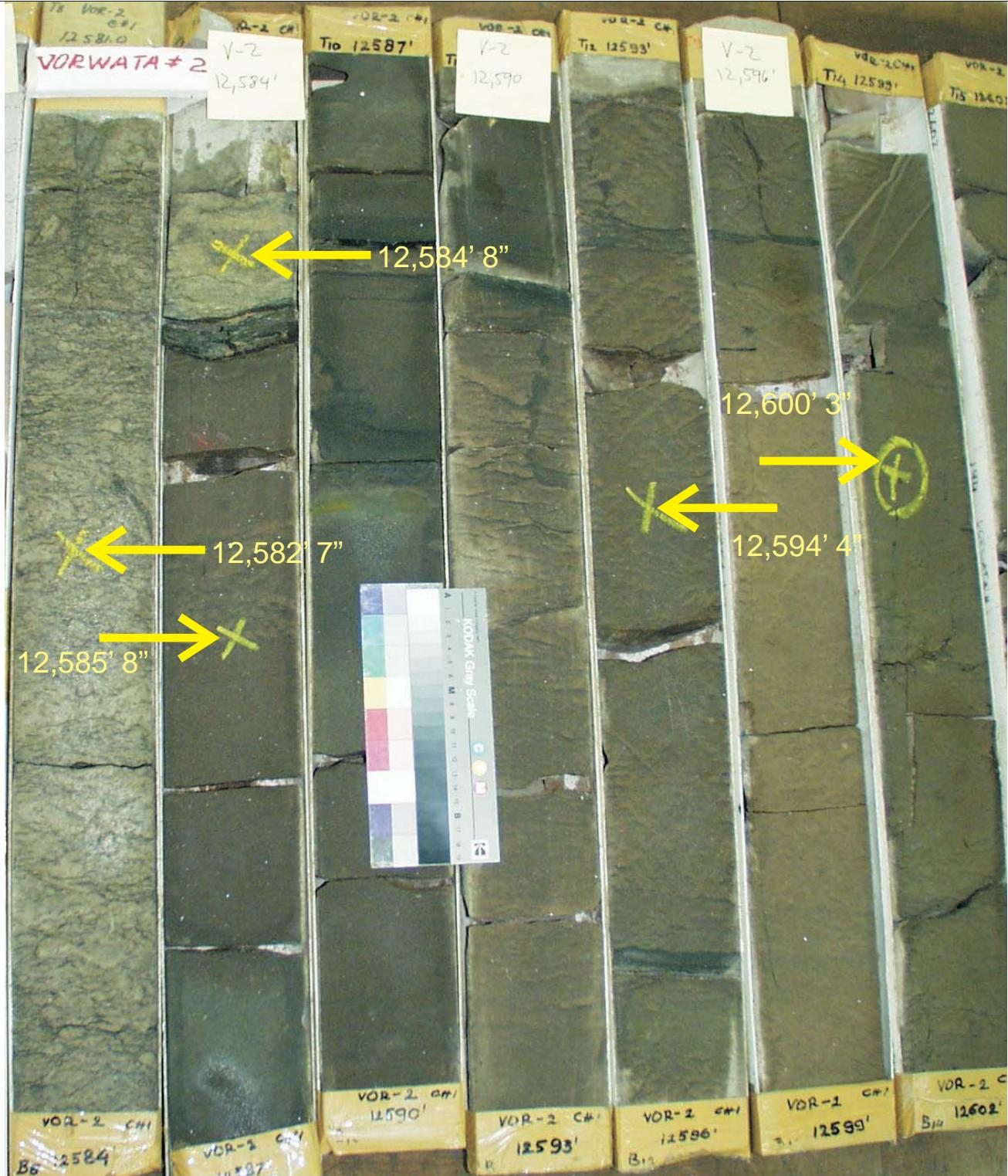
Sample Depth: 12582' 7"
Shifted Depth: 12595' 7"
He-Ø: 14.8%
k air: 19.8 mD (NOB 800 psia)

WHOLE CORE PLUG ANALYSES
WELL: VORWATA - 2
DEPTH: 12582' 7"

PLATE B:

Digital Whole Core Photographs
Digital Core Chip/Plug Photograph

Figure 36B: Core Plug/Chip Atlas for sample 12582' 7" from Vorwata-2.



WHOLE CORE PLUG ANALYSES

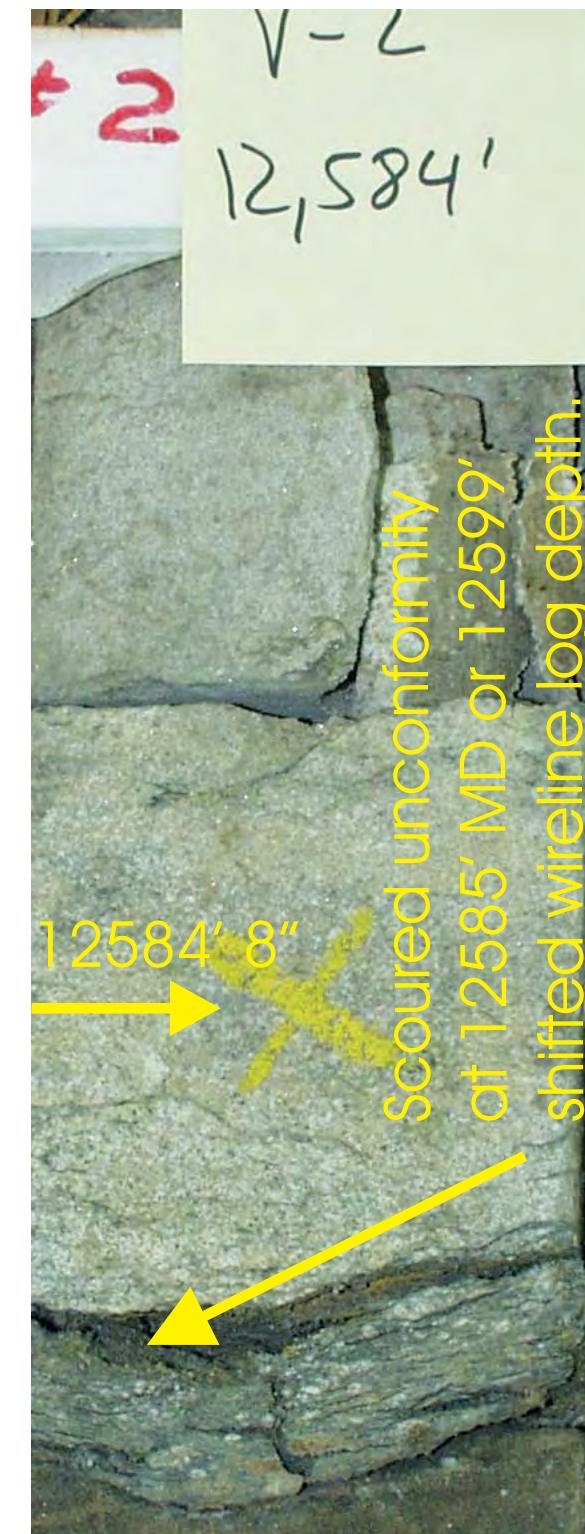
WELL: VORWATA - 2

DEPTH: 12584' 8"

PLATE A:

Digital Whole Core Photographs

Figure 37A: Core Plug/Chip Atlas for sample 12584' 8" from Vorwata-2.



Sample Depth: 12584' 8"
Shifted Depth: 12597' 8"
He-Ø: 12.4%
k air: 28.3 mD (NOB 800 psia)

Figure 37B: Core Plug/Chip Atlas for sample 12584' 8" from Vorwata-2.

WHOLE CORE PLUG ANALYSES

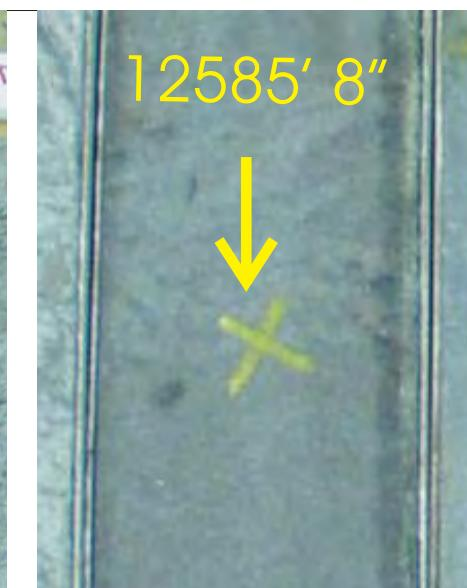
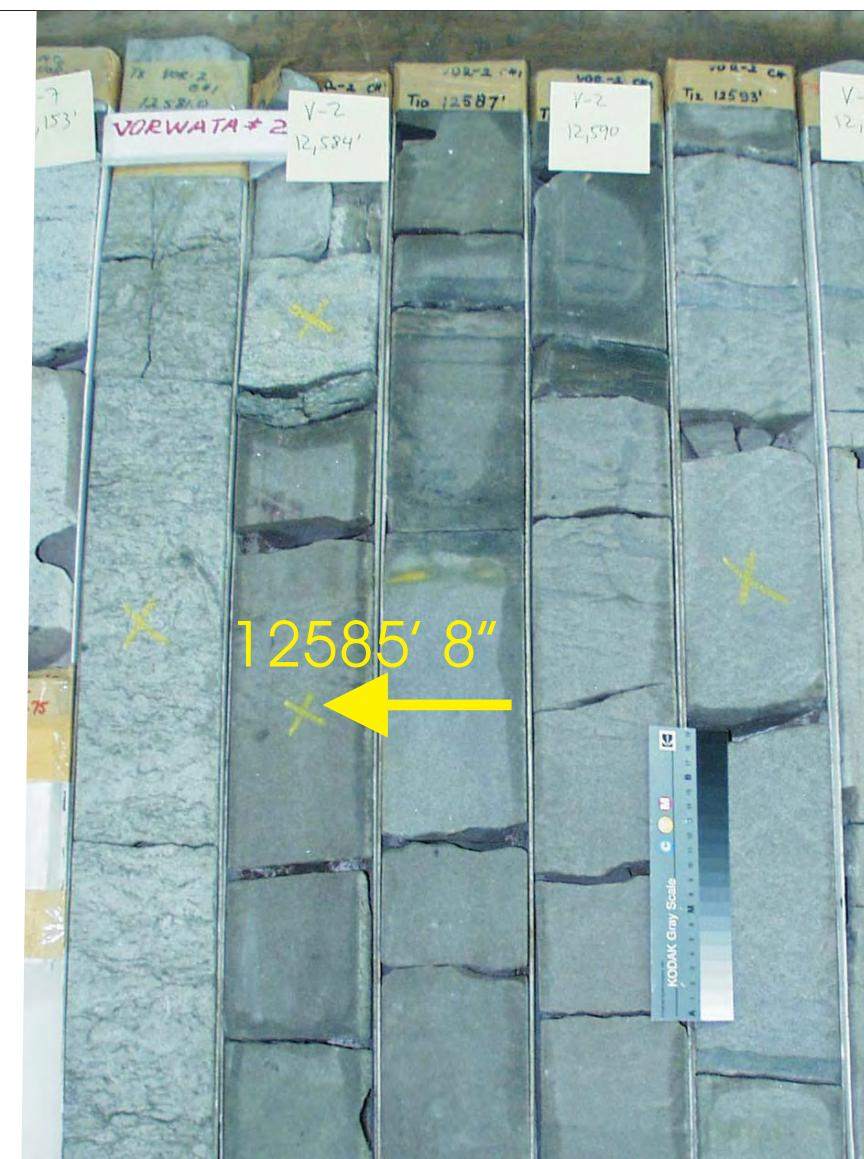
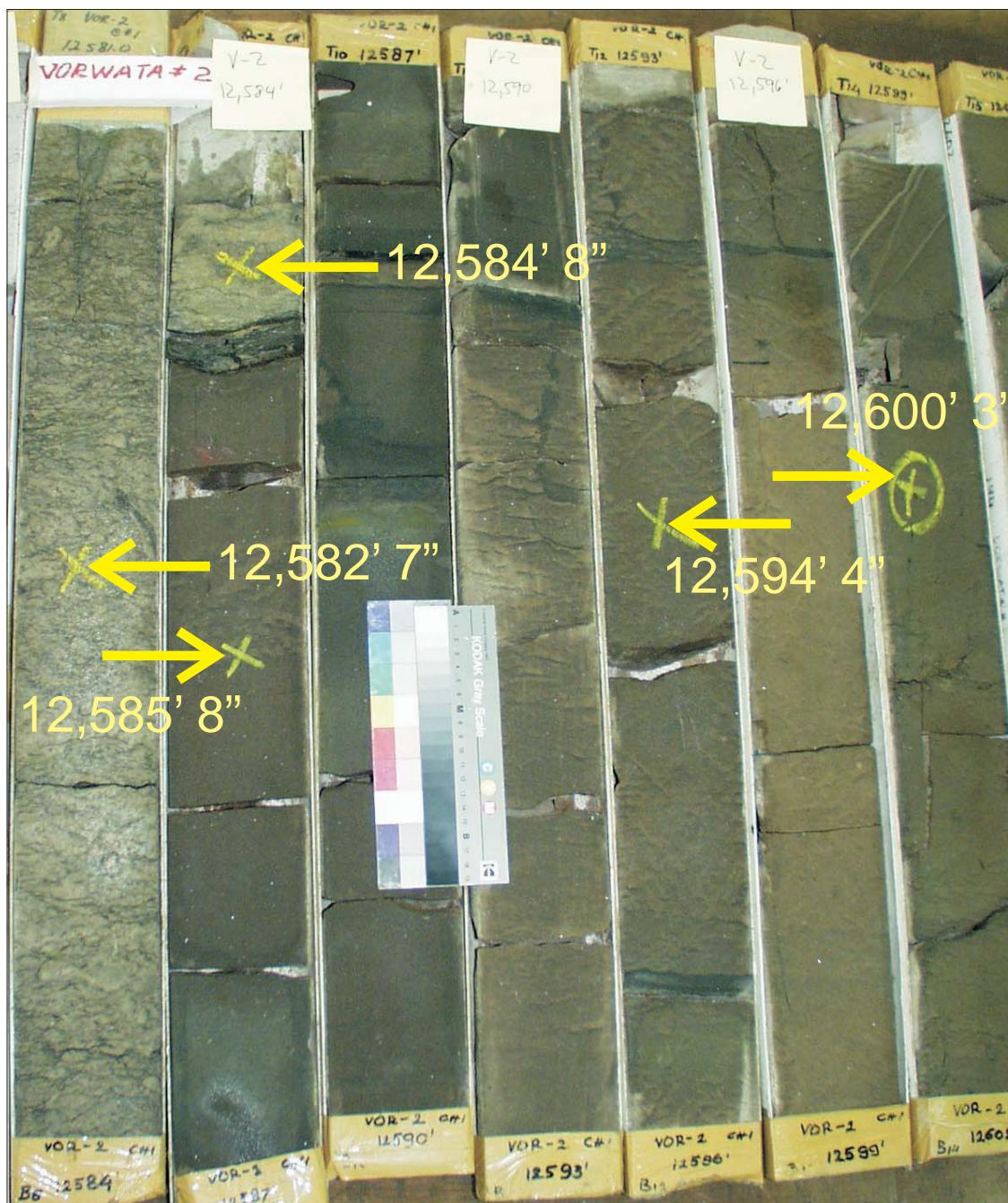
WELL: VORWATA - 2

DEPTH: 12584' 8"

PLATE B:

Digital Whole Core Photographs

Digital Core Chip/Plug Photograph



WHOLE CORE PLUG ANALYSES

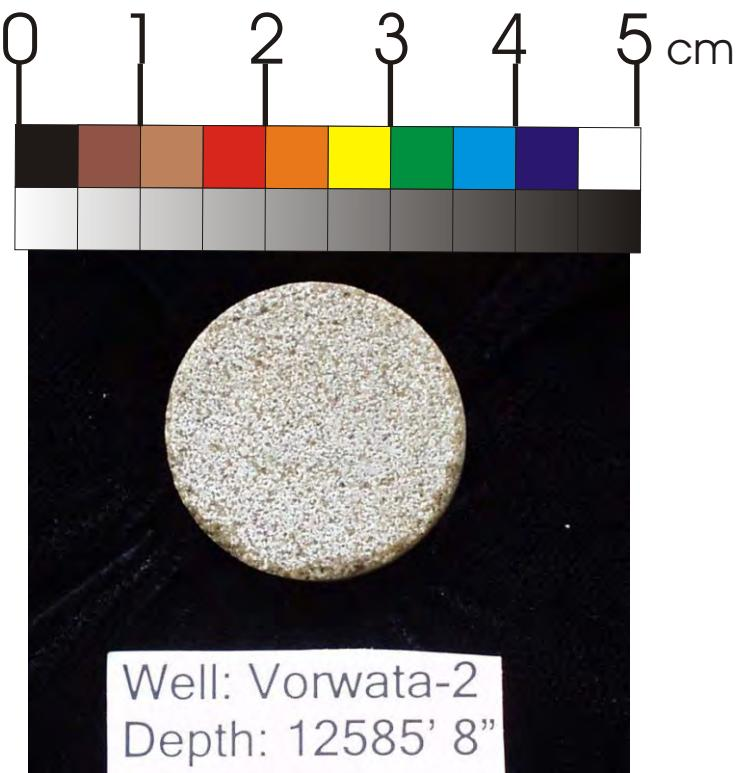
WELL: VORWATA - 2

DEPTH: 12585' 8"

PLATE A:

Digital Whole Core Photographs

Figure 38A: Core Plug/Chip Atlas for sample 12585' 8" from Vorwata-2.



Sample Depth: 12585' 8"
Shifted Depth: 12598' 8"
He-Ø: 15.2%
k air: 130 mD (NOB 800 psia)

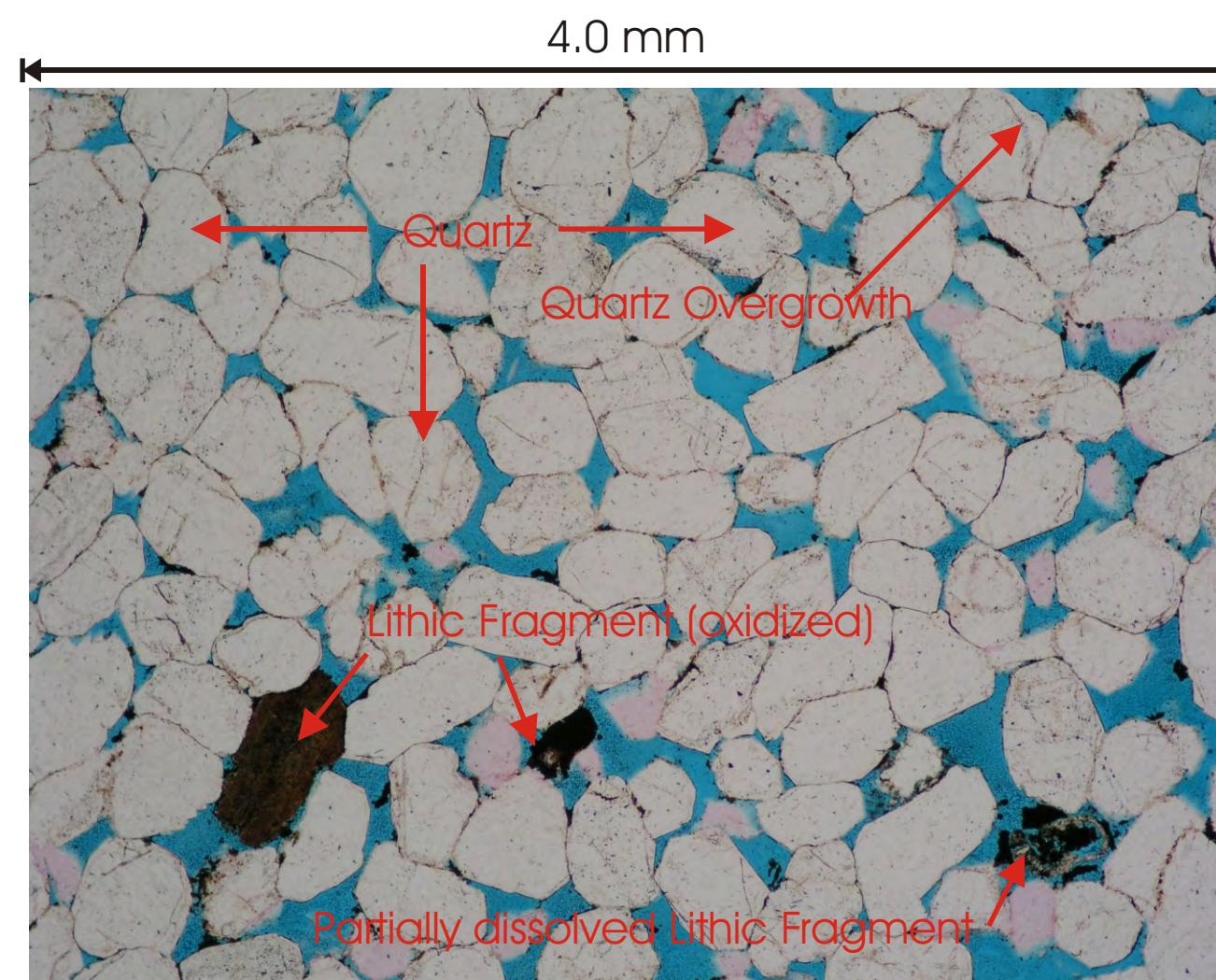
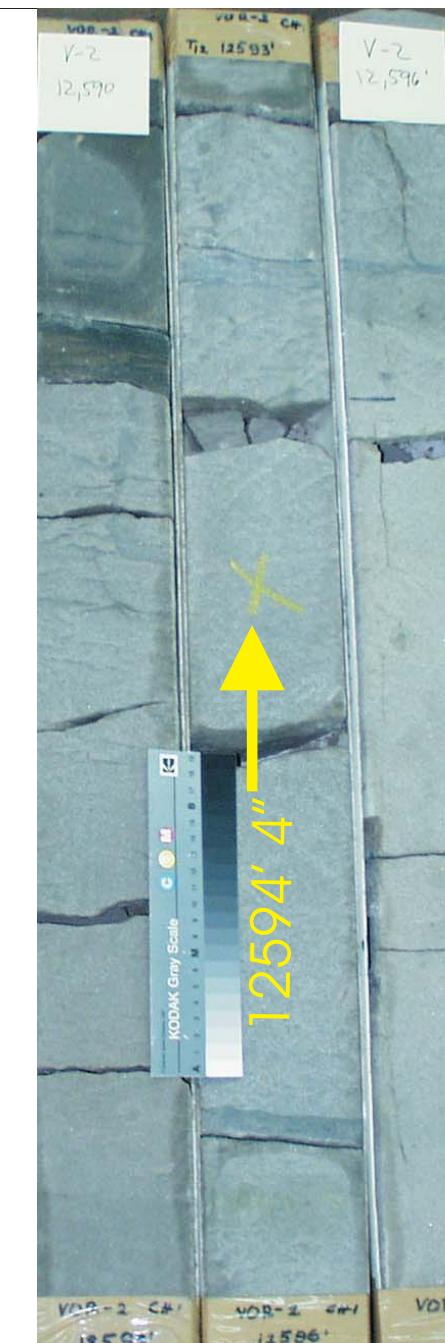
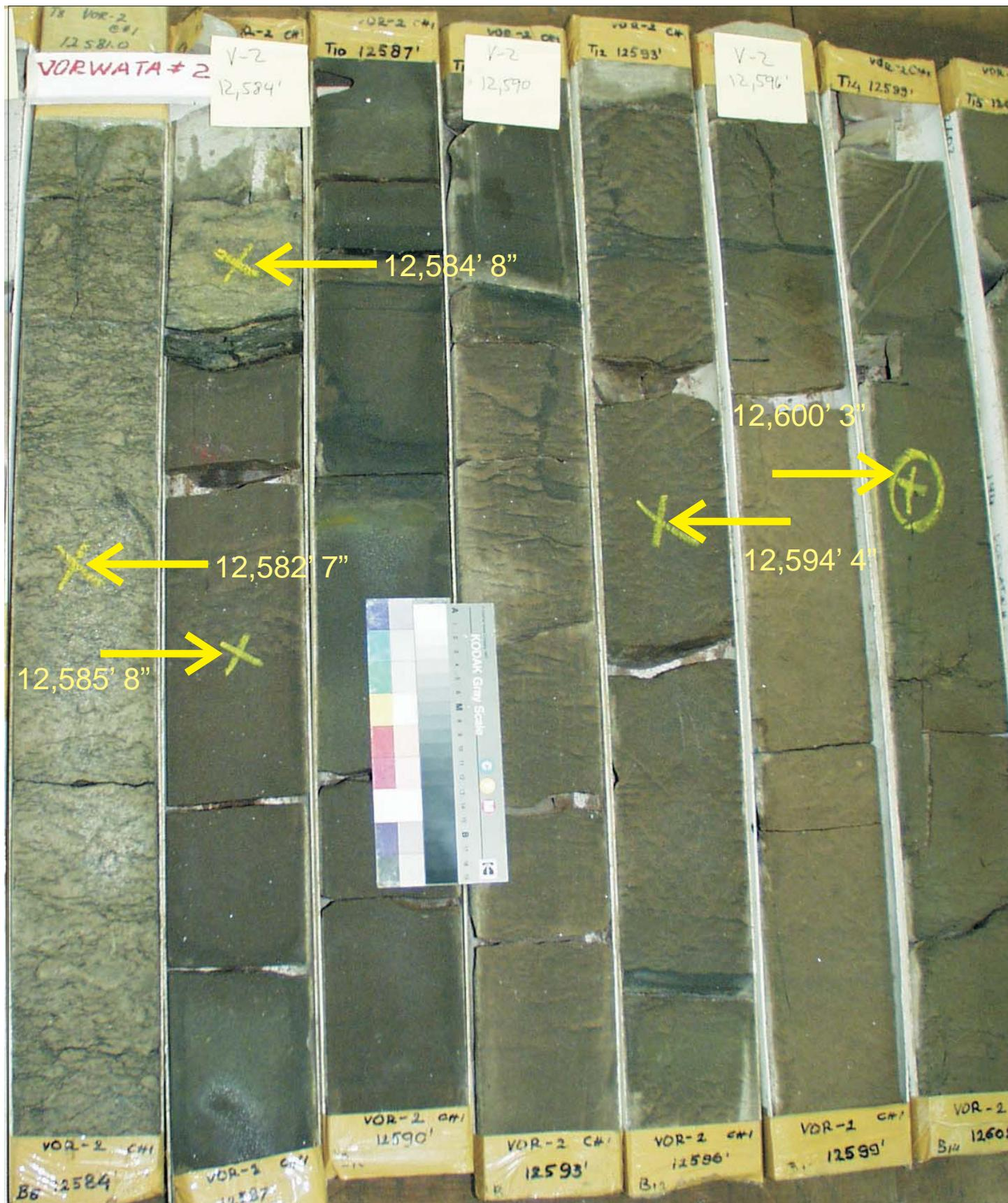


Figure 38B: Core Plug/Chip Atlas for sample 12585' 8" from Vorwata-2.

WHOLE CORE PLUG ANALYSES
WELL: VORWATA - 2
DEPTH: 12585' 8"

PLATE B:

Digital Core Chip/Plug Photograph
Petrographic Photomicrograph

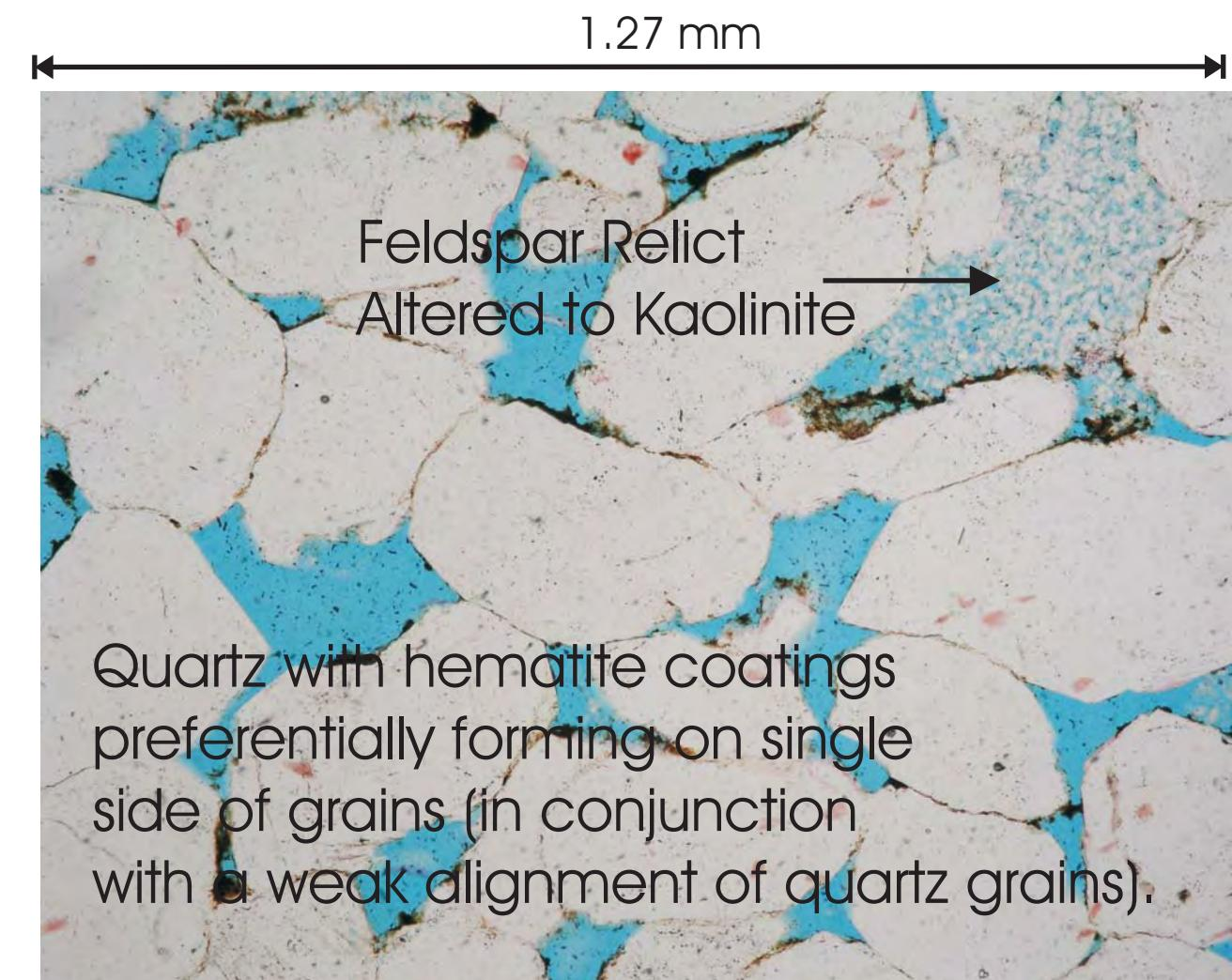


WHOLE CORE PLUG ANALYSES
WELL: VORWATA - 2
DEPTH: 12594' 4"

PLATE A:

Digital Whole Core Photographs

Figure 39A: Core Plug/Chip Atlas for sample 12594' 4" from Vorwata-2.



Sample Depth: 12594' 4"
Shifted Depth: 12607' 4"
He-Ø: 13.5%
k air: 477 mD (NOB 800 psia)

WHOLE CORE PLUG ANALYSES
WELL: VORWATA - 2
DEPTH: 12594' 4"

PLATE B:
Digital Whole Core Photographs
Digital Core Chip/Plug Photograph
Petrographic Photomicrograph

Figure 39B: Core Plug/Chip Atlas for sample 12594' 4" from Vorwata-2.

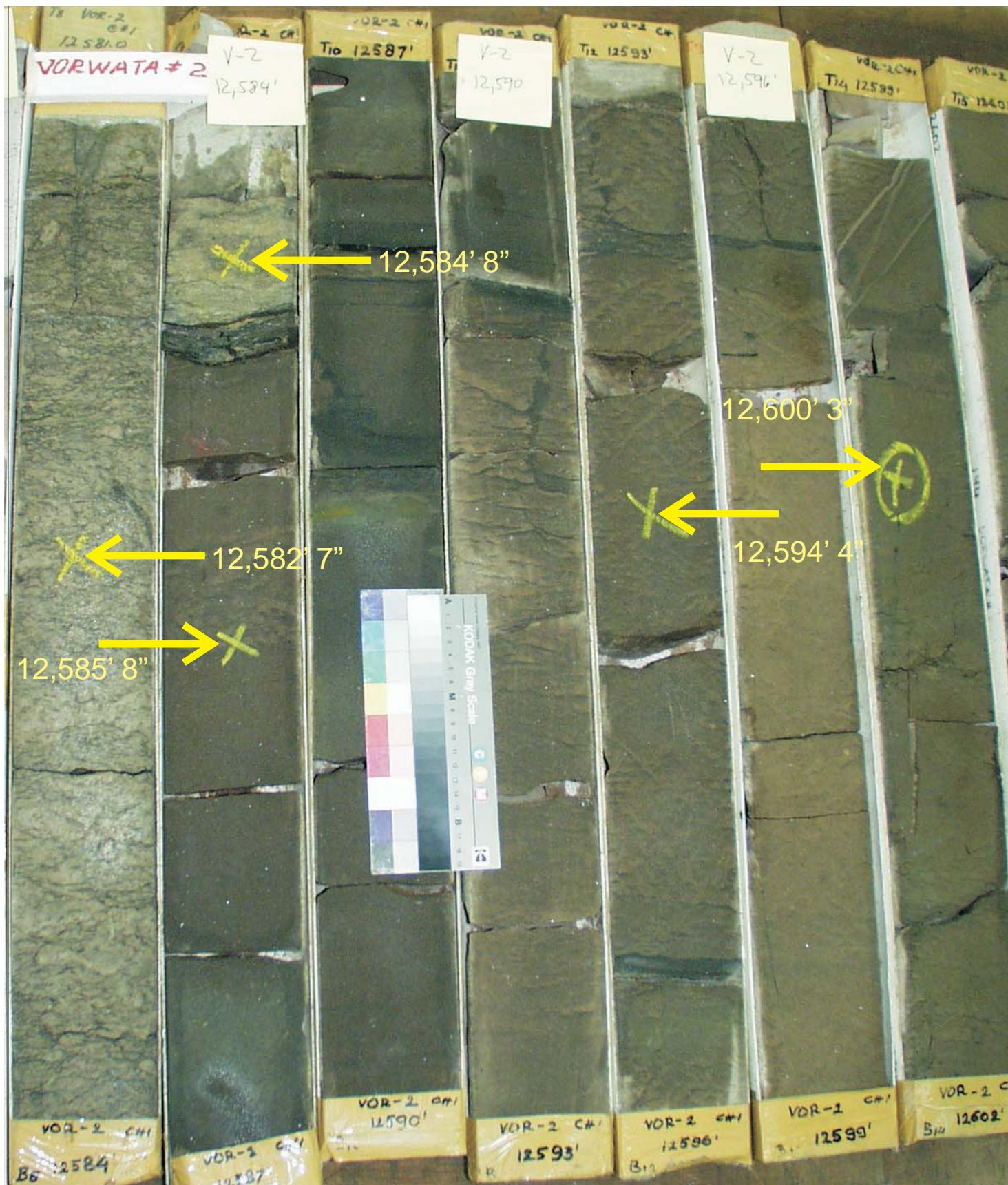
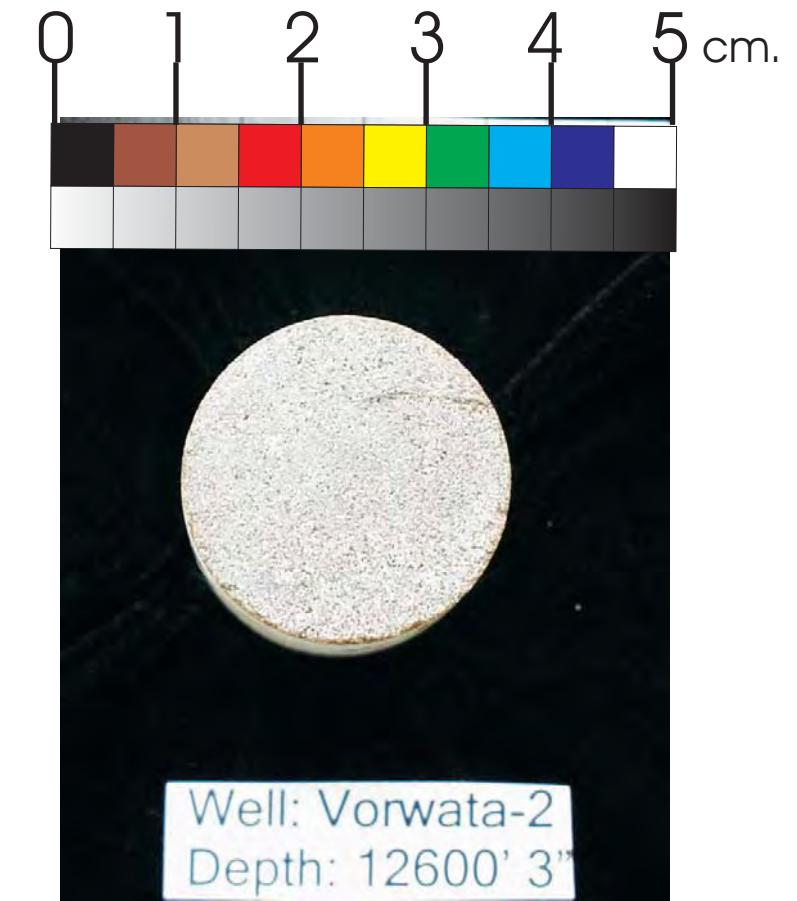
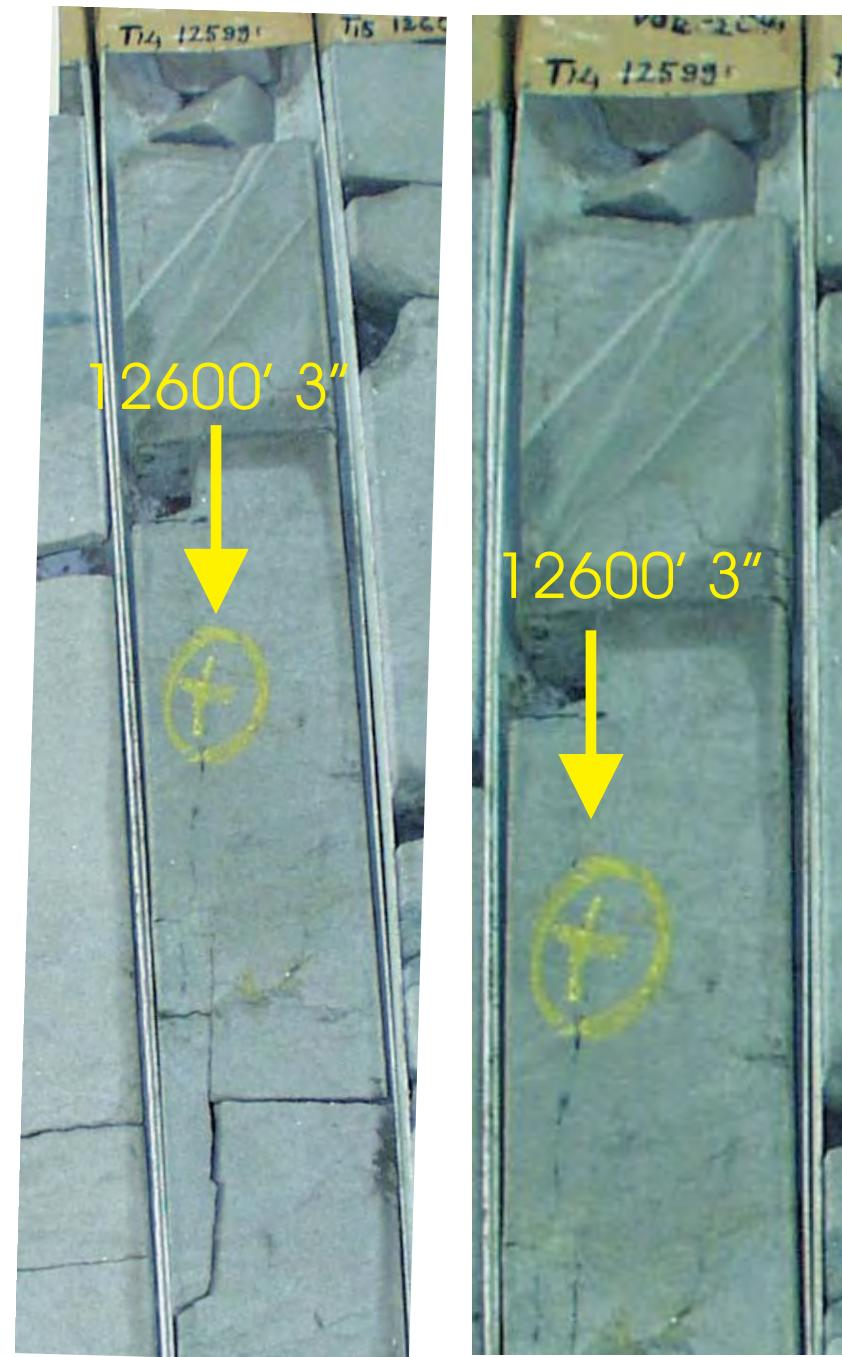
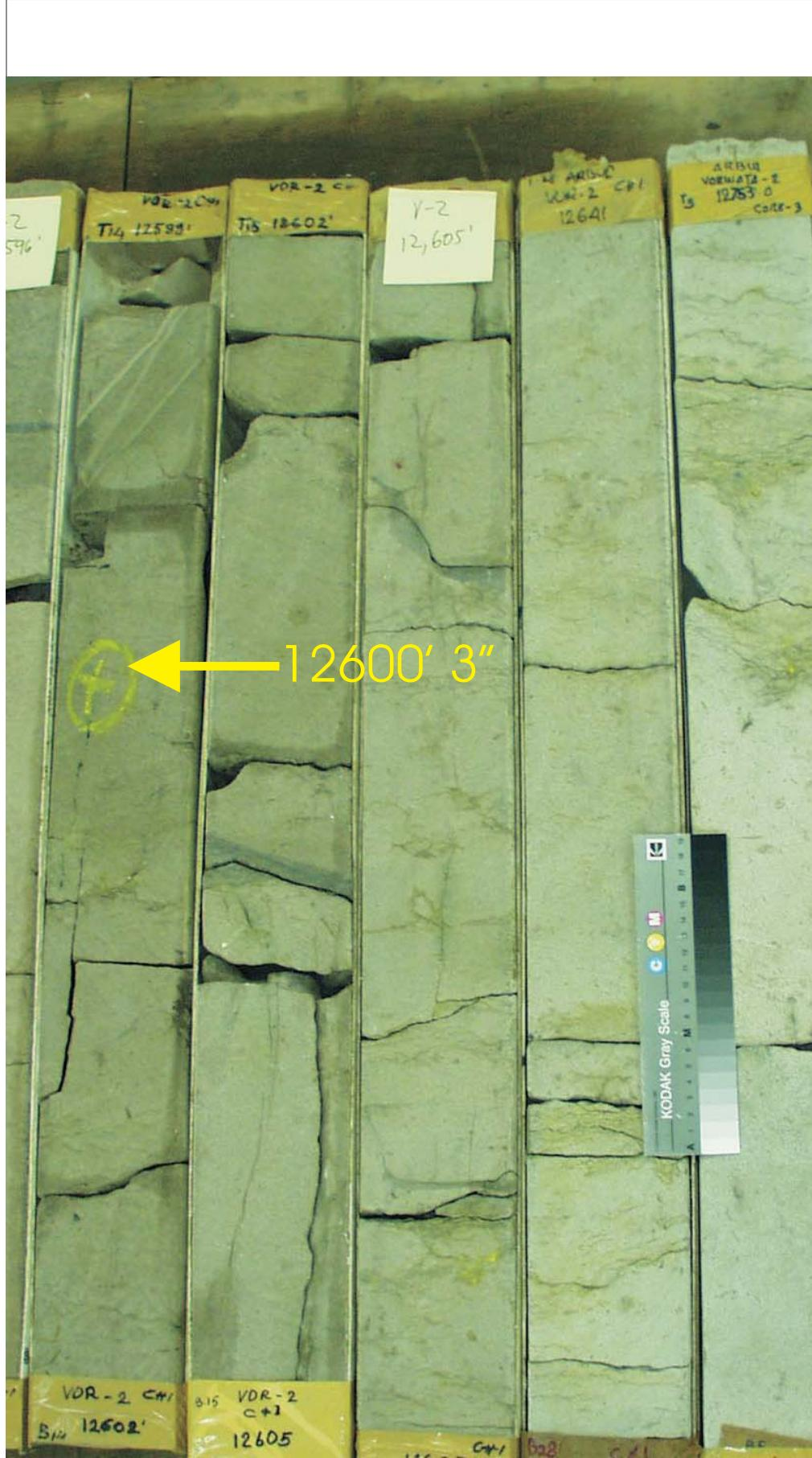


Figure 40A: Core Plug/Chip Atlas for sample 12600' 3" from Vorwata-2.

WHOLE CORE PLUG ANALYSES
WELL: VORWATA - 2
DEPTH: 12600' 3"

PLATE A:

Digital Whole Core Photographs



Sample Depth: 12600' 3"
 Shifted Depth: 12613' 3"
 He-∅: 13.1%
 k air: 134 mD (NOB 800 psia)

Figure 40B: Core Plug/Chip Atlas for sample 12600' 3" from Vorwata-2.

WHOLE CORE PLUG ANALYSES

WELL: VORWATA - 2

DEPTH: 12600' 3"

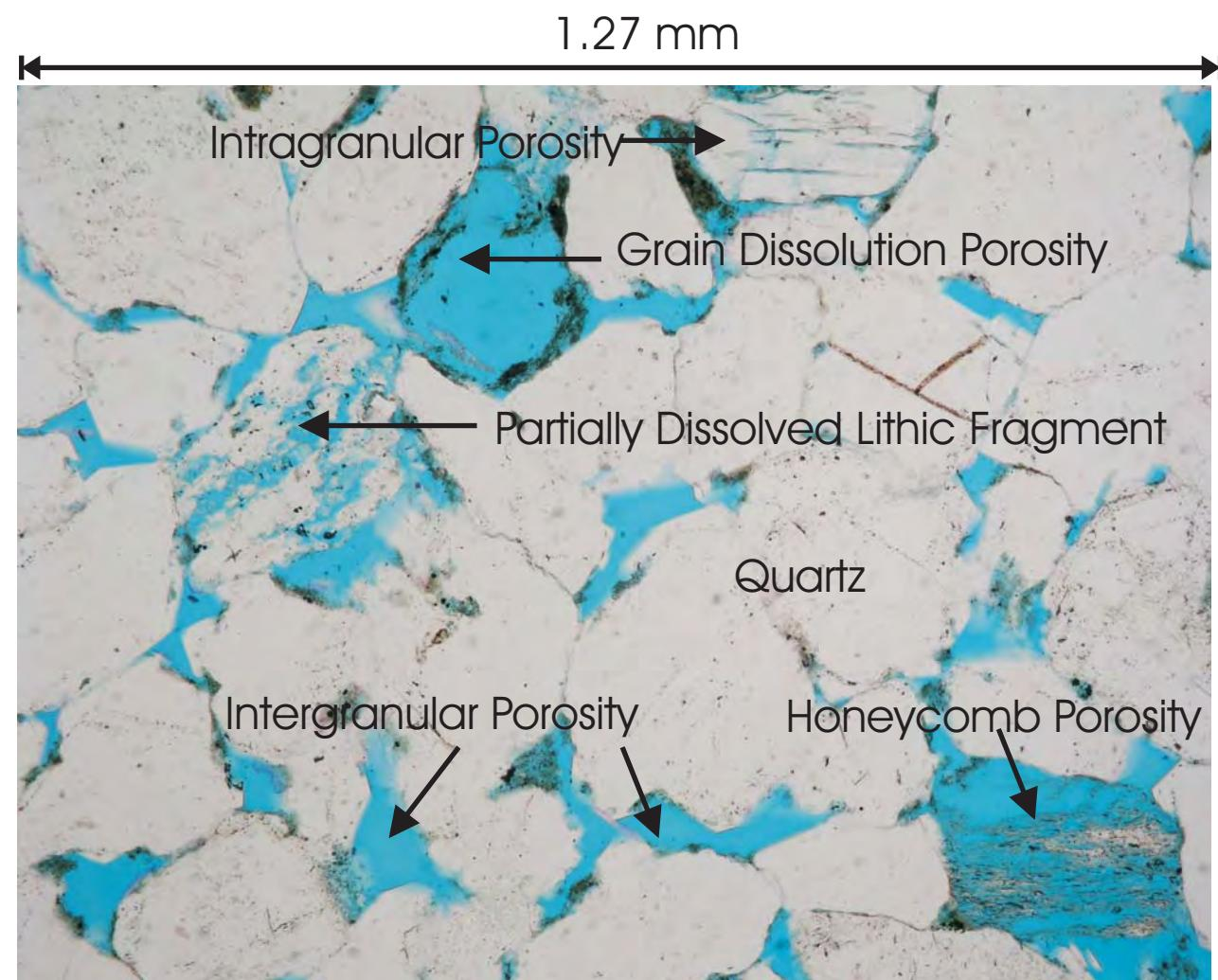
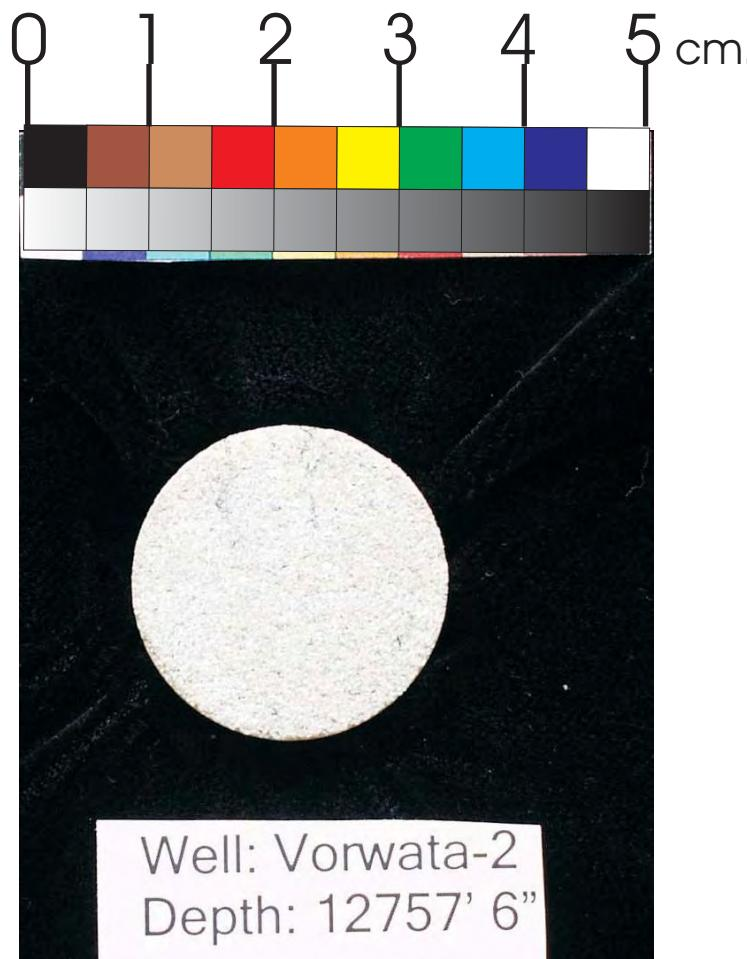
PLATE B:

Digital Whole Core Photographs

Digital Core Chip/Plug Photograph



Figure 41A: Core Plug/Chip Atlas for sample 12757' 6" from Vorwata-2.



Sample Depth: 12757' 6"
Shifted Depth: 12770' 6"
He-Ø: 15.9%
k air: 130 mD (NOB 800 psia)

WHOLE CORE PLUG ANALYSES
WELL: VORWATA - 2
DEPTH: 12757' 6"

PLATE B:

Digital Core Chip/Plug Photograph
SEM Photomicrograph

Figure 41B: Core Plug/Chip Atlas for sample 12757' 6" from Vorwata-2.

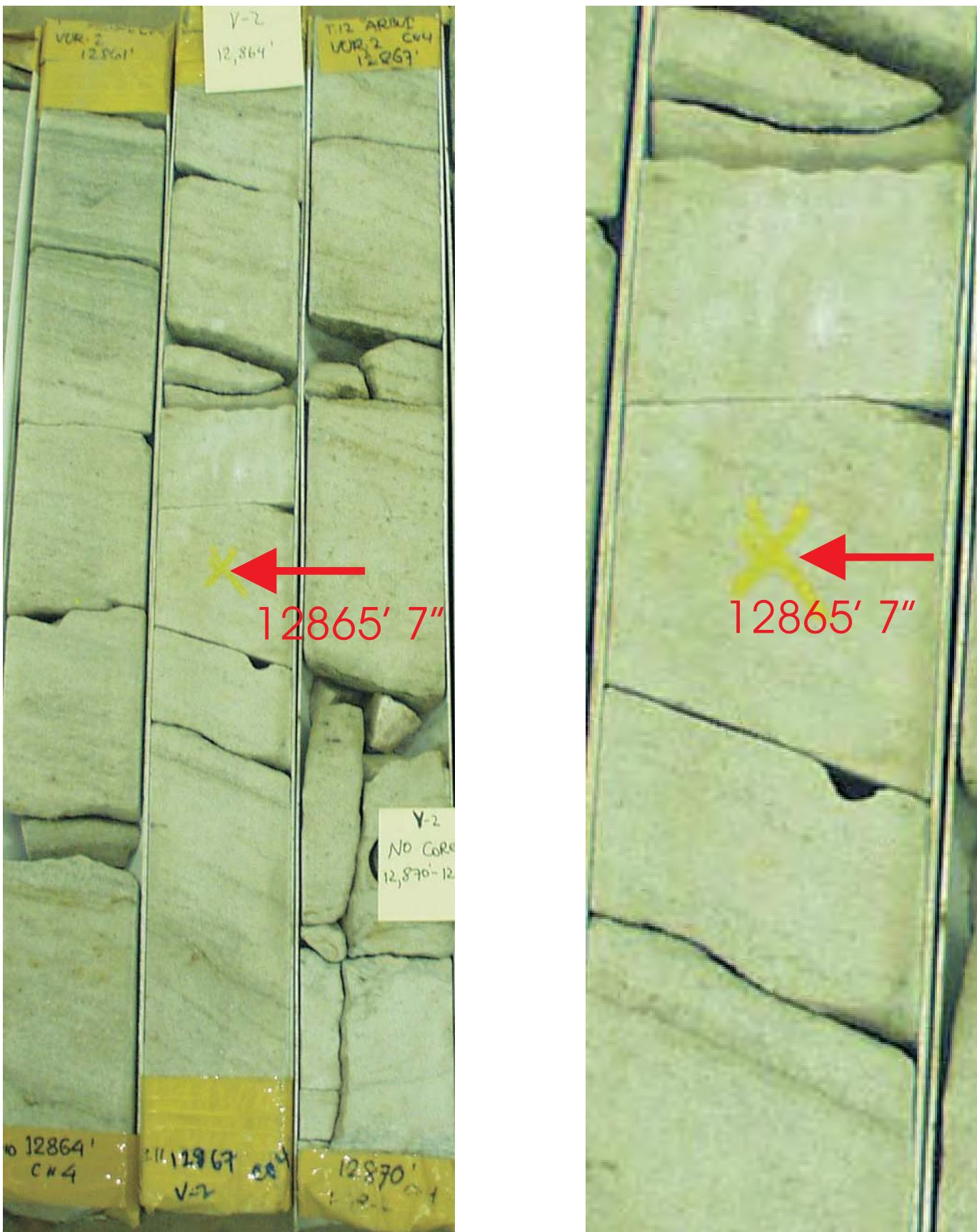
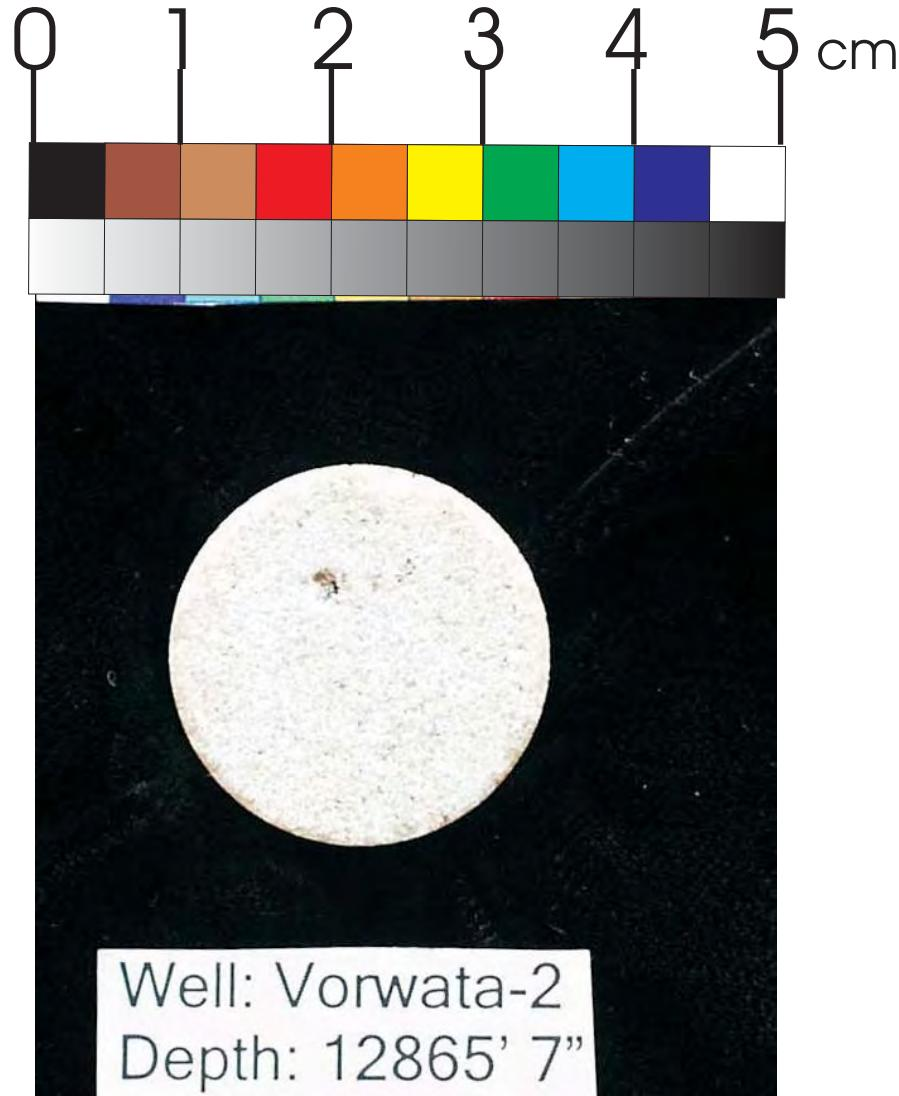


Figure 42A: Core Plug/Chip Atlas for sample 12865' 7" from Vorwata-2.

WHOLE CORE PLUG ANALYSES
WELL: VORWATA - 2
DEPTH: 12865' 7"
PLATE A:
Digital Whole Core Photographs



Well: Vorwata-2
Depth: 12865' 7"

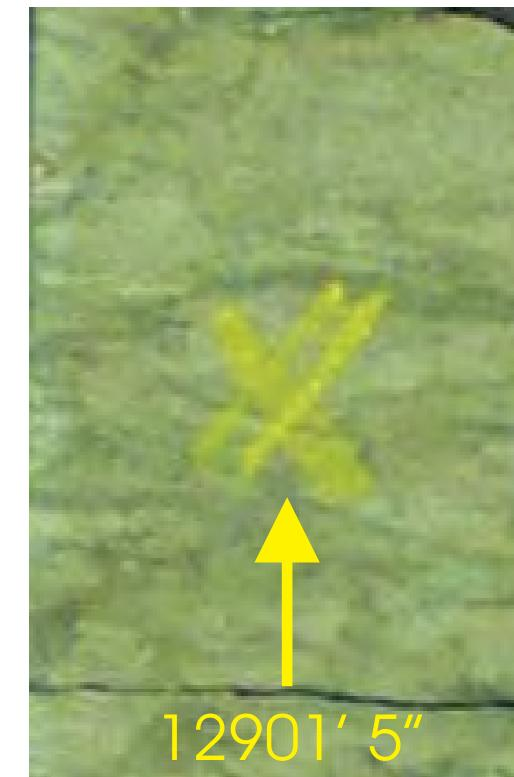
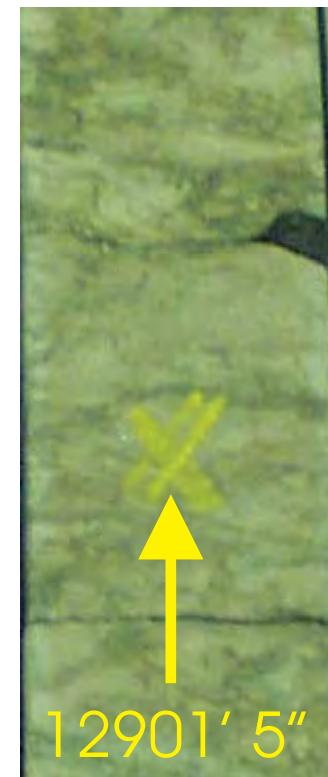
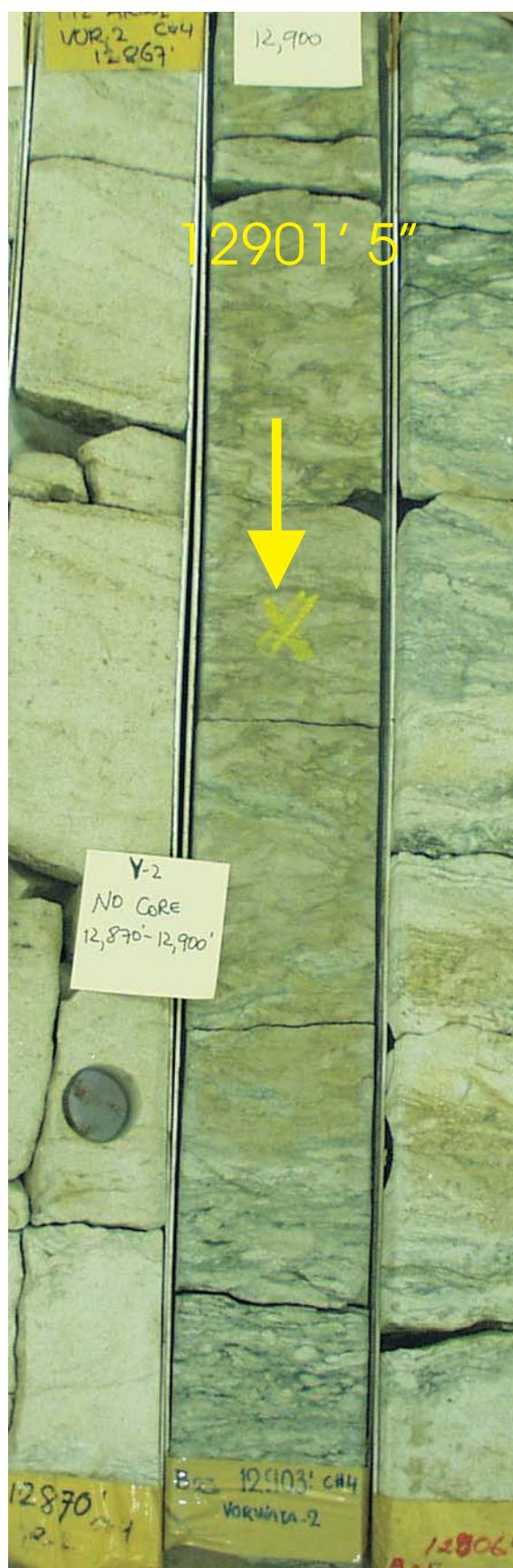
Sample Depth: 12865' 7"
Shifted Depth: 12878' 7"
He-Ø: 16.9%
k air: 1090 mD (NOB 800 psia)

WHOLE CORE PLUG ANALYSES
WELL: VORWATA - 2
DEPTH: 12865' 7"

PLATE B:

Digital Whole Core Photographs
Digital Core Chip/Plug Photograph

Figure 42B: Core Plug/Chip Atlas for sample 12865' 7" from Vorwata-2.

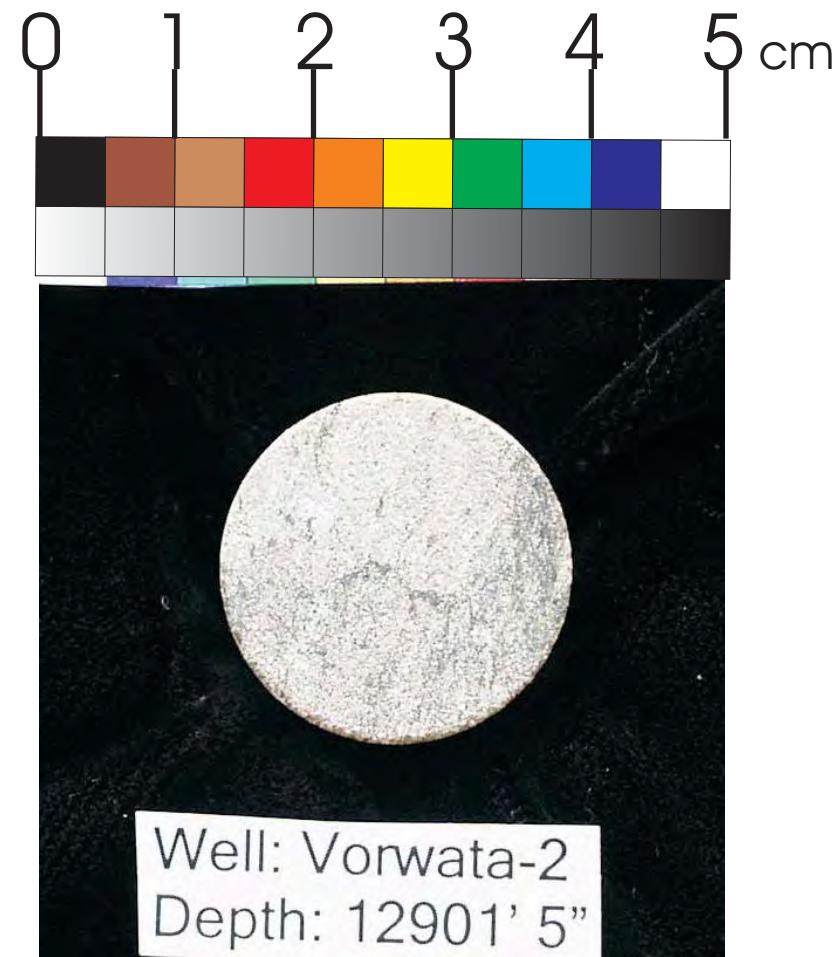


WHOLE CORE PLUG ANALYSES
WELL: VORWATA - 2
DEPTH: 12901' 5"

PLATE A:

Digital Whole Core Photographs

Figure 43A: Core Plug/Chip Atlas for sample 12901' 5" from Vorwata-2.



Sample Depth: 12901' 5"
Shifted Depth: 12914' 5"
He-Ø: 12.2%
k air: 0.32 mD (NOB 800 psia)

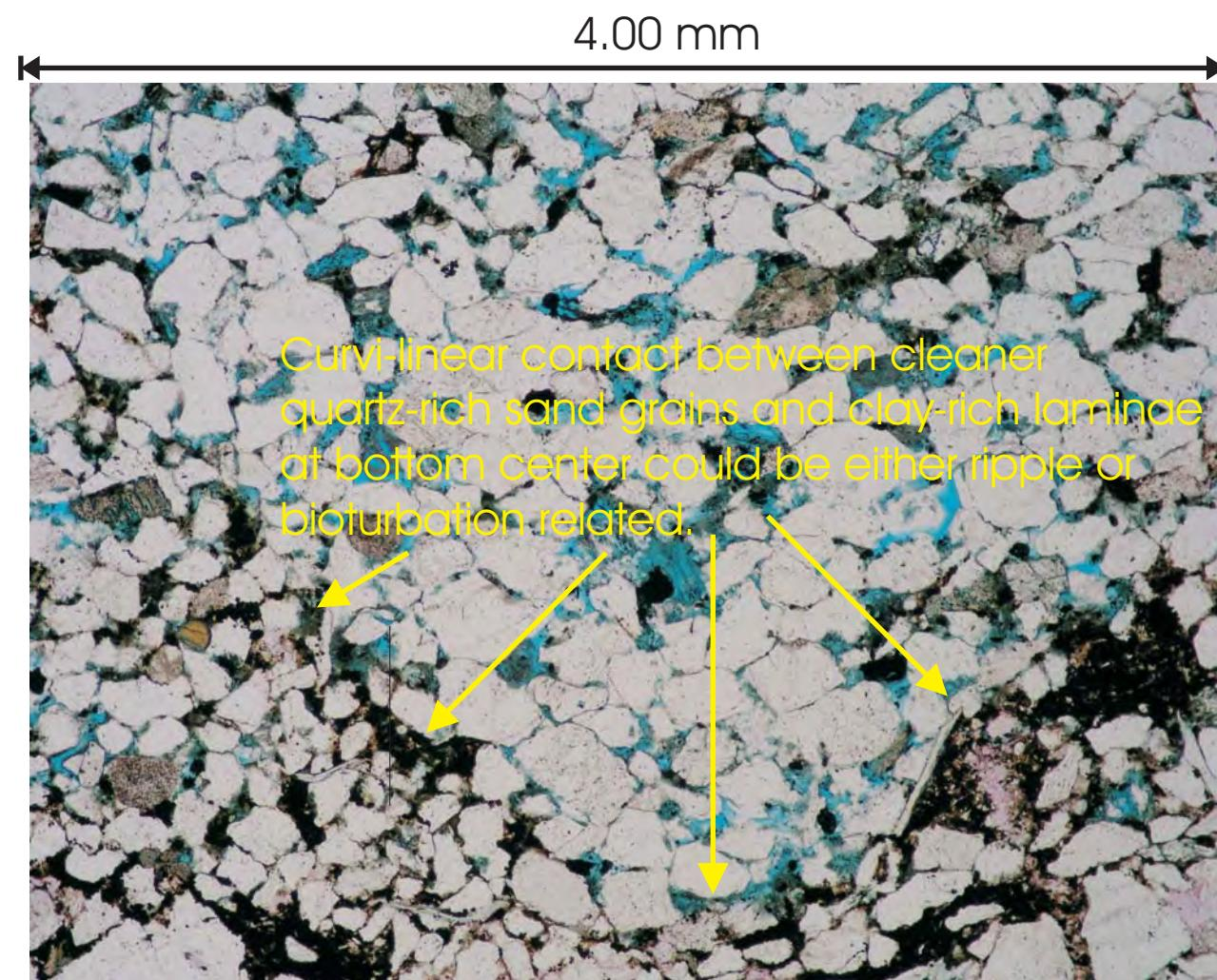
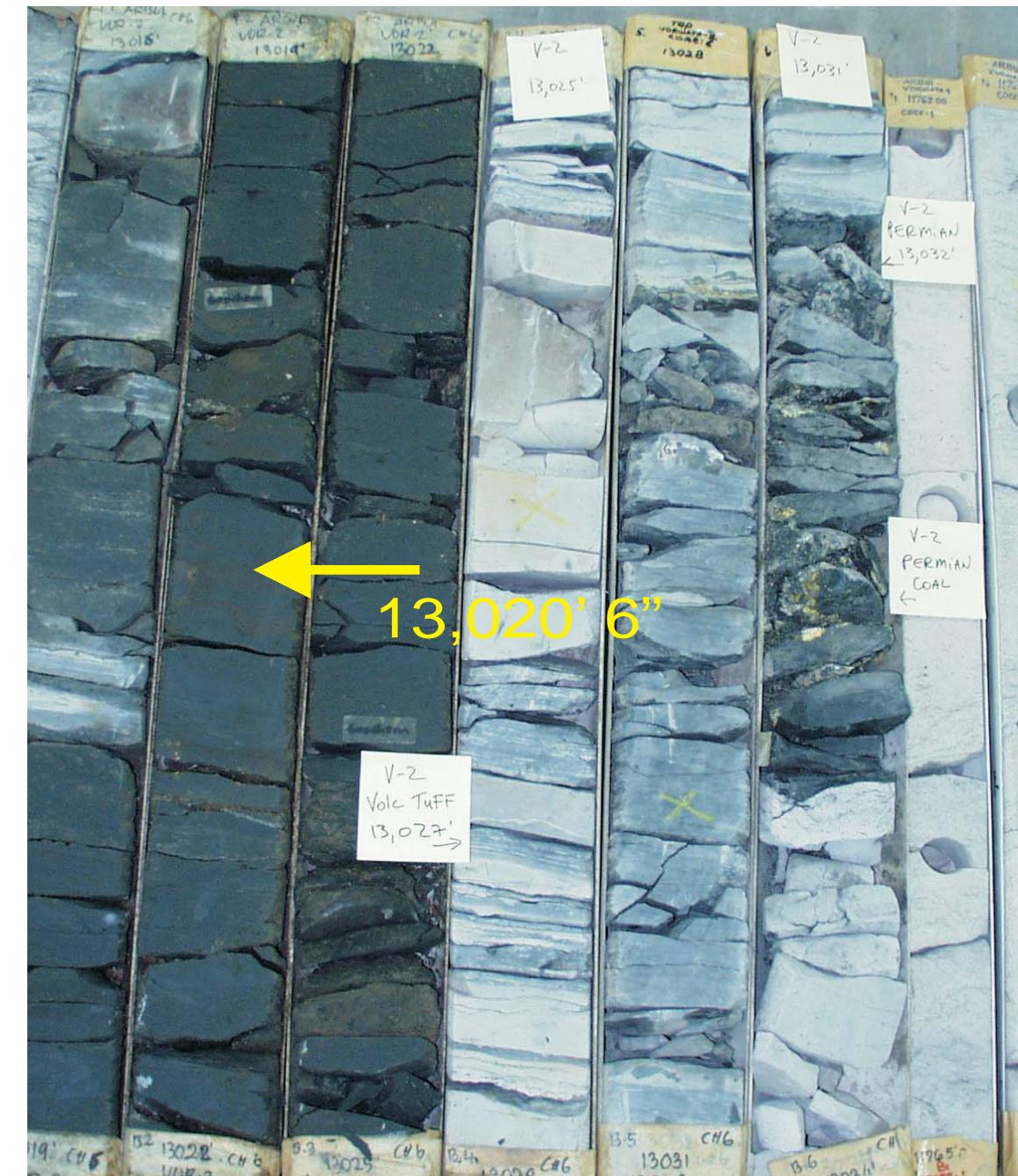
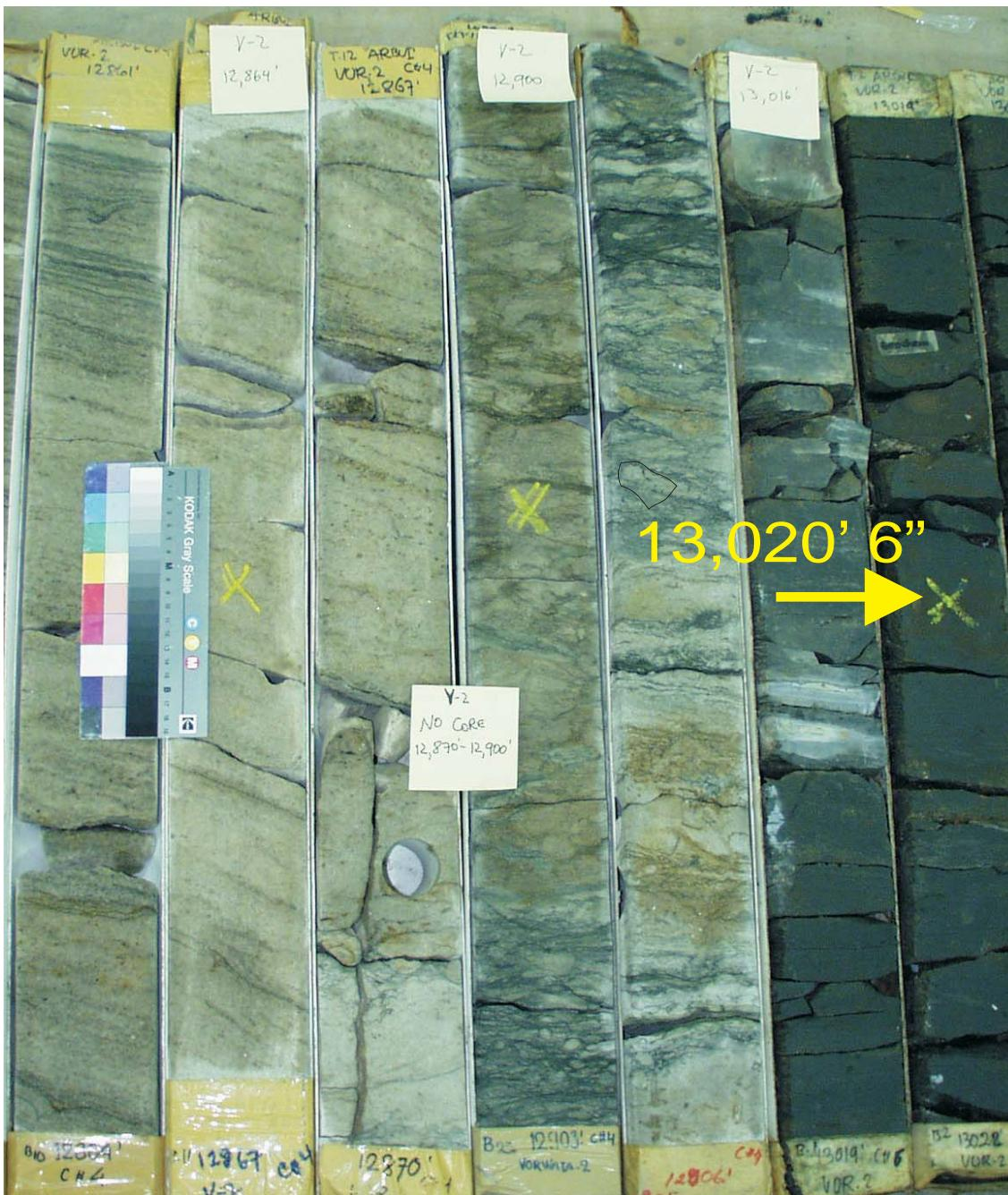


Figure 43B: Core Plug/Chip Atlas for sample 12901' 5" from Vorwata-2.

WHOLE CORE PLUG ANALYSES
WELL: VORWATA - 2
DEPTH: 12901' 5"

PLATE B:

Digital Core Chip/Plug Photograph
Petrographic Photomicrograph

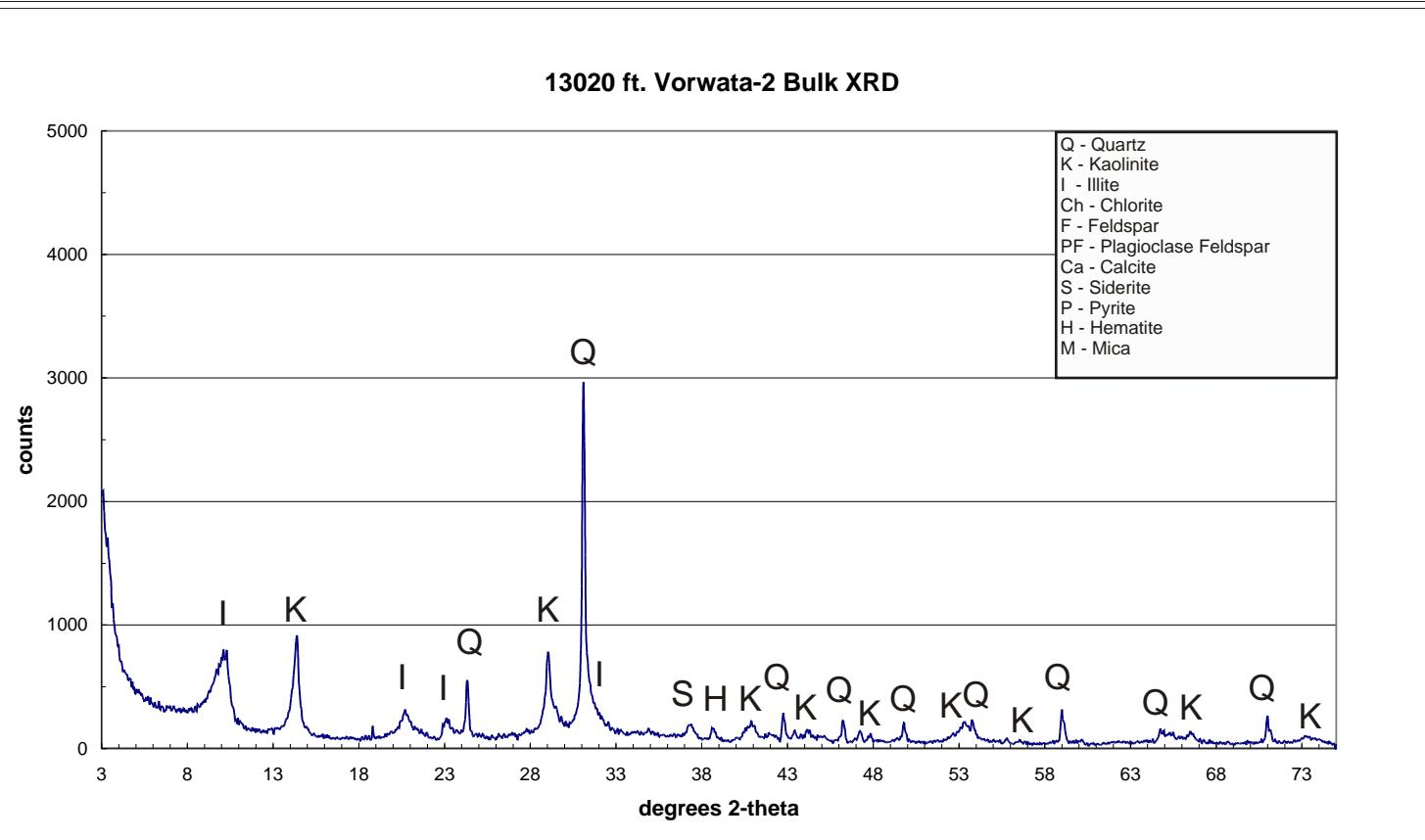


WHOLE CORE PLUG ANALYSES
WELL: VORWATA - 2
DEPTH: 13020' 6"

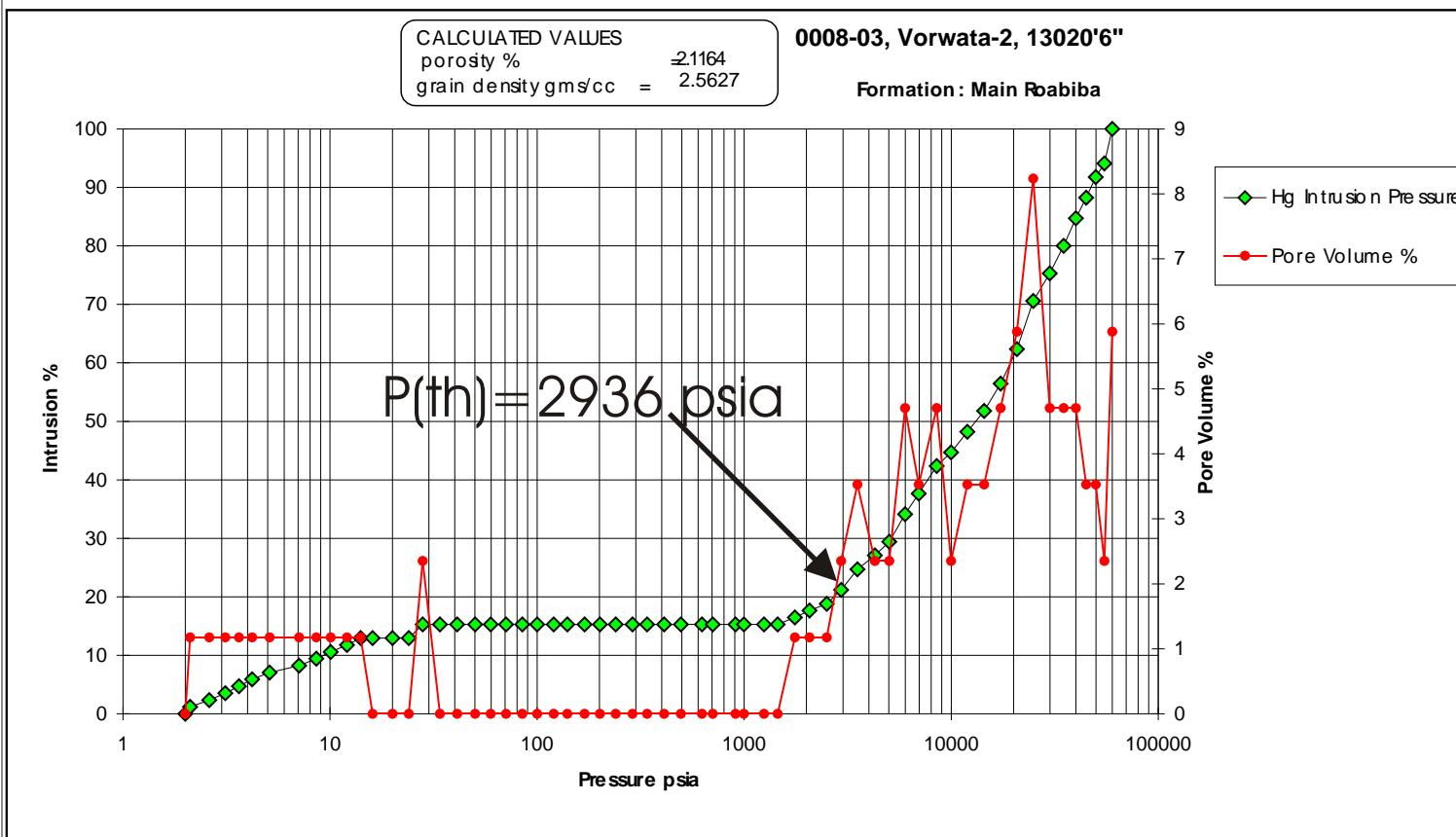
PLATE A:

Digital Whole Core Photographs

Figure 44A: Core Plug/Chip Atlas for sample 13020' 6" from Vorwata-2.



Bulk XRD showing a composition of illite, kaolinite, and quartz, with rare siderite.



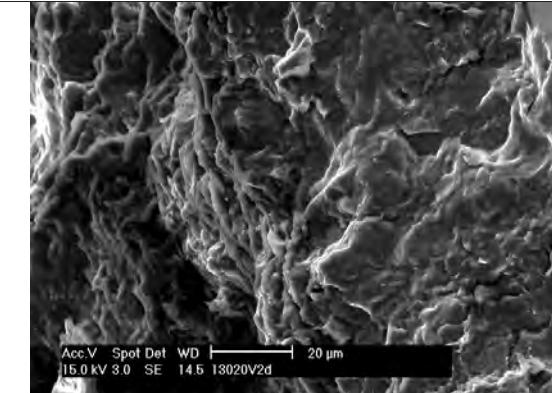
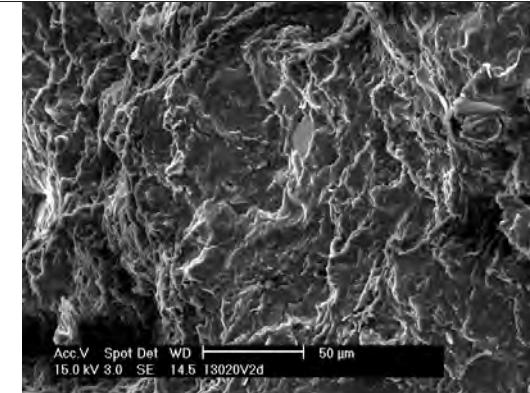
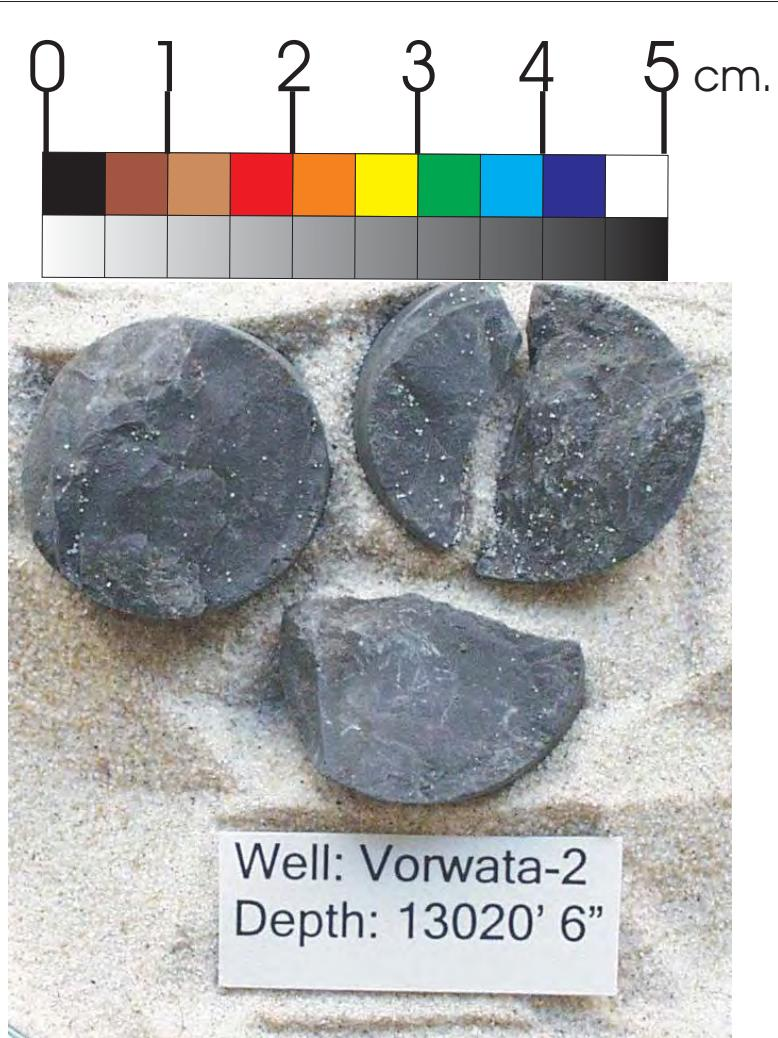
Sample Depth: 13020' 6"
Shifted Depth: 13033' 6"
MICP Entry Pressure: 1452 psia
MICP Threshold Pressure: 2936 psia
Lithology: Shale

WHOLE CORE PLUG ANALYSES
WELL: VORWATA - 2
DEPTH: 13020' 6"

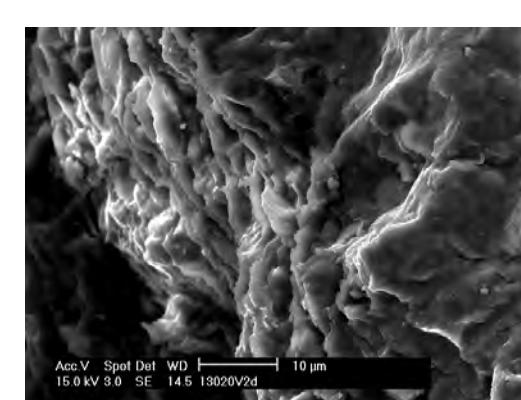
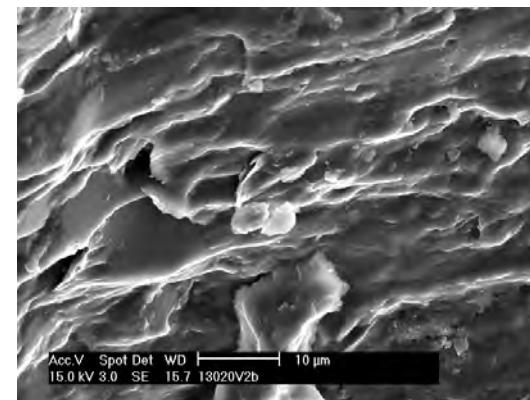
PLATE B:

BULK XRD
Mercury Injection Capillary Pressure

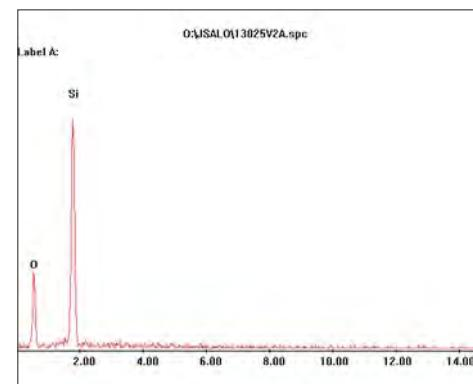
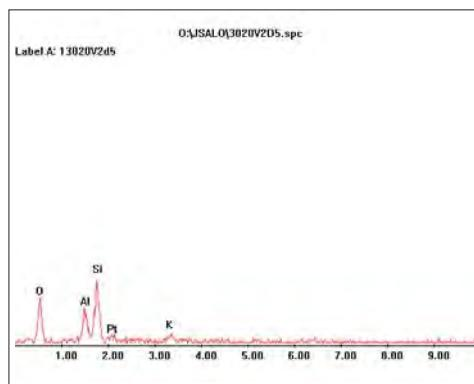
Figure 44B: Core Plug/Chip Atlas for sample 13020' 6" from Vorwata-2.



SEM images of illite mat and kaolinite, with occasional quartz silts and chlorite platelets, and rare authigenic siderte crystals.



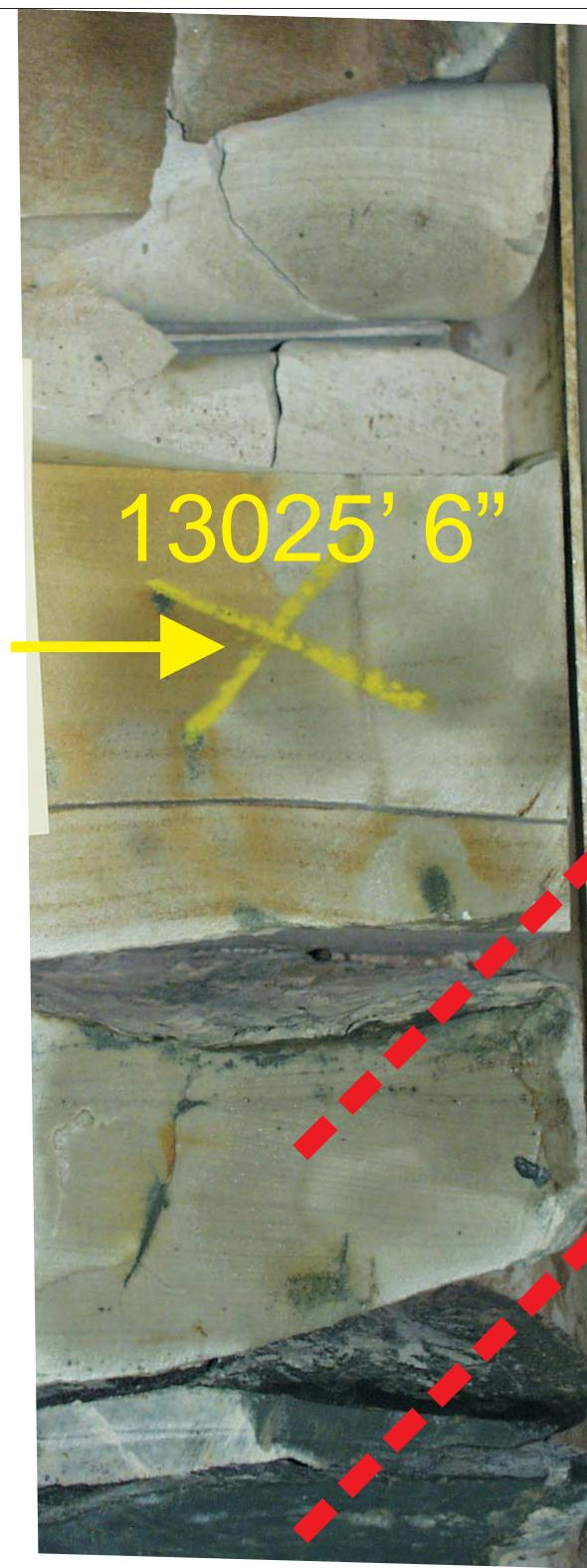
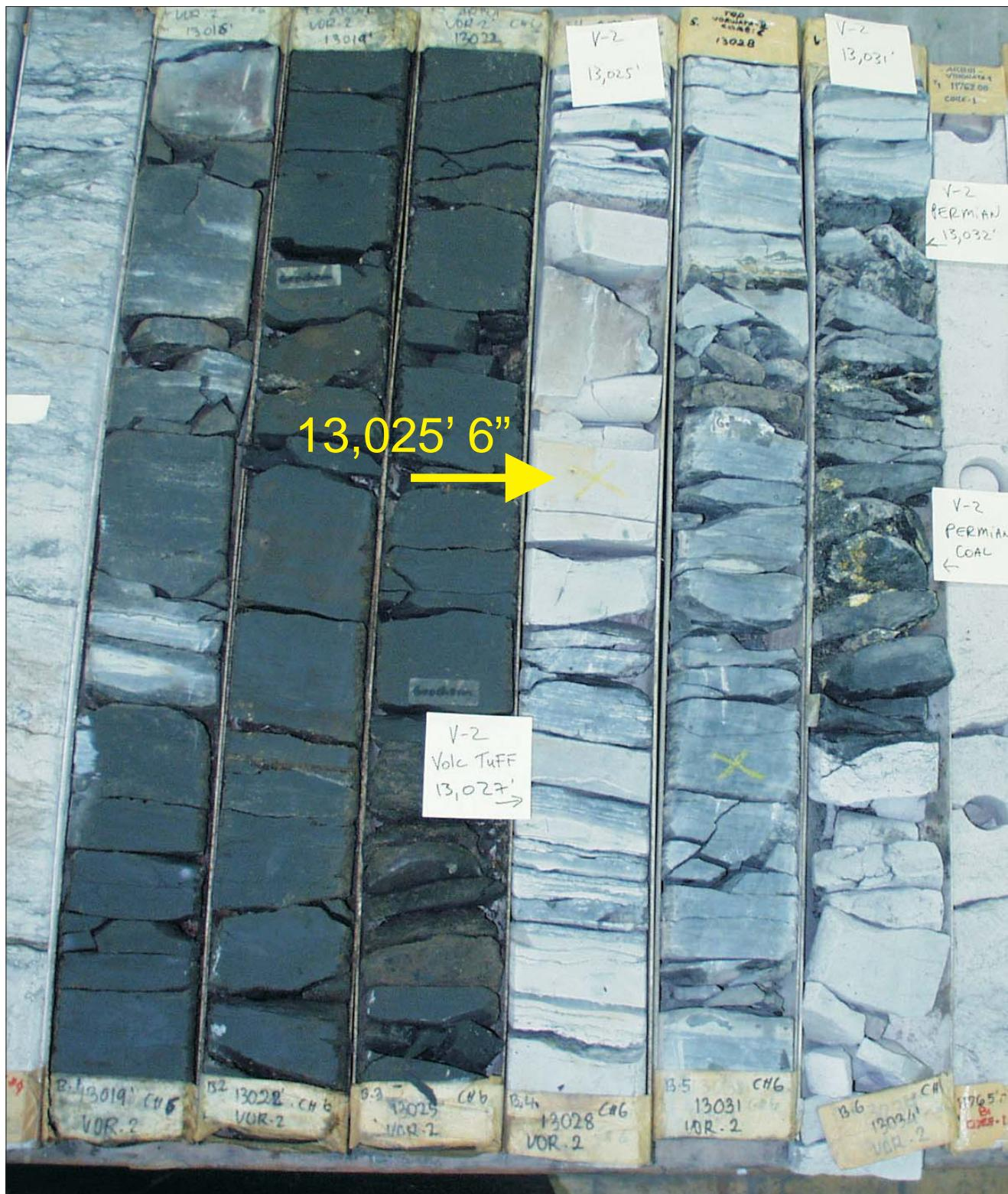
High magnification SEM images of the basal Roabiba Reservoir from the Vorwata-2 well. Illite and quartz components were verified with EDX analyses (below) made on individual grains.



WHOLE CORE PLUG ANALYSES
WELL: VORWATA - 2
DEPTH: 13020' 6"

PLATE C:
Digital Core Chip/Plug Photograph
FESEM Photomicrograph
FESEM EDX (SEM XRD)

Figure 44C: Core Plug/Chip Atlas for sample 13020' 6" from Vorwata-2.

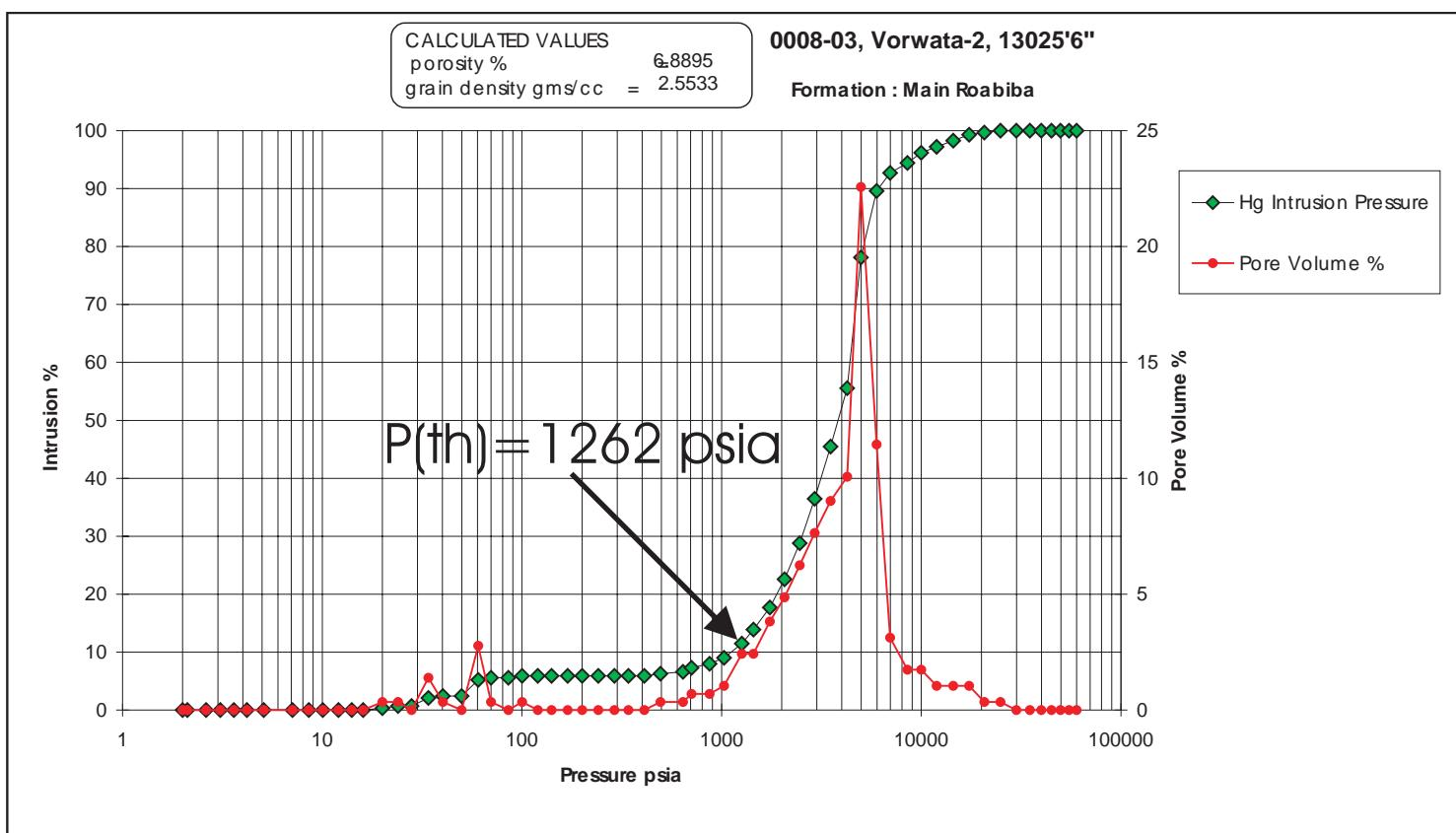
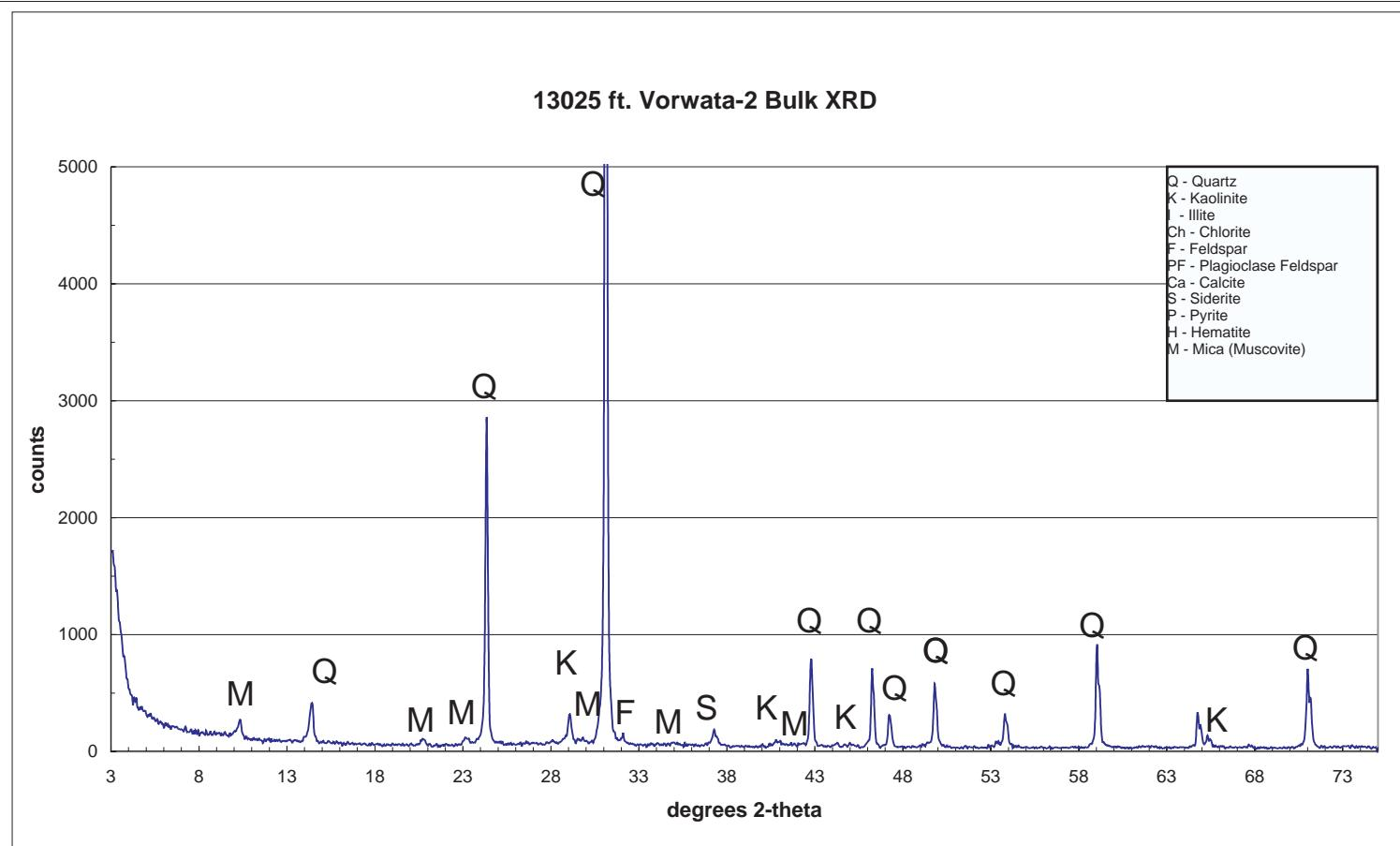
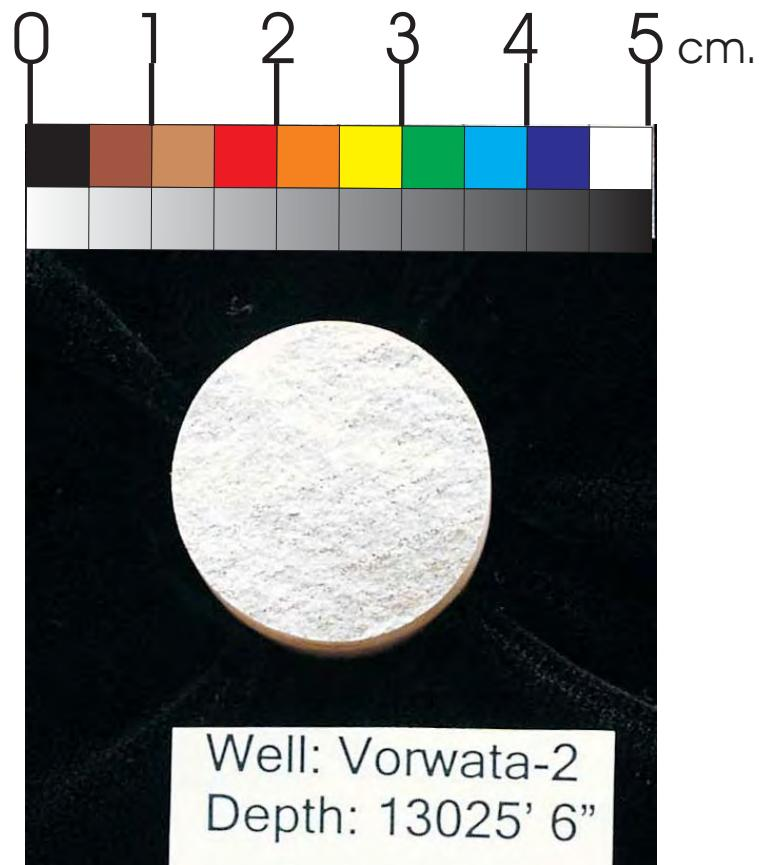


WHOLE CORE PLUG ANALYSES
WELL: VORWATA - 2
DEPTH: 13025' 6"

PLATE A:

Digital Whole Core Photographs

Figure 45A: Core Plug/Chip Atlas for sample 13025' 6" from Vorwata-2.



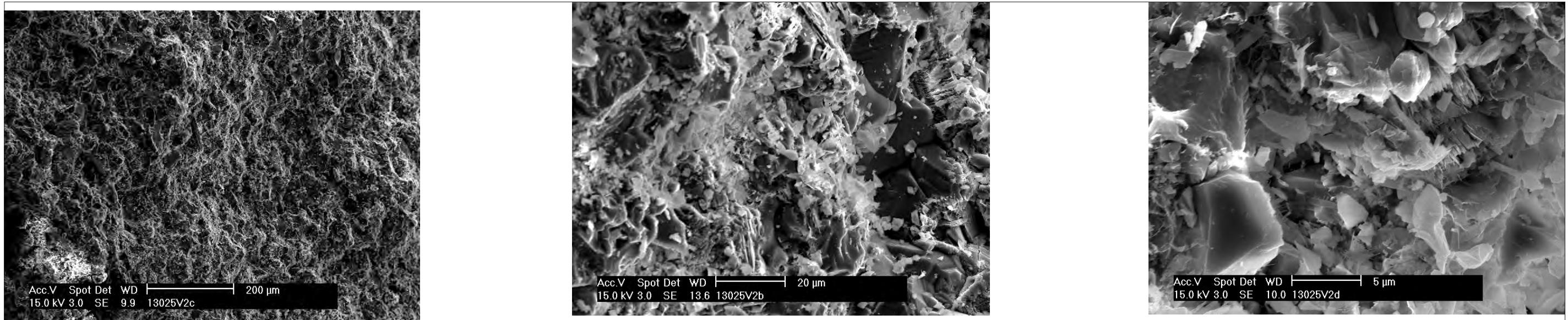
Bulk XRD indicates a quartz, kaolinite, and mica composition with traces of siderite.

Sample Depth: 13025' 6"
Shifted Depth: 13038' 6"
MICP Entry Pressure: 706 psia
MICP Threshold Pressure: 1262 psia
Lithology: Tuffaceous Shale

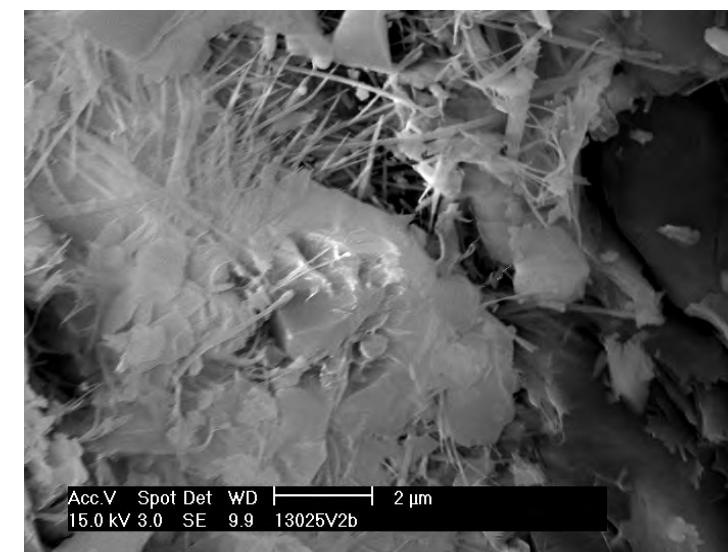
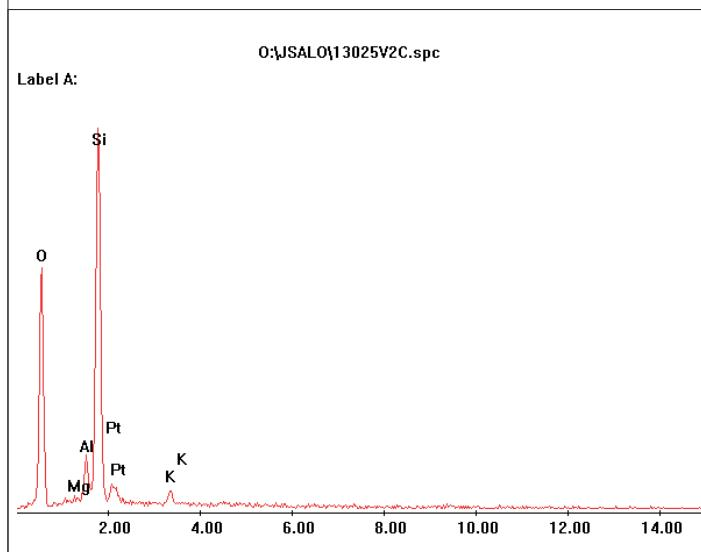
WHOLE CORE PLUG ANALYSES
WELL: VORWATA - 2
DEPTH: 13025' 6"

PLATE B:
Digital Core Chip/Plug Photograph
BULK XRD
Mercury Injection Capillary Pressure

Figure 45B: Core Plug/Chip Atlas for sample 13025' 6" from Vorwata-2.



SEM images of basal Roabiba Reservoir shales showing kaolinite, and illite/muscovite matrix with occasional quartz silts .



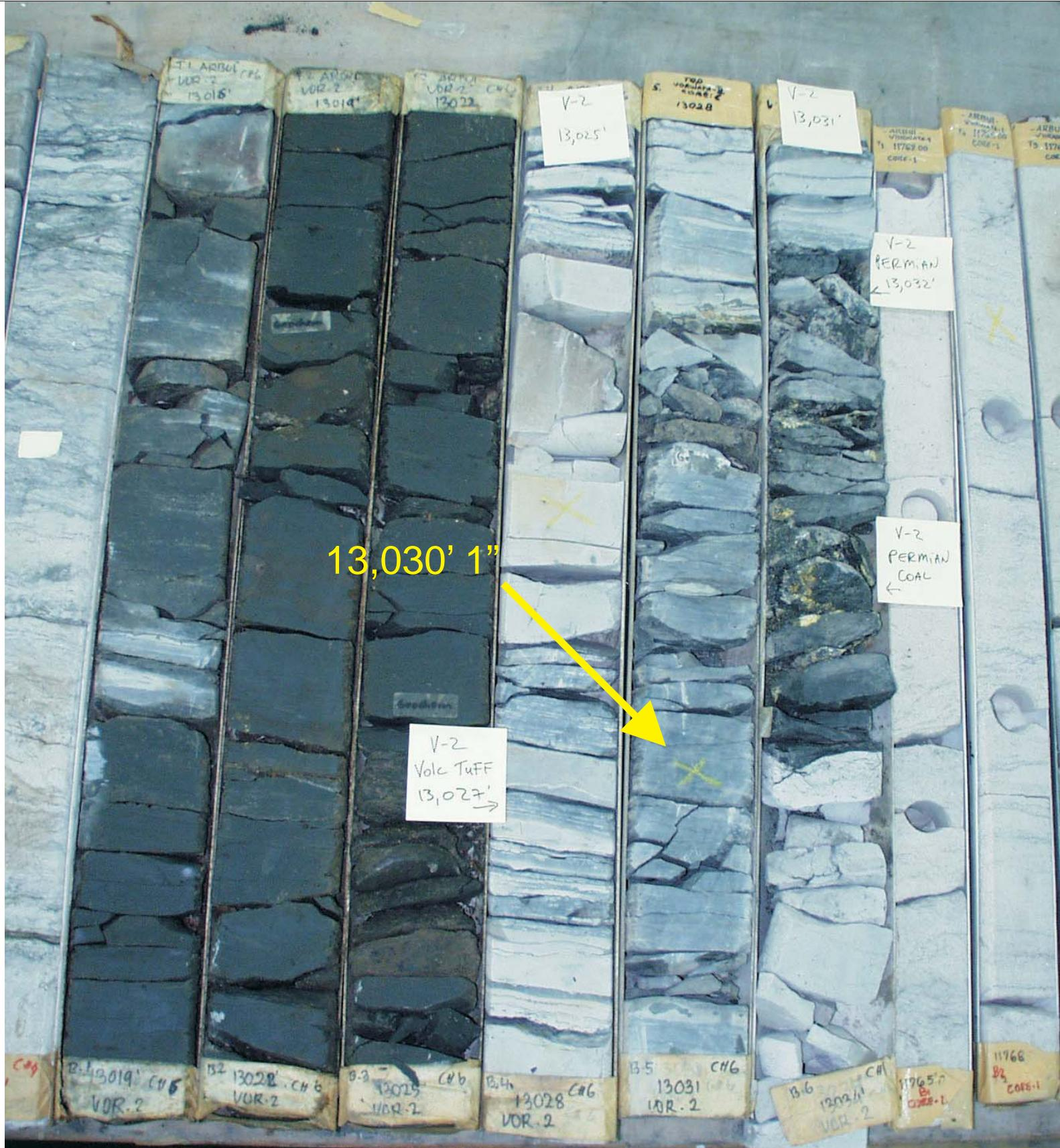
Wispy illite-smectite authigenic filaments are also present.
EDX indicates sample is primarily kaolinite and illite/muscovite.

Figure45C: Core Plug/Chip Atlas for sample 13025' 6" from Vorwata-2.

WHOLE CORE PLUG ANALYSES
WELL: VORWATA - 2
DEPTH: 13025' 6"

PLATE C:

FESEM Photomicrograph
FESEM EDX (SEM XRD)

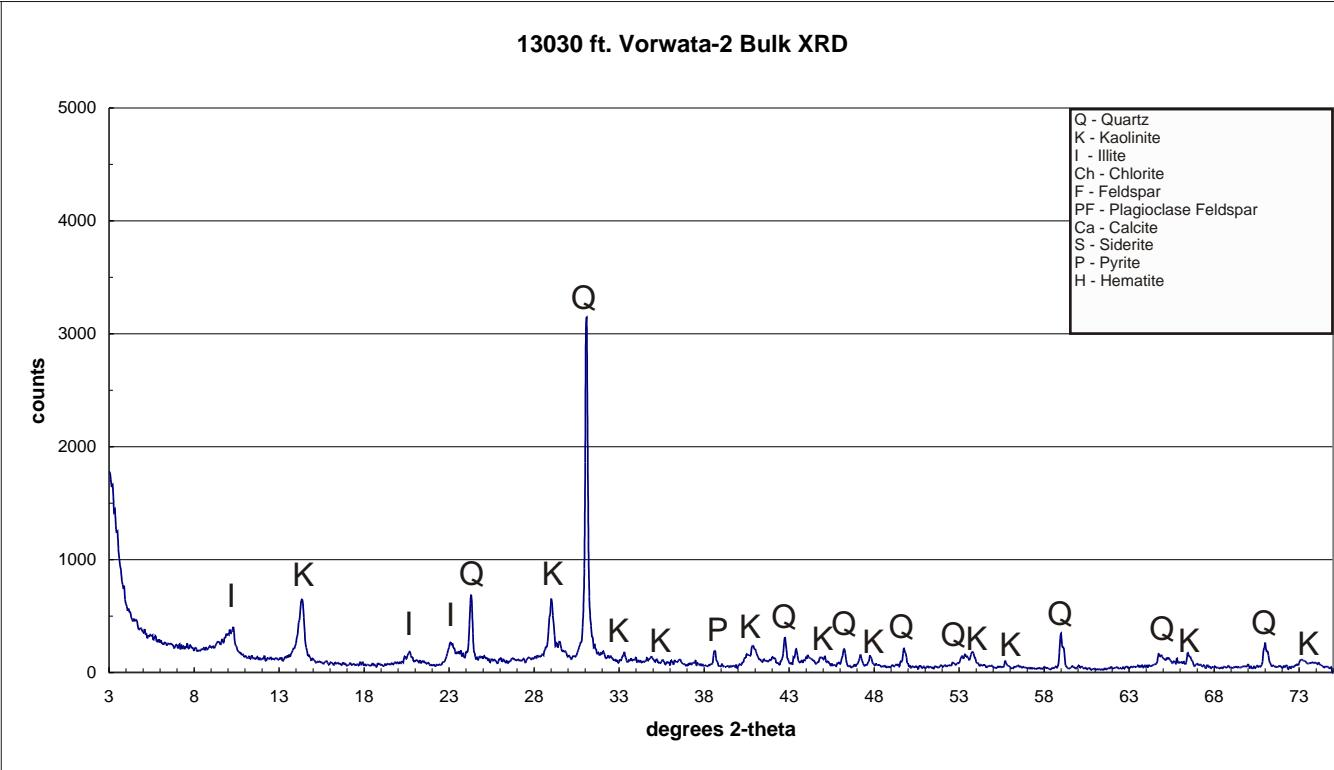


WHOLE CORE PLUG ANALYSES
WELL: VORWATA - 2
DEPTH: 13030' 1"

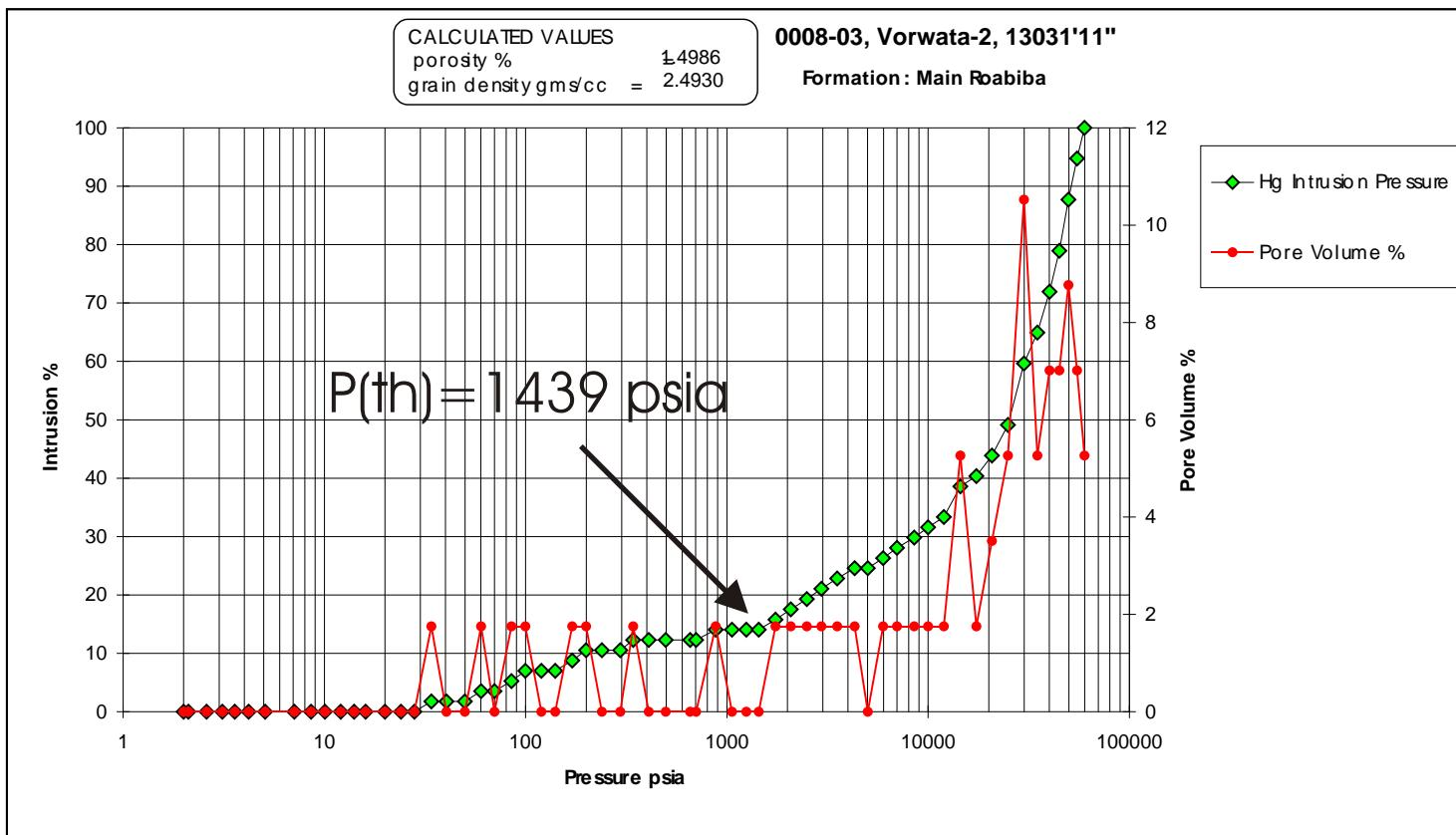
PLATE A:

Digital Whole Core Photographs
Digital Core Chip/Plug Photograph

Figure 46A: Core Plug/Chip Atlas for sample 13030' 1" from Vorwata-2.



Bulk XRD results indicating a bulk composition of illite, kaolinite, quartz, and minor chlorite.



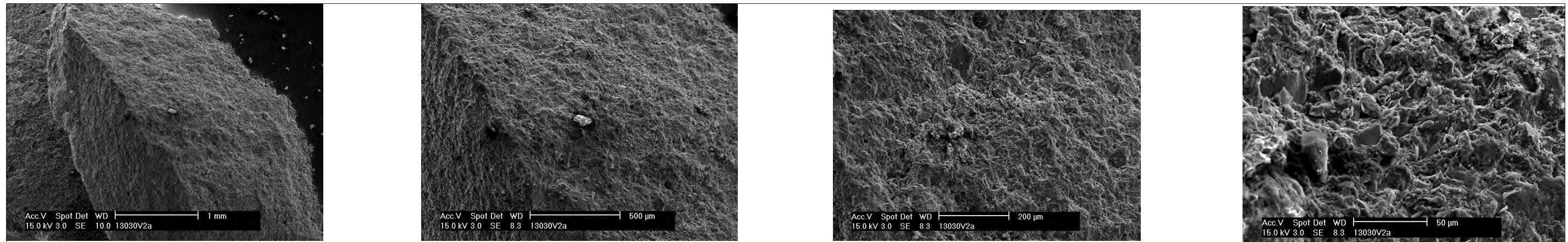
Sample Depth: 13030' 1"
Shifted Depth: 13042' 1"
MICP Entry Pressure: 702 psia
MICP Threshold Pressure: 1439 psia
Lithology: Shale

WHOLE CORE PLUG ANALYSES
WELL: VORWATA - 2
DEPTH: 13030' 1"

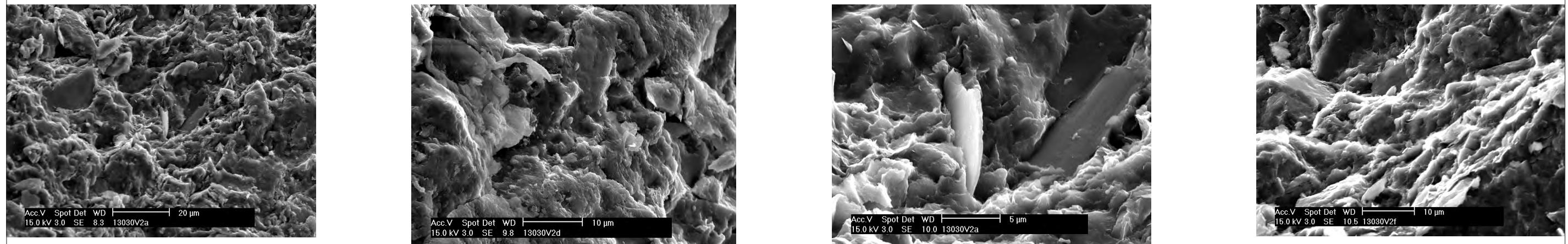
PLATE B:

BULK XRD
Mercury Injection Capillary Pressure

Figure 46B: Core Plug/Chip Atlas for sample 13030' 1" from Vorwata-2.



A series of SEM images showing illite-hydrated smectites and kaolinite matrix, with occasional quartz and rare potassic-feldspar silt grains scattered throughout.



High magnification SEM images of basal Roabiba reservoir shales. EDX indicates illite clay with some quartz present.

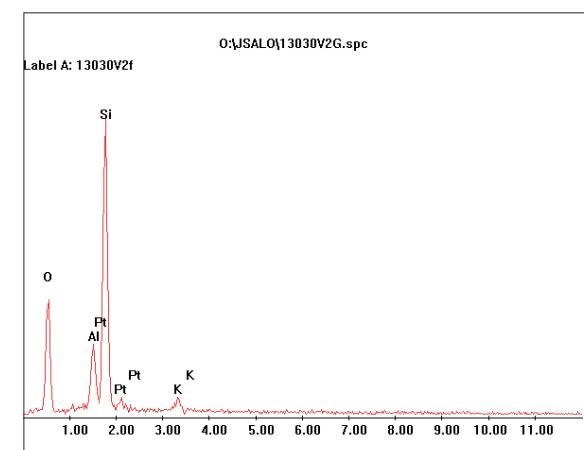
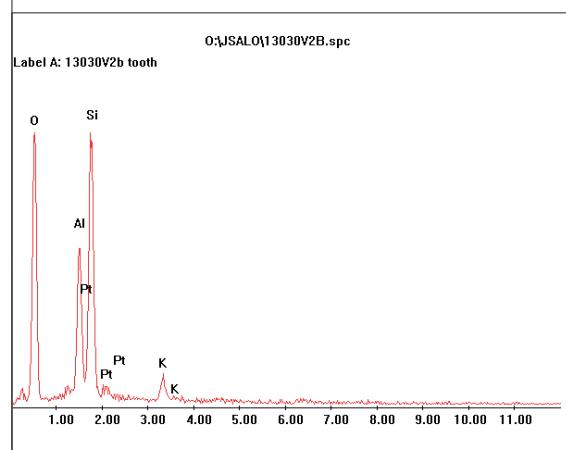


Figure 46C: Core Plug/Chip Atlas for sample 13030' 1" from Vorwata-2.

WHOLE CORE PLUG ANALYSES
WELL: VORWATA - 2
DEPTH: 13030' 1"

PLATE C:

FESEM Photomicrograph
FESEM EDX (SEM XRD)

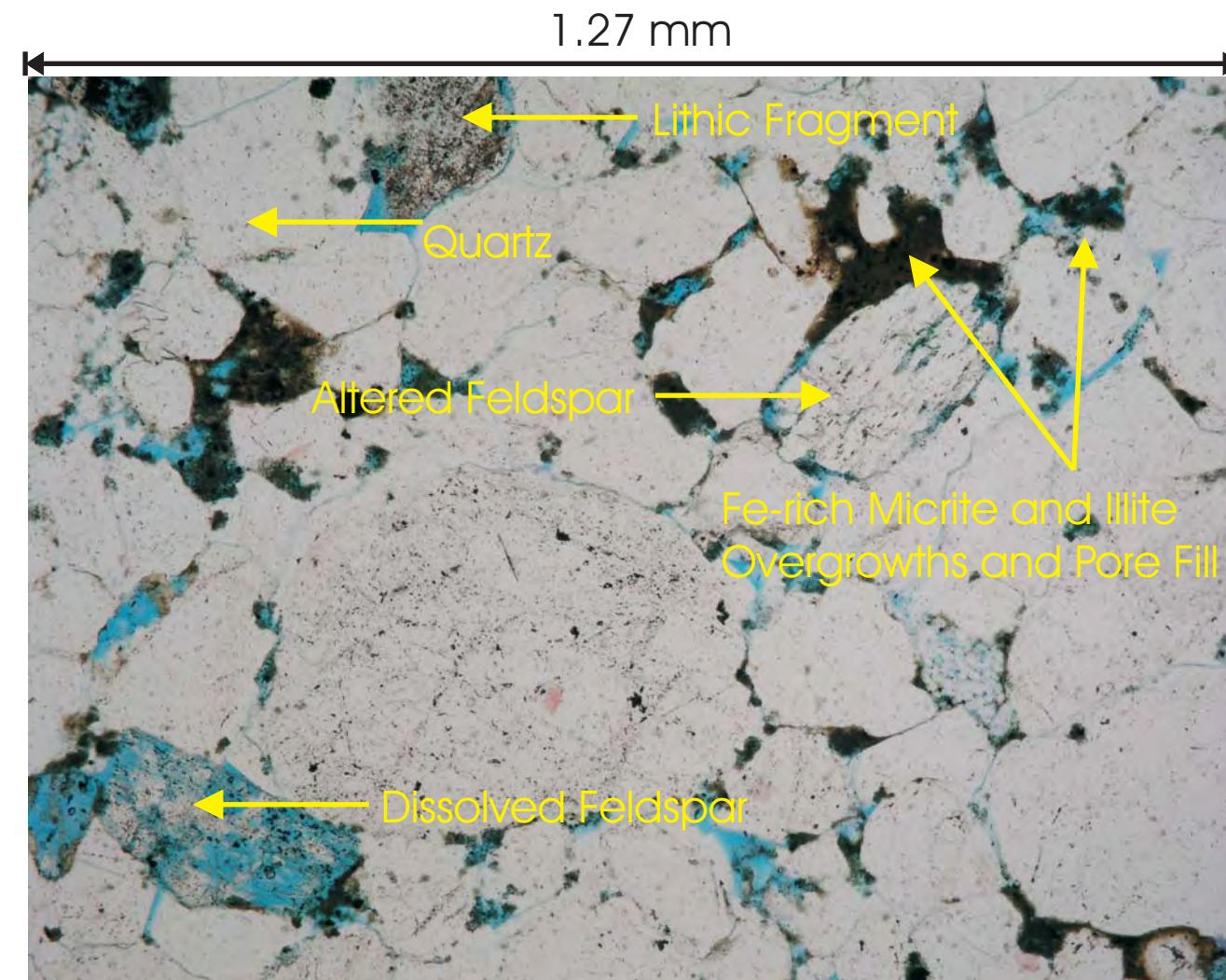


WHOLE CORE PLUG ANALYSES
WELL: VORWATA - 7
DEPTH: 13118' 3"

PLATE A:

Digital Whole Core Photographs

Figure 47A: Core Plug/Chip Atlas for sample 13118' 3" from Vorwata-7.



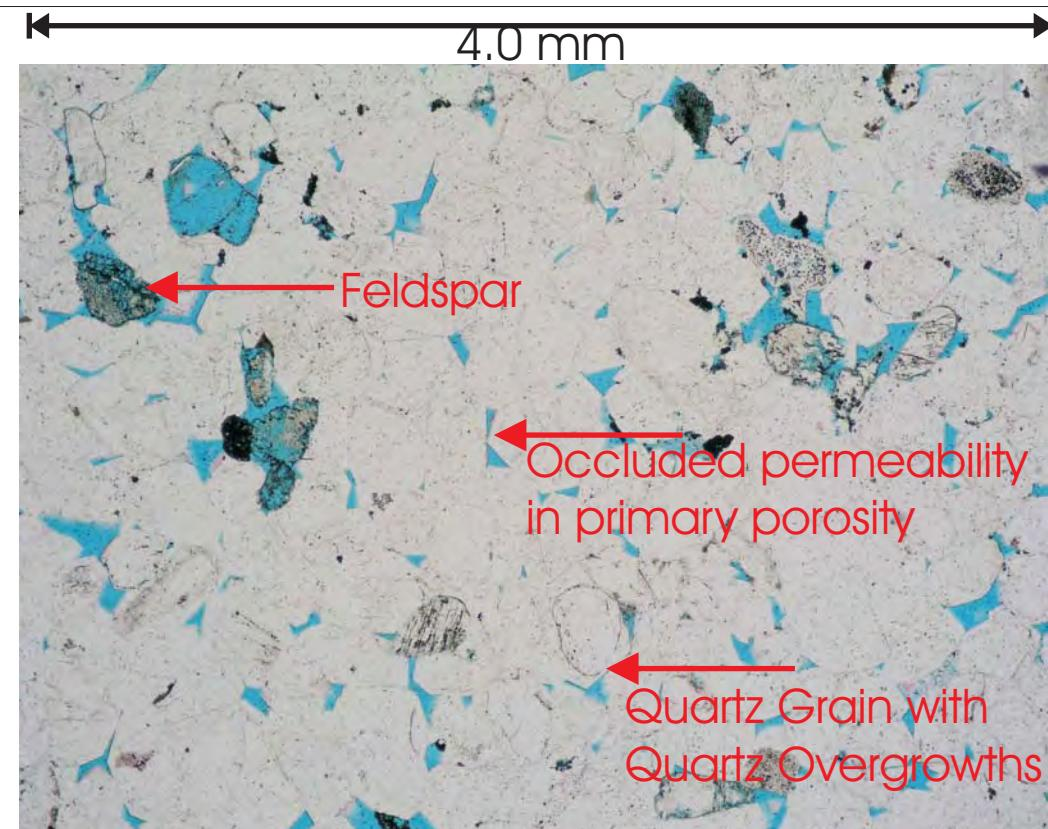
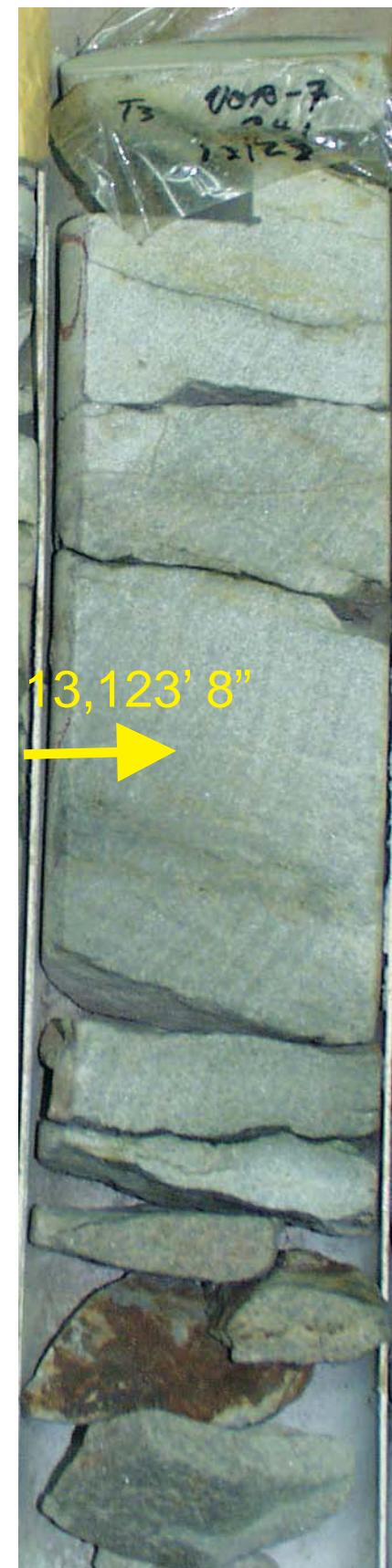
Sample Depth: 13118' 3"
Shifted Depth: 13132' 3"
He-∅: 9.9%
k air: 0.233mD (NOB 800 psia)

WHOLE CORE PLUG ANALYSES
WELL: VORWATA - 7
DEPTH: 13118' 3"

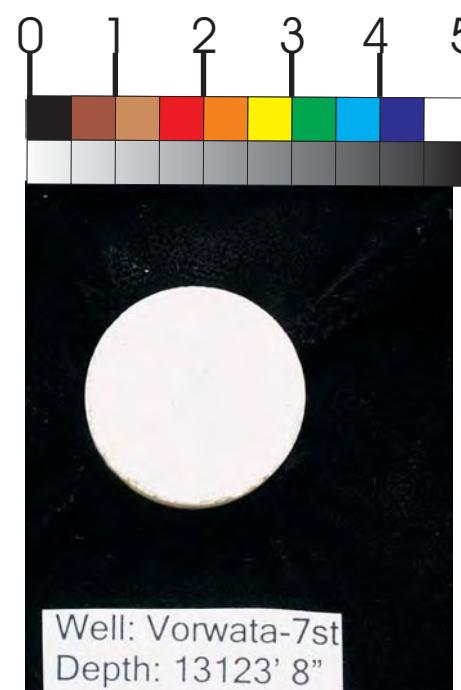
PLATE B:

Digital Core Chip/Plug Photograph
Petrographic Photomicrograph

Figure 47B: Core Plug/Chip Atlas for sample 13118' 3" from Vorwata-7.



Subarkosic sandstone core plug from the Roabiba Reservoir. Petrography shows quartz grains with quartz overgrowths, and occasional feldspar/relict altered feldspar grains. Occluded porosity is rarely interconnected resulting in poor permeability.

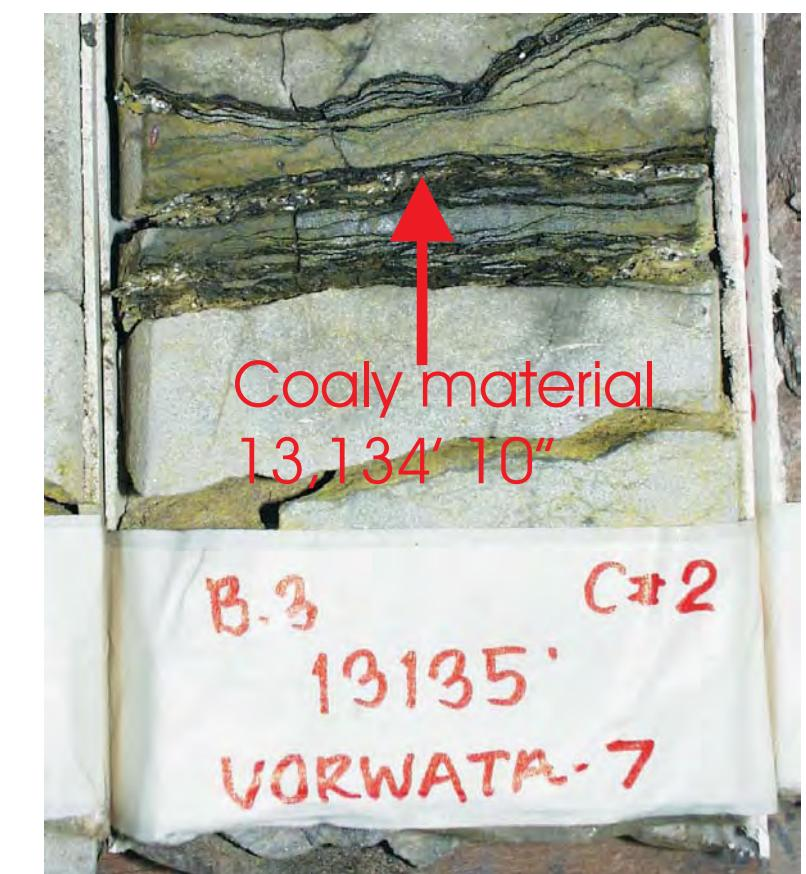
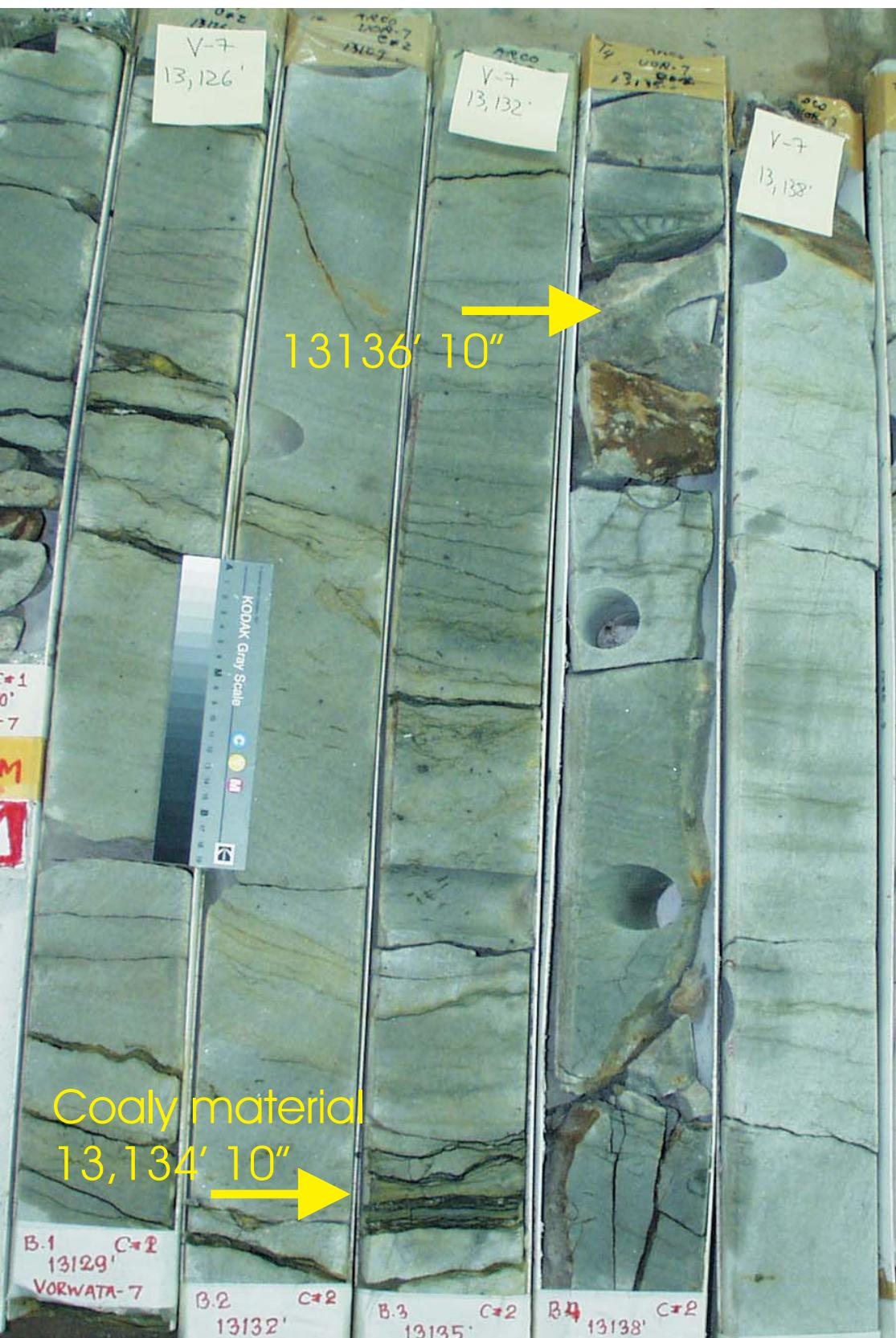


Sample Depth: 13123' 8"
Shifted Depth: 13137' 8"
He-Ø: 6.5%
k air: 0.868 mD (NOB 800 psia)

WHOLE CORE PLUG ANALYSES
WELL: VORWATA - 7
DEPTH: 13123' 8"

PLATE A:
Digital Whole Core Photographs
Digital Core Chip/Plug Photograph
Petrographic Photomicrograph

Figure 48A: Core Plug/Chip Atlas for sample 13123' 8" from Vorwata-7.

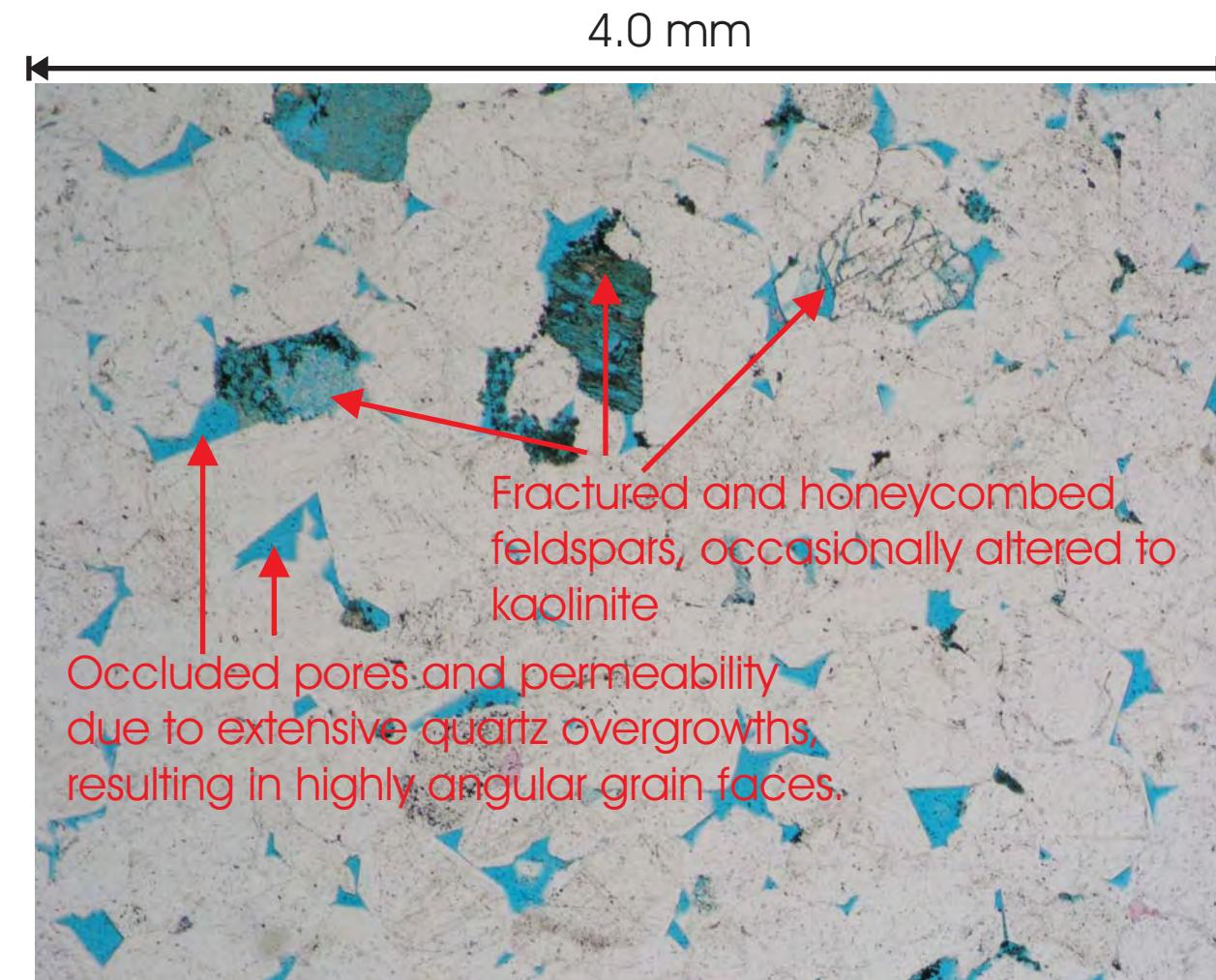


WHOLE CORE PLUG ANALYSES
WELL: VORWATA - 7
DEPTH: 13136' 10"

PLATE A:

Digital Whole Core Photographs

Figure 49A: Core Plug/Chip Atlas for sample 13136' 10" from Vorwata-7.

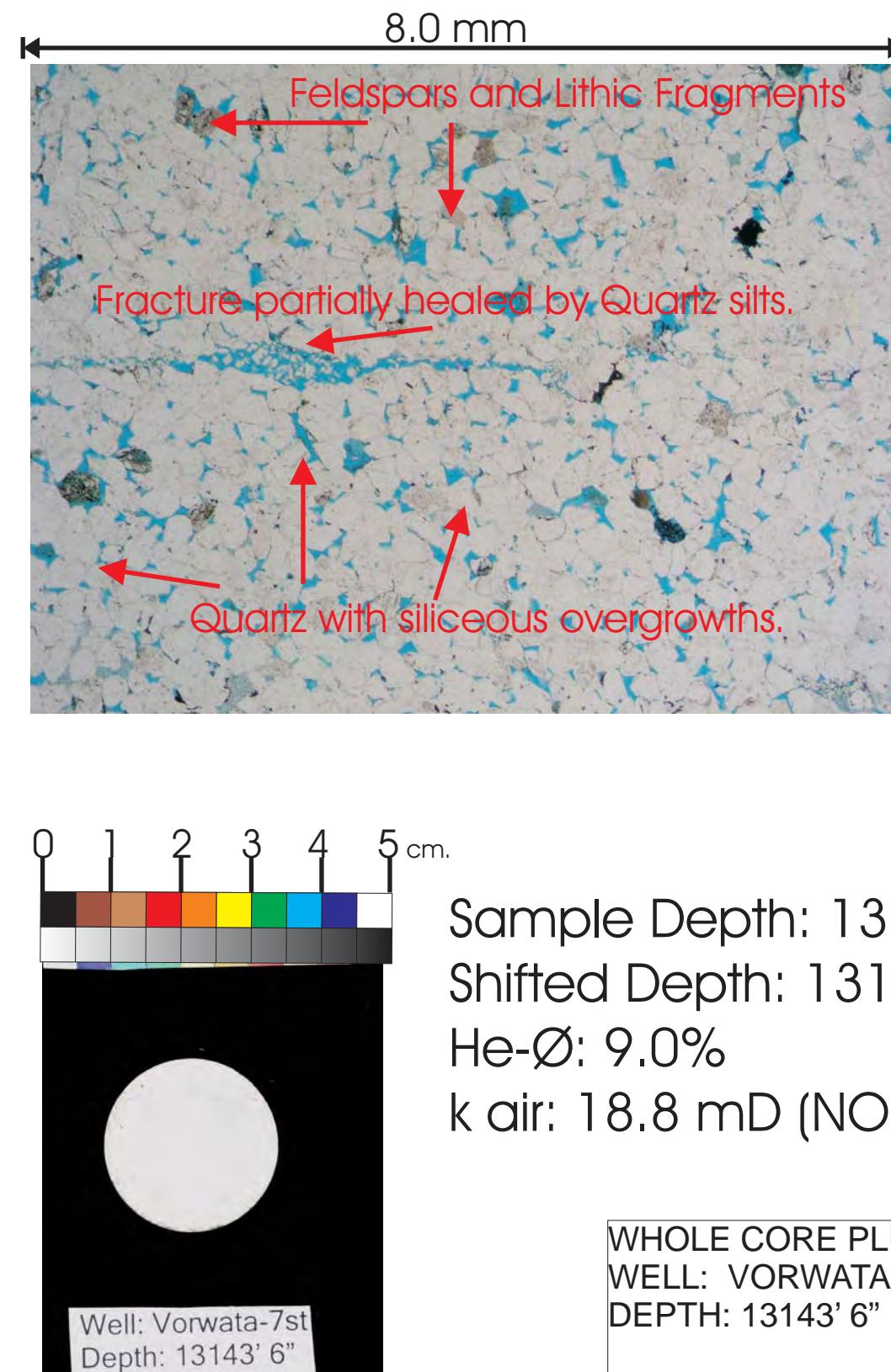


Sample Depth: 13136' 10"
 Shifted Depth: 13150' 10"
 He-Ø: 8.5%
 k air: 7.14 mD (NOB 800 psia)

WHOLE CORE PLUG ANALYSES
 WELL: VORWATA - 7
 DEPTH: 13136' 10"

 PLATE B:
 Digital Core Chip/Plug Photograph
 Petrographic Photomicrograph

Figure 49B: Core Plug/Chip Atlas for sample 13136' 10" from Vorwata-7.

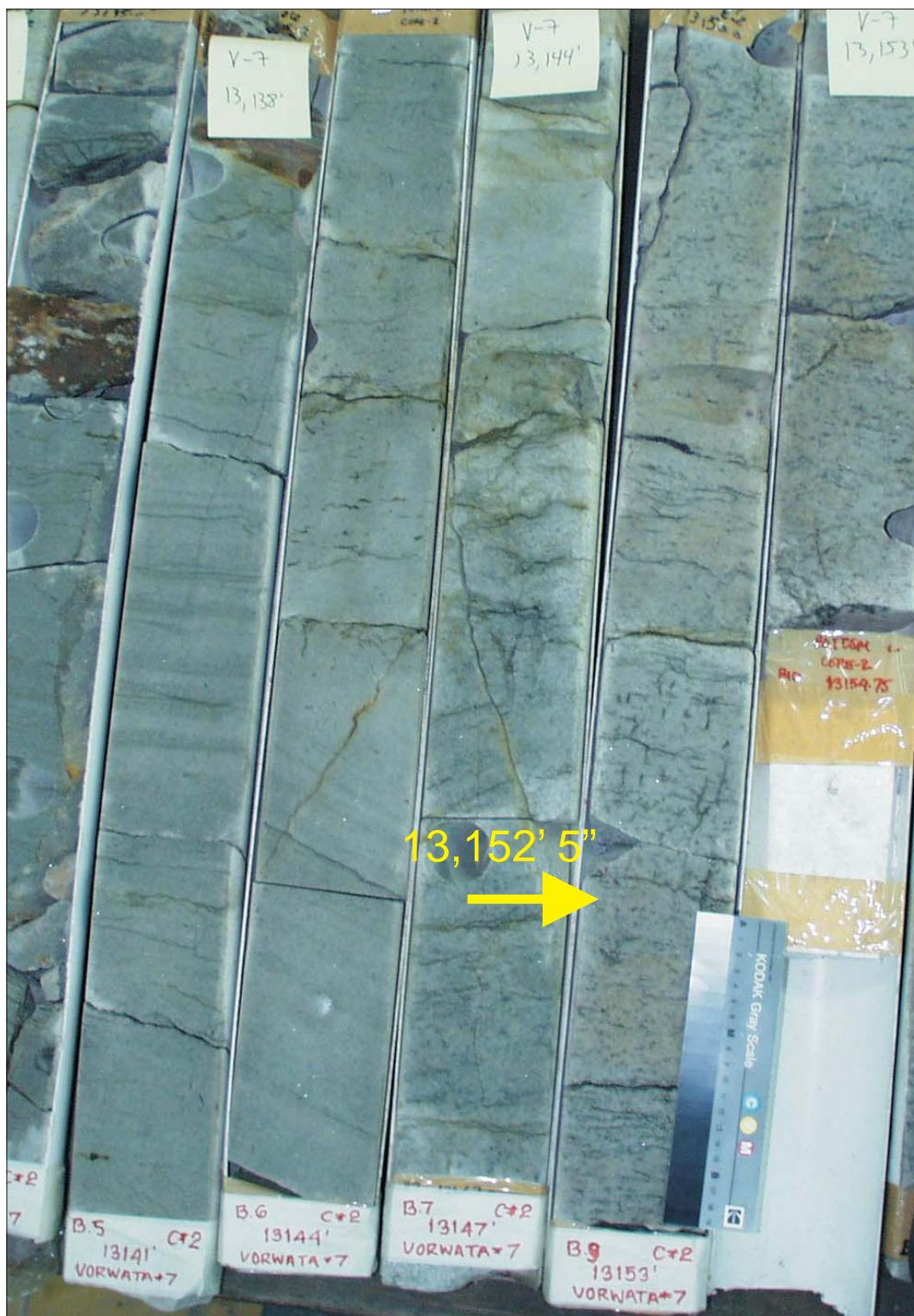


Sample Depth: 13143' 6"
Shifted Depth: 13157' 6"
He-Ø: 9.0%
k air: 18.8 mD (NOB 800 psia)

WHOLE CORE PLUG ANALYSES
WELL: VORWATA - 7
DEPTH: 13143' 6"

PLATE A:
Digital Whole Core Photographs
Digital Core Chip/Plug Photograph
Petrographic Photomicrograph

Figure 50A: Core Plug/Chip Atlas for sample 13143' 6" from Vorwata-7.

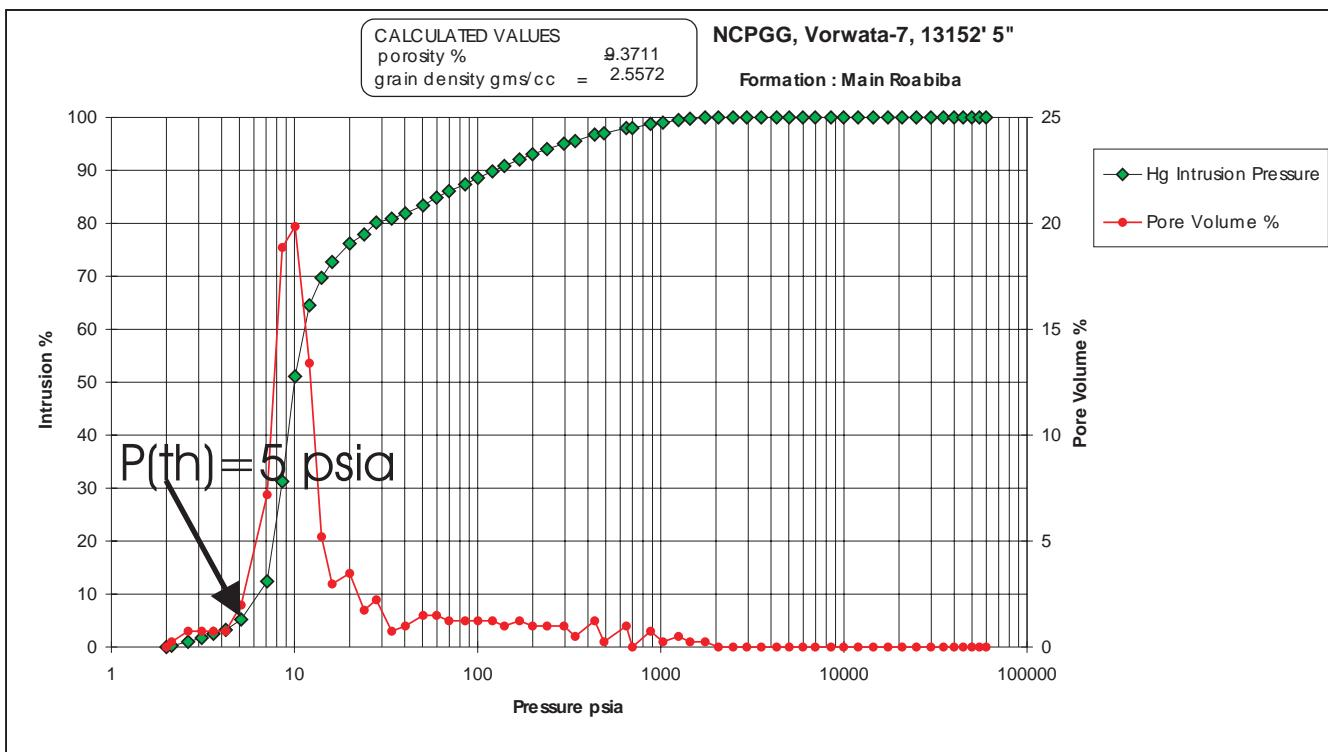
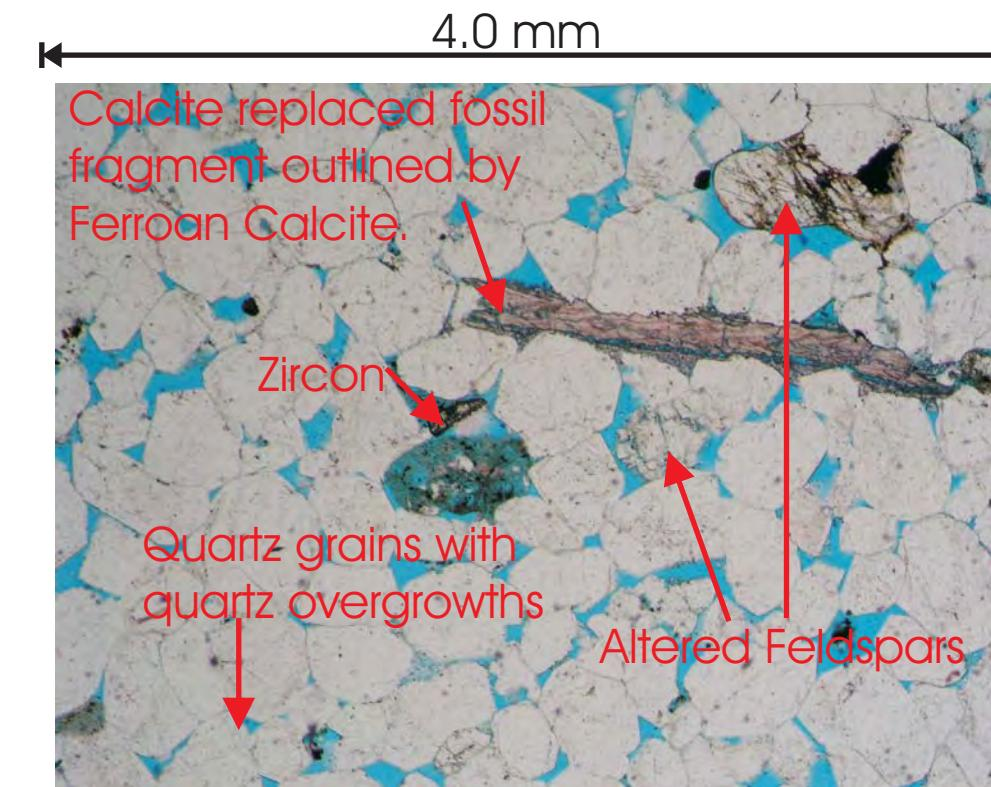
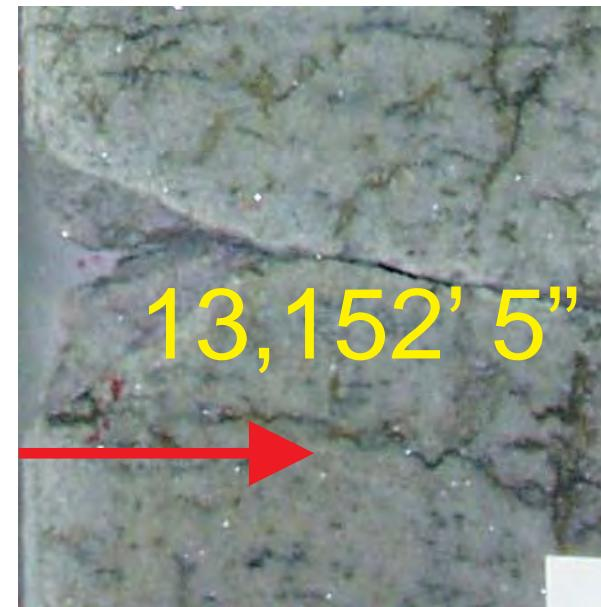


WHOLE CORE PLUG ANALYSES
WELL: VORWATA - 7
DEPTH: 13152' 5"

PLATE A:

Digital Whole Core Photographs

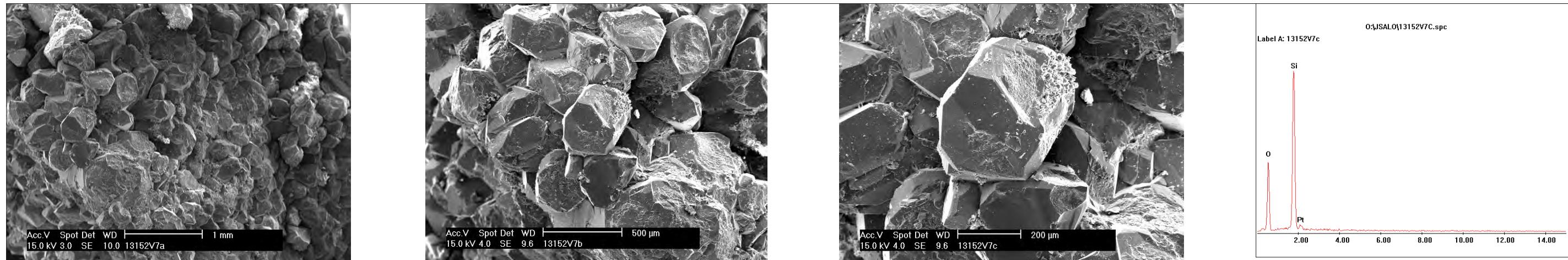
Figure 51A: Core Plug/Chip Atlas for sample 13152' 5" from Vorwata-7.



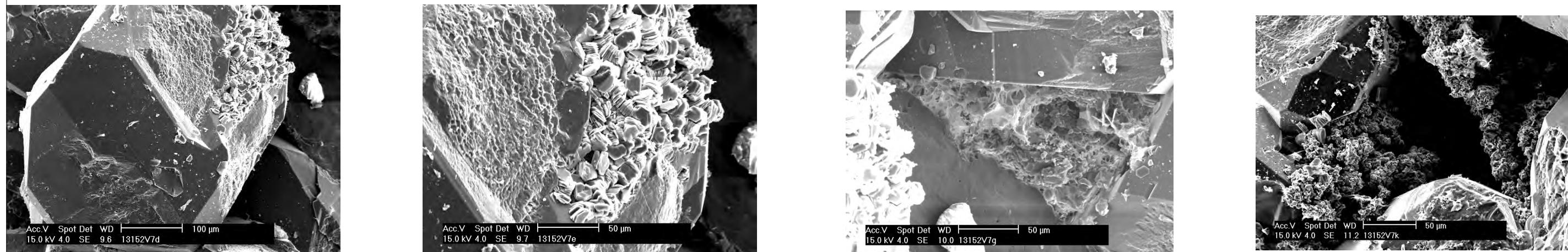
Sample Depth: 13152' 5"
Shifted Depth: 13166' 5"
MICP Entry Pressure: 3 psia
MICP Threshold Pressure: 5 psia
Lithology: Sandstone (Roabiba)

Figure 51B: Core Plug/Chip Atlas for sample 13152' 5" from Vorwata-7.

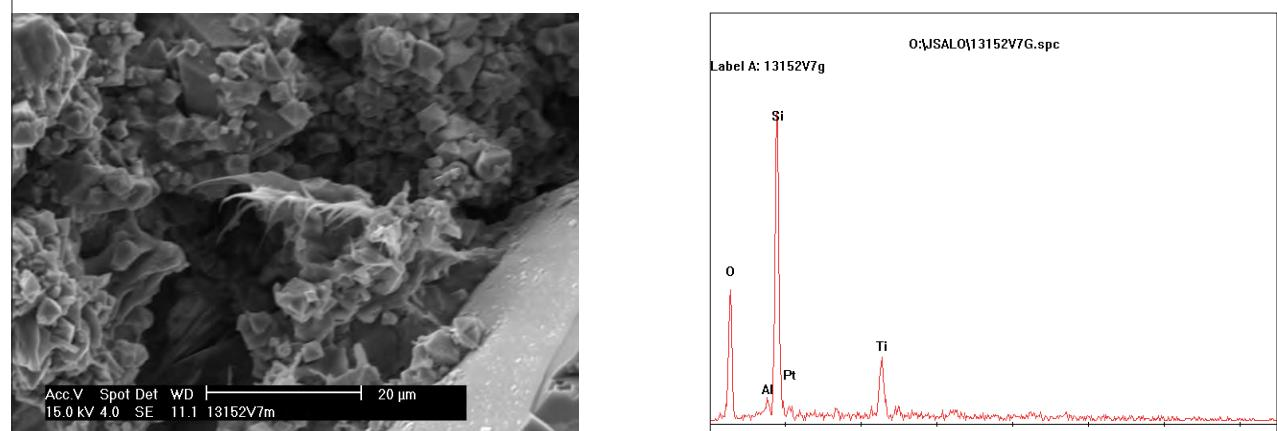
WHOLE CORE PLUG ANALYSES
WELL: VORWATA - 7
DEPTH: 13152' 5"
PLATE B:
Digital Whole Core Photographs
Digital Core Chip/Plug Photograph
Petrographic Photomicrograph
Mercury Injection Capillary Pressure



Quartz grains with common quartz overgrowths, and weak alignment, quartz composition confirmed with EDX analysis.



Increased SEM magnification showing kaolin clay platelets forming in intergranular pore spaces, and also exhibiting microporosity within the kaolinite.



Sample Depth: 13152' 5"
Shifted Depth: 13166' 5"
He-∅: 10.7%
k air: 131 mD (NOB 800 psia)

WHOLE CORE PLUG ANALYSES
WELL: VORWATA - 7
DEPTH: 13152' 5"

PLATE C:

FESEM Photomicrograph
FESEM EDX (SEM XRD)

Figure 51C: Core Plug/Chip Atlas for sample 13152' 5" from Vorwata-7.

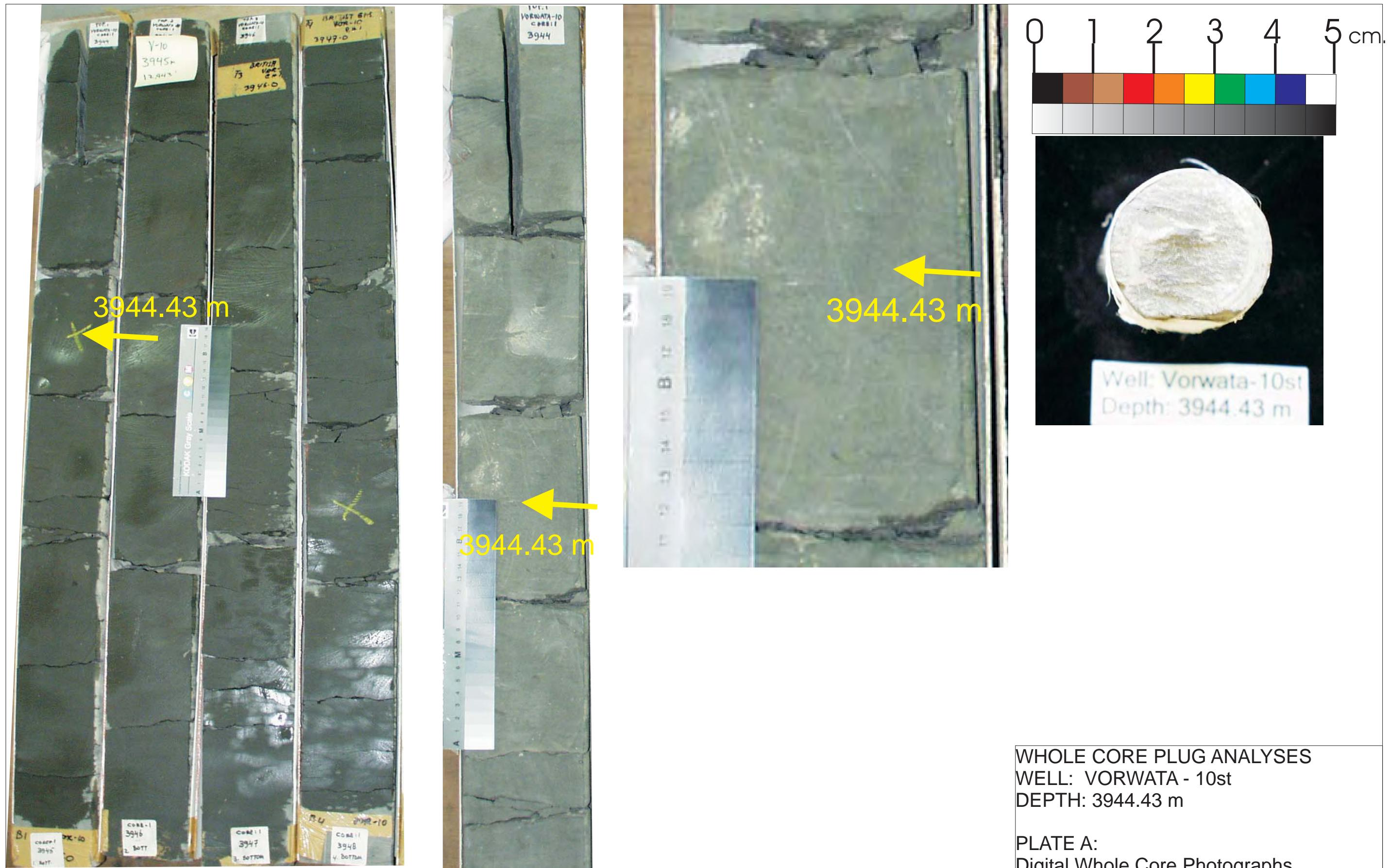
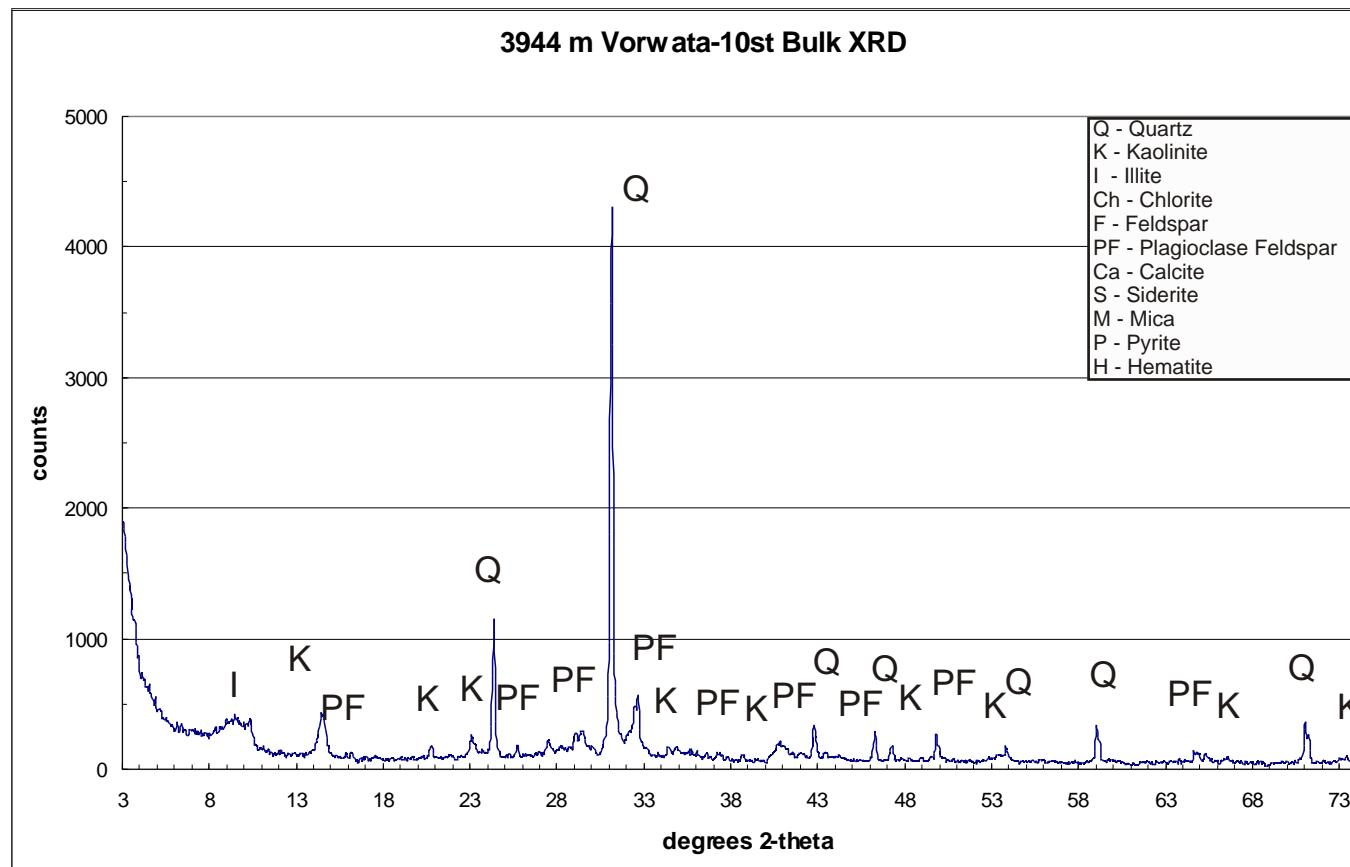
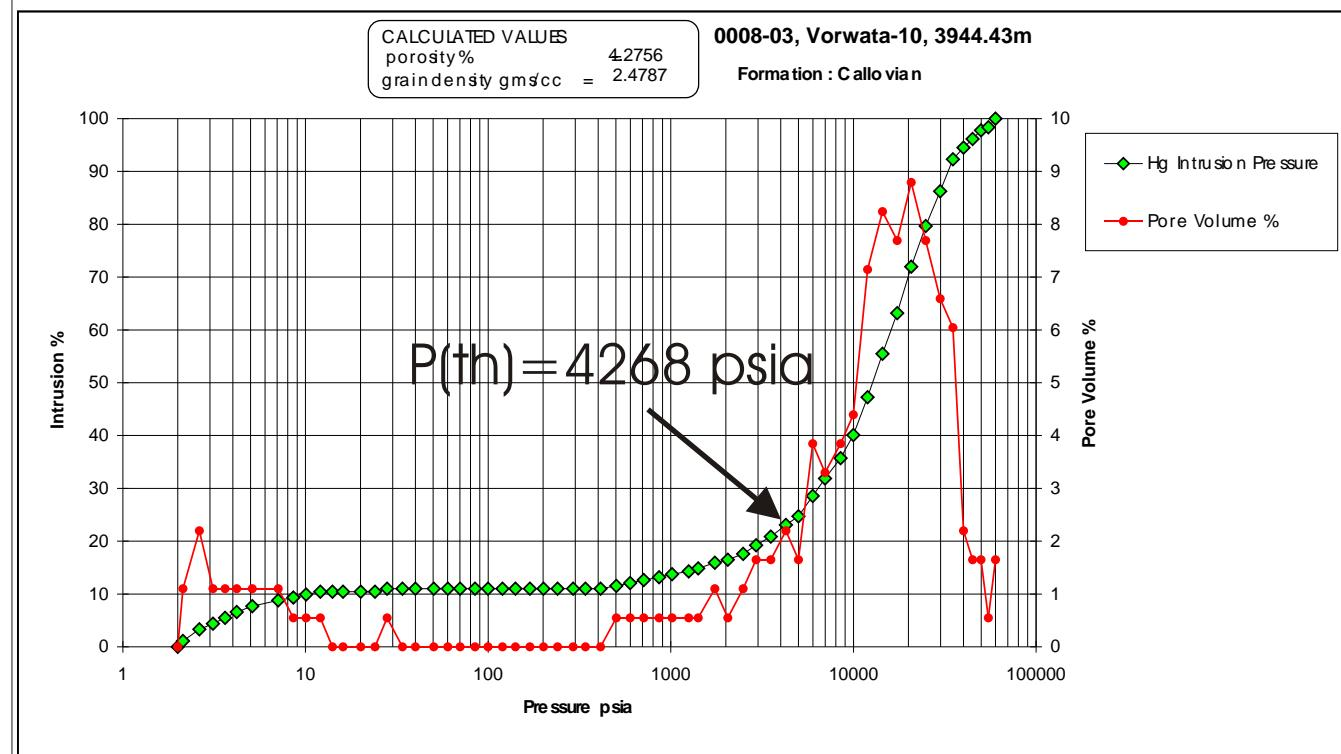


Figure 52A: Core Plug/Chip Atlas for sample 3944.43m from Vorwata-10.



Bulk XRD indicating primarily quartz, kaolinite, and mixed-layer illite and kaolinite, with additional K-feldspar content in the Pre-Ayot Shale seal at 3944m on the Vorwata-10 well.



Sample Depth: 3944.43 m
Shifted Depth: 12941.7 ft
MICP Entry Pressure: 598 psia
MICP Threshold Pressure: 4268 psia
Lithology: Shale

Figure 52B: Core Plug/Chip Atlas for sample 3944.43m from Vorwata-10.

WHOLE CORE PLUG ANALYSES
WELL: VORWATA - 10st
DEPTH: 3944.43 m

PLATE B:

BULK XRD
Mercury Injection Capillary Pressure

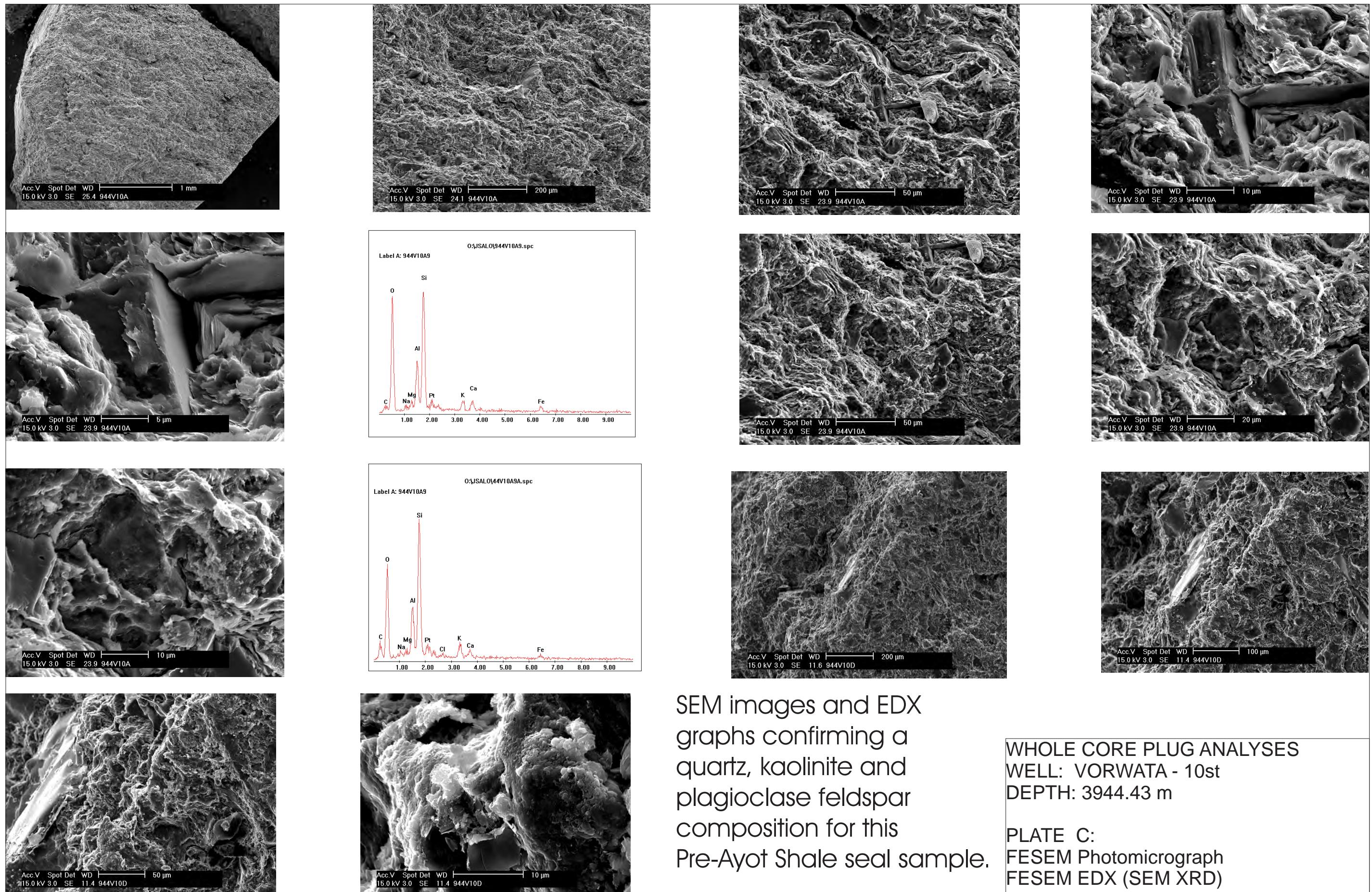
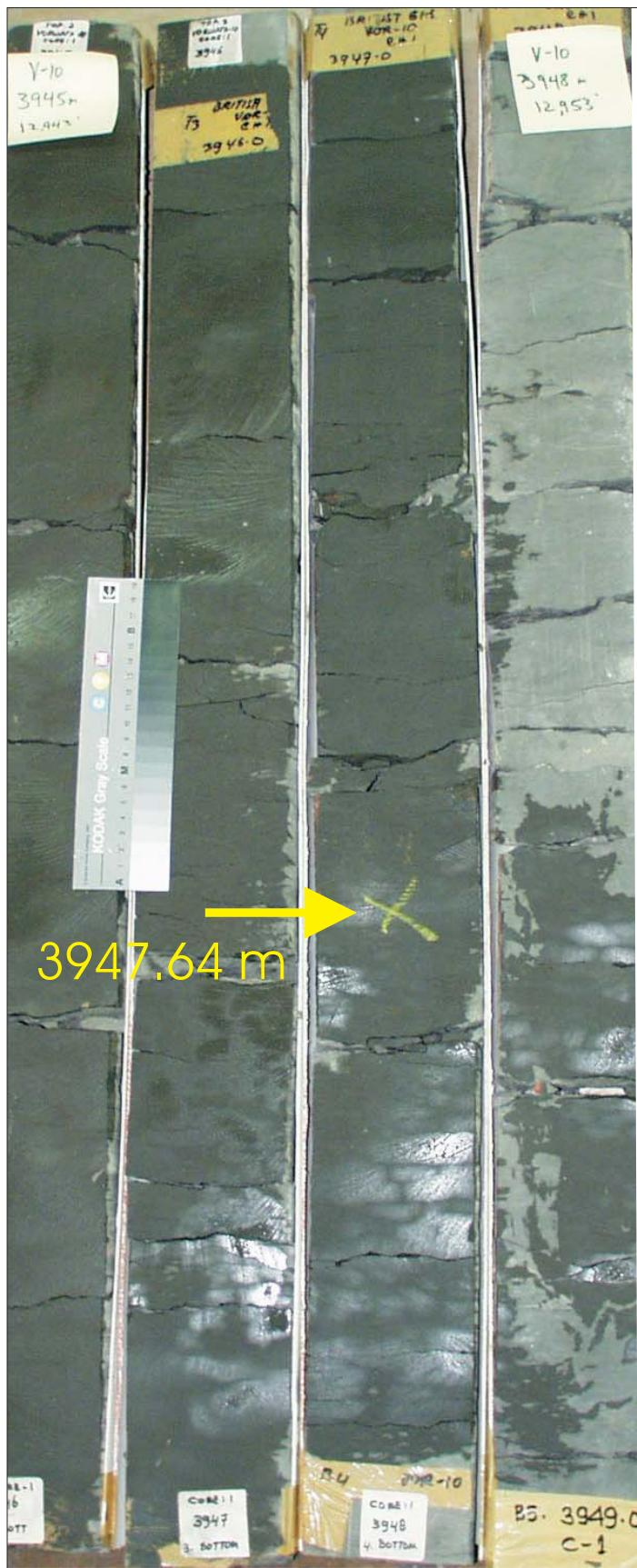


Figure 52C: Core Plug/Chip Atlas for sample 3944.43m from Vorwata-10.

SEM images and EDX graphs confirming a quartz, kaolinite and plagioclase feldspar composition for this Pre-Ayot Shale seal sample.

WHOLE CORE PLUG ANALYSES
WELL: VORWATA - 10st
DEPTH: 3944.43 m

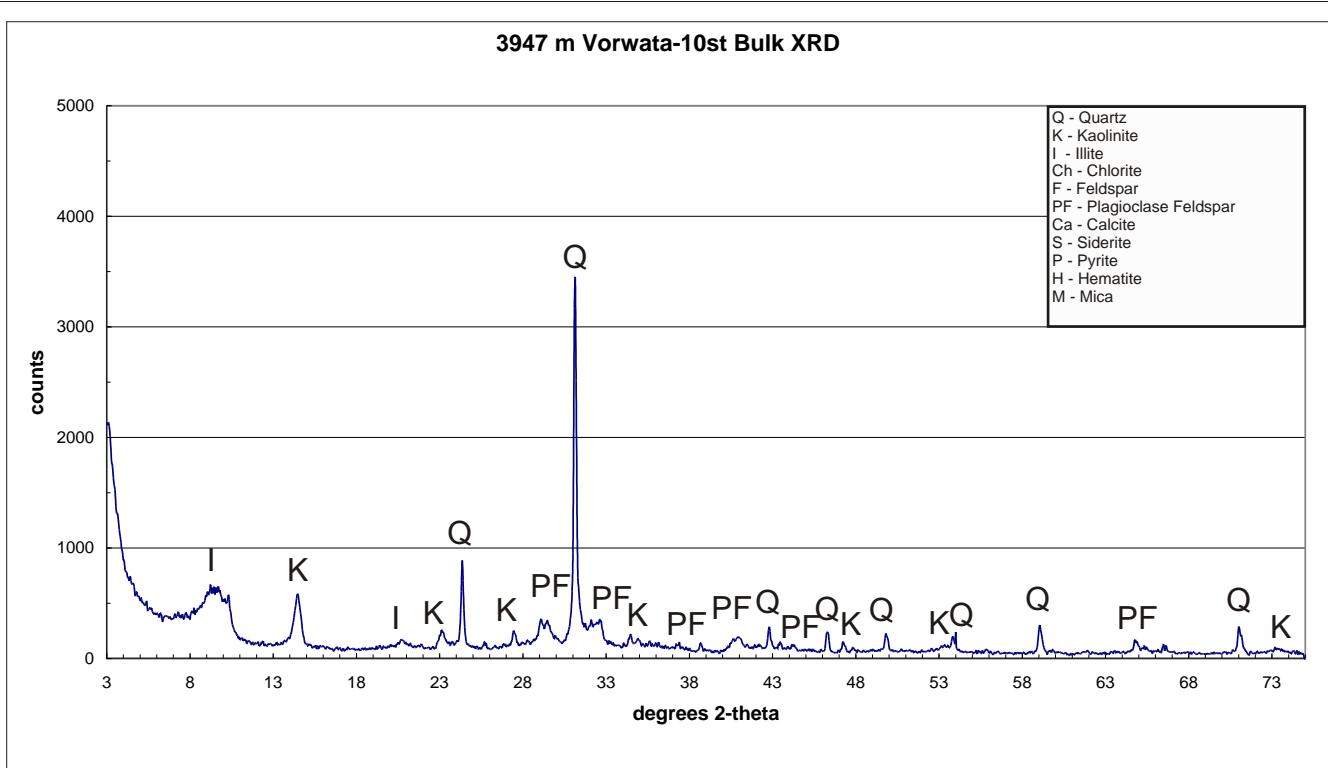
PLATE C:
FESEM Photomicrograph
FESEM EDX (SEM XRD)



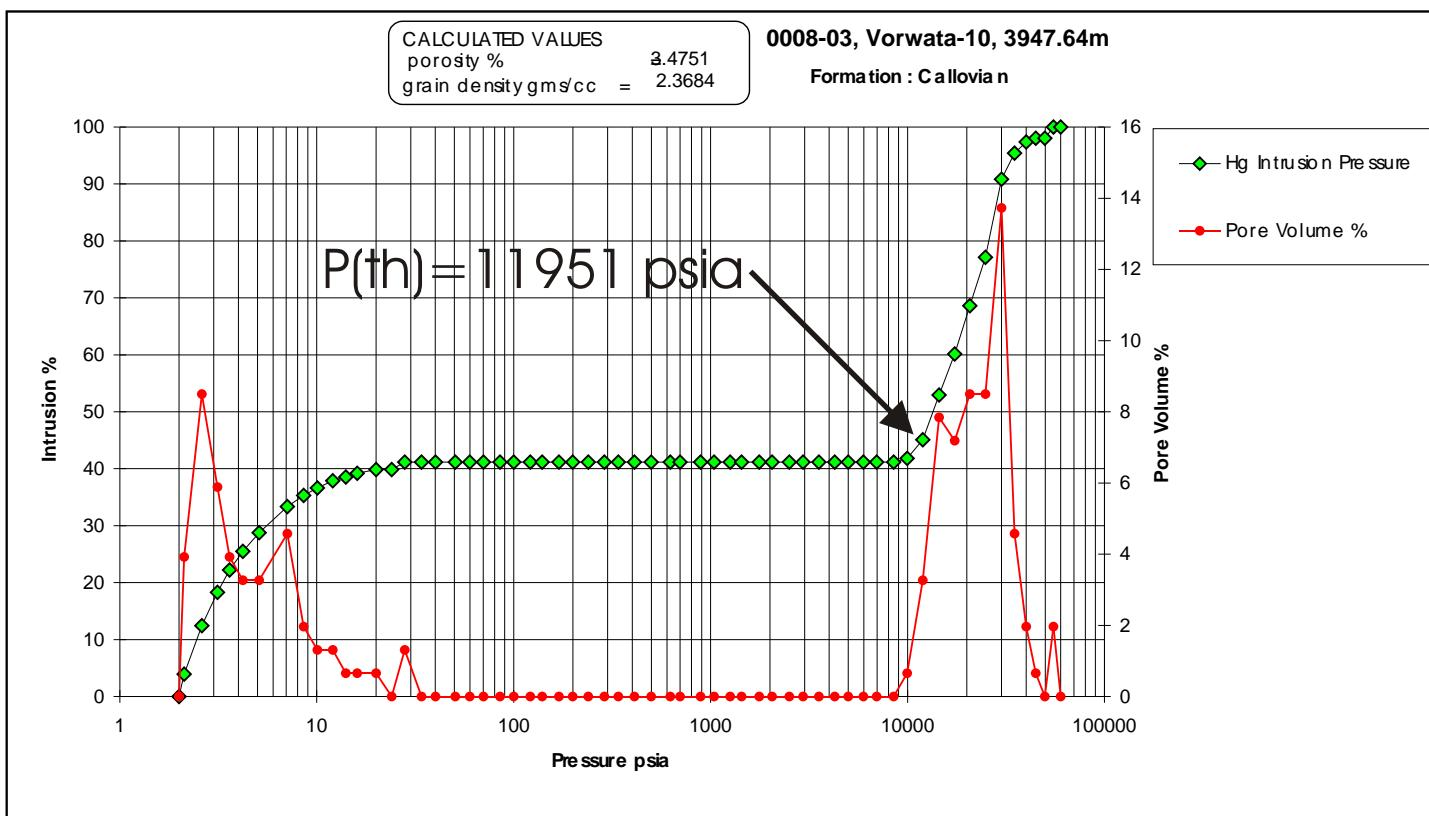
WHOLE CORE PLUG ANALYSES
WELL: VORWATA - 10st
DEPTH: 3947.64 m

PLATE A
Digital Whole Core Photographs
Digital Core Chip/Plug Photograph

Figure 53A: Core Plug/Chip Atlas for sample 3947.64m from Vorwata-10.



Bulk XRD indicating primarily a quartz, illite, kaolinite and plagioclase feldspar composition.

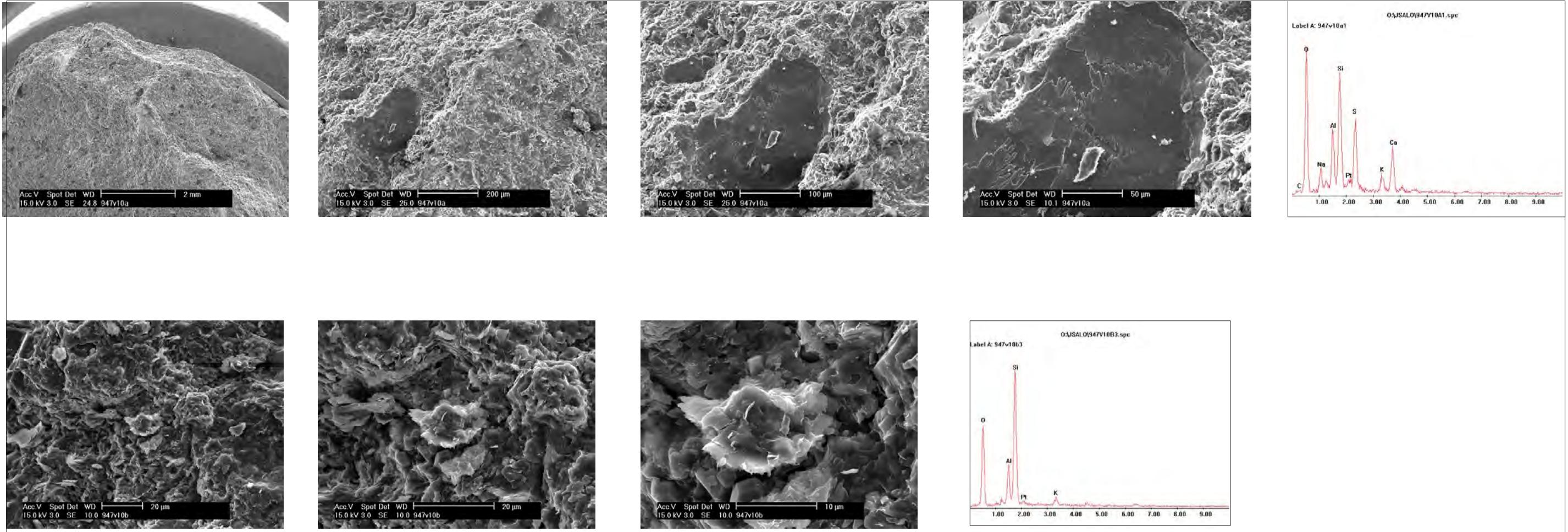


Sample Depth: 3947.64 m
Shifted Depth: 12592.2 ft
MICP Entry Pressure: 8507 psia
MICP Threshold Pressure: 11951 psia
Lithology: Shale

WHOLE CORE PLUG ANALYSES
WELL: VORWATA - 10st
DEPTH: 3947.64 m

PLATE B:
BULK XRD
Mercury Injection Capillary Pressure

Figure 53B: Core Plug/Chip Atlas for sample 3947.64m from Vorwata-10.



SEM Images and EDX confirm the composition of primarily quartz, illite, kaolinite, and plagioclase feldspar. Illite 'flower' and 'corn-flake' platelets quite common. Traces of calcite are present on the top-most EDX bulk elemental composition analysis.

Figure 53C: Core Plug/Chip Atlas for sample 3947.64m from Vorwata-10.

WHOLE CORE PLUG ANALYSES

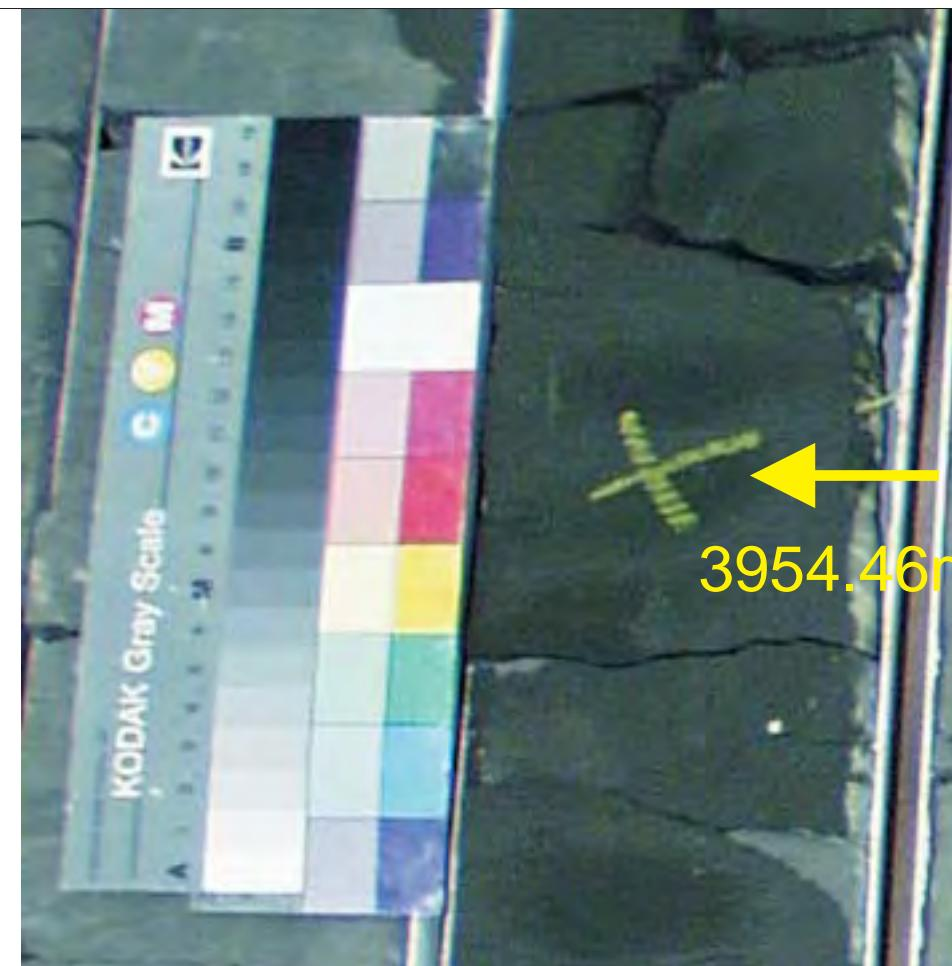
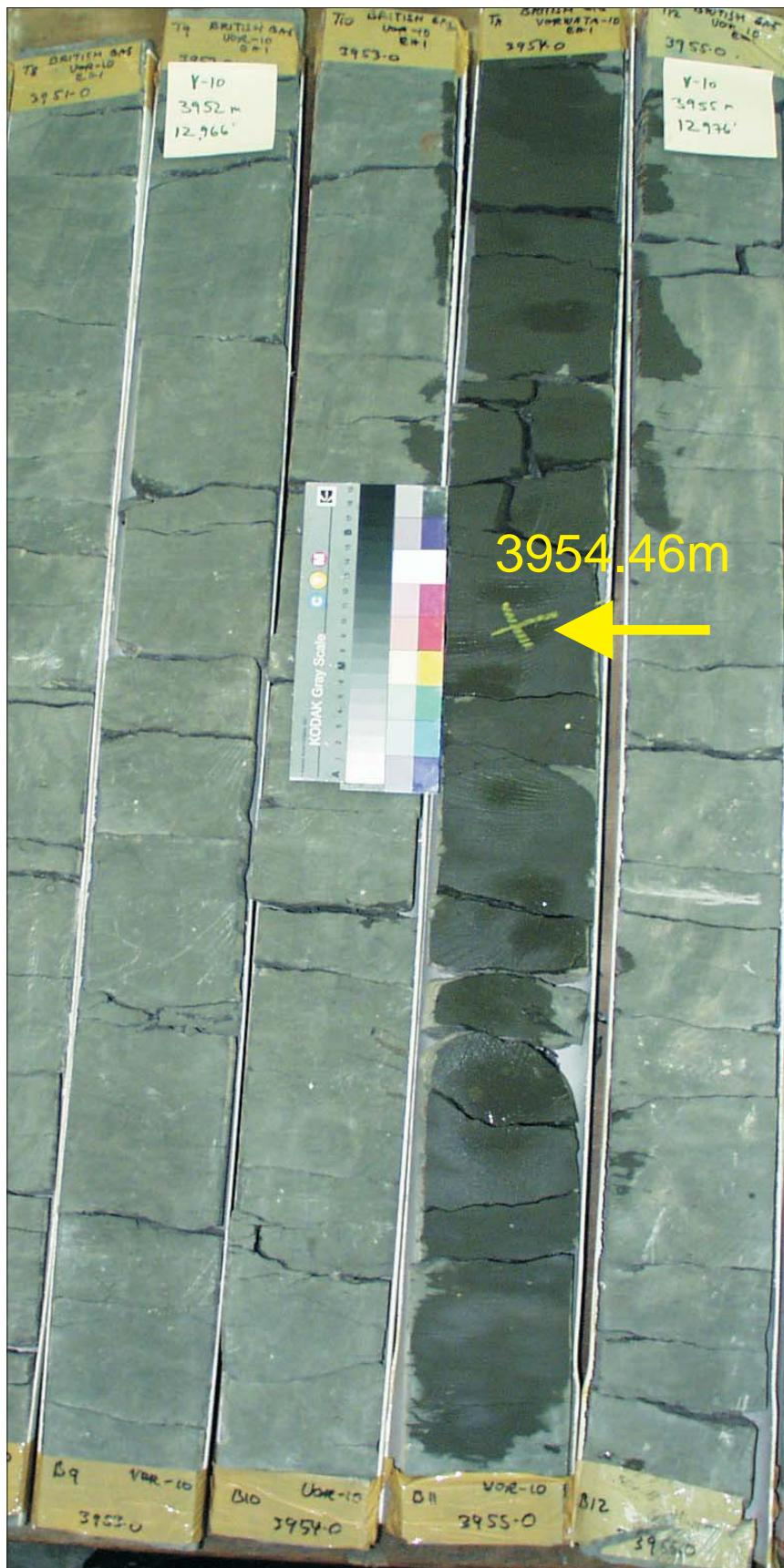
WELL: VORWATA - 10st

DEPTH: 3947.64 m

PLATE C:

FESEM Photomicrograph

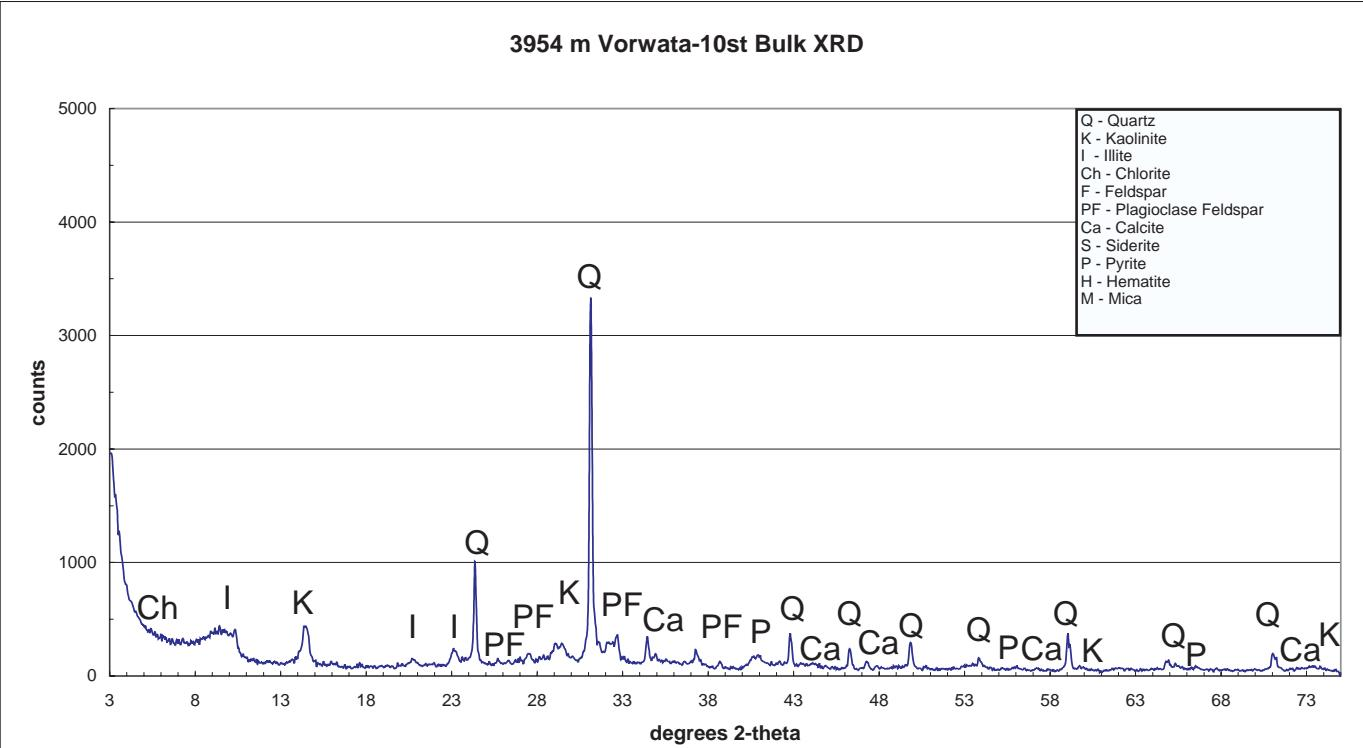
FESEM EDX (SEM XRD)



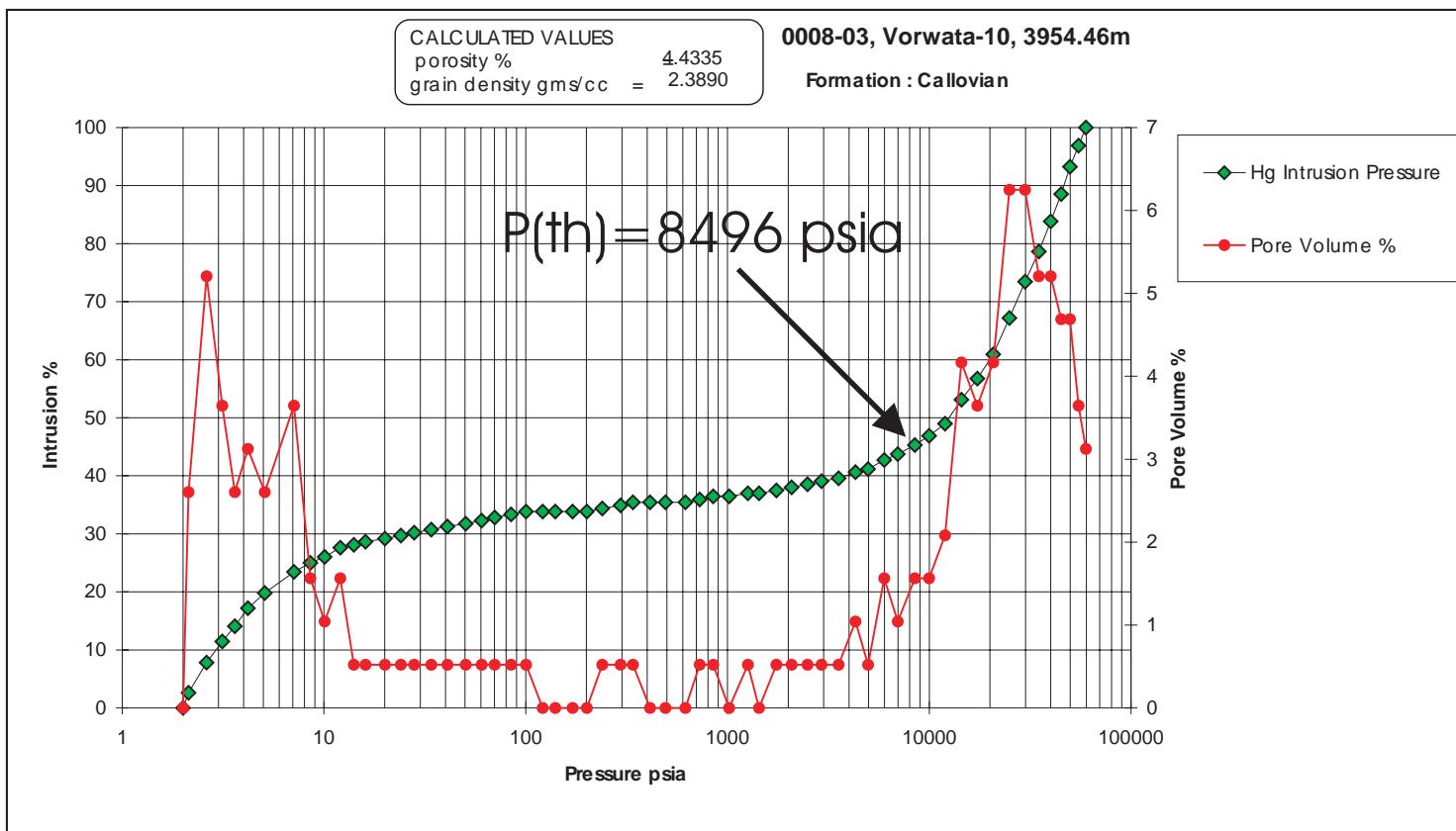
WHOLE CORE PLUG ANALYSES
WELL: VORWATA - 10st
DEPTH: 3954.46 m

PLATE A
Digital Whole Core Photographs
Digital Core Chip/Plug Photograph

Figure 54A: Core Plug/Chip Atlas for sample 3954.46m from Vorwata-10.



Bulk XRD indicates a primarily quartz, illite, kaolinite, composition with minor plagioclase feldspar, calcite, and chlorite present.



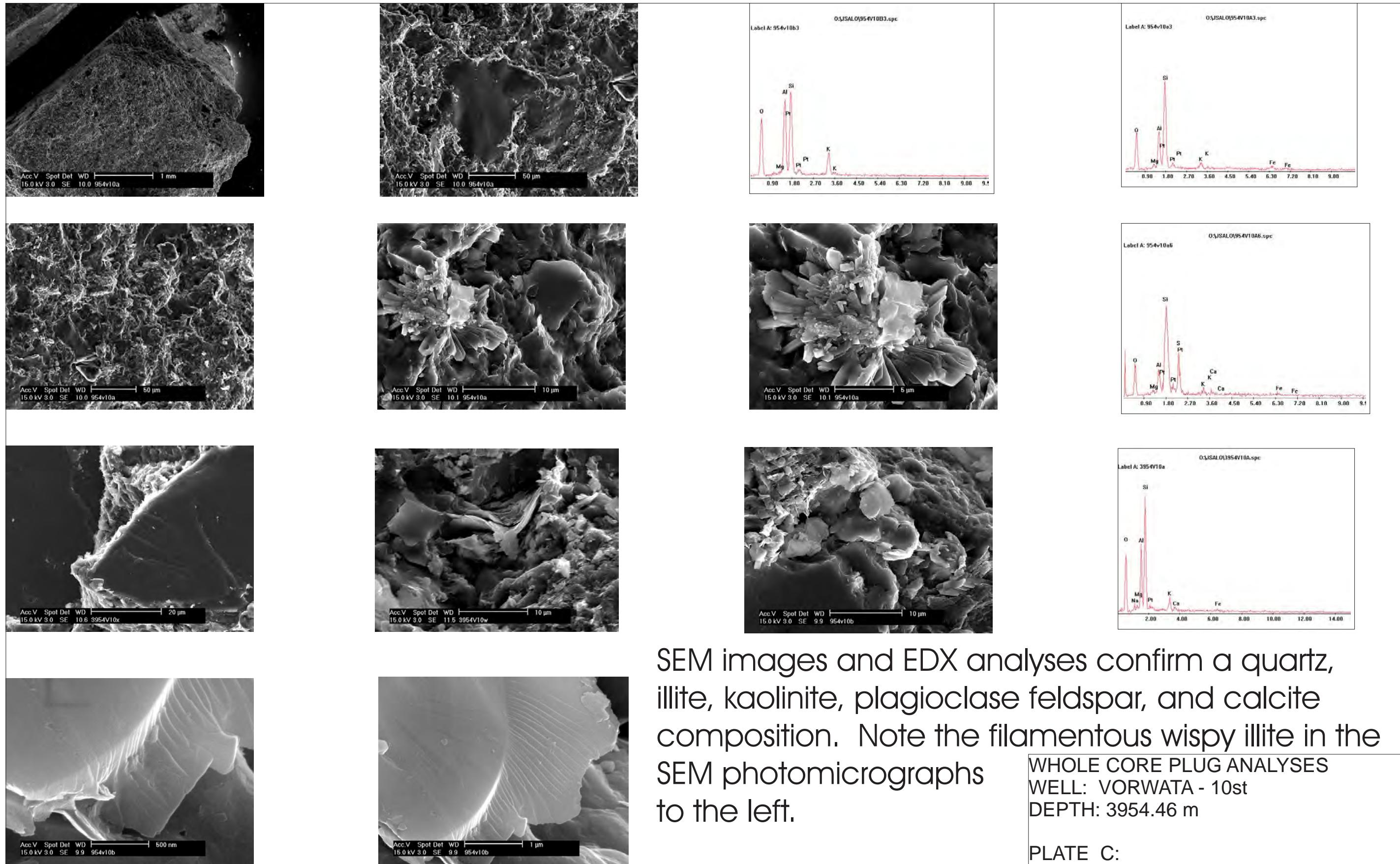
Sample Depth: 3954.46 m
Shifted Depth: 12974.6 ft
MICP Entry Pressure: 727 psia
MICP Threshold Pressure: 8496 psia
Lithology: Shale

WHOLE CORE PLUG ANALYSES
WELL: VORWATA - 10st
DEPTH: 3954.46 m

PLATE B

BULK XRD
Mercury Injection Capillary Pressure

Figure 54B: Core Plug/Chip Atlas for sample 3954.46m from Vorwata-10.



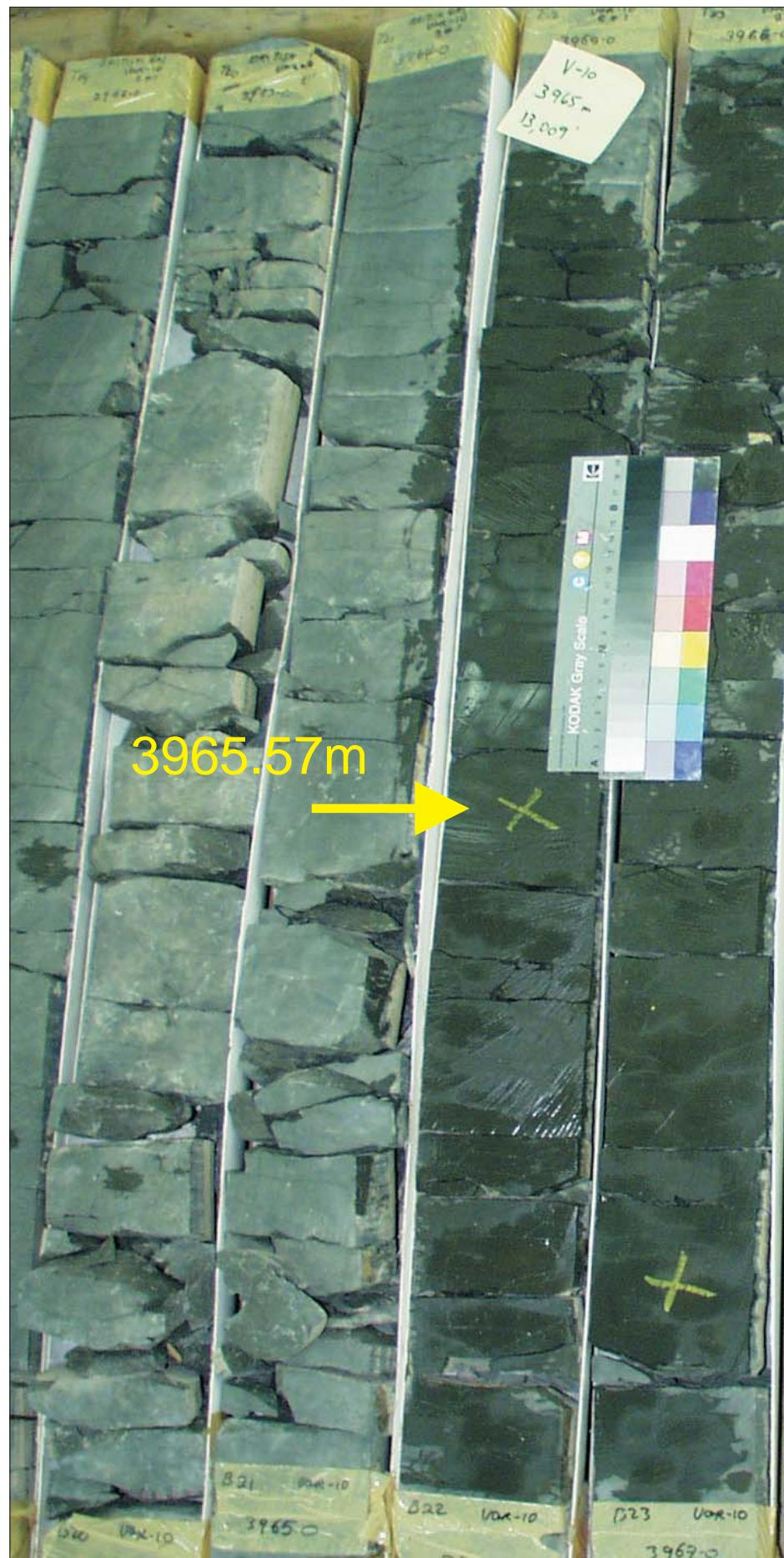
SEM images and EDX analyses confirm a quartz, illite, kaolinite, plagioclase feldspar, and calcite composition. Note the filamentous wispy illite in the SEM photomicrographs to the left.

WHOLE CORE PLUG ANALYSES
WELL: VORWATA - 10st
DEPTH: 3954.46 m

PLATE C:

FESEM Photomicrograph
FESEM EDX (SEM XRD)

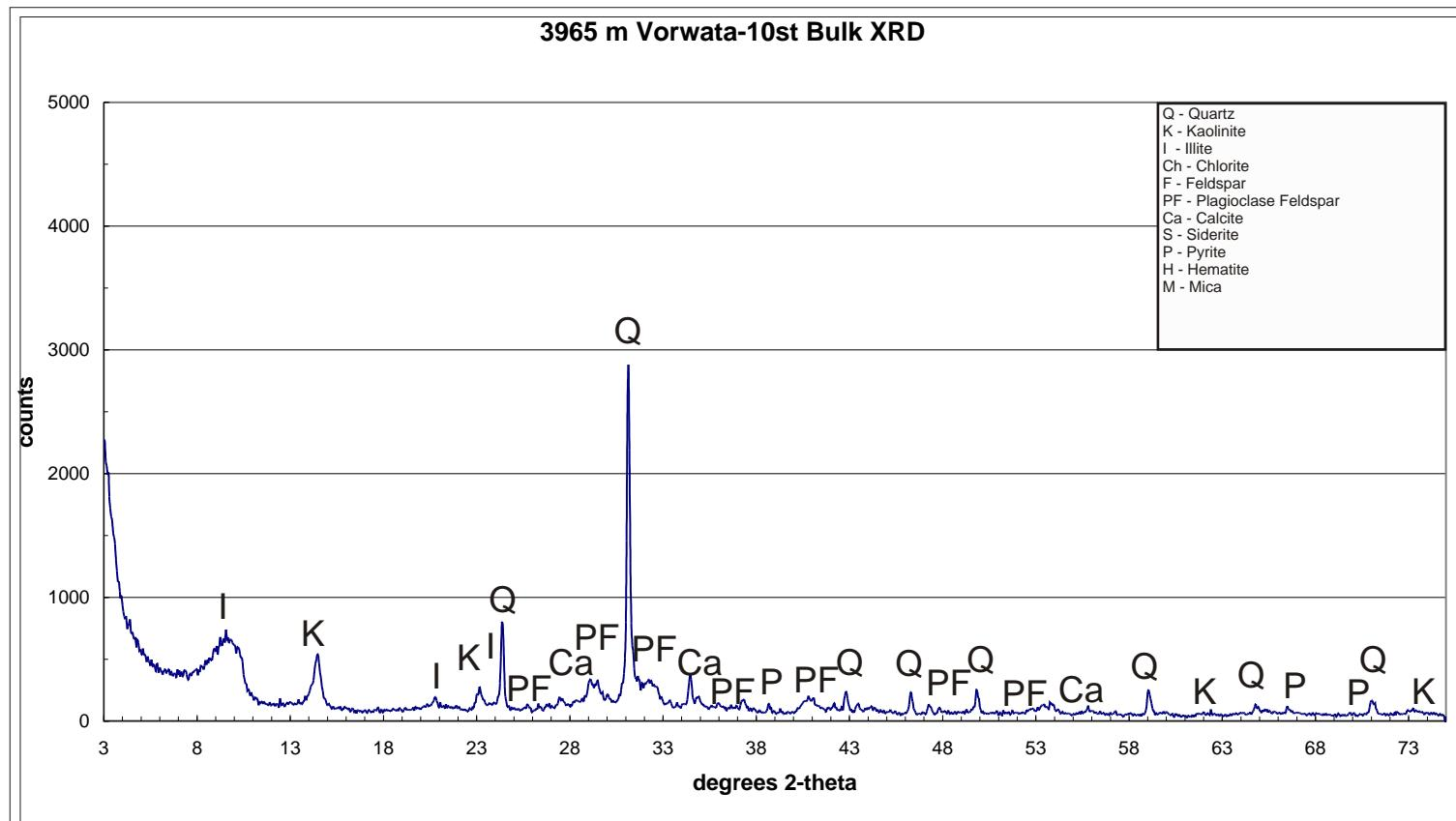
Figure 54C: Core Plug/Chip Atlas for sample 3954.46m from Vorwata-10.



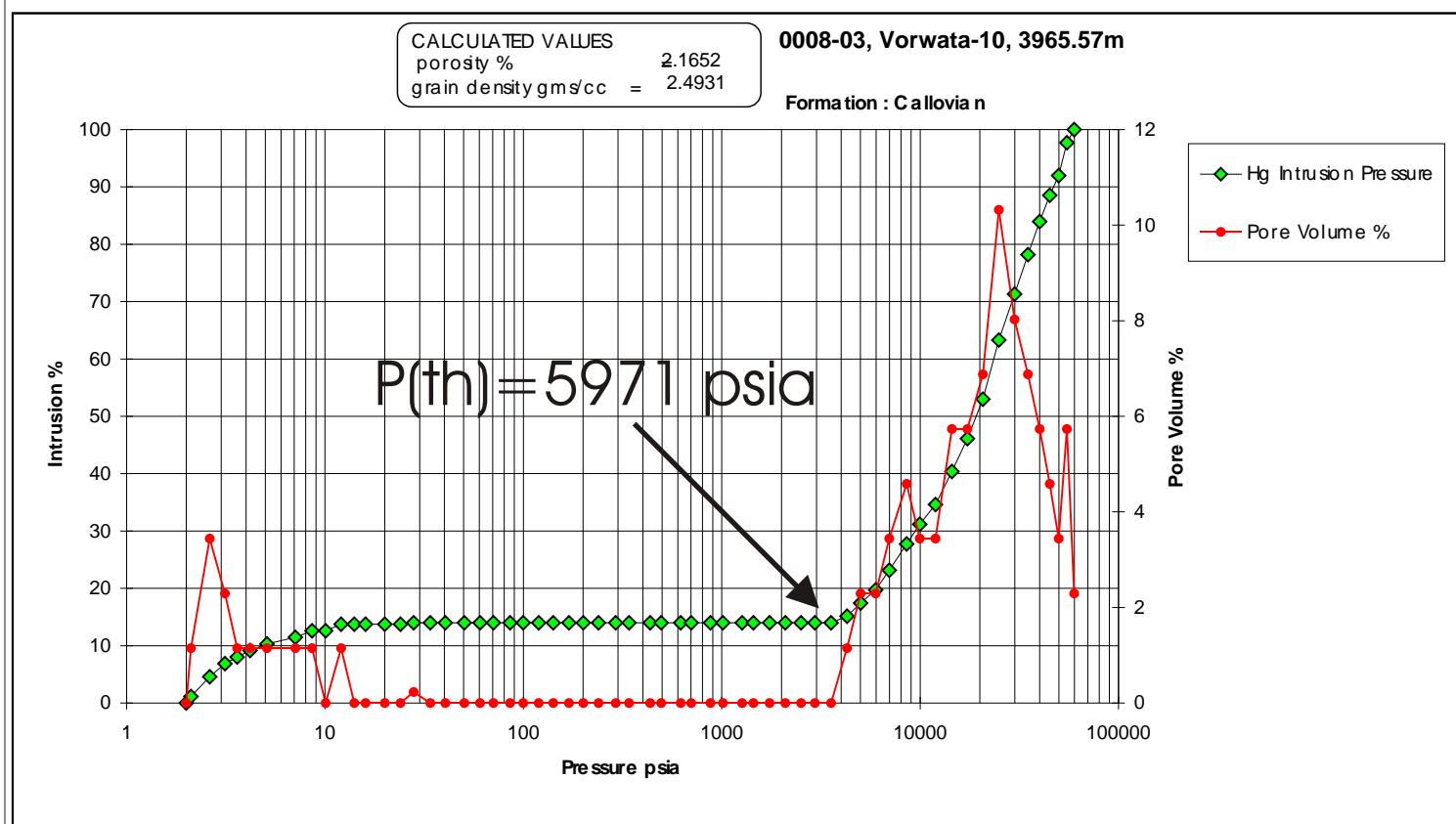
WHOLE CORE PLUG ANALYSES
WELL: VORWATA - 10st
DEPTH: 3965.57 m

PLATE A
Digital Whole Core Photographs
Digital Core Chip/Plug Photograph

Figure 55A: Core Plug/Chip Atlas for sample 3965.57m from Vorwata-10.



Bulk XRD analysis indicating a mineral composition of quartz, kaolinite, illite, plagioclase feldspar, and pyrite, with minor calcite present. Abundant ultra-fine quartz silts and mica, primarily muscovite, were visible in the core chip with x36 power microscopy as discrete bedded, oriented, microlaminations. Portion of the core chip powdered for Bulk XRD contained the quartz but not the mica microlaminations.



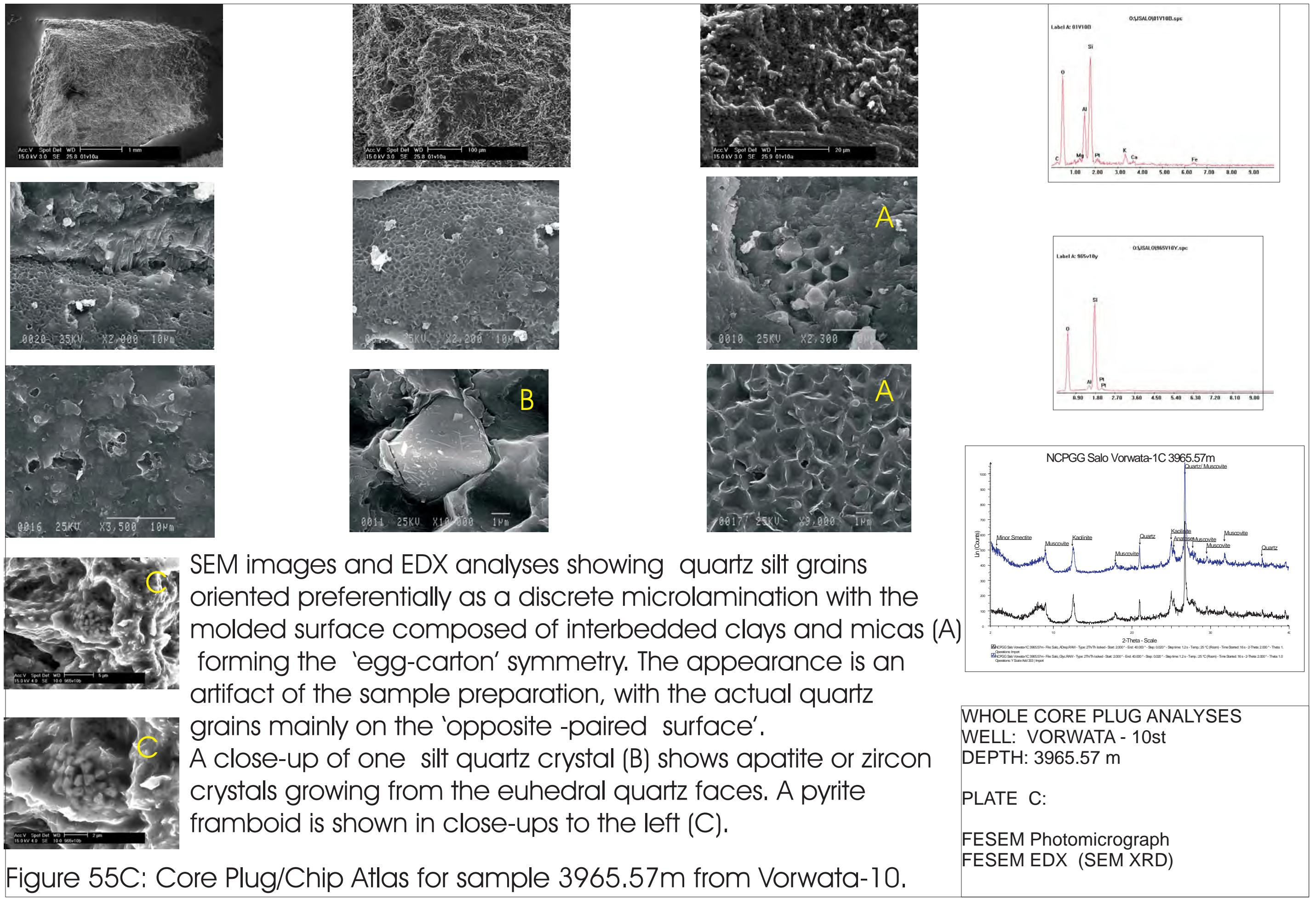
Sample Depth: 3965.57 m
Shifted Depth: 13011.0 ft
MICP Entry Pressure: 4279 psia
MICP Threshold Pressure: 5971 psia
Lithology: Shale

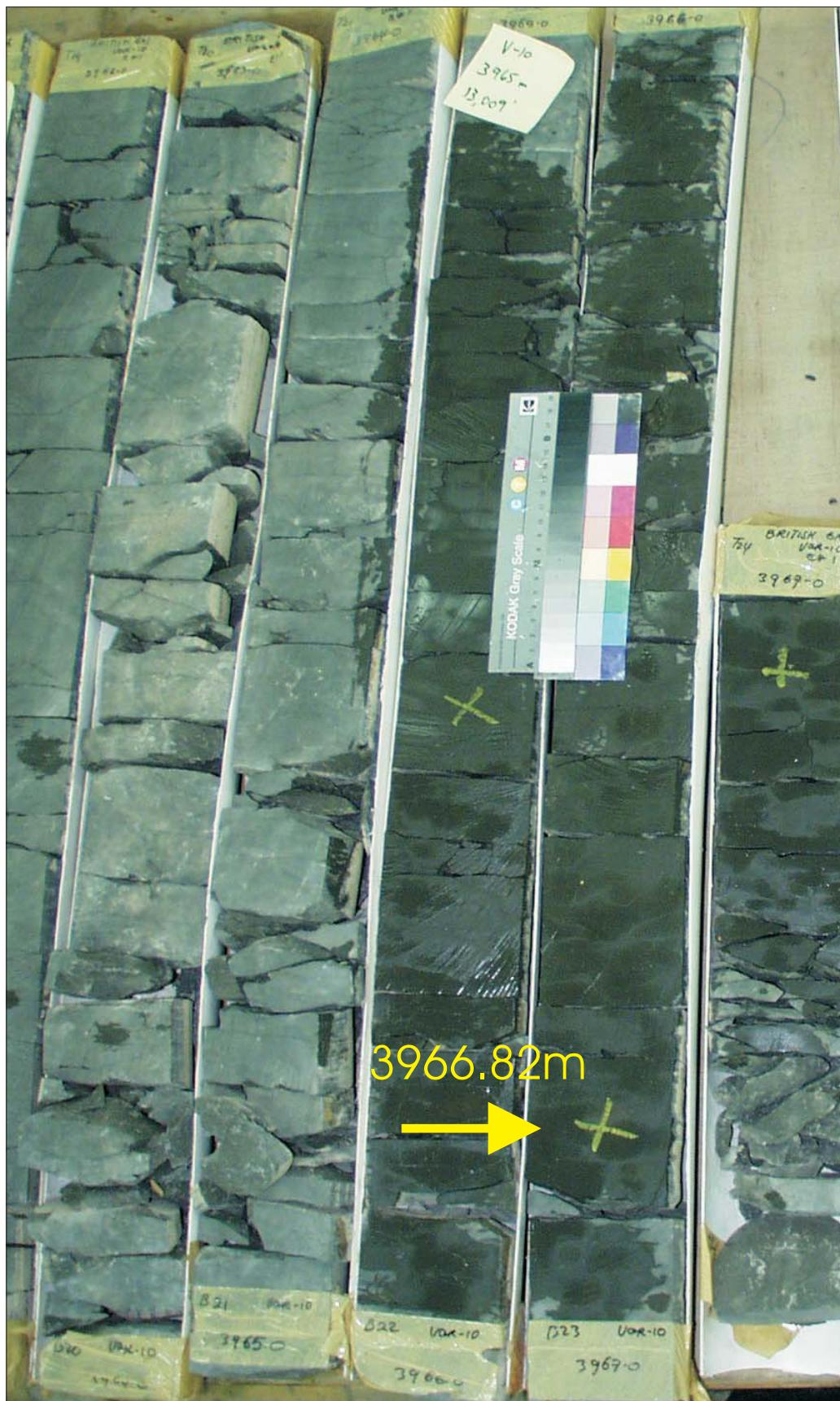
WHOLE CORE PLUG ANALYSES
WELL: VORWATA - 10st
DEPTH: 3965.57 m

PLATE B

BULK XRD
Mercury Injection Capillary Pressure

Figure 55B: Core Plug/Chip Atlas for sample 3965.57m from Vorwata-10.





WHOLE CORE PLUG ANALYSES

WELL: VORWATA - 10st

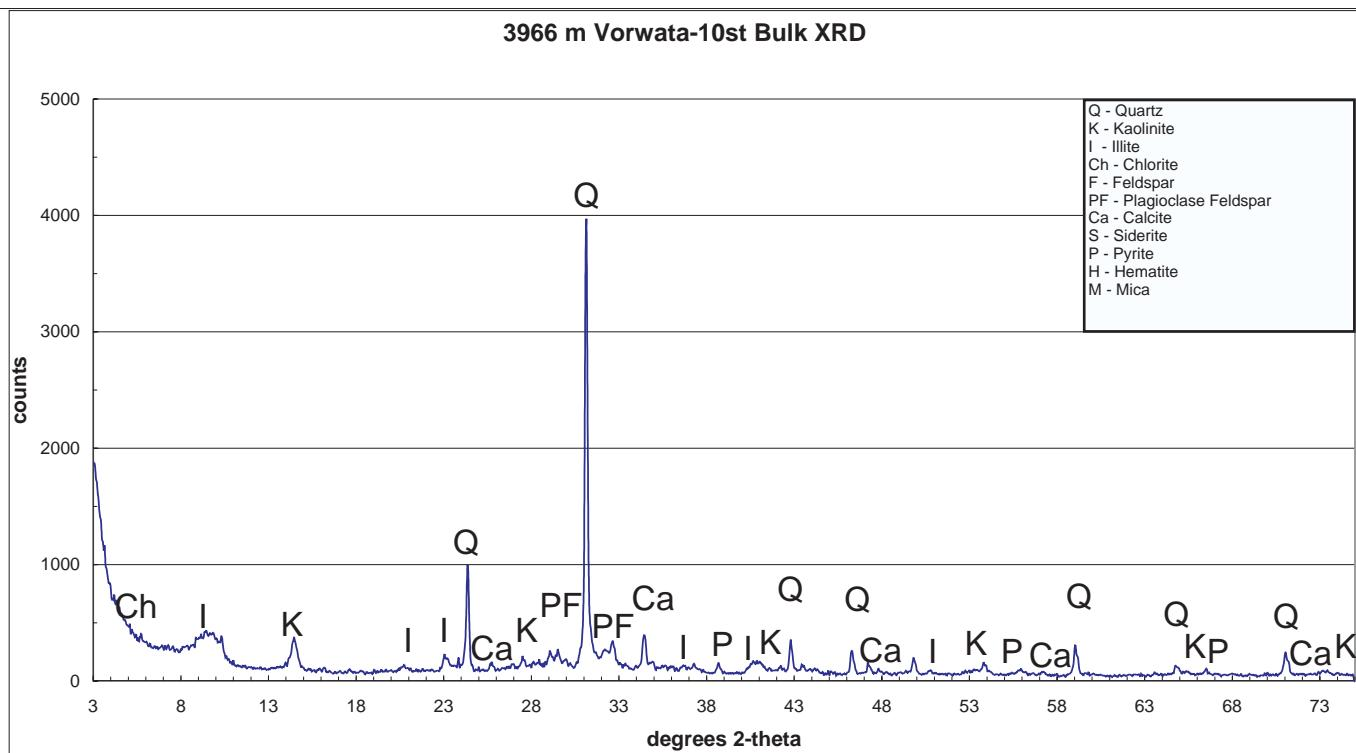
DEPTH: 3966.82 m

PLATE A

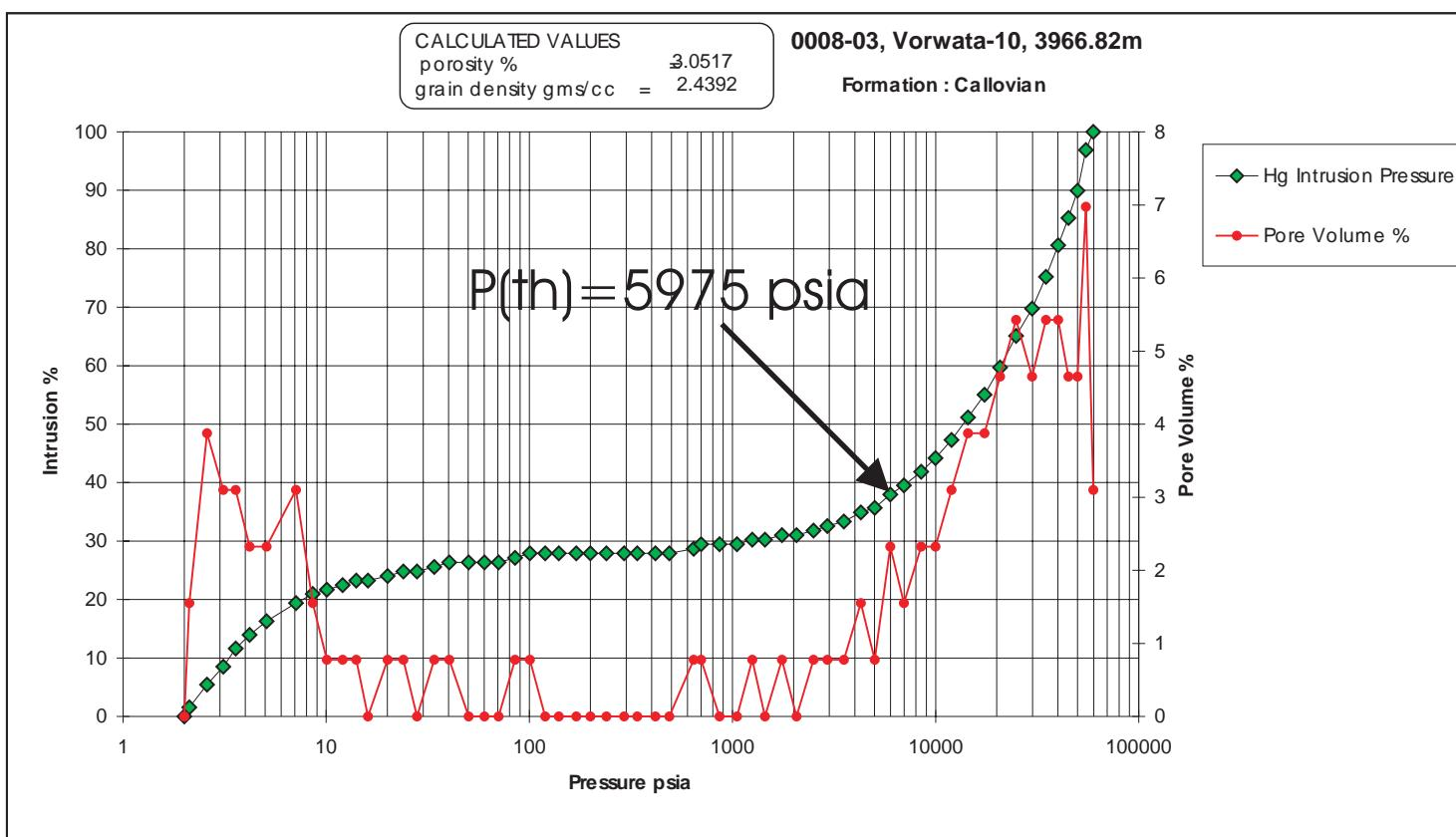
Digital Whole Core Photographs

Digital Core Chip/Plug Photograph

Figure 56A: Core Plug/Chip Atlas for sample 3966.82m from Vorwata-10.



Bulk XRD showing quartz, illite, kaolinite, and calcite mineralogy, with minor chlorite and pyrite present.



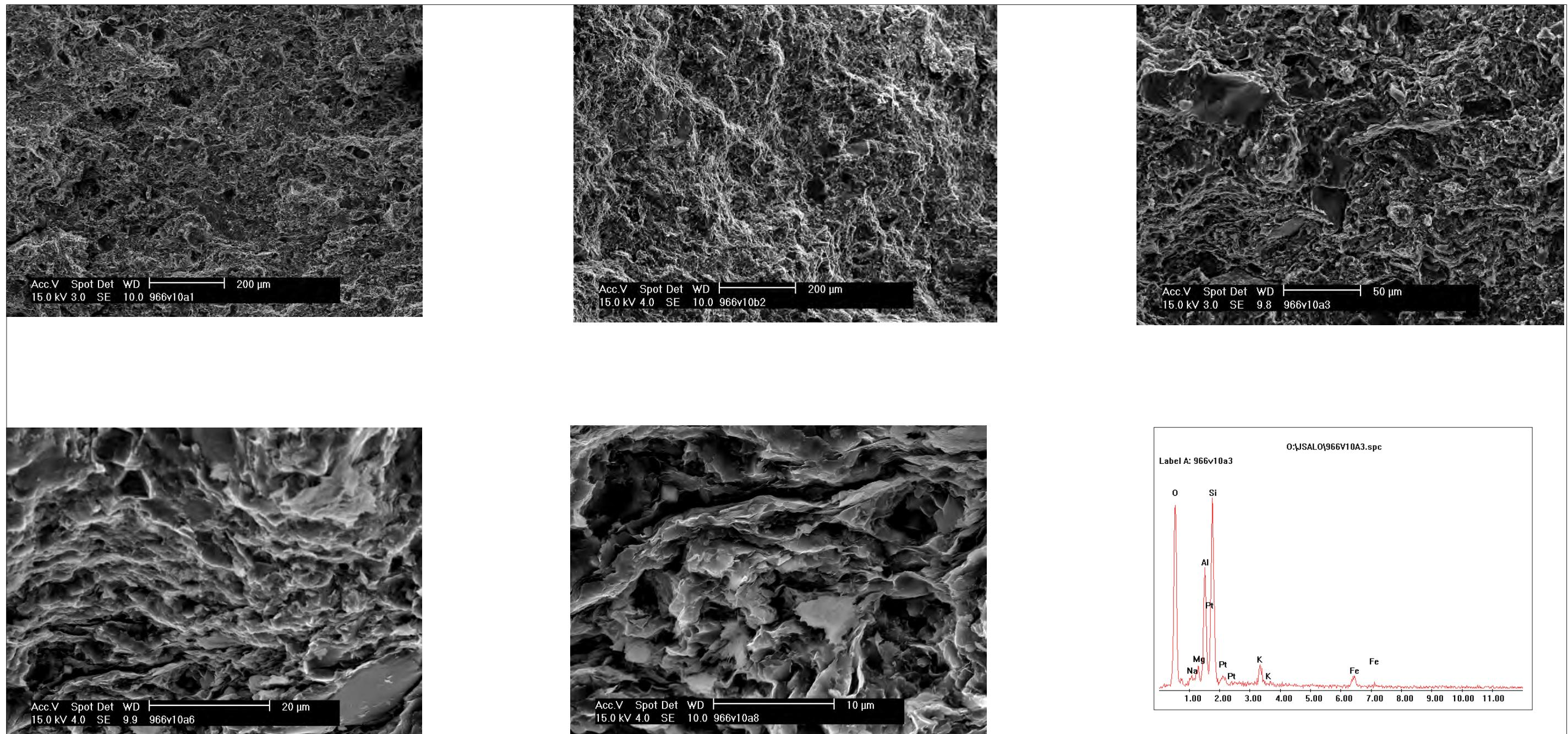
Sample Depth: 3966.82 m
Shifted Depth: 13015.1 ft
MICP Entry Pressure: 1053 psia
MICP Threshold Pressure: 5975 psia
Lithology: Shale

WHOLE CORE PLUG ANALYSES
WELL: VORWATA - 10st
DEPTH: 3966.82 m

PLATE B

BULK XRD
Mercury Injection Capillary Pressure

Figure 56B: Core Plug/Chip Atlas for sample 3966.82m from Vorwata-10.



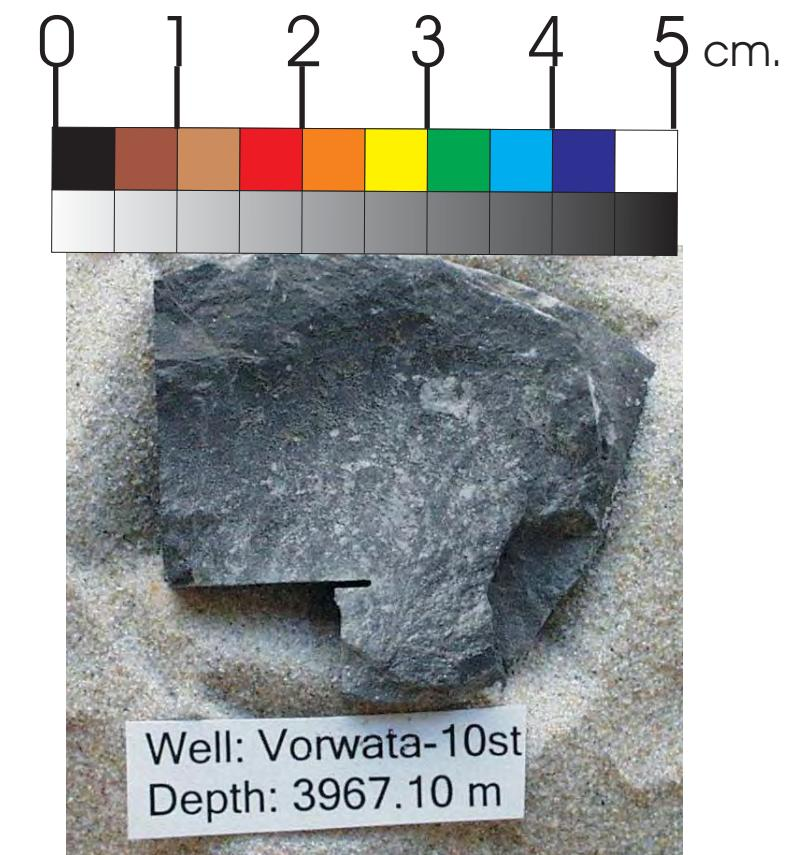
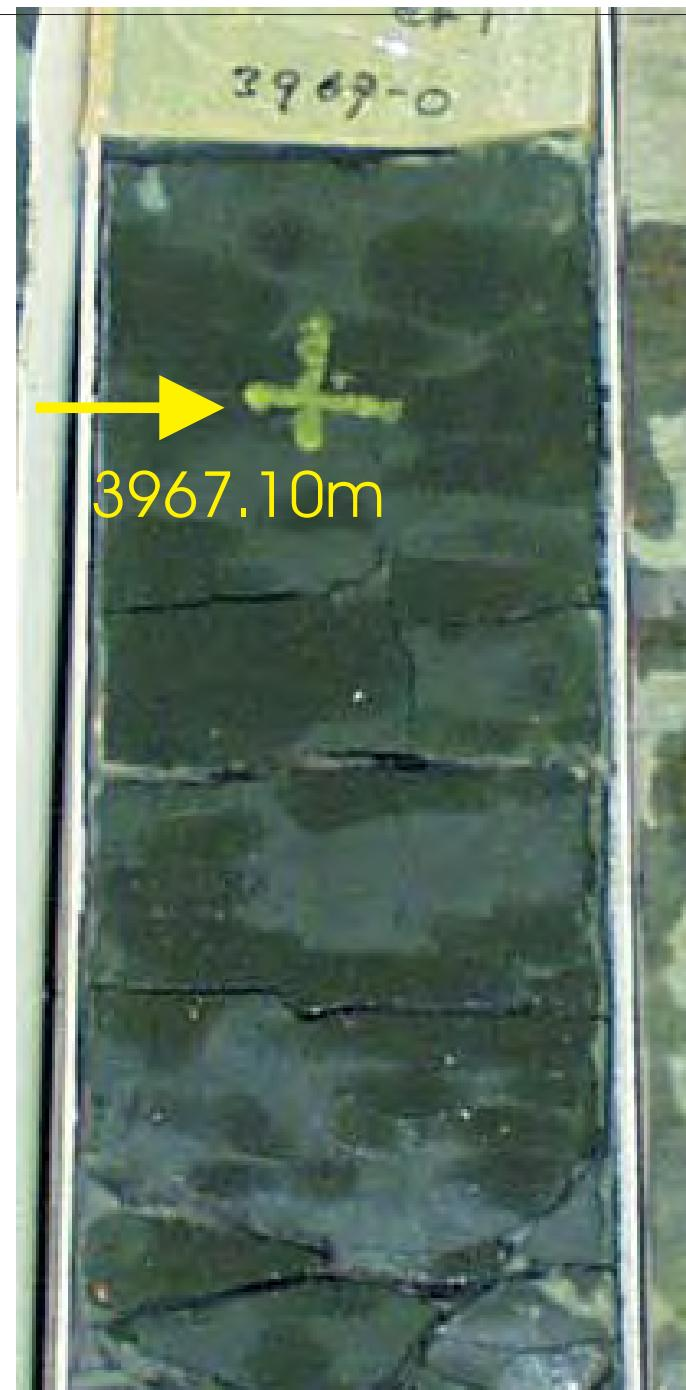
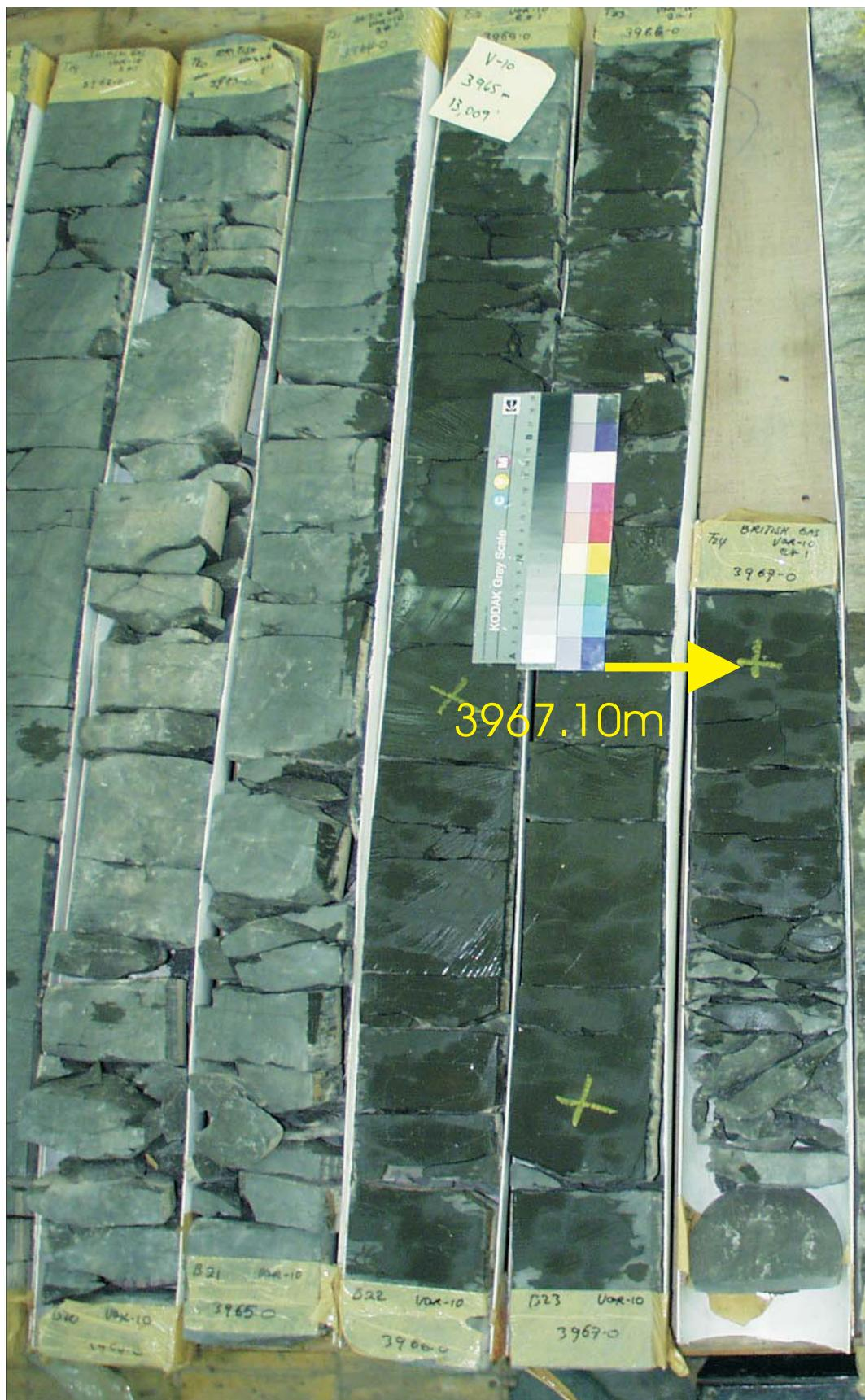
SEM photomicrographs and EDX analysis showing primarily quartz, illite, kaolinite, and chlorite mineralogy, with 'corn-flake' textured illite platelets appearing most pronounced.

Figure 56C: Core Plug/Chip Atlas for sample 3966.82m from Vorwata-10.

WHOLE CORE PLUG ANALYSES
WELL: VORWATA - 10st
DEPTH: 3966.82 m

PLATE C:

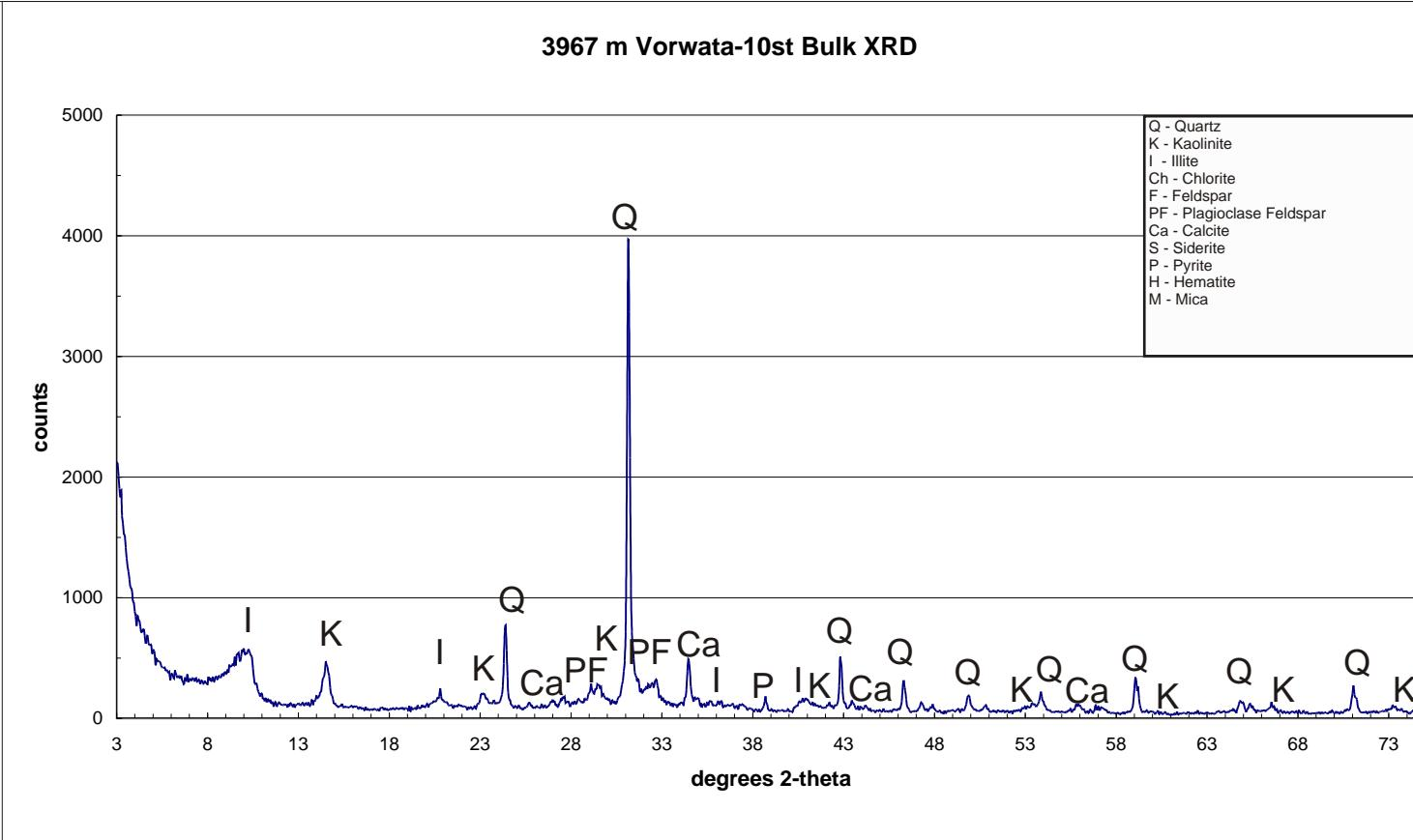
FESEM Photomicrograph
FESEM EDX (SEM XRD)



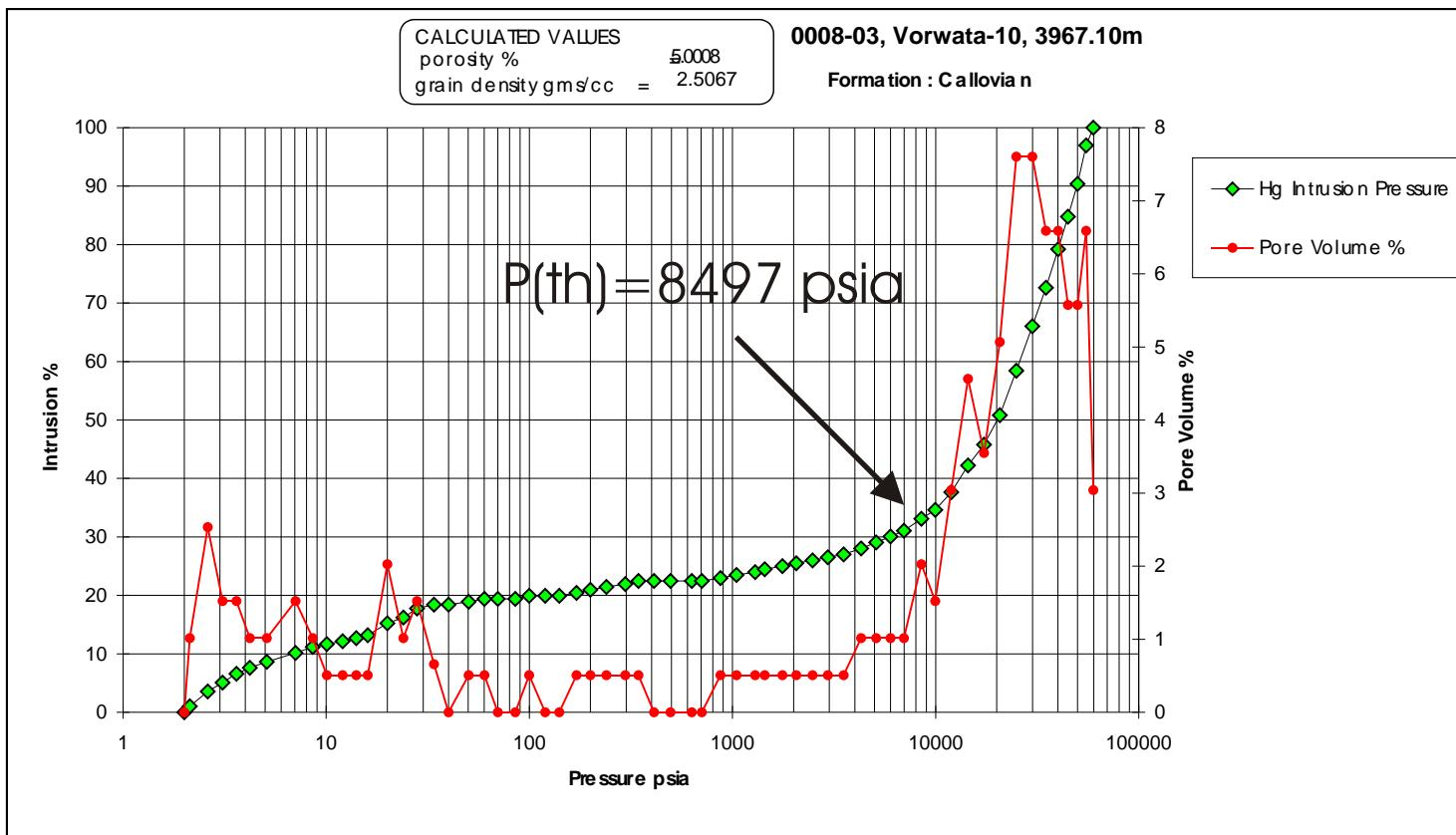
WHOLE CORE PLUG ANALYSES
WELL: VORWATA - 10st
DEPTH: 3967.10 m

PLATE A
Digital Whole Core Photographs
Digital Core Chip/Plug Photograph

Figure 57A: Core Plug/Chip Atlas for sample 3967.10m from Vorwata-10.



Bulk XRD showing predominantly quartz, illite, and kaolinite composition, with minor calcite and plagioclase feldspar present.



Sample Depth: 3967.10 m
Shifted Depth: 13016.1 ft
MICP Entry Pressure: 705 psia
MICP Threshold Pressure: 8497 psia
Lithology: Shale

WHOLE CORE PLUG ANALYSES
WELL: VORWATA - 10st
DEPTH: 3967.10 m

PLATE B

BULK XRD
Mercury Injection Capillary Pressure

Figure 57B: Core Plug/Chip Atlas for sample 3967.10m from Vorwata-10.

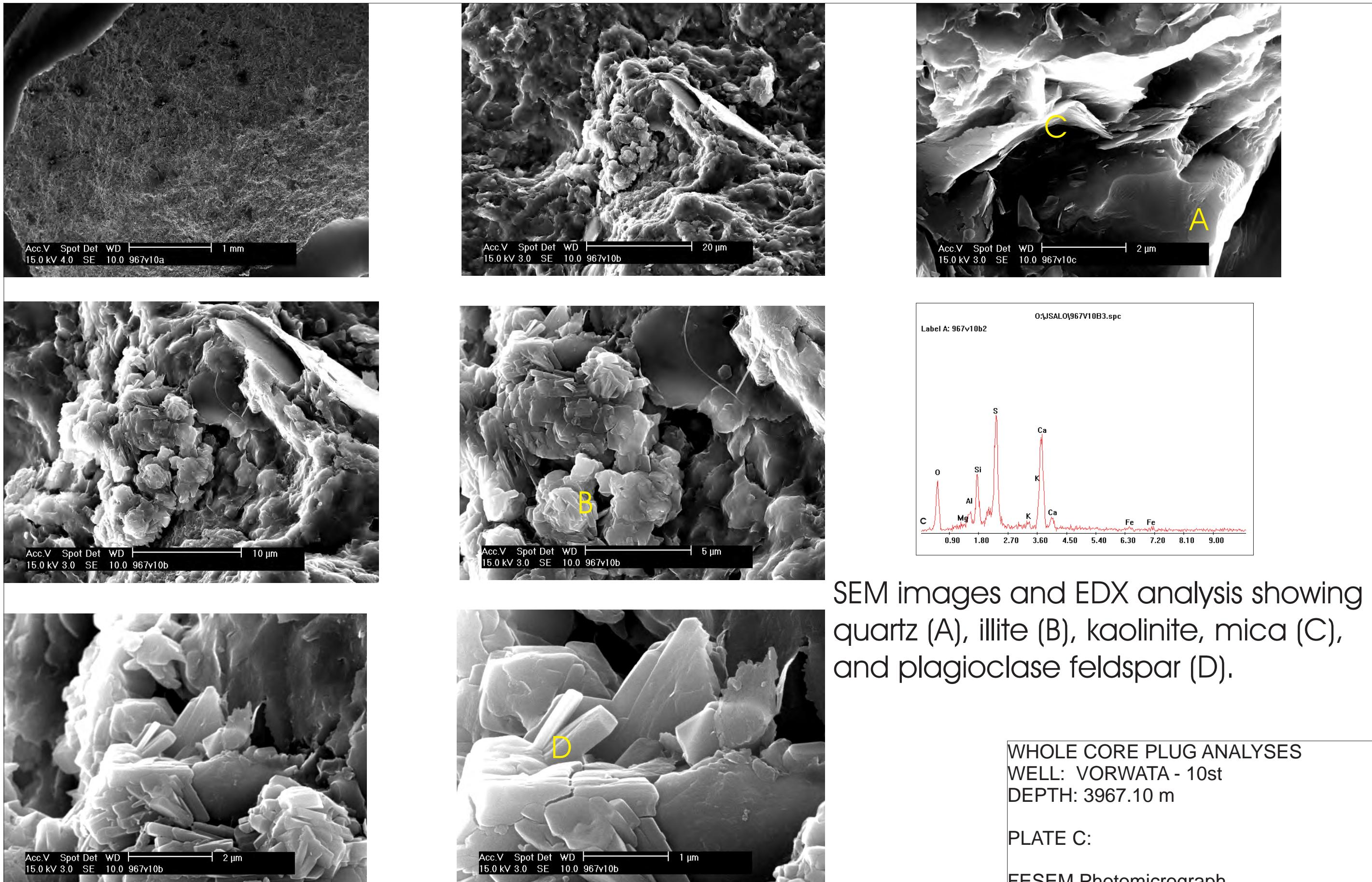


Figure 57C: Core Plug/Chip Atlas for sample 3967.10m from Vorwata-10.

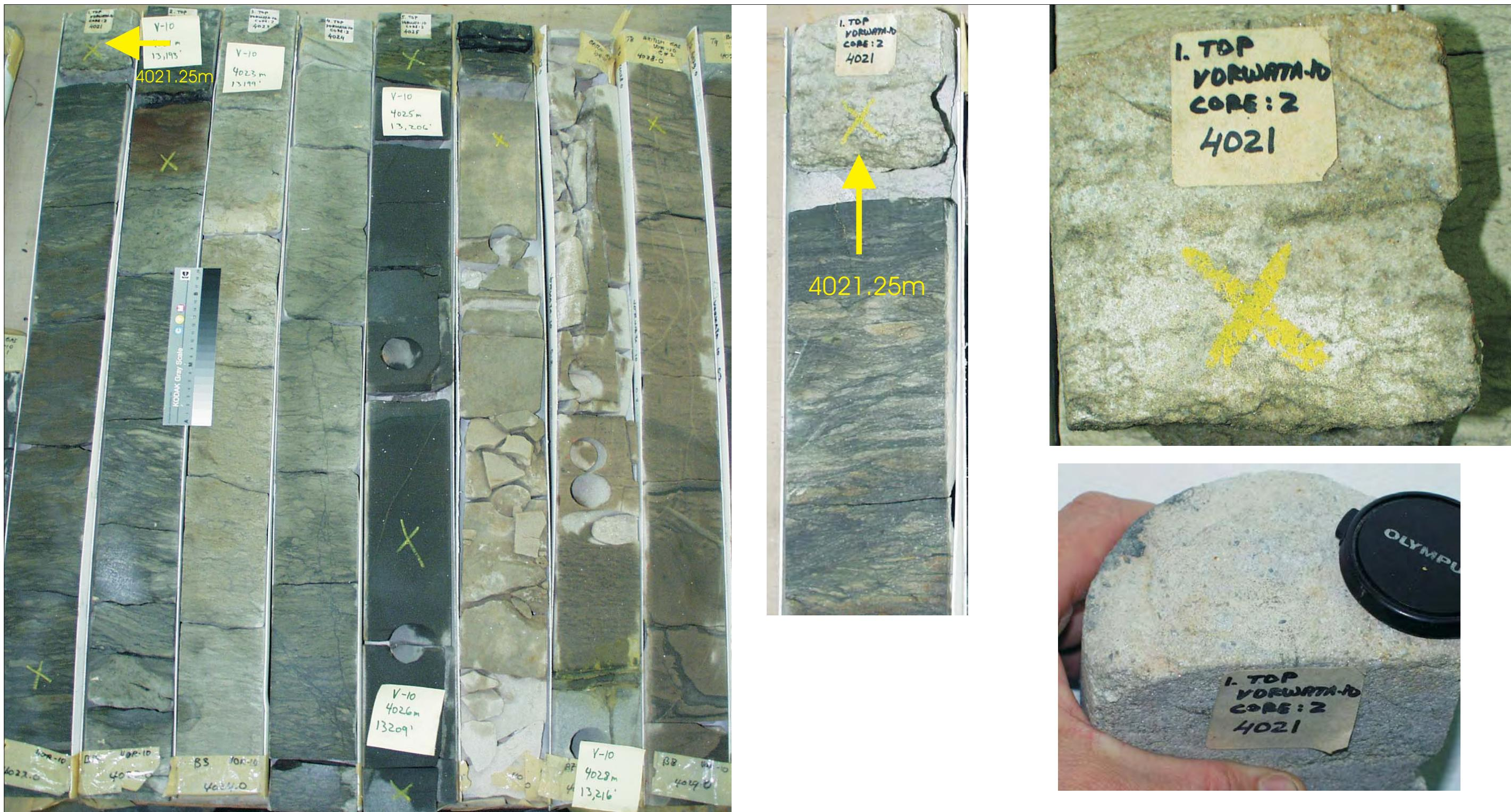


Figure 58A: Core Plug/Chip Atlas for sample 4021.25m from Vorwata-10.

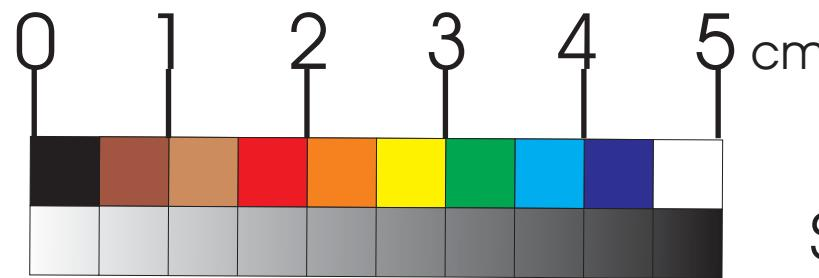
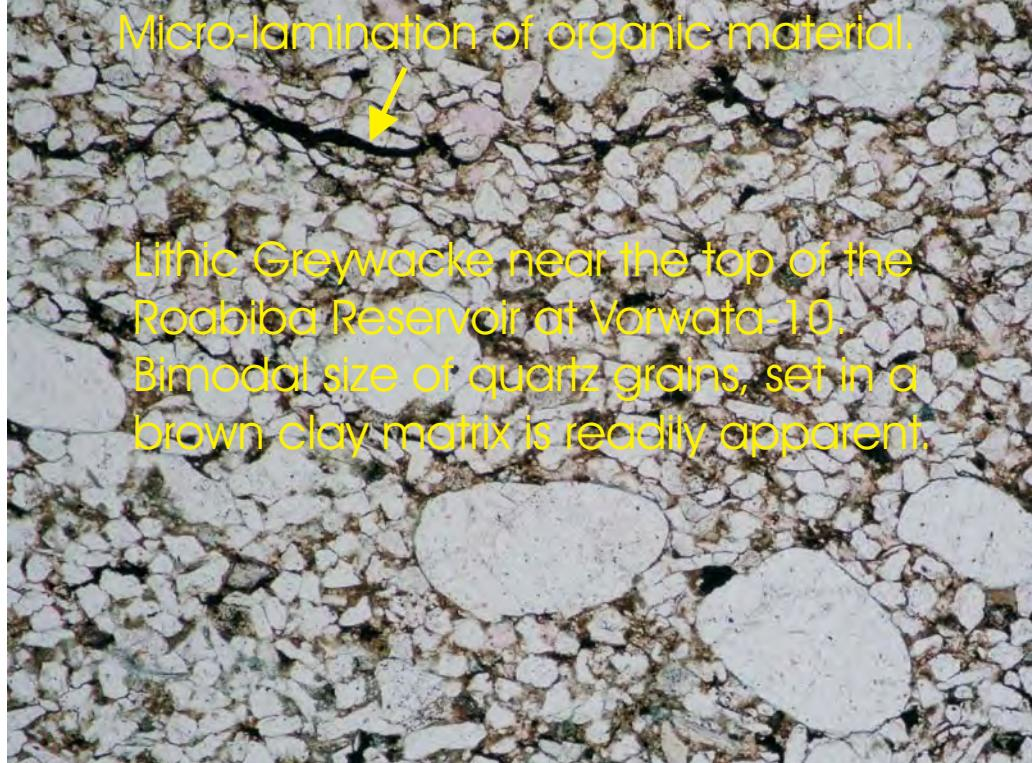
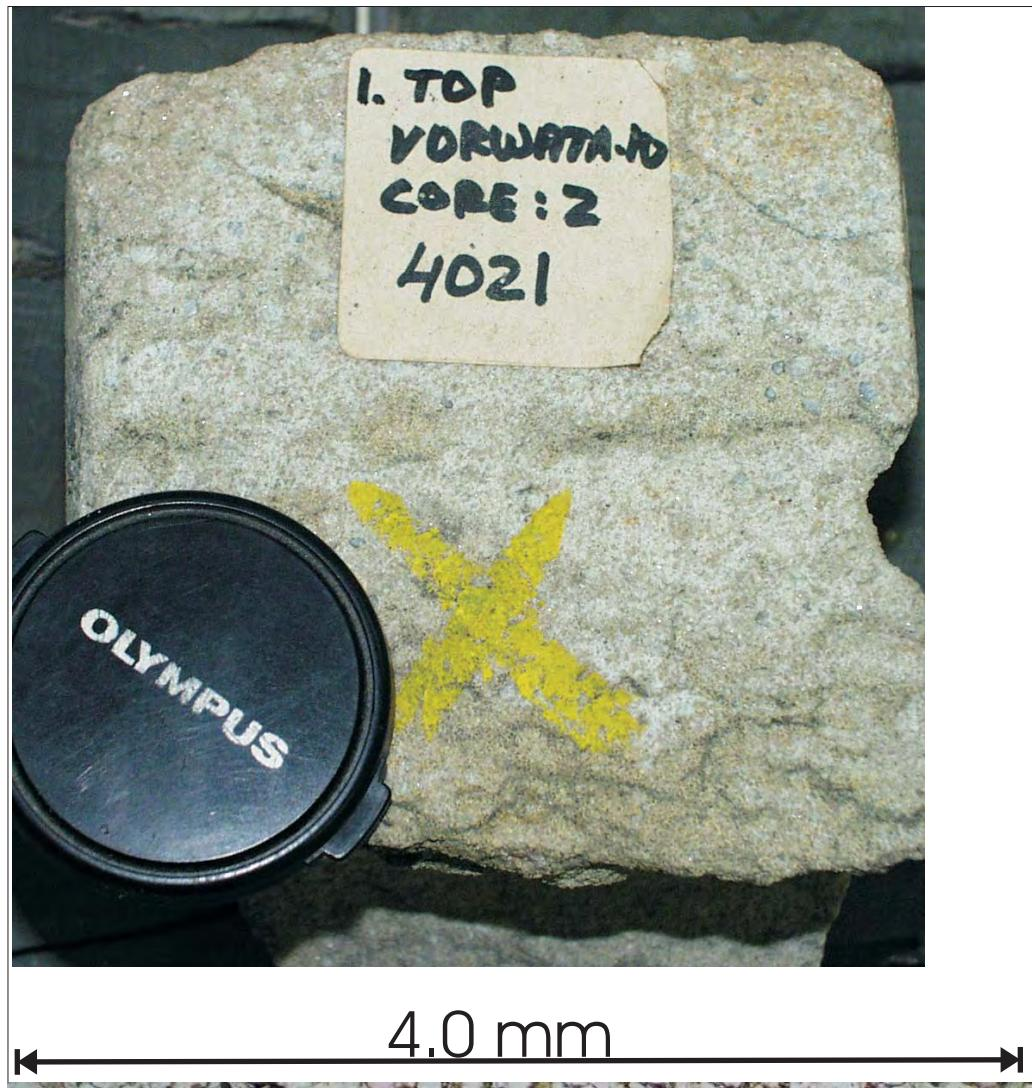
WHOLE CORE PLUG ANALYSES

WELL: VORWATA - 10st

DEPTH: 4021.25 m

PLATE A:

Digital Whole Core Photographs

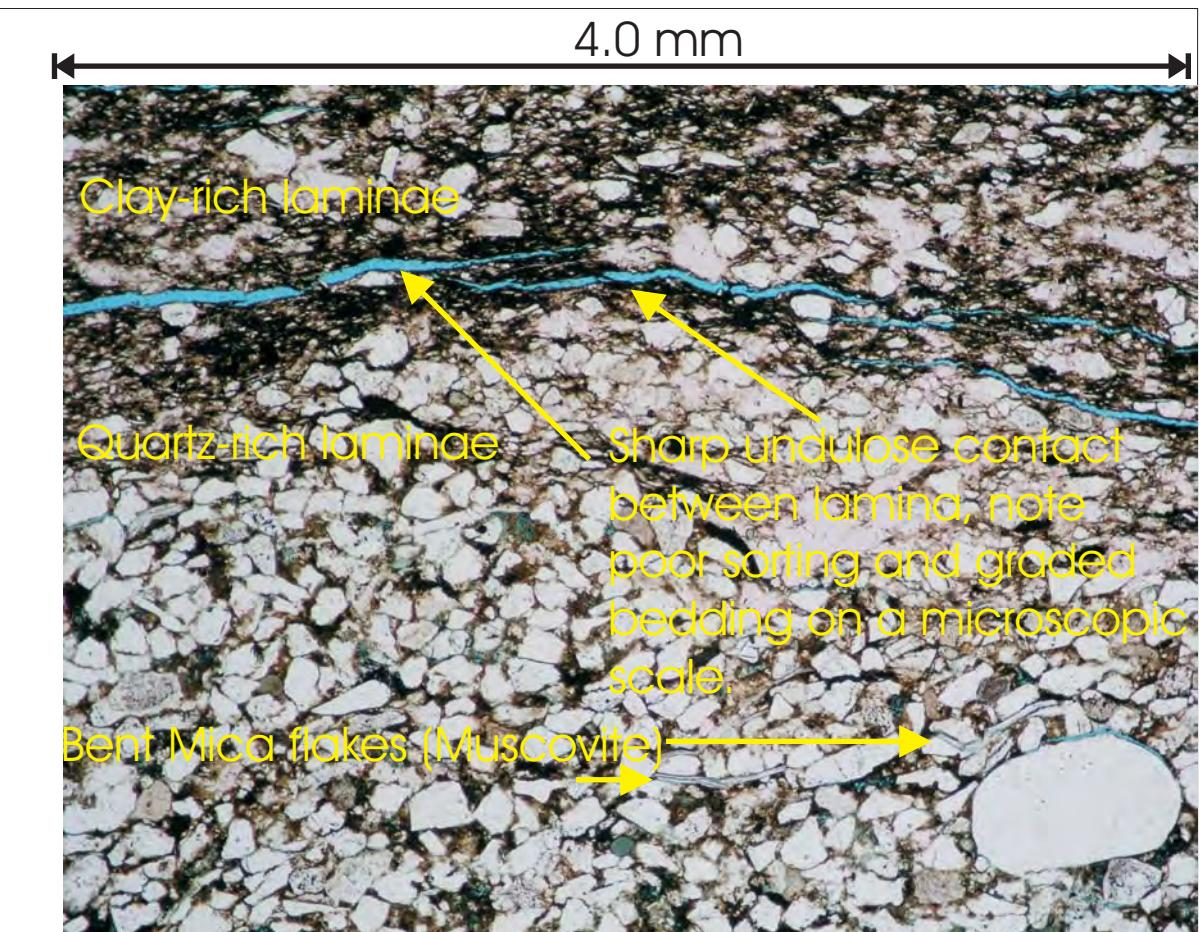
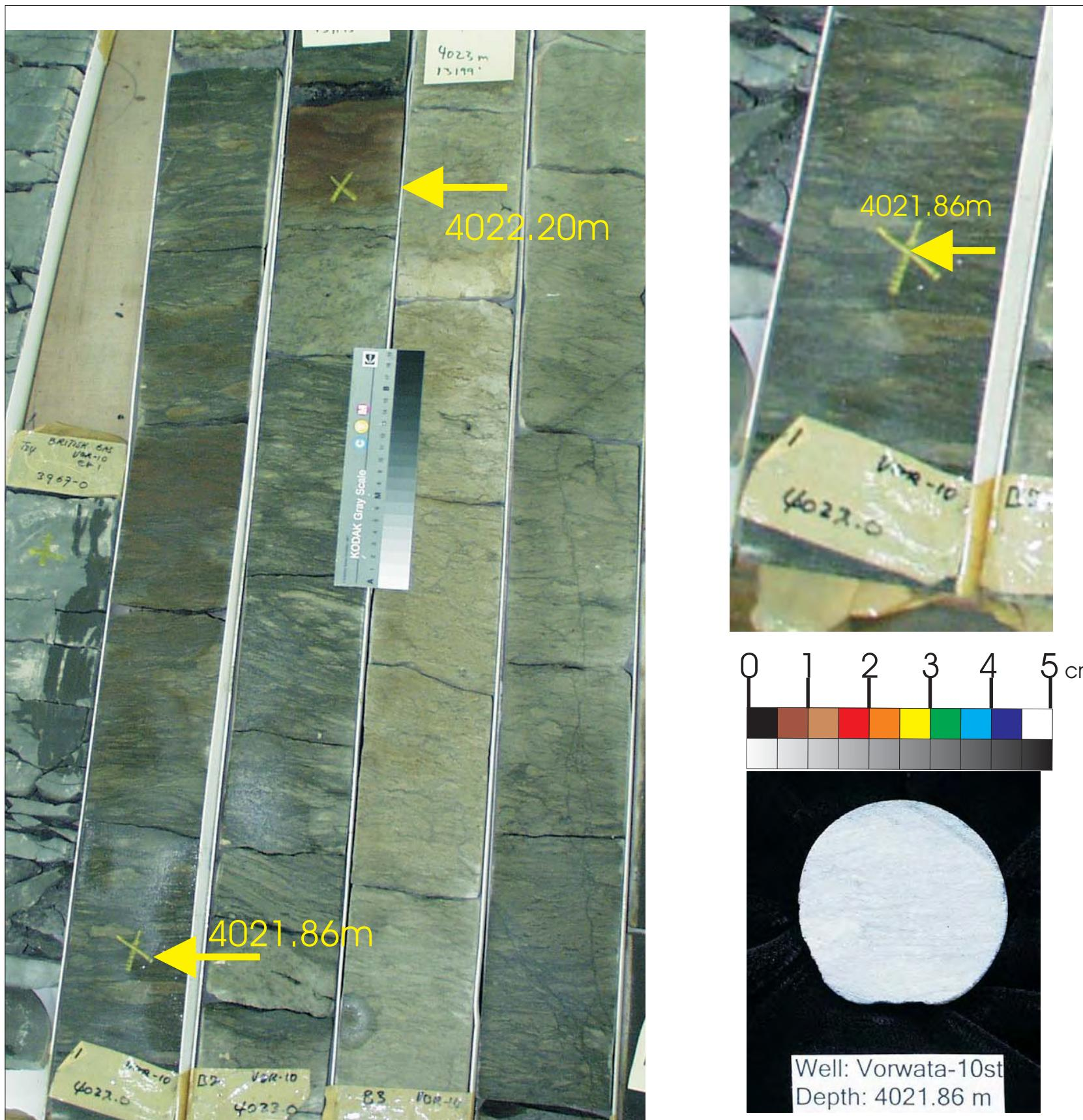


Sample Depth: 4021.25 m
Shifted Depth: 13193.7 ft
He-Ø: 8.2%
k air: 0.318mD (NOB 800 psia)

WHOLE CORE PLUG ANALYSES
WELL: VORWATA - 10st
DEPTH: 4021.25 m

PLATE B:
Digital Whole Core Photographs
Digital Core Chip/Plug Photograph
Petrographic Photomicrograph

Figure 58B: Core Plug/Chip Atlas for sample 4021.25m from Vorwata-10.



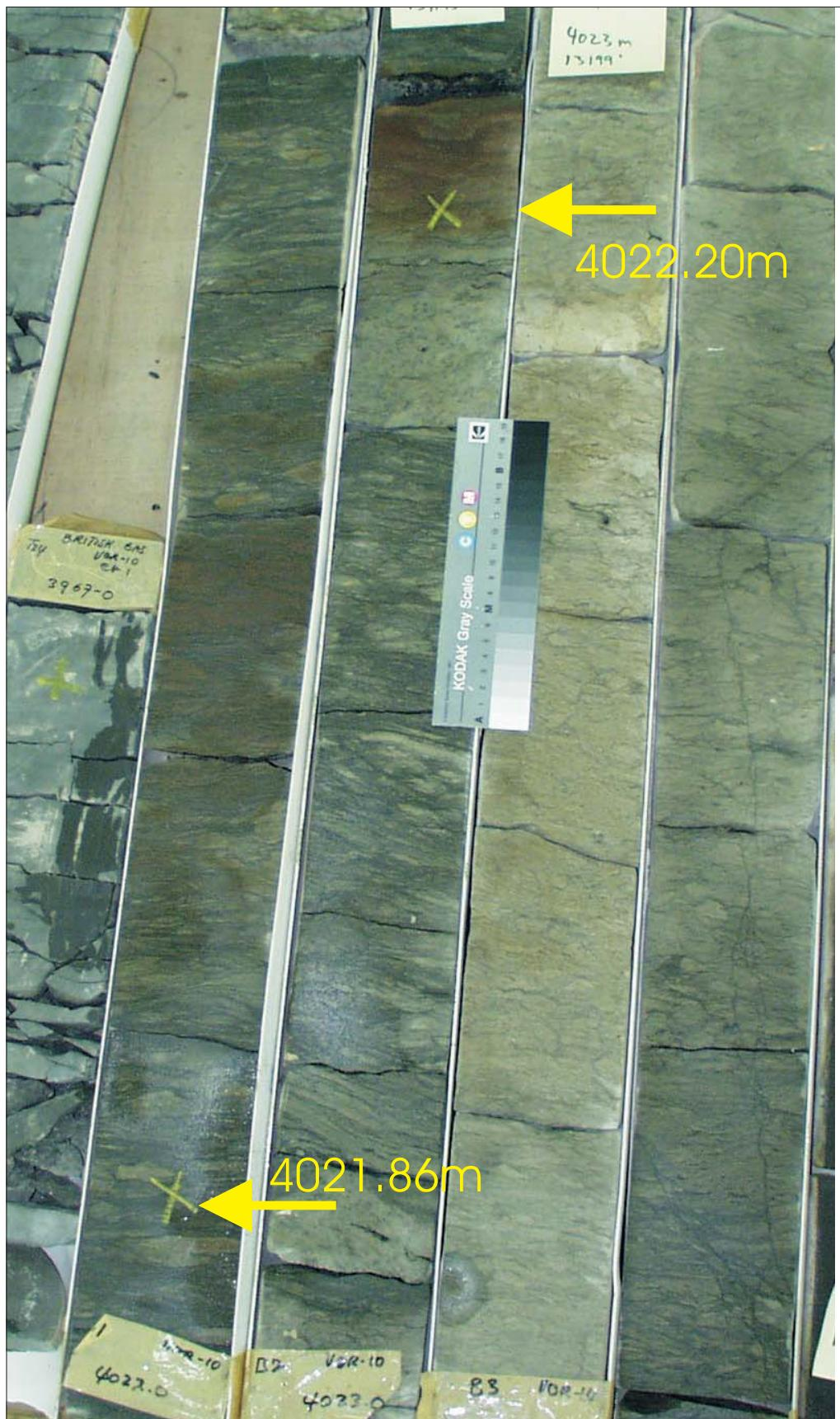
Open fracture with blue staining is probably a sampling artifact.

Sample Depth: 4021.86 m
Shifted Depth: 13195.7 ft
He-Ø: 5.7%
k air: 271mD (sc)

WHOLE CORE PLUG ANALYSES
WELL: VORWATA - 10st
DEPTH: 4021.86 m

PLATE A:
Digital Whole Core Photographs
Digital Core Chip/Plug Photograph
Petrographic Photomicrograph

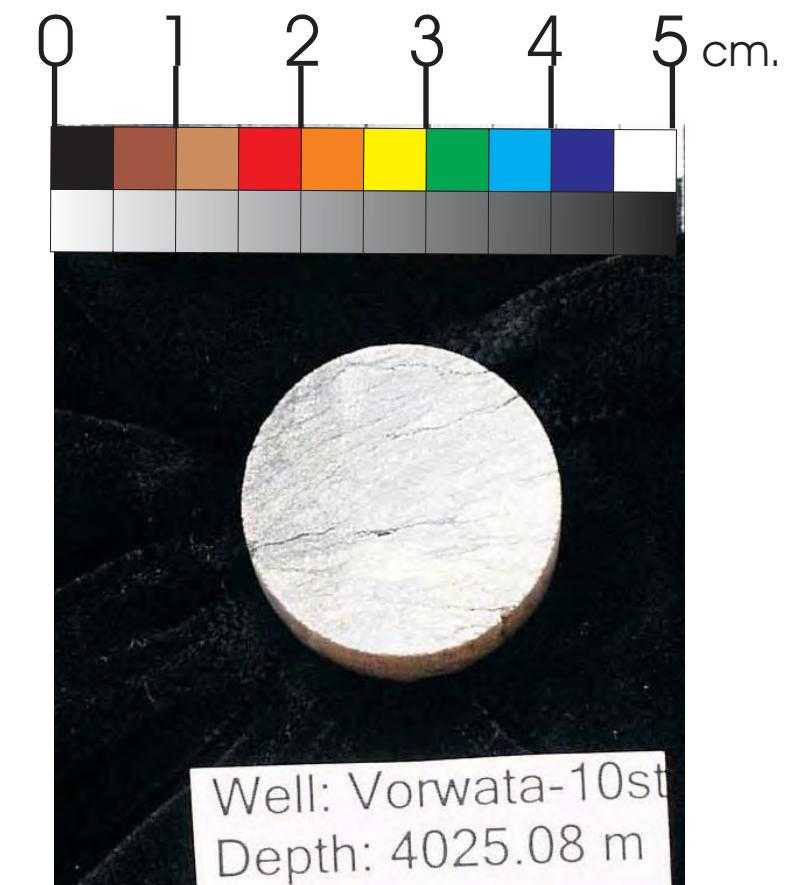
Figure 59A: Core Plug/Chip Atlas for sample 4021.86m from Vorwata-10.



Sample Depth: 4022.20 m
 Shifted Depth: 13196.8 ft
 He-∅: 7.7%
 k air: 96.24mD (sc)

WHOLE CORE PLUG ANALYSES
 WELL: VORWATA - 10st
 DEPTH: 4022.20 m
 PLATE A
 Digital Whole Core Photographs
 Digital Core Chip/Plug Photograph

Figure 60A: Core Plug/Chip Atlas for sample 4022.20m from Vorwata-10.

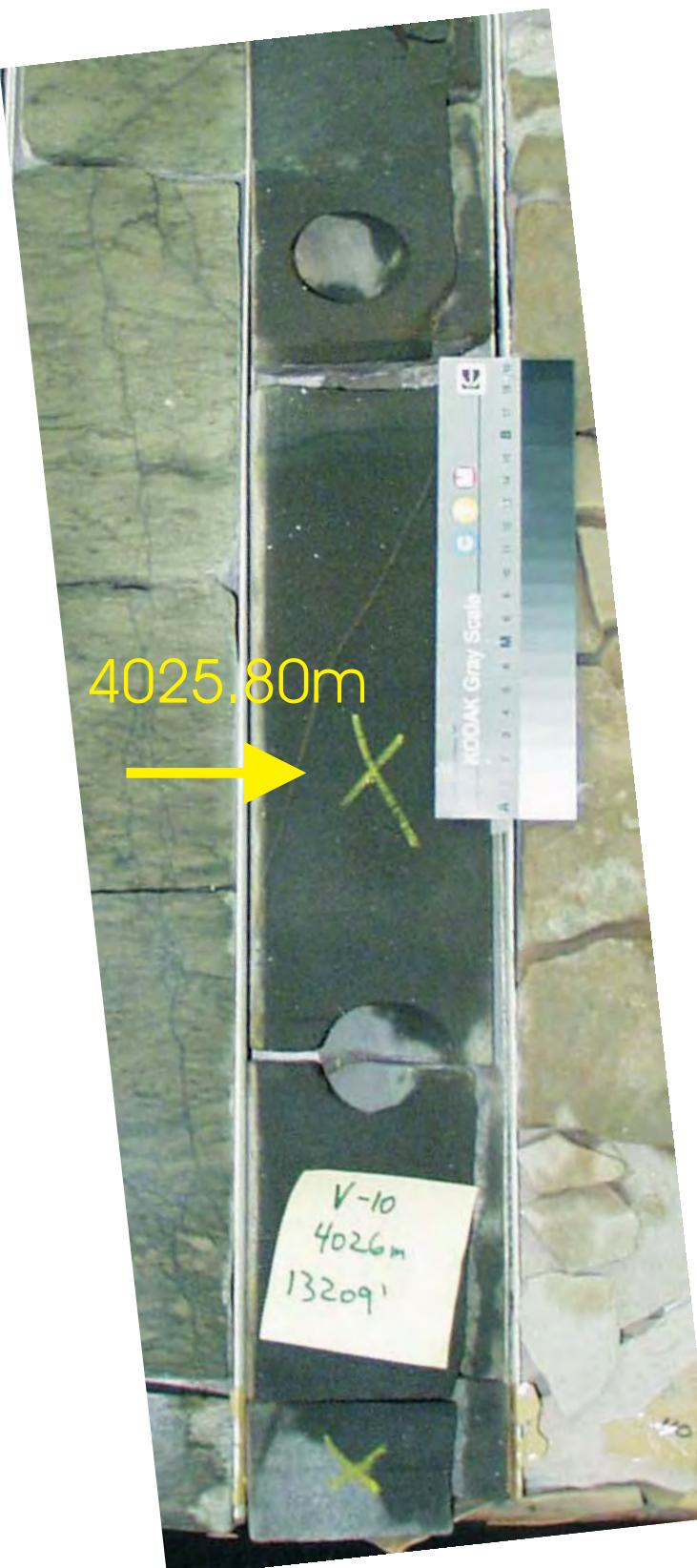


Sample Depth: 4025.08 m
Shifted Depth: 13206.3 ft
He-∅: 7.6%
k air: 40.7 mD (NOB 800 psia)

WHOLE CORE PLUG ANALYSES
WELL: VORWATA - 10st
DEPTH: 4025.08 m

PLATE A
Digital Whole Core Photographs
Digital Core Chip/Plug Photograph

Figure 61A: Core Plug/Chip Atlas for sample 4025.08m from Vorwata-10.

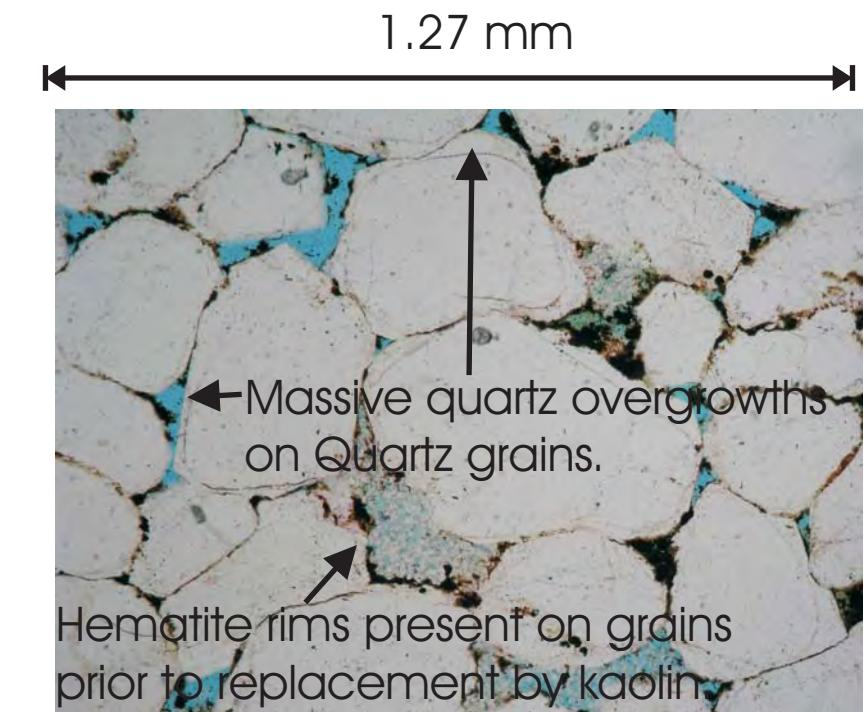
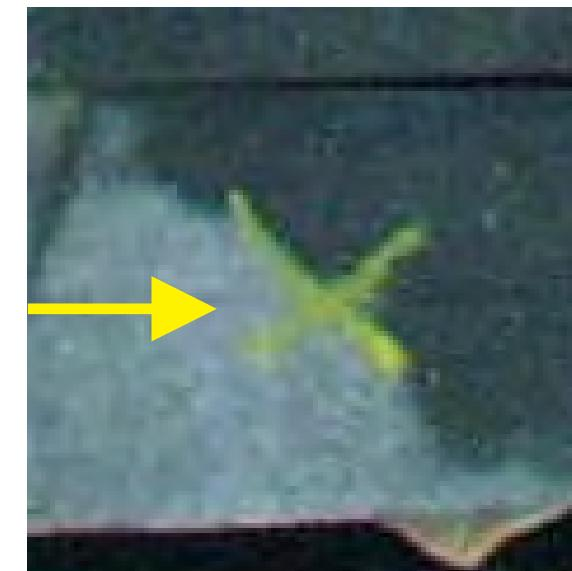
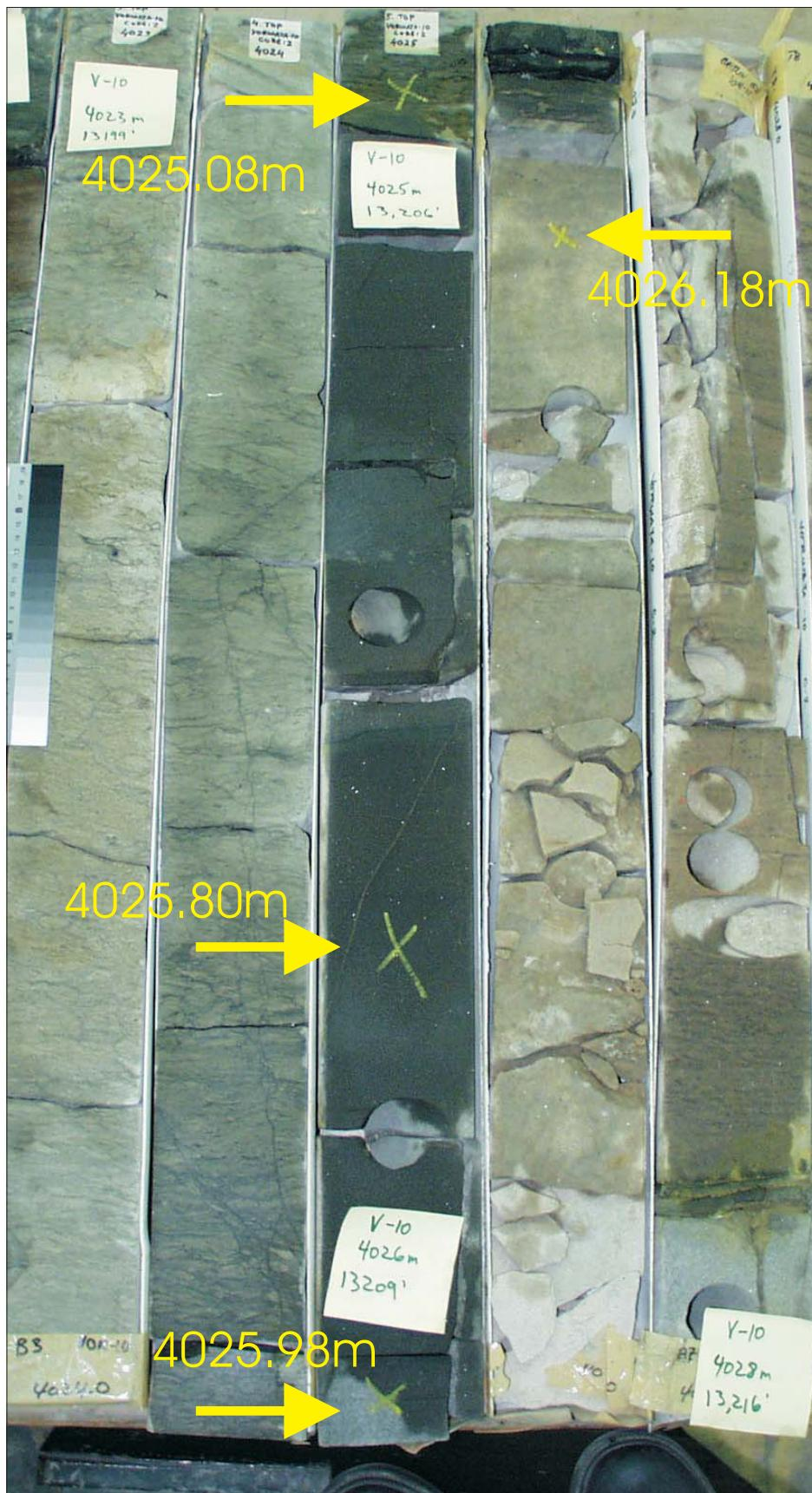


Sample Depth: 4025.80 m
Shifted Depth: 13208.6 ft
He-Ø: 11.2%
k air: 290.95mD (NOB 800 psia)

WHOLE CORE PLUG ANALYSES
WELL: VORWATA - 10st
DEPTH: 4025.80 m

PLATE A
Digital Whole Core Photographs
Digital Core Chip/Plug Photograph

Figure 62A: Core Plug/Chip Atlas for sample 4025.80m from Vorwata-10.

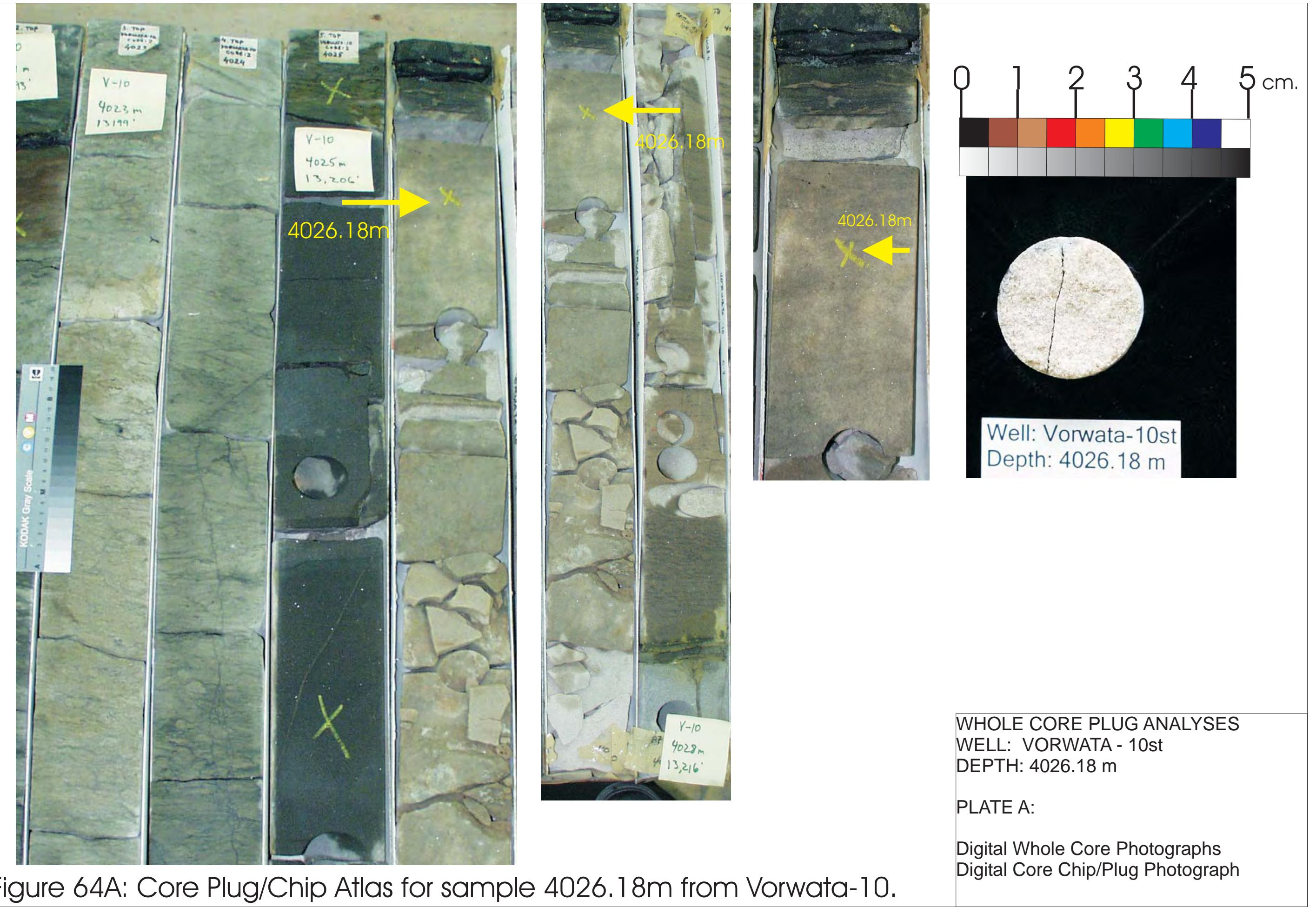


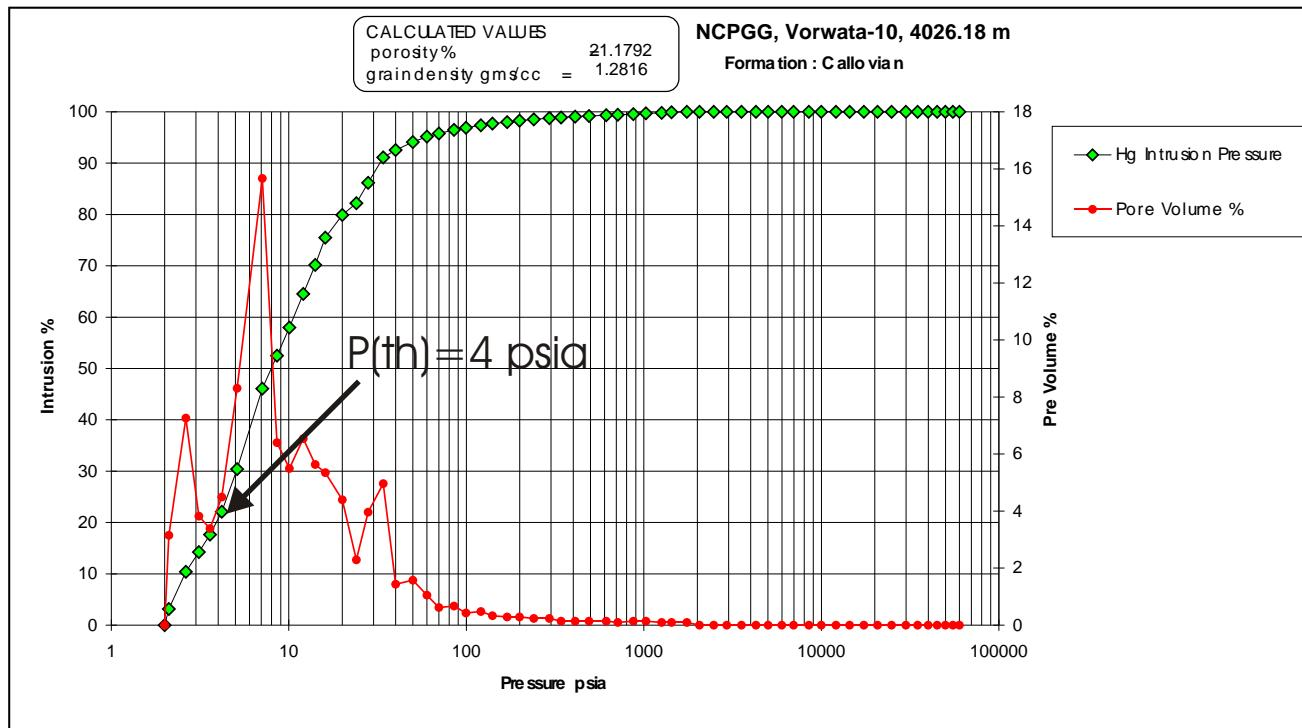
Sample Depth: 4025.98 m
 Shifted Depth: 13209.2 ft
 He-Ø: insufficient/broken sample
 k air: insufficient/broken sample

WHOLE CORE PLUG ANALYSES
WELL: VORWATA - 10st
DEPTH: 4025.98 m

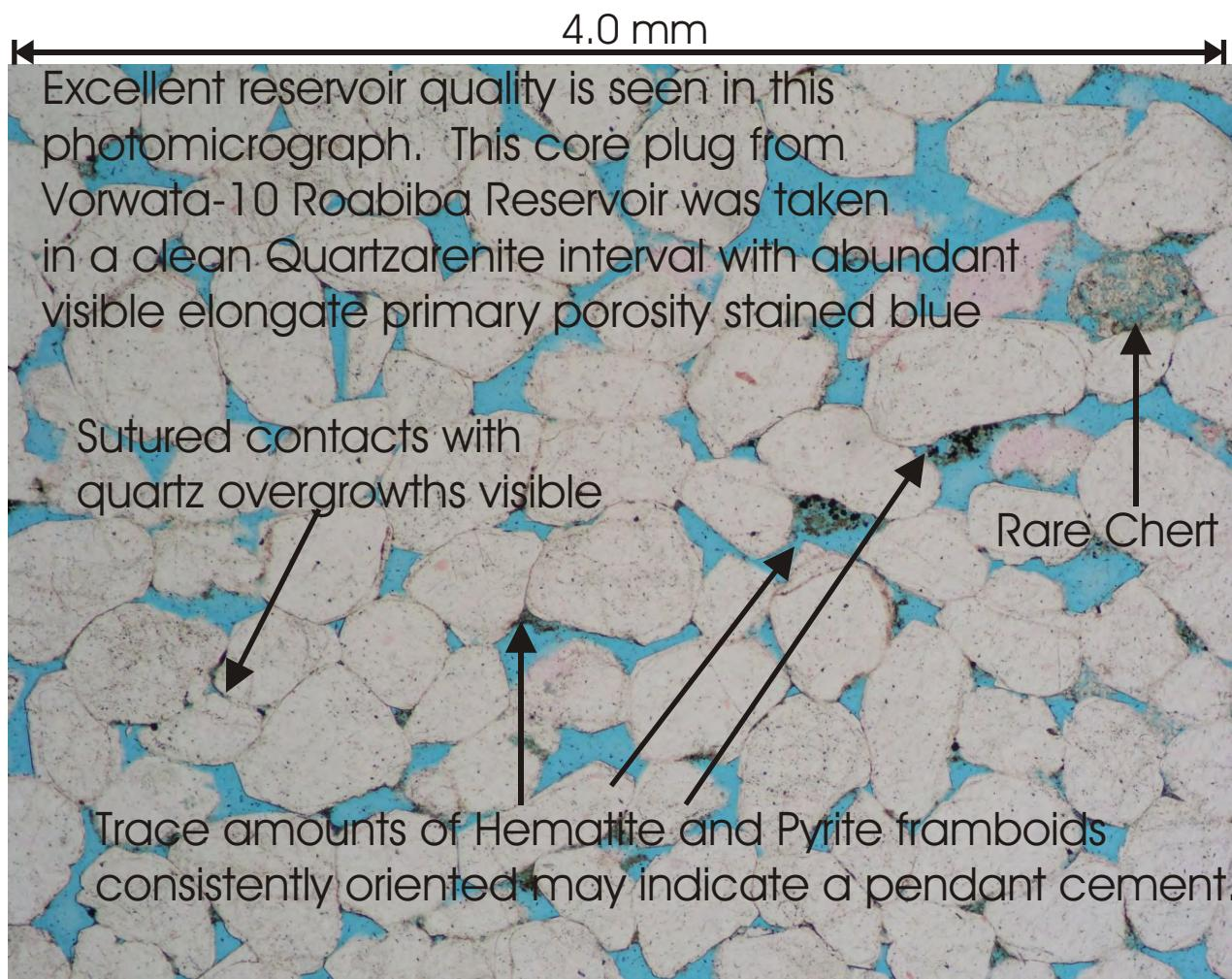
PLATE A:
 Digital Whole Core Photographs
 Digital Core Chip/Plug Photograph
 Petrographic Photomicrograph

Figure 63A: Core Plug/Chip Atlas for sample 4025.98m from Vorwata-10.





Sample Depth: 4026.18 m
Shifted Depth: 13209.9 ft
MICP Entry Pressure: 3 psia
MICP Threshold Pressure: 4 psia
Lithology: Sandstone (Roabiba)



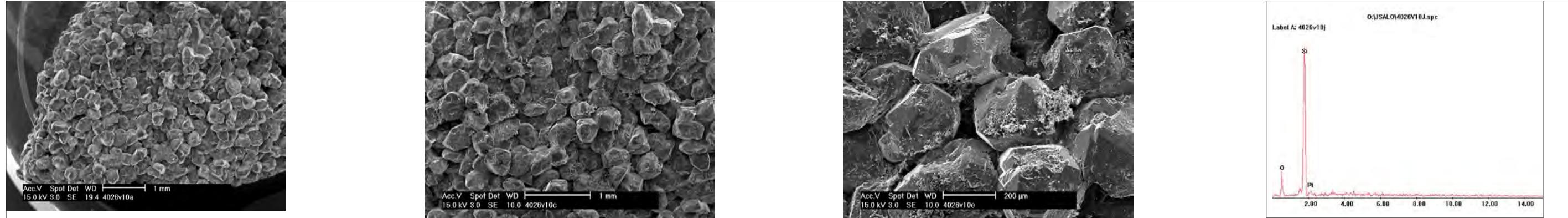
Sample Depth: 4026.18 m
Shifted Depth: 13209.9 ft
He-Ø: 14.5%
k air: 1080 mD (NOB 800 psia)

Figure 64B: Core Plug/Chip Atlas for sample 4026.18m from Vorwata-10.

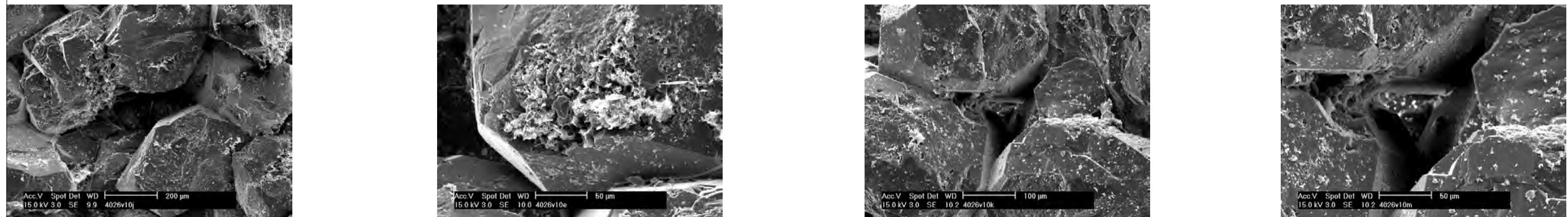
WHOLE CORE PLUG ANALYSES
WELL: VORWATA - 10st
DEPTH: 4026.18 m

PLATE B:

Mercury Injection Capillary Pressure
Petrographic Photomicrograph



SEM images showing extremely clean subrounded Quartz grains in this Roabiba Reservoir quartzarenite interval. EDX confirms quartz-rich composition.



SEM images at higher magnification showing excellent intergranular porosity with rare kaolin platelets clinging to grain crystal faces.



WHOLE CORE PLUG ANALYSES

WELL: VORWATA - 10st

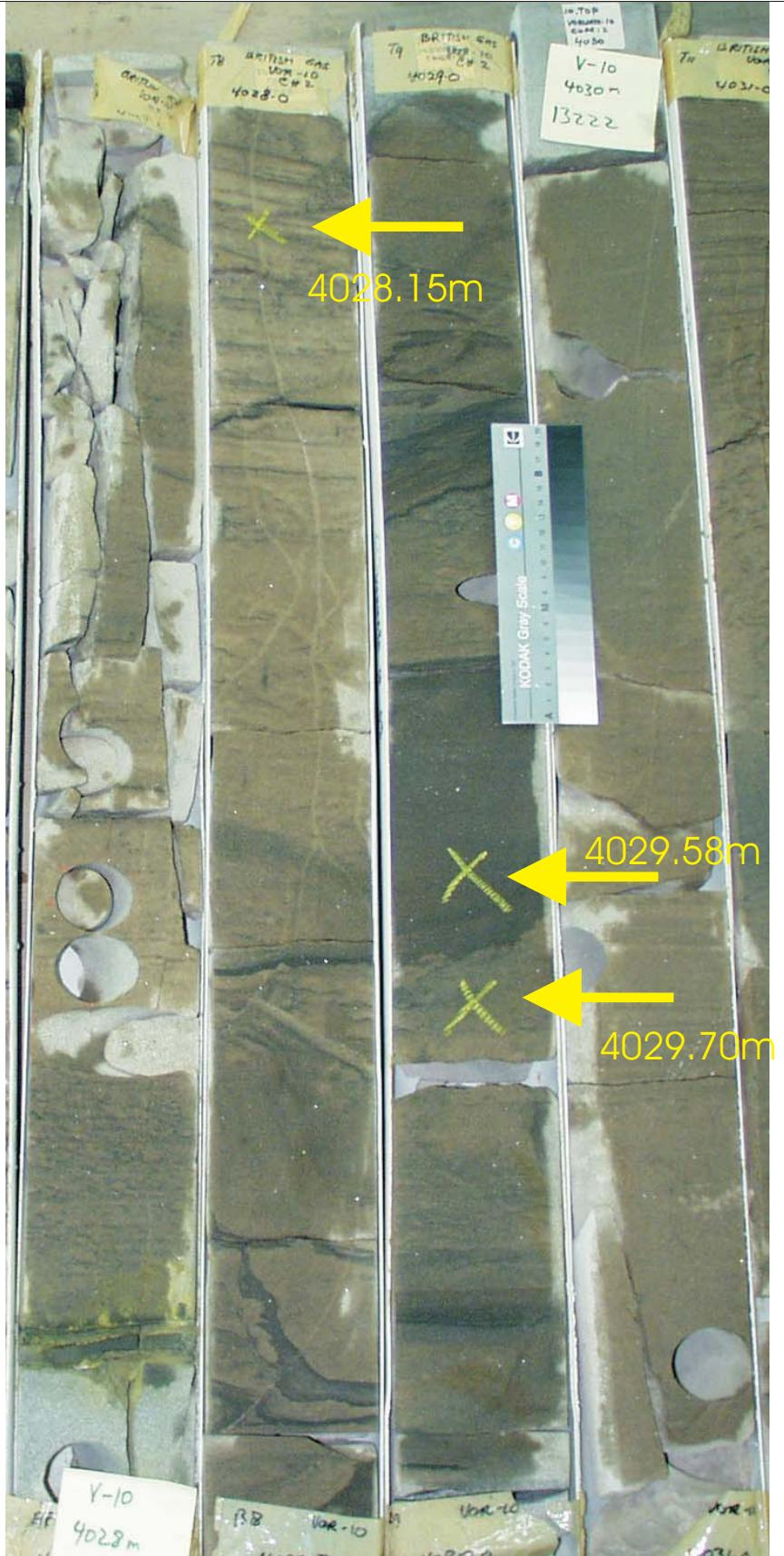
DEPTH: 4026.18 m

PLATE C:

FESEM Photomicrograph

FESEM EDX (SEM XRD)

Figure 64C: Core Plug/Chip Atlas for sample 4026.18m from Vorwata-10.



Sample Depth: 4028.15 m
Shifted Depth: 13216.4 ft
He-Ø: 14.8%
k air: 979 mD (NOB 800 psia)

WHOLE CORE PLUG ANALYSES
WELL: VORWATA - 10st
DEPTH: 4028.15 m

PLATE A
Digital Whole Core Photographs
Digital Core Chip/Plug Photograph

Figure 65A: Core Plug/Chip Atlas for sample 4028.15m from Vorwata-10.

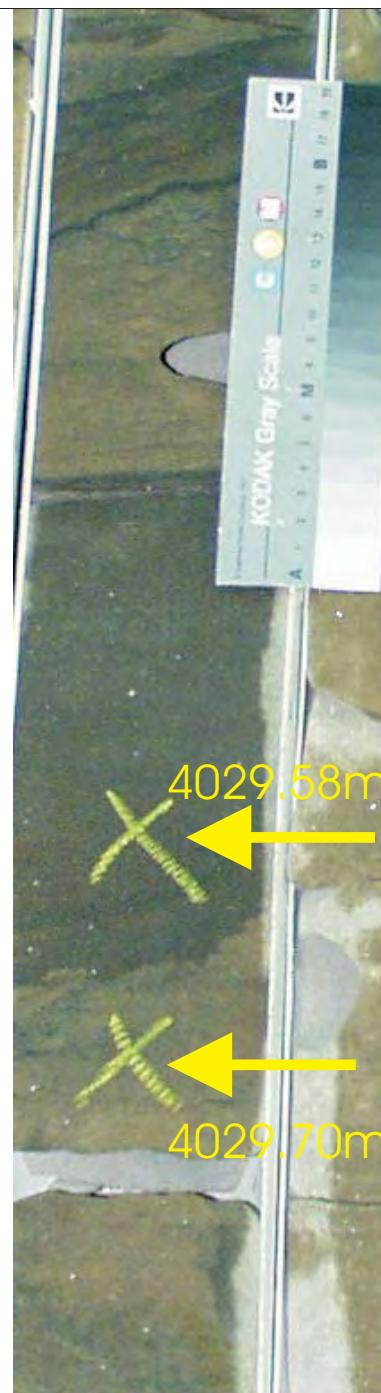
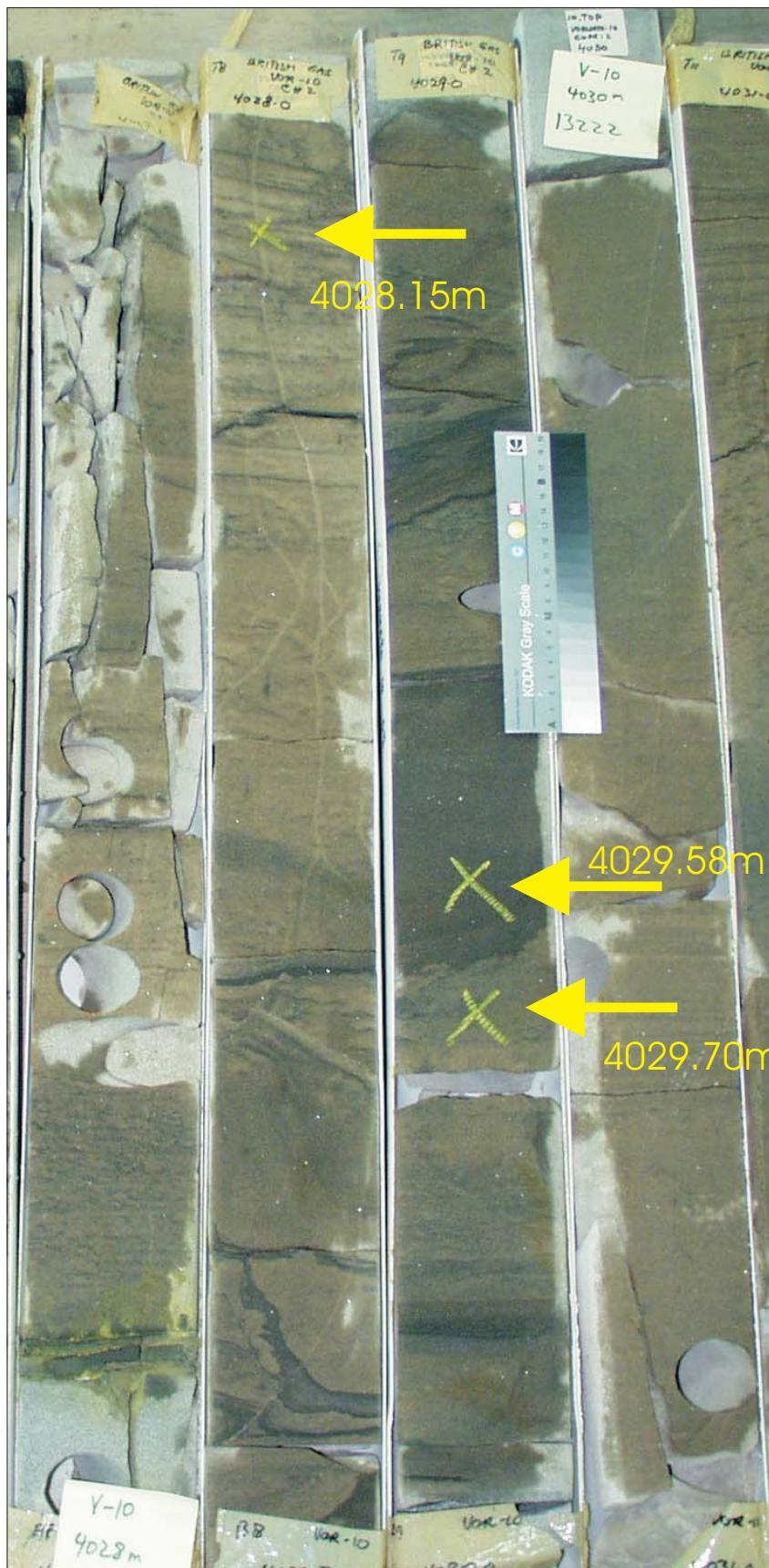


Sample Depth: 4029.58 m
Shifted Depth: 13221.1 ft
He-Ø: 14.4%
k air: 576 mD (NOB 800 psia)

WHOLE CORE PLUG ANALYSES
WELL: VORWATA - 10st
DEPTH: 4029.58 m

PLATE A
Digital Whole Core Photographs
Digital Core Chip/Plug Photograph

Figure 66A: Core Plug/Chip Atlas for sample 4029.58m from Vorwata-10.



Sample Depth: 4029.70 m
 Shifted Depth: 13221.4 ft
 He-∅: 14.8%
 k air: 1339.4 mD (sc)

WHOLE CORE PLUG ANALYSES
 WELL: VORWATA - 10st
 DEPTH: 4029.70 m

 PLATE A
 Digital Whole Core Photographs
 Digital Core Chip/Plug Photograph

Figure 67A: Core Plug/Chip Atlas for sample 4029.70m from Vorwata-10.

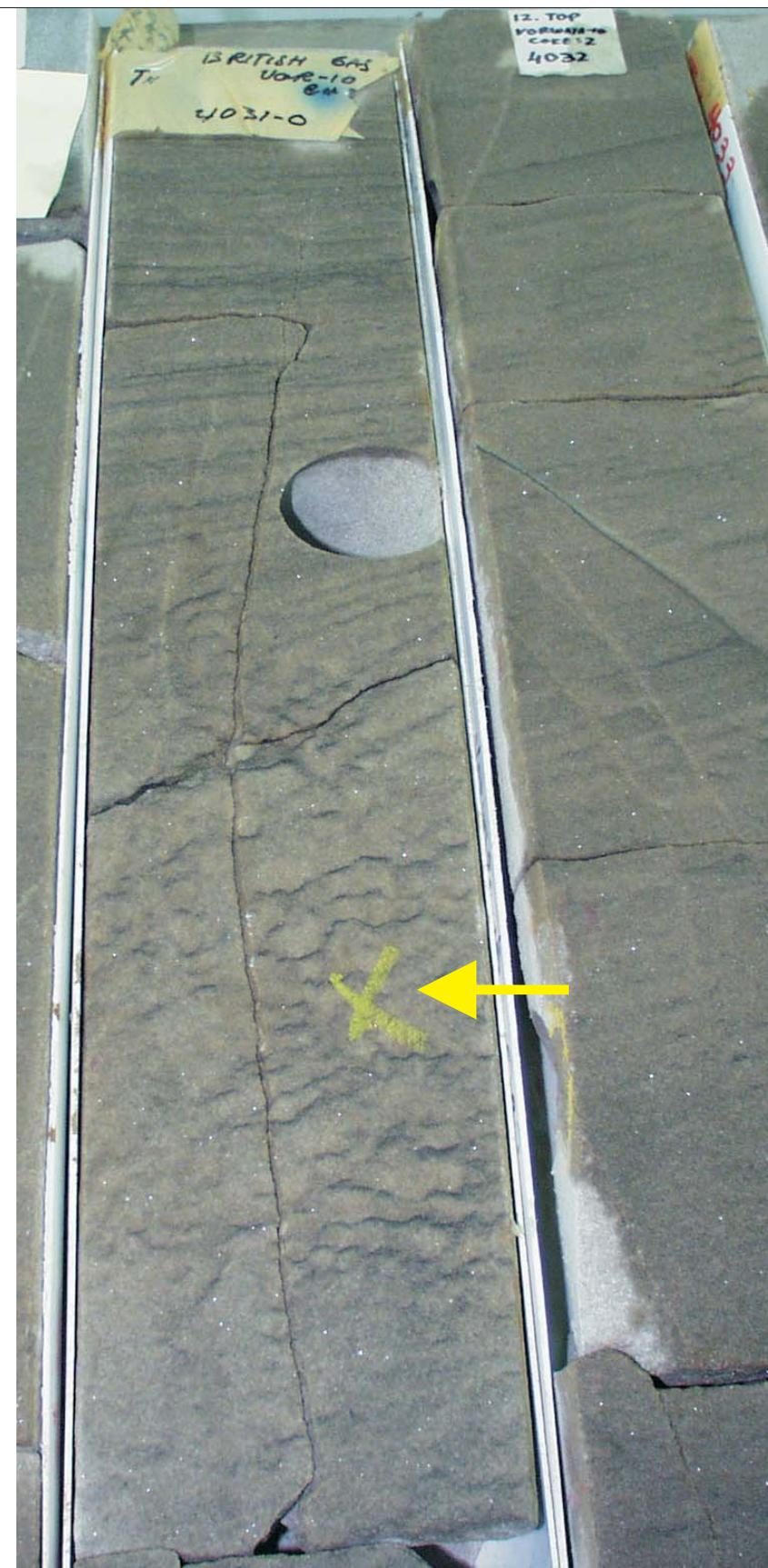
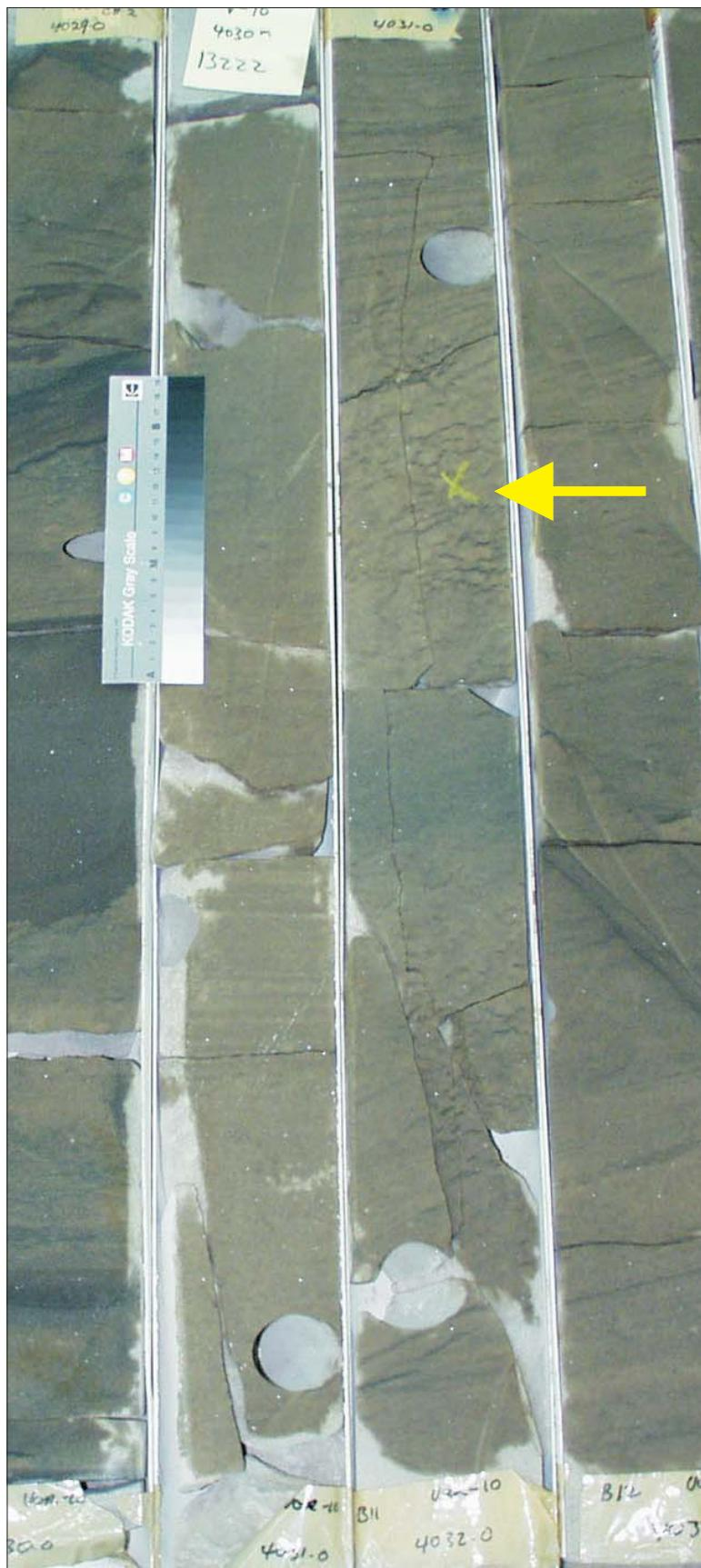


Figure 68A: Core Plug/Chip Atlas for sample 4031.55m from Vorwata-10.

WHOLE CORE PLUG ANALYSES

WELL: VORWATA - 10st

DEPTH: 4031.55 m

PLATE A:

Digital Whole Core Photographs



Well: Vorwata-10st
Depth: 4031.55 m

Sample Depth: 4031.55 m
Shifted Depth: 13227.5 ft
He-Ø: 11.9%
k air: 226 mD (NOB 800 psia)

Figure 68B: Core Plug/Chip Atlas for sample 4031.55m from Vorwata-10.

WHOLE CORE PLUG ANALYSES

WELL: VORWATA - 10st

DEPTH: 4031.55 m

PLATE B:

Digital Whole Core Photographs

Digital Core Chip/Plug Photograph



Figure 69A: Core Plug/Chip Atlas for sample 4034.51m from Vorwata-10.

WHOLE CORE PLUG ANALYSES

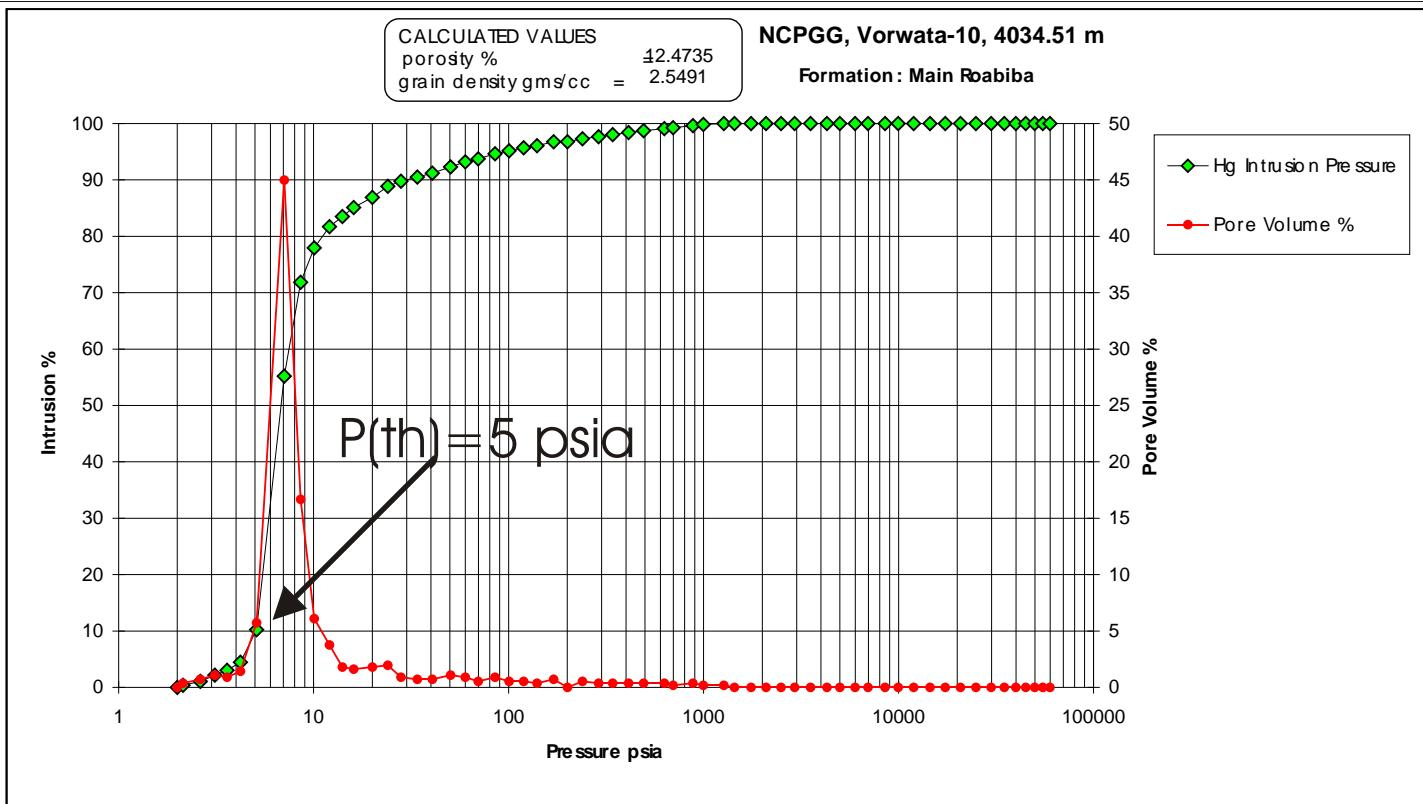
WELL: VORWATA - 10st

DEPTH: 4034.51 m

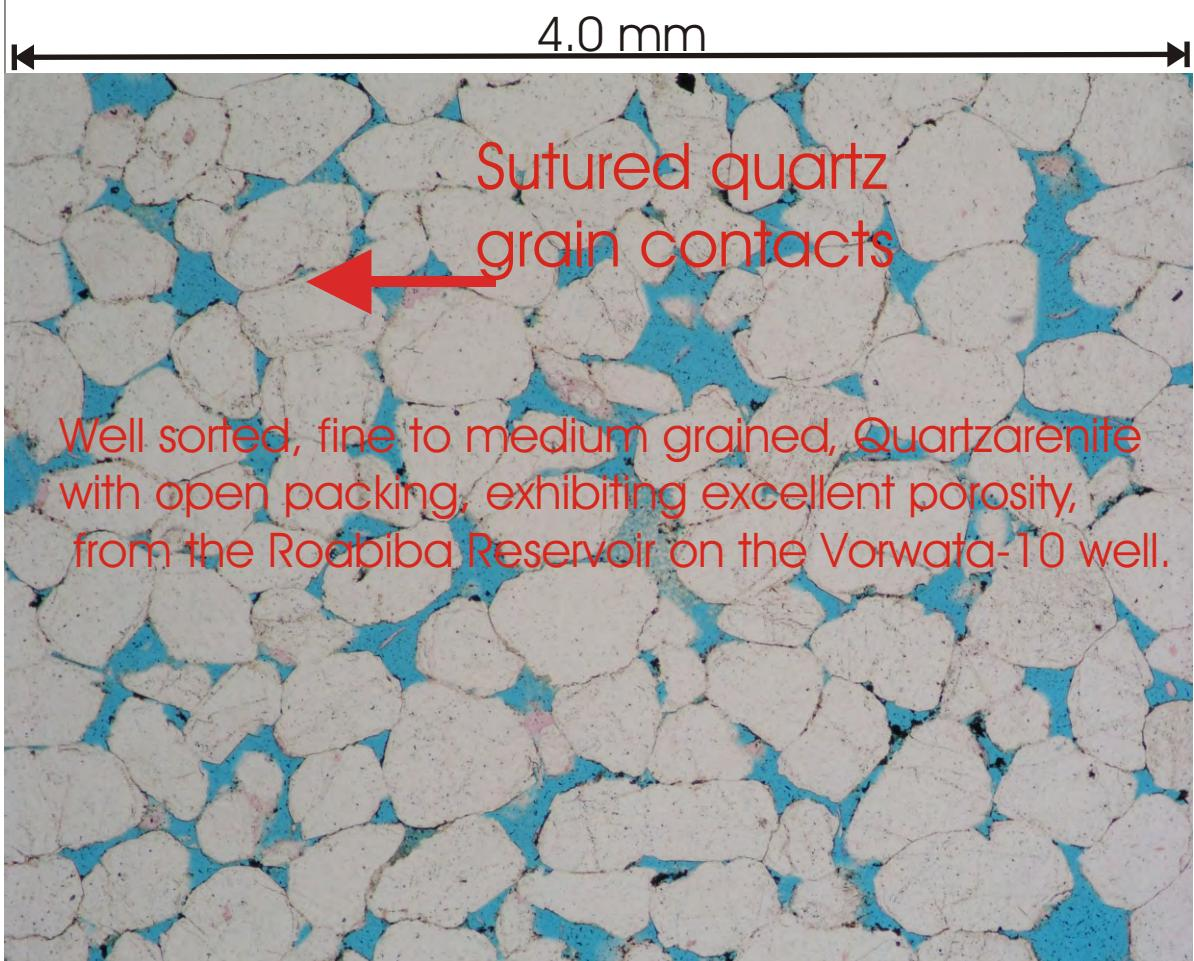
PLATE A:

Digital Whole Core Photographs

Digital Core Chip/Plug Photograph



Sample Depth: 4034.51 m
 Shifted Depth: 13237.2 ft
 MICP Entry Pressure: 2 psia
 MICP Threshold Pressure: 5 psia
 Lithology: Sandstone (Roabiba)

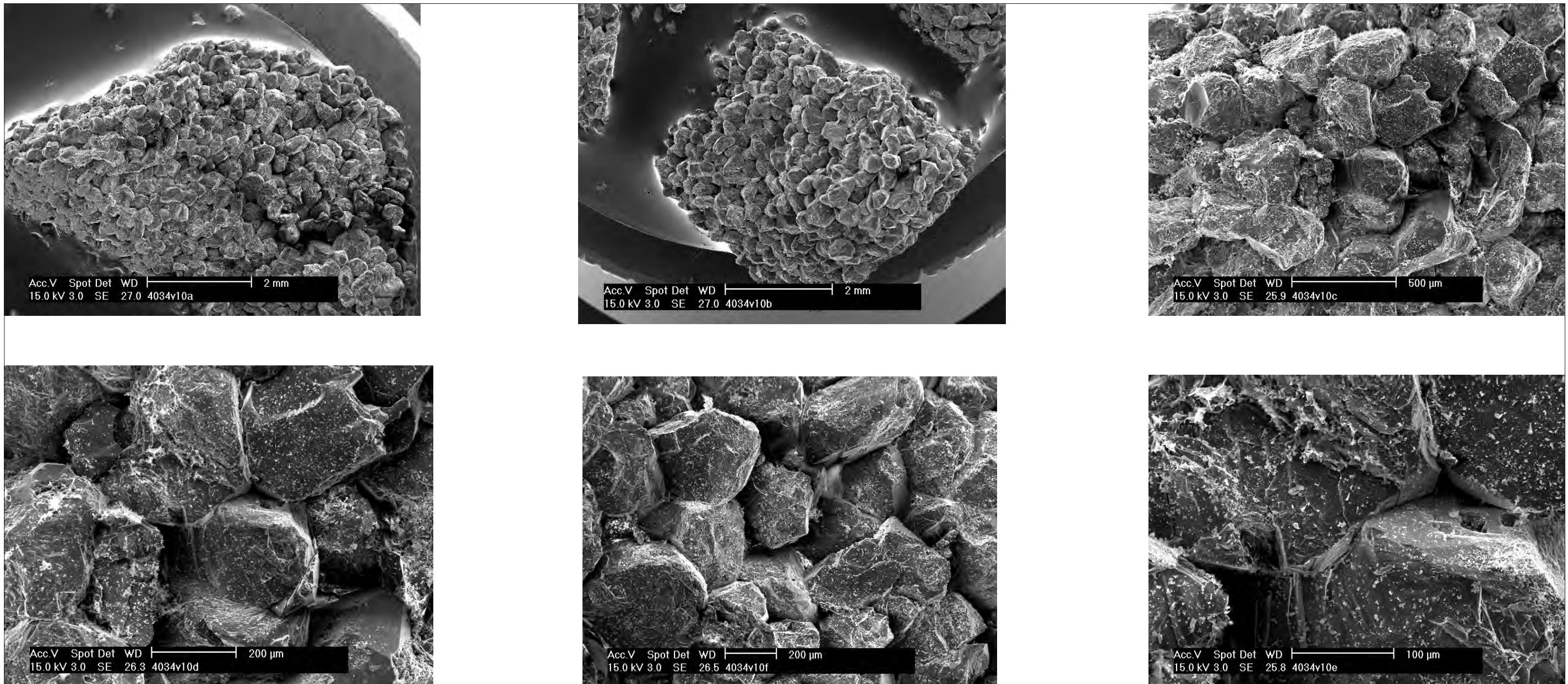


Sample Depth: 4034.51 m
 Shifted Depth: 13237.2 ft
 He-∅: 12.9%
 k air: 954 mD (sc)

Figure 69B: Core Plug/Chip Atlas for sample 4034.51m from Vorwata-10.

WHOLE CORE PLUG ANALYSES
 WELL: VORWATA - 10st
 DEPTH: 4034.51 m

 PLATE B:
 Petrographic Photomicrograph
 Mercury Injection Capillary Pressure



Fine to medium grained quartzarenite composed of primarily subrounded quartz grains with open packing. The EDX shows the Roabiba Reservoir at this depth in the Vorwata-10 well to be composed of mainly quartz.

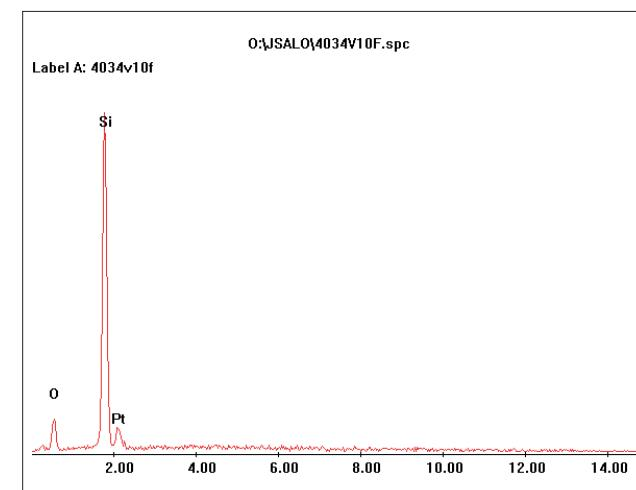
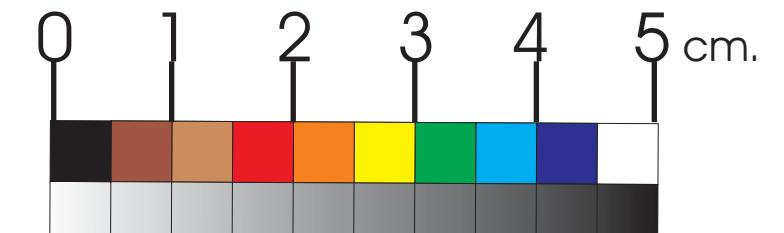
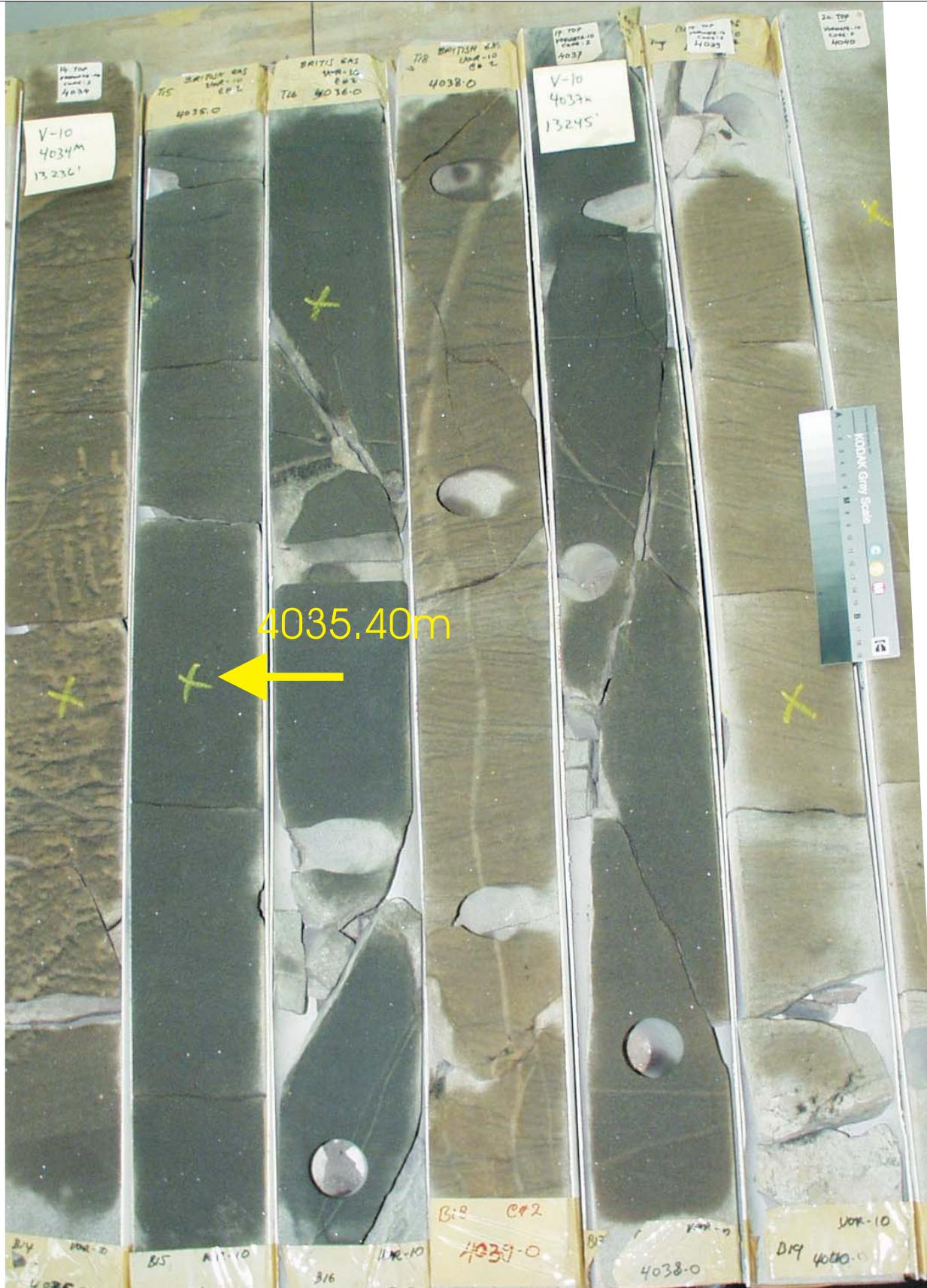


Figure 69C: Core Plug/Chip Atlas for sample 4034.51m from Vorwata-10.

WHOLE CORE PLUG ANALYSES
WELL: VORWATA - 10st
DEPTH: 4034.51 m

PLATE C:

FESEM Photomicrograph
FESEM EDX (SEM XRD)



Well: Vorwata-10st
Depth: 4035.40 m

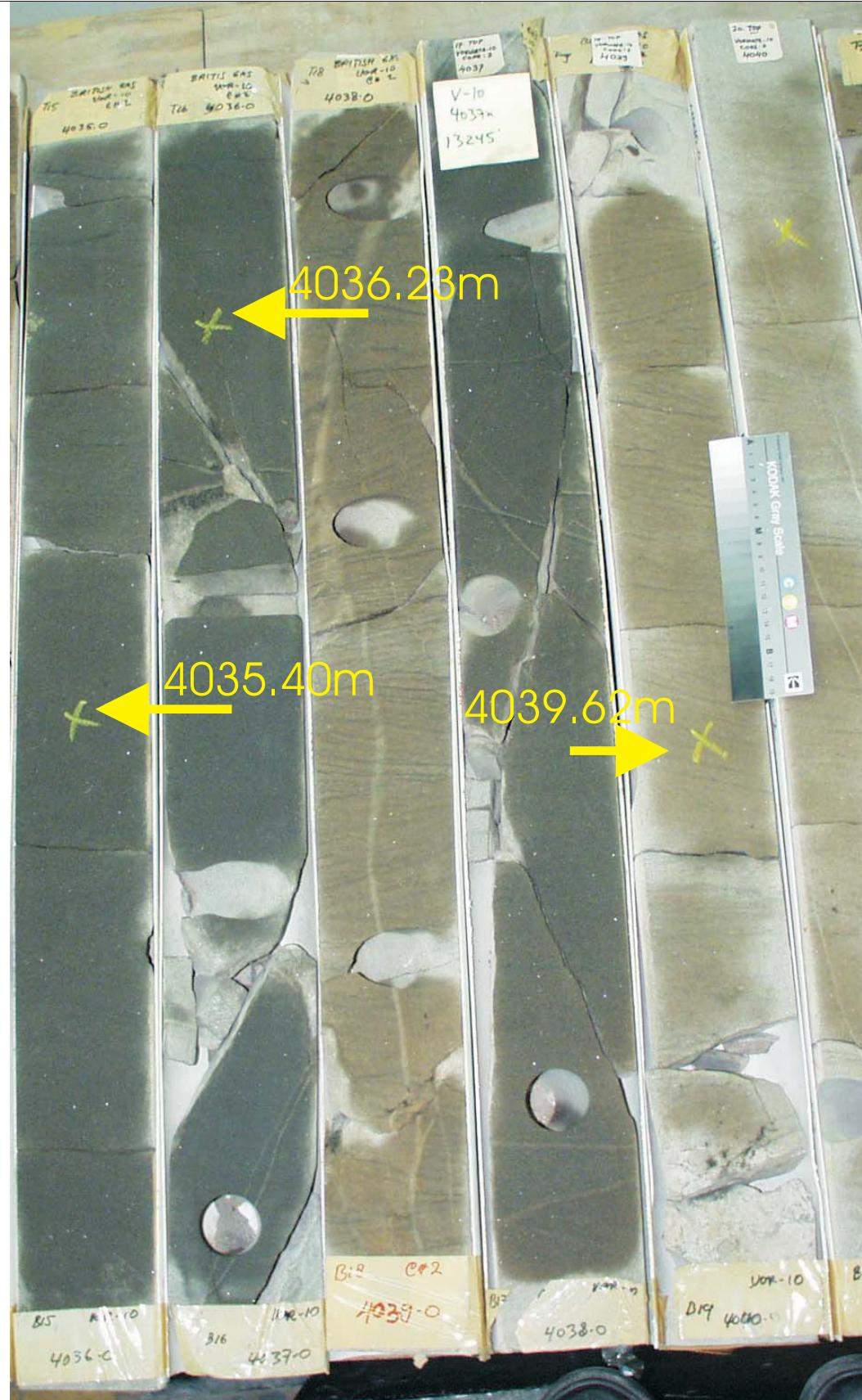
Sample Depth: 4035.40 m
Shifted Depth: 13240.1 ft
He-Ø: 12.7%
k air: 506 mD (sc)

WHOLE CORE PLUG ANALYSES
WELL: VORWATA - 10st
DEPTH: 4035.40 m

PLATE A:

Digital Whole Core Photographs
Digital Core Chip/Plug Photograph

Figure 70A: Core Plug/Chip Atlas for sample 4035.40m from Vorwata-10.



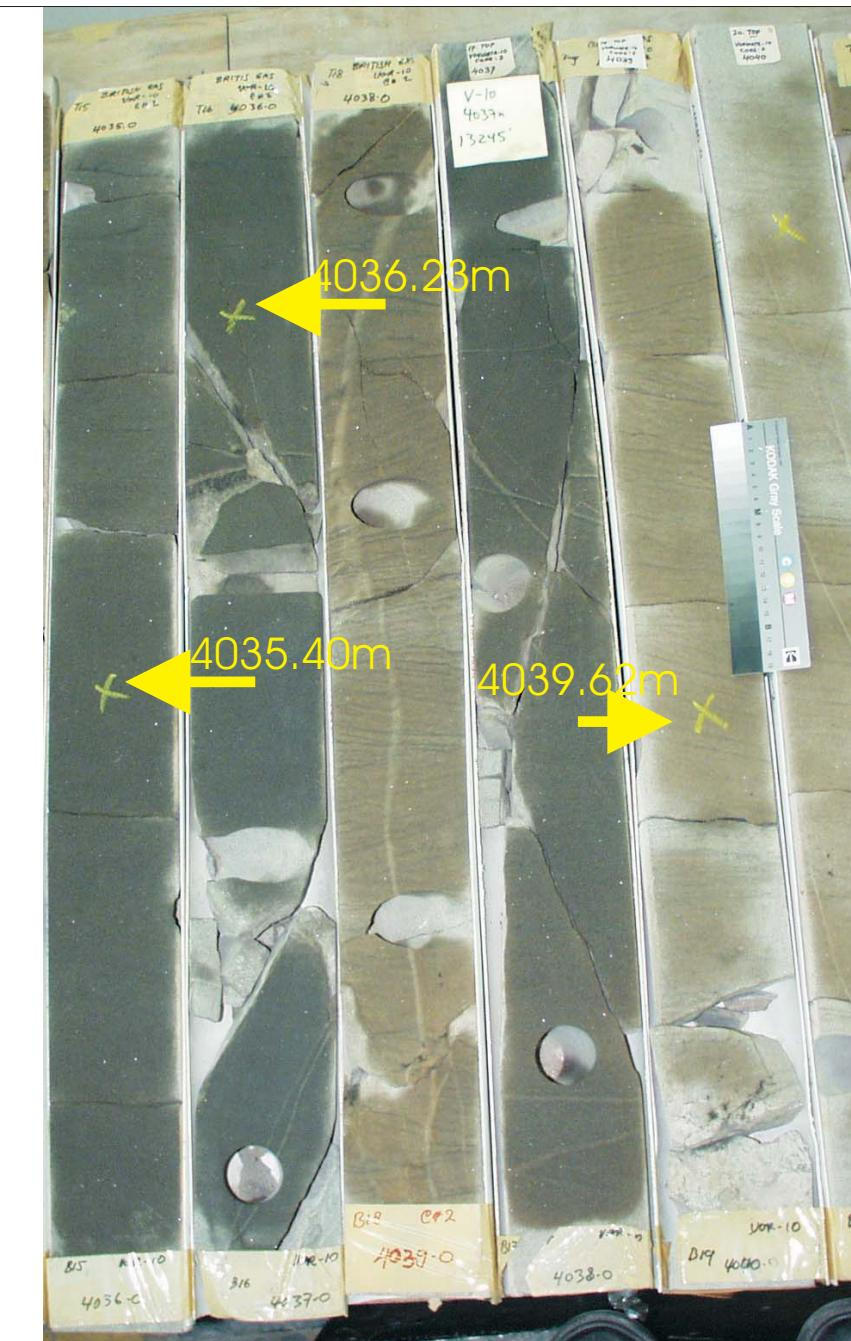
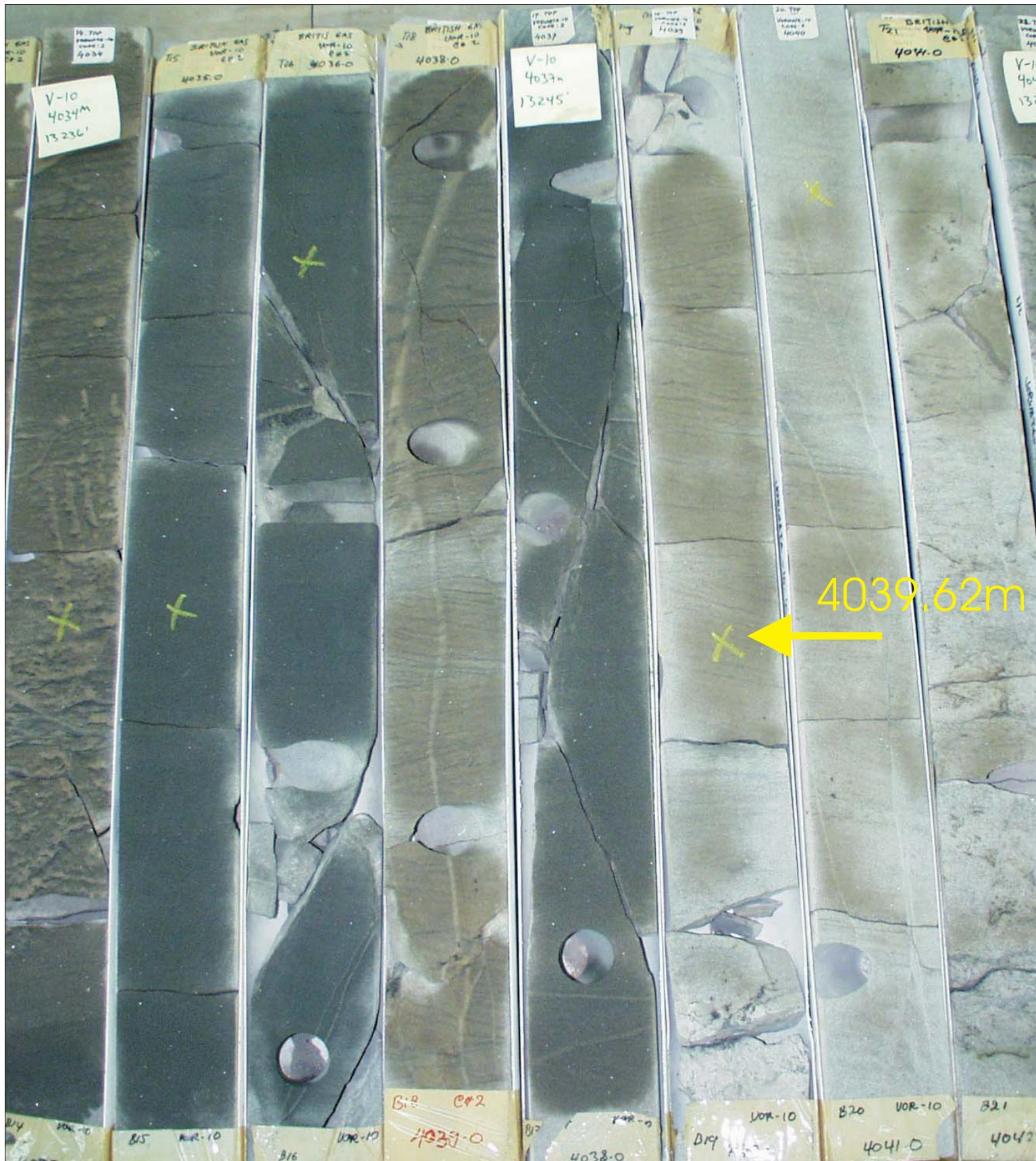
Sample Depth: 4036.23 m
 Shifted Depth: 13242.9 ft
 He-Ø: 12.9%
 k air: 298 mD (NOB 800 psia)

WHOLE CORE PLUG ANALYSES
WELL: VORWATA - 10st
DEPTH: 4036.23 m

PLATE A:

Digital Whole Core Photographs
 Digital Core Chip/Plug Photograph

Figure 71A: Core Plug/Chip Atlas for sample 4036.23m from Vorwata-10.

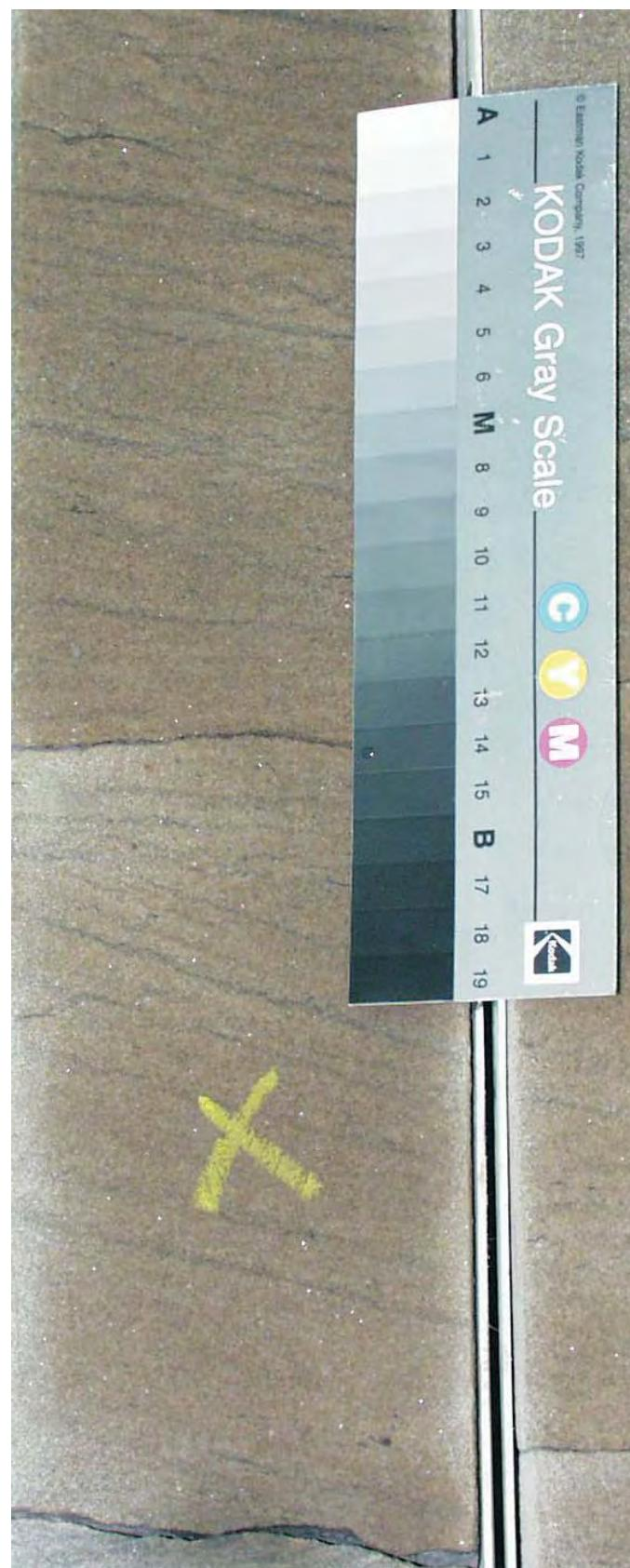


WHOLE CORE PLUG ANALYSES
WELL: VORWATA - 10st
DEPTH: 4039.62 m

PLATE A:

Digital Whole Core Photographs

Figure 72A: Core Plug/Chip Atlas for sample 4039.62m from Vorwata-10.



Sample Depth: 4039.62 m
Shifted Depth: 13254.0 ft
He-Ø: 13.47%
k air: 339.6 mD (NOB 800 psia)

WHOLE CORE PLUG ANALYSES

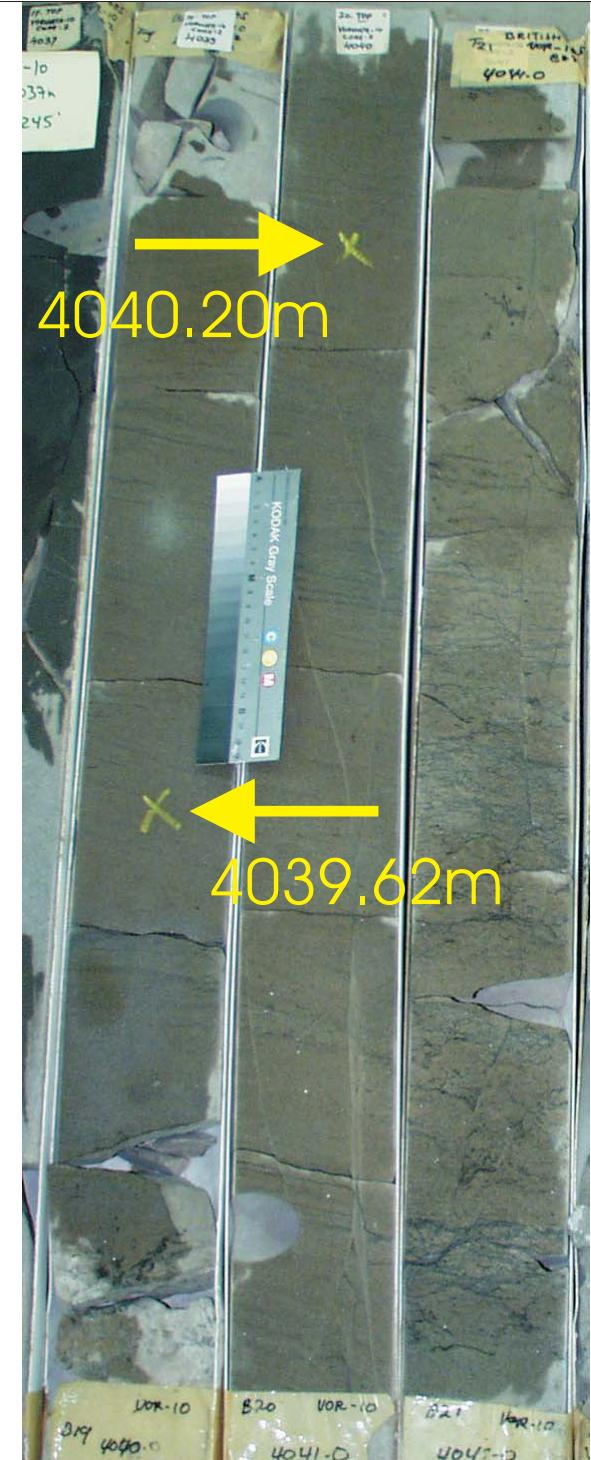
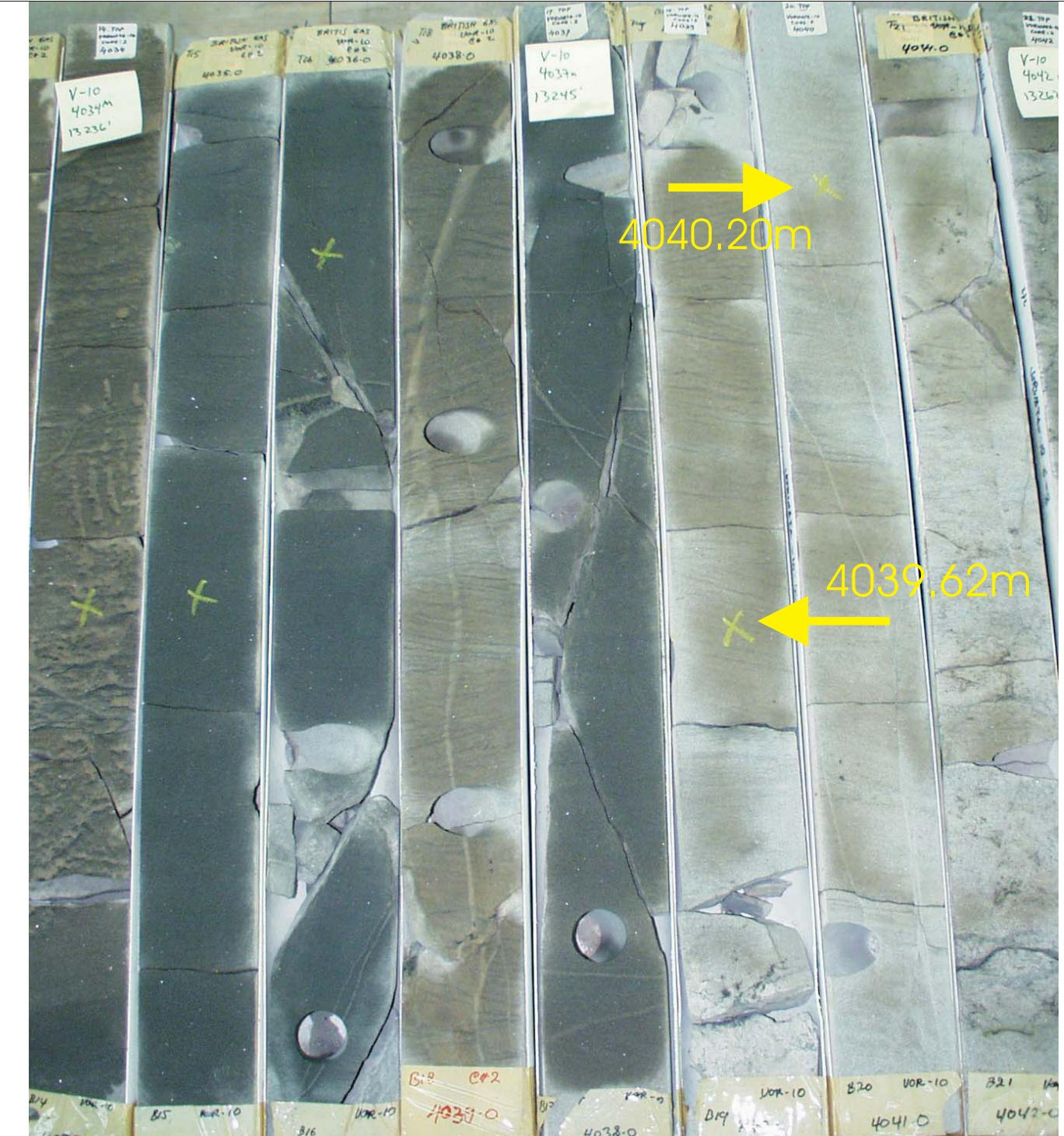
WELL: VORWATA - 10st

DEPTH: 4039.62 m

PLATE B:

Digital Whole Core Photographs
Digital Core Chip/Plug Photograph

Figure 72B: Core Plug/Chip Atlas for sample 4039.62m from Vorwata-10.

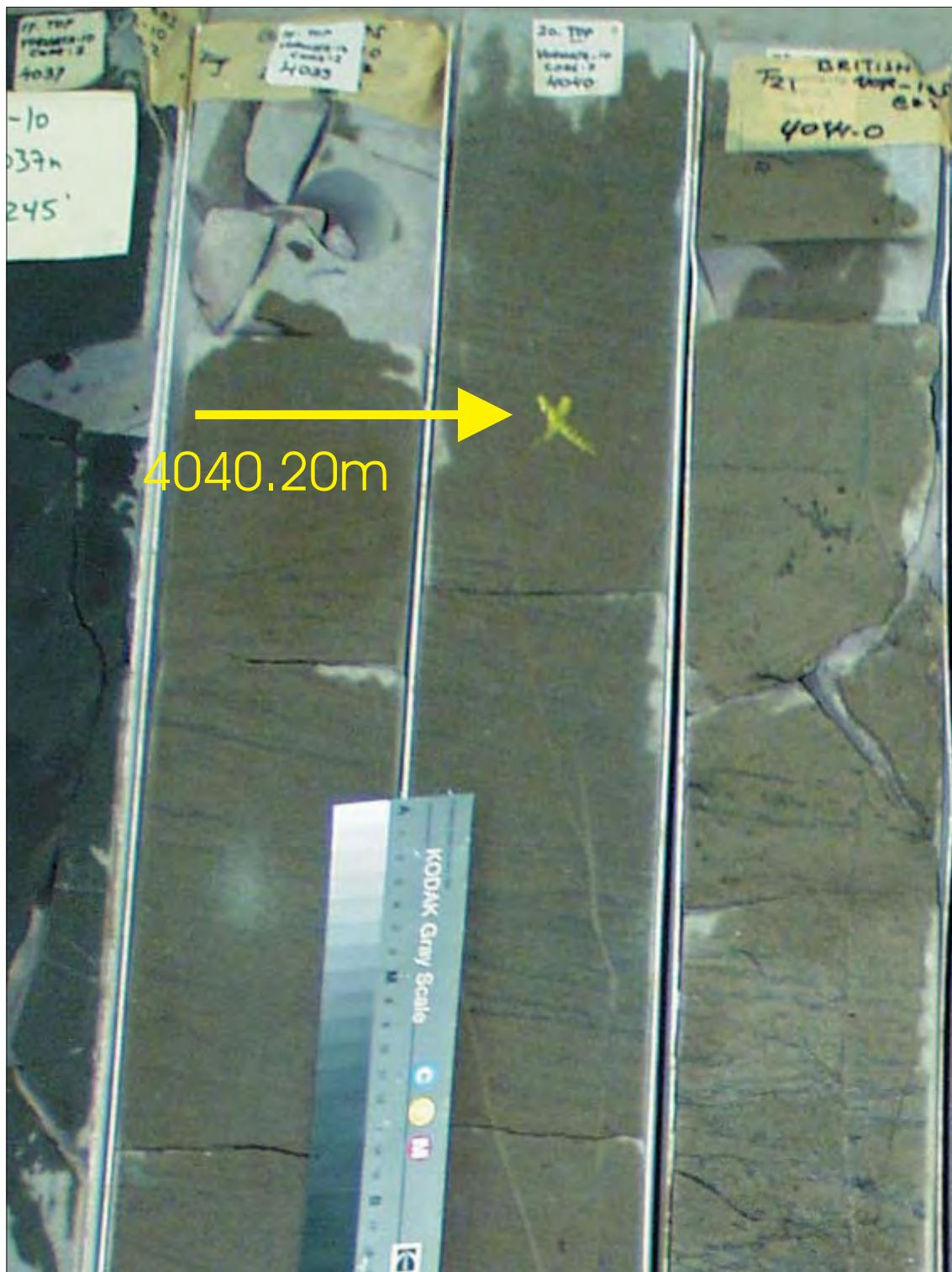


WHOLE CORE PLUG ANALYSES
WELL: VORWATA - 10st
DEPTH: 4040.20 m

PLATE A:

Digital Whole Core Photographs

Figure 73A: Core Plug/Chip Atlas for sample 4040.20m from Vorwata-10.



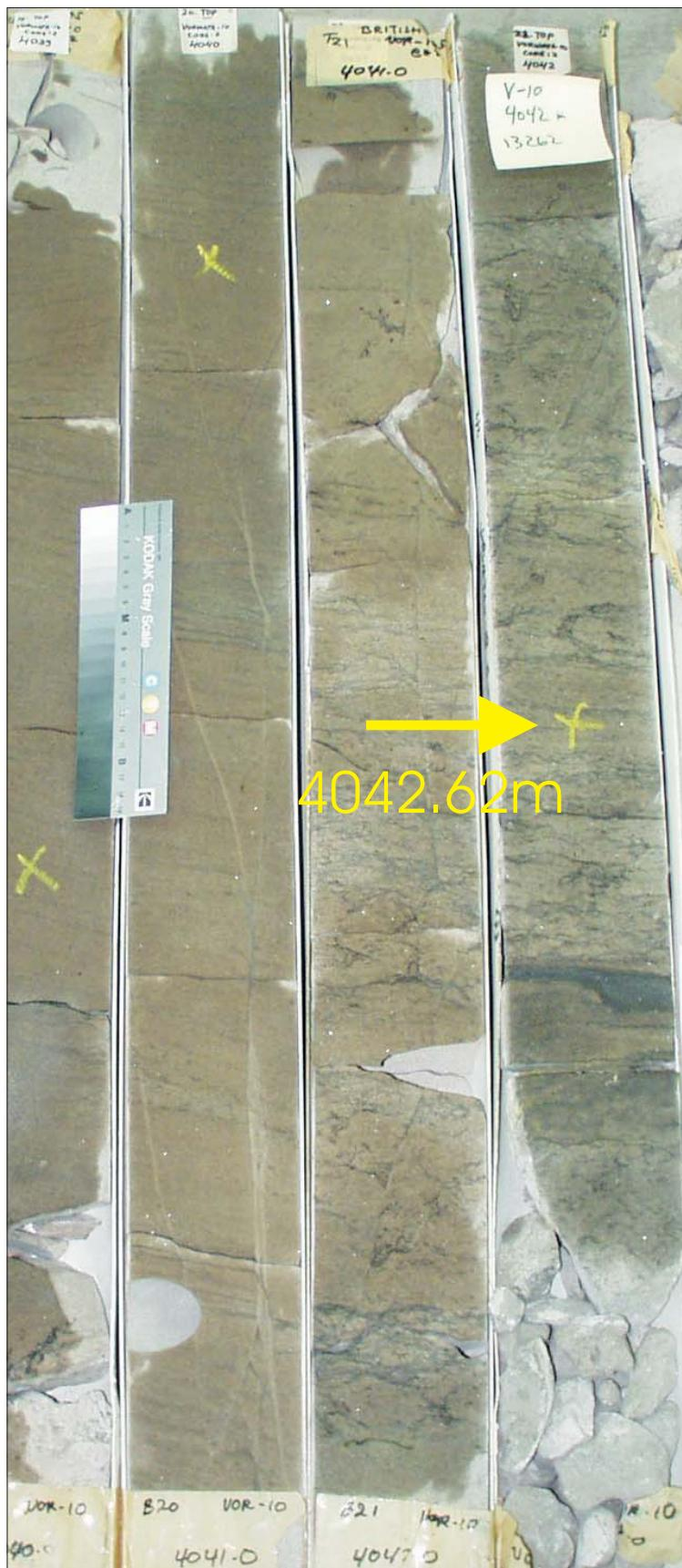
Sample Depth: 4040.20 m
Shifted Depth: 13255.9 ft
He-Ø: 14.06%
k air: 239.7 mD (sc)

Figure 73B: Core Plug/Chip Atlas for sample 4040.20m from Vorwata-10.

WHOLE CORE PLUG ANALYSES
WELL: VORWATA - 10st
DEPTH: 4040.20 m

PLATE B:

Digital Whole Core Photographs
Digital Core Chip/Plug Photograph



WHOLE CORE PLUG ANALYSES
WELL: VORWATA - 10st
DEPTH: 4042.62 m

PLATE A:

Digital Whole Core Photographs

Figure 74A: Core Plug/Chip Atlas for sample 4042.62m from Vorwata-10.



Sample Depth: 4042.62 m
Shifted Depth: 13263.8 ft
He-Ø: 12.42%
k air: 73.4 mD (NOB 800 psia)

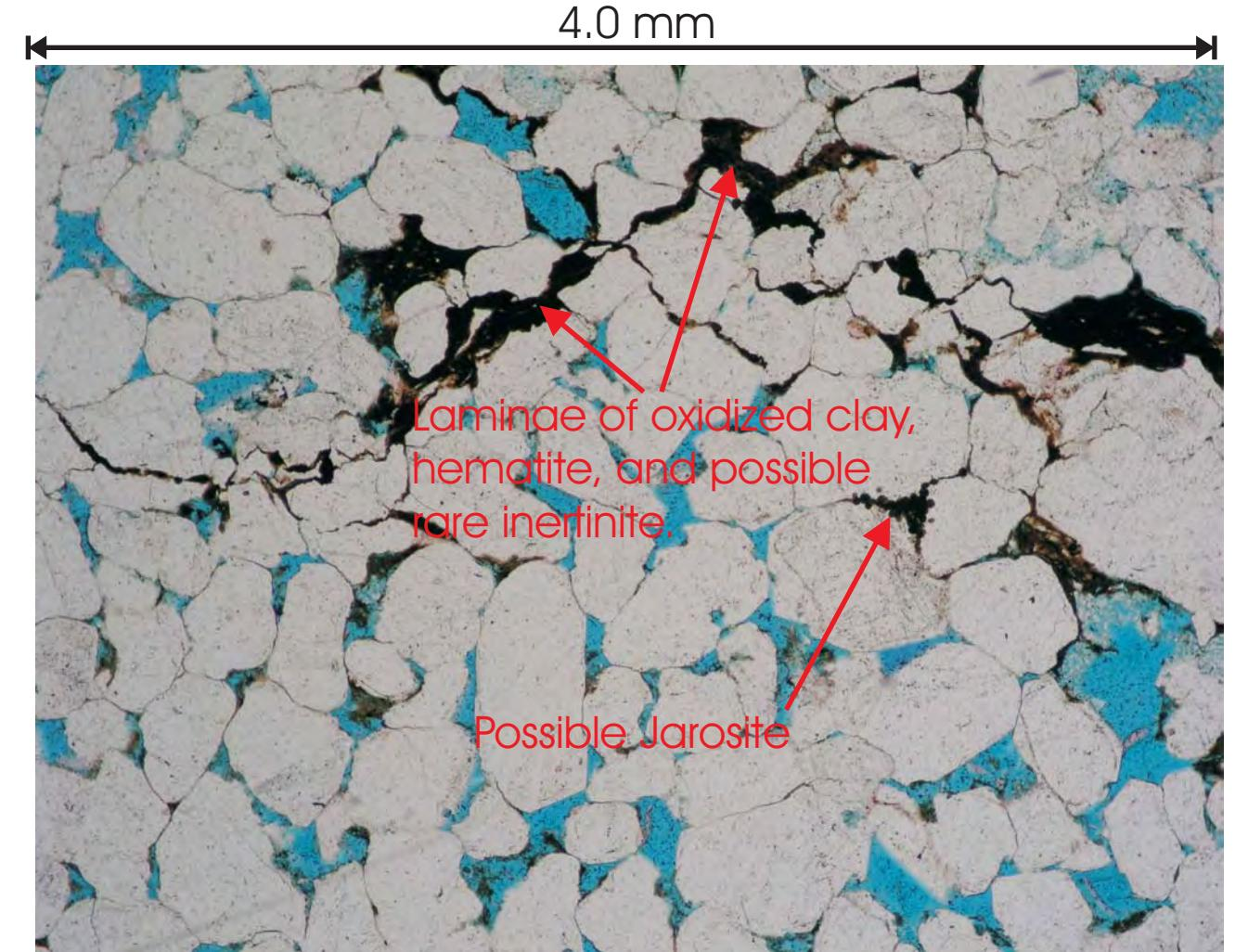
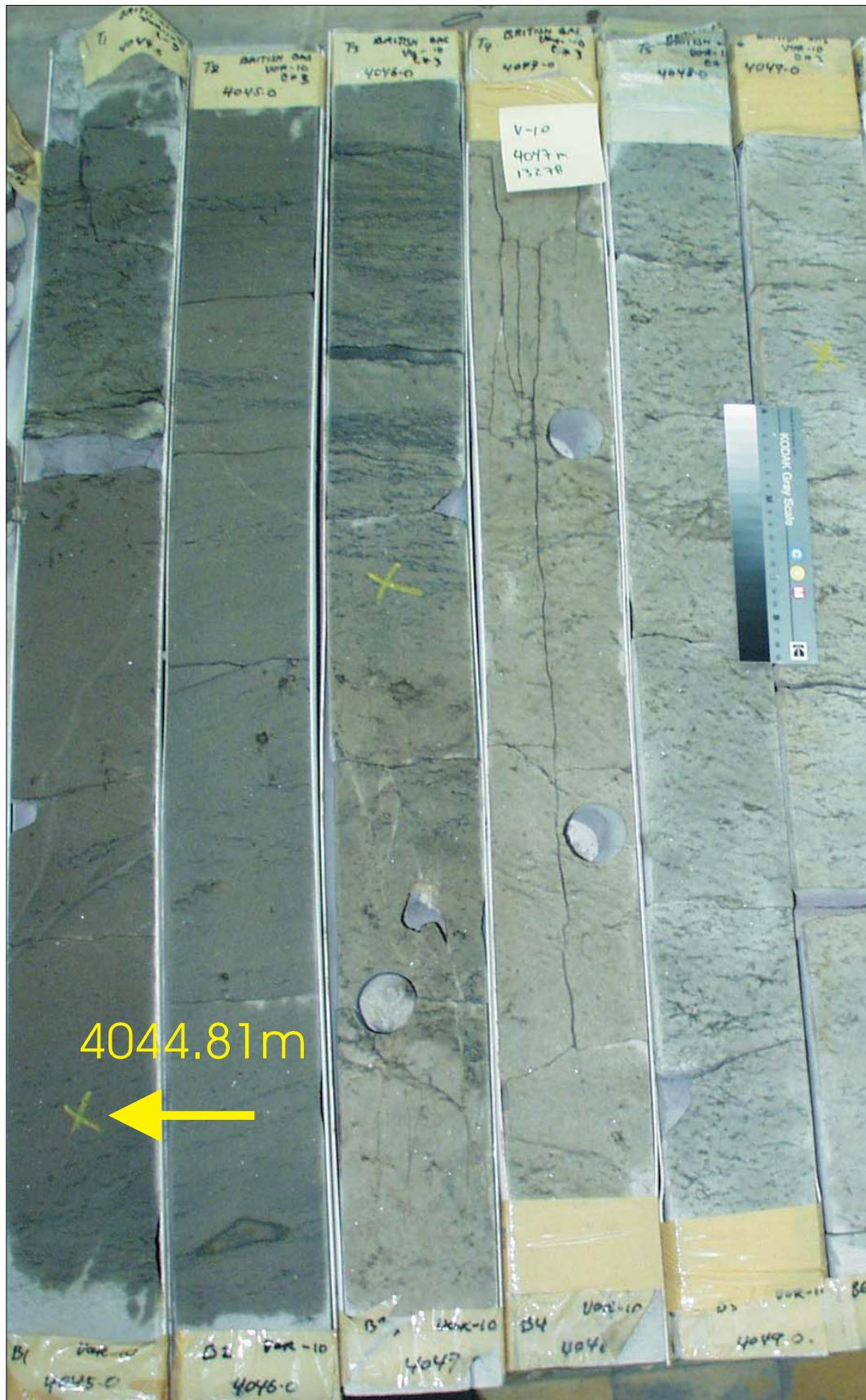


Figure 74B: Core Plug/Chip Atlas for sample 4042.62m from Vorwata-10.

WHOLE CORE PLUG ANALYSES
WELL: VORWATA - 10st
DEPTH: 4042.62 m

PLATE B:
Digital Whole Core Photographs
Digital Core Chip/Plug Photograph
Petrographic Photomicrograph

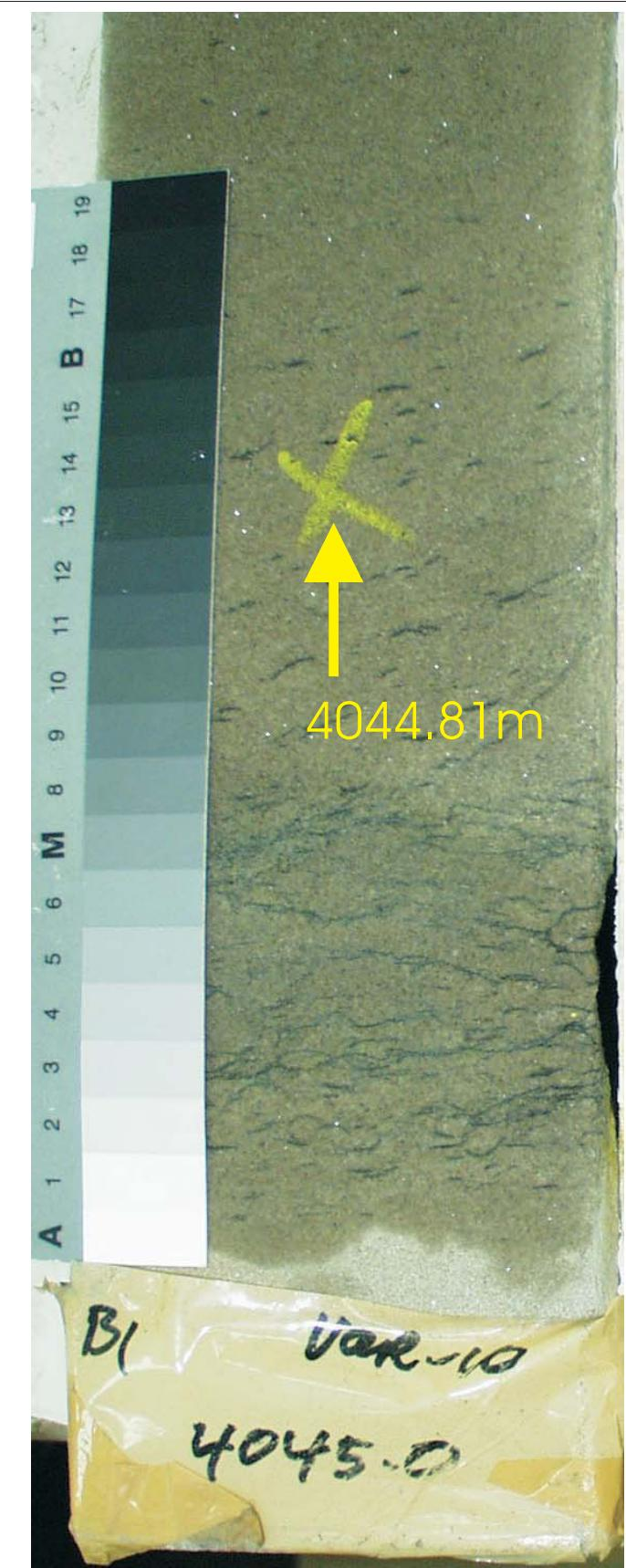


WHOLE CORE PLUG ANALYSES
WELL: VORWATA - 10st
DEPTH: 4044.81 m

PLATE A:

Digital Whole Core Photographs

Figure 75A: Core Plug/Chip Atlas for sample 4044.81m from Vorwata-10.



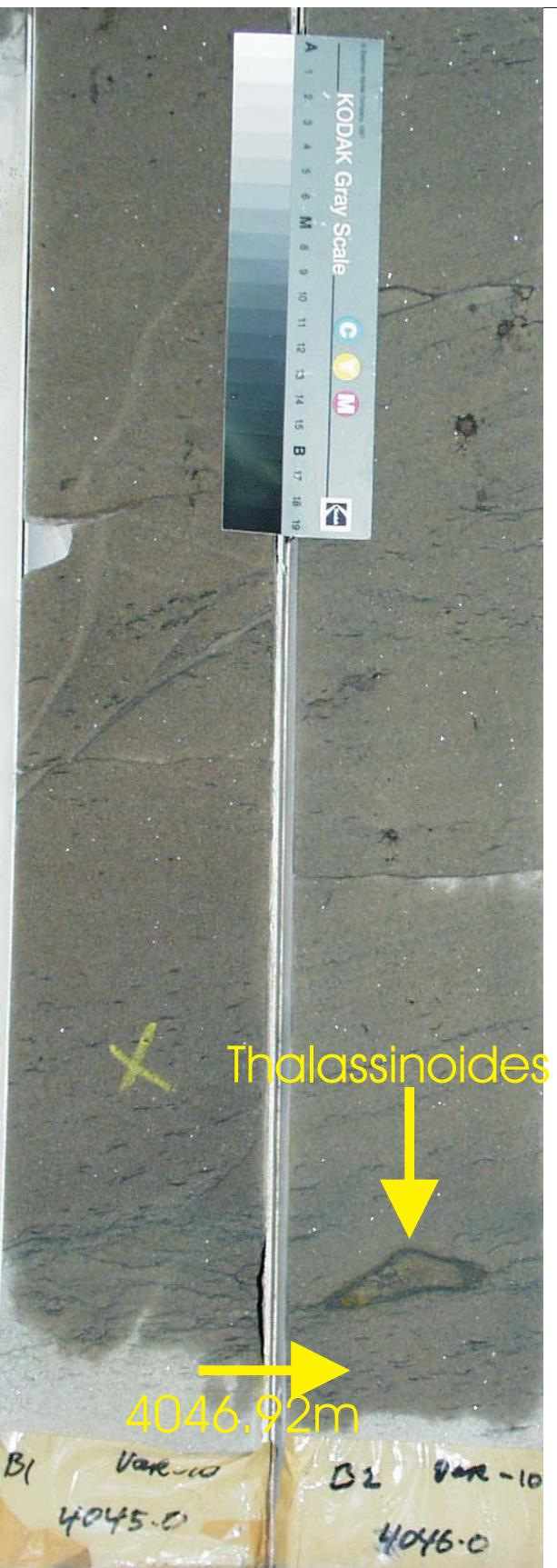
Sample Depth: 4044.81 m
Shifted Depth: 13271.0 ft
He-∅: 14.5%
k air: 545 mD (NOB 800 psia)

WHOLE CORE PLUG ANALYSES
WELL: VORWATA - 10st
DEPTH: 4044.81 m

PLATE B:

Digital Whole Core Photographs
Digital Core Chip/Plug Photograph

Figure 75B: Core Plug/Chip Atlas for sample 4044.81m from Vorwata-10.

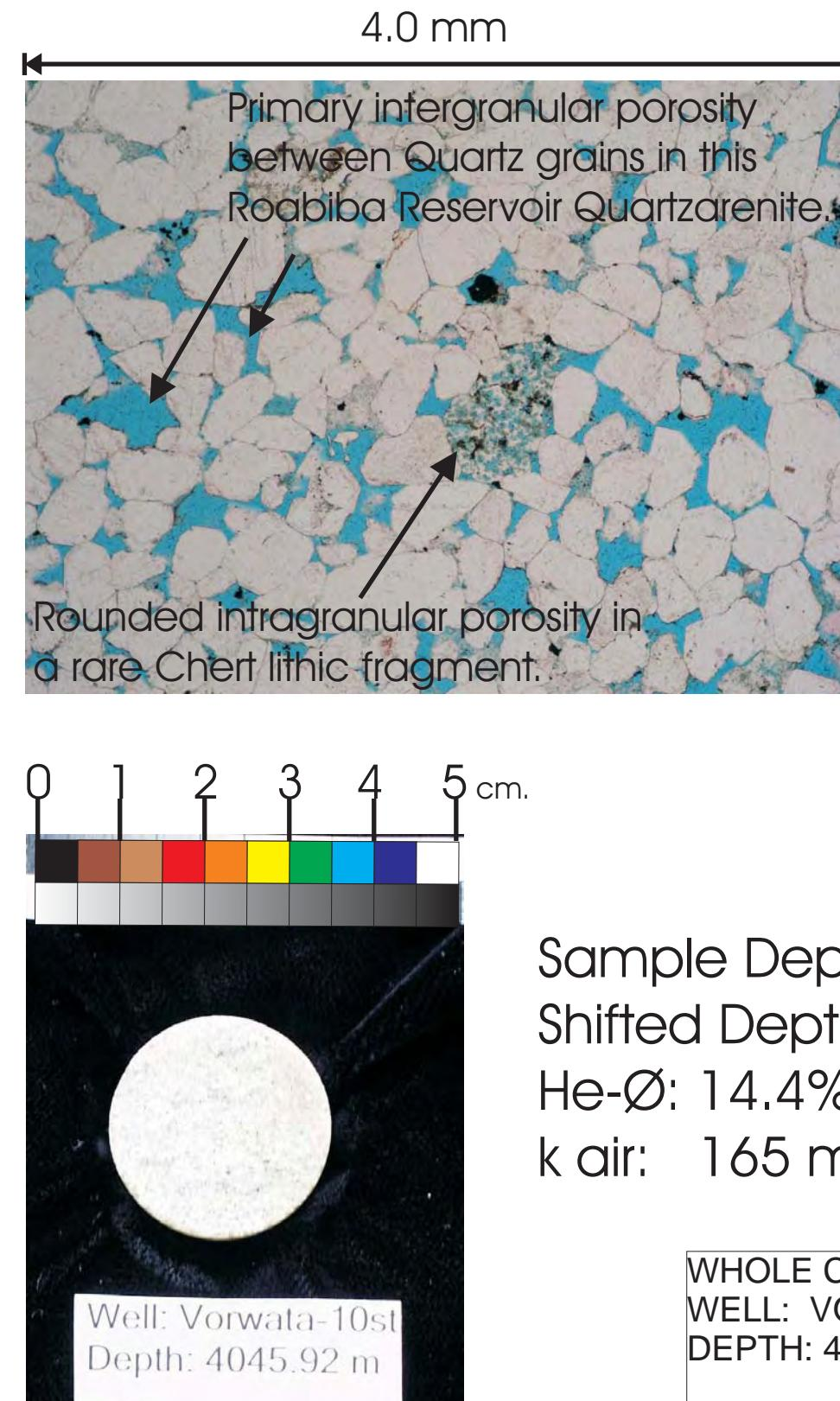
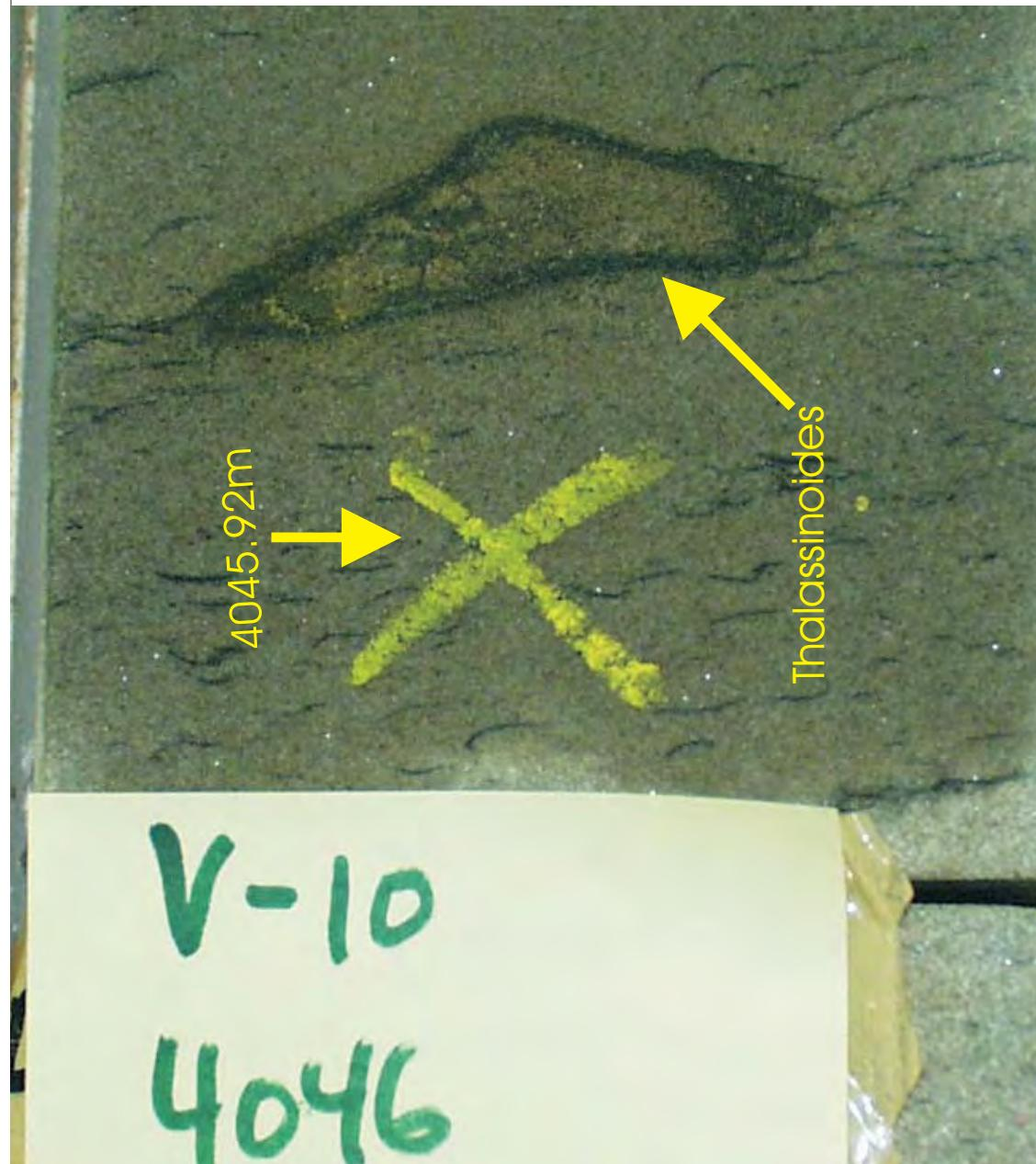


WHOLE CORE PLUG ANALYSES
WELL: VORWATA - 10st
DEPTH: 4045.92 m

PLATE A:

Digital Whole Core Photographs

Figure 76A: Core Plug/Chip Atlas for sample 4045.92m from Vorwata-10.



Sample Depth: 4045.92 m
Shifted Depth: 13274.7ft
He-∅: 14.4%
k air: 165 mD (NOB 800 psia)

WHOLE CORE PLUG ANALYSES

WELL: VORWATA - 10st

DEPTH: 4045.92 m

PLATE B:

Digital Whole Core Photographs
Digital Core Chip/Plug Photograph
Petrographic Photomicrograph

Figure 76B: Core Plug/Chip Atlas for sample 4045.92m from Vorwata-10.

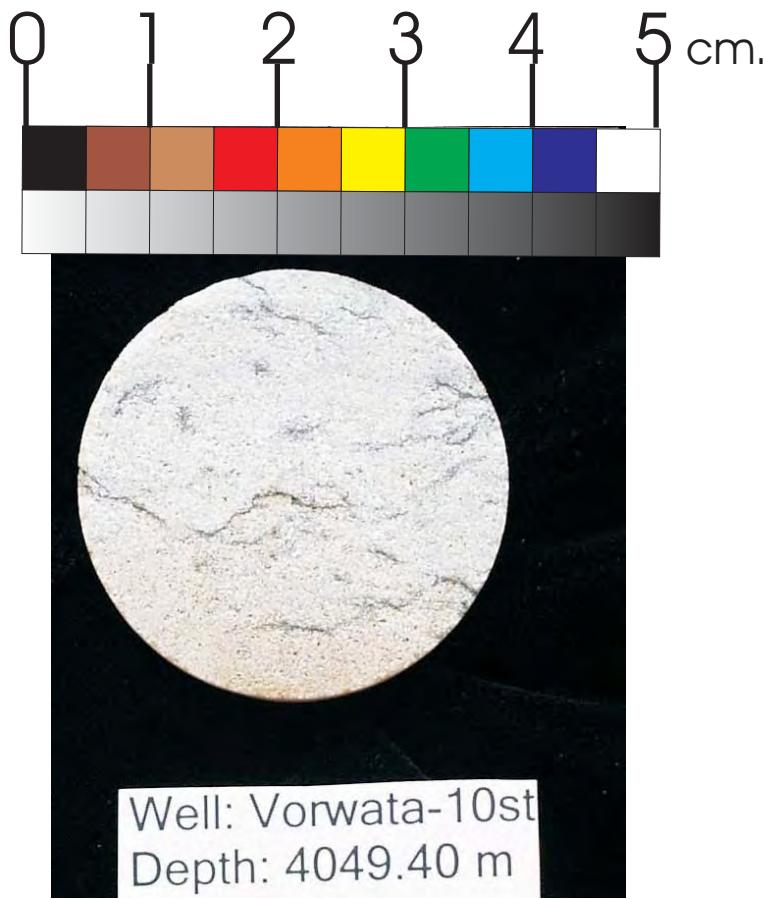


WHOLE CORE PLUG ANALYSES
WELL: VORWATA - 10st
DEPTH: 4049.40 m

PLATE A:

Digital Whole Core Photographs

Figure 77A: Core Plug/Chip Atlas for sample 4049.40m from Vorwata-10.



Sample Depth: 4049.40 m
Shifted Depth: 13286.1 ft
He-∅: 10.33%
k air: 26.75 mD (sc)

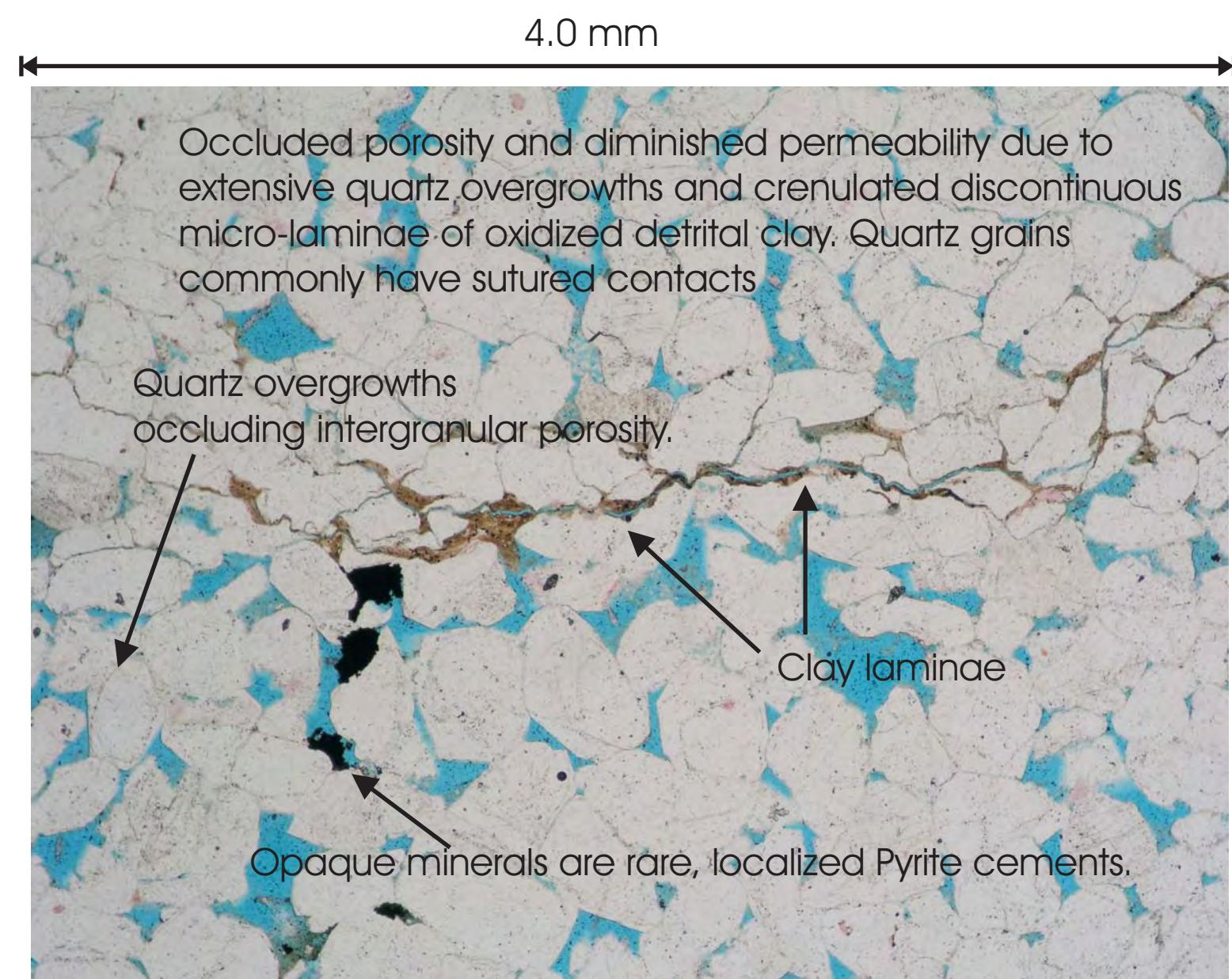


Figure 77B: Core Plug/Chip Atlas for sample 4049.40m from Vorwata-10.

WHOLE CORE PLUG ANALYSES

WELL: VORWATA - 10st

DEPTH: 4045.92 m

PLATE B:

Digital Core Chip/Plug Photograph
Petrographic Photomicrograph

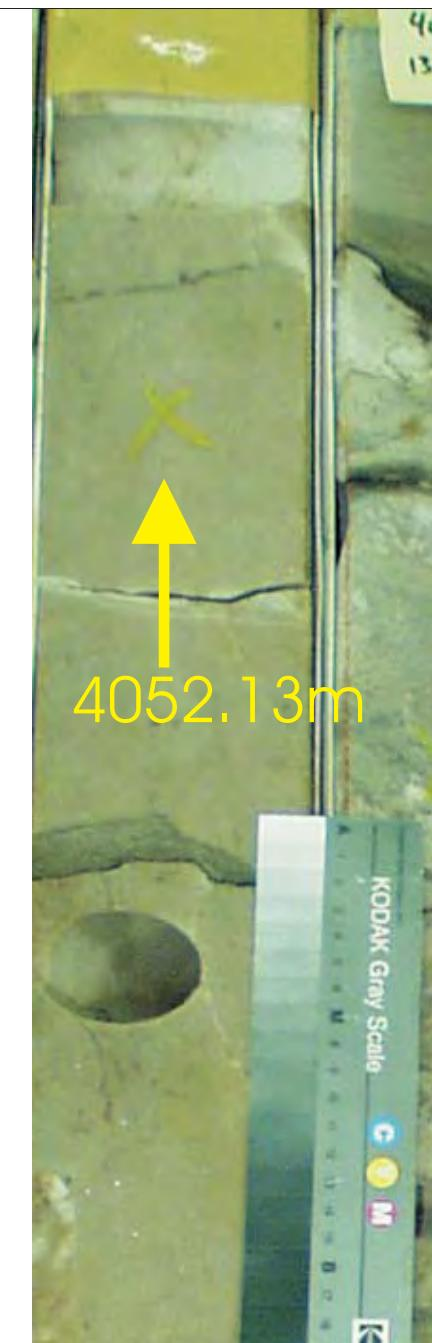
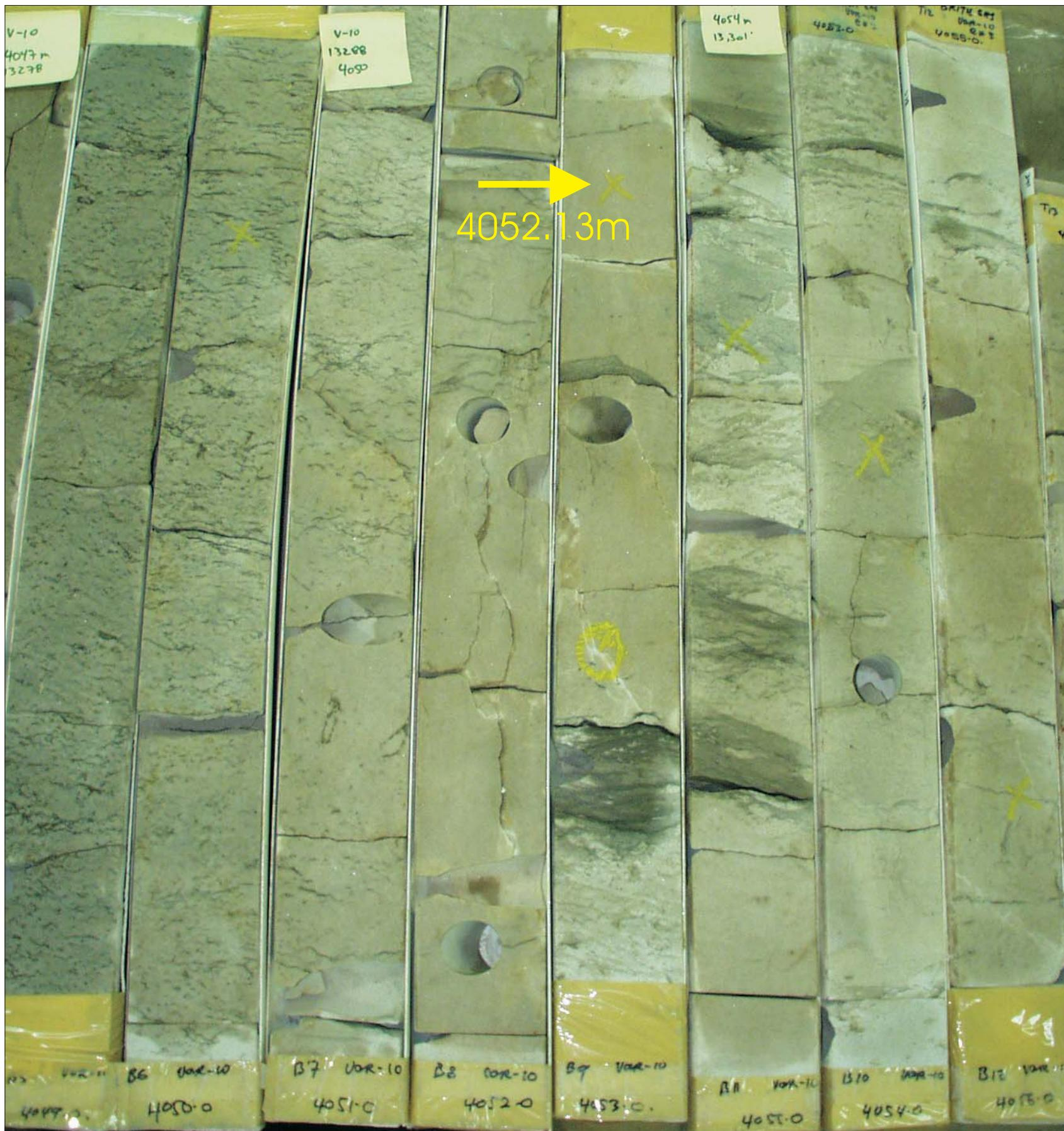


Figure 78A: Core Plug/Chip Atlas for sample 4052.13m from Vorwata-10.

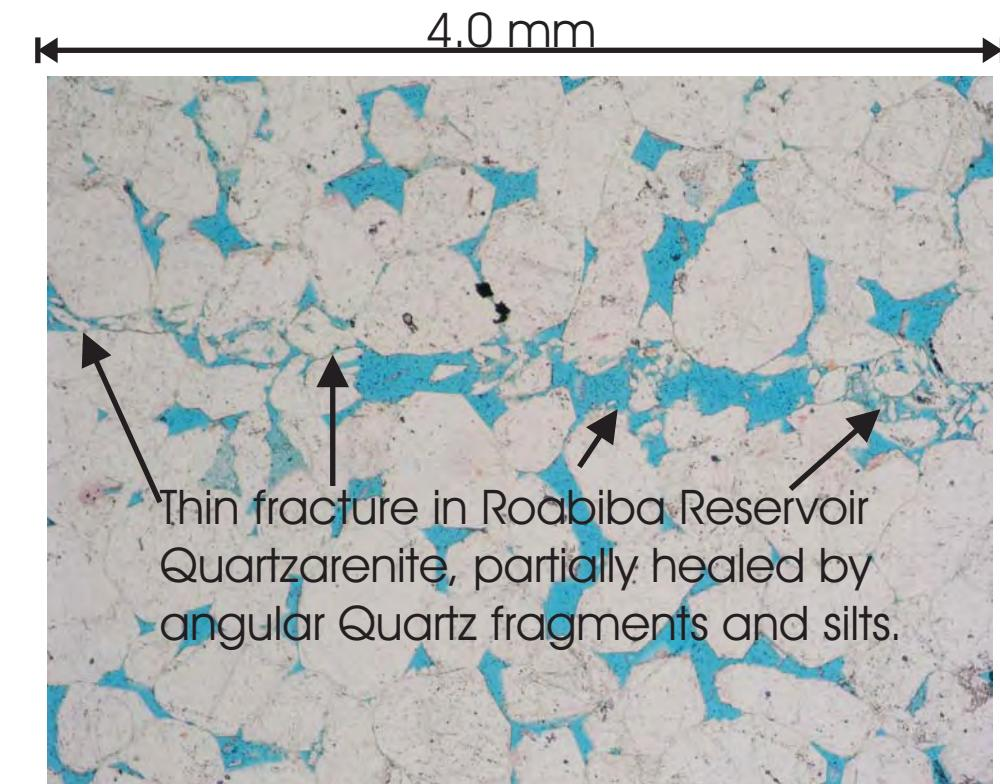
WHOLE CORE PLUG ANALYSES

WELL: VORWATA - 10st

DEPTH: 4052.13 m

PLATE A:

Digital Whole Core Photographs



Sample Depth: 4052.13 m
Shifted Depth: 13295.0 ft
He-Ø: 12.1%
k air: 673.94 mD (sc)

Figure 78B: Core Plug/Chip Atlas for sample 4052.13m from Vorwata-10.

WHOLE CORE PLUG ANALYSES

WELL: VORWATA - 10st

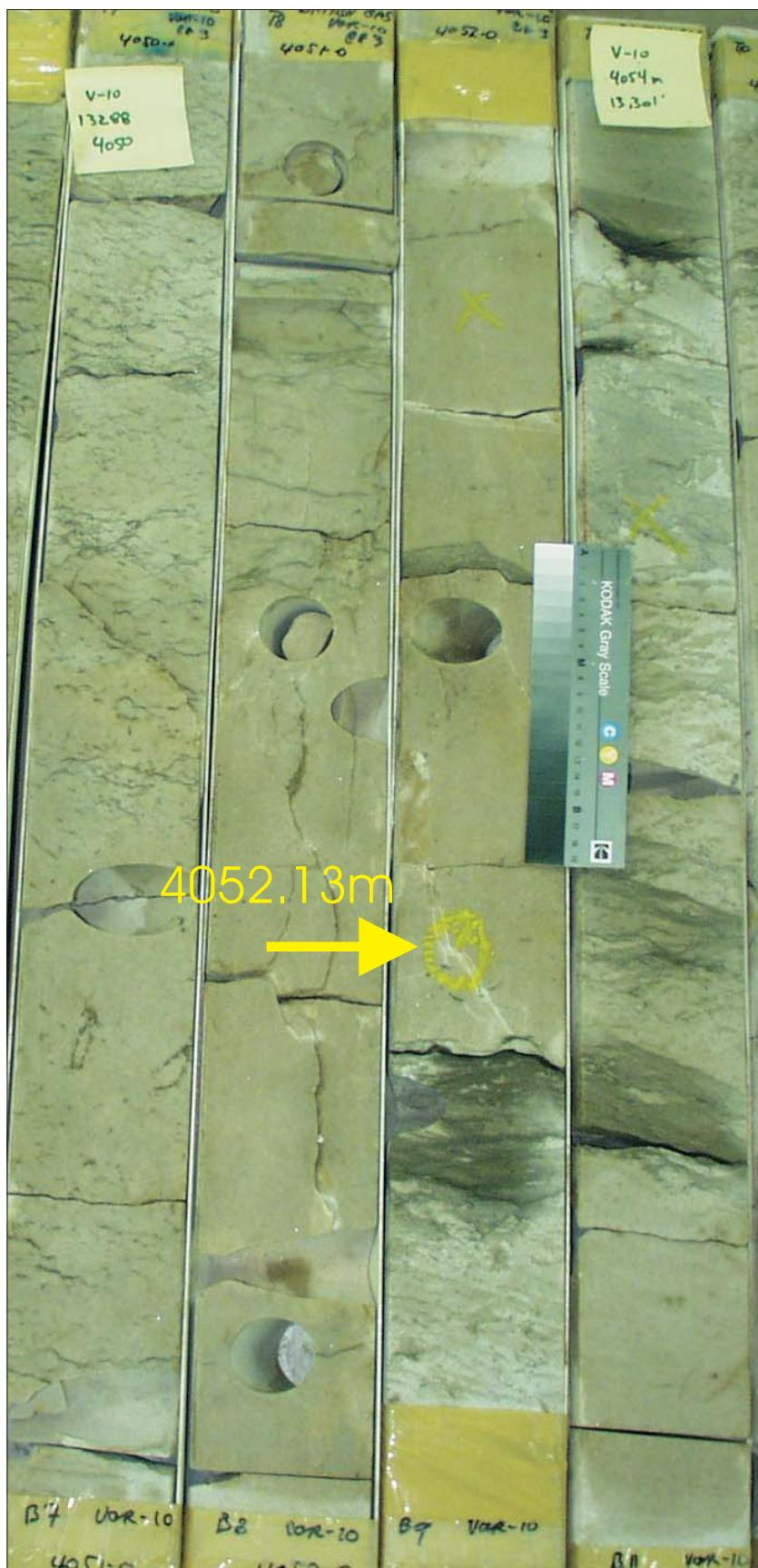
DEPTH: 4052.13 m

PLATE B:

Digital Whole Core Photographs

Digital Core Chip/Plug Photograph

Petrographic Photomicrograph

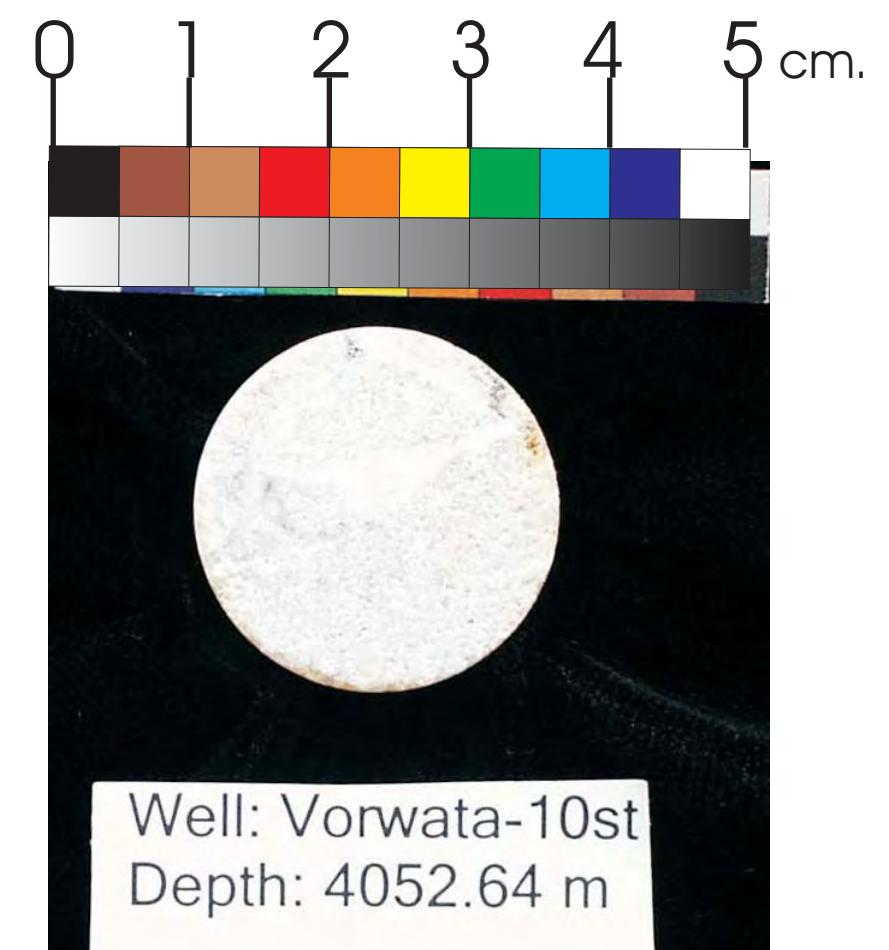
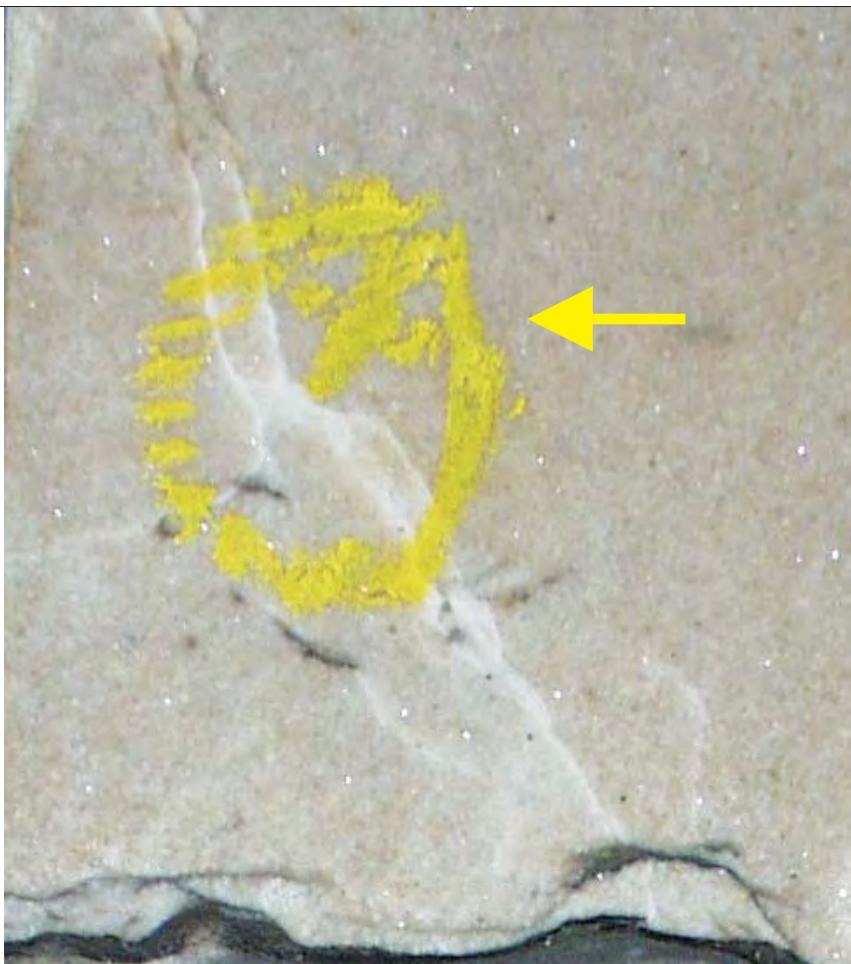


WHOLE CORE PLUG ANALYSES
WELL: VORWATA - 10st
DEPTH: 4052.64 m

PLATE A:

Digital Whole Core Photographs

Figure 79A: Core Plug/Chip Atlas for sample 4052.64m from Vorwata-10.



Sample Depth: 4052.64 m
Shifted Depth: 13295.2 ft
He-Ø: 11.3%
k air: 298 mD (NOB 800 psia)

Figure 79B: Core Plug/Chip Atlas for sample 4052.64m from Vorwata-10.

WHOLE CORE PLUG ANALYSES

WELL: VORWATA - 10st

DEPTH: 4052.64 m

PLATE B:

Digital Whole Core Photographs

Digital Core Chip/Plug Photograph



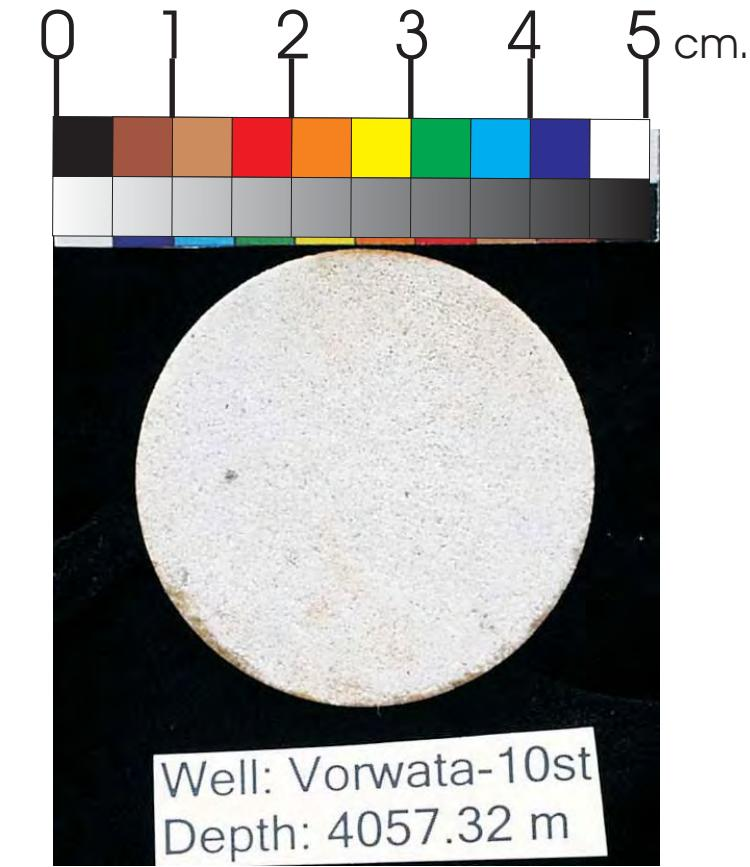
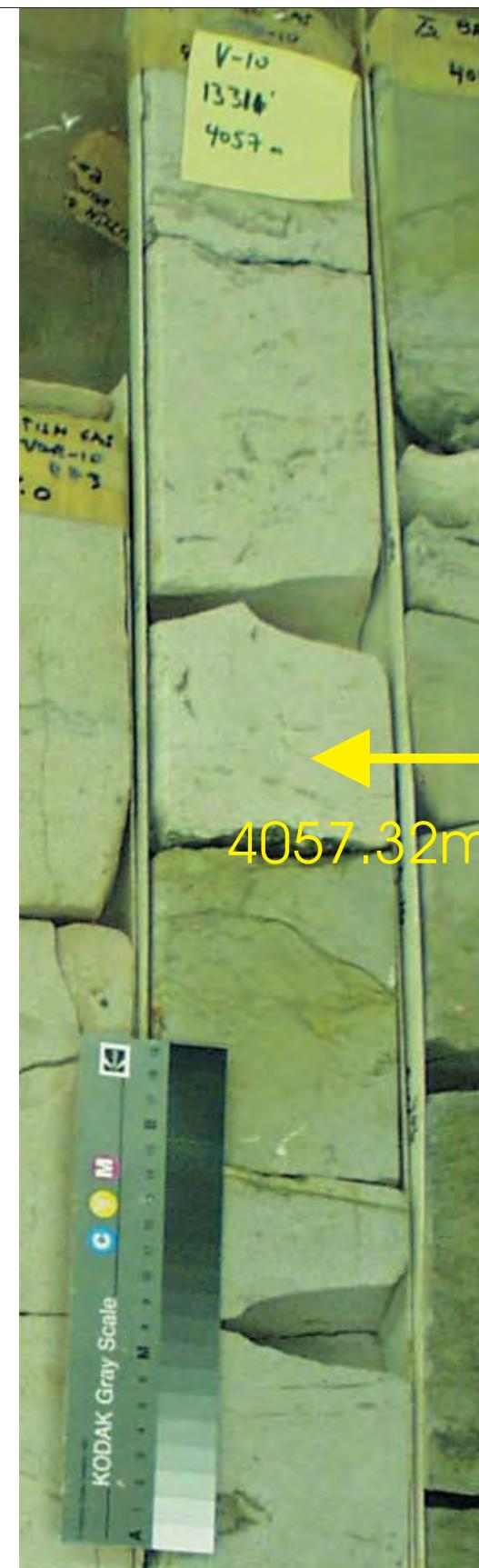
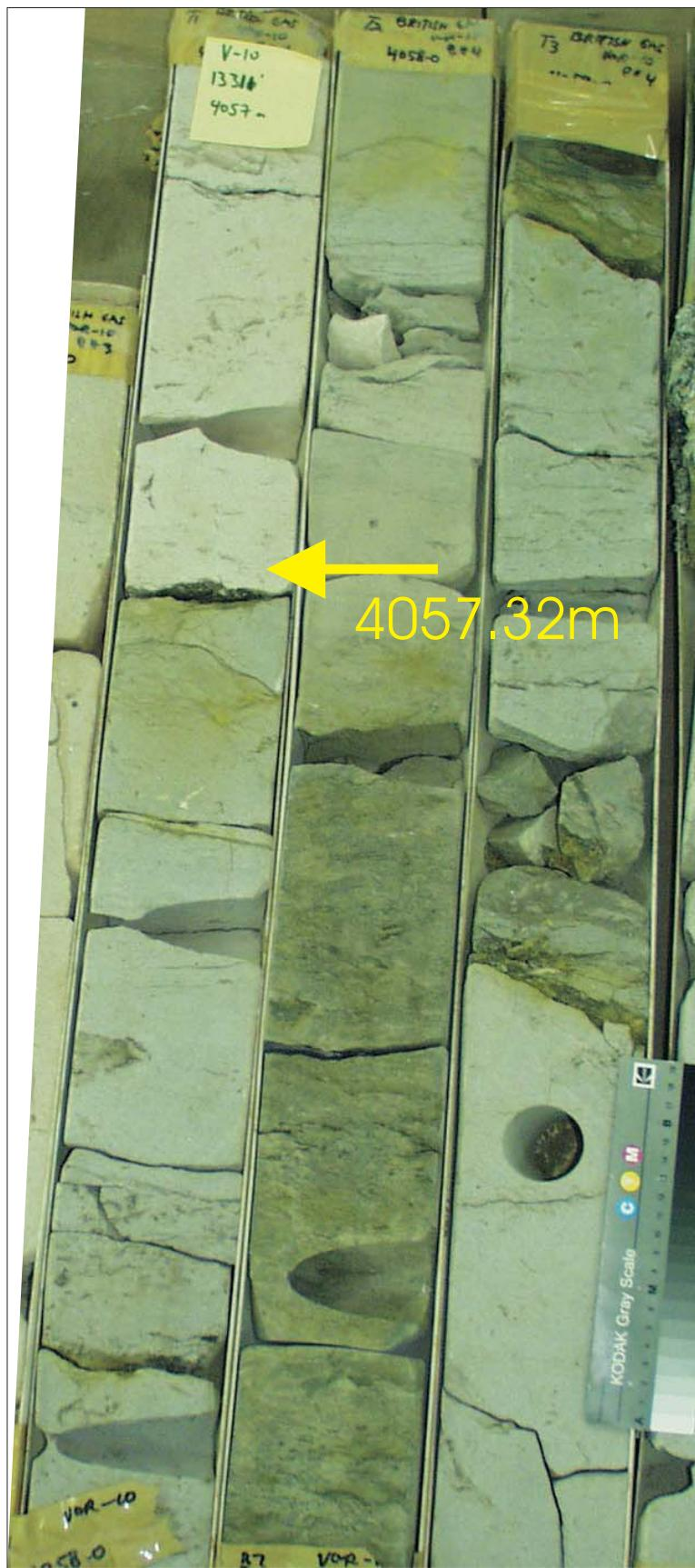
Sample Depth: 4056.02 m
Shifted Depth: 13307.8 ft
He-Ø: 17.1%
k air: 18.36D (sc)

WHOLE CORE PLUG ANALYSES
WELL: VORWATA - 10st
DEPTH: 4056.02 m

PLATE A:

Digital Whole Core Photographs
Digital Core Chip/Plug Photograph

Figure 80A: Core Plug/Chip Atlas for sample 4056.02m from Vorwata-10.



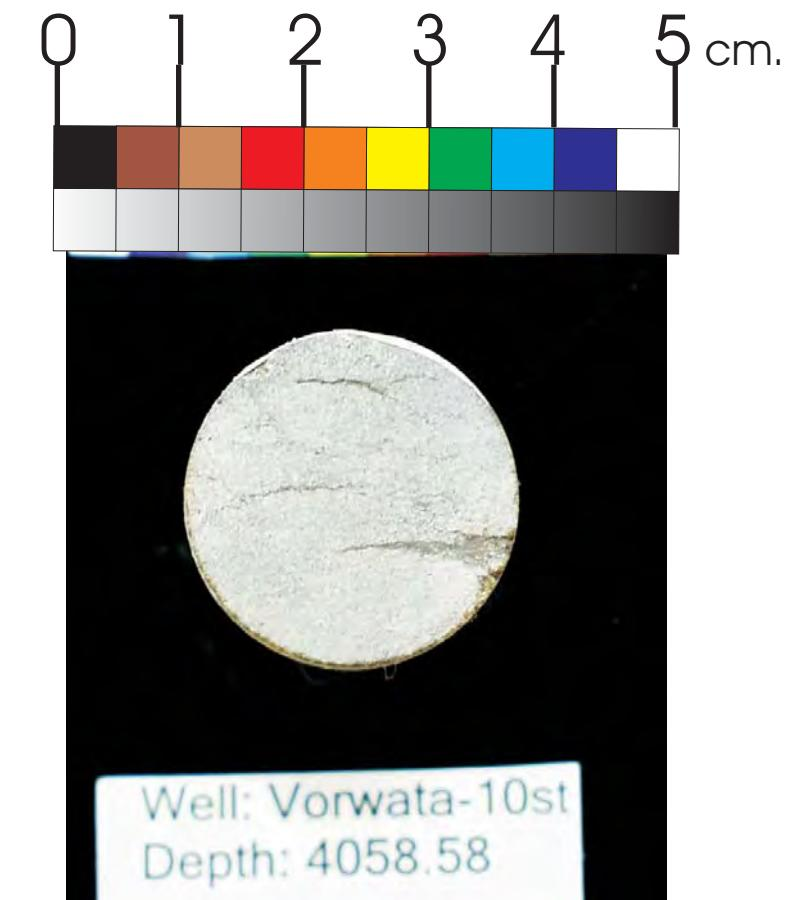
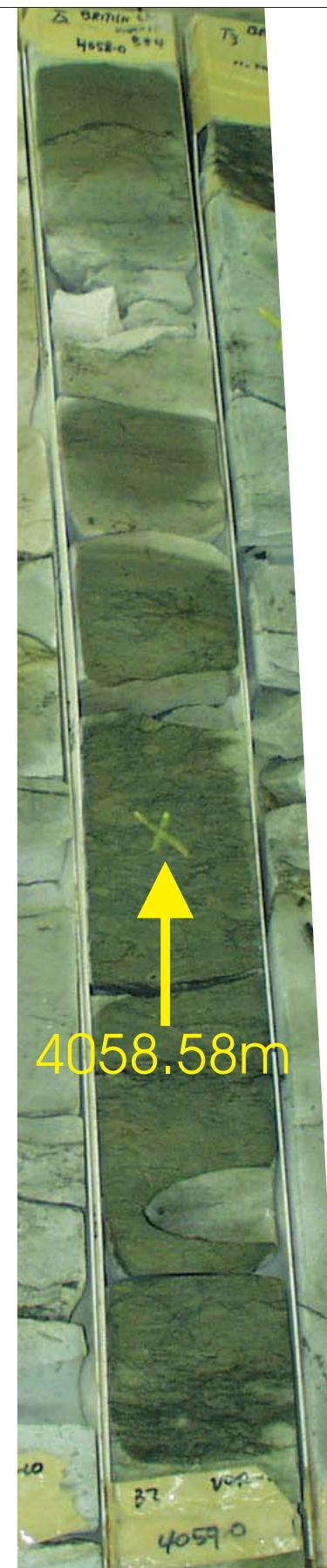
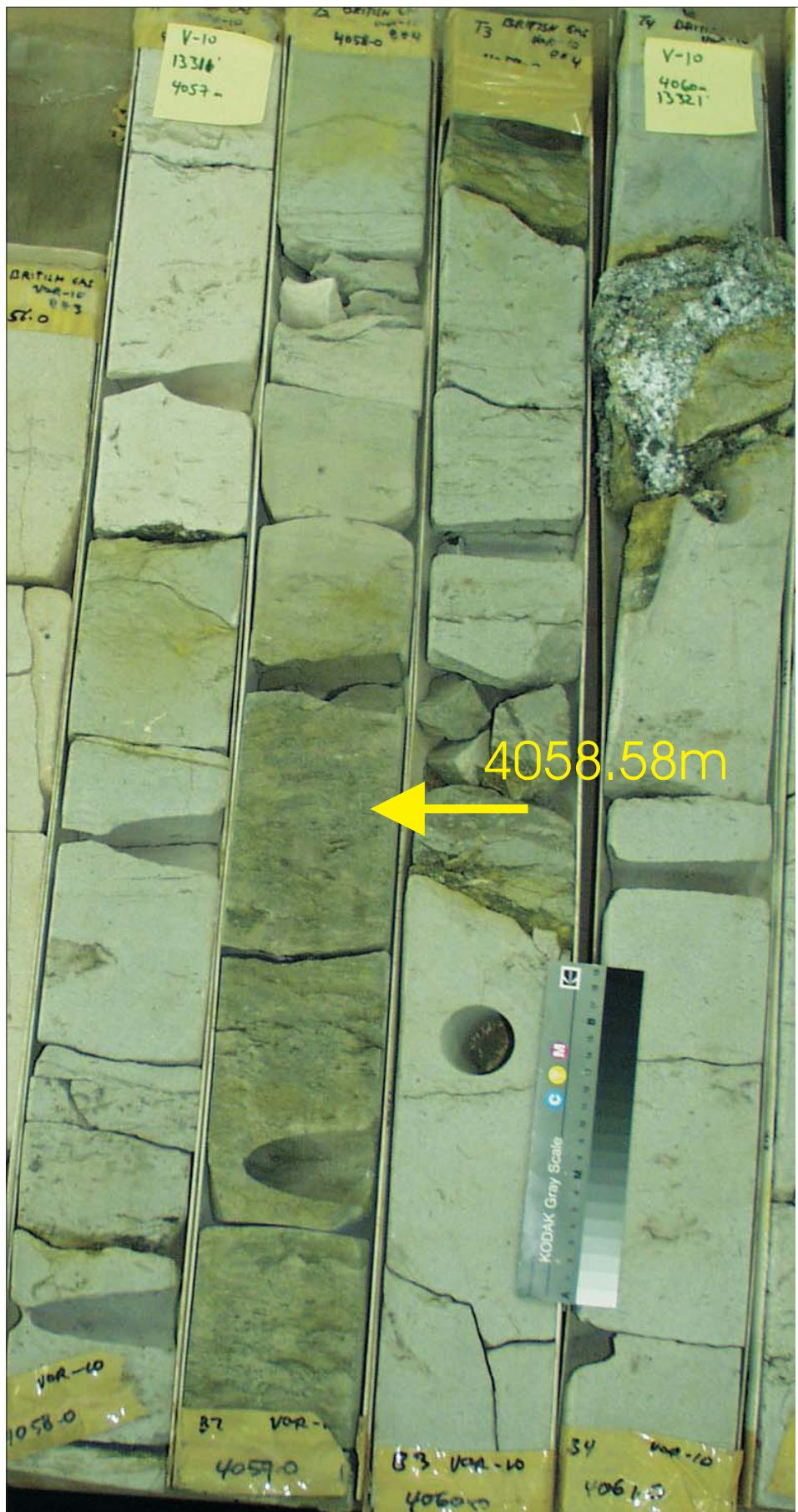
Sample Depth: 4057.32 m
Shifted Depth: 13312.1 ft
He-∅: 12.7%
k air: 14.06 mD (sc)

WHOLE CORE PLUG ANALYSES
WELL: VORWATA - 10st
DEPTH: 4057.32 m

PLATE A:

Digital Whole Core Photographs
Digital Core Chip/Plug Photograph

Figure 81A: Core Plug/Chip Atlas for sample 4057.32m from Vorwata-10.



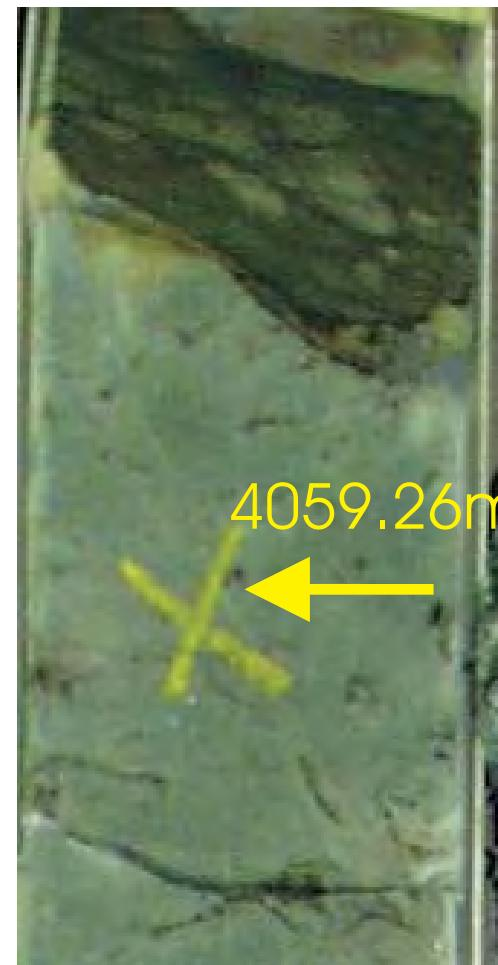
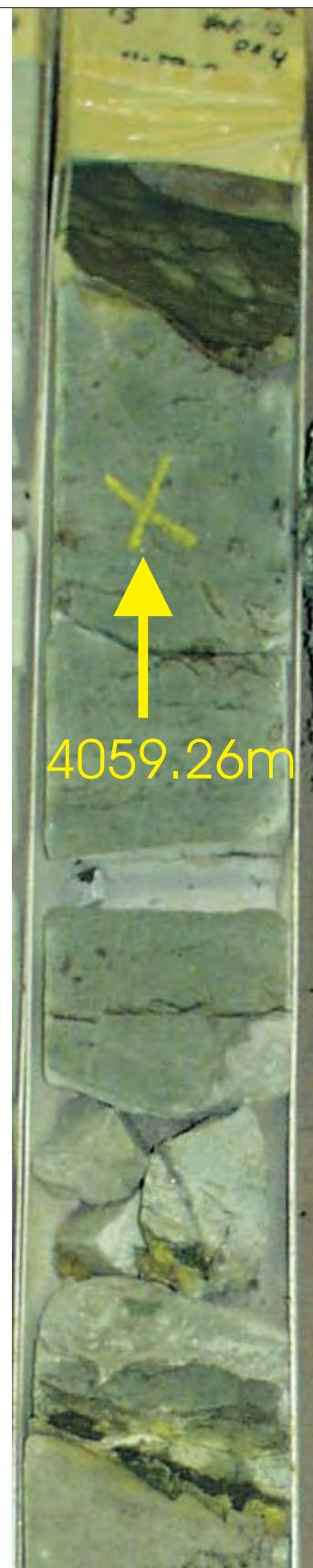
Sample Depth: 4058.58 m
 Shifted Depth: 13316.2 ft
 He-Ø: 6.7%
 k air: 0.18 mD (NOB 800 psia)

WHOLE CORE PLUG ANALYSES
 WELL: VORWATA - 10st
 DEPTH: 4058.58 m

PLATE A:

Digital Whole Core Photographs
 Digital Core Chip/Plug Photograph

Figure 82A: Core Plug/Chip Atlas for sample 4058.58m from Vorwata-10.



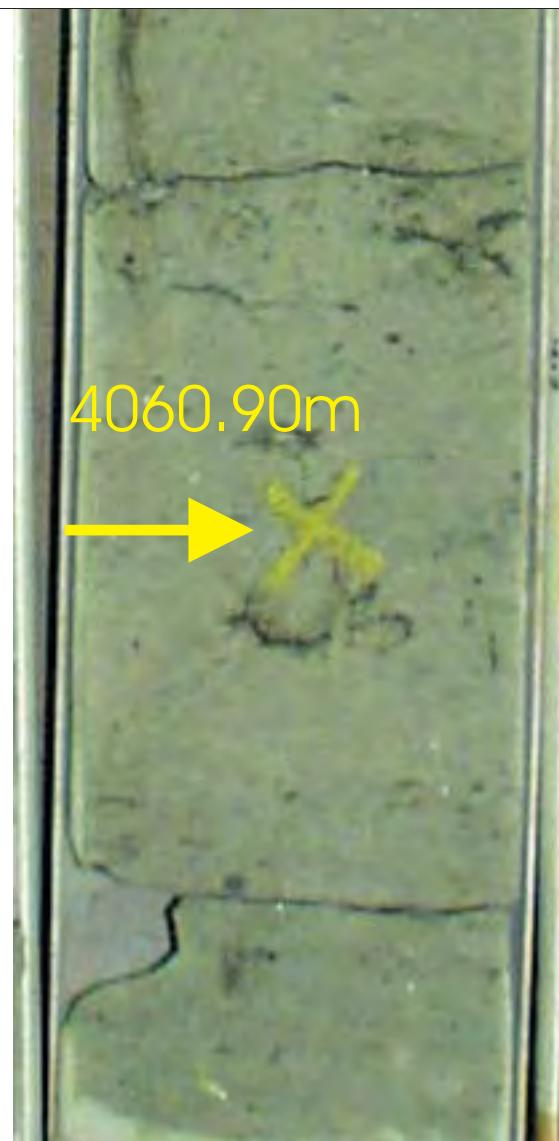
Sample Depth: 4059.26 m
Shifted Depth: 13318.4 ft
He-∅: 9.4%
k air: 4.59 mD (NOB 800 psia)

WHOLE CORE PLUG ANALYSES
WELL: VORWATA - 10st
DEPTH: 4059.26 m

PLATE A:

Digital Whole Core Photographs
Digital Core Chip/Plug Photograph

Figure 83A: Core Plug/Chip Atlas for sample 4059.26m from Vorwata-10.



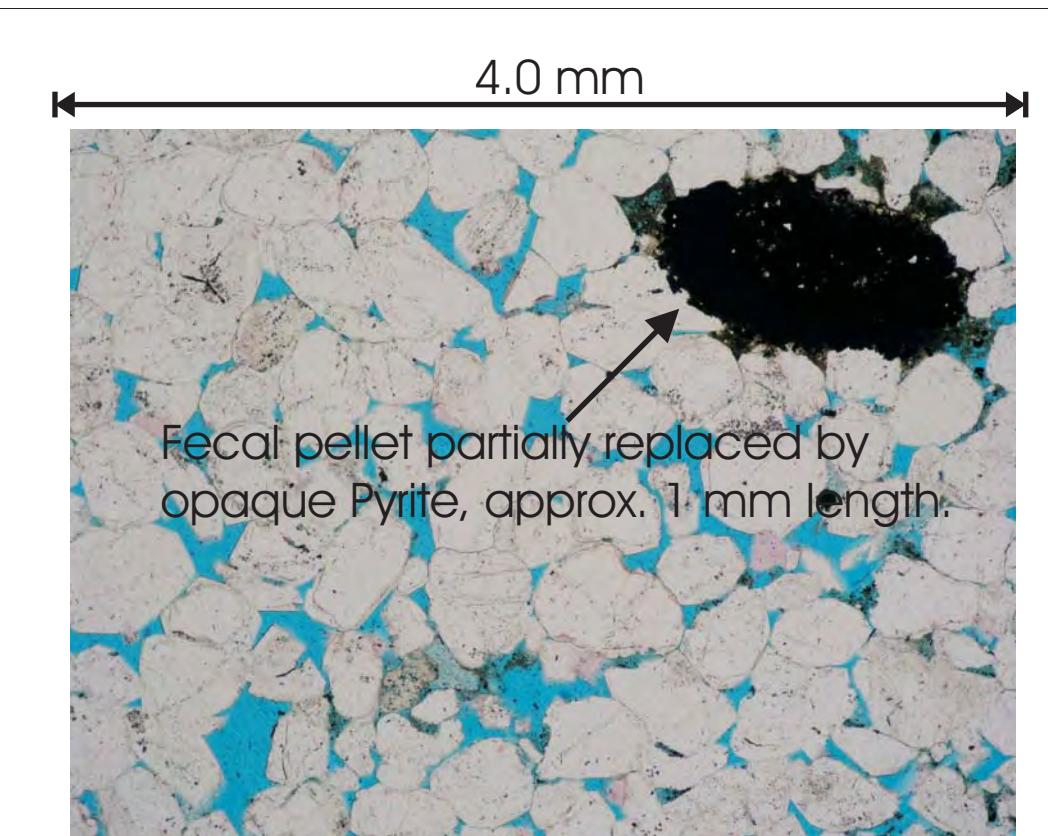
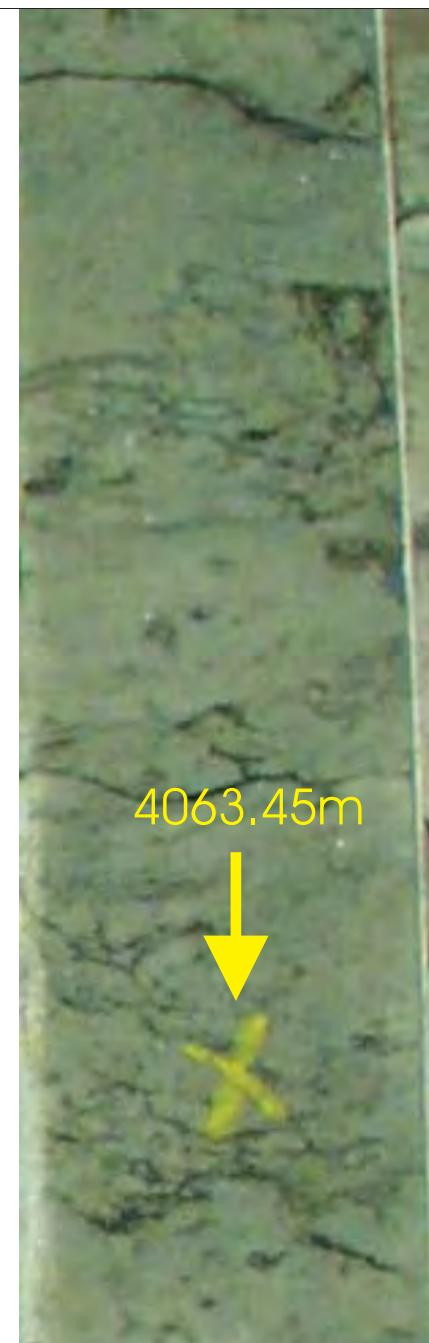
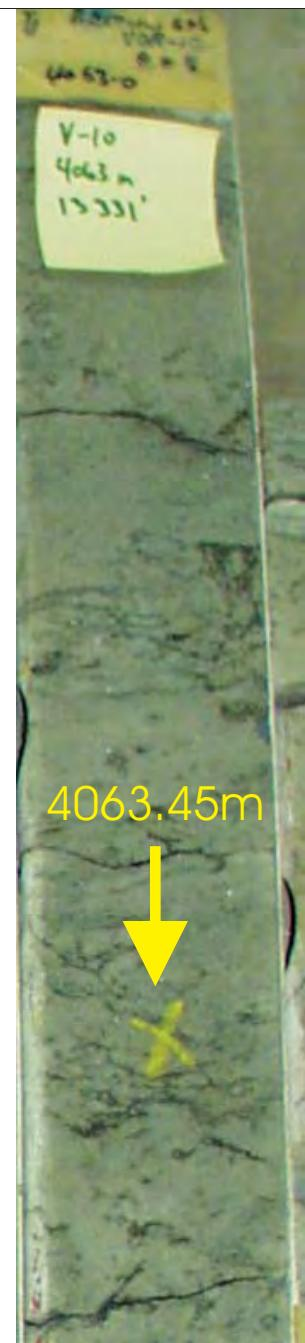
Sample Depth: 4060.90 m
Shifted Depth: 13323.8 ft
He-∅: 12.0%
k air: 10.6 mD (sc)

WHOLE CORE PLUG ANALYSES
WELL: VORWATA - 10st
DEPTH: 4060.90 m

PLATE A:

Digital Whole Core Photographs
Digital Core Chip/Plug Photograph

Figure 84A: Core Plug/Chip Atlas for sample 4060.90m from Vorwata-10.



Sample Depth: 4063.45 m

Shifted Depth: 13332.2 ft

He-Ø: insufficient/broken

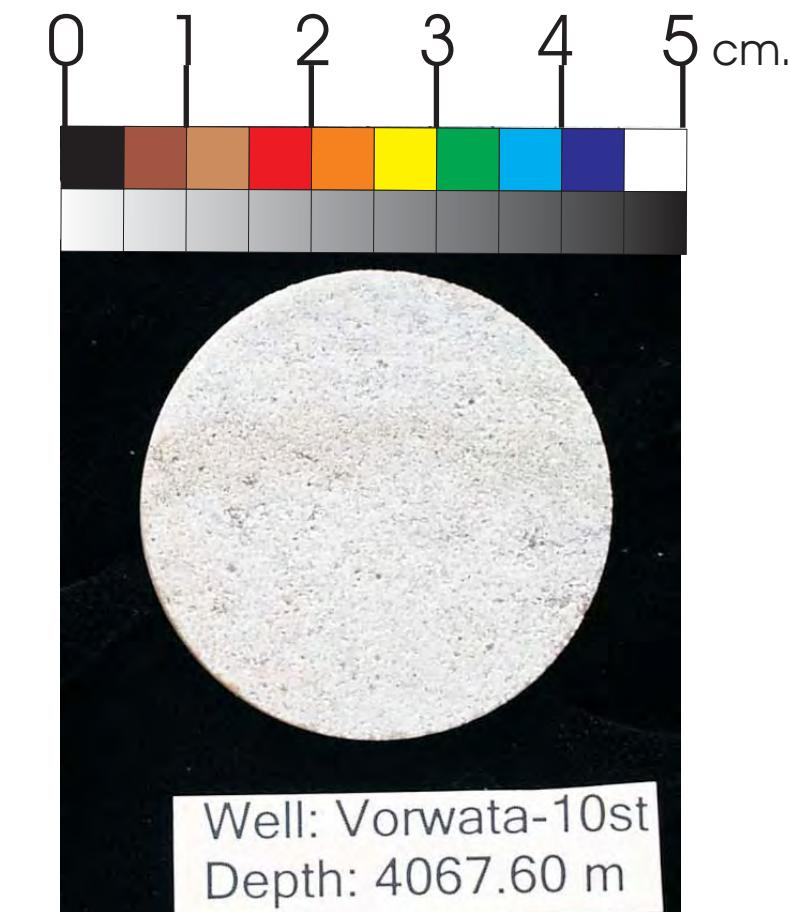
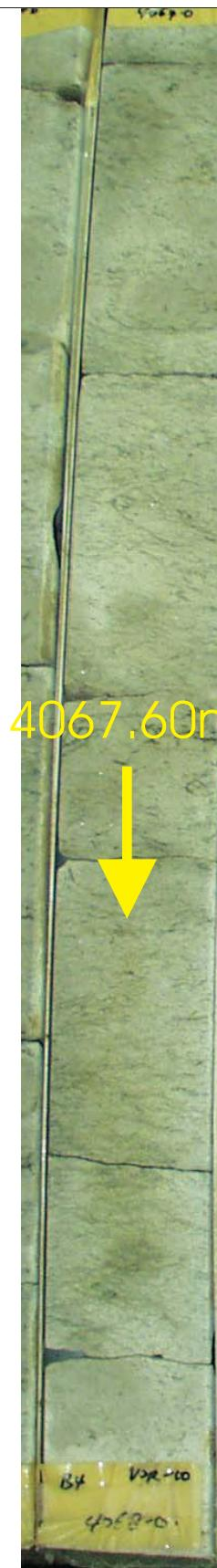
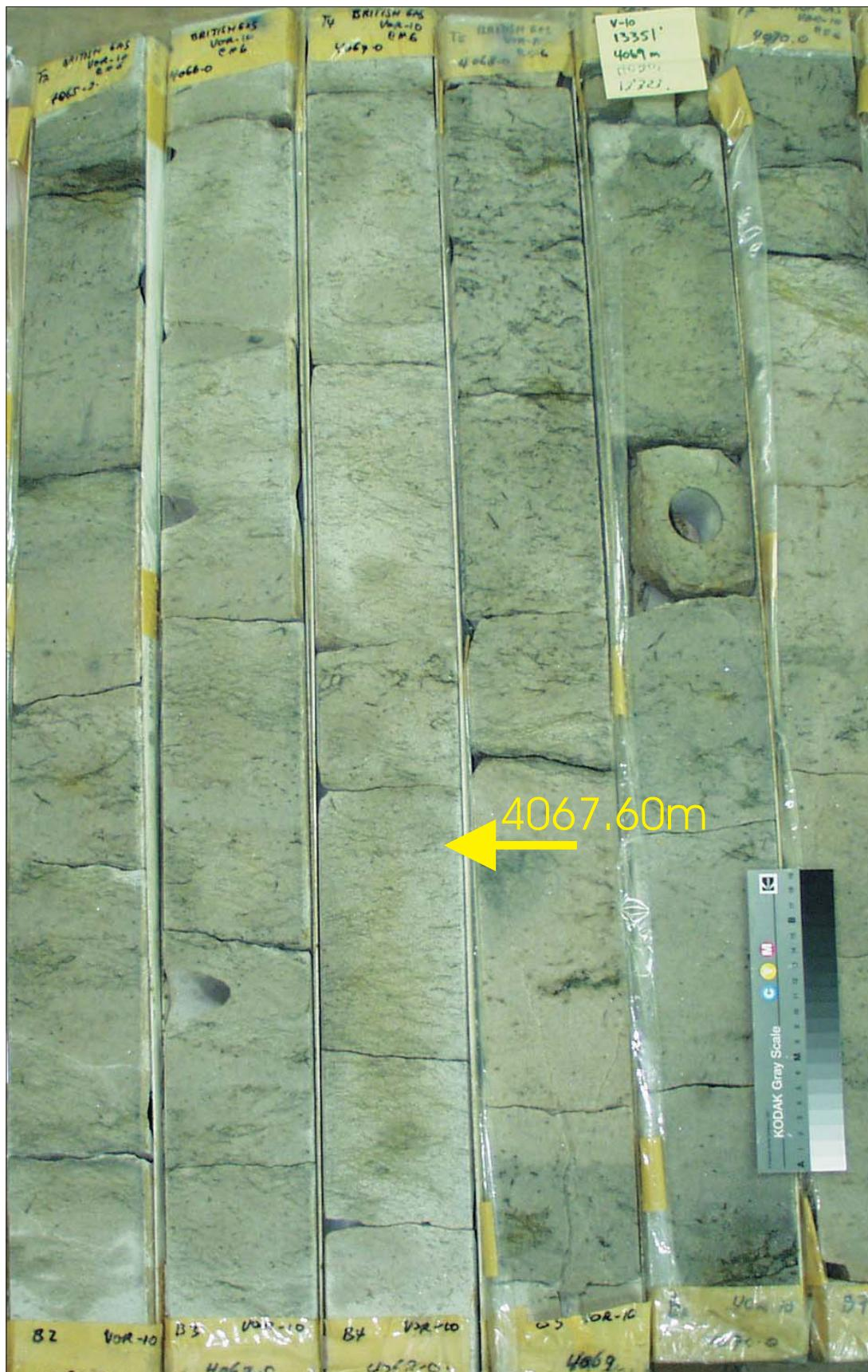
k air: insufficient/broken

WHOLE CORE PLUG ANALYSES
WELL: VORWATA - 10st
DEPTH: 4063.45 m

PLATE A:

Digital Whole Core Photographs
Petrographic Photomicrograph

Figure 85A: Core Plug/Chip Atlas for sample 4063.45m from Vorwata-10.



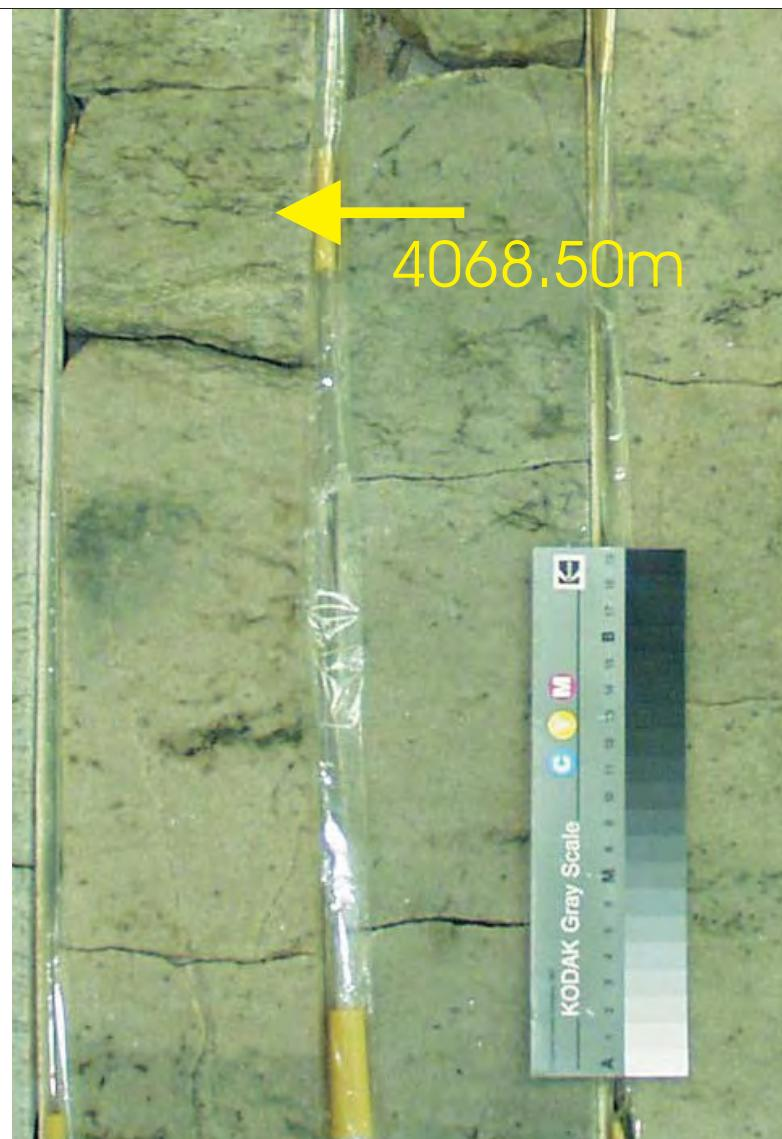
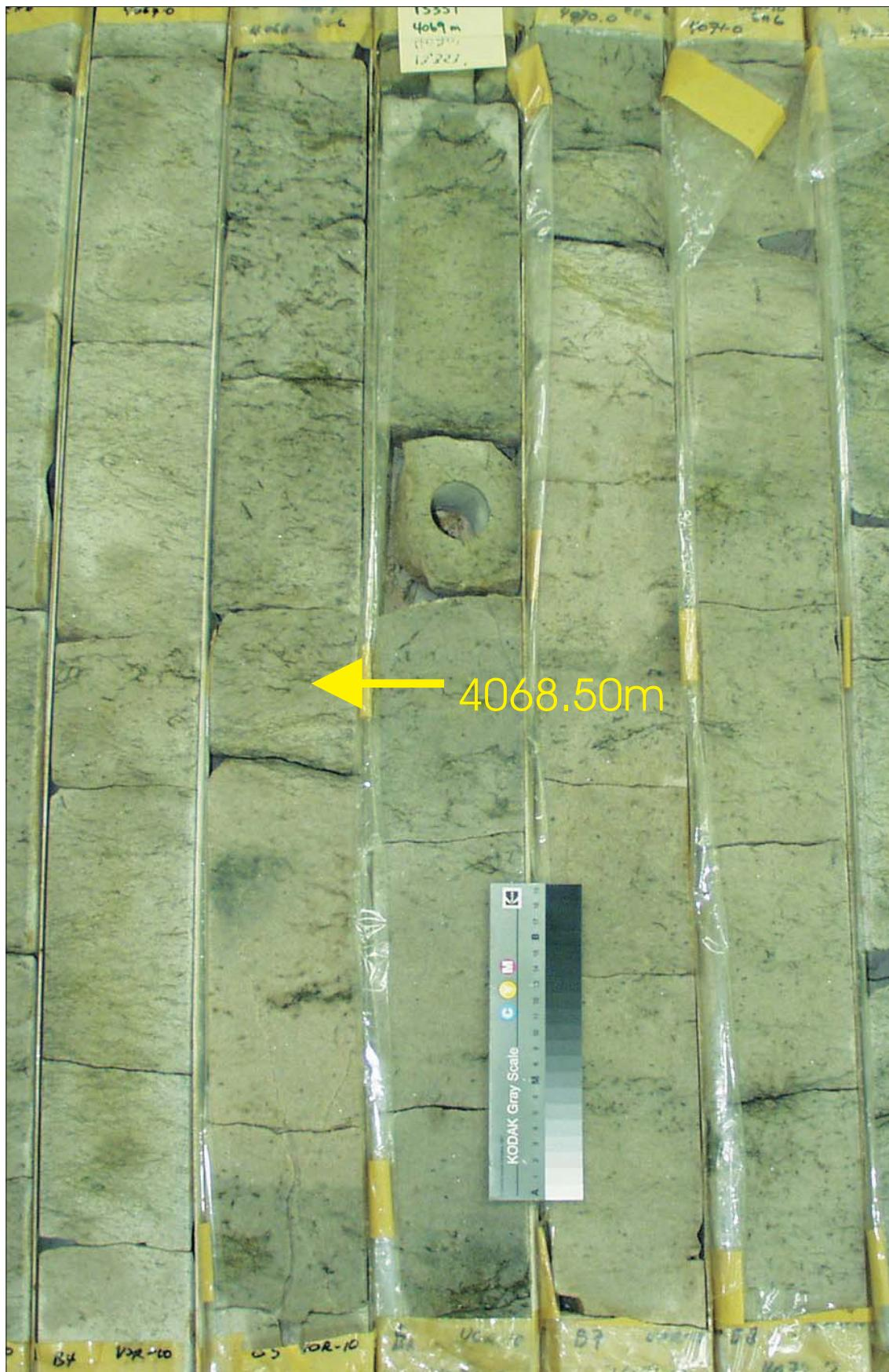
Sample Depth: 4067.60 m
Shifted Depth: 13345.8 ft
He-Ø: 9.97%
k air: 11.46 mD (sc)

WHOLE CORE PLUG ANALYSES
WELL: VORWATA - 10st
DEPTH: 4067.60 m

PLATE A:

Digital Whole Core Photographs
Digital Core Chip/Plug Photograph

Figure 86A: Core Plug/Chip Atlas for sample 4067.60m from Vorwata-10.



Sample Depth: 4068.50 m
Shifted Depth: 13348.7 ft
He-Ø: 13.77%
k air: 521 mD (sc)

WHOLE CORE PLUG ANALYSES
WELL: VORWATA - 10st
DEPTH: 4068.50 m

PLATE A:

Digital Whole Core Photographs
Digital Core Chip/Plug Photograph

Figure 87A: Core Plug/Chip Atlas for sample 4068.50m from Vorwata-10.

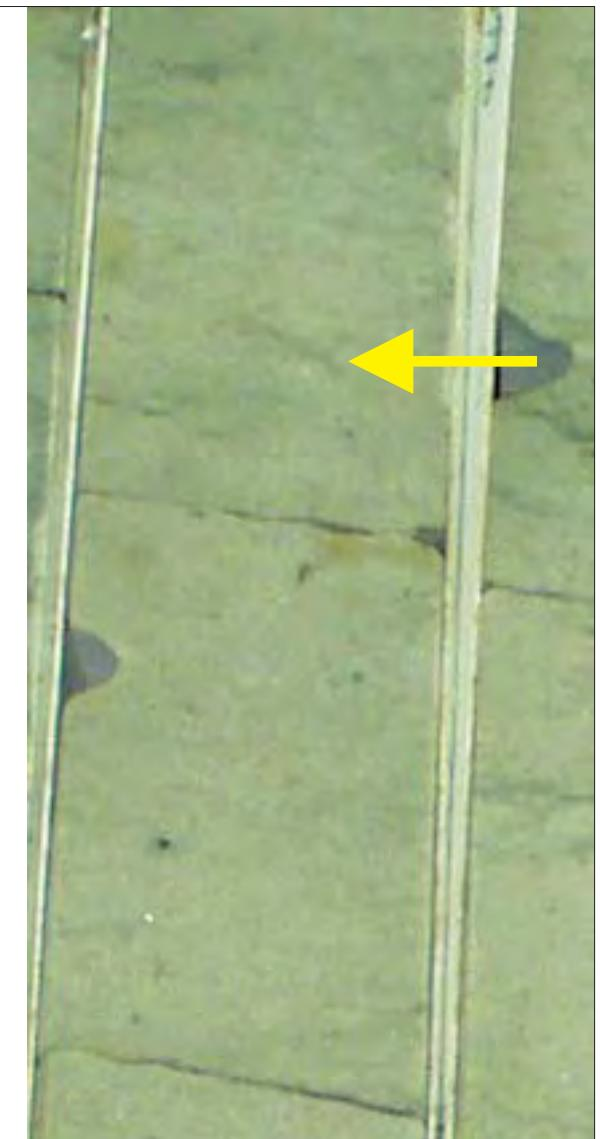
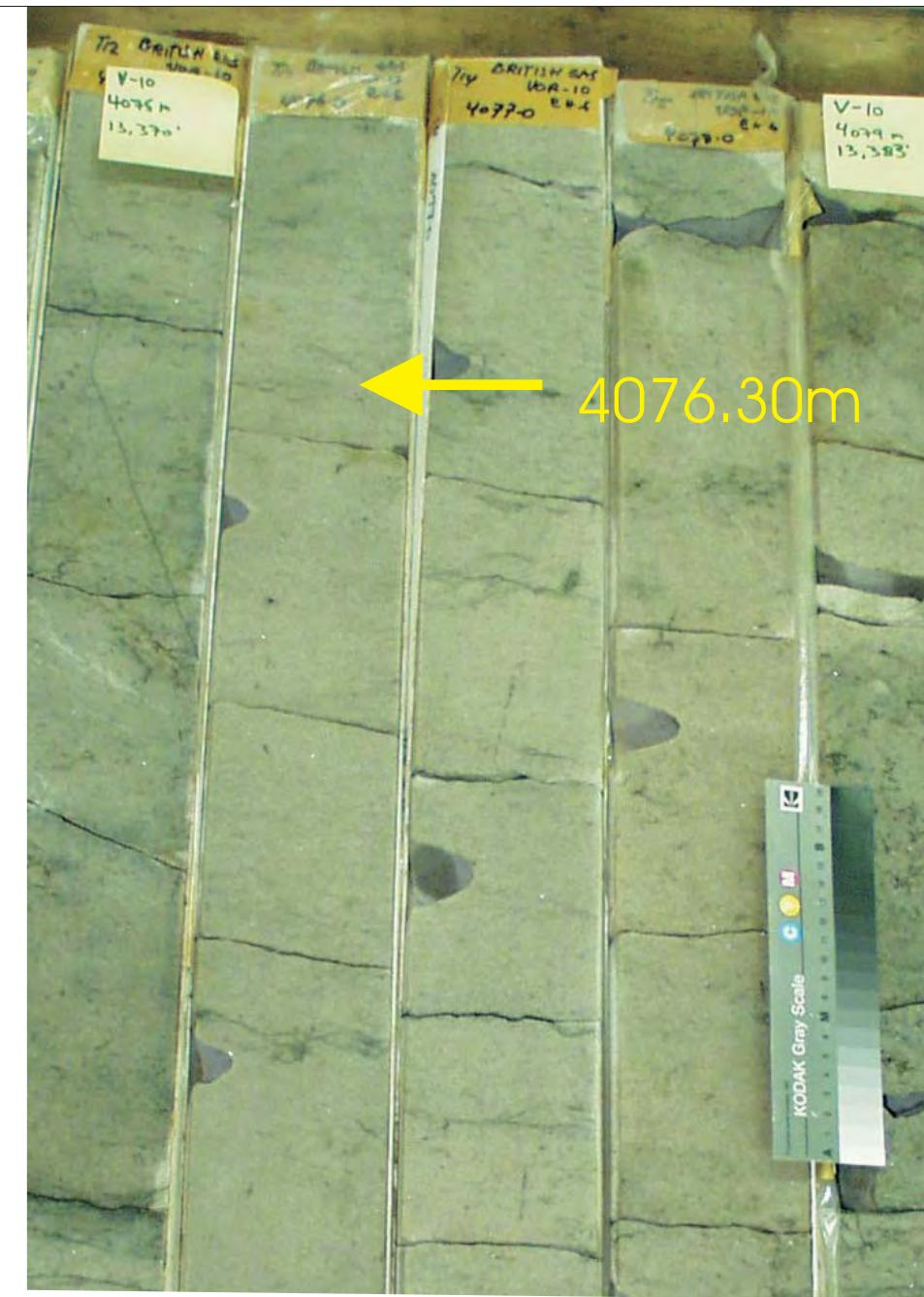
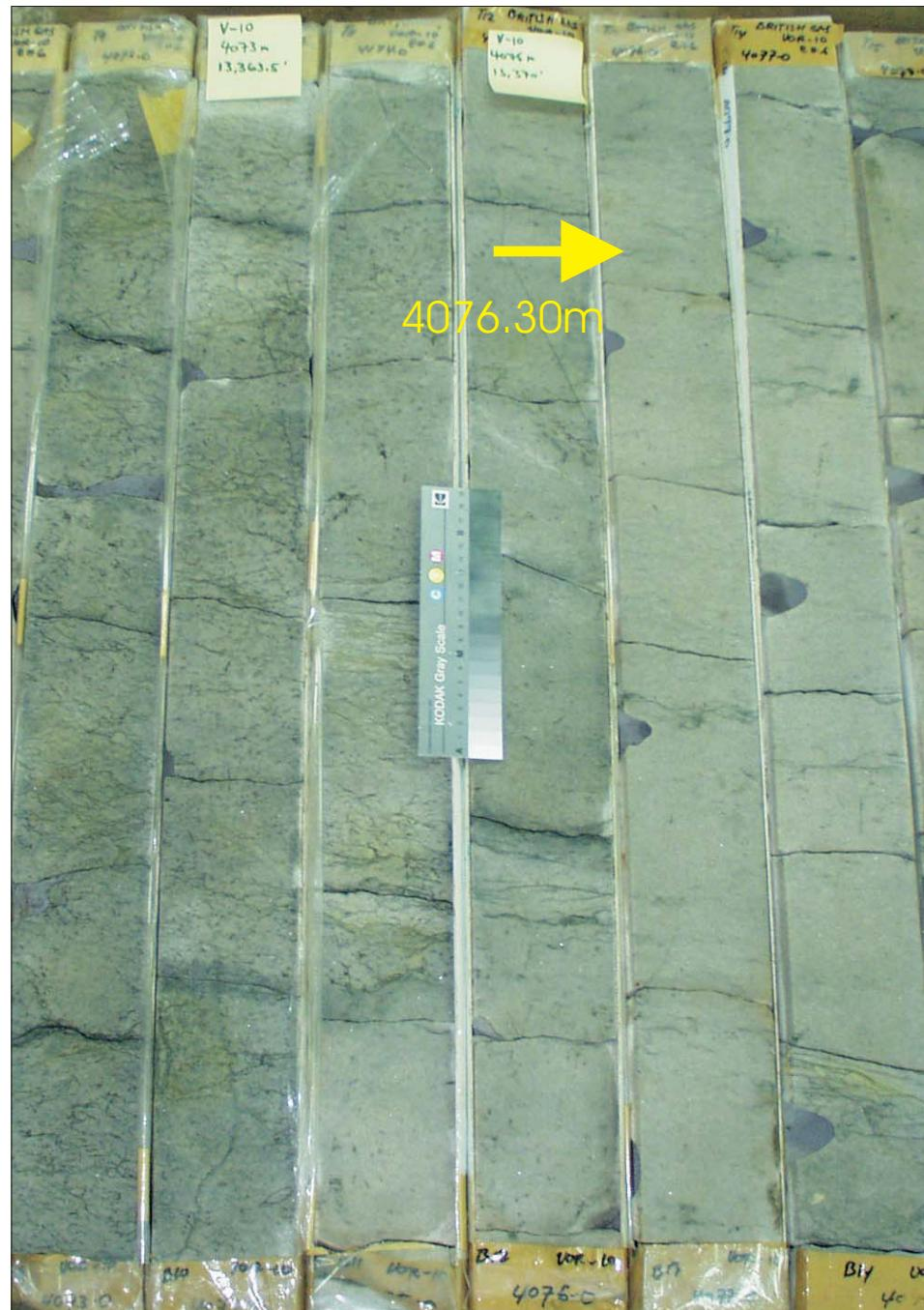
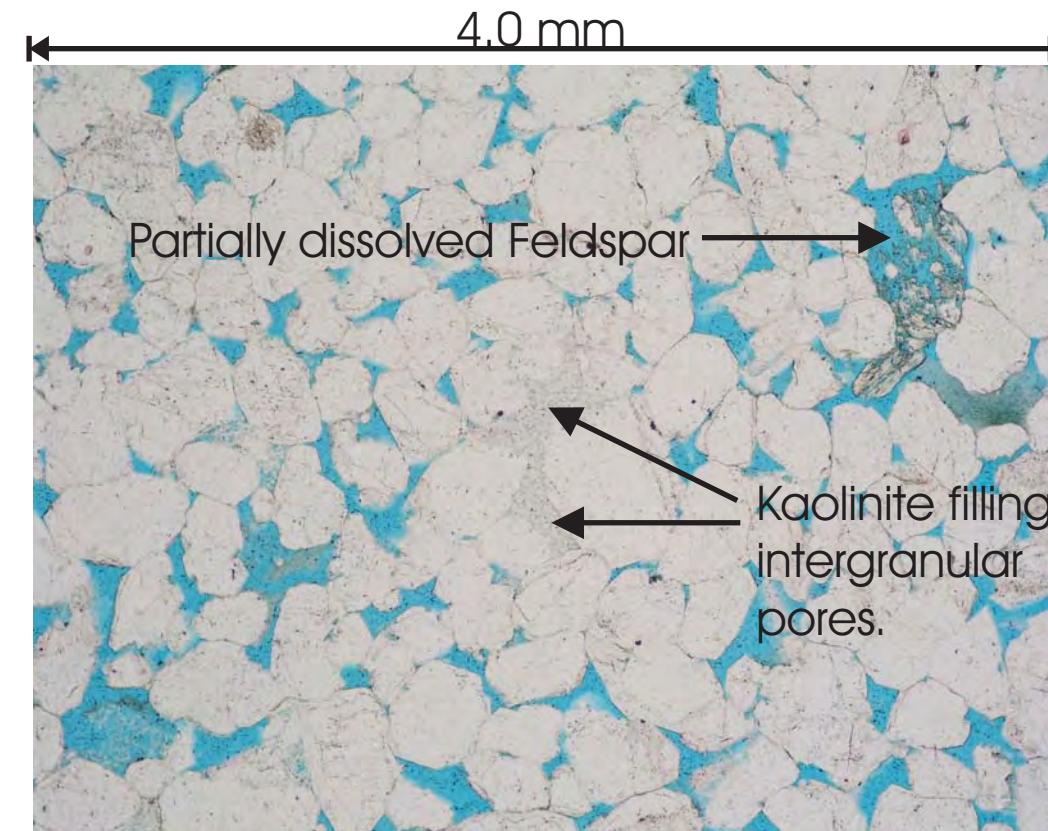


Figure 88A: Core Plug/Chip Atlas for sample 4076.30m from Vorwata-10.

WHOLE CORE PLUG ANALYSES
WELL: VORWATA - 10st
DEPTH: 4076.30 m

PLATE A:

Digital Whole Core Photographs
Digital Core Chip/Plug Photograph



Sample Depth: 4076.30 m
 Shifted Depth: 13374.3 ft
 He-Ø: 14.24%
 k air: 6.43 mD (sc)

Figure 88B: Core Plug/Chip Atlas for sample 4076.30m from Vorwata-10.

WHOLE CORE PLUG ANALYSES

WELL: VORWATA - 10st

DEPTH: 4076.30 m

PLATE B:

Digital Core Chip/Plug Photograph
Petrographic Photomicrograph

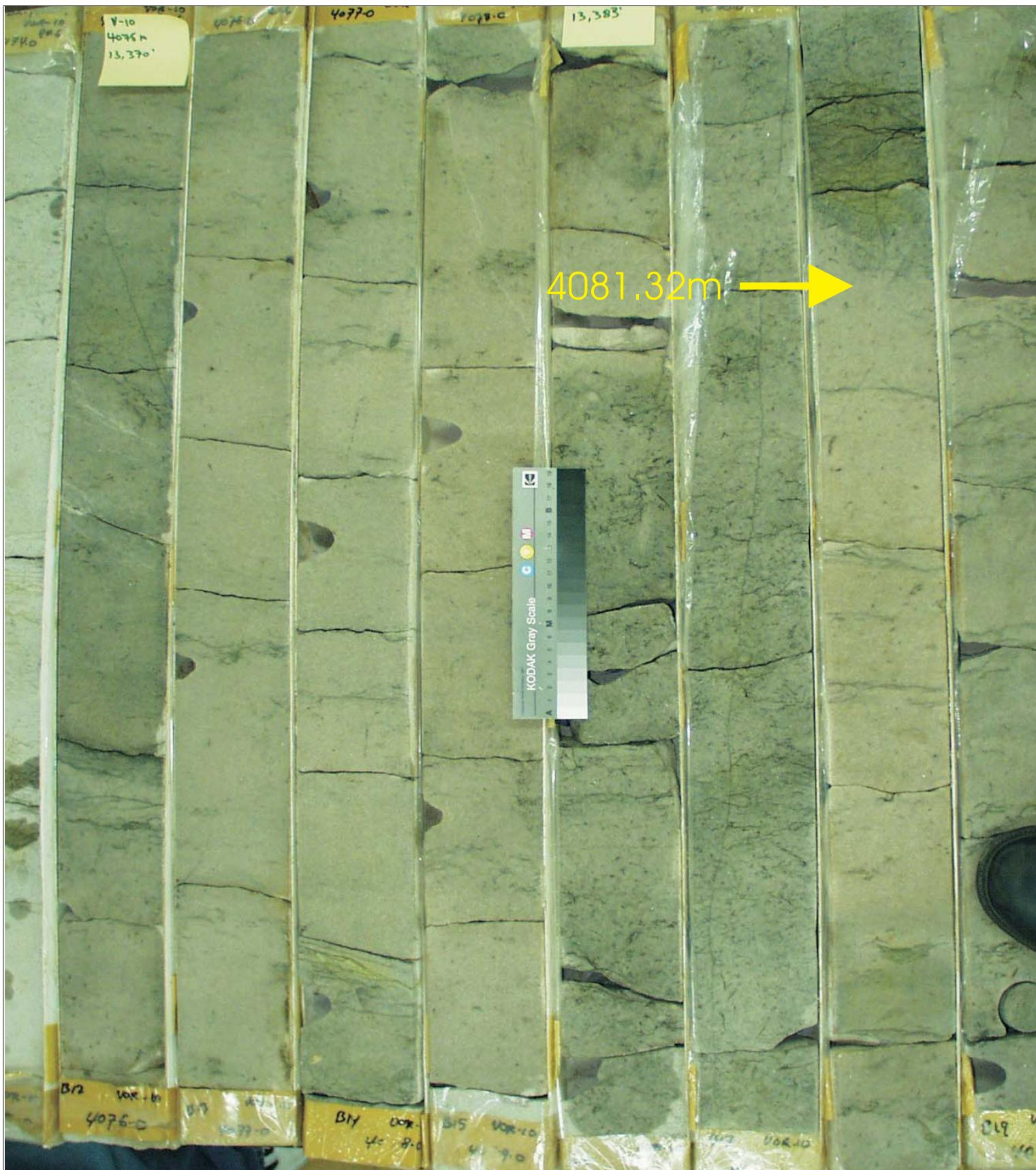


Figure 89A: Core Plug/Chip Atlas for sample 4081.32m from Vorwata-10.

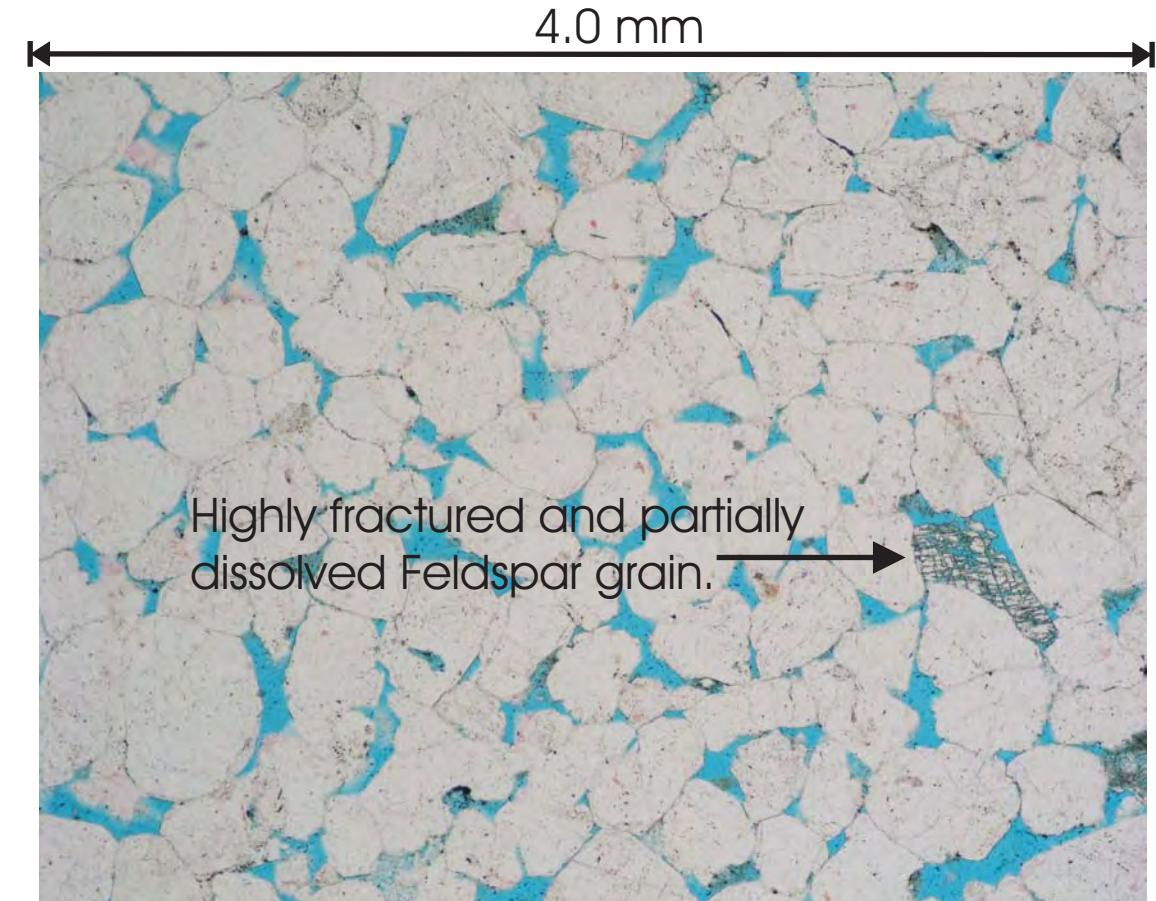
WHOLE CORE PLUG ANALYSES
WELL: VORWATA - 10st
DEPTH: 4081.32 m

PLATE A:

Digital Whole Core Photographs
Digital Core Chip/Plug Photograph



Sample Depth: 4081.32 m
Shifted Depth: 13390.8 ft
He-Ø: 10.5%
k air: 80.1 mD (NOB 800 psia)



Quartzarenite from the water-wet interval of the Roabiba Reservoir in the Vorwata-10 well.

Figure 89B: Core Plug/Chip Atlas for sample 4081.32m from Vorwata-10.

WHOLE CORE PLUG ANALYSES

WELL: VORWATA - 10st

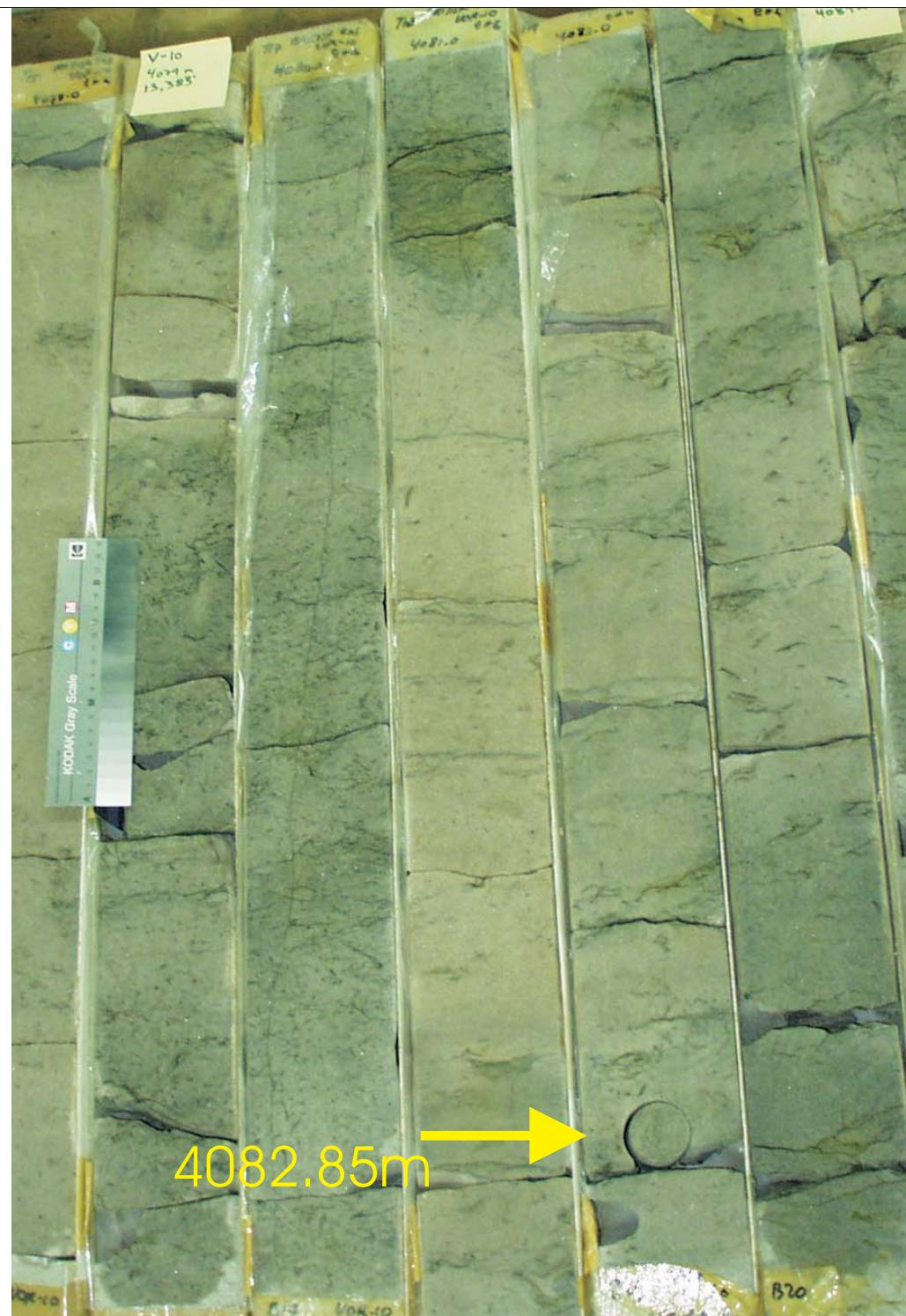
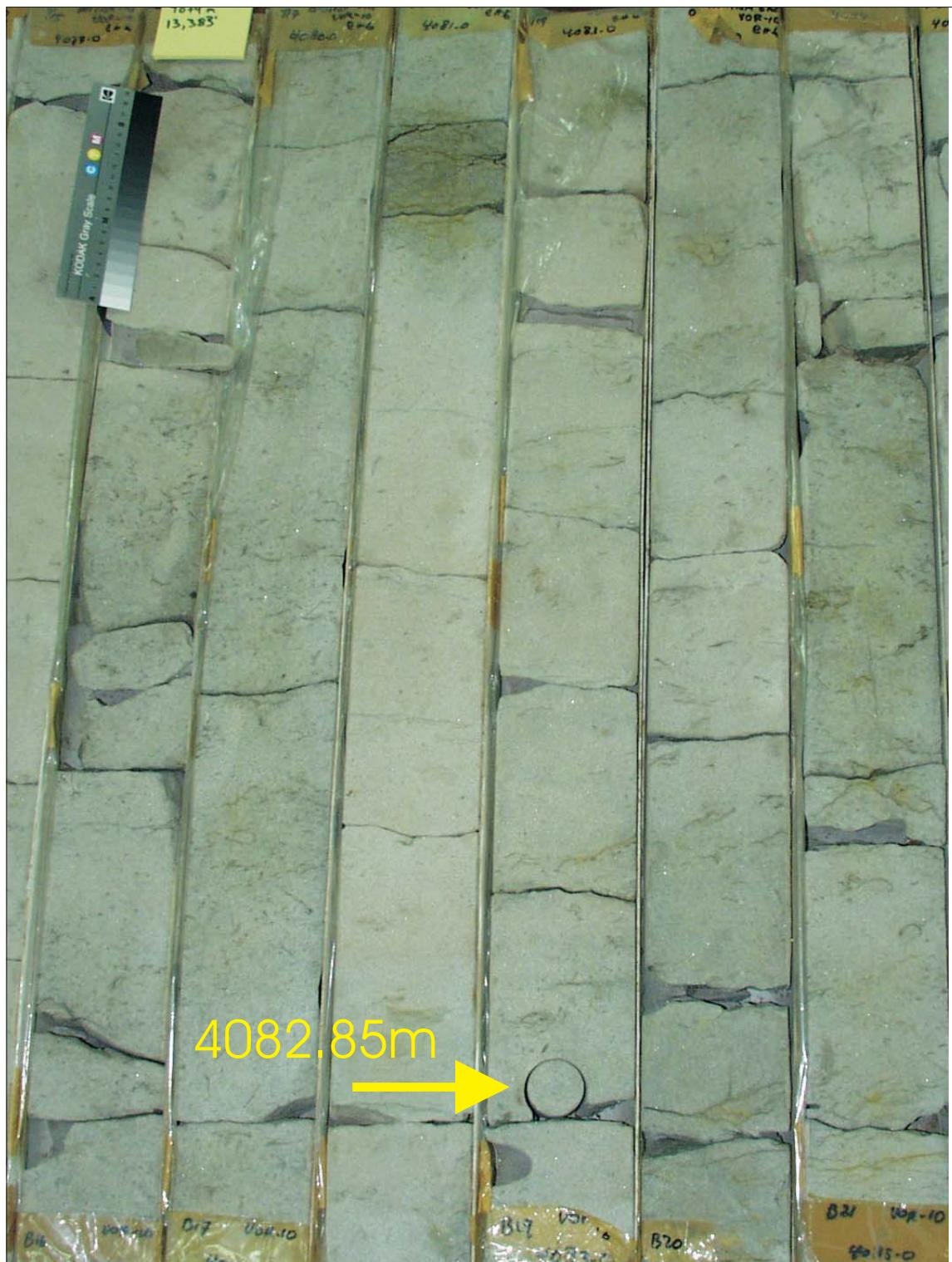
DEPTH: 4081.32 m

PLATE B:

Digital Whole Core Photographs

Digital Core Chip/Plug Photograph

Petrographic Photomicrograph



WHOLE CORE PLUG ANALYSES

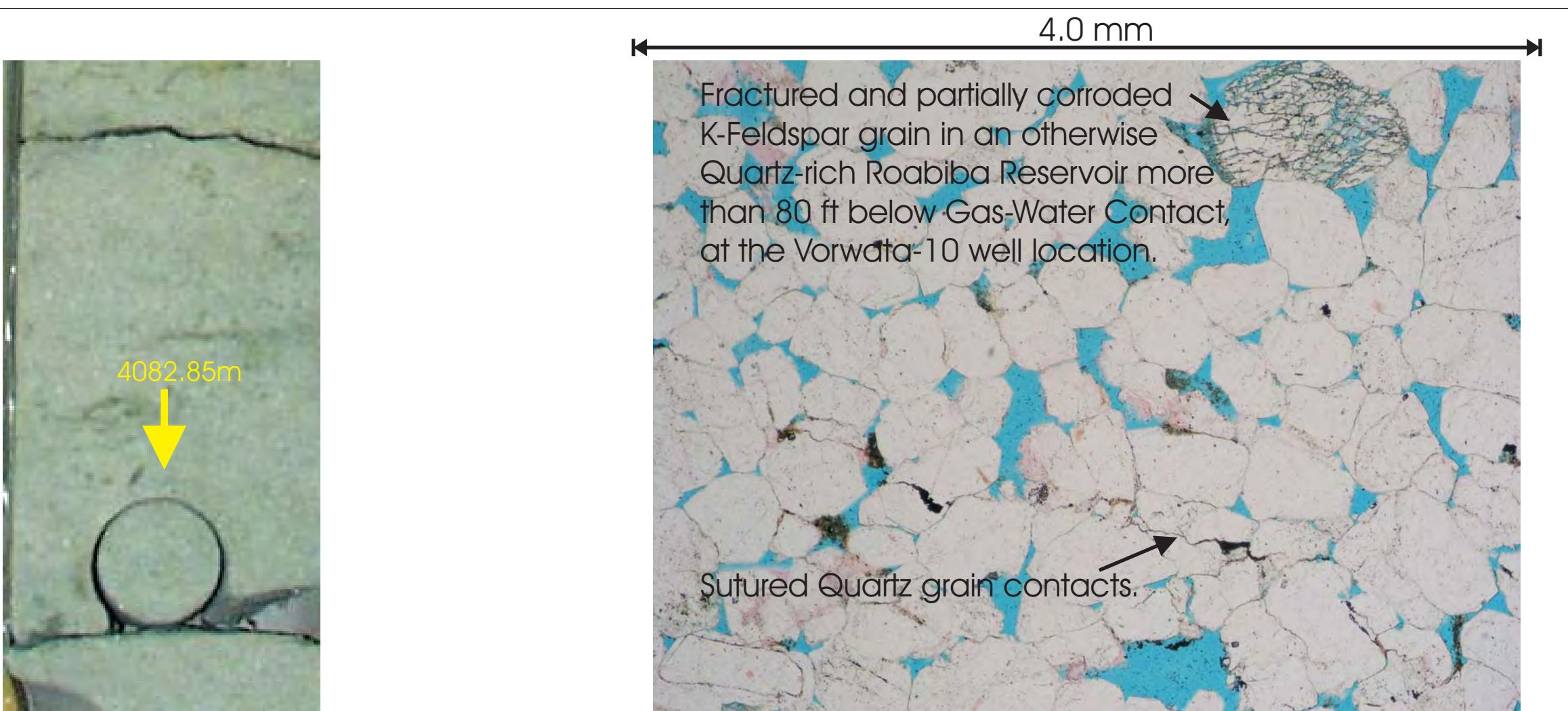
WELL: VORWATA - 10st

DEPTH: 4082.85 m

PLATE A:

Digital Whole Core Photographs

Figure 90A: Core Plug/Chip Atlas for sample 4082.85m from Vorwata-10.



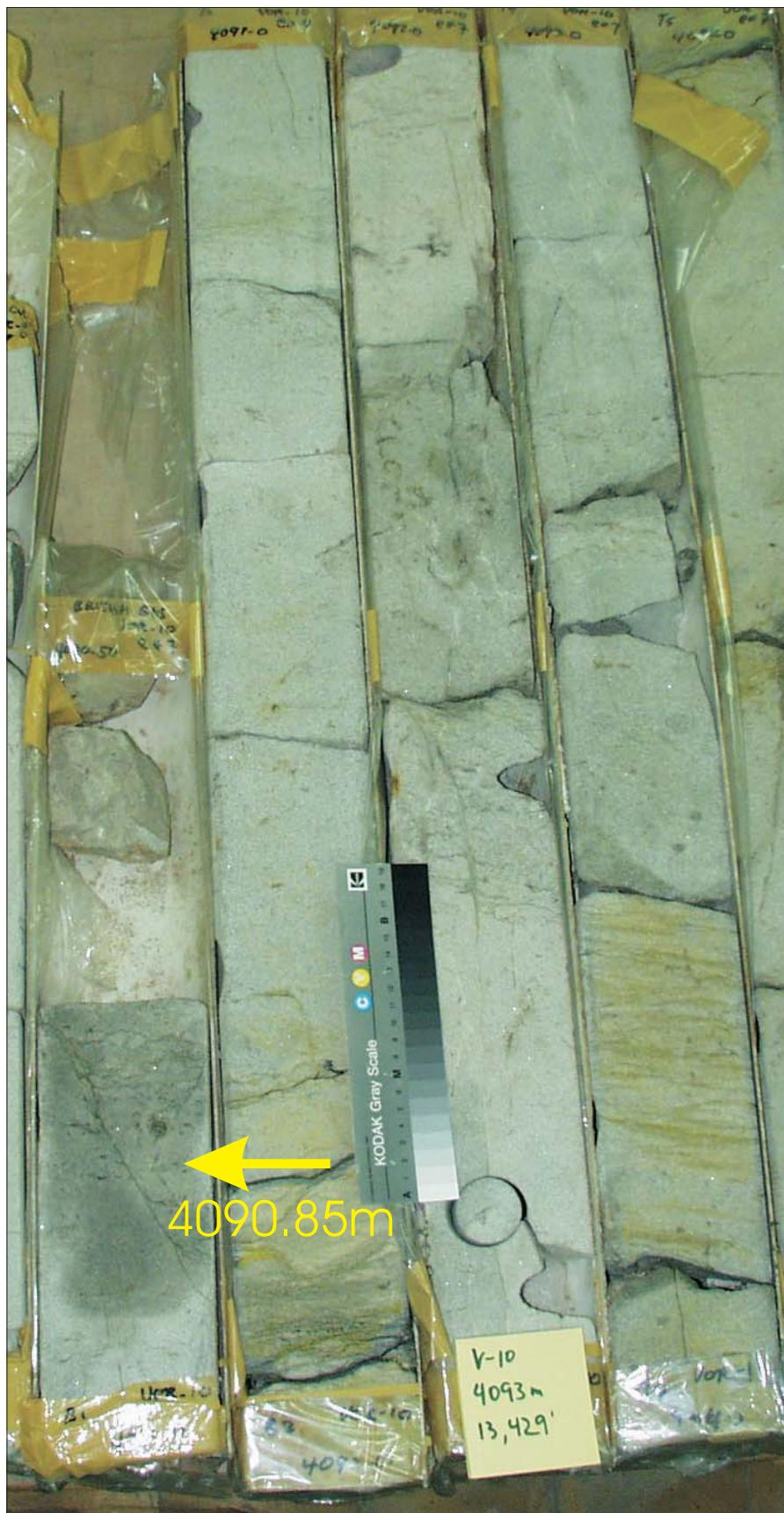
Sample Depth: 4082.85 m
 Shifted Depth: 13395.8 ft
 $\text{He-}\emptyset$: insufficient/broken
 k_{air} : insufficient/broken

Figure 90B: Core Plug/Chip Atlas for sample 4082.85m from Vorwata-10.

WHOLE CORE PLUG ANALYSES
 WELL: VORWATA - 10st
 DEPTH: 4082.85 m

PLATE B:

Digital Whole Core Photographs
 D Petrographic Photomicrograph



WHOLE CORE PLUG ANALYSES
WELL: VORWATA - 10st
DEPTH: 4090.85 m

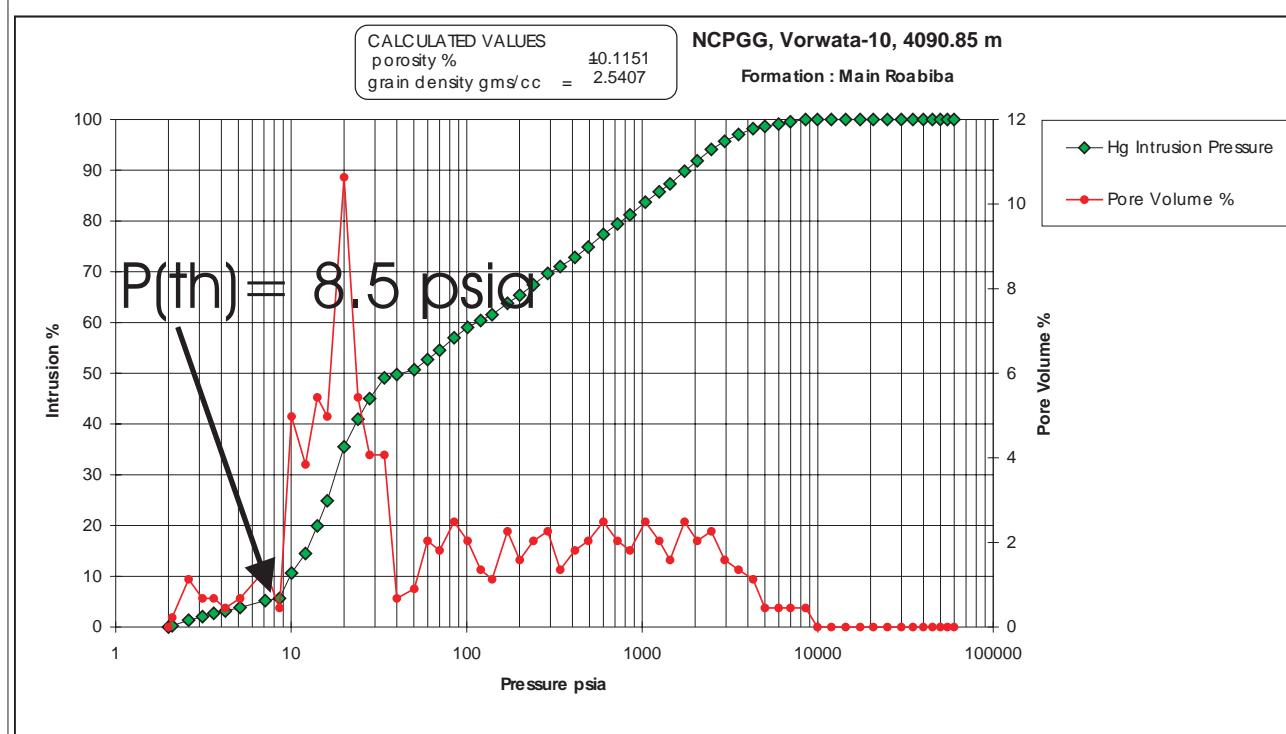
PLATE A:

Digital Whole Core Photographs

Figure 91A: Core Plug/Chip Atlas for sample 4090.85m from Vorwata-10.



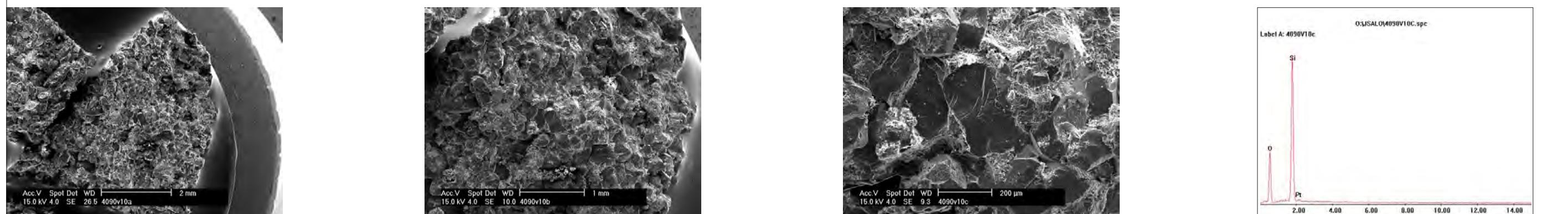
Sample Depth: 4090.85 m
Shifted Depth: 13422.1 ft
He-Ø: 11.3%
k air: 5.89 mD (NOB 800 psia)



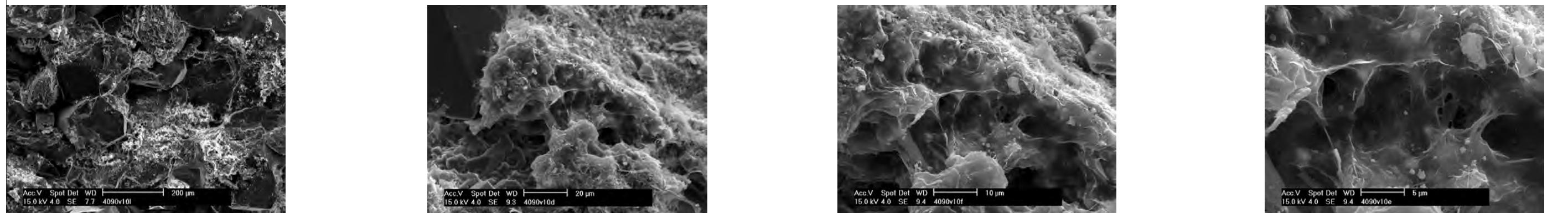
Sample Depth: 4090.85 m
Shifted Depth: 13422.1 ft
MICP Entry Pressure: 2 psia
MICP Threshold Pressure: 8.5 psia
Lithology: Sandstone (Roabiba)

WHOLE CORE PLUG ANALYSES
WELL: VORWATA - 10st
DEPTH: 4090.85 m
PLATE B:
Digital Whole Core Photographs
Digital Core Chip/Plug Photograph
Petrographic Photomicrograph
Mercury Injection Capillary Pressure

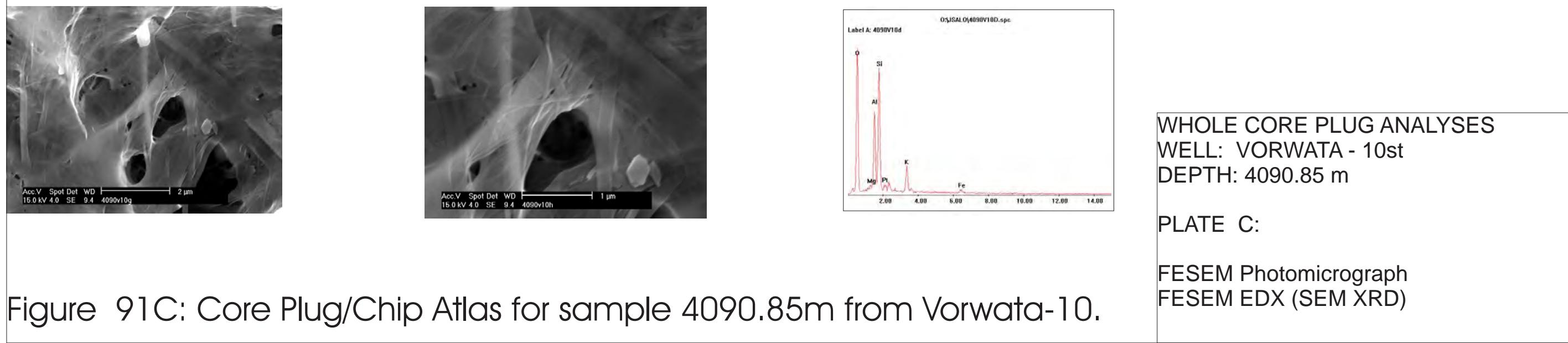
Figure 91B: Core Plug/Chip Atlas for sample 4090.85m from Vorwata-10.

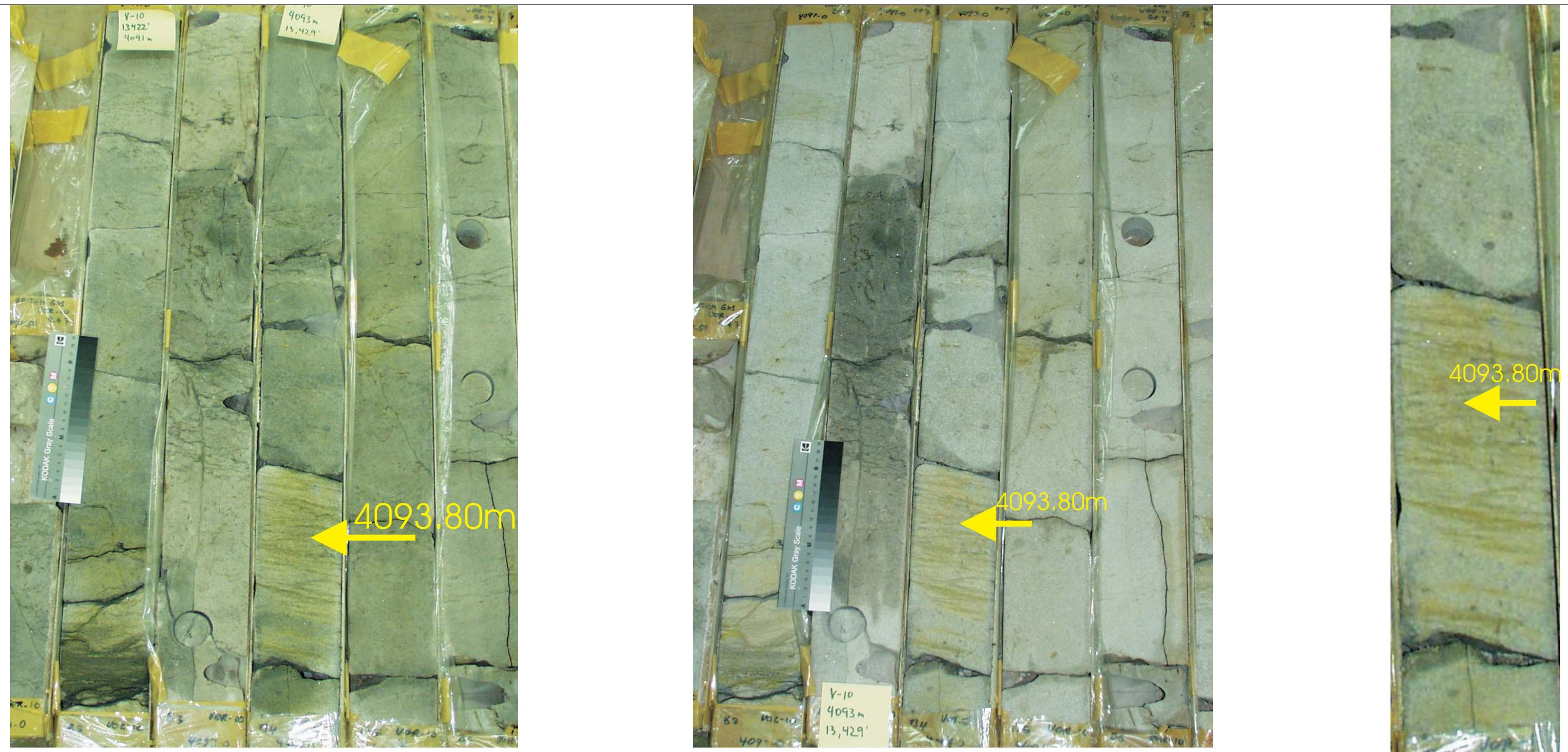


Sublitharenite Roabiba core plug sample, imaged with SEM, from more than 100 ft below the established GWC at the Vorwata-10 location. EDX shows composition is predominantly quartz.



High magnification SEM photomicrographs show wispy illite clay occluding some porosity. EDX confirms illitic composition of clays with microporosity of one micron or less.



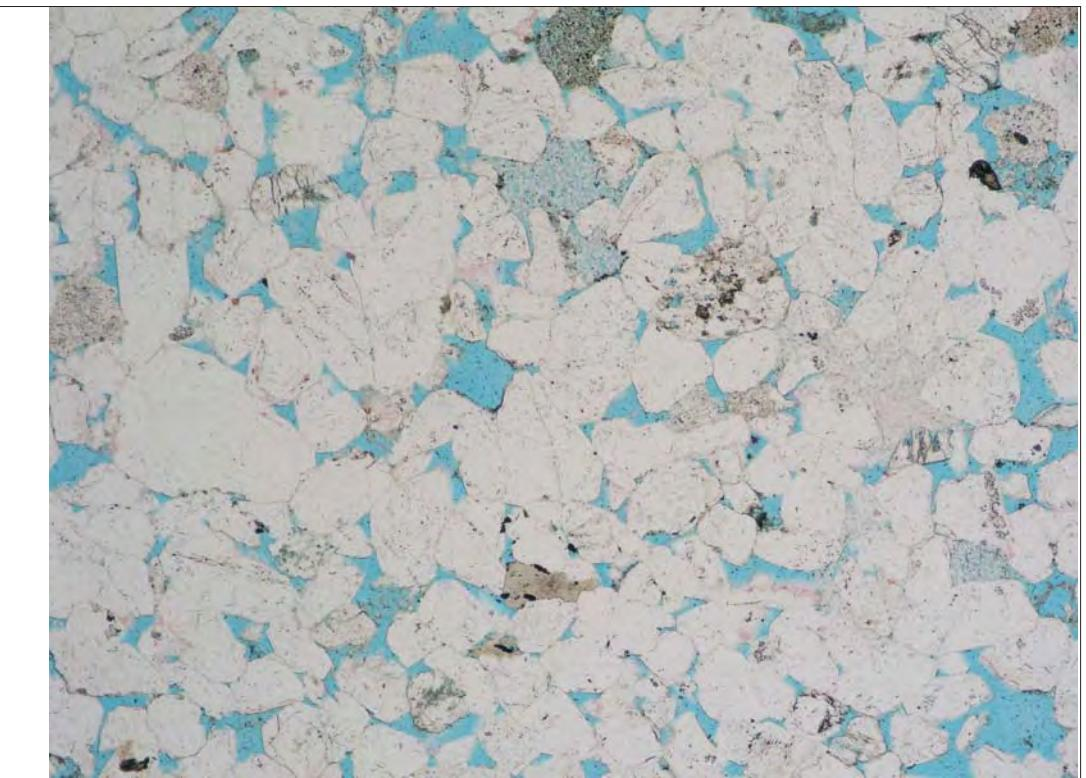


WHOLE CORE PLUG ANALYSES
WELL: VORWATA - 10st
DEPTH: 4093.80 m

PLATE A:

Digital Whole Core Photographs

Figure 92A: Core Plug/Chip Atlas for sample 4093.80m from Vorwata-10.



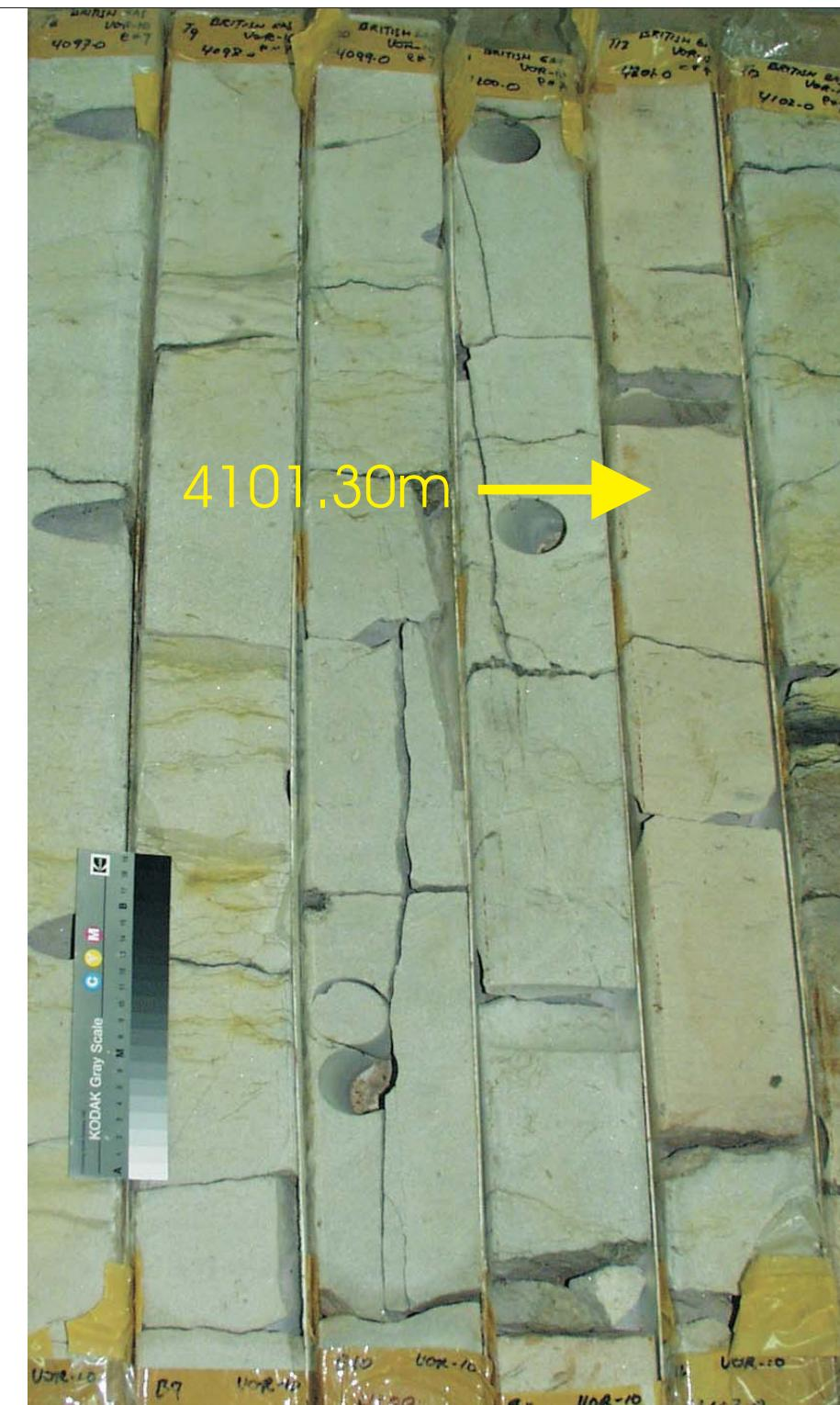
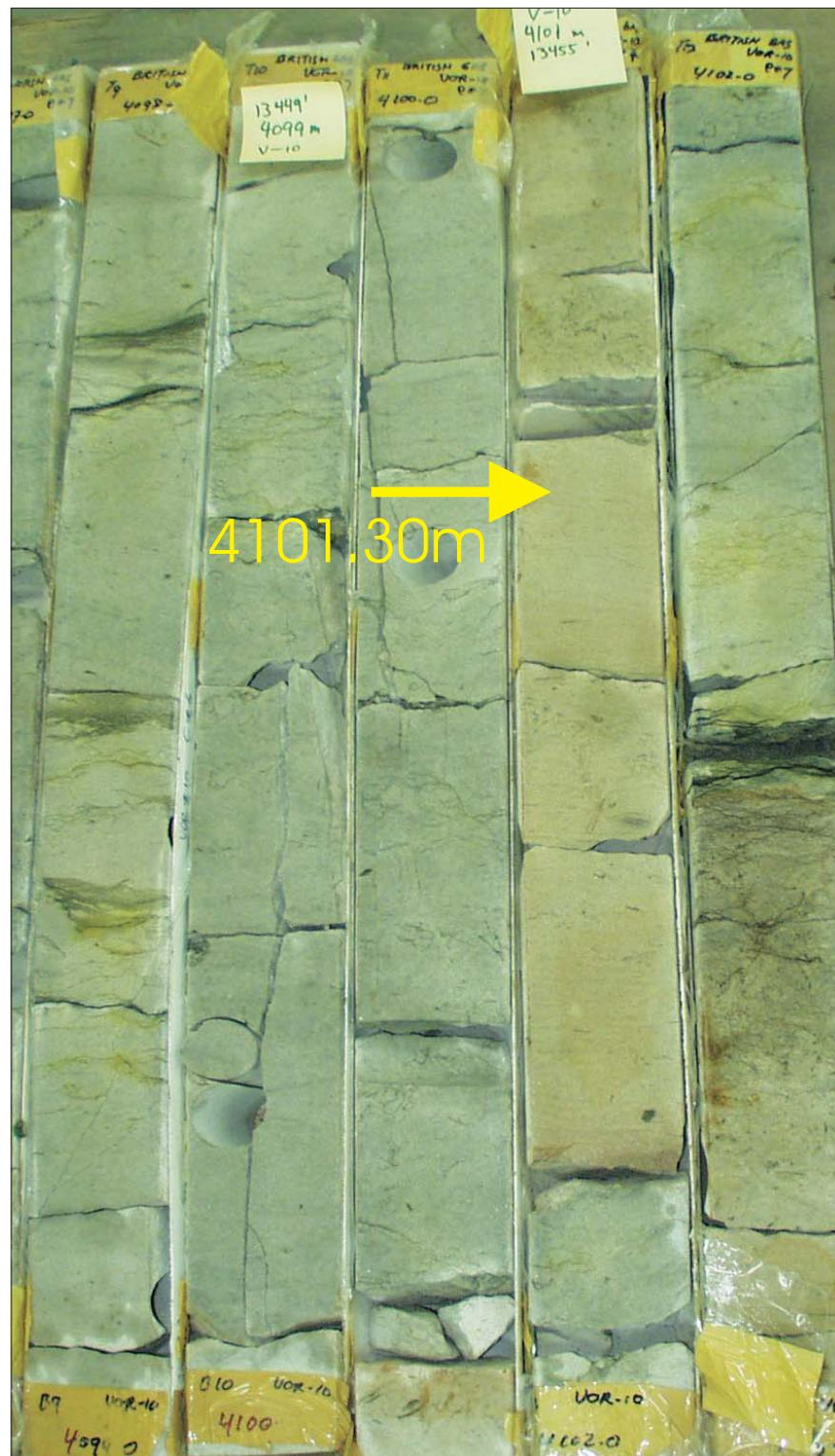
Sample Depth: 4095.50 m
Shifted Depth: 13437.3 ft
He-Ø: insufficient/broken
k air: insufficient/broken

Figure 93A: Core Plug/Chip Atlas for sample 4095.50m from Vorwata-10.

WHOLE CORE PLUG ANALYSES
WELL: VORWATA - 10st
DEPTH: 4095.50 m

PLATE A:

Digital Whole Core Photographs
Petrographic Photomicrograph

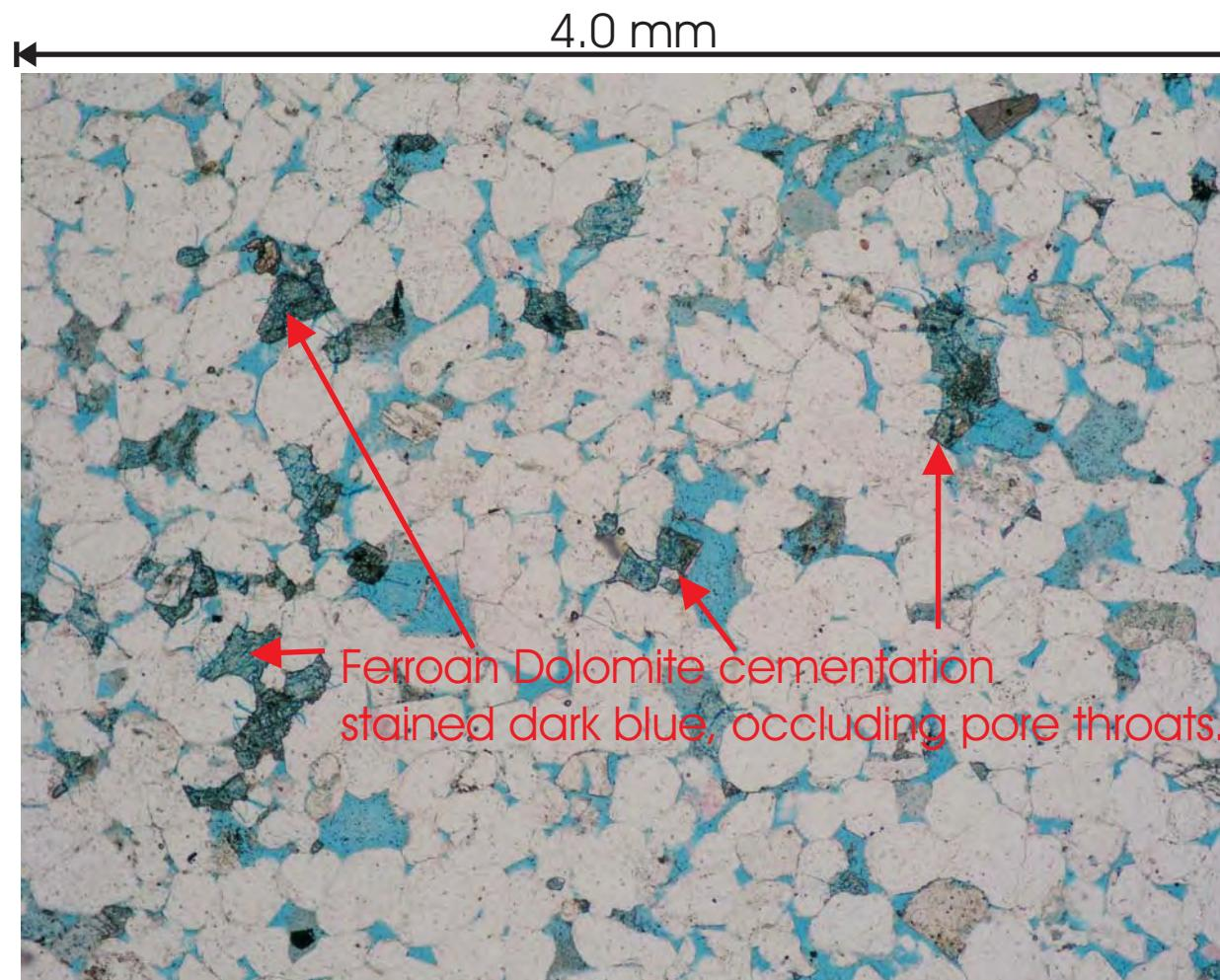
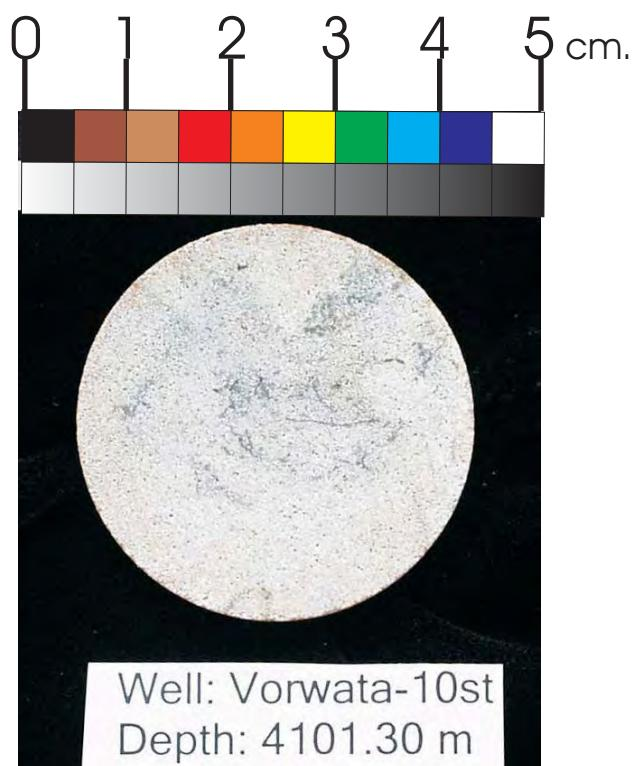


WHOLE CORE PLUG ANALYSES
WELL: VORWATA - 10st
DEPTH: 4101.30 m

PLATE A:

Digital Whole Core Photographs

Figure 94A: Core Plug/Chip Atlas for sample 4101.30m from Vorwata-10.



Photomicrograph of carbonate cemented quartzarenite in the lower portion of the Bajocian Roabiba Reservoir. Ferroan dolomite cement is stained dark blue, and limits the permeability of this interval with otherwise good visible porosity.

Sample Depth: 4101.30 m
Shifted Depth: 13456.4 ft
He-Ø: 11.36%
k air: 18.17 mD (sc)

WHOLE CORE PLUG ANALYSES

WELL: VORWATA - 10st

DEPTH: 4101.30 m

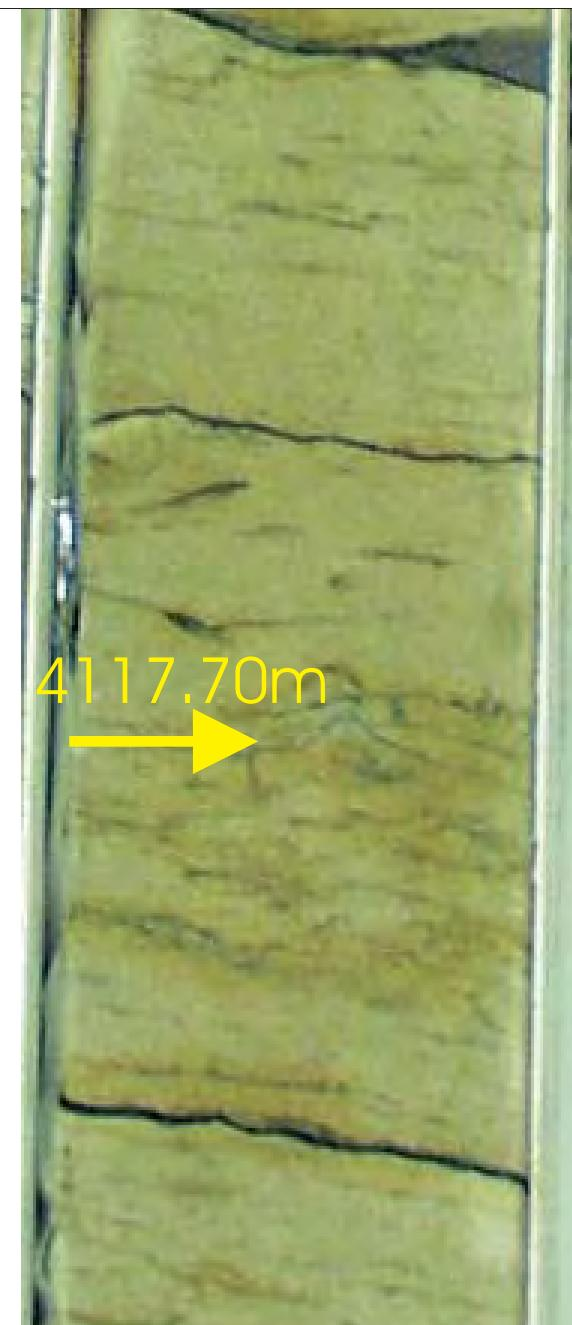
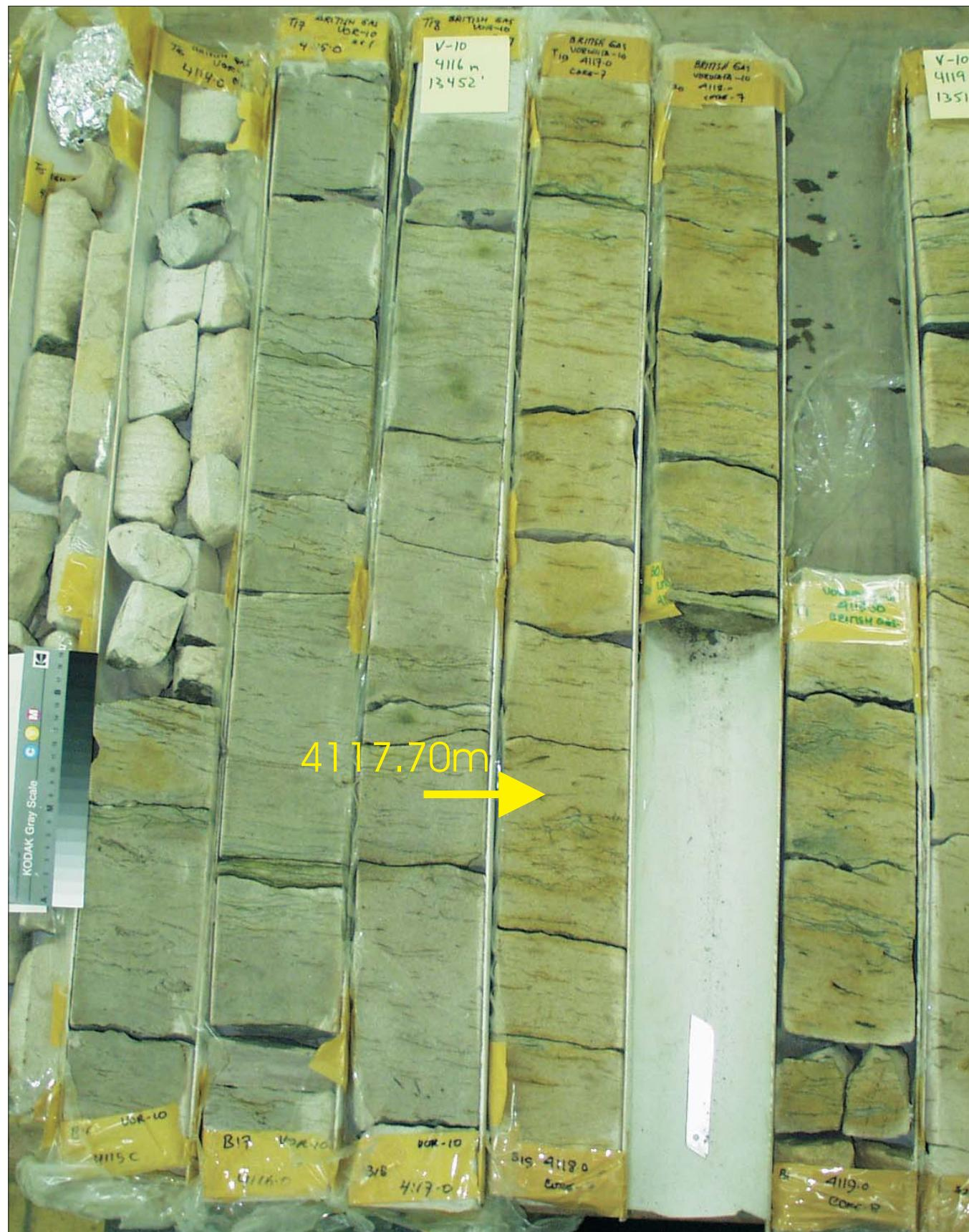
PLATE B:

Digital Whole Core Photographs

Digital Core Chip/Plug Photograph

Petrographic Photomicrograph

Figure 94B: Core Plug/Chip Atlas for sample 4101.30m from Vorwata-10.

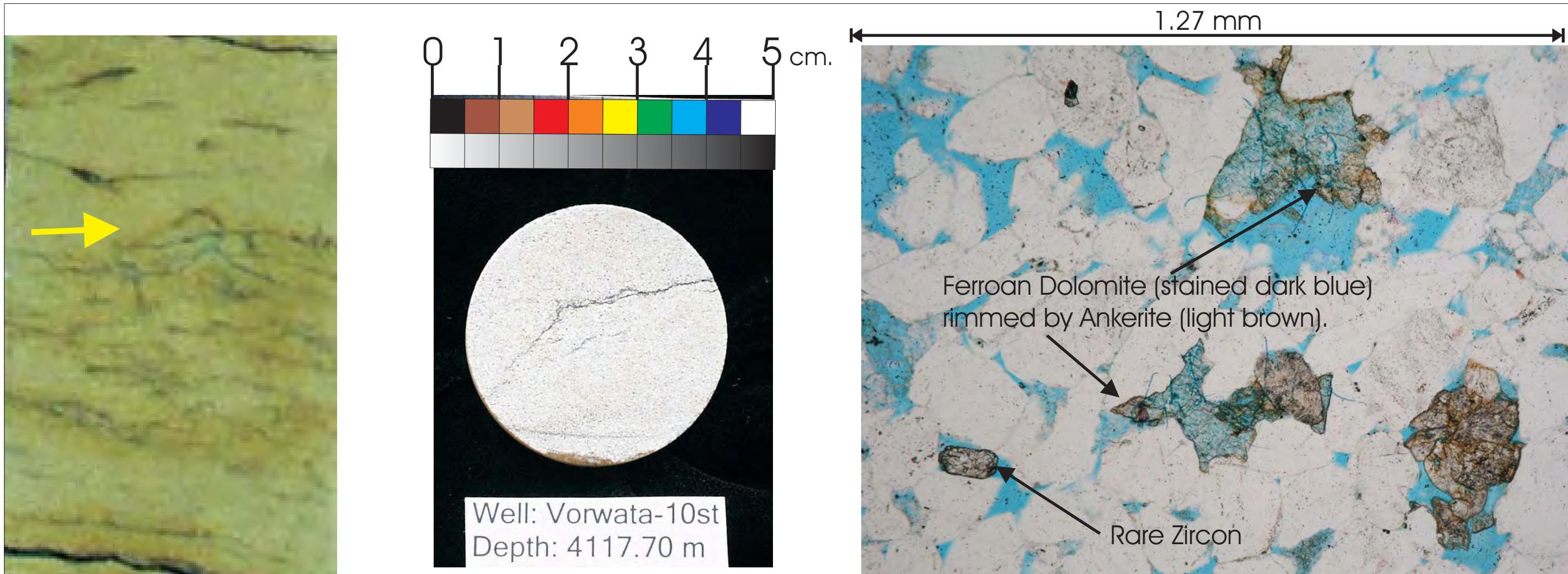


WHOLE CORE PLUG ANALYSES
WELL: VORWATA - 10st
DEPTH: 4117.70 m

PLATE A:

Digital Whole Core Photographs

Figure 95A: Core Plug/Chip Atlas for sample 4117.70m from Vorwata-10.



Sample Depth: 4117.70 m
 Shifted Depth: 13510.2 ft
 He-Ø: 15.53%
 k air: 840.8 mD (sc)

Figure 95B: Core Plug/Chip Atlas for sample 4117.70m from Vorwata-10.

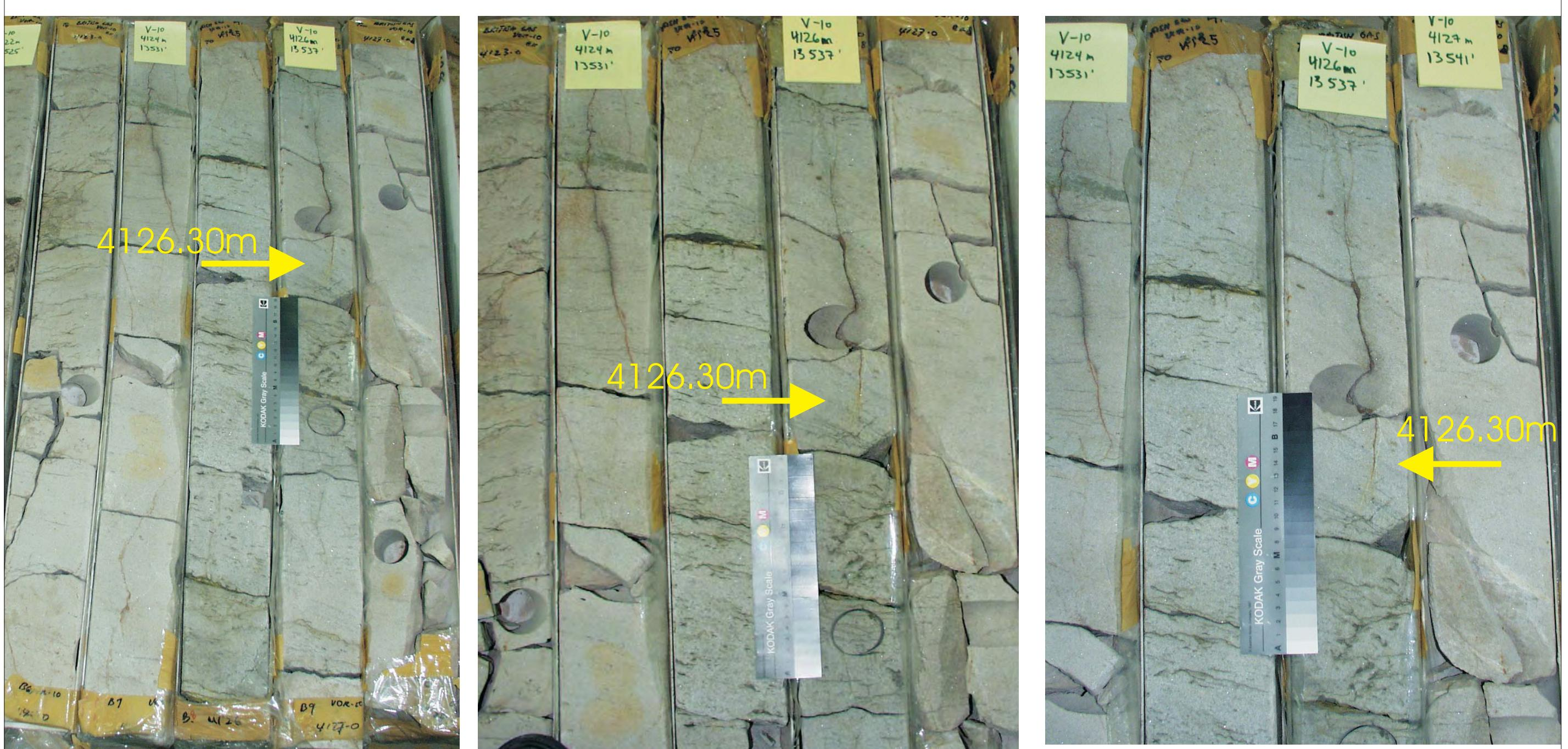
WHOLE CORE PLUG ANALYSES

WELL: VORWATA - 10st

DEPTH: 4117.70 m

PLATE B:

Digital Whole Core Photographs
 Digital Core Chip/Plug Photograph
 Petrographic Photomicrograph

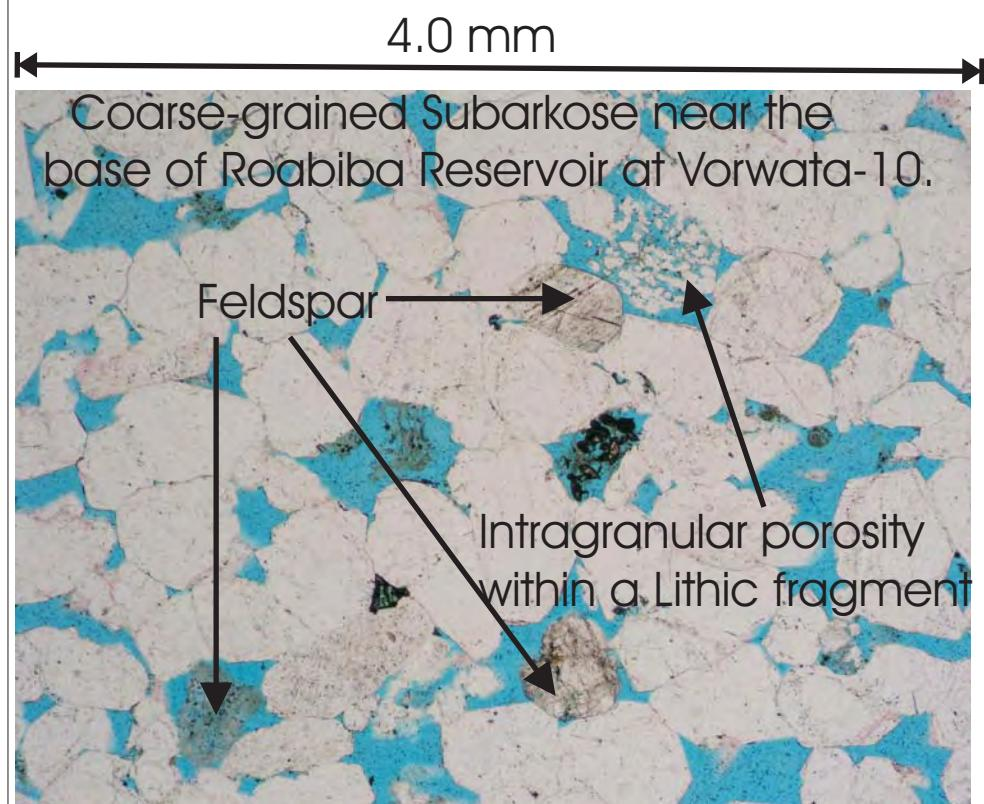
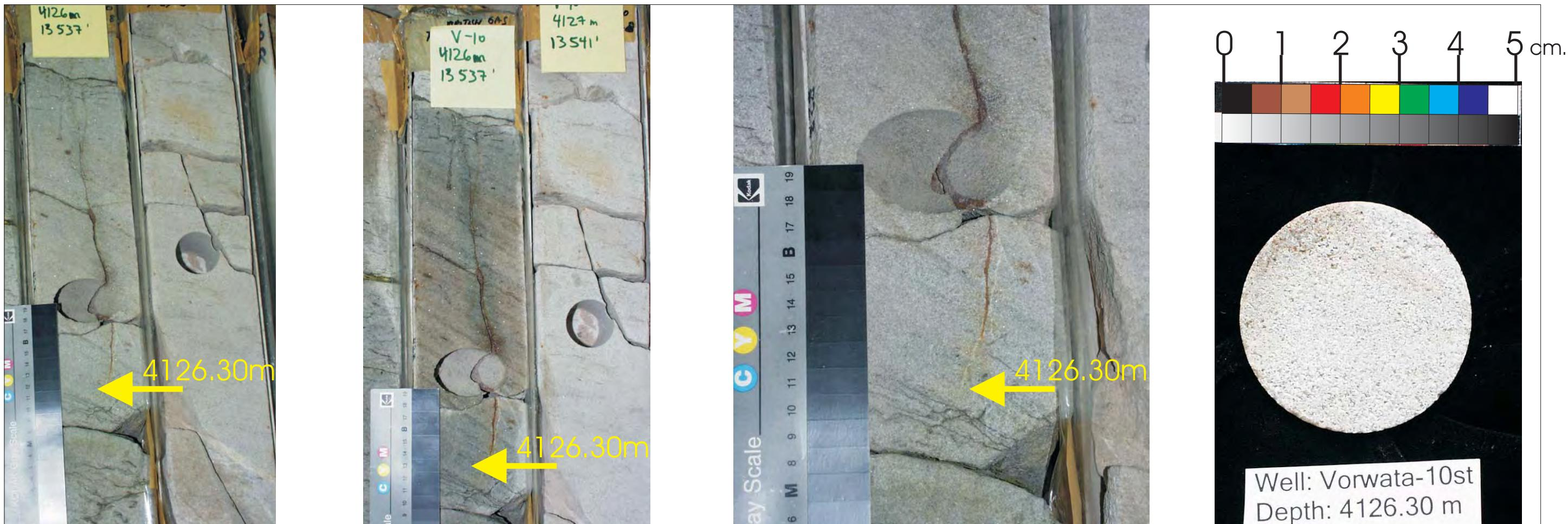


WHOLE CORE PLUG ANALYSES
WELL: VORWATA - 10st
DEPTH: 4126.30 m

PLATE A:

Digital Whole Core Photographs
Digital Core Chip/Plug Photograph

Figure 96A: Core Plug/Chip Atlas for sample 4126.30m from Vorwata-10.



Sample Depth: 4126.30 m
Shifted Depth: 13538.4 ft
He-∅: 14.86%
k air: 42.3 mD (sc)

WHOLE CORE PLUG ANALYSES
WELL: VORWATA - 10st
DEPTH: 4126.30 m

PLATE B:
Digital Whole Core Photographs
Digital Core Chip/Plug Photograph
Petrographic Photomicrograph

Figure 96B: Core Plug/Chip Atlas for sample 4126.30m from Vorwata-10.



Figure 97A: Core Plug/Chip Atlas for sample 4126.69m from Vorwata-10.

WHOLE CORE PLUG ANALYSES

WELL: VORWATA - 10st

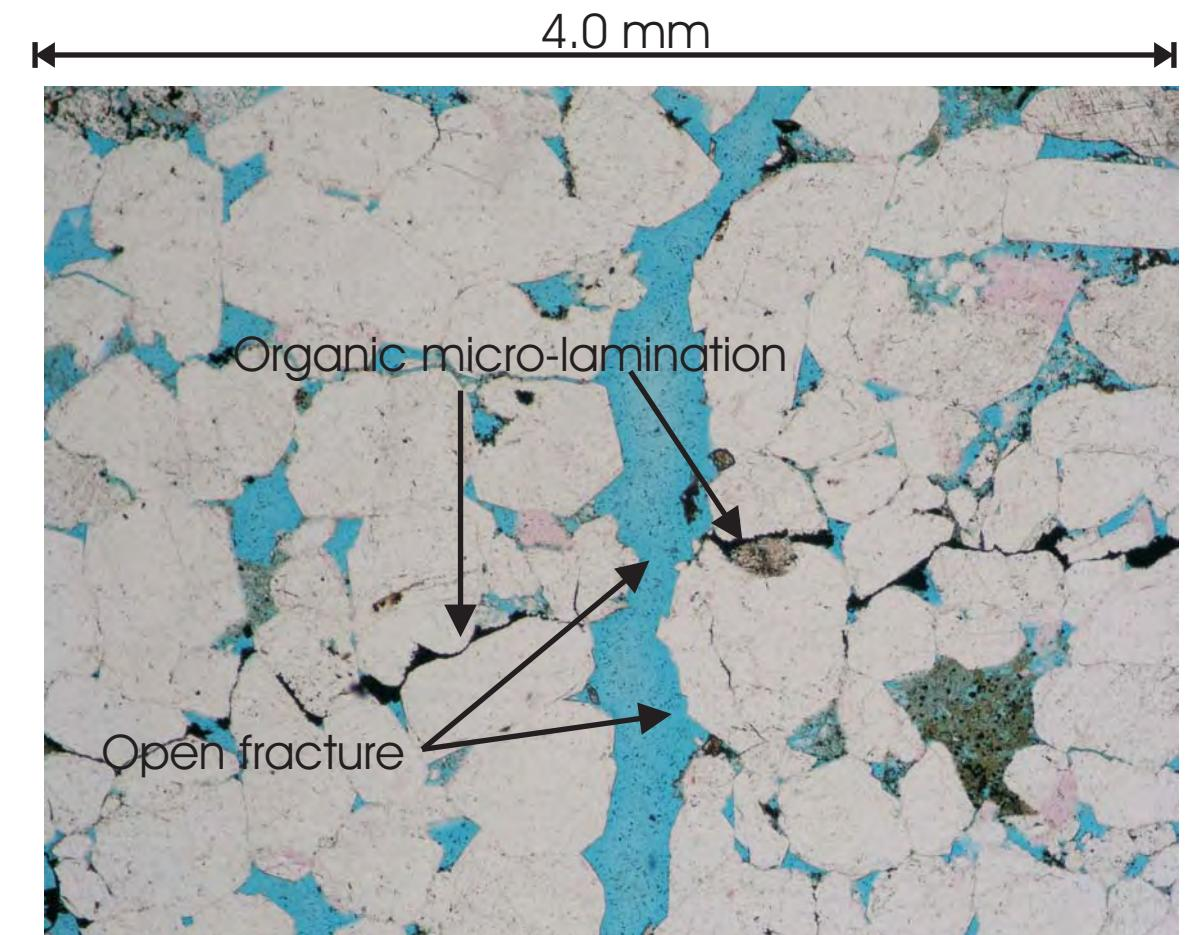
DEPTH: 4126.69 m

PLATE A:

Digital Whole Core Photographs



Sample Depth: 4126.69m
Shifted Depth: 13539.7 ft
He-Ø: 13.69%
k air: 463.8 mD (NOB 800 psia)



Open fractures have enhanced the permeability of this subarkosic basal interval of the Roabiba Reservoir on Vorwata-10. Orientation of bedding is indicated by micro-lamination of opaque organic material (possibly inertinite)

WHOLE CORE PLUG ANALYSES
WELL: VORWATA - 10st
DEPTH: 4126.69 m

PLATE B:
Digital Whole Core Photographs
Digital Core Chip/Plug Photograph
Petrographic Photomicrograph

Figure 97B: Core Plug/Chip Atlas for sample 4126.69m from Vorwata-10.

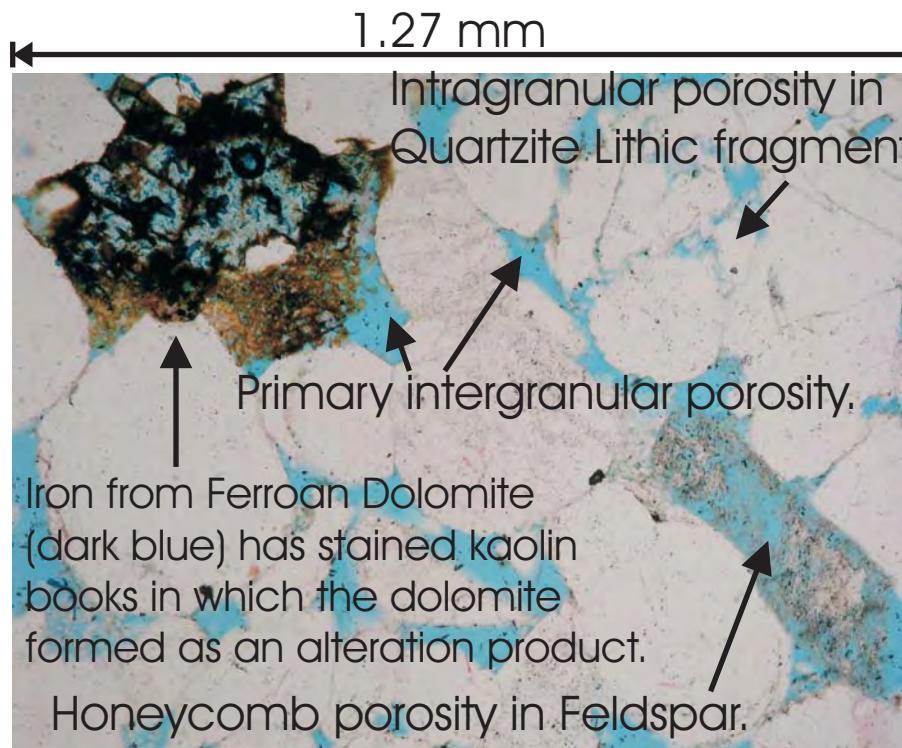


Figure 98A: Core Plug/Chip Atlas showing photographs and analyses results from sample depth 4128.92m from the Vorwata-10 well.



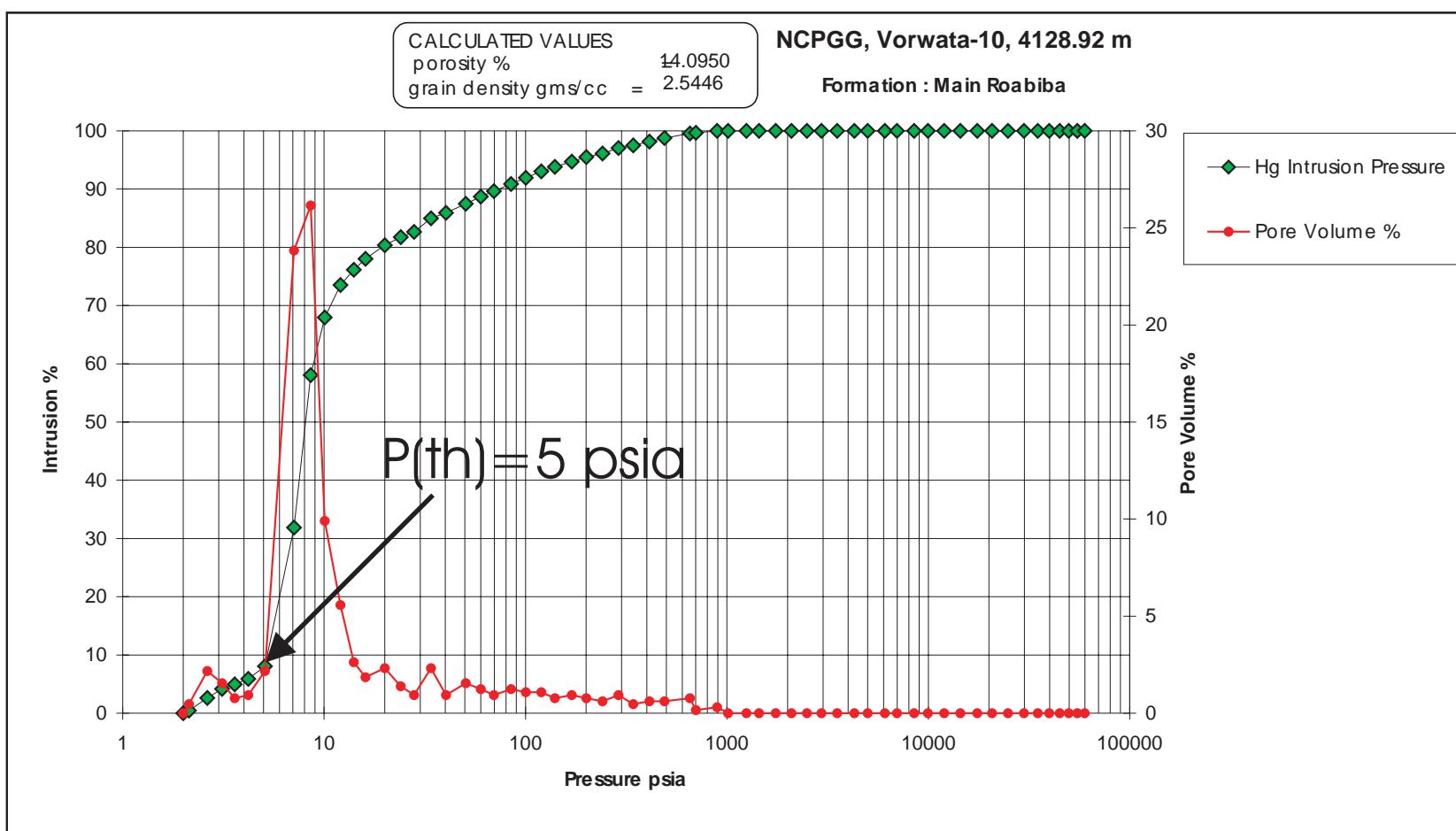
FIGURE 99:
WHOLE CORE PLUG ANALYSES
WELL: VORWATA - 10st
DEPTH: 4128.92 m

PLATE A:
Digital Whole Core Photographs



Sample Depth: 4128.92 m
Shifted Depth: 13547.0 ft
He-Ø: 15.7%
k air: 475.0 mD (NOB 800 psia)

Sample Depth: 4128.92 m
Shifted Depth: 13547.0 ft
MICP Entry Pressure: 3 psia
MICP Threshold Pressure: 5 psia
Lithology: Sandstone (Roabiba)



WHOLE CORE PLUG ANALYSES

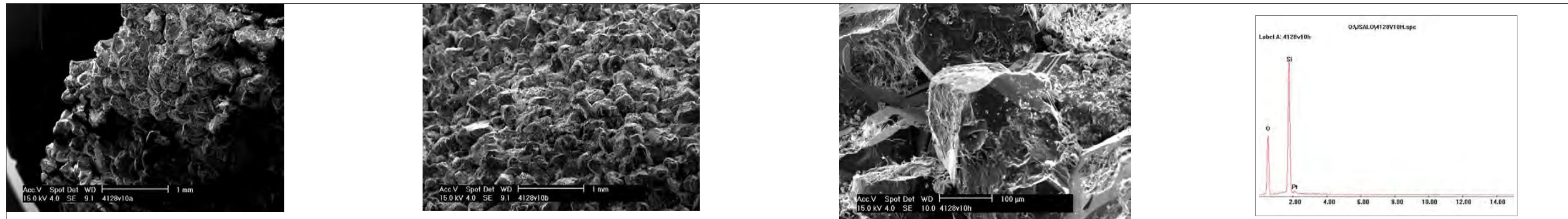
WELL: VORWATA - 10st

DEPTH: 4128.92 m

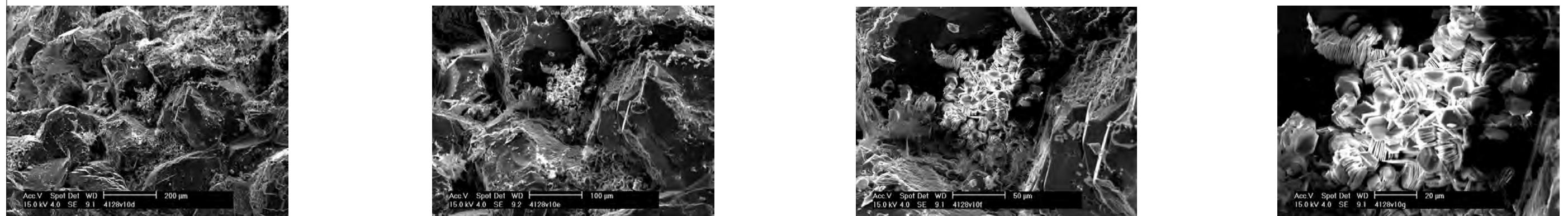
PLATE B:

Digital Core Chip/Plug Photograph
Petrographic Photomicrograph
Mercury Injection Capillary Pressure

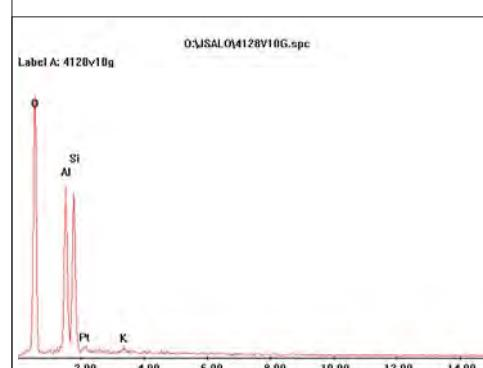
Figure 98B: Core Plug/Chip Atlas showing photographs and analyses results from sample depth 4128.92m from the Vorwata-10 well.



Quartzarenite core plug sample from the base of the deepest core in the Roabiba Reservoir at Vorwata-10. SEM images confirm medium grained quartz sandstone with occasional replacement of grains by kaolin books (possibly an alteration product of feldspar).



EDX analysis confirms composition of kaolinite grain nested between quartz grains. Helium porosity (with 800 psi Net Over-Burden confining pressure) was 15.7%, and air permeability was 475 mD. This sample is the deepest core plug sample obtained from Roabiba Reservoir cores, and is almost 250 ft below the GWC (i.e. Gas-Water Contact).



WHOLE CORE PLUG ANALYSES
WELL: VORWATA - 10st
DEPTH: 4128.92 m

PLATE C:

FESEM Photomicrograph
FESEM EDX (SEM XRD)

Figure 98C: Core Plug/Chip Atlas showing photographs and analyses results from sample depth 4128.92m from the Vorwata-10 well.

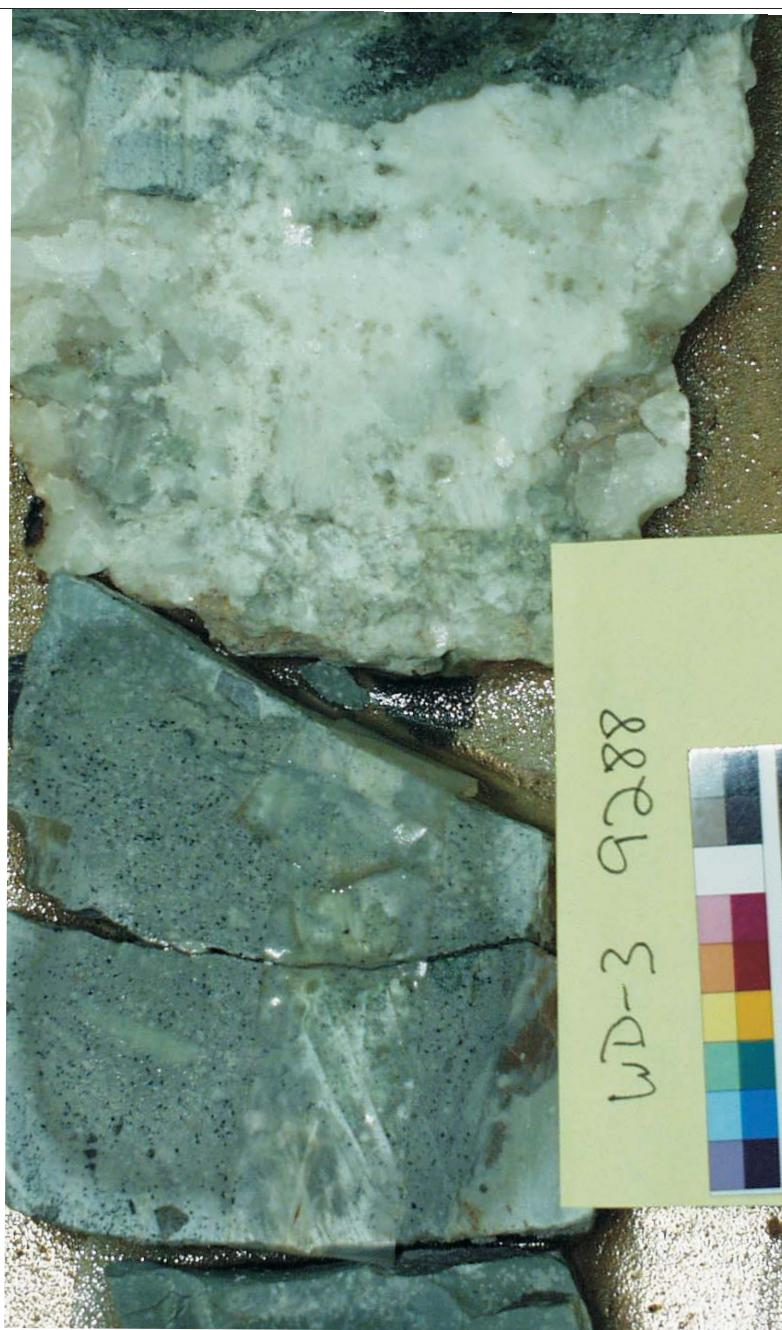
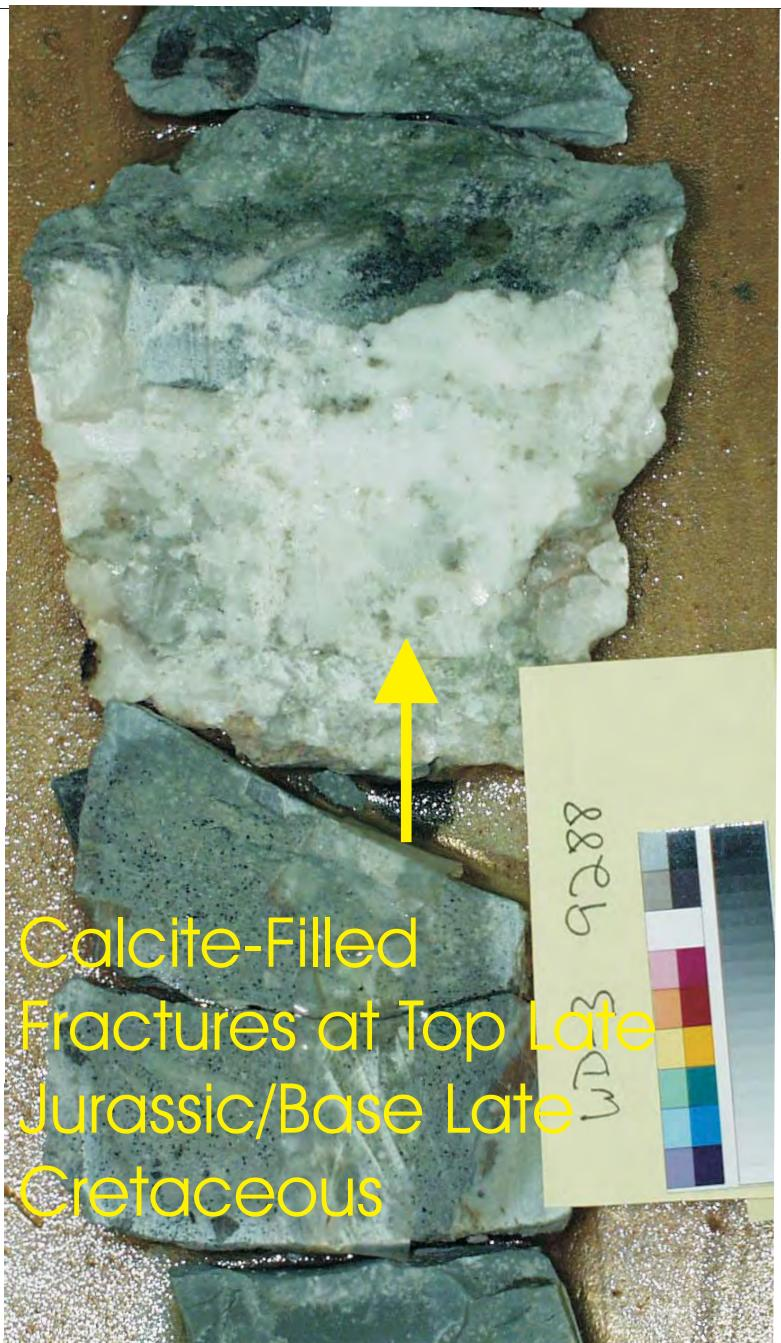


Figure 99A: Core Atlas illustrating the faults/fractures in cores from Wiriagar Deep wells, in regional seal lithologies. Whole core photographs of open fractures/faults cross-cutting the Upper Late Jurassic Shale/Base Late Cretaceous Marl unconformity, from the Wiriagar Deep-3 well.

FIGURE 99:
Digital Whole Core Photographs
Of Faults and Fractures on Wiriagar Deep
Wells.



Figure 99B: Core Atlas illustrating the faults/fractures in cores from Wiriagar Deep wells, in regional seal lithologies. Significant slickensided fault cored at Wiriagar Deep-1 well, in the shale seal of the Paleocene Sand-Prone Upper Member, produced a gas kick of 2445 units during the coring. Open fault, acting as a hydrocarbon conduit, was confirmed on FMI imaging also (depth 6805' to 6811').

FIGURE 99:

Digital Whole Core Photographs
Of Faults and Fractures on Wiriagar Deep
Wells.

**Whole Core
Digital
Photographs**

(Photography by
J. Salo)

**Core Plug/Chip
Digital
Photographs**

(Photography by
J. Salo)

**Petrographic
Photomicrograph
Images**

(Petrography by
S.E.Phillips)

Bulk XRD

(XRD analysis by
J. Salo)

**MICP Pressure
Plots**

(MICP interpretation
by J.Salo)

**SEM
Photomicrograph
Images**

(SEM preparation,
analysis, and images
by J.Salo, Figure 55C
by J. Salo and P. Uwins)

SEM EDX

(SEM EDX analysis and
interpretation by J.Salo,
Figure 55C by J. Salo
and P. Uwins)

**He Porosity and
Air Permeability
Data**

(Poro-perm analysis
by Amdel or Core
Laboratories)

Core Plug/Chip Atlas Guide

(Some or all of the analyses listed in this guide were carried out on
the whole core plugs/chips presented in this "Core Plug/Chip Atlas").

Figure Number 100 Core Plug Atlas Guide

**Core Plug/Chip
Sample and Analyses
Information Legend**